Handbook of Thermoset Resins

Debdatta Ratna

SMITHERS
iSmithers

Handbook of Thermoset Resins

Debdatta Ratna

*i*Smithers – A Smithers Group Company

Shawbury, Shrewsbury, Shropshire, SY4 4NR, United Kingdom
Telephone: +44 (0)1939 250383 Fax: +44 (0)1939 251118
http://www.rapra.net

First Published in 2009 by

***i*Smithers**

Shawbury, Shrewsbury, Shropshire, SY4 4NR, UK

A catalogue record for this book is available from the British Library.

ISBN: 978-1-84735-410-5 (hardback)
978-1-84735-411-2 (softback)

Typeset by Argil Services
Printed and bound by Lightning Source Inc.

Preface

This book is dedicated to thermoset resins, an important class of polymer materials. Unlike thermoplastics, thermoset resins are characterised by a curing reaction, which converts the low molecular weight liquid resins (easy to process) into solid three- dimensional network structures. The main advantage of a thermoset over a thermoplastic is that a wide range of properties can be achieved by simply adjusting the crosslink density of the thermoset network, without changing the chemical structure. As a student of polymer science and a researcher in the field of thermoset resins, I always felt the lack of a self-sufficient book dedicated to thermoset resins. That is why I decided to compile my fundamental understanding and long research experience in this specialised field and present it in the form of a book when I was invited to do so by Ms. Frances Gardiner (Smithers Rapra Technology, UK) after the publication of my Rapra Review Report (No. 185) on Epoxy Resins. I am thankful to her and her team for their cooperation and encouragement.

The major part of this book was written when I was a visiting scientist to the Institute of Composite Materials (IVW), Technical University, Kaiserslautern, Germany. Alexander von Humboldt foundation, Germany, was the sponsor for my fellowship and Professor J. Karger-Kocsis was my host, who has advised and encouraged me during my entire research stay in Germany. Dr. Thomas Abraham, who was a post doctoral fellow from the very beginning of my tenure in IVW, had helped me a lot to prepare the large number of figures for the book. Dr. Wanjale joined as a post doctoral fellow in IVW at a later part of my tenure and also helped me to a certain extent. I would like to acknowledge all of their contributions. I wish to thank Dr. Narayana Das, Director, Naval Materials Research Laboratory (NMRL), Dr. B.C. Chakraborty, Head of polymer division, NMRL and my other colleagues of NMRL for their encouragement and supports.

I have divided this book into seven chapters. It starts with a general introduction to thermosets, which includes network concept, additives and techniques/instrumentations (their principles) used to characterise a thermoset resin. The chemistry, properties and applications of individual thermoset resins are discussed in Chapters 2 and 3. Chapters 4 and 5 deal with the modification of thermoset resins for improvement in fracture toughness. The thermoset-based composites and nanocomposites are

discussed in Chapters 6 and 7, respectively. With such broad technical content covering the basic concepts and recent advances, I am sure this book will serve as a useful textbook-cum-handbook for the students, researchers, engineers, R&D scientists from academia, research laboratories and industries. It will be extremely useful for the scientists and researchers to make a knowledge-base in the subject as well as to plan their future works because I have not only presented the review of the recent advances in this book but also highlighted the future directions of research in the various areas of thermoset resins. The bounty of information garnered in this book will serve as a fountainhead for further exiting development in the field of thermoset resins in general and thermoset nanocomposites in particular.

I would like to dedicate this book in the memory of my father late Lakshmikanta Ratna. The best wishes of my mother (Snehalata Ratna), in-laws, sisters, Sunilda and other well wishers have always been the driving force and heaven's light (Almighty's blessing) has been the guide behind this creation. I am thankful to my father-in-law Shri Nirmalendu Sathpathi for not only his moral support but for his editorial assistance. For writing this book, I had to utilise much of the quality time, which I generally give, to my family. Hence I am sincerely thankful and indebted to my wife (Sujata) and sons (Saptarshi and Debarshi) for their patience and for always being the source of inspiration, without which this book would have not been in reality.

Debdatta Ratna

Summer 2009

Contents

1 General Introduction to Thermoset Networks

1.1 Introduction

Nature has long demonstrated the propensity to synthesise polymers, as exemplified by natural macromolecules such as proteins, carbohydrates, and natural rubber. The first synthetic polymer (phenol-formaldehyde resin) was developed by Baekeland in 1909 [1]. Modification of natural polymers using sulfur, i.e., vulcanisation of natural rubber, was discovered much before the development of synthetic polymer by Goodyear in 1839 [2]. All these activities were carried out without understanding macromolecular concepts. The macromolecular hypothesis was proposed by Staudinger in 1920. With the development of polymer science and technology, polymers started to be used in various applications if other materials could not be used or as replacements for conventional materials. Polymers are therefore comparatively new materials, and have proved to be suitable substitutes for conventional materials in diverse applications. The driving force for replacement of conventional materials by polymers is their obvious advantages: light weight, low cost, ease of processing, and wide scope of modifications to tailor the desired properties.

Synthetic polymers can be classified into thermoplastic polymers and thermoset polymers. The former soften on heating and stiffen on cooling repeatedly. Thermosetting polymers undergo a chemical reaction ('curing') on heating and are converted into an infusible and insoluble material. The infusibility and insolubility of the cured polymer arise due to the formation of a three-dimensional (3D) network structure, as discussed below. Thermoset polymers can be grouped on the basis of molecular weight into thermoset resins (low molecular weight) and rubber or elastomer (high molecular weight). Low molecular weight thermoset polymers, i.e., thermoset resins, are the subject of this book.

1.2 Network Concept

The term 'network' is widely used to describe the structure of solid-state materials. A molecular or atomic network structure is the basis of the mechanical coherence of such materials. A lattice is an example of a network of ions in which the electrostatic

ionic forces keep the cations and anions together. When a solid is melted or dissolved in any solvent, the network structure is broken and structural integrity lost. Diamond is a classic example of a covalent network, in which each carbon atom is covalently bonded to its neighbours, forming a tetrahedral structure. The structure is basically a macromolecular 3D network responsible for its remarkable hardness in contrast to the other allotrope, graphite.

Polymer networks or crosslinked networks are molecular-based networks whose network structures depend entirely on covalent bonding or on physical interactions between the macromolecules. Just like in diamond, each pair of adjacent junction points in the network are separated by only one covalent bond. In a polymer network, two junction points are separated by linear sub-chains of several bonds or many covalent bonds. When the connectivity from the junction point is through chemical bonds, they are called 'chemical crosslinks', as found in thermosets. The crosslinks generated due to the entanglement of long polymer chains are known as 'physical crosslinks'. In case of thermoset polymers, the crosslinks are chemical crosslinks.

1.3 Gelation

When a thermoset resin cures, it encounters an interesting phenomenon: gelation. The gel point is considered to be a point in polymerisation where network structure first occurs with unit probability. The question is: what is the molecular basis of gelation? The basic condition of a compound to be a precursor of a polymer is that the functionality of the compound must be ≥2. When two molecules with a functionality of 2 react with each other, the product will always have a functionality of 2 because, out of the total functionality of 4, 2 are lost due to the reaction. A linear polymer is formed due to polymerisation of a difunctional monomer. If the functionality is >2, branching will be generated and the number of reactive functionality will increase with an increase in the branch points (**Figure 1.1**). For example, if a trifunctional molecule reacts with a difunctional molecule, the reactive functionality of the intermediate will be 3, and when the first intermediate reacts with another trifunctional monomer, the functionality will be 4. If we assume that all the functional groups are equally reactive (irrespective of the attachments), then the intermediate will react preferentially and a network will be formed before completion of the reaction (**Figure 1.1**). If we consider a reaction between a difunctional monomer and monomer of functionality f, then the number of reactive groups (N_r) in an intermediate molecule with n branch point can be expressed as:

$$N_r = n(f-1)+2 \tag{1.1}$$

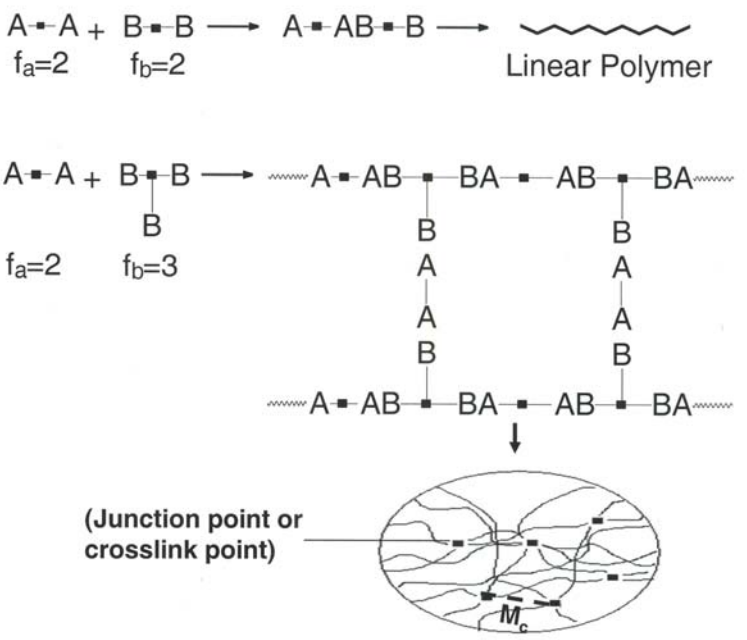

Figure 1.1 Schematic representation of network formation during a reaction between two molecules with functionality of >2

The gelation phenomena in polymerisation reactions were described by Flory and Stockmayer [3–5]. In the case of a polymerisation reaction of A and B with functionality f_a and f_b, respectively, the number of paths which can lead from a randomly chosen A group from the f_a functional groups is (f_a–1). Similarly, one B group can react in (f_b–1) number of ways with any one of the A groups. If P_a and P_b are the extent of reaction of A and B groups, P_a and P_b are the probabilities per path for A and B groups, respectively. Hence the gel point can be statistically expressed as:

$$(f_a - 1)p_a(f_b - 1)p_b = 1 \tag{1.2}$$

The statistical approach for deriving the above equation is based on the assumption that all A and all B groups have the same probabilities of reacting and there is no intramolecular reaction. In the case of a mixture of reactants of different functionalities, the functionality should be replaced by an average functionality. Thus, expressing **Equation 1.2** in terms of average functionality we get:

$$(f_{an} - 1)p_a(f_{bn} - 1)p_b = 1 \tag{1.3}$$

where f_{an} and f_{bn} are the number average functionalities of A and B, respectively.

The number average degree of polymerisation (DP_n) is defined as the ratio of number of units (number of molecules initially present) to the number of molecules present after the reaction. DP_n can be expressed as:

$$DP_n = \frac{N_a + N_b}{N_a + N_b - N_x} \tag{1.4}$$

where N_x is the number of A or B groups reacted. N_x can be expressed in terms of extent of reaction as follows:

$$N_x = N_a f_{an} p_a = N_b f_{bn} p_b \tag{1.5}$$

Combining **Equations 1.4** and **1.5** we get:

$$DP_n = \frac{N_a + N_b}{N_a + N_b - N_a f_{an} p_a} = \frac{1}{1 - p_a \dfrac{1}{\dfrac{1}{f_{an}} + \dfrac{1}{r f_{bn}}}} \tag{1.6}$$

where r is the molar ratio of A and B, i.e., N_a/N_b

Similarly,

$$DP_w = 1 + \frac{p_a p_b f_{an} f_{bn} \{p_a (f_{an} - 1) + 2\}}{\{1 - p_a p_b (f_{an} - 1)(f_{bn} - 1)\}(p_a f_{an} + p_b f_{bn})} \tag{1.7}$$

For the resins, which self-polymerise without a curing agent, namely resole type phenolic resin or cyanate ester resin ($p_a = p_b$, r = 1 and $f_a = f_b$), Equations 1.6 and 1.7 can be written as:

$$DP_n = \frac{1}{1 - p_a \dfrac{f_{an}}{2}} \tag{1.8}$$

$$DP_w = \frac{1 + p_a}{1 - p_a (f_{an} - 1)} \tag{1.9}$$

Carothers proposed the criterion for gelation that $DP_n \to \infty$ at gel [6]. This criterion is based on the percept that all the units in a polymerising mixture are connected to form a single network. This is inconsistent with a random polymerisation because it groups cannot organise in such a way that only two per original molecule react. Thus, the

more acceptable criterion for gelation is the weight average degree of polymerisation $DP_w \rightarrow \infty$, which means that average degree of polymerisation per unit is infinite. The condition $DP_n \rightarrow \infty$ means average DP per molecule is infinite because the number of molecules reduces to zero. Thus, gelation is accompanied with a divergence in DP distribution in which the weight averages or higher averages become infinite.

1.4 Cure Characteristics

Cure kinetics of the resin must be studied for effective utilisation of the potential of a thermoset resin. Cure kinetics of the thermosetting resins has been investigated using various thermal and spectroscopic techniques [7–11]. The principle of these techniques will be discussed in **Section 1.10**. When a thermoset resin cures, gradual conversion of functional groups due to a chemical reaction takes place. Hence, the first step of cure kinetics is to define the conversion or extent of curing (α). The extent of curing is determined from the disappearance of functional groups using Fourier-transform infrared or nuclear magnetic resonance (NMR) spectroscopic analysis, and from the heat of reaction using differential scanning calorimetry (DSC). For example, α can be determined from the infrared (IR) absorbance of the reactive groups using the following relationship [7]:

$$\alpha = 1 - \frac{A^t}{A^0} \tag{1.10}$$

A_t and A_0 are the normalised absorbance of the functional groups before the reaction and after reaction time t. Absorbance of a group which does not participate in reaction is used as a reference for normalisation.

The extent of curing can be expressed in terms of heat of reaction as follows:

$$\frac{d\alpha}{dt} = \frac{1}{H_0}\frac{dH}{dt} \tag{1.11}$$

where H_0 is the total heat released during complete curing and H is the heat released from the onset of polymerisation up to time t. If the curing reaction involves only one chemical reaction, then the crosslinking reaction will be characterised by a single heat of reaction and the extent of curing will be the same as the number of reacted groups determined by spectroscopic analysis. However, if the curing reaction involves several chemical reactions, then the heat of reaction determined by DSC will represent the mean value. Details about DSC measurement and analysis are discussed in **Section 1.10.6.1.**

Several models have been proposed to describe the curing of thermoset resins [11–13]. The phenomenological model developed by Kamal [14] is mostly used for isothermal kinetic analysis. The general equation for an n^{th} order reaction [15, 16] can be written as:

$$\frac{d\alpha}{dt} = K_1(1-\alpha)^n \tag{1.12}$$

where K_1 is the rate constant and n is the order of the reaction. In many curing reactions, the new groups (produced as a result of curing) catalyse the curing reaction. For instance, the hydroxyl groups formed during the curing of epoxy resin catalyse the epoxy/amine reaction. The equation for an autocatalytic curing reaction can be represented as:

$$\frac{d\alpha}{dt} = (K_1 + K_2\alpha^m)(1-\alpha)^n \tag{1.13}$$

where K_2 expresses the rate constant for an autocatalytic curing reaction, m and n are the kinetic exponents of the reaction, and (m + n) gives the overall order of the curing reaction. When $K_2 = 0$, the equation reduces to a non-catalytic one. From the isothermal DSC experiment, the extent of reaction and reaction rate data must be determined and adjusted with kinetic equations. The initial rate of reaction, i.e., reaction rate at $\alpha = 0$, is used to determine K_1.

The kinetic constants K_1 and K_2 can be correlated to temperature according to the Arrhenius equation given below:

$$K_i = A\exp\left(\frac{E_i}{RT}\right) \tag{1.14}$$

K_i and E_i are the rate constant and the activation energy, respectively. A is a constant, R is the universal gas constant, and T is the absolute temperature. Thus, the kinetic model as discussed above allows calculation of activation energy (E), using linear regression on data obtained at different temperatures. Typical plots showing the effect of temperature on reaction rate and conversion of free radically polymerised unsaturated polyester are shown in **Figures 1.2a** and **1.2b**, respectively.

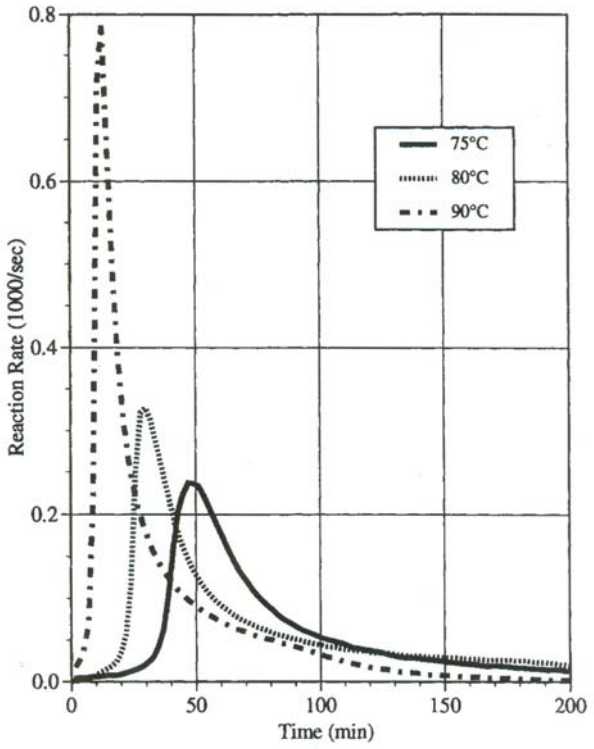

Figure 1.2a Isothermal reaction rate versus time plot of a free radical-polymerised unsaturated polyester resin. Reprinted with permission from S.V. Muzumdar and L.J. Lee, *Polymer Engineering and Science*, 1996, **36**, 7, 943 © 1996, John Wiley and Sons Publishers.

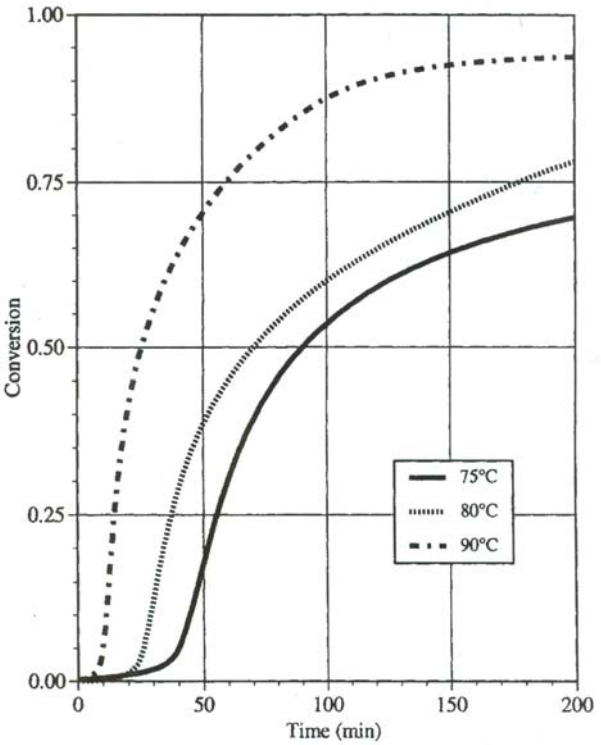

Figure 1.2b Conversion profile *versus* time plot of a free radical-polymerised unsaturated polyester resin. Reprinted with permission from S.V. Muzumdar and L.J. Lee, *Polymer Engineering and Science*, 1996, **36**, 7, 943 © 1996, John Wiley and Sons Publishers.

1.5 Effect of Vitrification on Polymerisation Rate

The polymerisation or curing rate is a function of conversion and temperature, and can be defined as:

$$r = f(x, T) = k(x, T)\, f1(x) \tag{1.15}$$

where k is the overall rate constant and $f_1(x)$ is a measure of the dependence of curing rate on the concentration of functional groups. Unlike the reaction for synthesis of small molecules, a polymerisation reaction is associated with an increase in the viscosity of the medium. As the viscosity of the medium increases, the rate of diffusion of the molecules decreases, and hence there will be competition between reactivity-control and diffusion-control reactions. At a critical conversion (α_c), at which the T_g of the network approaches the curing temperature, the reaction becomes totally diffusion-

controlled. At this stage, a conversion from a rubbery gel to glassy gel takes place, and the process is called 'vitrification'. Due to a significant decrease in free volume, the rate of diffusion will be significantly reduced at this stage. A semi-empirical relation can be used to express the rate constant [17, 18], as given in **Equation 1.16**:

$$K_d = K_r \exp\left[-D(\alpha - \alpha_c\right] \tag{1.16}$$

K_r is the reactivity rate constant, D is a constant, and α_c is the critical extent of curing at which the glassy state is attained. Because switching from a reactivity-controlled reaction takes place gradually, the overall rate constant k (x, T) can be expressed using the Rabinovitch model [13] in terms of the Arrhenius rate constant (k) or reactivity rate constant (k_r) and diffusion rate constant (k_d) as follows [19, 20]:

$$\frac{1}{k(\alpha,T)} = \frac{1}{k_r(\alpha,T)} + \frac{1}{k_d(\alpha,T)} \tag{1.17}$$

The ratio of K (α, T) to K_r (α, T) is defined as the diffusion factor f (α) for the rate of the curing. Hence, by combining **Equation 1.16** and **1.17** and rearranging, we get:

$$f_\alpha = \frac{K(\alpha,T)}{K_r(\alpha,T)} = \frac{1}{1+\exp\left[D(\alpha-\alpha_c\right]} \tag{1.18}$$

During the initial stage of curing, α is much smaller than α_c ($\alpha << \alpha_c$) f_α is close to unity, and curing is reactivity-controlled.

Hence, a generalised autocatalytic and non-catalytic kinetic equation can be expressed, as shown next in **Equations 1.19** and **1.20**, respectively.

$$\frac{d\alpha}{dt} = (K_1 + K_2\alpha^m)(1-\alpha)^n \frac{1}{1+\exp\left[D(\alpha-\alpha_c\right]} \tag{1.19}$$

$$\frac{d\alpha}{dt} = K_1(1-\alpha)^n \frac{1}{1+\exp\left[D(\alpha-\alpha_c\right]} \tag{1.20}$$

1.5.1 Modelling from the Pressure, Volume and Temperature Approach

Most of the models describing thermoset curing deal with the effect of temperature on the curing reaction. However, pressure is a critical parameter for the moulding of

thermoset resins. During curing, the volume of the resin decreases, and this is called 'cure shrinkage'. Processing of thermoset resins without application of pressure often leads to the generation of voids [21] as a result of cure shrinkage. Therefore, it is interesting to study the effect of pressure on the curing reaction. Unlike the many reports dedicated to the study of the effect of temperature on curing, there are only a few studies on the effect of pressure [22–25] on curing of thermoset resins. If curing is carried out at constant temperature, then volume change can be attributed to cure shrinkage and conversion in terms of volume [26] can be expressed as:

$$\alpha = \frac{v_t - v_1}{v - v_0} \tag{1.21}$$

where v_t and v_1 are the specific volume at time t and at t = 0, respectively, and v and v_0 are the final and initial specific volume, respectively.

The dependence of the rate constant on pressure at a constant temperature [26] can be expressed as follows:

$$K = K_0 \exp\left(-\frac{\Delta v}{RT} + \beta\right)(P - P_0) \tag{1.22}$$

where K and K_0 are the rate constant at pressure P and $P_{0,}$ respectively, Δv is the activation volume, and β is the compressibility factor. At the initial stage of curing when the reaction is reactivity-controlled, the increase in pressure increases the probability of the mutual approach of the reactive groups, and thereby enhances the rate of reaction. At a later stage of curing, when the reaction is diffusion-controlled, application of pressure further reduces the diffusion, leading to the reduction in reaction rate.

1.6 Effect of Cure Conversion on Glass Transition Temperature (Tg)

Amorphous polymers are characterised thermodynamically by a second-order transition known as 'glass transition'. The temperature at which the transition takes place is called the T_g. Unlike melting, glass transition is not sharp. Hence, we call it a glass transition region, i.e., a temperature range. At a temperature below the T_g, polymer materials are glassy (hard and strong). When the service temperature goes beyond the T_g, the polymer becomes soft and loses its dimensional stability. A drastic change in modulus (rigidity) takes place in the T_g region. Thus, the T_g of a thermoset has great significance with regards to design of the materials for a particular application. For load-bearing applications where dimensional stability is of prime

importance, the service temperature must be well below the T_g. The methods for experimental determination of T_g and its significance in different applications will be addressed in subsequent chapters. In this section, how one can predict the T_g of a thermoset resin as a function of conversion of curing reaction will be discussed.

With the advancement of a curing reaction, the T_g of the resin will increase, but the goal is to quantitatively predict the T_g of a resin as a function of cure conversion. Several models have been proposed to correlate the T_g with the conversion or extent of curing (α). With the increase in conversion, the concentration of reactive functionalities decreases, and crosslinks or junction points are formed, leading to the departure from Gaussian behaviour. Steric hindrance affects chain conformation at high crosslink densities. The models are based on the statistical description of network formation and calculation of the concentration of junction points of different functionalities as a function of conversion. However, one issue that complicates the calculation and which is not fully resolved is whether to consider all the junction points or only those which are elastically effective.

An equation (known as Dibenedetto equation) which has been successfully applied to correlate the experimental values of the T_g as a function of conversion for many thermosetting resin like epoxy, phenolics is given next [27]:

$$\frac{T_g - T_{g0}}{T_{g\infty} - T_{g0}} = \frac{\lambda\alpha}{1-(1-\lambda)\alpha} \tag{1.23}$$

where T_{g0} is the T_g of the resin mixture before cure, $T_{g\infty}$ is the T_g obtainable after maximum possible curing, and λ is an adjustable parameter. Pascault and Williams [28] derived similar equation using Couchman's analysis [29] considering the isoberic heat capacity change as a variable:

$$T_g = \frac{\alpha\Delta c_{p\infty} T_{g\infty} + (1-\alpha)\Delta c_{p0} T_{g0}}{\alpha\Delta c_{p\infty} + (1-\alpha)\Delta c_{p0}} \tag{1.24}$$

where Δc_{p0} and $\Delta c_{p\infty}$ are the change in heat capacity corresponding to T_{g0} and $T_{g\infty}$.

Comparing the two equations:

$$\lambda = \frac{\Delta c_{p\infty}}{\Delta c_{p0}} \tag{1.25}$$

During advancement of the curing reaction, it was observed that the change in heat capacity decreases. Montserrat [30] proposed an equation to correlate $\Delta c_p\left(T_g\right)$ with the T_g of the network:

$$\Delta c_p\left(T_g\right) = x + \frac{b}{T_g} \tag{1.26}$$

Neglecting the constant (x), which may be applicable for a particular case, we get:

$$\lambda = \frac{\Delta c_{p\infty}}{\Delta c_{p0}} = \frac{T_{g0}}{T_{g\infty}} \tag{1.27}$$

Combining **Equations 1.24** and **1.27** and rearranging we get:

$$\frac{1}{T_g} = \frac{(1-\alpha)}{T_{g0}} + \frac{\alpha}{T_{g\infty}} \tag{1.28}$$

This is an equation similar to the Fox equation, which is widely used to predict the T_g of a copolymer as a function of composition. However, this simple rule-of-mixture equation cannot precisely explain the experimental results obtained in actual systems. Hence, a modified equation has been proposed [31, 32]:

$$\frac{1}{T_g} = \frac{(1-\alpha)}{T_{g0}} + \frac{\alpha}{T_{g\infty}} + c\alpha(1-\alpha) \tag{1.29}$$

1.7 Crosslinked Density (Xc)

Crosslink density is an important parameter for a thermosetting system for tailor-making the properties of a crosslinked network. As crosslink density increases, the hardness, modulus, mechanical strength and chemical resistance increase, whereas percentage elongation at break, impact strength, toughness, resiliency, and low temperature flex tend to decrease. For example, when natural rubber is lightly crosslinked (low crosslink density), the network produces a highly flexible and resilient material. When the same rubber is highly crosslinked, it generates a brittle material. X_c is expressed as the number of crosslinks per unit volume or molecular weight between the two crosslink points (M_c). The methods for determination of crosslink density are discussed below.

X_c can be determined from swelling study using the Flory–Rehner theory [3]. Unlike thermoplastics, which dissolve in a solvent having a close proximity of solubility parameters, the crosslinked network swells by absorbing solvent. As more and more solvent is adsorbed by the polymer network, the network expands progressively. The driving force towards swelling is the increase in entropy of mixing of solvent with polymer. However, during the swelling process, the network chains are forced to attain more elongated, less probable configurations. As a result, like pulling a spring from both ends, a decrease in chain configurational entropy is produced by swelling. This effect reduces the entropy and opposes the swelling. Considering the forces arising from the entropy effect as discussed above and the enthalpy component, i.e., heat of mixing, the equilibrium condition according to the Flory–Rehner theory can be expressed as shown below:

$$\ln(1-\nu_p)+\nu_p+\chi\nu_p^2+V_s X_c\left[\nu_p^{1/3}-\frac{\nu_p}{2}\right]=0 \tag{1.30}$$

$$X_c=\frac{\ln(1-\nu_p)+\nu_p+\chi\nu_p^2}{V_s\left[\nu_p^{1/3}-\frac{\nu_p}{2}\right]}$$

Hence (1.31)

$$\overline{M}_c=\frac{d_p V_s\left[\nu_p^{1/3}-\frac{\nu_p}{2}\right]}{\ln(1-\nu_p)+\nu_p+\chi\nu_p^2} \tag{1.32}$$

$$\chi=k+\frac{V_s}{RT}(\delta_s-\delta_p)^2 \tag{1.33}$$

d_p = Density of cured resin

V_s = Molar volume of solvent

ν_p = Volume fraction of polymer in the swollen network

χ_c = Crosslinked density

$\overline{M}_c$ = Molecular weight between two crosslink points

X = Flory–Huggins interaction parameter

δ_s = Solubility parameter of solvent

δp = Solubility parameter of resin

R = Universal gas constant

T = Temperature (= 295 K)

K = Constant specific to solvent

Estimation of the crosslink density of a thermoset network can be obtained from the storage modulus values in the rubbery plateau region. In principle, the crosslink density of a cured thermoset network could be calculated from the theory of rubber elasticity. The shear modulus G of a crosslinked rubbery network is given by [33]:

$$G = \frac{r_1^2}{r_f^2}\frac{dRT}{M_c}\left(1 - \frac{2M_c}{M_n}\right) \tag{1.34}$$

where d is the density, R is the universal gas constant, T is the absolute temperature, M_c is the molecular weight between crosslinks, M_n is the chain backbone molecular weight, and r_1^2/r_f^2 is the ratio of the mean square end-to-end distance of the polymer chain in the sample to the same quantity in a randomly coiled chain. The ratio is often assumed to be unity. For a highly crosslinked system, M_c/M_n is negligible. Hence, **Equation 1.34** can be written as:

$$M_c = \frac{dRT}{G} = \frac{3dRT}{E'} \tag{1.35}$$

Thus, M_c can be determined from the dynamic storage modulus value at a temperature at least 30 °C higher than the T_g. The details for determination of the dynamic modulus using dynamic mechanical analysis are given in **Section 1.9.6.3**.

1.8 Additives for Thermoset Resins

1.8.1 Antioxidants

Thermoset resins (and polymers in general) are susceptible to degradation through oxidation reactions during processing at a high temperature, during thermal treatment, and outdoor exposure. Oxidation of polymers results in changes in molecular structures, causing a loss in mechanical properties (e.g., tensile, flexural and impact strength) of the cured resin network and physical characteristics (e.g., gloss, finish,

colour) of the resin surface. The extent of oxidative degradation of polymer chains depends on the processing or service conditions and the chemical structure of the polymer. Aliphatic chains degrade more easily compared with aromatic structures. This degradative reaction must be prevented to increase the life expectancy of polymer or thermoset materials. The additives used to protect polymer materials from oxidative degradation are called 'antioxidants'. β-carotene and α-tocophenol are examples of natural antioxidants.

To know how antioxidants function, the mechanism of the oxidation process must be known. The oxidation reaction is believed to proceed through a free-radical mechanism [34–37] (**Figure 1.3**). The main feature of the oxidation mechanism is the initial peroxidation of the polymer substrate through the reaction of alkyl peroxyl radical ($ROO\cdot$) with the substrate, which produces hydroperoxide (RCOOH). The peroxide is the major free-radical generator for continuing free radical-initiated oxidation. The generation of free radicals and propagation of the oxidative degradation process is represented in **Figure 1.3**.

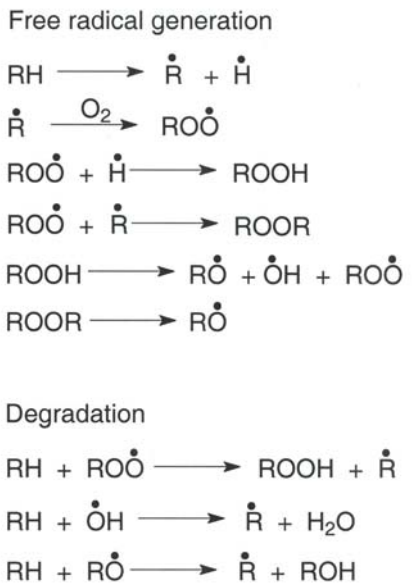

Figure 1.3 Free-radical mechanism of oxidative degradation of polymers

Antioxidants interfere with the free-radical oxidative cycle to inhibit or retard the oxidation mechanism. On the basis of the mechanisms by which antioxidants function, they can be classified into two categories: primary or chain-breaking antioxidants, and secondary or preventive antioxidants. Chain-breaking antioxidants are of two types: chain-breaking donor (CB-D) antioxidants and chain breaking acceptor (CB-A)

antioxidants. The former operate through a stabilisation reaction by reducing ROO· to ROOH (**Figure 1.4**). The reaction is facilitated due to the higher stability of antioxidant free radicals (A·). These stable radicals do not participate in the propagation reaction and are converted into non-radical products. Hindered phenol (e.g., 2.6-*t*-butyl 4 methyl phenol) and amines (2,2,6,6-tetramethyl piperidine) are good examples of CB-D antioxidants. Chain-breaking acceptor antioxidants remove alkyl radicals from chain-propagating reactions, and are effective under oxygen-deficient conditions [36, 37]. Quinones are important examples of CB-A antioxidants. Preventive or secondary antioxidants stop the generation of free radicals and thereby reduce degradation [38, 39]. They decompose the hydroperoxide into non-radical products. Phosphites and sulfide esters are classic examples of secondary antioxidants. The use of primary and secondary antioxidants results in a synergistic effect with respect to stabilisation. Addition of a small amount of such additives (0.05–0.5 wt%) considerably increases the life of the material. Benzophenone and benzotriazole compounds absorb ultraviolet (UV) radiation (referred to as 'UV absorbers') and protect the polymer from the harmful degrading effect of UV light. Like heat, UV light initiates free-radical oxidation of the polymer chain. UV absorbers convert harmful UV radiation to a comparatively harmless heat. In the case of 2-hydroxy benzophenone, UV light is utilised for a reversible keto–enol transition [39].

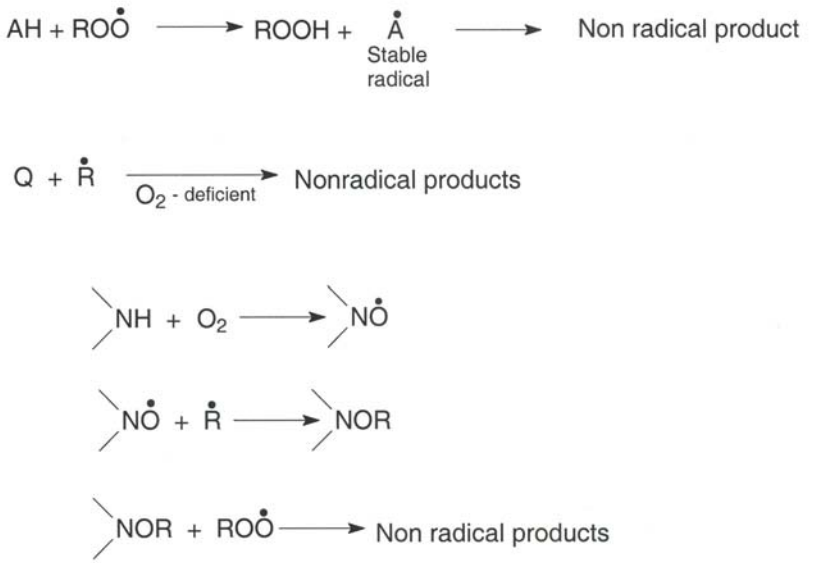

Figure 1.4 Mechanism of the antioxidant effect: formation of stable radicals or non-radical products

When selecting an antioxidant for a particular thermoset matrix, it should: (1) be

compatible with the matrix; 2) not degrade during curing or post-curing; and 3) not exude from the matrix after curing. However, loss of antioxidants due to leaching or diffusion cannot be avoided for the conventional antioxidants discussed above [40–42]. To solve the migration problem, reactive antioxidants that can be chemically anchored to polymer backbones have been explored [43–45].

1.8.2 Fillers

Fillers are solid additives mostly of inorganic type that are added to reduce the cost or to modify the physical properties (usually mechanical) of polymer materials. Fillers are mainly classified into two groups: inert fillers and reinforcing fillers. The latter can dramatically improve the mechanical properties of a polymer, and are used for the development of composite materials (composite materials are discussed in greater detail in subsequent chapters). Inert fillers do not significantly improve mechanical properties, and are used to reduce the cost and other properties (e.g., viscosity). Fillers impart hiding ability and help to reduce shrinkage stress, which is very important for adhesive and coating applications. Cure shrinkage results in the development of residual stress in the matrix. This effect is more prominent for resins with high cure shrinkage (e.g., phenolic resins, polyester resins). Inert filler improves the rigidity at the cost of toughness and strength. Fillers must be selected judiciously, and their size and shape manipulated accordingly to keep such loss in strength and toughness to a minimum. Aluminium powder, calcium carbonate, china clay, talc, and barium sulfate are commonly used as fillers.

1.8.3 Blowing Agents

Blowing agents are used to produce cellular products (e.g., foam). They are used mostly for phenolic and polyurethane resins. Chlorofluro carbon compounds (CFC) such as trichlorofluro methane (boiling point (bp), 23.8 °C) 1,1,1-trifluorodichloroethane (bp, 28.7 °C) and 1,1-dichloro-1-fluoro ethane (bp, 32 °C) are classic examples of blowing agents. A CFC is mixed with the polyol before the polymerisation reaction. During processing, liquid CFC change to gases and develop into foam. The frothed foam fills cavities quickly and imparts uniform cells. Though CFC are very successful as blowing agents, they are not environmentally safe. The concern over depletion of the ozone layer allegedly caused by the CFC has prompted polymer technologists to search for alternative blowing agents.

Addition of a small amount of water produces carbon dioxide by reaction with an isocyanate compound. The produced carbon dioxide is released and produces a cellular structure. Other classes of blowing agents such as sodium bicarbonate,

hydrazide derivatives, and azodicarbonamide decompose during processing and produce gases (e.g., carbon dioxide, nitrogen) which generate cellular structures. However, such blowing agents are chosen after consideration of the reaction conditions and decomposition temperature of the respective blowing agent. The processing temperature of the thermosetting resin system must be higher than the decomposition temperature of the blowing agent. For example, if sodium bicarbonate is selected as a blowing agent, the processing temperature must me >130 °C, and similarly for azodicarbonamide the processing temperature should be >200 °C. Bicarbonates and sulfonylhydazides are used in unsaturated polyester resin where metal catalysts are used as promoters. The catalyst reduces the decomposition temperature and ensures generation of gases at a lower temperature (less than the processing temperature).

1.8.4 Coupling Agents

The property of a polymer blend or a filled polymer system largely depends on the compatibility between the constituent polymers in the blends or between the polymer and filler in filled-polymer systems. Other terminologies such as 'wetting' and 'interfacial adhesion' are sometimes used to reflect compatibility. For filled polymer systems, the incompatibility generates weak interfaces, leading to a drastic reduction in mechanical properties. Coupling agents are used to improve the compatibility, wetting or interaction between the constituent polymers in the blends, or between the polymer and filler in filled polymer systems. Coupling agents have been found to be very successful for improving the properties of thermoplastic blends [46]. However, in thermosetting resin systems, coupling agents are mostly used to improve the wetting of filler by the resin matrices. Silane compounds such as trichlorovinyl silane, triethoxyvinyl silane, and γ-glycidoxypropyl-trimethoxy silane are examples of coupling agents for thermosetting resins [47].

1.8.5 Surfactants

Surfactants are added to a thermoset resin system to promote the dispersion of fillers in the resin matrix. Recently, surfactants have been used to disperse carbon nanotubes in polymer matrices [48–50]. Surfactants are of two types: neutral and ionic. Surfactants have many applications in coating industries for the development of a water-based resin system [51]. Surfactants are added to phenolic or polyurethane foam formulation in which they facilitate formation of small bubbles. The size and uniformity of bubble formation results in a fine cell structure. A surfactant reduces the surface tension of resin formulations and provides an interface between the highly polar resin and the non-polar blowing agent. The surfactant for a particular resin system must be selected carefully so that it is compatible with the resin and resistant

to the acidic or basic catalyst. When the foam develops, the surfactant protects the developing foam from collapse or rupture. However, it is important to optimise the concentration of surfactant as a function of foam properties to develop foam with desirable structure and properties.

1.8.6 Colorants

Thermoset resins can be coloured by introducing a chromophore group or by using a suitable additive (colorant). The first approach is expensive and the chemical modification may affect other physical properties of the resin. Using a colorant is comparatively easier and widely accepted. Colorants are generally divided into two classes: pigments (insoluble colorants) and dyestuffs (soluble colorants). As mentioned for other additives, the colorant should be stable under the processing condition and should have good covering power.

1.8.7 Other Additives

The additives that are usually added to thermoset resin systems to improve the flame-retardant features and toughness of network polymers are known as 'flame retardants' and 'toughening agents' (or 'flexibilisers'), respectively. The design of such additives to make a high-performance resin have been investigated extensively in recent years, and are discussed separately in subsequent chapters.

1.9 Processing of Thermoset Resins

1.9.1 Die Casting

Die casting is a very common and simple method to fabricate an object from liquid thermoset resins. The liquid resin is thoroughly mixed with the curing agent and other additives using a glass rod or mechanical stirrer. The resin mixture is subjected to a vacuum to remove air bubbles and poured into a preheated mould. The mould can be composed of aluminium, glass, or plaster of Paris. The resin takes the shape of the mould. The mould is kept in an oven to cure the resin for a specified time. Once curing is complete, the mould is cooled and the sample removed. The resin shrinks during curing, allowing easy removal of the cured product. When a thin aluminium mould is used, the sample can be recovered by tearing off the aluminium foil. The sample is post-cured if necessary. A flow diagram for a die casting process is shown

in **Figure 1.5**.

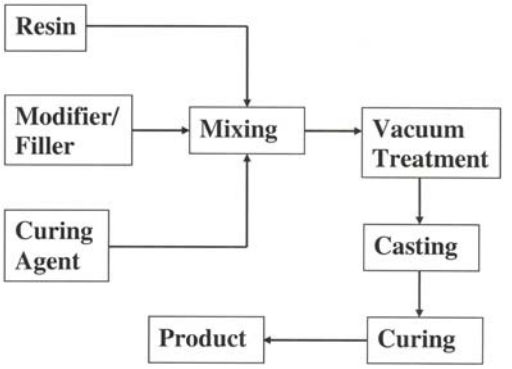

Figure 1.5 The die casting process for thermoset resins

1.9.2 Rotational Casting

Die casting is used to make a solid object, but hollow objects cannot be produced by this method. Hollow objects such as balls and dolls are made by rotational casting. The resin and curative mixture is placed in a hollow mould that can rotate simultaneously along the primary and secondary axes. The resin takes the shape of the mould. The shape is fixed due resin curing under rotation at elevated temperature. The mould is then cooled and opened to remove the product.

1.9.3 Compression Moulding

The compression moulding process is widely used to fabricate thermoset resin-based castings and composites. A typical mould used for compression moulding is shown in **Figure 1.6**. The mould consists of two halves: an upper (or male) and a lower (or female) half. The lower half usually contains a cavity, and the upper half has a projection which exactly fits into the cavity when the mould is closed. The gap between the projected upper half and the cavity in the lower half gives the shape of the moulded articles. The material in the mould is subjected to heat and pressure simultaneously using a hydraulic press with a heating facility. Moulding temperature can be up to 300 °C, and the pressure up to 80 kg/cm^2. Depending on thermal and rheological properties, pressure and temperature are adjusted. A sufficient amount of material must be put in so that the cavity is filled. As the mould closes down under pressure, the material is squeezed or compressed between the two halves, and excess material flows out of the mould as a thin film known as ‘flash’. The mould is cooled

and the product removed.

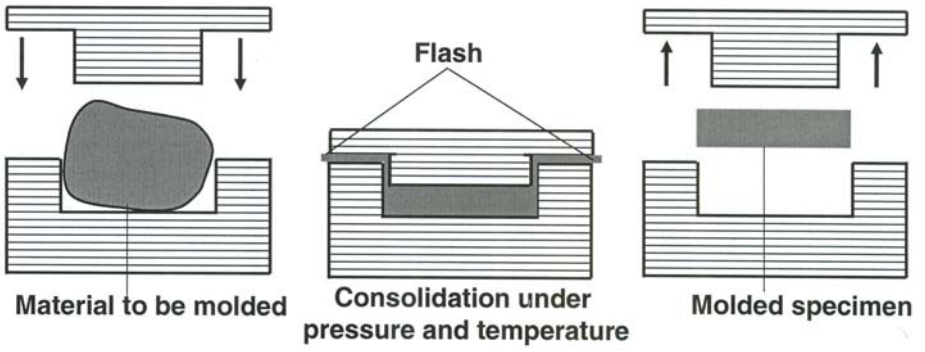

Figure 1.6 A typical mould used for compression moulding of thermoset resins

1.9.4 Reaction Injection Moulding Process (RIM)

RIM is a high-productivity parts-manufacturing process or a process used for the rapid and automated production of large, thin and complex-shaped parts. The difference between RIM and standard injection moulding (used for thermoplastics) is that RIM uses polymerisation in the mould (unlike cooling) to form a solid polymer in injection moulding. Polyurethane is the commonest system used for RIM [52]. A schematic representation of the RIM process is shown in **Figure 1.7**. In the RIM process, two or more low-viscosity reactant liquids (monomer, prepolymer, or both) are accurately metered according to chemical stoichiometry and mixed at high pressure (20–30 MPa), giving a turbulent flow condition in a hydraulically operated mixhead. Unlike standard polymerisation, which is initiated by heat, polymerisation in a RIM process is initiated by impingement mixing. Hence, activating polymerisation at a relatively low temperature (~40 °C) is often possible. The reactant mixture then flows under low pressure under laminar conditions into the mould cavity. The principal advantage of RIM is the ability to process low-viscosity liquid reactants (typically 0.1–1.0 Pa) using low temperatures and pressures, particularly during the mould-filling stage. Small-scale hydraulic equipment (lighter weight and lower cost of mould) can therefore be used. This facilitates the short production runs and prototype applications.

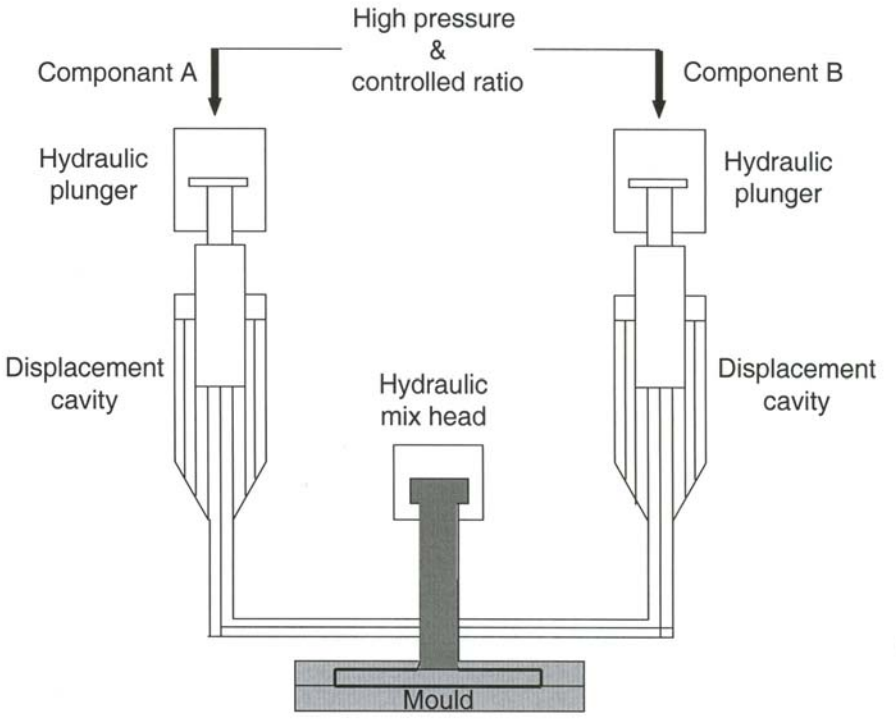

Figure 1.7 The RIM process (schematic)

1.10 Characterisation of Thermoset Resins

Thermoset resins are oligomers (low molecular weight) with reactive functional groups that undergo crosslinking with or without a crosslinker and form 3D networks. Thorough characterisation and analysis of uncured resins are necessary for quality control. Simultaneously, effective exploitation of these resins requires analysis of cure characteristics and characterisation of cured networks. In this section, the general methods/techniques used for characterisation of thermoset resins and composites are discussed.

1.10.1 Titration

Titration is an easy way to estimate the concentration of functional groups in the resin. A small amount of accurately weighed sample is dissolved in a suitable non-reactive

solvent and titrated with a suitable standard solution. For example, carboxyl groups and epoxy groups are titrated by standard alcoholic solution of potassium hydroxide and an acetic acid solution of hydrobromic acid solution, respectively. The degree of unsaturation in the structure is estimated by reacting the material with iodine and titrating back the excess iodine using an aqueous solution of sodium thiosulfate.

1.10.2 IR Spectroscopy

IR spectroscopic analysis is the primary tool to characterise a chemical compound, monomer or polymer. The atoms in a molecule are considered to undergo various motions such as stretching, bending, and rotation. The energy associated with a change in vibration level of a particular chemical bond corresponds to the energy of IR radiation (wave number 200 cm^{-1} to 4000 cm^{-1}). Different bonds absorb at different frequencies. By analyzing two monochromic beams passing through a sample and a reference, absorption can be readily detected. Instead of using a monochromatic beam, a polychromatic beam, after passage through a sample, can be analysed by means of a scanning Michelson interferometer. A spectrum is reconstructed from the information contained in the interferogram using a mathematical process known as a Fourier transformation. A particular chemical bond will have a characteristic IR absorption frequency that may change slightly due to interaction with other bonds. Whether certain functional groups are present in the monomer/polymer can be assessed by interpretation of IR spectra. Subtle interaction such as H-bonding can also be detected. Liquid samples are analysed as thin film cast in a sodium chloride cell, which is transparent at wave numbers up to 650 cm^{-1}. A polyethylene cell can be used for frequencies <600 cm^{-1}. Solid samples are analysed in a pellet form. In general, specimens are prepared by adding approximately 1 wt% of the sample to dry KBr powder. This mixture is pressed into a disc of about 15 mm diameter and 1.5–2 mm thickness. For thick or highly filled samples, analysis is carried out by attenuated total reflectance. In this method, the angle of incidence is adjusted so as to attain total internal refection. When a material is placed in contact with a reflecting substrate, the beam will lose energy at the frequency characteristic to the groups present in the sample.

1.10.3 NMR Spectroscopy

NMR spectroscopic analysis is a well-known powerful technique for elucidation and characterisation of the structure of thermoset resins. NMR spectroscopy is an extremely sensitive technique for evaluating the chemical environment of specific nuclei, which allows precise characterisation of the chemical structure of a thermoset resin. The sample is subjected to a magnetic field and radiofrequency (R/F) field. Under

the magnetic field, half-spin nuclei such as ^{1}H and ^{13}C dissociate into two energy states. Nuclei undergo Larmor precessional motion about the field of direction. When the frequency of the R/F field matches the precessional frequency, resonance occurs. The resonance frequency for a particular nucleus changes with its chemical environment. This is expressed by the chemical shift, expressed in relation to the resonance of tetramethylsilane (the reference). Uncured thermoset resins can be characterised by solution NMR. Cured resins can be characterised only by solid-state analysis. However, contrary to solution NMR where spectra usually consist of a series of very sharp lines due to averaging of all the anisotropic interactions by the molecular motion in the solution, very broad peaks are observed due to the anisotropic interactions between the nuclei for solid samples. This makes characterisation of cured thermoset networks extremely difficult.

1.10.4 Distribution of Molecular Weights

Unlike simple molecules, polymer molecules are large in size. The physical parameter typically used to describe polymer size is molecular weight. With the exception of a few naturally available polymers such as proteins and DNA, a polymer sample consists of chains of varying length. That is why we talk about average molecular weight and not absolute molecular weight for polymers.

The averages commonly used for molecular weights are number-average molecular weight ($\bar{M}_n$), weight-average molecular weight ($\bar{M}_w$), z-average molecular weight ($\bar{M}_z$) and viscosity-average molecular weight ($\bar{M}_v$). $\bar{M}_n$ is calculated like any other numerical average by dividing the sum of individual molecular weight values ($M_i N_i$) by the number of molecules (N_i).

$$M_n = \frac{\sum_{i=1}^{i=\infty} M_i N_i}{\sum_{i=1}^{i=\infty} N_i} \tag{1.36}$$

Any measurement that leads to the determination of number of molecules, functional groups or particles present in a given weight of sample allows calculation of $\bar{M}_n$. Most thermodynamic properties are related to the number of particles present and are therefore dependent on $\bar{M}_n$. Colligative properties dependent on the number of particles present are obviously related to $\bar{M}_n$. $\bar{M}_n$ values are independent of molecular size, and are highly sensitive to the presence of small molecules in the mixtures.

M_w is the second moment or second power average, as shown mathematically:

$$M_w = \frac{\sum_{i=1}^{i=\infty} M^2{}_i N_i}{\sum_{i=1}^{i=\infty} M_i N_i} \tag{1.37}$$

M_w is determined from experiments in which each molecule or chain makes a contribution to the measured results. The average is more dependent on the number of heavier molecules than is the $\overline{M}_n$, which is dependent simply on the total number of particles. Bulk properties associated with large deformations such as viscosity and toughness are particularly related to $\overline{M}_w$. It is determined by light scattering and ultracentrifugation techniques.

Melt elasticity is more closely dependent on $\overline{M}_z$, which can also be determined by ultracentrifugation. It is the third moment or third power average, and is shown mathematically as:

$$M_z = \frac{\sum_{i=1}^{i=\infty} M^3{}_i N_i}{\sum_{i=1}^{i=\infty} M^2{}_i N_i} \tag{1.38}$$

Although z+1 and higher-average molecular weights can be calculated, the major interests for all practical purposes lie with $\overline{M}_n$, $\overline{M}_w$ and $\overline{M}_z$. Because $\overline{M}_w$ is always greater than $\overline{M}_n$ except in a monodisperse system, the ratio $\overline{M}_w/M_n$ is a measure of polydispersity and is called the 'polydispersity index'. The most probable distribution for polydisperse polymers produced by condensation techniques is a polydispersity index of 2.0. Thus, for a polymer mixture, which is heterogeneous with respect to molecular weight, $\overline{M}_z > \overline{M}_w > \overline{M}_n$. As heterogeneity decreases, the various molecular weight values converge until for homogeneous mixtures, where $\overline{M}_n = \overline{M}_w = \overline{M}_n$. Various methods for the determination of molecular weights are discussed next.

1.10.4.1 Viscometry

Viscometry is the most widely used method for the characterisation of polymer molecular weight because it provides the easiest and most rapid means of obtaining molecular weight-related data, and requires only a minimum amount of instrumentation. The molecular weight thus obtained is $\overline{M}_v$. The most obvious characteristic of polymer

solutions is their high viscosity, even if the quantity of added polymer is very small. Viscometry does not yield an absolute value for molecular weight, so one must calibrate viscometry results with the values obtained for the same polymer and solvent by using an absolute technique such as light scattering photometry.

1.10.4.2 End-Group Analysis

End-group analysis is a chemical method used for calculating the $\bar{M}_n$ of a polymer sample whose molecules contain reactive functional groups at one end or both ends. $\bar{M}_n$ can be expressed as shown next:

$$\bar{M}_n = F / X \tag{1.39}$$

where F is the functionality (eq/mol) and X is the equivalent of functional groups present.

1.10.4.3 Vapour Pressure Osmometry

Vapour pressure osmometry is based on the principle that the vapour pressure of a solution is lower than the vapour pressure of the solvent (Rault's law). Drops of solvent and solution are kept in two thermister beads placed in a thermostated chamber saturated with solvent vapour. Solvent condenses on the solution bead and temperature increases due to liberation of latent heat of fusion. The increase in temperature is noted. The temperature change can be correlated with molecular weight, as given below:

$$\frac{\Delta T}{c} = k_s \left(\frac{1}{M_n} + A_2 c \right) \tag{1.40}$$

where ΔT is the increase in temperature, c is the concentration of the solution, and A_2 is a second virial coefficient. K_s is a constant determined by calibrating the instrument with a substance of known molecular weight. Thus, a plot of $\Delta T/c$ *versus* c will be a straight line. $\bar{M}_n$ and the second virial coefficient can be easily determined from the slope and intercept of the straight line, respectively.

1.10.4.4 Membrane Osmometry

For membrane osmometry, osmotic pressure is measured for a polymer solution of various concentrations. The equation relating osmotic pressure ( ) and molecular

weight and concentration can be written as follows [3, 5]:

$$\frac{\Pi}{c} = \frac{RT}{M_n} + \frac{A_2}{RTM_n}c \tag{1.41}$$

where R is the universal gas constant, T is the temperature, c is the concentration of the solution, and A_2 is a second virial coefficient. $\bar{M}_n$ can be determined from the slope ($RT/\bar{M}_n$) of the plot of Π/c *versus* c (straight line).

1.10.4.5 Light Scattering

The principal method for determining $\bar{M}_w$ is light scattering (although small-angle neutron scattering is now becoming important, particularly in the bulk state). The radiation is scattered when the size of an object begins to approach the wavelength of the radiation. . Many natural phenomena (e.g., rainbows, blue colour of the sky and sea) are connected to light scattering, which occurs when light beams encounter suspended matter. The molecular weight of a polymer can be determined using light scattering because the polymer molecule in solution can scatter a beam of light like suspended matter.

The basic equation used for molecular weight and molecular size can be written as [3, 5]:

$$\frac{kc}{\Delta\tau} = \frac{Hc}{R(\theta)} = \frac{1}{M_w P_\theta} + 2A_2c \tag{1.42}$$

where $\Delta\tau$ is the excess turbidity of the solution over that of pure solvent, c is the concentration of the solution, P_θ is the particle-scattering factor, and A_2, K and H are the second virial coefficient and light-scattering calibration constants, respectively.

$$P_\theta = \left[1 - \frac{16\pi^2 R_g^2 \sin^2\frac{\theta}{2}}{3\lambda^2}\right] \tag{1.43}$$

Hence, the key equation at the limit of zero angle and zero concentration, respectively, relating light scattering intensity to $\bar{M}_w$ and the z-average radius of gyration (R_g) may be written as:

$$\left(\frac{Hc}{R(\theta)}\right)_{\theta=0} = \frac{1}{M_w} + 2A_2c \tag{1.44}$$

$$\left(\frac{Hc}{R(\theta)}\right)_{c=0} = \frac{1}{M_w}\left[1 + \frac{16\pi^2 R_g^2 \sin^2\frac{\theta}{2}}{3\lambda^2}\right] \quad (1.45)$$

From Equation 1.45, it is clear that by plotting Hc/R(θ) *versus* c and Hc/R(θ) *versus* $\sin^2\theta$, $\bar{M}_w$ and R_g can be determined.

1.10.4.6 Gel Permeation Chromatography (GPC)

GPC is a powerful technique and an instrument exclusively used for the characterisation of molecular weight and molecular-weight distribution of polymers. GPC makes use of size exclusion. A dilute polymer solution is passed through a gel (usually made of crosslinked styrene-divinyl benzene copolymer) containing fine spherical beads. The gel contains voids as well very small pores (diameter, 50–100 Å). The pure solvent is initially passed through the column so that all the pores are filled with solvent. When a solution is passed through the column, the smaller molecules diffuse into the pores due to a concentration gradient. The bigger molecules cannot penetrate into all the pores and elute faster than the smaller molecules. As the mobile phase passes the porous particle, the separation between the smaller and larger molecules becomes greater. By calibrating the column with a polymer solution of known molecular weight (polystyrene standard), it is possible to determine the molecular weight of an unknown polymer sample. Data are collected as the height of chromatograph *versus* retention counts. The resultant data are then analysed (usually by computer software) to yield various molecular-weight averages. Thus, the entire distribution of molecular weight is determined in one experiment.

1.10.5 Morphological Characterisation

1.10.5.1 Scanning Electron Microscopy (SEM)

SEM is widely used to study the morphology (microstructure and nanostructure) of thermoset resin systems. SEM produces high-resolution images of a sample surface. Cryogenically fractured surfaces with a conductive coating of gold or carbon are used for analysis. The coating makes the insulating resin surface conducting to prevent charging. SEM images have a unique 3D appearance and are therefore used to characterise surface structure (homogeneity, phase morphology) and mode of failure (ductile, brittle). The principal of SEM is that primary electrons coming from the source strike the surface structure and are inelastically scattered by atoms in the

sample. The electrons emitted are detected to produce an image. Besides the emitted electrons, X-rays are also produced by interaction of the electrons with the sample. This feature is used to detect metallic elements by energy dispersive X-ray spectroscopy. SEM can provide resolution up to 1 nm, and hence is used for characterisation of nano-filled thermoset resins or nanocomposites (which are discussed in subsequent chapters).

1.10.5.2 Transmission Electron Microscopy (TEM)

TEM is also used to study morphology, particularly to study nano-scale dispersion of inorganic fillers or other polymeric components in the thermoset resin. Modern TEM can provide resolution up to 0.1 nm. Images are produced by focusing a beam of electrons onto a very thin specimen. The transmitted electrons carry information about the inner structure, which is captured to produce an image. Hence, specimen thickness should be very low (<80 nm) to ensure transmittance. There are several problems for characterisation of polymer samples by TEM. First, the preparation of such a thin sample is time-consuming and difficult for a highly flexible resin. Second, thermoset resin samples often produce poor contrast in TEM due to a weak interaction of electrons with the resin sample. This problem can be partially solved by using stains such as heavy metal compounds. The dense electron clouds of the heavy metal atoms interact strongly with the electron beam. Third, the resin sometimes decomposes in the electron beam due to the increase in temperature as a result of exposure to the electron beam. To avoid the decomposition of resins, cryogenic microscopy (cryo-TEM), which stores the sample in liquid nitrogen, is used.

1.10.5.3 Atomic Force Microscopy (AFM)

AFM is another powerful tool that has been used for the characterisation of the morphology of modified thermosets and thermoset-based composites [53, 54]. This technique has helped to image surface topography on a nanometric scale [55–57]. AFM has several advantages over TEM and SEM. AFM gives a 3D surface profile of the sample; and it does not need a high vacuum, conducting coating (needed for SEM) or exposure to a high-voltage electron beam (needed for SEM and TEM), which may degrade the surface of the resin sample. In AFM, a cantilever with a sharp tip at its end (typically composed of silicon or silicon nitride) with tip sizes of the order of 1 nm is used. The probe is brought close to the sample surface. The distance between the tip and the surface must be selected with appropriate care otherwise the tip may get damaged due to the collision of the tip with the sample surface. The van der Waal forces between the tip and the sample leads to a deflection of the cantilever. Typically, the deflection is measured applying a laser beam, which is reflected from

the top of the cantilever into an array of photodiodes. The sample is mounted on a piezoelectric holder in all the three space directions (x and y for scanning the sample; z for maintaining a constant force). Scanning in the x–y plane represents the topography of the sample. Contamination of the probe or substrate surface is a common problem in AFM, so special care must be taken in sample preparation and analysis.

Another unique feature of AFM is that it allows estimation of the adhesion of the filler with the matrix in a filled thermoset system. Adhesion strength can be determined using a probe with a specific spring constant by calibrating the cantilever. The changes in surface topology can be determined quantitatively by the root mean square (RMS) roughness calculation (R_{rms}). This is used in a range of applications, particularly if the surfaces show a degree of randomness. Because roughness analysis is based on the vertical axis i.e., z-axis, RMS height deviations can be expressed as:

$$R_{rms} = \sqrt{\frac{\sum (Z_i)^2}{n}} \tag{1.46}$$

where Z is the current and n is the number of points on the image. Mean roughness (R_a) can be determined from the arithmetic average of the absolute values of the surface height deviations measured from the main plane:

$$R_a = \sum_{j=1}^{n} \left| Z_j \right| \tag{1.47}$$

The analysis of surfaces can also be carried out in terms of power spectral density (PSD) by considering the surfaces as a superimposition of spatial waves [58]. The variation of height in real space can be considered in terms of power spectrum in frequency space through use of the Fourier transform, which is a well-known means of relating real space to frequency space. Surfaces are analysed by a series of line scans of N_x steps, yielding a profile h(x), for each value from 1 to N_y in the y direction. The power (P) is determined by taking the Fourier transform of each of these line scans and squaring the results. Once the power (P) is obtained, it may be used to derive one-dimensional power spectral density (1DPSD):

$$PSD = \frac{P}{\Delta f} \tag{1.48}$$

Δf is derived by progressively sampling the data from the image's fast Fourier transform centre [59]. 1DPSD is expressed in $(\text{length})^3$. Two-dimensional PSD (2DPSD) is determined by taking an annular average of the square of 2D Fourier transform.

1.10.5.4 X-ray Diffraction (XRD)

XRD is a fast and nondestructive test which is frequently used to characterise thermoset materials and their composites. Crystalline materials are characterised by sharp peaks, whereas amorphous materials show broad humps. Thus, the degree of crystallinity can be estimated. When a crystalline material such as clay is dispersed in a thermoset matrix, one can study the intercalation and exfoliation behaviour (see subsequent chapters). If the crystallites of the power are very small, the peaks of the pattern will be broadened. From this broadening one can determine an average crystallite size using the Debye–Scherrer equation:

$$d = \frac{0.9\lambda}{B\cos\theta} \tag{1.49}$$

Where B is the broadening of the diffraction line measured at half of its maximum intensity (radians), Θ is the Bragg angle, and λ is the wavelength of the X-ray.

1.10.6 Thermal Analysis

Thermal analysis is an essential tool to study the necessary thermal transitions in polymers, without which the processing and fabrication of polymeric materials is not possible. The thermal behaviour of a polymer has significant technological importance. For example, the T_g of rubber determines the lower limit of the use of rubber and the upper limit of the use of an amorphous thermoplastic. The most important techniques will be briefly discussed below.

1.10.6.1 Differential scanning Calorimetry (DSC)

DSC involves the measurement of relative changes in temperature and energy under isothermal or adiabatic conditions, i.e., the heat capacity of the sample at constant pressure. It is a technique measuring the energy necessary to establish a nearly zero temperature difference between a substance and an inert reference material because the specimen and reference are subjected to identical temperature regimens in the same environment (heated or cooled at a controlled rate).

Two types of DSC systems are commonly used: power compensation and heat-flux DSC. In the former, temperatures of the sample and reference are made identical by varying the power input to the two furnaces; the energy required to do this is a measure of enthalpy or heat capacity changes in the sample relative to the reference. In heat-flux DSC, a low resistance heat flow path connects the sample and the

reference. The assembly is enclosed in a furnace. The enthalpy or heat capacity change in a sample causes a difference in its temperature relative to the reference. DSC can be used for analyzing the uncured or partially cured thermosets because curing involves crosslinking which is accompanied by heat evolution that can be readily monitored.

DSC is widely used to obtain information about the T_g, melting point (T_m), crystallisation temperature (T_c), heat of crystallisation (H_c), heat of melting (H_f), and that heat absorbed or evolved during cure reactions or decomposition reactions. A typical DSC plot showing T_g, T_m and T_c is shown in **Figure 1.8**. During heating, as a solid sample melts and transforms to a liquid state, it absorbs more energy (endothermic) than that of the reference. Similarly, as the crystallisation takes place, excess energy is given out (exothermic). As a result, the melting and crystallisation processes appear as peaks (endothermic or exothermic) and the area under the curve gives a direct measure of the heat of fusion or crystallisation. The heat of curing and degradation can also be measured.

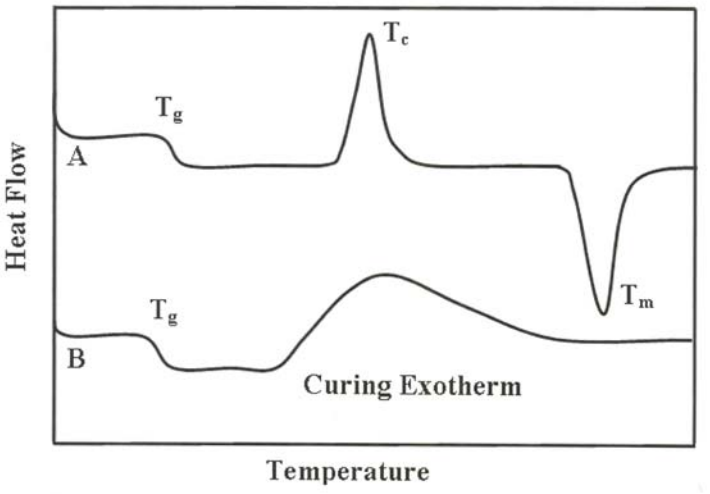

Figure 1.8 A typical DSC plot showing T_g, T_m and T_c of a polymer sample

1.10.6.2 Dynamic Mechanical Analysis (DMA)

DMA provides the most significant information on the viscoelastic behaviour of polymers in addition to thermal transitions. In principle, a sinusoidal strain or stress is applied to a sample and the response is monitored as a function of frequency and temperature. A viscoanalyser is commonly used to apply a displacement d(w) at the

upper end of a sample and measure the force F(w) transmitted to the fixed lower end. F(w) is measured by a dynamic force sensor, and d(w) is measured by displacement or acceleration sensor. By measuring the upstream displacement and downstream force, the measurement method can obtain the stiffness irrespective of the weight of the sample.

The strain of a viscoelastic body is out of phase with the applied stress by the phase angle δ. This phase lag is due to the excess time necessary for molecular motions and relaxations to occur. For a perfectly elastic material, the value of δ is 0°; for a perfectly viscous material, the value of δ is 90°. Polymers are viscoelastic and the value of δ falls between 0° and 90°. The phase angle [δ (w)], i.e., the phase shift between the dynamic force and dynamic displacement, can be calculated using the processing of the signals F (w), d (w) according to first Fourier transform. Like mechanical testing, DMA can be carried out using various modes like tension, flexure, shear or creep.

Viscoelastic properties may be expressed in terms of a dynamic storage modulus (E´), dynamic loss modulus (E´´) and mechanical damping factor (tanδ) . Mathematically, they are defined as follows:

$$E = \acute{o}_0 / \mathring{a}_0 \cos(\ddot{a}) \tag{1.50}$$

$$E'' = \sigma_0 / \varepsilon_0 \sin(\delta) \tag{1.51}$$

$$\tan \delta = E'/E' \tag{1.52}$$

The storage modulus is often associated with the 'stiffness' of a material, and refers to the energy stored in the sample elastically after applying the stress. The dynamic loss modulus is associated with the 'internal friction' arising out of the segmental motions, and is very sensitive to the different types of molecular motions, relaxation processes, transitions, morphology and other structural heterogeneities. Tan δ is the energy of dissipation during the stress cycle relative to the energy stored elastically in the material. A typical DMA plot of a cured thermoset resin is shown in **Figure 1.9**. From the figure, it can be seen that as temperature is increased, tan δ goes through a maximum in the transition region and then decreases in the rubbery region. The damping is low below T_g because the chain segments in that region are frozen. Below T_g, the deformations are thus primarily elastic and the molecular slips resulting in viscous flow are very low. Above T_g, in the rubbery region, the damping is low because the molecular segments are free to move, and consequently there is a little resistance to flow. Maximum damping occurs in a region where most of the chain segments take part in this cooperative micro-Brownian motion under harmonic stress. For thermosets, the position and height of the loss tangent peak in the relaxation spectra

of a polymer are indicative of the structure and the extent to which the polymer is crosslinked.

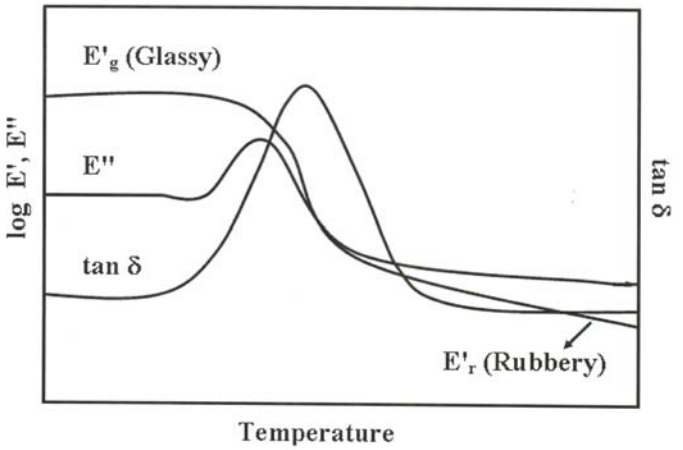

Figure 1.9 A typical DMA plot of a cured thermoset resin

1.10.6.3 Time–Temperature Superposition (TTS)

The principle of TTS lies in the equivalency of time (frequency) and temperature. Due to various limitations, one cannot carry out experiments at conditions such as at very low frequencies and very high temperatures or *vice versa*. TTS is used to obtain data at different conditions to save experimental time. The viscoelastic data of one temperature can be related to the higher or lower temperature using a shift factor (a_T) to the right side, or to the left side of the time axis using a reference temperature (T_{ref}). A fully overlapped curve can be obtained for any reference temperature; this is called a 'master curve'. It is also widely accepted that a minor vertical shift factor may also be applied to more accurately model master curves.

The related shift factor a_T is given by:

$$a_T = \frac{E'(T)}{E'(T_{ref})} \tag{1.53}$$

The master curve in the form of stiffness *versus* frequency can be created by fitting the experimentally determined shift factors to a mathematical model. With a multi-frequency measurement, frequencies beyond the measurable range of the DMA can be achieved by using the superposition method based on the Williams–Landel–Ferry (WLF) equation [60, 61]. For a temperature range above the T_g, it is generally

accepted that the shift factor–temperature relationship is best described by the WLF equation:

$$\log a_T = \log\left(\frac{f}{f_0}\right) = \frac{-C_1(T - T_{ref})}{C_2 + (T - T_{ref})} \tag{1.54}$$

where C_1 and C_2 are constants. The general values of the constants, $C_1 = 17.4$ and $C_2 = 51.6$ are used. For a temperature range below the T_g, the Arrhenius equation is generally considered to be suitable to describe the relationship between the shift factors of the master curve and the temperature. In the latter case, the activation energy (E_a) for shifting the curves can be obtained by the following equation:

$$\ln a_T = \frac{E_a}{R}\left(\frac{1}{T} - \frac{1}{T_{ref}}\right) \tag{1.55}$$

1.10.6.4 Thermogravimetric Analysis (TGA)

In TGA, change in the weight of the sample with respect to temperature and time is monitored when heated under a controlled programme. The programme is often of linear increase in temperature or time. This technique is quantitative, and is very useful to study curing reactions/degradations taking place while heating the sample. A TGA instrument consists of a thermobalance (which records weight with a sensitivity of about 1 μg and a capacity of about few hundred milligrams) and a furnace operated in the temperature range 50–800 °C with a heating rate up to 100 °C/min. The thermal stability of a material can be studied in an inert or oxidative atmosphere. TGA curves elucidate the decomposition mechanism. There are many factors that affect these curves. The primary factors are heating rate and sample size. As the heating rate and sample size increases, the decomposition temperature of the sample also increases. The particle size of the sample, the way in which it is packed, the crucible shape, and the gas flow rate can also affect the kinetics of the reaction. Thus, if comparing the thermal stability of two materials, an identical condition with respect to these variables must be maintained.

1.10.7 Rheological Characterisation

Rheology is the study of the flow of matter. The name derives from the Greek word ‘rheo’ which means ‘to flow’. A solid will usually respond to a force by deforming and storing energy elastically. A liquid, however, will flow and dissipate energy

continuously in viscous losses. A Newtonian liquid has a linear relationship between shear rate and shear stress. Complex fluids exhibit elastic and viscous responses, and show a non-linear relationship between shear rate and strain. One of the properties often observed within rheology is the viscosity that measures the resistance to flow. Some materials are intermediate between solids and fluids, and the viscosity is not sufficient to characterise them. A solid material can be described by its elasticity or resilience: when it is deformed, it will store the energy. For example, a spring regains its original shape after being deformed. The other extreme is a fluid, which stores no energy while deformed and just flows.

A viscoelastic material is intermediate and stores some energy and flows a little when deformed. In general, a polymer network is viscoelastic, with a complex shear modulus having elastic (solid-like) and viscous (liquid-like) components of similar magnitudes over a wide range of frequencies. Rheological testing provides a precise means for measuring intrinsic mechanical material properties that can be related to the processing characteristics and performance of a material. The rheological tests for thermosetting resins are carried out in a parallel plate rheometer. The resin system is placed in-between the plate and the strain is applied to it. The three rheological test modes (steady, dynamic, transient) are distinguished by the manner in which the strain is applied to the sample. A steady test uses continuous rotation to apply the strain and provide a constant shear rate. The resultant stress is then measured when the sample reaches a steady state. In a dynamic test, an oscillatory strain is applied to a sample and the resulting stress is measured. Dynamic tests can be made using free oscillations at the resonance frequency of the test material (e.g., torsion pendulum) or with sinusoidal (or other waveform) oscillations at a forced frequency chosen from a wide range. In a transient test, the response of a material as a function of time is measured after subjecting the material to an instantaneous change in strain, strain rate or stress.

The advantage of a dynamic test is that it allows measurement of the storage modulus (G´) and loss modulus (G´´) in addition to viscosity. Usually, the rheological properties of a viscoelastic material are independent of strain up to a critical level of strain. Beyond this critical strain level, behaviour is non-linear and moduli decline. Therefore, before carrying out the dynamic rheological experiment, the linear viscoelastic regimen must be defined. Strain sweep measurements are used to define the linear viscoelastic regimen A generalised plot of a strain sweep experiment is shown in **Figure 1.10**, in which the storage and loss moduli are plotted as a function of strain. The moduli remain almost unchanged up to a critical strain level, above which they tend to decrease. Hence, a strain level less than the critical strain must be used for determination of storage and loss moduli as a function of frequency.

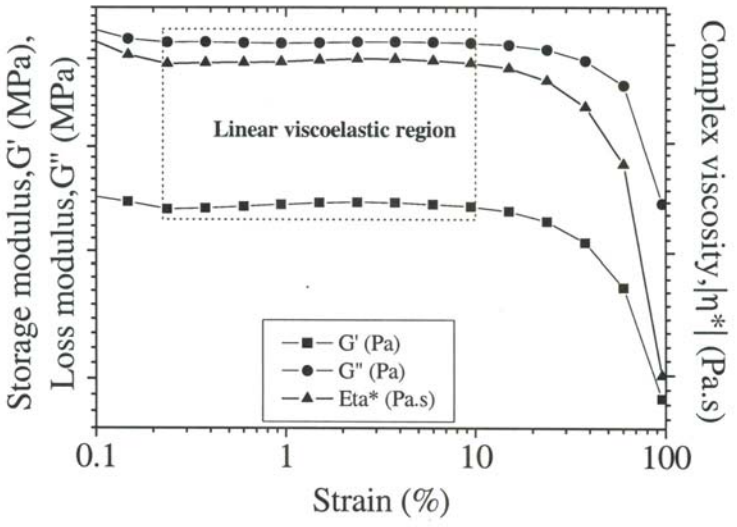

Figure 1.10 A generalised plot of a strain sweep experiment where storage and loss moduli are plotted as a function of strain

A generalised plot showing the change in storage and loss moduli as a function of frequency is shown in **Figure 1.11**. At low frequencies, G″ is higher than G′. G′ increases with increasing frequency because the molecules do not have sufficient time to relax. As a result, the difference between G′ and G″ decreases as the frequency increases. G′ intersects with G″ at a certain frequency within the transition zone. This crossover frequency between storage and loss moduli indicates the transition from liquid-like to solid-like behaviour. The crossover point is sometimes defined as a 'gelation' of a thermoset network.

The behaviour of thermoplastics during the melt processing is governed mainly by the molecular weight, molecular-weight distribution, degree of branching, and filler content of the polymer. For thermosetting polymers, the rheological changes occurring during the curing reaction can be measured as the resin transforms from a low melting solid to a low viscosity liquid, then through the gel point without disrupting the gel structure, and finally to a highly crosslinked stiff solid. The entire curing process can be simulated by the rheometer to provide guidelines for production (see Chapters 2 and 3).

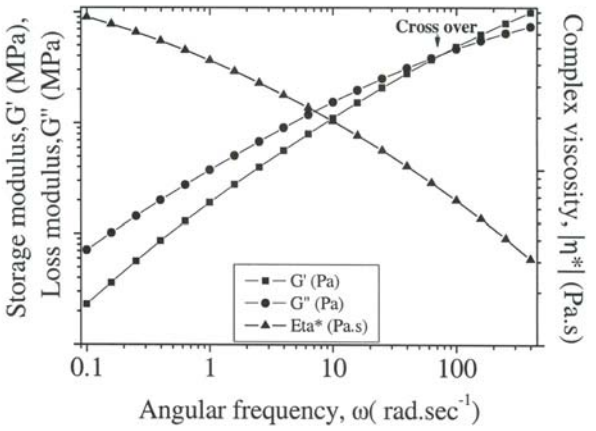

Figure 1.11 Generalised plots showing the change in storage and loss moduli of a polymer as a function of frequency obtained from a parallel plate rheometer

1.11 Testing and Evaluation of Thermoset Resins

With the development of polymer science and technology and proliferation of polymer-based products, the testing of materials and components has become an integral part of not only research and development, but also of product design and manufacturing. Testing is necessary for verification of the manufacturing process, design concept, quality control, and reproducibility of a process. It is also used to assess a new product, to prove the design concepts, and to ensure the safety and reliability of the products. Testing is carried out to assess the suitability of a material followed by testing as a component. However, component testing technology is a vast area, and is beyond the scope of this book. Testing of thermoset resins as a material is discussed briefly here. Detailed procedures for testing can be obtained from handbooks from the American Society for Testing and Materials (ASTM). For convenience, ASTM standards for the relevant tests are presented in **Table 1.1**.

1.11.1 Mechanical Properties

In virtually all applications, polymer materials have to be subjected to a loading force in some way or other. Hence, the assessment of mechanical properties is very important for the design of polymer materials for various applications. Polymer materials are more sensitive to the service temperature and other environmental effects compared with conventional materials. Hence, the data for mechanical properties, measured using conditions similar to a service environment, should be used for design rather than standard data available in the literature.

Table 1.1 ASTM standards for various tests used for the evaluation of thermoset resins	
Testing	**ASTM standard**
Tensile	D638 [62]
Flexural	D790 [63]
Fracture toughness	D5045-99 [64]
Pendulum impact	D256 [65]
Falling weight impact (dart)	D1709 [66]
Falling weight impact (tup)	D2444 [67]
Creep	D2990 [68] or D2991 [69]
Fatigue	D671 [70]
Heat deflection temperature	D648 [71]
Dielectric constant	D150 [72]
Arc resistance	D495 [73]
Dielectric strength	D149 [74]
Cone calorimetry	E1354-08 [75]
Limiting oxygen index	D2863 [76]

When an elastic body is subjected to a tensile or compressive stress, the strain changes proportionally with stress according to Hooke´s law, as given next:

$$\sigma = E\varepsilon \tag{1.56}$$

Where σ is the longitudinal stress, ε is corresponding strain, and E is called Young´s modulus (or the modulus of elasticity). Similarly, in shear deformation, the modulus is called the shear modulus or the modulus of rigidity (G). When a hydrostatic force is applied, a third elastic modulus is used: the modulus of compressibility or bulk modulus (K). It is defined as the ratio of hydrostatic pressure to volume strain. A deformation (elongation or compression) caused by an axial force is always associated with an opposite deformation (contraction or expansion) in the lateral direction. The ratio of the lateral strain to the longitudinal strain is the fourth elastic constant called Poisson's ratio (v). For a small deformation, elastic parameters can be correlated in the following way:

$$K = \frac{E}{3(1-2v)} \tag{1.57}$$

$$G = \frac{E}{2(1+\nu)} \tag{1.58}$$

In a rubbery network, Poisson's ratio is often close to 0.5 and hence shear modulus can be determined by dividing the elastic modulus by 3.

1.11.1.1 Tensile Test

The tensile test is most widely used to assess the performance of a material or identify the material for a particular application. The test indicates the ability of a material to withstand the pull-out forces, and is used to determine the extent of stretching before the break. The tensile test is carried out using ASTM D638 [62]. Dumbbell specimens of different size as specified by the standard can be used. The test is carried out using a universal testing machine (UTM) by fixing the specimen in two grips (one stationary and one movable) (**Figure 1.12**). Appropriate tightening and alignment is very important, otherwise the test may lead to erroneous results due to the slippage or breakage at the grip. Depending on the nature of sample, different speeds of testing can be used. The most commonly used speed of testing is 5 mm/min. Tensile strength is determined by dividing the force (measured by the load cell) by the cross-sectional area, and strain is calculated from the ratio of elongation to gauge length. Calculations of various parameters (e.g., stress, elongation, modulus) are done automatically using computerised instruments. The definition of elongation, elastic limit and modulus of elasticity as per ASTM standard are quoted below (with permission).

Elongation: the increase in length produced in the gauge length of the test specimen by a tensile load. It is expressed in units of length, usually millimeters [inches] (also known as extension).

Elastic limit: the greatest stress which a material is capable of sustaining without any permanent strain remaining upon complete release of the stress. It is expressed in force per unit area, usually megapascals.

Modulus of elasticity: the ratio of stress (nominal) to corresponding strain below the proportional limit of a material. It is expressed in force per unit area, usually megapascals (also known as elastic modulus or Young's modulus).

Figure 1.12 A tensile test setup with a dumb-bell-shaped specimen

Typical stress–strain plots observed in polymer materials are shown in **Figure 1.13**. The initial linear portion of the curve represents the elastic behaviour where stress is proportional to strain (Hooke's law). Up to the elastic limit, the strain is recoverable. Deformation is associated with the bending and stretching of interatomic bonds of the polymer chains. Beyond the elastic limit, permanent deformation or yielding takes place as a result of permanent displacement of molecules relative to each other. This strain is not recoverable completely and instantaneously. Due to a permanent deformation the strain increases, keeping the stress almost identical until failure. If the resin is highly crosslinked, then failure occurs without significant permanent deformation and is called 'brittle failure'. This is because the high crosslink density resists the displacement of molecules from their relative positions. A lightly crosslinked network exhibits a significant permanent deformation before failure. This type of failure is called 'ductile failure'. The area under the stress–strain curve is a measure of toughness. Naturally the area under the stress–strain curve is higher for a ductile (optimally crosslinked) material compared with a brittle (highly crosslinked) material. In some cases, the stress increases before failure due to the development of some order arrangements, such as strain-induced-crystallisation. The mechanical behaviour of polymers is best explained by the spring and dashpot model: the spring represents elastic behaviour and the dashpot represents viscous flow.

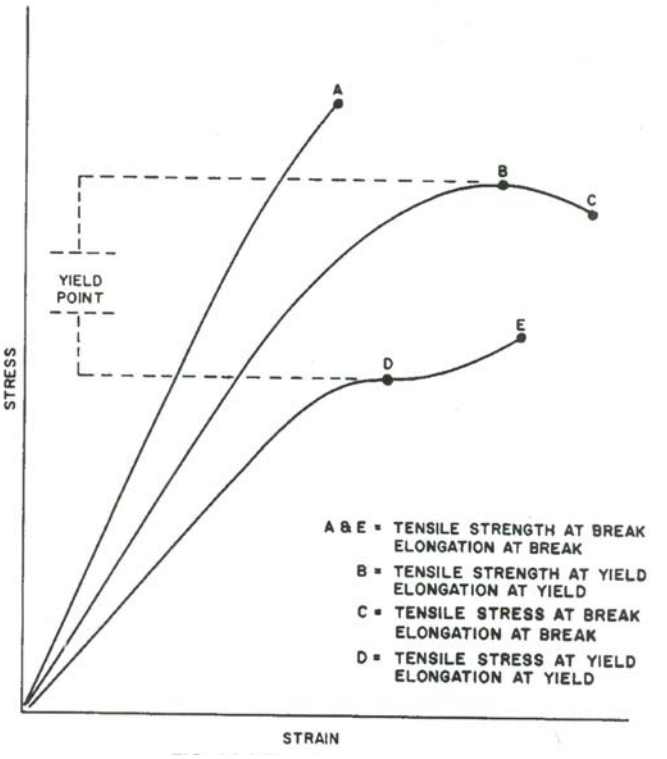

Figure 1.13 Tensile designations for plastic samples. Reprinted with permission from ASTM D256-04. © 2004 ASTM International

1.11.1.2 Flexural Test

Flexural properties give an indication of the response of a material under bending load. The test is carried out by a three-point bending method as per ASTM D790 [63]. The test setup for this is very simple; a rectangular sample is placed between two supports and the load is applied by means of a loading nose from the midway between the supports (**Figure 1.14**). Unlike the tensile test, the flexural test allows easy sample preparation and does not involve clamping of the sample. Very tight clamping of tensile specimens (which is necessary for the testing of high-strength materials) may generate stress concentration points, leading to erroneous results. In general, three test parameters are reported from a flexural test: flexural strength, flexural strain and flexural modulus. The area under the stress–strain curves reflects the toughness of a material. Flexural strength is the ability of a material to withstand bending force applied perpendicular to its longitudinal axis. The fracture strength (FS) is determined from the peak load (kg) using the following formula:

$$F.S = \frac{\frac{3}{2} \times peakload \times span \times 9.8}{width \times (thickness)^2} \tag{1.59}$$

Flexural strain reflects the flexibility of a material. Highly flexible resins like rubbery epoxy, polyurethane, and modified resins do not break even after a large deflection; determination of ultimate flexural strength is impractical for them. The relevance of mechanical tests depends on the form in which the material is going to be used. If a material is to be used as a beam, then a flexural test is more relevant than a tensile test.

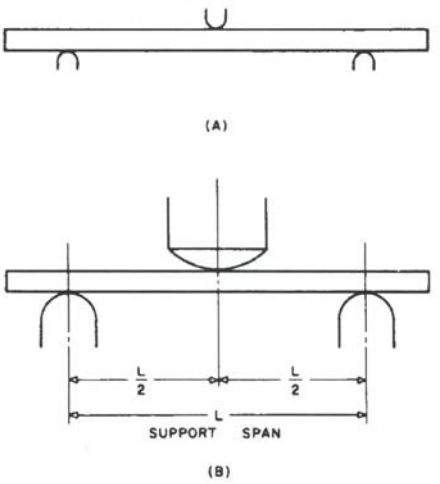

Figure 1.14 A test setup for a flexural test. Reprinted with permission from ASTM D790-07. © 2007 ASTM International

1.11.1.3 Creep Test

Consideration of creep properties is very important to predict the long-term load-bearing capacity, and to design polymer-based products for such applications. When a polymer material is subjected to a constant load, it deforms quickly to a strain depending on its physicochemical properties and then continues to deform slowly until failure. This property is called 'creep'. A plastic thread, very tightly tied

between the two supports, is found to often become loose after few weeks. This is a manifestation of creep. Creep is an inherent property of all polymers. Because of chemical crosslinks, a cured thermoset network exhibits much lower creep compared with a thermoplastic resin, and the creep decreases with an increase in the crosslink density of a thermoset network.

Creep measurements involve measuring a constant tensile or flexural load to a respective specimen (as discussed previously) and measuring the strain as a function of time. In a typical creep plot, percentage creep strain is plotted against time. The apparent creep modulus at a particular time can be calculated by dividing the stress by strain at that particular time. Creep compliance is determined by dividing the strain by stress. For a tensile test, the simplest way to measure extension is to make two gauge marks on the tensile specimen and note the distance between the marks at different intervals. However, accurate measurement of extension requires an optical or laser extensometer. In a flexural measurement, the strain is usually calculated with the help of a linear variable differential transformer system.

1.10.1.4 Fatigue Test

For many applications (e.g., pressure vessels, hinges, tubing, vibration equipment, automobiles) polymer materials must repeatedly encounter cyclic loading in terms of flexing, stretching, twisting or compressing. The fatigue test is intended to predict the behaviour of materials under such conditions. Like conventional loading, cyclic loading also generates mechanical deterioration, which leads to complete fracture in due course. For this test, a material is subjected to cyclic loading with a particular oscillating condition, and the number of cycles required to produce the failure is determined. Thus, stress is plotted as a function of the number of cycles. Fatigue life is defined as the number of cycles of deformation required to bring about the failure of the test specimen under a given set of oscillations. Thus, the fatigue life will be longer at low stress level, and will be shorter if the stress level is higher. The limiting stress below which the material will never fail is called the 'fatigue endurance limit'. The fatigue test can be carried out in tensile and flexural mode (ASTM D671 [70]). The flexural fatigue test is carried out in the constant deflection principle, and tensile fatigue is carried out in the constant load (stress) condition. In a flexural fatigue test, the specimen is held as a cantilever beam in a vice at one end, and bent by a concentrated load applied through a yoke fastened to the opposite end. In a tensile fatigue test, both ends of the specimen are mounted in the machine, and the same is rotated between two spindles. The typical specimen dimensions of a flexural fatigue test are given in **Figure 1.15**.

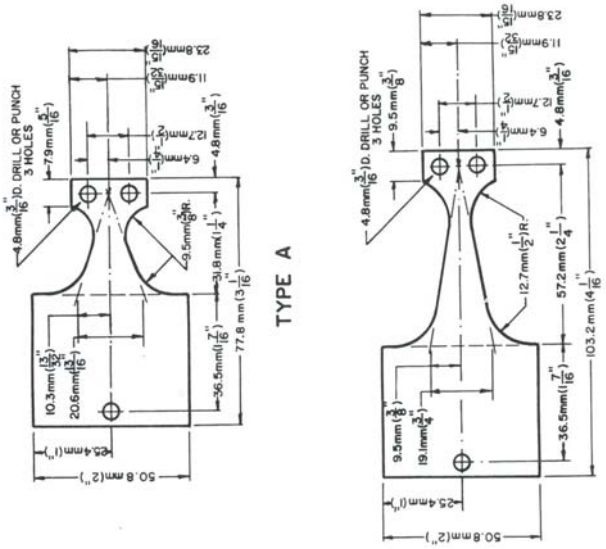

Figure 1.15 Dimensions of a constant force flexural fatigue specimen. Reprinted with permission from ASTM D671-93. © 1993 ASTM International

1.11.2 Fracture Toughness (K1c)

K_{1c} is one of the most important properties of a material. It is used to design materials for dynamic applications where the material must encounter many mechanical shocks and vibrations. The toughness of a material is defined as the energy absorbed by a material before fracture, and expressed as impact energy (G_{1c}). Fracture toughness describes the resistance of a material with a crack to fracture. Because it is almost impossible to make a material for practical purposes free from cracks/defects, fracture toughness analysis is extremely important for design applications. The fracture properties of a thermoset material are determined using ASTM D5045-99 [64]. The critical stress intensity factor, K_{1c} and the impact energy, G_{1c}, are determined. Tests are carried out with an UTM using a compact tension or bending mode. An initial crack is machined in a rectangular specimen and a natural crack generated by tapping on a fresh razor blade placed in the notch. A typical specimen configuration for bending and compact tension mode is shown in **Figure 1.16**. The parameters can be expressed mathematically as follows:

$$K_{IC} = \frac{P_Q}{BW^{1/2}} f(x) \tag{1.60}$$

$$G_{IC} = \frac{1-\nu^2}{E} K_{IC}^{\ 2} \tag{1.61}$$

Where P_Q is the critical load for crack propagation; B and W are the thickness and width of the specimen, respectively; E is the elastic modulus; and f (x) is a non-dimensional shape factor given by:

$$f(x) = 6\sqrt{x}\frac{(1.9 \ -x(1-x)\times(2.15-3.93x+2.7x^2)}{(1+2x)(1-x)^{3/2}} \tag{1.62}$$

The thickness of the specimen should be higher than the critical value below which the material shows plane stress behaviour. The K_{1c} and G_{1c} of a given material are functions of testing speed and temperature. The values may be different under cyclic load. Therefore, application of K_{1c} and G_{1c} in the design of service components should be made considering the differences that may exist between test conditions and field conditions.

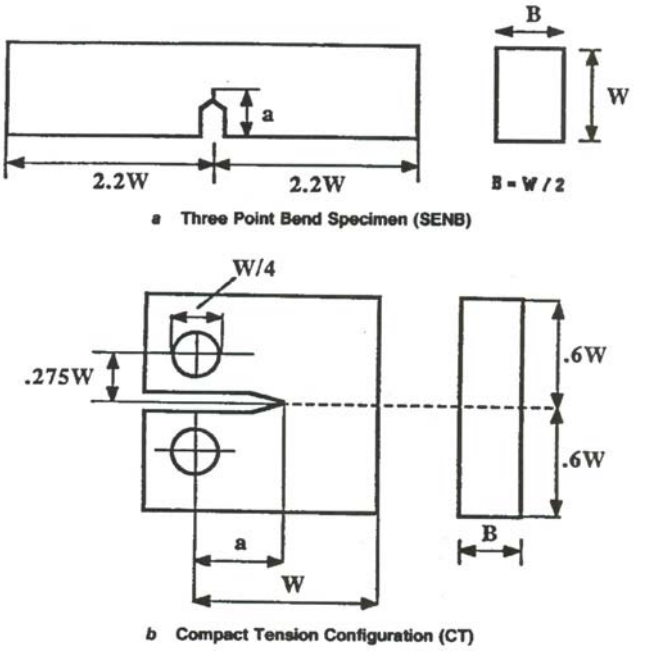

Figure 1.16 Typical specimen configurations for bending and compact tension mode for measurement fracture toughness. Reprinted with permission from ASTM E399-08. © 2008 ASTM International

1.11.3 Impact Test

Impact tests are used to determine the behaviour of a material subjected to shock loading in bending, tension and torsion. Impact tests can be divided into two classes: pendulum impact tests and drop-weight impact tests. Each test can be subdivided into non-instrumented and instrumented. A non-instrumented test displays only one feature: total impact energy. It cannot provide additional information on fracture behaviour, ductility, yielding or dynamic toughness. An instrumented test measures force continuously while the specimen is penetrated. Thus, in addition to the energy required to break the material, it provides a total load history, and failure during the impact event can be recorded.

1.11.3.1 Pendulum Impact Test

The pendulum impact test employs a pendulum type of hammer. It is carried out in four ways: Izod, Charpy, Chip and Tensile. The apparatus used for the pendulum test consists of a heavy base with a vice for clamping the specimen and a pendulum hammer swinging at a sample. The machine base must be kept on a rigid platform to prevent vibrational energy losses.

These Izod/Charpy tests are widely applied in industry due to the ease of sample preparation, and it is possible to generate comparative data very quickly. Both tests are done as per ASTM D256 [65] using a notched specimen. In the Izod test the specimen is fixed as a cantilever with the help of a vice (**Figure 1.17**). The Charpy test is also carried out in the same apparatus and specimen. The only difference is that in Charpy test the specimen is supported as a simple beam. The apparatus consists of a heavy base with a vice for clamping the specimen and a pendulum hammer swinging at a notched sample. The energy transferred to the material can be inferred by comparing the difference in height of the hammer before and after fracture. Depending on the instrument, the impact energy (J/m) or the load history during the impact event can be recorded. The test can be carried out using different combinations of impactor mass and incident impact velocity to generate data on damage tolerance as functions of impact parameters, which are helpful for the design of composite materials for a particular application [78].

The chip impact test is carried out in a similar way to the Izod test but without a notch. The test specimen is usually 25.4 mm long, 12.7 mm wide, and 1.65 mm thick. The tests are carried out using ASTM D4508 [79]. Because the test involves an un-notched sample, it reflects material toughness rather than the notch sensitivity measured for the Izod and Charpy tests.

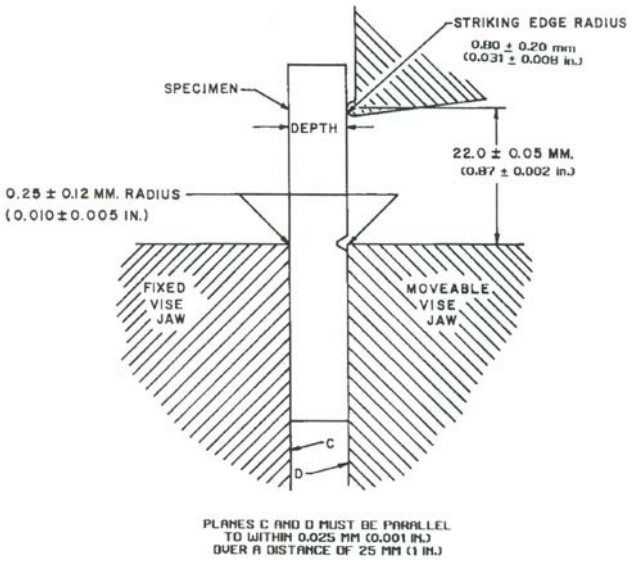

Figure 1.17 Relationship between vice, specimen and striking edge to each other for Izod test methods. Reprinted with permission from ASTM D256-04. © 2004 ASTM International

The tensile impact test is carried for un-notched samples in a test setup where one end of the specimen is mounted in the pendulum and other end is gripped by a crosshead member which travels with the pendulum until the instant of impact. The tensile force is exerted by the pendulum. The advantage of the tensile impact test over Izod or Charpy tests is that thinner and ductile samples can also be tested by the tensile impact test, whereas Charpy/Izod tests are limited to only thicker and rigid samples.

1.11.3.2 Falling Weight Impact Test

Another test used to evaluate thermoset resins and composites is the falling-weight or drop-weight impact strength. The falling weight may be a ball, a tup with a chemical nose, or a dart. Depending on the nature of weight and the application, two ASTM standards D5420 (ball, rigid specimen) [80] and D1709 (dart, film) [66] are used for testing thermoset materials. ASTM D2444 (tup) [67] is used for the evaluation of thermoplastic materials. In a dart impact test, the dart is allowed to fall on a specimen kept in a fixture with an annular hole typically ranging from 2.5 cm to 7.5 cm. The output of the load transducer can be directly fed into a signal processor, and the impact

energy or the entire loading history recorded using an instrumented machine. It can also be coupled with ultrasonic c-scan and microscopic techniques for post-failure analysis [81, 82]. The biggest advantage of the falling-weight impact test over the pendulum impact test is its ability to duplicate the multidirectional impact stresses that a structure or part would be subjected to in the actual service condition. It also enables specimens of different sizes and shapes and a part as a whole to be tested. For critical applications, rigorous testing must be carried out after considering service conditions to confirm the specified service life [83].

1.11.4 Heat Distortion Temperature (HDT)

The HDT (or the heat deflection temperature) indicates the temperature range over which the polymer material begins to soften and gets deformed under the application of load. Thus, the HDT can identify materials which lose their rigidity and load-bearing capacity over a narrow temperature range. This is commonly used for quality control and assessing materials for short-term heat resistance. The service temperature of a load-bearing component must be lower than the HDT of the composed material. The HDT is determined as per ASTM D648 [71]. The temperature at which a standard test bar deflects 0.25 mm under a load of 455 kPa or 1820 kPa is recorded as the HDT. The HDT is a single-point measurement and does not indicate the long-term heat resistance of the material.

1.11.5 Electrical Properties

A material conducts electricity due to the movement of charge carriers (e.g., electrons, ions) under an electric field. Metallic materials are very good conductors because they have loosely bound electrons, and the valance band and conduction band overlap with each other. However, thermoset plastics do not have free electrons, which is why they exhibit very low conductivity (typically $<10^{-8}$ $ohm^{-1}cm^{-1}$) and are considered to be insulators. In thermoset plastics, the outermost electrons of the atoms are covalently bonded. When an electric field is applied, the firmly bound charges in such materials can be displaced by only a limited extent from their equilibrium position depending on the amplitude of the electric field and polarity of the bonds in the polymer network. The bound charges exert an opposing force towards the displacement of charges, and the corresponding energy can be stored in the material. The ability to store energy in this way is called the ‘dielectric property’. The ratio of charge stored in an insulating material placed between two metallic plates to the charges stored when the insulating material is replaced by air or vacuum is called the ‘permittivity’ or ‘dielectric constant’ of the material. The dielectric constant of a material can be

determined using ASTM D150 [72]. The value of the dielectric constant increases with the increase in polarity of the polymer. For instance, typical values of the dielectric constant for more polar thermoset resins such as melamine and phenolic resins are 5.2–7.9 and 3.5–7.0 respectively, whereas the same values for epoxy and polyester resins are 3.5–5.4 and 4.3–5.1, respectively. Because of the higher dielectric constant compared with thermoplastic resins and other materials, they are widely used as insulators/dielectrics for various applications.

1.11.5.1 Electrical Conductivity

Thermosetting resins are inherently insulators and widely used in printed circuit boards and microelectronics. However, for many applications electrostatic dissipation (antistatic materials) or electromagnetic radiation shielding, the electrical conductivity of the cured resin is a crucial factor. The electrical properties of a thermoset network can be altered by blending with conducting fillers (e.g., carbon black, metallic powder) or conducting polymers (e.g., polyaniline, polythiophine). Recently, carbon nanotube (CNT) has drawn considerable attention for the development of conducting composites. Thermoset/CNT composites are discussed in Chapter 7. Hence, for both types of applications the measurement of electrical resistance or conductivity of thermoset materials is very important. Electrical resistance can be measured by a two-probe or a four-probe method. The alternating current (AC) electrical resistivity can be determined using AC impedance spectroscopy. Conductivity can be calculated from resistivity data using the following equation:

$$\sigma = (1/R)\,(t/A) \tag{1.63}$$

where t is the thickness of the thermoset resin film, A is the area of the electrode, and R is the resistance.

The resistance offered by a thermoset material is the combined effect of volume and surface resistances, which always act in parallel. Volume resistivity or specific volume resistance is the resistance to leakage of current through the body of the material, and is a function of thickness of the material. Volume resistivity is defined as the resistance between two electrodes covering opposite faces of a cube of dimension 1 cm. Surface resistance is the resistance to passage of current through the surface. Thus, surface conductivity is influenced by the surface finish and contamination. Samples having a rough surface or which are contaminated with oil or moisture display a lower value of surface resistance compared with samples with smooth and cleaned surfaces. Conductivity measurement is affected by the temperature and relative humidity of the atmosphere. Hence, for comparing the conductivity data for different samples, experiments must be carried out in similar conditions.

1.11.5.2 Dielectric strength

Ideally, an insulator should not allow current to pass through it. However, due to defects, every material is associated with some leakage, especially at higher voltage. The smaller the leakage, the better is the material. Such leakage generates heat and further increases the extent of leakage. This process slowly accelerates with time, leading to the total breakdown of the insulator. The minimum voltage at which dielectric breakdown occurs is called the 'breakdown voltage'. Dielectric strength is defined as the breakdown voltage per unit thickness, and is expressed as V/mil (1 mil = 1/1000 inch). Dielectric strength reflects the electrical strength of an insulator, and is thus an important characteristic of an insulating material. The higher the dielectric strength, the better is the insulator. The dielectric strength of phenolic resin is in the range 240–340 V/mil.

Dielectric strength is determined using ASTM D149 [74]. The measurement of dielectric strength is usually carried out by short-time method or a step-by-step method. In the former, voltage is increased continuously at a uniform rate until failure occurs. In step-by-step testing, definite voltages are applied to the sample for a definitive time, starting with a value that is one-half that obtained by short-time testing with equal increments of voltage until failure occurs. Because the step-by-step method is associated with longer exposure to the electric field, dielectric strength values obtained by this method are always lower that those obtained by the short-time test. However, a step-by-step method confirms the actual service condition compared with a short-time method, and thus the values are useful for designing thermoset materials for dielectric application.

1.11.5.3 Arc resistance

Themoset materials are used for switches, contact bushes and circuit breakers. For these applications, insulating materials are likely to be subjected to arcing. Arcing tends to produce a conducting carbonised path on the surface and destroys the insulator property. In cases of acrylic resins, instead of carbonisation, decomposition to ignitable gases takes place, resulting in failure in a short time. Thus, arc resistance is an important criterion for a thermoset material to be used for an insulator application. Arc resistance is the ability of a material to resist the action of a high-voltage electrical arc. The arc resistance of an insulator can be defined as the time in seconds that an arc may play across the surface without forming a conducting path or loss of integrity. The test to measure arc resistance can be conducted in various ways. ASTM D495 [73] describes the measurement of arc resistance. Resins that easily carbonise (e.g., phenolics) have poor arc resistance; unsaturated polyesters and melamine are extremely arc resistant.

1.11.6 Flammability and Smoke Tests

In general, polymers are flammable, but they can be suitably modified to significantly reduce flammability. Assessing the flammability of a polymer is extremely important from a safety viewpoint, especially if the material is likely to catch fire. There are many standards and governing regulatory bodies controlling the level of flame retardancy required for various applications, as described in earlier issue of a Rapra review report [84]. The three most commonly used flame tests are: underwriters laboratory test (UL-94), cone calorimetry, and limiting oxygen index (LOI) test. These are briefly described below.

1.11.6.1 UL-94 Flammability Test

The UL-94 test is carried out on a plastic sample (125 mm by 13 mm with various thicknesses up to 13 mm) suspended vertically above a cotton patch. The plastic is subjected to flame exposure for 10 s with a calibrated flame in a unit, which is free from the effect of external currents. After the first 10 s exposure, the flame is removed and the time for the sample to self extinguish recorded. Cotton ignition is noted if polymer dripping ensues; dripping is permissible if no cotton ignites. The second ignition is done for the same sample, and the self-extinguishing time and dripping characteristic recorded. If the plastic self-extinguishes in <10 s after each ignition with no dripping, it is classified as V-0. If it self-extinguishes in <30 s after each ignition with no dripping, it is classified as V-1, and if the cotton ignites it is classified as V-2. If the sample does not self-extinguish before burning completely, it is classified as failed (F).

1.11.6.2 Cone Calorimetry

Cone calorimetry experiments are done in an incident heat flask at 50 kW/m, and combustion behaviour is assessed according to ASTM E1354-92 [75]. During the test, materials are subjected to irradiated heat plus the feedback heat from the flame starting from the ignition of the volatile products. The aim is to simulate the conditions likely to occur in a real fire. Data are collected for first 250 s, this being regarded as representative of the initial stage of fire when it can still be stopped before becoming uncontrollable after flashover. The heat released is calculated from the consumption of oxygen due to combustion. Various parameters (peak heat release rate (HRR), mass loss rate, specific extinction area, ignition time (t_{ign}), carbon dioxide yield, carbon monoxide yield, specific heat of combustion) are calculated. The results obtained from the cone calorimeter are considered reproducible to within 10% error if measured at 50 kW/m^2. The average HRR is correlated to the heat released in a room where the

flammable materials are not ignited in the same time. Data should be reported for a minimum of three replicated experiments.

1.11.6.3 LOI Test

The LOI test is one of the oldest flammability tests (ASTM D2863 [76]) and frequently used to compare the flame-retardant properties of polymer samples. The method of operation is to select the desired initial concentration of oxygen based on past experience with a similar material. The gas is allowed to flow for 30 s to purge the system. The specimen is ignited so that entire tip is burning. The relative flammability is determined by adjusting the concentration of oxygen, which will permit the specimen to burn. The LOI is calculated from the following formula:

$$LOI = \frac{V_O}{V_N + V_O} \times 100 \tag{1.64}$$

where V_o is the volume of oxygen and V_N is the volume of nitrogen. Thus, the LOI of polymer sample 28 indicates that 28% of the oxygen/nitrogen mixture was required to be oxygen to support continued combustion of the sample.

References

1. A. Gardziella, L.A. Pilato and A. Knop, *Phenolic Resins*, 2nd Edition, Springer-Verlag, Heidelberg, Germany, 2000.

2. H.L. Fisher, *Chemistry of Natural and Synthetic Rubbers*, Reinhold Publishing Corporation, New York, NY, USA.

3. P.J. Flory, *Principles of Polymer Chemistry*, Cornell University Press, Ithaca, NY, USA, 1953.

4. W.H. Stockmayer, *Journal of Chemical Physics*, 1944, **12**, 125.

5. F.W. Billmeyer, *Textbook of Polymer Science*, 3rd Edition, Wiley, New York, NY, USA, 1984.

6. W.H. Carothers, *Transactions of the Faraday Society*, 1936, **32**, 39.

7. S.D. Senturia and N.F. Sheppard, *Advances in Polymer Science*, Ed., K. Dusek, 1986, **80**, 1.

8. J.B. Enns and J.K. Gillham, *Journal of Applied Polymer Science*, 1983, **28**, 2567.

9. S. Sourour and M.R. Kamal, *Thermochemica Acta*, 1976, **14**, 1, 41.

10. M.R. Dusi, C.A. May and C.J. Seferis in *Chemorheology of Thermosetting Polymers*, Ed., C.A. May, ACS Symposium Series No.227, ACS, Washington, DC, USA, 1983, p.301.

11. K. Horie, H. Hiura, M. Sauvada, I. Mika and H. Kambe, *Journal of Polymer Science: Polymer Chemistry Edition*, 1970, **8**, 1357.

12. K. Dusek, M. Ilavski and S. Lunak, *Journal of Polymer Science:, Polymer Symposium*, 1975, **53**, 29.

13. S.V. Muzumdar and L.J. Lee, *Polymer Engineering and Science*, 1996, **36**, 7, 943.

14. M.R. Kamal and S. Sourour, *Polymer Engineering and Science*, 1973, **13**,1, 59.

15. M.R. Keenan, *Journal of Applied Polymer Science*, 1987, **33**,1725.

16. T.J. Horong and E.M. Woo, *Angewandte Macromolecular Chemistry*, 1998, **260**, 1, 31.

17. C.S. Chern and G.W. Pohlein, *Polymer Engineering and Science*, 1987, **27**, 782.

18. V. Khanna and M. Chanda, *Journal of Applied Polymer Science*, 1993, **49**, 319.

19. E. Rabinovitch, *Transactions of the Faraday Society*, 1937, **33**, 1225.

20. I. Havlicek and K. Dusek in *Crosslinked Epoxies*, Eds., B. Sedlecek and J. Kahobek, Walter de Gruyter , Berlin, Germany, 1987, p.359.

21. K. Potter, *Resin Transfer Molding*, 1st Edition, Chapman and Hall, London, UK, 1997, p.196.

22. J. Pinoteck, S. Richter, S. Zschoche, K. Sahre and K.F. Arndt, *Acta Polymerica*, 1998, **49**, 192.

23. E. Haberstroh, W. Michaeli and E. Henze, *Journal of Reinforced Plastics and Composites*, 2002, **21**, 461.

24. N. Boyard, M. Vayer, C. Sinturel, R. Erre and D. Delaunay, *Journal of Applied Polymer Science*, 2003, **88**, 1258.

25. M. Zarreli, A.A. Skordos and I.K. Patridge, *Plastics, Rubber and Composites*, 2002, **31**, 377.

26. J. Ramos, N. Pagani, C.C. Riccardi, J. Borrajo, S.N. Goyanes and I. Mondragon, *Polymer*, 2005, **46**, 3323.

27. L.E. Nielsen, *Journal of Macromolecular Science: Part C Reviews of Macromolecular Chemistry*, 1969, **3**, 69.

28. J.P. Pascault and R.J.J. Williams, *Journal of Polymer Science, Part B*, 1990, **28**, 1, 85.

29. P.R. Couchman, *Macromolecules*, 1987, **20**, 1712.

30. S. Montserrat, *Polymer*, 1995, **36**, 435.

31. I. Havlicek and K. Dusek in *Crosslinked Epoxies*, Eds., B. Sedlacek and J. Kahovec, de Gruyter, Berlin, Germany,1987, p.417.

32. *Polymer Networks*, Ed., R.F.T. Stepto, Blackie Academic and Professional, New York, NY, USA, 1998.

33. A.V. Tobolsky, D.W. Carlson and N. Indictor, *Journal of Polymer Science*, 1961, **54**, 175.

34. H. Zweifel, *Macromolecular Symposia*, 1997, **115**, 181.

35. P.P. Nicholas, A.M. Luxader, L.A. Brooks and P.A. Hammes in *Kirk-Othmer Encyclopedia of Chemical Technology*, Ed., M. Grayson, Wiley, New York, NY, USA, 1978, p.128.

36. P.P. Klemchuk in *Ullman´s Encyclopedia of Industrial Chemistry*, Eds., W. Albrecht, H. Fuchs and W. Kittelmann, Wiley-VCH Verlag GmbH & Co KgaA, Weinheim, Germany, 2002, Section A3.

37. S. Al-Malaika in *Atmospheric Oxidation and Antioxidants, Volume 1*, Ed., G. Scott, Elsevier Publishers, Amsterdam, The Netherlands, 1993, Chapter 2.

38. J. Pospisil in *Developments in Polymer Stabilisation, Volume 1*, Ed. G. Scott, Applied Science Publishers, London, UK, 1979, Chapter 1.

39. R. Bagheri, K.B. Chakraborty and G. Scott, *Polymer Degradtion and Stability*, 1982, **4**, 1, 1.

40. G. Gungumus in *Plastic Additives Handbook*, 2nd Edition, Ed., R. Gachter and H. Muller, Hanser Publishers, Munich, Germany, 1997, Chapter 3.

41. Developments in *Polymer Degradation*, Ed., N. Grassie, Applied Science Publishers, London, UK, 1977.

42. J.W. Moison in *Polymer Permeability*, Ed., J.W. Comyn, Applied Science Publishers, London, UK, 1985, Ch. 4.

43. S. Al-Malaika, *Polymer Plastics Technology and Engineering*, 1990, **29**, 1, 73.

44. J. Pospisil in *Oxidation Inhibition of Organic Materials*, Eds., P. Klemchuk and J. Pospisil, CRC Press, Boca Ratan, FL, USA, 1996, Chapter 6.

45. S. Al-Malaika in *Chemical Reactions on Polymers*, Eds., J.L. Benham and J.F. Kinstle, ACS Symposium Series No.364, Washington, DC, USA, 1988, Chapter 29.

46. D. R. Paul and S. Newman, *Polymer Blends*, Academic Press, New York, NY, USA, 1978, p.2.

47. *Silane and other Coupling Agents - 2*, Ed., K.L. Mittal, VSP, Utrecht, The Netherlands, 2000.

48. X. Gong, J. Liu, S. Baskaren, R.D. Voise and J.S. Young, *Chemistry of Materials*, 2000, **12**, 1049.

49. T. Fukushima, A. Kosaka, Y. Ishimura, T. Yamamoto, T. Takigawa, N. Ishii and T. Aida, *Science*, 2003, **300**, 2072.

50. P.V. Kodgire, A.R. Bhattacharyya, S. Bose, N. Gupta, A.R. Kulkarni and A. Misra, *Chemical Physics Letters*, 2006, **432**, 480.

51. D. Ratna, A.K. Banthia and N.C. Maity, *Indian Journal of Chemical Technology*, 1995, **2**, 253.

52. C.W. Macosko, *RIM: Fundamentals of Reaction Injection Molding*, Hanser, Munich, Germany, 1989.

53. O. Gryshchuk, J. Karger-Kocsis, R. Thomann, Z. Konya and I. Kiricsi, *Composites Part A: Applied Science and Manufacturing*, 2006, **37**, 9, 1252.

54. M. Maiti and A.K. Bhowmick, *Polymer*, 2006, **47**, 6156.

55. E.A. Stefanescu, A. Dundigalla, V. Ferreiro, E. Loizou, L.Porcar, I. Negulescu, J. Garnoa and G. Schmidt, *Physical Chemisty Chemical Physics*, 2006, **8**, 1739.

56. E. Loizou, P. Butler, L. Porcar and G. Schmidt, *Macromolecules*, 2005, **38**, 2047.

57. D.Ratna, O. Becker, R. Krishnamurty, G.P. Simon and R. Varley, *Polymer*, 2003, **44**, 24, 7449.

58. G. Binnig, C.F. Quate and C.H. Gerber, *Physical Review Letters*, 1986, **56**, 930.

59. C.J. Buchko, K.M. Kozlo and D.C. Martin, *Biomaterials*, 2001, **22**, 1289.

60. T. Murayama, *Dynamic Mechanical Analysis of Polymeric Materials*, Materials Science Monograph 1, Elsevier Science, New York, NY, USA, 1978.

61. J.D. Ferry, *Viscoelastic Properties of Polymers*, John Wiley, New York, NY, USA, 1980.

62. ASTM D638-08, *Standard Test Method for Tensile Properties of Plastics*, 2008.

63. ASTM D790 07e1, *Standard Test Methods for Flexural Properties of Unreinforced and Reinforced Plastics and Electrical Insulating Materials*, 2007.

64. ASTM D5045-99 (2007)e1, *Standard Test Methods for Plane-Strain Fracture Toughness and Strain Energy Release Rate of Plastic Materials*, 2007.

65. ASTM D256-06ae1, *Standard Test Methods for Determining the Izod Pendulum Impact Resistance of Plastics*, 2006.

66. ASTM D1709 – 08, *Standard Test Methods for Impact Resistance of Plastic Film by the Free-Falling Dart Method*, 2008.

67. ASTM D2444-99 (2005), *Standard Test Method for Determination of the Impact Resistance of Thermoplastic Pipe and Fittings by Means of a Tup (Falling Weight)*, 2005.

68. ASTM D2990-01, *Standard Test Methods for Tensile, Compressive, and Flexural Creep and Creep-Rupture of Plastics*, 2001.

69. ASTM D2991-84, *Recommended Practice for Testing Stress-Relaxation of Plastics*, 1984. (Withdrawn 1990 – no replacement)

70. ASTM D761, *Specification for Enclosures and Servicing Units for Tests Above and Below Room Temperatures*. (Withdrawn 1951 – no replacement)

71. ASTM D648-07, *Standard Test Method for Deflection Temperature of Plastics Under Flexural Load in the Edgewise Position*, 2007.

72. ASTM D150-98 (2004), *Standard Test Methods for AC Loss Characteristics and Permittivity (Dielectric Constant) of Solid Electrical Insulation*, 2004.

73. ASTM D495-99 (2004), *Standard Test Method for High-Voltage, Low-Current, Dry Arc Resistance of Solid Electrical Insulation*, 2004.

74. ASTM D149-97a (2004), *Standard Test Method for Dielectric Breakdown Voltage and Dielectric Strength of Solid Electrical Insulating Materials at Commercial Power Frequencies*, 2004.

75. ASTM E1354-08a, *Standard Test Method for Heat and Visible Smoke Release Rates for Materials and Products Using an Oxygen Consumption Calorimeter*, 2008.

76. ASTM D2863-08, *Standard Test Method for Measuring the Minimum Oxygen Concentration to Support Candle-Like Combustion of Plastics (Oxygen Index)*, 2008.

77. ASTM E399-08, *Standard Test Method for Linear-Elastic Plane-Strain Fracture Toughness K Ic of Metallic Materials*, 2008.

78. N.K. Naik, S.V. Borade, H. Arya, M. Sailendra and S.V. Prabhu, *Journal of Reinforced Plastics and Composites*, 2002, **21**, 1347.

79. ASTM 4508-06, *Standard Test Method for Chip Impact Strength of Plastics*, 2006.

80. ASTM D5420-04, *Standard Test Method for Impact Resistance of Flat, Rigid Plastic Specimen by Means of a Striker Impacted by a Falling Weight (Gardner Impact)*, 2004.

81. M.L. Karasek, L.H. Strait, M.F. Amateau and J.P. Runt, *Journal of Composites Technology and Research*, 1995, **17**, 11.

82. D. Hui *in the Proceedings of the ICCM/9 Conference on Composite Behaviour*, 1993, **5**, 321.

83. D. Ratna, *Epoxy Composites: Impact Resistance and Flame Retardancy*, Rapra Review Report No.185, 2005, **16**, 5, 1.

84. J. Innes and A. Innes, *Plastic Flame Retardance: Technology and Current Developments*, Rapra Review Report No.168, Rapra Technology, Shrewsbury, UK, 2003.

2 Chemistry, Properties and Applications of Thermoset Resins

2. Introduction

Thermosetting resins are characterised by a crosslinking reaction, which leads to the formation of a three-dimensional (3D) network structure. The basics of network structure and various evaluation methods for thermosetting resins were discussed in Chapter 1. The greatest advantage of thermoset resins is that they are processed from a low molecular weight compound (resin) unlike the high molecular weight macromolecules in the case of thermoplastics. This is why thermoset-based products can be moulded, in general, at a much lower temperature and pressure compared with thermoplastics. Another distinct characteristic of thermosetting resins is that their properties are not only dependent on the chemistry and molecular weight of the resin (as in the case of thermoplastics) but are also largely dependent on the crosslink density of the resin network. A wide range of properties can be achieved by simply adjusting the crosslink density of a network without changing the chemical structure.

In this chapter the chemistry, properties and applications of individual thermosetting resins will be discussed. For convenience, a list of various thermosetting resins to be discussed and their precursors and field of applications are presented in **Table 2.1**.

Table 2.1 Important thermosetting resins and their field of application		
Resin	**Precursor**	**Applications**
Phenolic resin	Phenol and formaldehyde	Wood adhesive, moulding compounds, foundry binders, laminate mouldings, electrical laminates, ablative coating casting and fibre composites for household appliances, automotive, aircraft construction and accessories, electrical and lighting industries
Unsaturated polyester	Dicarboxylic acids, diols and reactive diluents e.g.,, styrene	Surface coating, fibre composites for mechanical equipment and building construction, electrical and lighting industries
Epoxy	Epichlorohydrin and bisphenols	Engineering adhesives, paints and surface coating, electrical laminates, fibre composites for automotive, marine construction and aerospace applications.
Vinyl ester	Epoxy resin and acrylic or methacrylic acid	Fibre composites for mechanical equipment and building construction, marine construction, electrical industries
Melamine	Melamine and formaldehyde	Coatings, moulding compounds, wood materials processing, friction linings, textile auxiliaries
Urea	Urea and formaldehyde	Moulding compounds, textile auxiliaries, wood materials, foundry binder, foams
Furan	Furfuryl alcohol	Refractory materials processing, fibre composites, moulding compounds, grinding wheels, acid-resistant cements
Polyurethane (PU)	Diisocyanate and hydroxyl-functionalised oligomer (polyol)	Coating, adhesive, encapsulating materials, acid-resistant cements, foams, adhesives
Polyimide	Diamines and dianhydride	Coating and composite for high-temperature applications
Cyanate ester	Cyanogen halide and alcohol or phenol	Fibre composites for aircraft, rocket, missiles and re-entry vehicles
Bismaleimide	Bismaleic acid and amine	Fibre composites for aircraft, rockets, missiles and re-entry vehicles

2.1 Phenolic resins

Phenolic resin or phenol formaldehyde (PF) resin is considered to be the first polymer material produced commercially from a low molecular weight compound. In other words, phenolic resins were the first truly synthetic resins to be exploited commercially. The concept of producing high molecular weight substances from oligomeric resins (phenolic resin) with or without filler was first discovered by Leo H. Baekeland. This pioneering concept has been subjected to continued technological development and perfection over the years, and has reached the sophisticated thermoset resin composite technology available today.

Phenolic resins are prepared by a step-growth polymerisation of formaldehyde and phenol or phenol derivative using an acid or a base catalyst. The product type and the quality largely depend on the ratio of the reactants used and the nature of the catalyst. Phenolic resins are available in two varieties: 1) novolac, which is a thermoplastic type and can be used as it is or can be cured with hexamethylene tetramine (HMTA) to get a crosslinked structure. This can also be viewed as a reactive intermediate, and can be transformed into other groups so different types of structures can be generated; and 2) resole, which is a multifunctional reactive compound and can be cured thermally without a catalyst or an acid catalyst.

2.1.1 Novolac

Novolac is produced by the reaction of formaldehyde with an excess amount of a phenol or a phenol derivative in the presence of an acid catalyst. The ratio of phenol to formaldehyde used is in the range 1.49 to 1.72. The reaction in acid medium involves initial protonation of hydrated formaldehyde followed by electrophilic substitutions in the *ortho* and *para* position (electron-rich position unlike the *meta* position). At low temperature, only addition of formaldehyde to phenol occurs and *o*- or *p*-methylol phenols are formed. At higher temperature, the condensation reactions of methylol phenol with phenol and/or methylol phenol occur, leading to the formation of a prepolymer and the desired resin [1, 2]. Water is formed as a byproduct. The reaction scheme is shown in **Figure 2.1**. The condensation of methylol phenol can generate three types of methylene bridges: *o*,*o*´ (condensation of two *o*-methylol phenols), *o*, *p* (condensation of an o-methylol phenol with a *p*-methylol phenol) and *p*, *p*´ (condensation of a p-methylol phenol with a p-methylol phenol. The reaction in the presence of a strong acid such as sulfuric acid or phosphoric acid produces the distribution methylene linkages (*o*,*o*´:*o*,*p*:*p*,*p*´) close to the statistical value 1:2:1. However, a weak acid catalyst like oxalic acid leads to the formation of more *p*,*p*´ linkages. A typical distribution of methylene linkages obtained for the synthesis of novolacs using sulfuric acid and oxalic acid are 25.9:48.5:25.9 and 23.3:49.1:27.6, respectively [3].

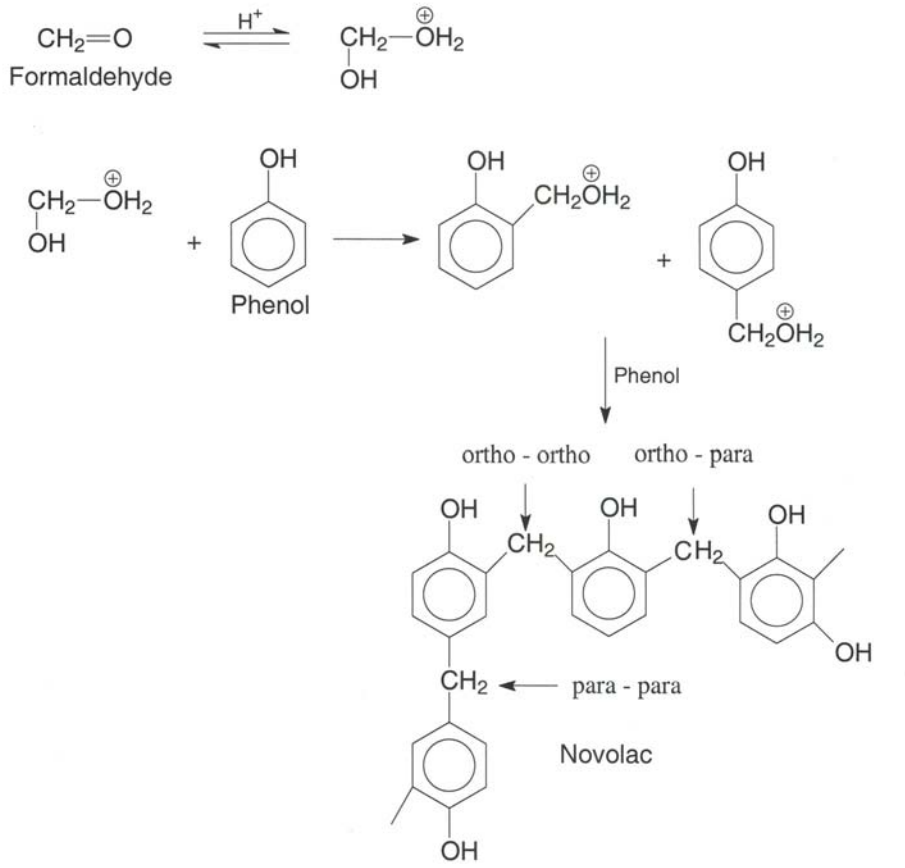

Figure 2.1 Reaction mechanism for the synthesis of novolac-type phenolic resin

To achieve the selectivity in the mixture of products with different methylene bridges is a critical issue. It is reported that the selectivity of the p-isomer can be boosted by using β-cyclodextrin or crown ether [4]. The basic mechanism is that the additive form complexes with the phenoxide ions and encourages preferential attack at the p-position due to the steric hindrance caused by the attack at o-position. Ortho selectivity can be increased by using a metallic catalyst such as salts of zinc, magnesium, or lead. When the reaction is carried out in the presence of metallic salts, the metal ion forms

a chelate intermediate (**Figure 2.2**). The chelate intermediate is further transformed into *o*-methylol phenol as confirmed by ^{1}H-NMR spectra [5]. Thus, high ortho resins are formed with 47–49% *o*,*o´* and *o*,*p* methylene bridges each, and <5% of *p*,*p* methylene bridges.

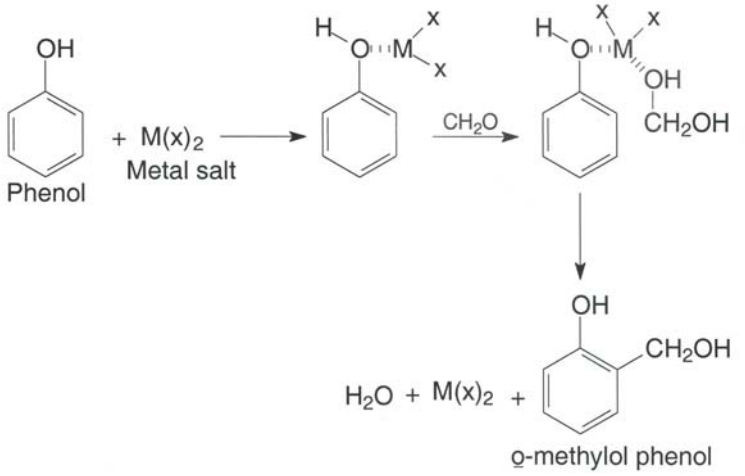

Figure 2.2 Formation of chelate intermediate for the phenol/formaldehyde reaction in the presence of a metal salt catalyst

2.1.2 Synthesis of Resole

Resole is produced by reaction of a phenol or a phenol derivative with an excess amount of formaldehyde in the presence of a base catalyst. The reaction in basic medium proceeds through the addition of formaldehyde with the phenoxide ion, leading to the formation of *o*- or *p*-monomethylol phenol (along with some di- or trimethylol phenol) as established by complexation via cyclodextrin or crown ether [2]. The reaction scheme for the synthesis of resole is shown in **Figure 2.3**.

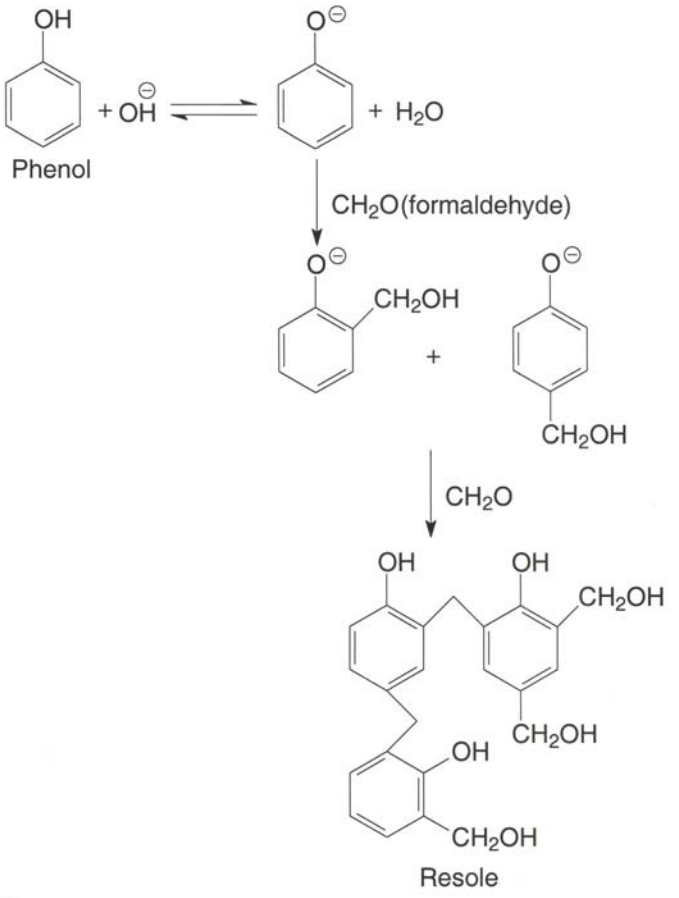

Figure 2.3 Reaction scheme for the formation of resole-type phenolic resin

2.1.3 Difference Between Novolac and Resole

Novolac and resole are the products of phenol and formaldehyde, and are known as 'phenolic resin'. The differences between novolac and resole are as follows:

Novolac is produced using excess phenol and an acid or metal salt catalyst, whereas resole is produced using excess formaldehyde and a basic catalyst.

Novolacs are mostly supplied in the solid form, whereas resoles are mostly supplied as a solution (using water or alcohol as a solvent).

Novolac is not self-curing; it requires an extra curing agent, whereas resole is self-curable without an additional catalyst.

Novolac has a long shelf-life, whereas resole has a limited shelf life (<1 year).

Novolac can be used as a thermoplastic and can be readily modified by reacting with the terminal hydroxyl groups. Modification of resole is comparatively difficult due to a gelling problem.

2.1.4 Characterisation of Phenolic Resin

From the previous discussion it is clear that the produced resin may vary with respect to branching, molecular-weight distribution, methylene linkages, and free phenol content. Hence a thorough analysis and characterisations are necessary for quality control. Molecular weight and molecular-weight distribution are analysed by gel permeation chromatography (GPC). However, because of the presence of mixtures of different methylene bridges, producing a standard calibration curve is difficult. The molecular weight of novolac can also be determined from ^{1}H-NMR analysis. The ratio of intensity of aliphatic to aromatic protons (r) is used to determine the molecular weight from the following equations [6]:

$$r = \frac{2n-2}{3n+2} \tag{2.1}$$

$$M_w = 106n + 200 \tag{2.2}$$

Here n is the number phenolic units in the chain. The methylene bridges are characterised by ^{13}C-NMR spectroscopic analysis. The characteristics peaks for *o*, *o´*, *o*, *p* and *p*, *p* methylene carbons are 30, 35 and 40 ppm. The free phenol is characterised from peaks at 115 ppm and 120 ppm. The free phenol content of a resin sample is determined by dissolving the sample in acetone and gas chromatographic analysis of the solution using m-cresol as an internal standard. The –OH and –CO functional groups are characterised by Fourier transform infra red spectroscopy (FT-IR) from their characteristic peaks at 3350–3500 cm^{-1} and 1730 cm^{-1}, respectively [7].

2.1.5 Crosslinking of Phenolic Resins

When resole solution is subjected to a thermal cure with or without an acid catalyst, the molecular weight increases leading to an intermediate gel state (B-stage), which

is insoluble in the solvent (water or alcohol). As the solvent evaporates the curing proceeds further, leading to the formation of a rigid crosslinked structure.

Unlike resole, novolac is not self-curing. It requires extra formaldehyde for curing to take place. Novolac is usually cured with HMTA, which is a condensation product of formaldehyde and ammonia. HMTA is added at 8–15% [8]. Under this curing condition, HMTA decomposes to generate formaldehyde which converts novolac to a crosslinked network structure (**Figure 2.4**). The mechanism of HMTA-cured novolac has been studied extensively, but numerous possible intermediates complicate the analysis. Dargavililleand co-workers [9] de Bruyn and co-workers [10] and Zang and co-workers [11, 12] employed monomers and dimers to analyse their curing reactions with hexamine. The proposed mechanism occurs in two stages: formation of initial intermediates such as benzoxazines and benzyl amines, and further reactions of these initial intermediates into methylene bridges with residual traces of amines, imides, imines, methyl phenol and others. When the amount of methylene is low, hexamine provides only one methylene bridge to the 4, 4 site and many reactive sites remain and react to form more methylene bridges for crosslinking. Hence, more methylene bridges are formed compared with the composition with higher hexamine content.

Decomposition of the intermediates is also affected by the pH of the medium. Novolac is acidic and hexamine is alkaline. Hence the resultant pH of the mixture depends on the composition. At low hexamine concentration, the pH remains acidic and facilitates the decomposition of intermediates. Another factor is the *ortho*:*para* ratio of novolac. The strategy to make preferential *ortho*- or *para*-substituted products was discussed in **Section 1.1.1**. The *para*-bridged intermediate decomposes more readily than the *ortho*-bridged intermediate, which is more stable due to the possibility of formation of six-membered rings. Thus when novolac with many *ortho* sites is reacted with a higher amount of hexamine, a stable network with high nitrogen content is formed. The reaction of novolac with many vacant para sites with a low amount of hexamine produces a network with low nitrogen content. Because the presence of nitrogen increases the thermal stability and flame retardancy of the resin, a sufficiently high amount of hexamine should be used for curing novolac.

Markovic and co-workers [13] investigated the effects of the phenol to formaldehyde ratio used for the preparation of novolac and the nature of methylene linkages on the curing behaviour of the novolac/HMTA system using rheological studies. Cure kinetics were described by a third-order phenomenological equation, which took into account the self-acceleration effect that arises from the chemical reaction and phase separation. The reaction rate was found to increase with an increase in phenol to formaldehyde ratio. For the same phenol to formaldehyde ratio, the reaction rate increased with an increase in *o*, *o´* methylene linkages (**Table 2.2**).

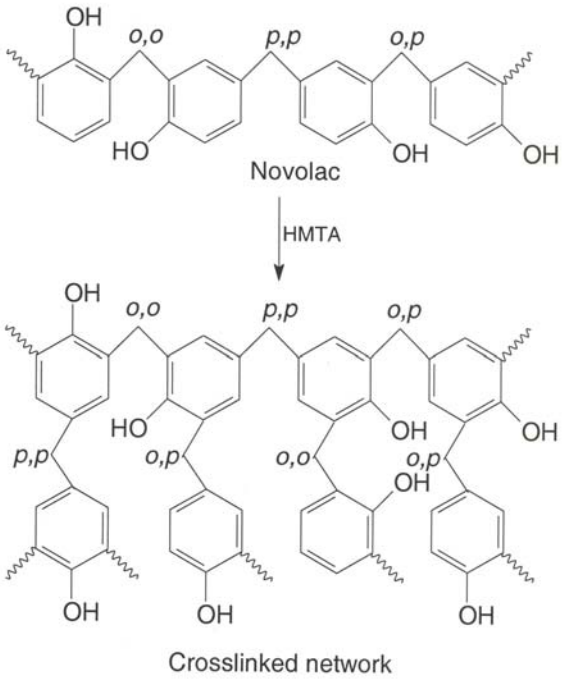

Figure 2.4 Crosslinking of novolac using HMTA

Various hydroxymethyl derivatives (e.g.,, bismethylol cresol, bisphenol A tetramethylol) can be used as the curing agents instead of hexamine. The networks produced by these curing agents display much higher impact strength and bending strength compared with hexamine-cured networks.

Table 2.2 Effect of phenol to formaldehyde ratio and content of *o*, *o´* isomer on reaction rate [13]

Phenol to formaldehyde ratio	Molecular weight [$] (g/mole)	Content of *o-o´* isomer (%)	Reaction rate (per min)	Gel point (min)
1:0.75	406	26.05	0.061	4.4
1:0.79	492	27.20	0.071	2.5
1:0.85	813	26.58	0.093	0.5
1:085	712	70.17	0.107	1.0

[$]Determined by ^{1}C-NMR spectroscopy

2.1.6 Properties of Phenolic Resins

Phenolic resins offer many useful properties such as high mechanical strength, long-term thermal and mechanical stability, excellent fire, smoke and toxicity characteristics, and excellent thermal insulating capability. Because of its aromatic structure, phenolic resin offers flame- and smoke-resistance. Smoke density (ASTM E662) of phenolic resin is 16 compared with 480-515 for epoxy and 530 for vinyl ester. The cured resins exhibit a glass transition temperature (T_g) of >150°C. Phenolic resins are widely used as moulding compounds. The thermomechanical properties of commercial phenolic moulding compounds are presented in **Table 2.3** [14].

Table 2.3 Mechanical properties of phenolic moulding compounds [14]

Moulding compound	Tensile strength (MPa)	Tensile modulus (GPa)	Strain at break (%)	Flexural strength (MPa)	Compressive strength (MPa)
RX-630	82.7	13.8	0.6	193	275.8
RX-660	55.2	11.7	0.5	137.9	227.5
RX-865	68.9	17.2	0.4	186	241.3
XB-22	75.8	7.6	1.0	151.7	234.4

2.1.7 Applications of Phenolic Resins

Phenolic resins are mainly used in wood materials and insulating products. Such materials are mostly used in the building and automotive industries. In wood composites, about 10% binder resin is used which is mostly the aqueous solution of resole type phenolic resins. The driving force for such application is that phenolic resins can offer durable bonding that is resistant to heat and moisture. Phenolic-bonded wood materials exhibit good resistance to moisture and other environmental effects, and retain these properties even after lengthy exposure. Acoustic and thermal insulating materials should retain a constant level of functional properties over long periods of time. For example, materials used as insulating materials and in automobile constructions should provide a load-bearing and/noise damping function throughout the life of the product or vehicle. Phenolic resin-bonded textile mats are used for

such purposes. The other applications are moulding compounds, foundry/refractory materials, abrasives, and friction linings. Phenolic resin moulding compounds continue to be in electrical and household appliance areas. One of the oldest fields of application for phenolic resin-glass fabric prepregs is the production of fishing rods [15].

The resin content in abrasive and friction lining materials is about 10%, whereas binder content is much less (approximately 2%) in foundry materials. For friction lining applications (e.g., automobile braking operation), the surface temperature of the lining may increase up to 800 °C for a short time due to tremendous friction. Phenolic resins are most suitable for such applications because of their high thermal stability.

Phenolic resin is soluble in low boiling alcohol, impregnated papers, and fabric. It can be made easily by soaking the fabric in resin solution followed by drying and curing. Such impregnated papers are used as separators in lead–acid storage batteries and fuel cells to separate positive and negative electrodes. Phenolic resin as an impregnation material offers adequate insulation, high resistance to acids, oxidation and mechanical strength. Because of inherent fire-retardant properties, they are used to make heat- and fire-resistant panels.

Honeycomb structures and paper honeycombs also represent an application for phenolic resins as impregnating and dipping agents. Honeycomb structures are very effective for development of lightweight structures. Though epoxy and vinyl ester resins are used for such applications, phenolic is also preferred due to its inherent fire-resistant property and low cost. Honeycomb structures were initially intended for only high-tech applications such as the flooring and interior paneling of aircrafts, but such structures find application even in passenger and freight train cars to reduce the weight penalty. Sliding doors for subways and ship buildings are other applications. The panels must be coated with suitable flame-retardant materials to reach the required fire protection standard.

Braking straps and friction pads are used in power shift transmissions, ship winch transmission, and automobile clutches. Special types of papers impregnated with special phenolic resins are used for this application. Adequate adhesion of the paper to the metal parts is required to satisfy the parameters required for friction lining compounds. In general, phenolic resins in combination with epoxy resins are used to develop a wide range of friction lining materials. Another application of impregnated fabric is in the foundry industry (e.g., to filter aluminium melts). For the preparation of such impregnated fabric, woven glass fabrics is passed through an impregnating bath containing an aqueous solution of resole, dried and finally cured in stages up to 300 °C.

Because of their high aromatic content, phenolic resins absorb a lot of heat for their degradation. This is why they are used as an ablative material in re-entry vehicles. When a space vehicle re-enters the earth's atmosphere, due to tremendous friction with air, a lot of heat is generated. Phenolic resins can absorb the heat at the cost of its degradation, and stops the vehicle from deteriorating as a result of the extremely high temperature.

Phenolic resins are used as an alternative to conventional precursor (pitch, tar) materials for the development and production of carbon-based engineering materials (e.g., glassy carbon, carbon fibres, carbon–carbon composites [16–18]). This application is related to the high yield of carbon (60–70%) produced as a result of pyrolysis. Glassy carbon, which is prepared by pyrolyzing phenolic resin at about 600 °C at a heating rate of 2–5 °C per hour, exhibits distinct properties such as thermal resistance up to 3000 °C, very low density, alkali resistance, gas permeability and biocompatibility. Because of high thermal stability, carbon-based engineering materials are not only used for conventional applications like electrode materials, slip ring seals and bearing materials, but also in nuclear reactors, missiles and rocket engineering. Carbon–carbon composites are made by curing the carbon fibre/phenolic prepreg followed by carbonisation at 500–1000 °C by heat/pressure and densification by chemical vapour deposition or chemical vapour infiltration. During carbonisation, the precursor is converted to a porous carbon fibre matrix. The unique feature of carbon–carbon composite is that the matrix and reinforcement phases are carbon. The carbon–carbon composites are suitable if high temperature strength and high strength to weight ratio are of utmost importance. They can work at very high temperature (2200 °C) as well as at subzero temperatures. Another important property that carbon–carbon composites exhibit is very low high temperature creep. On reentry of the space shuttle, the nose cone and leading edges of the shuttle experience hot gases rushing through the nozzle/cone at high velocity, stressing and eroding the nozzle wall. Carbon–carbon composites can resist high temperature erosion without burning away. Most carbon–carbon composites are used in commercial and military aircraft brakes, and in rockets and missiles.

Phenolic resins exhibit excellent dimensional stability with a constant use temperature range of 180–200 °C, excellent resistance to chemicals, moisture, and heat; and favorable behaviour against fire and smoke. The predominant consideration in the use of phenolic resins as a matrix resin in fibre-reinforced composites is fire behaviour. Phenolic-based composites perform better under fire conditions compared with epoxy- or vinyl ester-based composites. This is due to their delayed ignitability coupled with low heat release, low smoke evolution with little or no toxic gas emission, and capability to provide significant strength retention (70%)

at a service temperature of 300 °C over 1–2 hours. Thus, phenolic composites with exceptional fire resistance are suitable for use in demanding critical applications where the safety of passengers during egress in the case of fire is most important. The possible applications are composites for aircraft interiors, mass transportation, and marine/offshore areas.

2.1.8 Phenolic Resin as Additives

2.1.8.1 Additives for Rubber

Phenolic resins are useful additives for rubbers. Rubbers also belong to the category of thermoset polymers but, unlike thermosetting resins, they are high molecular weight polymers. Depending on the nature of rubber and the phenolic resin modifier, they can function as curing or vulcanising agents, tackifier, and reinforcing agents. The phenolic modifier can be incorporated into the rubber using the same methodology used for incorporating carbon black and other rubber additives. In general, rubbers are cured by sulfur for commercial purposes. *Para*-aminophenol resole-type phenolic resins can be used to cure butyl rubber (containing less unsaturation) in the presence of a Lewis acid catalyst [19].

Unlike natural rubber, filled synthetic rubber compounds (e.g., styrene butadiene rubber (SBR), ethylene propylene diene rubber (EPDM)) exhibit inherent low tack. The tack property is very important for tyre applications where multiple layers must adhere to each other. The lack of adequate tack may lead to failure of the final product. Long-chain and branched alkyl phenol-based novolac resins have been recommended as tackifier.

2.1.8.2 Modifier for Poly(Ethylene Oxide) (PEO)

PEO can coordinate alkali metal ions strongly and is used as a solid polymer electrolyte [20–22]. However, conventional PEO–Li salt complexes show conductivities of the order of 10^{-5} S/cm, which is not sufficient for battery, capacitor and fuel-cell applications. A high crystalline phase concentration limits the conductivity of PEO-based electrolytes. Apart from high crystallinity, PEO-based electrolytes suffer from low cation transport number (t_+), ion-pair formation and inferior mechanical properties. Peter and co-workers [23] reported the modification of PEO with phenolic resin for improvement in mechanical properties and conductivity.

Ratna and co-workers [24, 25] recently proposed PEO/novolac blends for use as a crystallisable switching segment for shape memory application. A material is said to show a shape memory effect [26] if it can be deformed and fixed into a temporary shape and recover its original permanent shape only on exposure of external stimuli such as heat or light. Thermally induced shape memory effect is more common if the recovery takes place with respect to a certain critical temperature. The crystalline PEO acts as a switching segment because when the system is heated the PEO melts, so the system becomes deformable and can be given a temporary shape. On cooling, the melted PEO crystallises and the temporary shape gets fixed. When the system is reheated, the PEO melts and shape recovery takes place. In this context, blends of novolac with low and high molecular weight (unsaturated polyester; UPE) PEO containing 0–30 wt% of novolac have been investigated [24, 25]. Other studies on PEO/phenolic blends with phenolic as a major component have also been investigated [27–29].

The interaction between PEO and novolac was corroborated by FT-IR spectroscopy [24]. The FT-IR spectra of PEO, novolac, and blend containing 20% novolac are presented in **Figure 2.5**. Novolac shows a broad band consisting of two peaks at 3500 cm^{-1} and 3350 cm^{-1} which are assigned to the non-associated free hydroxyl groups and self-associated hydroxyl groups, respectively. In the blend, the band corresponding to the self-associated –OH group remains unchanged, but the same corresponding to the non-associated –OH group is shifted to 3300 cm^{-1}. The bands corresponding to the ether groups (1200–1300 cm^{-1}) become broader compared with those in PEO. This clearly indicates that there are polar interactions between the –OH groups of PEO with either chain of PEO via H-bonding (**Figure 2.6**).

The crystallisation behaviour of PEO/novolac blends containing various concentrations of novolac is shown in **Figure 2.7**. The crystallisation temperature gradually decreases with increasing concentration of novolac. This is because amorphous novolac disturbs the crystallisation of PEO, as will be discussed shortly using cross-polarised optical microscopy (CPOM). Thus shape memory polymers (SMP) with adjustable switching temperature can be made by using a correct blend composition as a crystallisable switching segment. A shape memory system functions only if the switching temperature matches the switching temperature. For example, medical applications require the switching temperature to be about 37 °C. Hence by using the PEO/phenolic blend composition as a switching component, the application PEO-based shape memory polymers can be broadened.

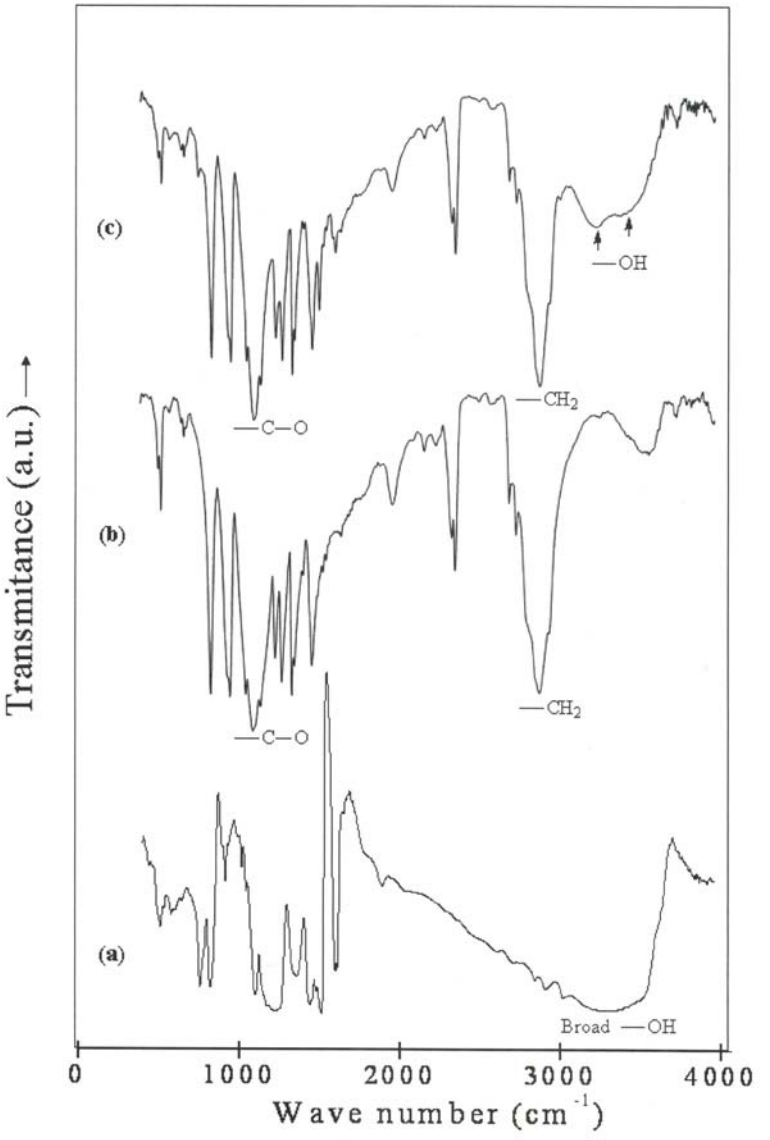

Figure 2.5 FT-IR spectra of a) novolac b) PEO and c) PEO/novolac blend (80/20 w/w). Reproduced with permission from D. Ratna, T. Abraham and K. Kocsis, *Journal of Applied Polymer Science*, 2008, 108, 2156 © 2008, John Wiley and Sons Publishers

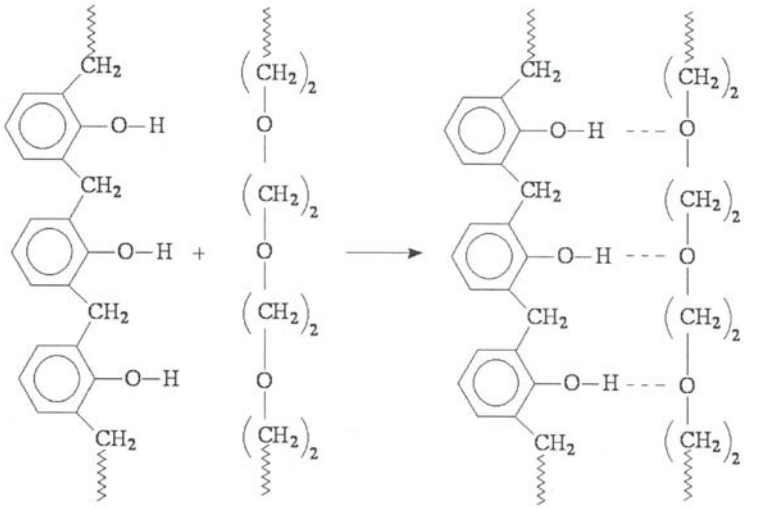

Figure 2.6 Polar interactions between the –OH groups of PEO with the ether chain of PEO via H-bonding

The CPOM photographs of PEO and blends containing 20 wt% and 30 wt% novolac are presented in **Figure 2.8**. When the PEO melt is cooled, small circular spherulites are formed, which subsequently impinge upon one another, producing a typical Maltese cross (a regular isotropic three-dimensional shape; **Figure 2.8**). In the case of blends, the spherulites are characterised by many anisotropic, non-spherulitic shapes with jagged edges. The sizes of spherulites decrease with increase in novolac concentration in the blends. This can be attributed to disturbance of radial orientation caused by amorphous novolac during crystallisation. The blends with higher concentration of novolac (>20 wt%) show a leaf-like structure due to anisotropy of the total crystallisation process. Hence the optimum phenolic concentration is 20 wt% in the blend because an adequate overall crystallinity of the blend is essential for triggering the shape memory effect.

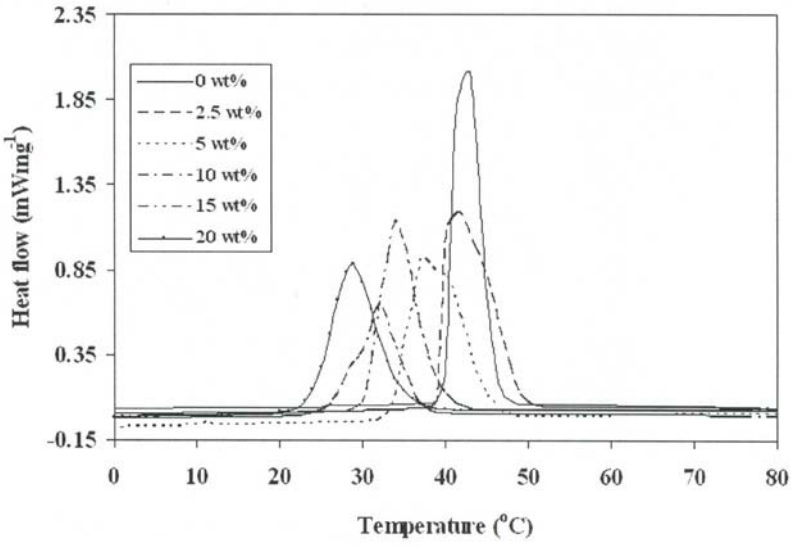

Figure 2.7 Crystallisation behaviour of PEO/phenolic blends with varying concentration of phenolic resin. Reproduced with permission from D. Ratna, T. Abraham and K. Kocsis, *Journal of Applied Polymer Science*, 2008, 108, 2156 © 2008, John Wiley and Sons Publishers

Differential scanning calorimetry (DSC) scans of novolac (UPE = 989 g/mole) and PEO/novolac (70/30 *w/w*) blends are shown in **Figure 2.9**. The blend displays a single T_g (approximately –20 °C) in-between the T_g of novolac (55 °C) and the T_g of PEO (–62 °C). This indicates that the amorphous phase of PEO is compatible with novolac and the crystalline phase remains separate as evident from the melting peak. The theoretical T_g value for the blend was calculated by using the Fox equation [30] as given next:

$$\frac{1}{T_g} = \frac{(1-C)}{T_{g1}} + \frac{C}{T_{g2}} \qquad \text{(Equation 2.3)}$$

where T_g is the glass transition temperature of the blend, T_{g1} = glass transition temperature of the phenolic resin, T_{g2} = glass transition temperature of PEO, and C is the weight fraction of PEO. The T_g of the blend shows a positive deviation with respect to the value calculated by the Fox equation (–38 °C), which can be attributed to the crystallinity and inter-association H-bonding as confirmed by FT-IR analysis discussed previously.

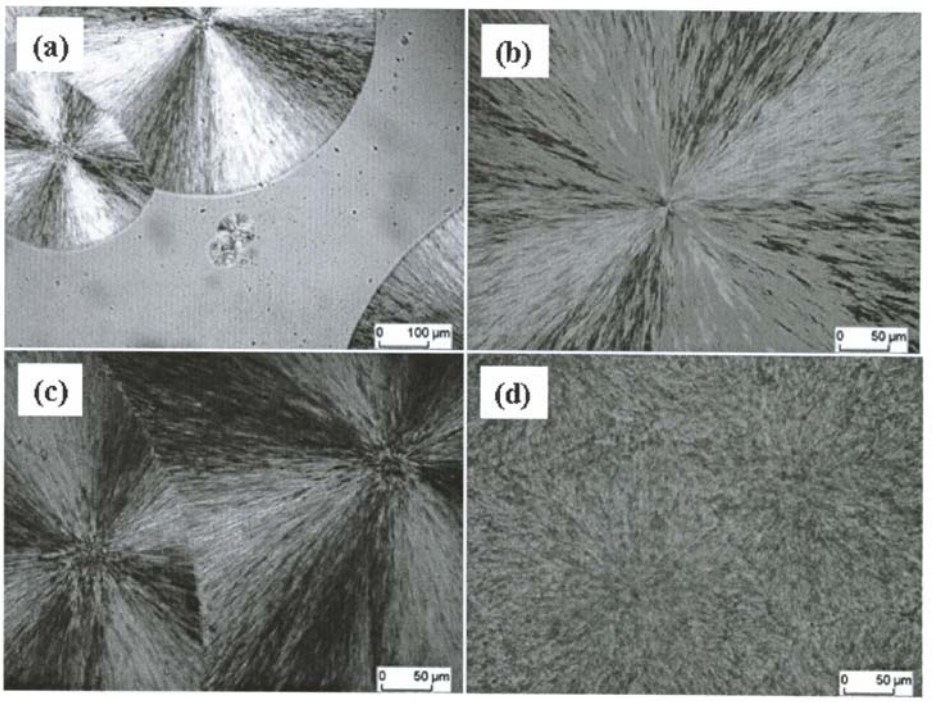

Figure 2.8 Cross-polarised optical microscope images of PEO blends a) at the beginning of crystallisation b) spherullites with Maltese cross section c) PEO+20 wt% novolac d) PEO+30 wt% novolac

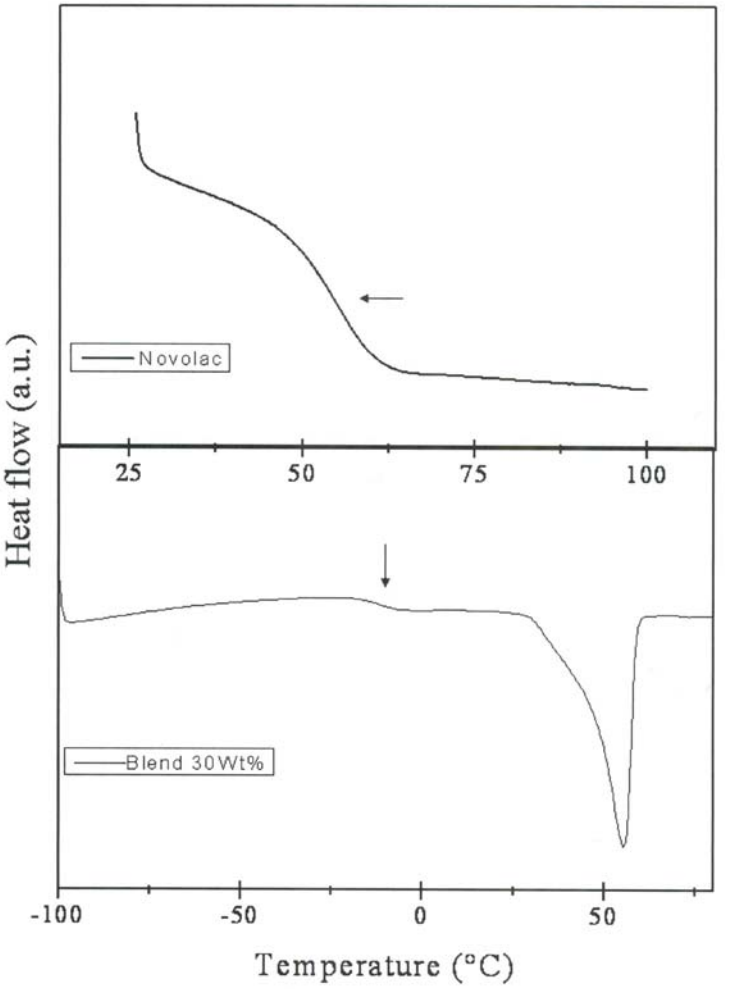

Figure 2.9 DSC scans of novolac and PEO/novolac (70/30 *w/w*) blend. Reproduced with permission from D. Ratna, T. Abraham, K. Kocsis, *Journal of Applied Polymer Science*, 2008, 108, 2156 © 2008, John Wiley and Sons Publishers

2.2 Amino Resins

Amino resins are the resins produced by the reaction between amino group-containing compounds and formaldehyde. The most popular amino resins are urea–formaldehyde (UF) resins and melamine–formaldehyde (MF) resins. Amino resins are considered to supplement and complement phenolic resins [31, 32]. UF and MF resins are prepared

by reacting formaldehyde with urea and melamine, respectively. The general reaction scheme for the synthesis of UF and MF resins is shown in **Figure 2.10**. Liquid amino resins are prepared by reacting the corresponding methylol intermediate in n-butanol or methanol.

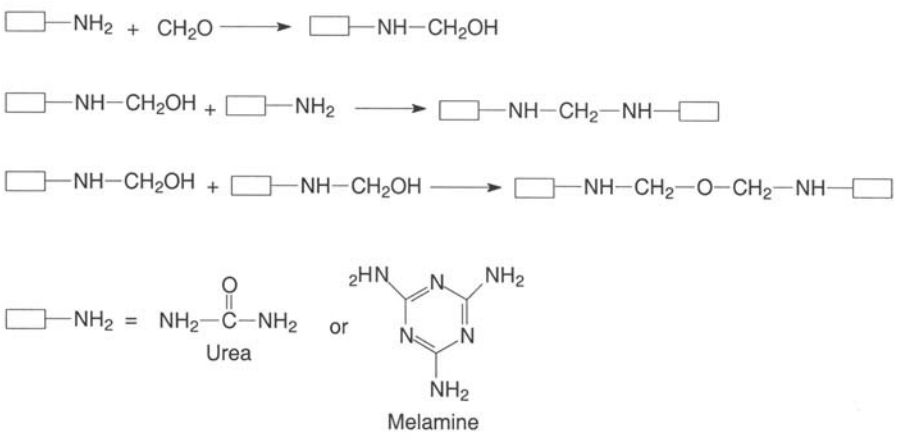

Figure 2.10 The general reaction scheme for synthesis of UF and MF resins

Amino resins are used as curing agents for the resins containing carboxyl, hydroxyl and amide groups. Amino resins can be used in all possible applications in which phenolic resins are used (section 2.1.7). Unlike phenolic resins, which are dark-brown in colour, amino resins are light in colour. Hence amino resins have replaced phenolic resins in applications where bright colour and aesthetic appearances are needed. MF resin shows the best performance in terms of water resistance and toughness. However, use of MF resin is restricted due its high cost. The first commercial production of MF resin was started by American Cyanamid Corporation (USA) in 1939. The well-known applications of phenolic resins are in domestic plugs and switches. UF resins have largely replaced phenolic resins for such purposes due to their better anti-tracking properties and wider colour range.

2.3 Furan Resins

Furan resins are also a low-volume consumption resin like amino resins, and are used as supplements to phenolic resins [33, 34]. They are prepared by the reaction between a phenol and furan compounds such as furfural, furfuryl alcohol, and furan. Furan compounds can be used in place of formaldehyde in the conventional production of phenolic resins. The most popular and viable furan resins are prepared from furfuryl

alcohol (FFA). FFA undergoes homopolymerisation through an addition reaction in acid medium, leading to the formation of a furan resin (**Figure 2.11**). Like other thermosetting resins, furan resin undergoes crosslinking in the presence of a strong acid and forms a 3D network. The crosslinking involves the reaction with a methylene bridge (**Figure 2.11**).

Like amino resins, furan resins can also be used in all possible applications where phenolic resins are used as discussed in section 2.1.7.

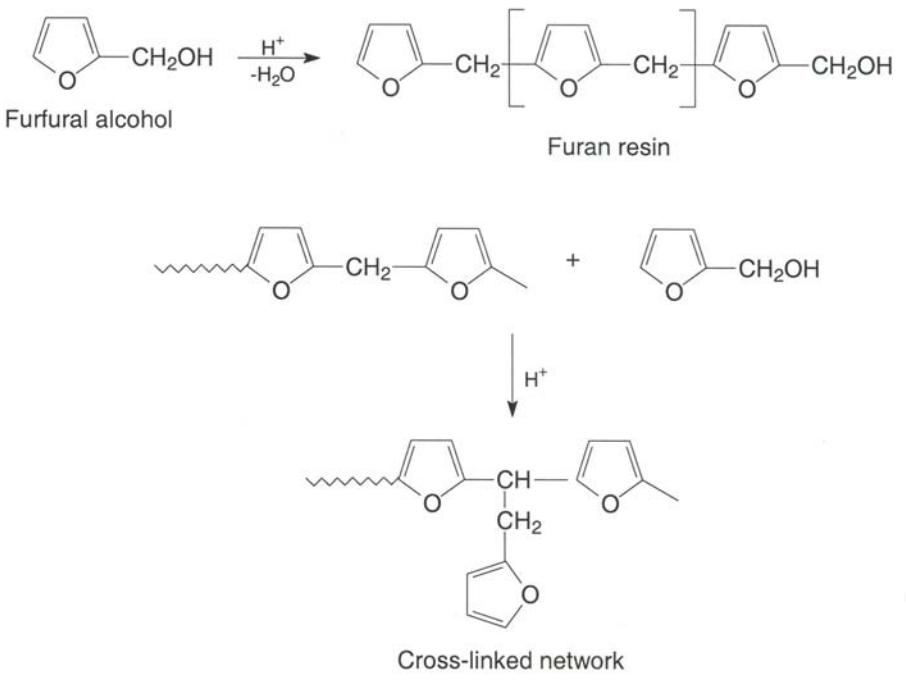

Figure 2.11 Reaction schemes for the synthesis and crosslinking of furan resin

2.4 Epoxy Resins

Epoxy resins are a class of thermosetting resin materials characterised by two or more oxirane rings or epoxy groups within their molecular structure [35–38]. The commonest epoxy resin is the diglycidyl ether of bisphenol A (DGEBA), which is prepared by the reaction of epichlorohydrin (ECD) and bisphenol A (BPA) (**Figure 2.12**).

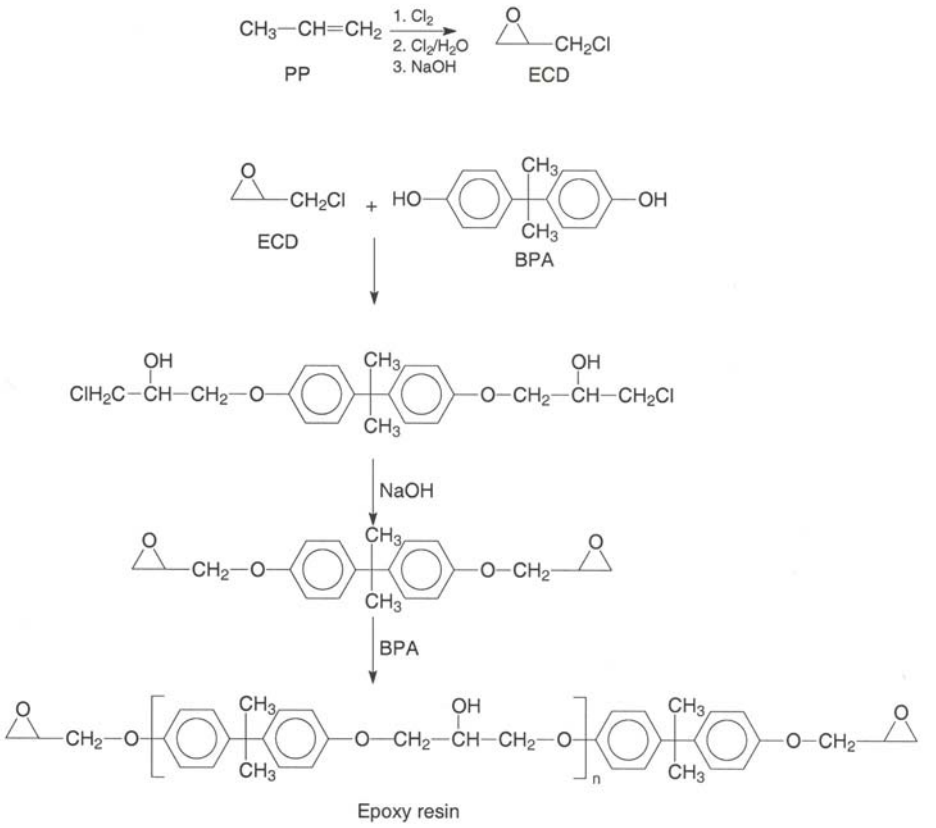

Figure 2.12 Reaction schemes for the synthesis of DGEBA-type epoxy resin

ECD is prepared from polypropylene (PP) by reacting chlorine with sodium hydroxide. ECD is allowed to react with BPA in the presence of sodium hydroxide. The first step is cleavage of the oxirane ring of ECD by the hydroxyl group of BPA. The second step is cyclisation in base medium, leading to the formation of an epoxy-ended intermediate. The intermediate then undergoes chain extension with BPA to produce an epoxy resin. A wide variety of resins can be produced by adjusting the concentration of the reactants. A liquid resin can be further chain-extended with BPA to make a solid resin of higher molecular weight. Thus epoxy resins are available in various consistencies from low viscous liquid to a tack-free solid.

There are undoubtedly more publications and reports based on the basic and applied research on epoxy resins than for any other commercially available thermosetting

resin. The broad interest in epoxy resins originates from the versatility of epoxy group towards a wide variety of chemical reactions and the useful properties of the network polymers [38–40] such as high strength, very low creep, excellent corrosion- and weather-resistance, elevated temperature service capability, and adequate electrical properties. Therefore, a detailed discussion on epoxy resins will be presented in a separate chapter (Chapter 3).

2.5 Unsaturated Polyester Resins

The second synthetic thermoset resin discovered in early 1940 (after phenolic resin) was unsaturated polyester (UPE) resin. UPE consists of an unsaturated polyester, a monomer, and an inhibitor. UPE gained wide industrial applications due to their low viscosity, which offers easy processability, low cost and rapid cure schedules.

2.5.1 Unsaturated Polyesters

Polyesters are macromolecules made by reacting a diacid or dianhydride with a dihydroxy compound (diols). To make unsaturated polyesters, maleic anhydride or fumeric acid is used in addition to a saturated acid, which provides unsaturation in the structure. The most commonly used anhydrides are maleic anhydride (unsaturated) and phthalic anhydride (saturated). The commonest diols are ethylene glycol or propylene glycol. Use of an unsaturated anhydride is very critical to provide unsaturation in the structure, which is utilised to cure the resin by free-radical polymerisation. The chemical reaction for the synthesis of UPE is shown in **Figure 2.13**.

Fumerate double bonds (planar *trans* configuration) react faster with the reactive monomer compared with the double bonds of maleate ester because maleate esters are slightly distorted from the planar configuration, which suppresses their ability to copolymerise with styrene. Hence fumeric acid is preferable to maleic anhydride as an unsaturated anhydride precursor for the formation of a uniform network with better properties. However, maleic anhydride is mostly used because of two reasons: (i) maleic acid offers lower cost and easier handling, and (ii) most maleate double bonds isomerise to a more stable fumerate form during resin synthesis at high temperature [41, 42]. It was reported that the extent of isomerisation depended on the structure of glycol [43, 44]. For instance, isomerisation is reported to be 95% with propylene glycol, 39% with 1,4 butylene glycol, and 35% with 1,6 hexamethylene glycol at 180 °C. ^{13}C-NMR analysis is used to study the isomerisation. The nature of acids and catalyst also has an important role in isomerisation [45, 46].

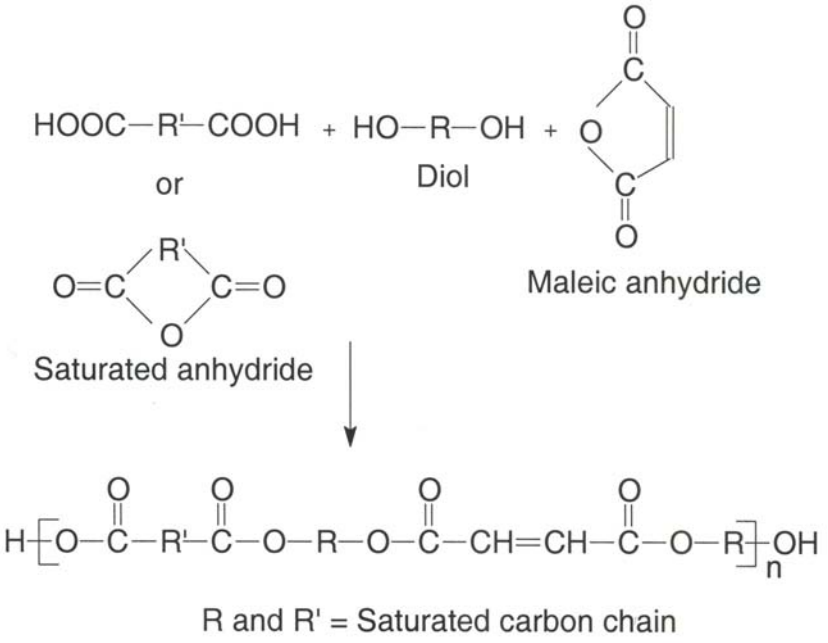

Figure 2.13 Reaction scheme for the synthesis of UPE resin

The rate of polyester synthesis by polycondensation depends on the chemical structure of the reactants (diacid and diol) and the stoichiometry of the reactants. In general, glycol is used in slight excess to compensate for the potential loss of glycol via evaporation. The reaction takes place in two stages: formation of monoester followed by polycondansation at higher temperature. The reaction is reversible and water is produced as a byproduct. Hence it is necessary to remove the water from the reaction mixture to push the reaction forward. Water is removed continuously from the reaction mixture by application of vacuum or by using a solvent such as xylene, which forms an azeotrope with water in the vapour state. A Dean and Stark apparatus is used for the synthesis. The azeotrope vapour is allowed to condense in a receiver tank, where they are separated from each other due to the difference in density. Xylene forms the upper layer (which is fed back continuously to the reactor) and water forms the bottom layer (which is removed through an opening at the bottom of the tank). The progress of the reaction is monitored through the amount of water produced and the acid value (mg of potassium hydroxide required to neutralise 100 g of resin) of the reaction mixture. The acid value is checked by withdrawing a small amount of sample from the reactor and it analysing using a standard titration method. The typical molecular weight of UPE is 3000–5000 g/mole with an acid value of the product of <20. Polymerisation is the first growth step, so the UPE of the polymer

is highly sensitive to the purity of the reactants. At high temperature, alcoholysis or acidolysis of the polyester chains by hydroxyl or carboxyl groups of the monomers and/or oligomers occurs. This process is called 'transesterification'. The tranesterification reaction allows the redistribution of UPE and functional groups in UPE. A reaction scheme for transesterification is shown in **Figure 2.14**.

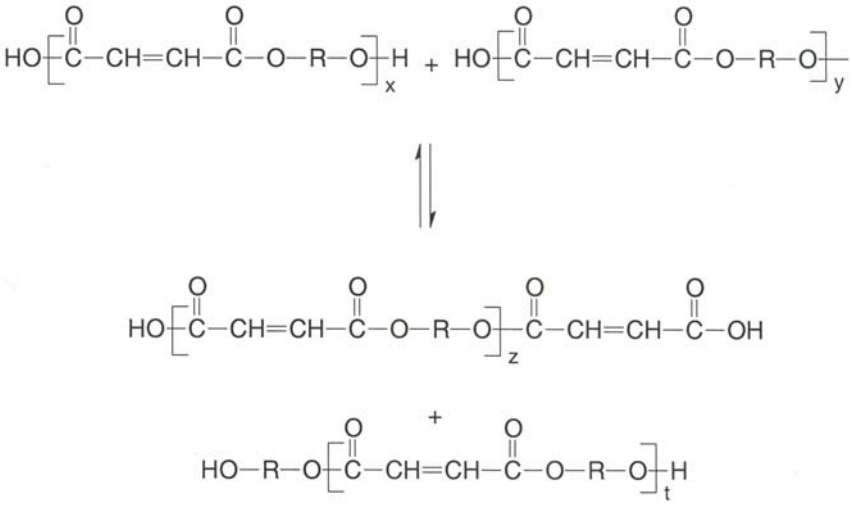

Figure 2.14 Reaction scheme for a trans-esterification reaction

2.5.2 Polyester Structure

A linear structure of polyester is expected from the reaction of acid and alcohol (**Figure 2.13**). However, branching in a polyester structure takes place as a result of side reactions. Such side reactions were first investigated by Ordelt and co-workers [47–49]. The electron-deficient double bond (due to the presence of electron-withdrawing carbonyl groups) of maleic anhydride can react with the hydroxyl groups of glycol or oligomers via Michel addition. The reaction of glycol with the double bonds produces short branches, whereas involvement of hydroxyl groups of oligomer or macromolecules leads to the formation of long branches (**Figure 2.15**). Because the hydroxyl groups of a glycol are more reactive than those of the monoesters, mostly short branches are formed. Thus the side reactions produce branching and reduce the double bond functionality of the unsaturated polyester. This is why the double-bond functionality of a maleic anhydride-based polyester is less than the theoretical value calculated based on the concentration of maleic acid in the polyester. Hence the

polyester structure is characterised by main-chain end groups (carboxyl or hydroxyl), double-bond functionality (maleate or fumerate) in the backbone, and side-chain end groups (mostly hydroxyl). It is necessary to analyse and characterise the structure of UPE with respect to functional groups and branching for quality control. Functional groups are identified by FT-IR analysis from the characteristics peaks: carboxylic acid (1710 cm^{-1}), ester (1730 cm^{-1}), double bond (1640 cm^{-1}), ether (1100–1250 cm^{-1}) and hydroxyl (3350–3500 cm^{-1}). Maleate and fumerate double bonds are identified by ^{1}H-NMR analysis. The vinylic proton of maleic acid absorbs at 6.55 ppm, whereas the same for fumeric acid absorbs at a higher chemical shift (6.98 ppm) [50].

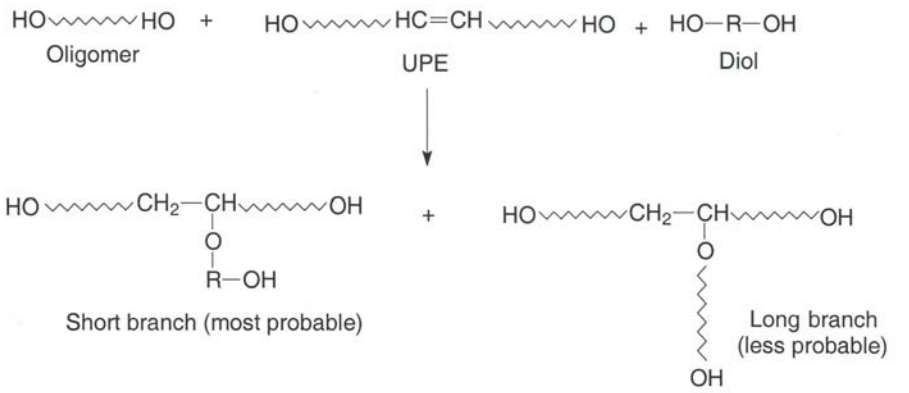

Figure 2.15 Mechanism for the formation of long and short branches in UPE resin

Carboxyl and hydroxyl groups can be estimated by standard titration methods. For the estimation of carboxyl groups, the sample is directly titrated with a standard alcoholic potassium hydroxide solution. To determine hydroxyl number, the sample is refluxed for 1 h with acetylating mixture (pyridine/acetic anhydride) and the excess acetic anhydride titrated back. The overall average functionality (f_n) (carboxyl and hydroxyl) is the sum of average carboxyl functionality (c_n), main-chain hydroxyl functionality (h_n) and branching-chain hydroxyl functionality (b_n).

$$f_n = c_n + h_n + b_n \tag{2.4}$$

$$c_n + hn = 2 \tag{2.5}$$

b_n can be determined by considering the Ordelt reaction, as given next [51, 52]:

$$b_n = \left[\frac{2M_{n,index}X_{Ordelt}}{2M_{c=c} + 2mX_{Ordelt} - M_{n,index}X_{Ordelt}} \right] \tag{2.6}$$

$$M_{n,index} = \frac{112{,}200}{I_H + I_c} \tag{2.7}$$

Hence combining **Equations 2.4**, **2.5** and **2.6** we get:

$$f_n = 2 + \left[\frac{2M_{n,index}X_{Ordelt}}{2M_{c=c} + 2mX_{Ordelt} - M_{n,index}X_{Ordelt}} \right] \tag{2.8}$$

where X_{Ordelt} = Ordelt saturation degree of polyester or ratio of moles of saturated double bonds to moles of initially introduced double bonds, $M_{\text{C=C}}$ = molar mass per mole of double bond on polyester chain, m = molar mass of branches, I_{C} = carboxyl value, and I_{H} = hydroxyl value.

2.5.3 Polyesterification Kinetics

The first studies on the kinetics and mechanisms of polyesterification reactions were carried out by Flory [53]. The studies indicated a third-order self-catalysed and a second-order acid-catalysed reaction. For a self-catalysed reaction, the rate of the reaction is associated with second-order dependence on carboxyl group concentration and first-order dependence on hydroxyl group concentration. For an acid-catalysed reaction, the order is one with respect to carboxyl group concentration and hydroxyl group concentration. A model proposed by Lin and Hsieh [54] also suggested an overall order of 3 for a self-catalysed reaction. However, they suggested first-order dependence of the rate of reaction on carboxyl group concentration, and second-order dependence of the rate of reaction on hydroxyl group concentration. For an acid-catalysed reaction, the overall order is 2, and is dependent only on carboxyl group concentration.

The catalytic activity of the acid catalyst is due to hydrogen ions [55]. In the presence of a strong acid catalyst (e.g., *p*-toluene sulfonic acid), hydrogen ions are produced mainly from the added acid. Thus the polyesterification is a second-order reaction. In the absence of an acid catalyst, hydrogen ions are formed from the ionisation of dicarboxylic acid, and the order of the reaction is 2.5 [55]. More complicated rate equations are proposed by considering the reverse reaction, and the effect of dielectric constant of the medium on ionisation of diacid [56, 57].

The difference in kinetics may originate from the fact that some studies were carried out under a constant oil bath, and others were carried out at constant reaction temperature. Polyesterification is an endothermic process (even though the polyesterification reaction is exothermic because the condensates are evaporated continuously). Hence there is a large and rapid temperature drop, especially in the early stages of the reaction [56]. Thus the data generated from the experiments at a constant oil-bath temperature are expected to be different from data generated from the experiment at a constant reaction temperature.

Chen and Wu [57] proposed a rate equation considering that: 1) the hydroxyl group is a stronger proton acceptor than the carboxylic acid group; 2) variation in the dielectric constant of the reaction mixture affects the dissociation constant of dicarboxylic acid; and 3) there is a possibility of reverse reaction due to unremoved water. The rate equation can be expressed as follows:

1. For a self-catalysed reaction

$$\frac{d[RCOOR^1]}{dt} = K_a \exp(\alpha p)[RCOOH]^2[R^1OH] - K_h[H_2O][RCOOR^1] \quad (2.9)$$

where [RCOOR], [RCOOH] and [R´OH] is the concentration of polyester, carboxylic acid groups and hydroxyl groups, respectively.

Considering that α is the conversion of the acid group ($[COOH]_0$ – [COOH]/$[COOH]_0$) and r is the ratio of diol to diacid at the beginning of the reaction (r = $[OH]_0/[COOH]_0$) we obtain:

$$\frac{d\alpha}{dt} = K_a C_0^{\,2} \exp(x\alpha)(1-\alpha)^2(r-\alpha) - K_h[H_2O]\alpha \quad (2.10)$$

K_a and K_h are forward and reverse rate constants, respectively, x is a constant related to the dielectric constant, and $[H_2O]$ is the concentration of unremoved water.

2. For an acid-catalysed reaction

$$\frac{d[RCOOR^1]}{dt} = K_{ac}[AH]\exp(x\alpha)[RCOOH][R^1OH] - K_h[H_2O][RCOOR^1] \quad (2.11)$$

Equation 2.12 can be expressed in terms of r and α as follows:

$$\frac{d\alpha}{dt} = K_{ac}C_0[AH]\exp(x\alpha)(1-\alpha)(r-\alpha) - K_{hc}[H_2O]\alpha \quad (2.12)$$

K_{ac} and K_{hc} are forward and reverse rate constants, respectively, for an acid-catalysed reaction, x is a constant related to dielectric constant, and $[H_2O]$ is the concentration of unremoved water.

Kuo and Chen [58] applied the previous equation to the reactions of adipic acid and three diols (ethylene glycol, 1,4 butane diol, 1,6 hexandiol) for the self-catalysed and acid-catalysed reaction. They reported that the experimental data fitted well with the previous equation, and that the activation energy decreased with an increase in the chain length of diols. Beigzadeh and co-workers [59] used the equation of Chen and Wu [57] for a two-stage production system. In the first stage, an excess amount of diol was allowed to react with the saturated acid until the acid value reached 10 and then the unsaturated acid was added. It was assumed that at the end of first stage the oligomers formed were new diols and could react with the diacid in a similar way. They also reported good fitting of experimental data with the Chen and Wu model [57] but did not find such good fittings with other models.

2.5.4 Types of Polyester

Polyester resins can be grouped broadly into two major categories based on compositions and applications: general purpose polyester resin and speciality polyester resin.

2.5.4.1 General Purpose Resin

General purpose resins are made from low-cost raw materials and used without modification. The main criteria are that the resin can be offered at a reasonable (competitive) cost and should provide a network structure with reasonable physical properties in a reasonable time. For general purpose UPE resins, the cost of the materials is a major consideration rather than how well they perform (performance). In general, propylene glycol, diethylene glycol, phthalic anhydride and minimum amount of maleic anhydride are used for the synthesis of general purpose polyester resin. A typical formulation of general purpose polyester resins is given in **Table 2.4**. Diethylene glycol is used not only to reduce the cost but also to improve the cure rate. For further reduction in cost, hydrolysed poly(ethylene terepthalate) residue and other mixed acids or glycol byproducts are used. To reduce the amount of maleic anhydride, dicyclopentadiene is typically coupled with maleic anhydride in the initial steps. Dicyclopentadiene improves the solubility of polyester resin in styrene, which is used as a reactive diluent. These resins are cooked to a lower UPE, which allows the use of fewer amounts of reactive diluents to achieve the desired viscosity.

Table 2.4 Typical formulation of general Purpose UPE	
Ingredients	**Molar concentration Type 1 Type II**
Propylene glycol	2.1 1.75
Diethylene glycol	0 0.35
Maleic anhydride	0.6-0.8 1.75
Pthalic anhydride	1.4-1.2 0.25

2.5.4.2 Speciality Polyester Resins

In speciality polyesters, raw materials are selected judiciously to improve the properties and performance of the resin with compromise of the cost. Speciality resins are used if high mechanical strength, and resistance to chemicals and corrosion, is required. Use of a non-polar glycol such as polypropylene glycol and poly(butylene glycol) contributes towards the water resistance and corrosion resistance. Three types of speciality resins are used: isopthalic resin, chlorendic resin, and BPA fumerate resin. Typical formulations of speciality UPE resins are given in **Table 2.5**.

Table 2.5 Typical formulations for speciality UPE resins			
Precursor	**Isopthalic**	**BPA-fumarate**	**Chlorendic**
Maleic anhydride	1.0		1.0
Fumaric acid		2.0	
Isopthalic acid	1.0		
Chlorendic anhydride			1.0
Propylene oxide	2.15		2.15
Propoxylated BPA		2.05	

Isopthalic resins are based on isopthalic acid and maleic anhydride. Incorporation of isopthalic acid causes an increase in UPE of the resulting polyester, which exhibits good mechanical properties, chemical resistance, and thermal resistance. The correlation between corrosion resistance and polyester structure is not well established. In general, if the ester is sterically crowded and there are fewer ester groups in the chain, good chemical resistance and corrosion resistance are achieved [60].

BPA fumarate resins are prepared by the reaction of propoxylated BPA with fumeric acid. The use of BPA results in a significant reduction in the number of ester linkages and makes the resin comparatively non-polar. This resin therefore shows very good corrosion resistance and chemical resistance. BPA fumerate resin-based composites

can be suitable for replacement of metallic materials for many industrial applications (e.g., pipes, tanks, panels) if materials have to serve under a corrosive environment.

Chlorendic resins are prepared by reacting propylene glycol with a combination of endomethylenehexachloropthalic anhydride (chlorendic anhydride) and phthalic anhy-dride. This resin shows excellent corrosion resistance and fire retardancy (due to the presence of chlorine) when used as a matrix for fibre-reinforced composites. Chlorendic resins are used in applications that require exceptional resistance to acidic and oxidising environments. In recent years, BPA fumarate resins have been extensively replaced by chlorendic resins for various industrial applications.

2.5.5 Reactive Diluents or Monomers

The unsaturated polyesters discussed previously are used in combination with a suitable comonomer which serves as a reactive diluent. The objective of adding a comonomer is to reduce the viscosity, adjust the cure schedule, and improve the mechanical properties of the resulting networks. In principle any monomer that can be polmerised using free radicals can be used for UPE resins, but commercial resins mostly contain styrene or, in some cases, divinyl benzene. The wide acceptance of styrene as a reactive diluent is due to low cost and better solubility of polyesters in styrene compared with other monomers and well-understood polymerisation kinetics (high reactivity with the 1,2-disubstituted double bonds of polyester). The good solubility of polyester and styrene is crucial for the formation of a homogeneous network after curing. Poor binary styrene–polyester miscibility has been cited as a significant cause of heterogeneous morphology observed during curing at low and high temperature [61–63]. Miscibility of UPE in styrene at a constant temperature depends on the physicochemical properties of the UPE, such as chemical composition, UPE, polydispersity index, polar end groups, and concentration of ester groups in the chain [64].

Buffa and Borrajo [65] synthesised UPE with varying concentration of adipic acid and pthalic anhydride, and carried out a thermodynamic analysis of miscibility. They found that the miscibility of UPE in styrene increases with increasing concentration of adipic acid. A similar composition effect was reported by Lecoinite and co-workers [66] using UPE prePolymers of similar molecular weights and distributions, where the polyester backbone chemical structure was changed using different proportions of neopentyl glycol and diethylene glycol. Buffa and Borrajo [65] also investigated the effect of UPE of polyester on styrene miscibility. Studies on UPE resins of similar chemical structure and different molecular weights (620, 1205, 1700 and 2740 g/mole) indicated that UPE miscibility in styrene changes in the following order: 1700>1205>2740>620 [65] (**Figure 2.16**). That is, miscibility increases with increasing

UPE and decreases beyond an optimum value (1700 g/mole). This can be explained by considering the relative influence of three contributions of chemical structure arising out of the change in UPE of UPE of identical composition. First, an increase in the UPE of UPE with a fixed comonomer composition lowers the concentration of highly polar hydroxyl and carboxyl groups. This effect increases the miscibility of UPE in styrene. Second, an increase in UPE of UPE with a fixed comonomer composition increases the concentration of polar ester groups (in the backbone), which reduces miscibility. Third, an increase in UPE reduces miscibility due to an entropy factor [67]. Up to an optimum UPE, the first factor predominates, leading to an increase in miscibility. Beyond the optimum molecular weight, the second and third factors predominate. Thus by the judicious selection of composition and by adjusting UPE, a good UPE miscibility in styrene or other reactive diluents can be achieved.

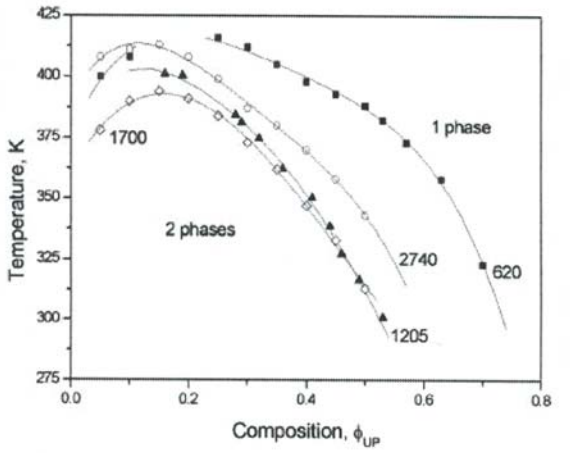

Figure 2.16 Unsaturated polyester molecular weight effects on the experimental T *versus* composition cloud point curves of a UPE resin. Study on resins of similar chemical structure and four molecular weights (620, 1205, 1700 and 2740 g/mole) indicated that UPE miscibility in styrene changed in the following order: 1700>1205>2740>620. Reproduced with permission from F. Baffa and J. Borrajo, *Journal of Applied Polymer Science*, 2006, **102**, 6064 © 2006, John Wiley and Sons Publishers

The neat polyester is highly viscous (2–80 Pa-s) and very difficult to process. Addition of monomer reduces the viscosity about 10-times (0.2–0.5 Pa-s) and makes the resin easy to process. Polyester resin offers better processability compared with other thermoset resins (e.g., epoxy). In general, the mole ratio of polyester to monomer is maintained in the range 1.9 to 2.4. Further increase in styrene content reduces

the crosslink density and leads to a reduction in tensile and flexural properties, and an increase in curing time. The properties of unsaturated resins depend on the concentration of styrene, and this can be further perfected by replacing certain fractions of styrene with a comonomer. For instance, the undiluted isopthalic resin in the cured state exhibits a T_g less than room temperature (–20 °C to 5 °C). By diluting with styrene, networks with different T_g can be produced. Use of a sufficiently higher amount of styrene generated a cured network [68] with reasonably high T_g (60–70 °C) and low moisture content. Small amounts of comonomers like α-methyl styrene or vinyl toluene can be used to alter the curing reaction and reduce volatility [69, 70]. Partial substitution of styrene by acrylates improves the weather resistance of the resulting UPE resin. Use of a combination of styrene and acrylonitrile instead of styrene resulted in improvement in mechanical properties of the cured resin. Acrylonitrile increases the miscibility of polyester in styrene by increasing the polarity, and readily polymerises with styrene.

The main problem of styrene is high emission, which restricts applications in closed compartments (e.g., naval application). Styrene emission is a health hazard (threshold value of 50 ppm). The need to reduce the volatile organic compound (VOC) is not only expressed in government regulations, but also equally and persuasively by various environmental concerns. The evaporation of styrene can be reduced by the addition of waxes or pyrogenic silicic acid with hydrophilic and hydrophobic end groups. However, such additives may affect the interfacial properties of composites made out of polyester resins. Some styrene-less UPE resin formulations using diacrylate monomers have been reported [71]. However, mostly styrene is used as a reactive diluent in UPE resins.

2.5.6 Inhibitors

Another important ingredient of UPE resins is the inhibitor, which is added to prevent premature gelling or to increase UPE through free-radical polymerisation. The type and concentration of inhibitor is very important to ensure a good shelf-life and the desired pot life. It must not significantly affect the final thermomechanical properties of the cured networks. The most commonly used inhibitors are p-benzoquinone, hydroquinone, and phenothiazine. The addition of a very small amount of inhibitor (<500 ppm) increases the shelf-life by more than one year. The concentration of inhibitor should be kept to a minimum otherwise subsequent crosslinking with peroxide initiators will be difficult. The inhibitors scavenge free radicals, which may be generated in the unsaturation sites or in the monomer. The driving force for this process is the greater stability of an inhibitor radical due to resonance. Being highly stable, the initiator radicals do not participate in the chain reaction. The possibilities of increase in UPE/viscosity and gelling during storage can therefore be avoided.

2.5.7 Curing of UPE Resin

Curing of UPE resin takes place through the free-radical polymerisation of unsaturated resin and monomer. Organic peroxides, azine compounds and azo compounds are used to to generate free radicals. The UPE industry is dominated by the use of peroxides: methyl ethyl ketone peroxide (MEKP), bezoyl peroxide (BPO) and *t*-butyl peroxide (TBO). MEKP decomposes at room temperature, whereas BPO and TBO decompose at 70 °C and 140 °C, respectively. To ensure room-temperature or low-temperature curing at a reasonable rate, accelerators (which accelerate the decomposition of peroxides) are used. In general, transition metal oxides are used as the accelerators for curing UPE resins. The most commonly used accelerators are cobalt napthenate and cobalt octoate. Such accelerated decomposition generates only one radical instead of two, as shown next:

$$ROOH + Co^{+2} \longrightarrow RO^{\cdot} + OH^{-} + CO^{+3} \qquad (2.13)$$

The free radicals initiate the chain reaction which propagates through the unsaturated sites of the polyester and monomer. This leads to the formation of a network structure which is insoluble and infusible (**Figure 2.17**). The cobalt compound, when present in excess, reacts with the free radicals and converts them into ions.

$$RO^{\cdot} + Co^{+2} \longrightarrow RO - + CO^{+3} \qquad (2.14)$$

Consequently, the radicals are destroyed and the curing reaction cannot proceed. This is why accelerators are added in a very small amount (0.02 wt%, and never more than 0.3 wt %).

As discussed in earlier sections, UPE resins are a mixture of an unsaturated polyester, styrene and an inhibitor. When the resin is mixed with a peroxide initiator and activator (cobalt octoate/napthenate), free radicals are formed. At the initial stage, all or most of the free radicals generated are consumed by the inhibitor. The driving force for the preferable reaction of free radicals with the inhibitor is the higher stability of inhibitor radicals. Once the inhibitor molecules are depleted, free radicals, produced from the initiator, initiate polymerisation of the polyesters. Styrene serves as an agent to link the adjacent polyester molecules. The curing of UPE resin (polyester + styrene) involves different types of reactions:

(i) Intermolecular crosslinking of polyester without linking through styrene monomer

(ii) Intermolecular crosslinking of polyester through styrene monomer

(iii) Intermolecular crosslinking of polyester molecules without involving styrene

(iv) Intramolecular crosslinking of polyester molecules linking through styrene monomer

(v) Chain branching on the polyester molecules

(vi) HomoPolymerisation of styrene.

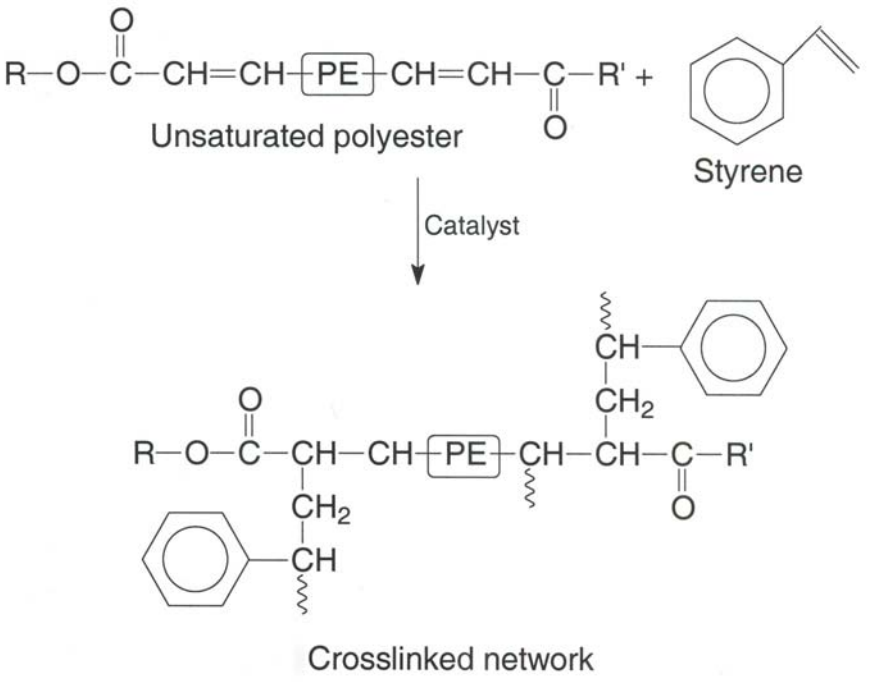

Figure 2.17 Crosslinking of UPE resin

Overall cure kinetics are affected by the possible reactions mentioned previously. However, chain branching and homopolymerisation of styrene do not contribute towards network formation. The long-chain molecules formed due to intramolecular and intermolecular reaction tend to form spherical-type structures with high cyclisation and crosslink density, and are called 'microgel particles' [72]. The pendent double bonds on the polyester molecules are buried inside these primary microgels or located near the surface of the microgels. The buried double bonds participate in the crosslinking reaction, causing further advancement of the curing reaction and increasing the crosslink density of the microgels [73]. Finally, macrogelation takes place by intermolecular microgelling and microgel clustering. Phase separation may occur depending on the polyester structure and its compatibility with styrene. The

factors that affect miscibility with styrene have been discussed in an earlier section. Muzumdar and co-workers [74] investigated the chemorhelogy and kinetics of the crossliking reaction. The results are shown in **Figure 2.18**, where the viscosity, conversion and radical concentration are plotted as a function of time. In the induction stage, no crosslinking takes place due to the consumption of radicals by the inhibitor, and consequently viscosity remains almost constant. The sharp increase in viscosity takes place in the macrogelation stage.

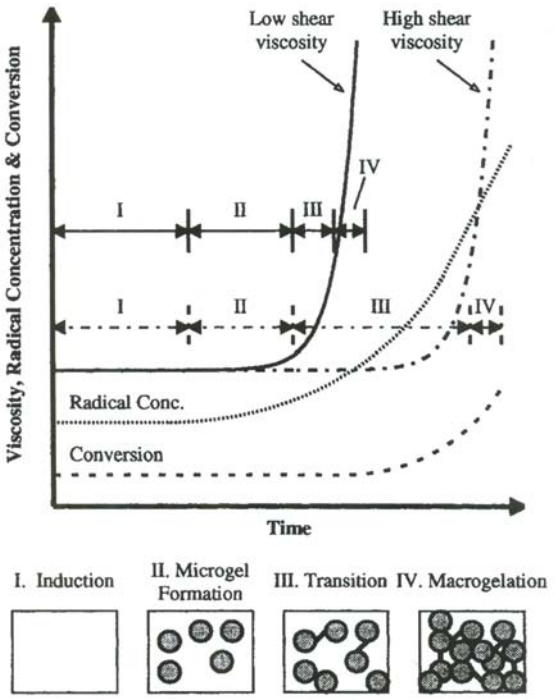

Figure 2.18 Mechanism of viscosity build-up in UPE-styrene coPolymerisation (schematic). Reproduced with permission from S.V. Muzumdar and L.J. Lee, *Polymer Engineering Science,* 1996, **36**, 7, 943 © 1996. ©1996, John Wiley and Sons Publishers

The kinetics of crosslinking reaction has been investigated. The crosslinking reaction is reported to be an autocatalytic reaction, as discussed in Chapter 1. The reaction rate is affected by the styrene content of the resin. Zlatanic and co-workers [75] carried out detailed rheological studies of acrylate-terminated UPE resins of different compositions e.g., poly [(tetramethylene maleate)-*co*-(tetramethylene phthalate)]

(BMPA), poly [(tetra methylene fumerate)-*co*-(tetramethylene phthalate)] (BFPA) and poly [(tetramethylene phthalate)-*co*-(tetramethylene succinate)] (BPSA). A typical rheological plot (G´ and G´´ versus time) of a BFPA sample [75] at 30 °C is shown in **Figure 2.19**. Rheokinetic studies indicate that the crosslinking follows an autocatalytic reaction. The rate constants obtained from autocatalytic model for BMPA and BMPA samples are 0.036–0.075 min^{-1} and 0.006–0.008 min^{-1}, respectively. A similar trend was observed using equilibrium swelling experiments of cured samples [76]. This is expected because the fumerate double bond (planar *trans* configuration) is more reactive than the double bond of maleate ester (distorted from the planar configuration). The effect of initiator concentration (benzoyl peroxide/*N*,*N*-dimethylaniline system) on rheokinetics was also studied by Zlatanic and co-workers [75]. The rate of rheological conversion (β) i.e., (dβ/dt) *versus* β plot is shown in **Figure 2.20**. The results indicate that the increase in BPO concentration significantly changes the rate of the reaction up to 1.5 wt% concentration of BPO. Beyond 1.5 wt% of BPO concentration, the influence of increase on BPO concentration on the rate of crosslinking is less.

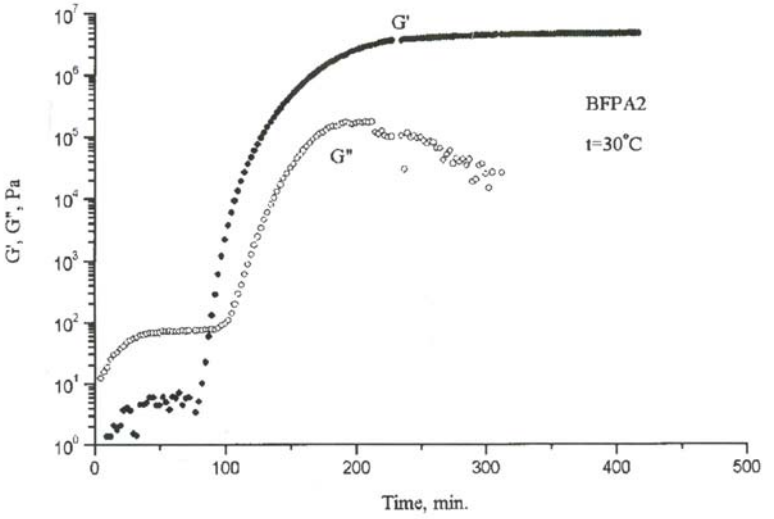

Figure 2.19 Storage and loss dynamic shear moduli (G' and G") for the reaction mixture BFPA, plotted logarithmically as a function of total reaction time at 30 °C. Reproduced with permission from A. Zlatanic, B. Dunjic and J. Djonlagic, *Macromolecular Chemistry and Physics*, 1999, **200**, 2048 © 1999. ©1999, Wiley-VCH Verlag

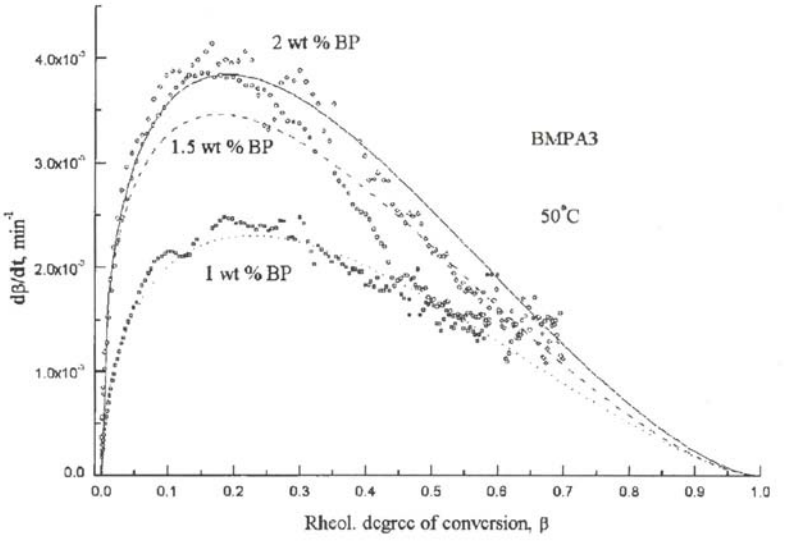

Figure 2.20 Influence of benzoyl peroxide (BP) concentration on the rate of rheological conversion for the reaction mixture BMPA at 50 °C. Symbols: experimental value, line: calculated values. Reproduced with permission from A. Zlatanic, B. Dunjic and J. Djonlagic, *Macromolecular Chemistry and Physics*, 1999, **200**, 2048 © 1999. ©1999, Wiley-VCH Verlag

2.5.8 Properties of UPE Resins

UPE resins are mostly used in the form of fibre-reinforced composites. The properties of such composites will be discussed in Chapter 6. In this section, the properties of neat resins (castings) will be discussed. **Table 2.6** shows a comparison of properties of different types of cured polyester resins. Isopthalic resins exhibit better tensile and flexural properties compared with orthopthalic acid-based general purpose resin. This is because isopthalic resins are more linear with higher UPE compared with orthopthalic acid based resins. BPA fumarate and chlorendic resins have a rigid structure as manifested by their high heat distortion temperature (HDT). This is due to a more aromatic backbone in BPA fumerate and chlorine in chlorendic resins. Consequently, they are highly brittle, leading to the poor mechanical performance. However, because of a rigid structure, BPA fumarate and chlorendic resins offer excellent chemical resistance and corrosion resistance.

Table 2.6 Themomechanical properties of speciality polyester resins						
Resin type	**Tensile strength (MPa)**	**Tensile modulus (GPa)**	**Elongation (%)**	**Flexural strength (MPa)**	**Flexural modulus (GPa)**	**HDT (°C)**
General Purpose	55	3.4	2.1	80	3.9	80
Isophthalic	75	3.5	3.3	130	3.6	90
BPA-fumarate	40	2.8	1.4	110	3.4	130
Chlorendic	20	3.4	1.2	120	3.9	140

2.5.9 Application of UPE Resin

UPE resins can be used as clear castings or in combination with particulate fillers or fibres. The resin was developed to meet the demand of lightweight materials in military application. The first functional use of UPE was in radome. Because of the obvious advantages of easy processability and low cost, it was used in a wide range of applications in civil sectors such as tanks, pipes, and electronic gears. Some of the important products based on cast UPE resins are encapsulation of electronic assembly, buttons, door handles, knives, umbrellas, industrial wood and furniture finishing. A filled resin system using limestone, silica, and china clay are used for floor tiles. The major use of UPE is as a matrix for fibre-reinforced composites. Such composites have wide applications in automobile and construction industries such as boats, water-skis and television antennae. Examples of applications of UPE resins are presented in **Table 2.7**.

UPE resin-based fibre reinforced plastics (FRP) are used extensively in the hull construction of various types of sail and motor boats, fishing boats, and naval vessels. UPE are preferred in such applications compared with epoxy due to their better water resistance and lower cost. UPE resin-based FRP are used for various applications in transportation industries (e.g., passenger cars, buses, trucks, construction equipment). Because of their light weight, they have been replacing metallic materials for structural applications in the transportation sector (e.g., floor pans, radiator support, equipment housing). The use of UPE composites in decorative components for transportation applications is less common because they cannot compete with reaction injection moulding (RIM)-processed polyurethane (PU) and engineering thermoplastic in terms quality of finish.

Table 2.7 Applications of unsaturated polyester resins	
Industries/fields	**Product**
Automotive industry, construction industry, household appliances, electrical appliances, military application, aircraft and aerospace industries	Automobile parts like hood, fenders, panels, bodies, aircraft components, furniture, electrical encapsulation, household articles, fibre composites for boat and other marine applications, solar energy panels, building panels, fuel tanks, radomes, tractor parts, transformer cover, electrical panels, helmet, grating, printed circuit board, Fenders, air conditioner panels, refrigerator parts, pressure tank, pipe and tubing, satellite dish antennae

In the construction industries, UPE-based FRP has been replacing aluminium, stainless steel and wood because of its low cost, and ease of cleaning and working. The examples for such applications are solar panels, wall liners, automobile components, liners for truck trailers and railroad cars. UPE-FRP products are used to make sanitary ware as replacements for conventional materials such as porcelainised cast iron due to their obvious advantages of lower cost and easier installation. The other related applications are bath tubs, showers, toilets and sinks.

2.6 Vinyl Ester (VE) Resins

Vinylester (VE) resins are prepared by an addition reaction between epoxy resin (difunctional or multifunctional) with an unsaturated carboxylic acid such as acrylic acid or methacrylic acid [77]. The simplest form of VE is the product of the reaction between one mole of diglycidyl ether of BPA and 2 moles of methacylic acid (**Figure 2.21**). The reaction is carried out at about 100 °C using a catalyst such as triphenyl phosphine. To stop the polymerisation of methacylic acid, an inhibitor such as hydroquinone is used. By changing the nature of base epoxy resin, various types of VE resins can be produced. The vinyl-ended prepolymer is then dissolved in styrene to produce a polymerisable resin similar to an unsaturated polyester resin. Styrene content is adjusted to provide a wide range of viscosities, typically 0.1–4 Pa-s.

VE resin exhibits desirable mechanical properties like epoxy and simultaneously offers processability like a polyester resin. Like UPE resins, VE resins are cured using a free-radical intiator in combination with an accelerator [78–80]. The commonest room temperature curing VE resin system consists of MEKP (1-2 wt%) and cobalt

napthenate (0.2–0.4 %). The BPO and dimethyl aniline system is used to achieve better corrosion resistance. The BPO system requires a higher temperature compared with MEKP. Thus, depending on the initiator systems, different curing conditions and gel time will vary widely. The analysis of the curing reaction indicates that the initial fractional rate of styrene conversion of dimethacrylate double bonds is greater than that of the styrene double bonds. However, the fractional rate of styrene conversion increases with time and exceeds the dimethacrylate fractional conversion rate at the end of the reaction. The homoPolymerisation of styrene continues after the dimethacrylate reaction terminates. Ultimately, the conversion of styrene is always greater than that of dimethacrylate.

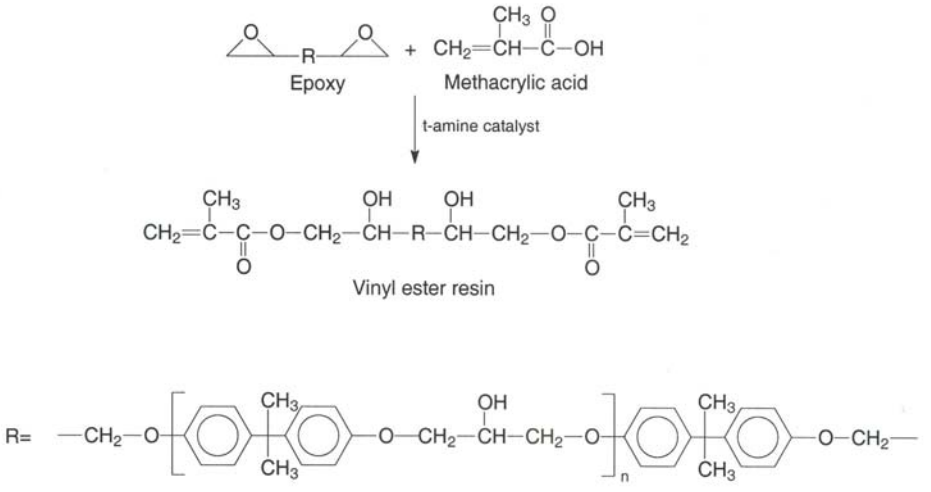

Figure 2.21 Reaction schemes for the synthesis of a VE resin

2.6.1 Properties of VE Resins

Unlike UPE resins, unsaturation occurs only at the end in VE resins resulting in fewer crosslinks compared with UPE resin networks. Because of fewer crosslinks and ether linkages in the structure, VE resin networks exhibit better flexibility compared with UPE resins. During the reaction of epoxy resins with carboxylic acid, several hydroxyl groups are formed along the VE chain. These hydroxyl groups allow H-bonds to form with the similar groups present in the glass fibre. That is why VE resins offer better adhesion with glass fibres or other polar substrates as compared with UPE resin. However, such adhesion occurs more in epoxy resins because more hydroxyl groups are present.

VE resins offer much better corrosion resistance compared with general purpose UPE resins. The better corrosion resistance originates from the large number of atoms between the ester groups, low concentration of ester groups, and the steric hindrance offered by the pendent methyl group of methacrylic acids.

2.6.3 Applications of VE Resins

VE resins can be used for all possible applications discussed for UPE resins. Specifically, VE resins have replaced metals and UPE-based FRP for corrosion-resistant applications. Applications include use in tanks, piping and ducts primarily for handling dilute acids, solvents and fuels, corrosion-resistant mixing vessels, precipitation vessels, scrubbers and process columns. In electrical industries, VE resin-based FRP are used to make components for electrcity generating stations, transmission and distribution, televisions, and antennae. They are also used for making electrical maintenance equipment such as ladders, and booms. Better water resistance makes them suitable for use in air conditioners, humidifiers and other household appliances. VE resins perform better in underwater applications than epoxy resins. Thus VE resins are extensively used for marine applications. Examples are hull construction of various types of sail and motor boats, fishing boats, and naval vessels.

2.7 PU

PU are polymers containing urethane linkages and are available in thermoplastic and thermosetting forms. In 1935, Otto Bayer and coworkers invented PU as a product of the polyaddition reaction between a macroglycol and a diisocyanate. PU are made as castable PU elastomers, PU thermoplastic elastomers and PU engineering thermoplastics. The precursors of standard PU formulations are polyol, polyisocynate, extender and modifier (which are optionally used).

2.7.1 Polyols

Polyols are hydroxyl-functionalised oligomers having a UPE in the range 300–9,000 g/mole and functionality of 1–6 equivalent per mole. Linear and low functionality (f = 2–3 eq/mole) generates flexible (low modulus) PU, whereas branched and high functionality (f = 3–6 eq/mole) polyols lead to hard PU systems (high modulus). Depending on the backbone structure, polyols are classified into two groups: polyether polyol and polyester polyol. Polyether polyol comprises about >80 % of global PU. Polyether polyol is prepared by the addition reaction of epoxide with a molecule with active hydrogen [81–83] or by ionic polymerisation of alkylene oxide [84–86].

Polyester polyols are produced by an esterification reaction of a carboxylic acid and a glycol. Unlike in chain-growth polymerisation, the UPE of the product of a step growth polymerisation is highly sensitive to the stoichiometry of the reactants. Thus high molecular weight linear polyester polyols are prepared using high-purity acids and are used to produce PU with improved properties, which are not achievable by using polyether polyol. Low molecular weight branched polyester polyols are prepared by glycolysis (*trans* esterification) of recycled byproducts with glycols. The various polyols used for PU synthesis are listed in **Table 2.8**. The chemical structures of some commonly used polyols are shown in **Figure 2.22**.

Table 2.8 Polyol and isocyanate compounds commonly used for the synthesis of PU resin

Isocyanate	Polyol
4,4´-Diphenylmethane diisocyanate (MDI) 2,4-, 2,6- Toluene diisocyanate (TDI) 1,6-Hexamethylene diisocyanate (HDI) 1,5-Napthalene diisocyanate 4,4´-Dicyclohexyl methane diisocyanate 3-Isocyanatomethyl-3,5,5-trimethylcyclohexyl isocyanate (isophorone diisocyanate) *para*-phenylene diisocyanate 2,2,4-Trimethyl-1,6-hexamethylene diisocyanate 3,3´-Dimethyl-diphenylmethane 4,4´-diisocyanate	Poly(ethylene oxide) (PEO) Poly (propylene oxide) (PPO) Poly (tetramethylene oxide) (PTMO) Poly caprolactone (PCL) diol 1,4 polybutadiene diol Poly (ethylene adipate) Poly (dimethyl siloxane) Polyisobutylene diol

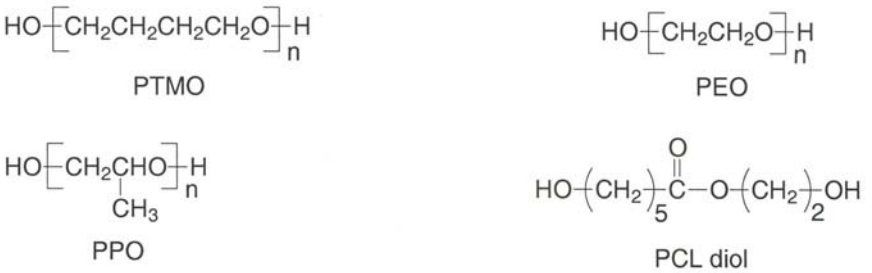

Figure 2.22 Chemical structures of polyols used for PU synthesis

2.7.2 Isocyanates

The second component for PU is a monomer containing two or more isocyanate functional groups. The isocyanate compounds commonly used for the synthesis of PU are listed in **Table 2.8**. In general, aromatic isocynates, especially 2,4-, 2,6-toluene diiso cyanate (TDI), 4,4′-diphenylmethane diisocyanate (MDI) and 1,6.hexamethylene diisocyanate (HDI) (**Figure 2.23**) are used for the synthesis of thermosetting PU. The high reactivity of isocyanates does not allow use as a one-component system. Isocyanates are highly toxic, which is a concern for storage of these materials. To circumvent this, they are reacted with phenols, oximes, alcohols, or dibutyl malonate; these substances are called 'blocking agents' [87–91]. A blocking agent must be selected in such a way that the blocked isocyanate undergoes deblocking in the reaction condition and generates isocyanate, which reacts with polyol; or the blocking agent should be eliminated by the polyol during the reaction. The reaction between blocked isocyanate and the polyol is shown in **Figure 2.24**. The rate, extent and mechanism of reaction depend on the chemical nature of the blocking agent and polyol, catalyst, and polarity of the solvent.

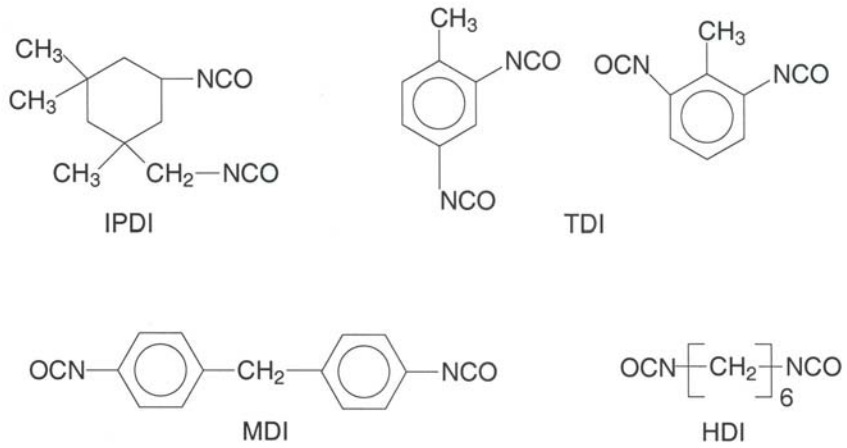

Figure 2.23 Chemical structures of common isocyanates used for PU synthesis

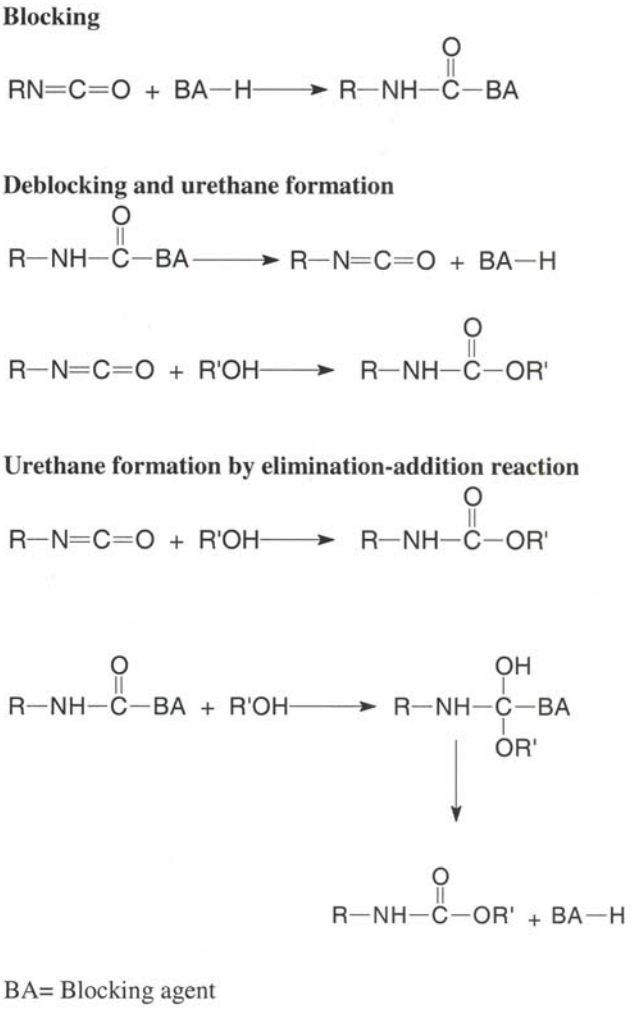

Figure 2.24 The chemistry of blocking of isocyanate and reaction of blocked isocyanate with the polyol

2.7.3 PrePolymers

The synthesis of PU is shown in **Figure 2.25**. The polyol is first reacted with excess di- or polyisocyanate to get an isocyanate-terminated intermediate, known as a 'prepolymer'. If all the hydroxyl groups are capped with isocynates and no free isocyanate remains in the mixture, then the intermediate is called a 'full' prepolymer. Such prepolymers are formed if the isocyanate groups on the polyisocyanate have

different reactivity, as in the case of 2,4 TDI and the ratio of equivalent of isocyanate to hydroxyl (f_{NCO}/f_{OH}) is close to 2. If the isocyanate groups are similar in reactivity or the functionality ratio (f_{NCO}/f_{OH}) is >2, then isocyanate groups will not be consumed fully and some amount of isocyanate will remain free. Prepolymers are analysed for isocyanate content using standard methods.

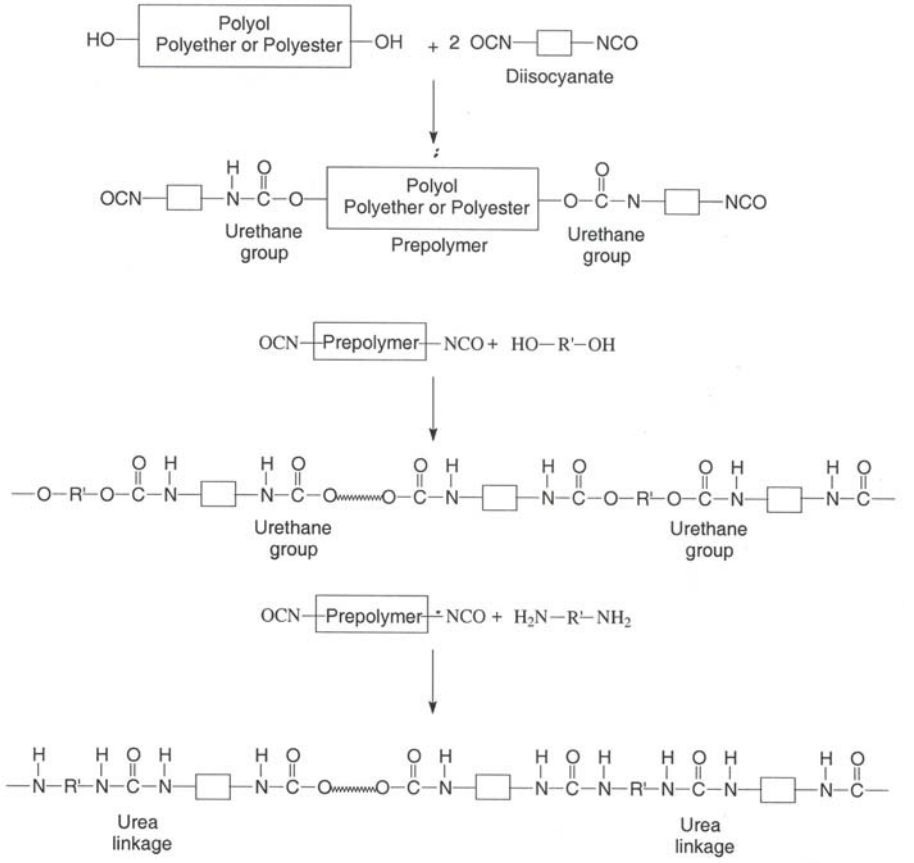

Figure 2.25 Synthesis of PU resin from polyol and diisocyanate

2.7.4 Extenders

The prepolymer is then reacted with a chain extender to get the desired polyurethane (**Figure 2.25**). The choice of extender has an important role in deciding the ultimate mechanical properties of the resulting PU. Most diols having a UPE <500 g/mole

can be used (**Table 2.9**). Extenders are of two types: diol- or triol-based extenders and amine-based extenders. A diol extender produces urethane linkages and an amine extender produces urea linkages. Incorporation of urea linkages enhances the mechanical properties of the PU networks. The chemicals structures of various diol and amine extenders are shown in **Figure 2.26**. Water can also be used as an extender. Water reacts with excess isocyanate and produces carbondioxide and amine (**Figure 2.27**). The amine further reacts with the prePolymer to form urea linkages.

Table 2.9 Glycol and amine extenders commonly used for PU synthesis

Glycol extender	Amine extender
Difunctional	Diethyl toluene diamine
1,4-Butane diol (1,4-BD)	*t*-Butyl toluene diamine
1,6-Hexane diol	4,4´-Methylene-bis-(2-chloroaniline) (MOCA)
Ethylene glycol	4,4´-Methylene-bis-(3-chloro-2,6-diethyl aniline)
Dimethylol propionic acid (DMPA)	Trimethylene glycol di-*p*-aminobenzoate
4,4´ Bis-(2- hydroxyethoxy) biphenyl (BEBP)	4,4` Diaminodiphenyl methane (DDM)
Trifunctional	4,4´-Methylene-bis-(2-carbomethoxy aniline)
Glycerol	4-Chloro-3,5-diamino-isobutylbenzoic acid ester
1,1,1 Trimethylol propane	
1,2,6 Hexane triol	

The extender forms the hard segment of the PU. With an increase in the concentration of hard segments the hardness, modulus, tear strength and chemical resistance of the PU system increase. Percentage elongation at break, resiliency, and low-temperature flex tend to decrease as a result of the increase in the concentration of the hard segment. Resiliency and low-temperature flex properties can be increased by increasing the UPE of the macrodiol. The extender should be selected keeping in mind the applications in which the PU materials are going to be used.

When the difunctional precursors (diisocyanate, polyol and extender) are allowed to react in a stoichiometric amount, a thermoplastic PU is formed. Thermosetting PU are made by using excess diisocyanate (excess diisocyanate reacts with a urethane structure to form allophanate bonds) or by using a trifunctional extender like glycerin or trimethylol propane [92–94]. The unique feature of PU resin is that the change in UPE between crosslink offers a wide change in properties, especially the strain (which reflects flexibility). For example, a PU system with a molecular weight between two

crosslinks (M_c) of 1890 g mole^{-1} shows a strain of 300%, whereas when the M_c is increased to 10,000 g mole^{-1}, a strain value of 750% is achieved [95].

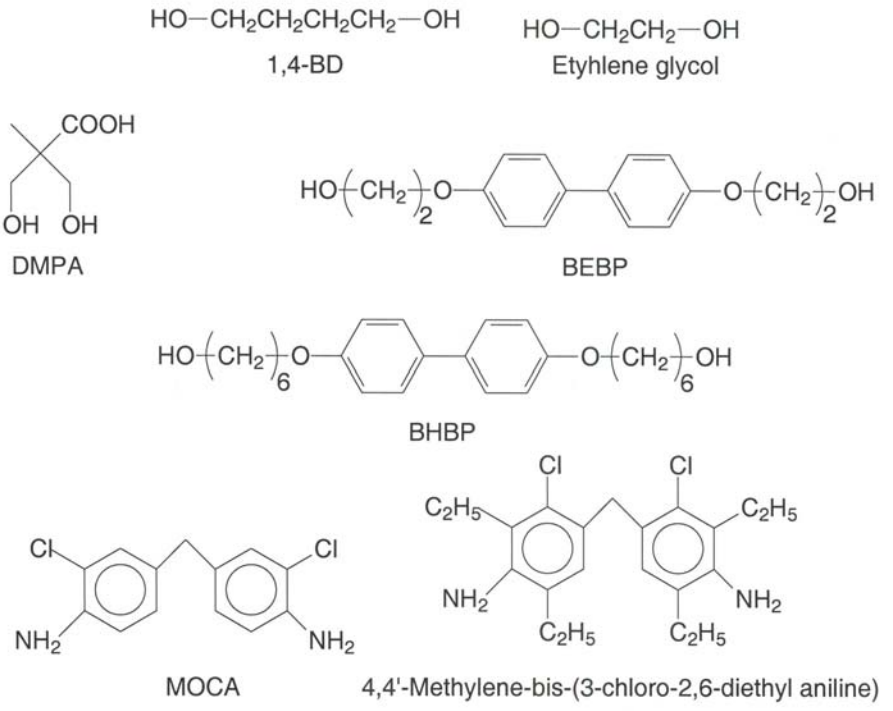

Figure 2.26 Chemical structures of some common alcohol- and amine-based extenders used for PU synthesis

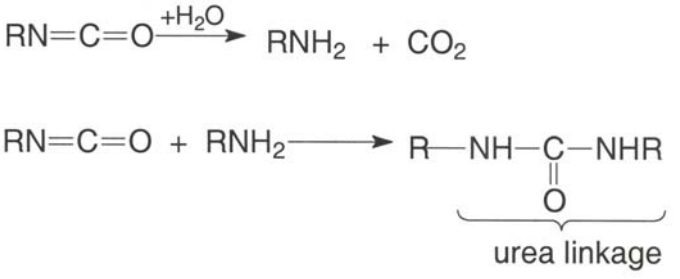

Figure 2.27 Reaction of isocyanate with water

2.7.5 Application of PU Resins

2.7.5.1 General Applications

PU are used in various forms, namely foam (flexible or rigid), elastomer sheet, coating, adhesives and sealants.

The major use of rigid foams is for refrigeration insulation such as in domestic refrigerators and cold storage rooms. They are also used in building and construction industries. The examples are roof or wall insulation for domestic and industrial buildings. Rigid foams are also used for insulated trailors, trucks and railway cars. Flexible foams are used in furniture, cushioning for transportation and sitting and bedding applications because of their lightweight and excellent cushioning properties. Bedding applications include mattresses, topper pads, convertible sofas and mattresses of variable size and densities.

PU coatings are known for their excellent abrasion resistance and weather resistance. They are used for coating of equipment, textiles and leather. Because of their better water resistance compared with epoxy, they replace epoxy for surface coating and paint in marine industries. Automotive coating includes clear top coating, plastic parts coating and body primers. PU coatings are also used for coating military and civilian aircraft.

PU elastomers processed by RIM are widely used in automotive industries. Examples are bumper covers, external body panels, modular windows and exterior and interior trims. Such elastomers are also used in equipment housing, sports equipment and furniture. Castable PU elastomer sheets are used as vibration damping materials and acoustic window materials for various naval and civil applications. Because of higher water resistance, PU elastomers are preferable as encapsulant materials for underwater electronics.

Cellular castable PU elastomers are used extensively in footwear industries. The introduction of multicolour, multi-density microcellular PU products has further broadened their applications. Non-celluar products are widely used as bushings, gaskets, hoses, belts, shock damping mounts and moulded parts for automobiles. PU sealants are used for household appliances, toys, and in ships and submarines.

The largest consumer of PU adhesive is the textile industry. Applications include textile lamination, integral carpet manufacture and rebonding of foam. Rebonded foam is made using scrap PU foam bonded with a urethane prepolymer and used primarily as carpet underlay. PU adhesives are used to bond film to film, film to foil

and film to paper in various packaging constructions. Other uses of PU adhesives are for laminating composite panels in truck and car applications, polycarbonate headlamp assemblies, and door panels. PU adhesives have replaced neoprene-based adhesive for footwear applications.

2.7.5.2 Shape Memory Applications

PU are potential materials for shape memory applications which have drawn considerable attention in recent years [96, 97]. Suitably designed PU exhibit an excellent shape memory effect. A material is said to show shape memory effect if it can be deformed and fixed into a temporary shape and recover its original permanent shape only on exposure of external stimuli such as heat or light. Thermally induced shape memory effect is more common if the recovery takes place with respect to a certain critical temperature. The most widely used shape memory material is Ni–Ti alloy (Nitinol). Shape memory alloys (SMA) exhibit outstanding properties such as small size and high strength, and have found wide technical applications. However, they have obvious disadvantages such as high manufacturing cost, limited recoverable deformation and appreciable toxicity. PU offers deformation to a much higher degree and a wider scope of varying mechanical properties compared with SMA or ceramics, in addition to its inherent advantages of being cheap, lightweight and easy to process. In the case of SMA, the maximum recoverable strain is 8%, whereas in PU it can be 800% [15]. PU are also biocompatible, non-toxic and can be made biodegradable.

Potential applications for shape memory PU exist in almost every area of daily life: from self-repairing auto bodies to kitchen utensils, from switches to sensors, from intelligent packing to tools [98]. Other potential applications are drug delivery [99], biosensors, biomedical devices [100, 101], microsystem components [102], and smart textiles [103]. Because PU can be made biodegradable, they can be used as short-term implants so removal by surgery can be avoided. Some important applications are discussed next.

Shape memory PU and polymers in general have tremendous applications in biology and medicine [104, 105] especially for biomedical devices which may permit new medical procedures. Because of the ability to memorise a permanent shape that can be substantially different from an initial temporary phase, a bulky device could be introduced into the body in a temporary shape (e.g., string) that could go through a small laparoscopic hole and then be expanded on demand into a permanent shape at body temperature.

Shape memory PU has been proposed as a candidate for aneurysm coils [106]. An intracranial aneurysm can go undetected until the aneurysm ruptures, causing

hemorrhaging within the subarachnoid space surrounding the brain. The typical treatment for large aneurysms is remobilisation using platinum coils. However, in about 15% of the cases treated by platinum coils, the aneurysm eventually re-opens as a result of the bio-inertness of platinum. One solution is to develop suitable materials with increased bio-activity (e.g., SMP) to use as coil implants.

Another example of a biomedical application is a microactuator made from thermosetting PU, which has been used to remove blood clots [107]. A microactuator with a permanent shape of a cone-shaped coil can be elongated to a straight wire and fixed before surgery and delivered to an occlusion through a catheter. On triggering the shape recovery using an optical heating method, the original coil shape is recovered and blood flow restored.

Recently, the concept of cold hibernated elastic memory utilising SMP in open cellular structures was proposed for space-bound structural applications [108]. The concept of cold-hibernated elastic memory can be extended to various new applications such as microfoldable vehicles, shape determination and microtags [109]. Recent studies on shape memory PU-based conductive composites using conducting polymers and carbon nanotubes show considerable promise for application as electroactive and remote sensing actuators [110].

The previous discussion indicates the tremendous application of shape memory PU. Extensive work has been carried out for the development of shape memory PU in the last few years, and is reviewed next.

2.7.5.3 Shape Memory PU

SMP are available from Mitsubisi, (Tokyo, Japan). The effect of processing the thermomechanical properties of shape memory PU have been investigated [111]. There was a significant variation in rubbery modulus for the sample cooled at different rates during processing. Thus thermomechanical properties of these materials can be adjusted for various medical applications. The thermal and dynamic mechanical properties of thermosetting Mitsubishi PU materials are given in **Table 2.10**. The exact compositions of these SMP have not been published, but they seem to consist of a complex combination of short amorphous polyester and polyether soft segments, short diol extender and aromatic urethane hard segments. The materials were synthesised by polymerising alternatively hard segment (diphenylmethane diisocyanate) and soft segment (polyol) and various interactions among the segments led to domain formation; hard segment worked as pivoting point for shape recovery and soft segment could mainly absorb external stress applied to the polymer.

Table 2.10 Thermal and viscoelastic properties of DiAPLEX ® (Mitsubishi) thermoset shape memory PU [111]

Trade name	T_s (°C)	T_g § (°C)	Tan $ peak temperature (°C)	E_g $ (Pa)	E_r $ (Pa)
MP3510	35	31	46.1	5.2E8	1.6E6
MP4510	45	42	54.1	7.0E8	1.7E6
MP5510	55	52	65.2	8.1E8	1.9E6

E_g and E_r are glassy modulus and rubbery dynamic modulus
§ determined by differential scanning calorimetry
$ determined by dynamic mechanical analysis

The T_g of PU materials can be controlled in a wide range from –30 °C to 100 °C using different kinds of urethane ingredients (diisocyanate, polyol, chain extenders) and by adjusting their molar ratios [112, 113]. To have an effective shape memory property, the glassy hard segments should maintain the shape through inter- or intra-Polymeric chain attractions such as H-bonding or dipole–dipole interaction, together with physical crosslinking, but soft segments could freely absorb external stress by unfolding and extending their molecular chains. If the stress exceeds and breaks the interactions among hard segments, shape memory will be lost and original shape cannot be restored. Therefore, precise control of composition and structure of hard and soft segments is very important to satisfy the conditions required for various applications. In segmented PU, the hard segment acts as the physical crosslink, and hard segment concentration should be sufficiently high (>20 wt%) to generate a shape memory effect [114]. Optimum shape memory properties were achieved at 35–40 wt% of hard segment concentration [115].

Shape memory PU can be classified into two catergories: amorphous and crystalline. The compositions and properties of different types of amorphous PU reported in recent literature are summarised [116–120] in **Table 2.11**. Wang and Yuen [121] synthesised a series of thermoplastic PU using aromatic chain extenders such as 4,4-bis(4-hydroxyhexoxy)-isopropylene or naphthoxy diethanol, in addition to 1,4-BD. They reported an improvement in shape memory properties as a result of introduction aromatic structure into the main chain. Yang and co-workers [122] compared the mechanical, dynamic mechanical and shape memory properties of PU block coPolymers with planar shape hard segment (1,6-diphenyl diisocyanate (PDI)) and bent shape hard segment (MDI). The PDI-based PU showed superior properties compared with MDI-based PU (**Table 2.11**) as a result of better interaction among hard segments due to the planar shape of PDI.

Table 2.11 Compositions and properties of amorphous PU

Polyol UPE, (g/mole)	Isocyanate	Extender	Hard segment (wt%)	T_g (°C)	Recovery (%)	Reference
PTMG 650	MDI	1,4-BD	31 to 86	-13 to 38	95	116
PTMG 2000	MDI	1,4-BD	12 to 50	-	90	117
PTMG	MDI	1,4-BD	20 to 50	-15 to 2	95	115
PTMG	MDI	1,4-BD	30 to 35	0 to -15	85	122
PTMG	PDI	1,4-BD	20 to 25	-1 to -17	96	122
PTMG 1000,2000	MDI	1,4-BD + BES + BPE/ ND	52 to 73	83 to107	>90	121
BHBP	TDI + HDI	1,3-BD	21 to 41	10 to 35		118
PTMG 1800	MDI	1,4-BD	30	-10	>80	120
PTMG 1000,2000	MDI	1,4-BD	35	-10 to 30	>80	119

BES = bis(2-phenoxyethanol)-sulfone
ND = naphthoxy diethanol
BPE = 4,4´-bis(4-hydroxy)-isopropylane

The compositions and properties of crystalline PU materials are presented in **Table 2.12**. Polycaprolactone (PCL) has been extensively used for synthesis of PU with crystalline soft phase. PCL is first converted to PCL diol and the diol used to synthesise PU-based SMP [123, 124]. The PCL segment undergoes microphase separation and forms the soft switching segment. The recovery temperature, T_r (the temperature at which fast recovery takes place) can vary from 40 °C to 60 °C depending on the soft phase/hard phase composition and UPE of PCL. The relationship between the shape memory effect and molecular structure has been investigated: the high crystallinity of the soft segment region at room temperature was a necessary prerequisite for segmented PU to demonstrate shape memory behaviour. However, the crystallisation of PCL segments is hindered by incorporating them into multiblock copolymers. Crystallisation was not observed when PCL-diol had a number average molecular

weight <2000 g/mole and the optimum molecular weight in terms shape memory properties was 5000–6000 g/mole [125].

Table 2.12 Structure and properties of crystalline shape memory PU					
Hard segment	**Soft segment (SS)**	**% SS**	**Switching temperature °C**	**Recovery (%)**	**Reference**
MDI/1,4- BD	PCL	70	44-55	82	98
MDI/1,4- BD	PCL/PVC blend (6/4)	38-62	18-48	92	125
HDI/4,4´-dihydroxybiphenyl	PCL	30-80	38-58	90	126
MDI/BEBP	PCL	57-70	41-50	80	127
MDI/DMPA	PCL	70	45	95	128
PVC: Polyvinyl chloride					

The major issues related to the developments of such PU-based SMP are to achieve maximum crystallisation and stable hard segment domains. Various strategies such as incorporation of mesogenic segment [126] and ionic groups [127] have been adopted to enforce microphase separation (**Table 2.12**). Mesogenic segments were incorporated in the PU by partially replacing 1,4-BD in PU formulation by 4,4´-bis (2-hydroxyethoxy) biphenyl (BEBP) [126]. The improvement in solubility and shape fixity were observed as a result of incorporation of mesogenic groups. Influence of ionic groups on the crystallisation behaviour of segmented PU using PCL-diol of various molecular weights (4000, 20200, 58500, 71600 g/mole) was also investigated [127]. Ionomers were synthesised by using dimethylol propionic acid (DMPA) in addition to 1,4 BD [128]. Crystallisation studies indicate that crystallisation rate increases as a result of incorporation of ionic groups for PU made from PCL-4000 whereas for samples having a higher molecular weight of PCL the crystallisation rate increases. The ionomers show higher tensile strength, modulus and fatigue resistance compared with the corresponding non-ionomers due to the Columbic forces between the ionic centres within the polymer backbone.

For PU with crystalline soft segments, the crosslinking (introduced in the structure), decreases the crystallisation of the soft segment and upgrades the mechanical properties of the resulting crosslinked structure (**Table 2.13**). Buckley and co-workers [129] reported a novel thermosetting PU using 1,1,1-trimethylol propane as a crosslinker. Improvement in creep, and increase in recovery temperature and recovery window

were observed due to the introduction of crosslinking. Xu and co-workers [130] synthesised hybrid PU, crosslinked with Si–O–Si linkages, formed through hydrolysis and condensation of ethoxy silane groups. The Si–O–Si linkages not only act as the netpoints but also act as inorganic fillers for reinforcement. Ping and co-workers [131] reported PCL-based biodegradable PU. Thermosetting PU with shape memory and hydrogel properties were also investigated [132, 133]. They can be made by making graft copolymers of PU and other hydrophilic polymers (e.g., polyacrylamides, polyacrylates) or by introducing hydrophilic groups into the crosslinked PU backbone [132, 133].

Table 2.13 Effect of crosslinking on mechanical and shape memory properties of crosslinked PU [92, 93]

Hard phase	Soft phase	Crosslinker	E´ GPa	σ MPa	T_m °C Soft phase	% recovery
MDI,1,4-BD, DMPA	PCL Mn ~4000	Nil	0.2	18	50.3	80
MDI,1,4-BD, DMPA	PCL Mn ~4000	Glycerin 6 wt%	0.5	40	46.9	90
E` and σ are storage modulus and tensile strength, respectively, at room temperature						

2.8 Polyimides

Polyimides are a class of high-temperature resin with a –CO-NR-CO– backbone that predominantly consists of a ring structure [134–137]. Because of this ring structure, polyimides offer outstanding thermal stability. Commercial polyimide materials were introduced by DuPont in the early 1960s with trade name of Kapton and Vespel. In general, polyimides are made by reacting a dianhydride with an aromatic amine (**Figure 2.28**). In the first step, a polyamic acid intermediate is formed, which further polymerises to form polyimides. They are generally prepared using *N*-methyl pyrrolidone (NMP) or dimethyl acetamide (DMAc) as a solvent. An appropriate amount of diamine is dissolved in the solvent at room temperature under nitrogen. The dianhydride is then added as a solid or slurry in the solvent while stirring. The reaction is allowed to continue till all the amine is consumed. Depending on the reactivity of the raw materials, it may take 5–30 hours to prepare the polyamic acid solution. The polyamic acid solution on further heat treatment is converted to polyimide. The polyamic acid solution can be used to prepare polyimide powder, thin films, adhesive tape or impregnated fibres.

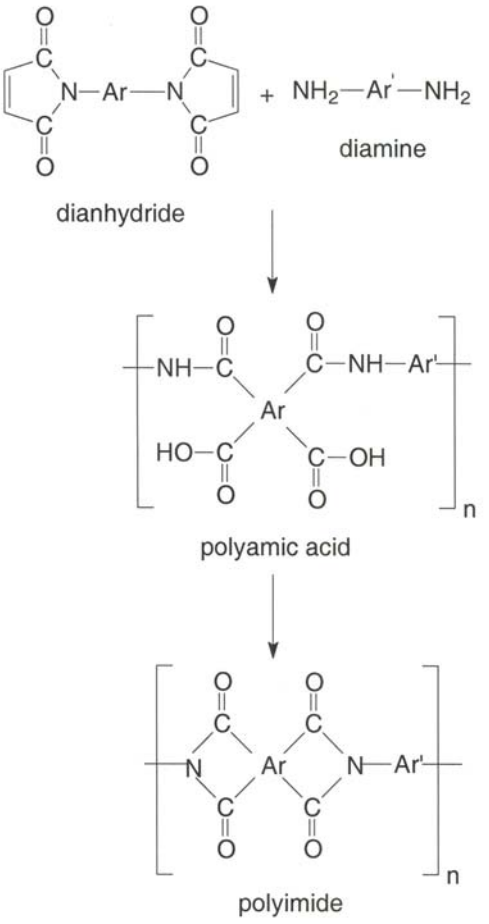

Figure 2.28 A general reaction scheme for polyimide synthesis

The high molecular weight polyimides are called 'condensation polyimide' or 'thermoplastic polyimide'. Thermoplastic polyimides exhibit high T_g, good toughness and excellent thermal and thermo-oxidative stability. Typical properties of some thermoplastic polyimides are given in **Table 2.14**. However, it is very difficult to process these materials because of their high softening or melting temperature. To solve the processing problem or to make the materials more tractable without significant sacrifice in thermal stability, extensive works have been done in last few decades. This has led to the development of polyamide-imides, polyester-imide, polybismalenimides and polyether imides [138]: detailed discussion of these materials is beyond the scope of this book. Another class of polyimides developed to address processability issues is known as 'addition polyimides' or 'thermosetting polyimides'.

Table 2.14 Properties of commercial thermoplastic polyimides						
Polyimide	**T_g, (°C)**	**Service temperature °C (max)**	**Tensile strength MPa (Mod, GPa)**	**Flexural strength, MPa (Mod, GPa)**	**G_{IC}, (J/m²)**	**Impact strength (J/m)**
Torlon (BP Amoco)	267	225	186(4.4)	211(4.5)	3900	133.5
Kapton H (DuPont)	360	316	173(3.0)	-	2000	23
Lark TPI (NASA Lange Centre)	265	300	166(3.6)	-	-	21.4
Vespel SP-1 (DuPont)	360	287	72	83(3.2)	2000	-
Pyramil PI (HD Micro-system)	400	316	113 (2.5)	-	-	-

2.8.1 Addition polyimides

Addition polyimides were introduced in the late 1970s and have been investigated extensively in last few decades [139–158]. These materials are low molecular weight imide oligomers with unsaturated functional groups (capable of undergoing an addition reaction) located in the terminal or pendant position. Mostly, the materials contain unsaturated end caps and in some cases they can also be present as pendant groups in the backbone. Schematic representations of such polyimide oligomers are shown in **Figure 2.29**. The materials are synthesised in a similar way as discussed for condensation polyimides, using an aromatic compound with the desired unsaturated group. A general method for the preparation of addition polyimides is shown in **Figure 2.30**. A wide variety of polyimides can be synthesised by changing the unsaturated functional group (depicted as X in **Figure 2.30**), for example vinyl, nadic, acetylene, and phenyl ethynyl. Polyimides are characterised easily by FT-IR analysis by two characteristic bands at 1790 cm^{-1} for symmetrical carbonyl stretching, and at 1710–1730 cm^{-1} for asymmetrical carbonyl stretching. Disappearance of the characteristic anhydride carbonyl peak at 1860 cm^{-1} indicates completion of the reaction.

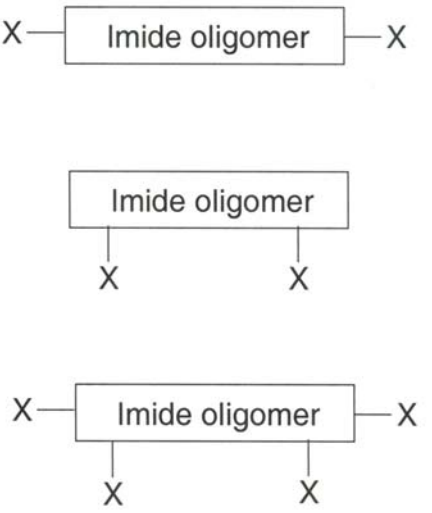

Figure 2.29 Representations of polyimide resins with terminal and pendant reactive groups

Because the resins are oligomeric in nature, addition polyimides exhibit excellent processability during the fabrication of castings or composites. Thermosetting polyimide resins with different end-capping groups and their precursor materials are presented in **Table 2.15**. Upon thermal cure, the unsaturated groups undergo complex reactions, including isomerisation, chain extension, branching, and addition, leading to the formation of a network structure. The curing reactions of such polyimides are not completely understood. The reaction involves the formation of double bonds or a polyene structure. Because the reactions are addition reactions volatiles are not evolved as a byproduct.

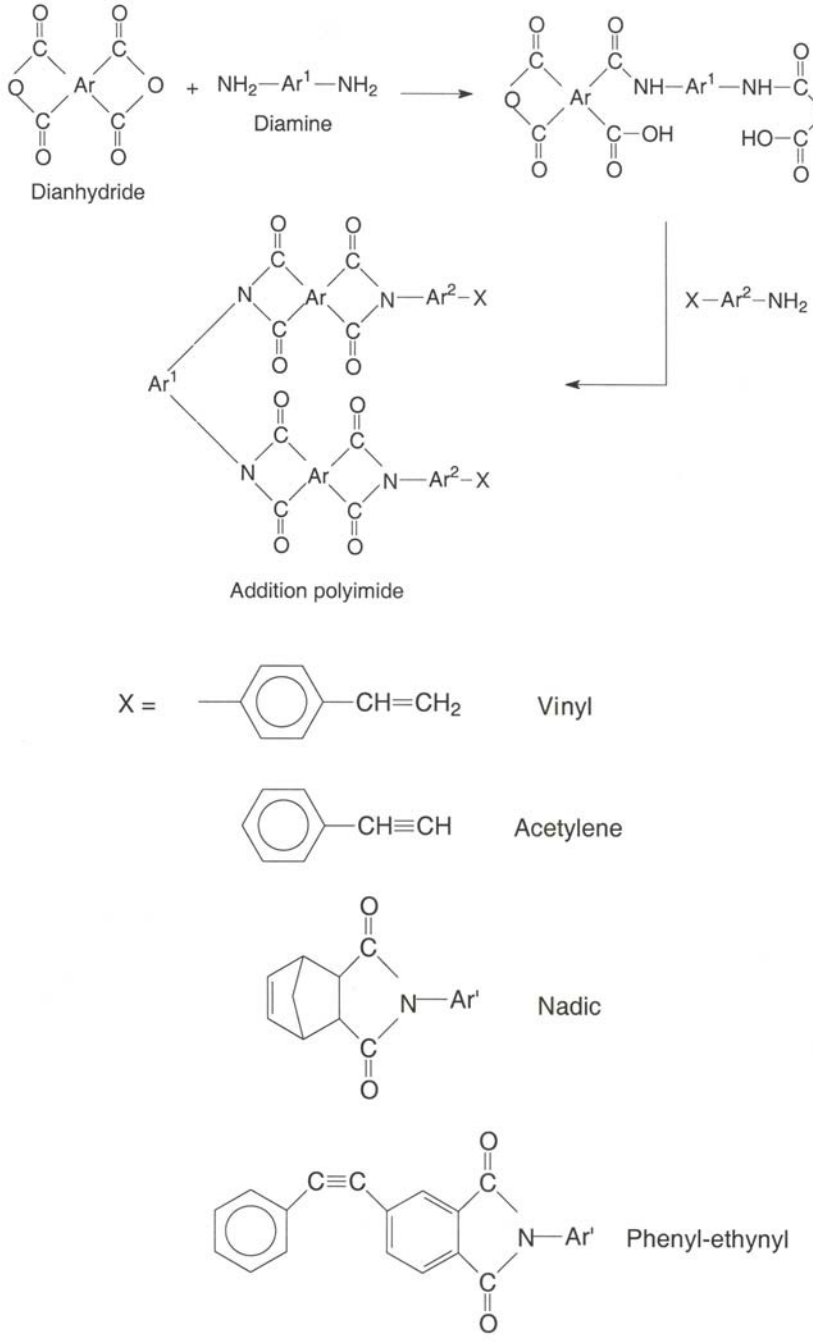

Figure 2.30 A general reaction scheme for the synthesis of addition polyimides with different end groups

Table 2.15 Precursors, end groups and thermal properties of addition polyimides

Polyimide	Precursor	End cap	T_g/T_{ms} °C	Reference
PETI-5	3,4′-Oxydianiline, 1,3-bis (3-amino phenoxy benzene) and 3,3′,4,4′-biphenyl tetracarboxylic dianhydride encapped with 4-phenylethynyl pthalic anhydride	Phenyl ethynyl	270/250	[141-143]
PMR-I (PMR 15, PMR 30, PMR 50)	Monomethyl ester of 5-norbornene-2,3 dicarboxylic acid (Nadic ester), dimethyl ester of 3,3′,4,4′-benzophenone tetracarbo xylic acid dianhydride (BTDA) and 4,4′-methylene dianiline Mole ratio 2:2.087:3.087	Nadic	340(395)/316	[144-146]
LARC-RP46	Modified PMR-I formulation: replacement of MDA by 3,4′-oxydianiline	Nadic	280(395)/300	[147, 148]
PMR-II 6F PMR	BTDA of PMR (I) is replaced by half ester of 4,4′-(hexafluoroisopropylidene)-dipthalic acid (HFDE)	Nadic	350(390)/316	[149, 150]
PMR-II 3F PMR	BTDA of PMR (I) is replaced by 4,4′-(2,2,2-Trifluoro-1-phenylethyledine) dipthalic anhydride (3FDA)	Nadic	370(380)/350	[151]
PMR-12F-71	Nadic ester, HFDE, 2,2′-bis (trifluoromethyl)-4,4′-diaminobiphenyl (BTDB)	Nadic	280 (318)/343	[154]
V-CAP-50	*p*-Amino styrene, HFDE, MDA	Vinyl	311(362)/275	[156, 157]
V-CAP-12F-71	*p*-Amino styrene, HFDE, BTDB	Vinyl	310(385)/316	[157, 158]
PE Ultem 3000	2,2′,3,3′-Biphenyltetracarboxylic dianhydride, 4-phenylethylnyl pthalic anhydride, *m*-phynelyne diamine	Phenyl ethynyl	230/250	[157, 158]

T_{ms} = upper use service temperature; T_g values reported in brackets indicate values obtained after post-curing

2.8.2 In situ Polymerisation of Monomeric Reactants (PMR)

In general, polyimide oligomers are prepared by using high boiling solvents such as NMP or DMAC. Removal of these solvents from the final polymer product is very difficult. The presence of traces of such solvents causes a significant deterioration of the properties of polyimide networks. To circumvent this problem, the PMR approach has been adopted. The half esters of tetracarboxylic acid such as 3,3´,4,4´-benzophenone tetracarboxylic acid anhydride (BTDA) and nadic anhydride are prepared by dissolving the anhydride in methanol or ethanol. The amine (4, 4´-methylene dianiline) is added and the mixture stored as a solution or in impregnated form. The formation of half esters reduces the reactivity of the anhydride, and the mixture of half ester and aromatic amine can be stored for a long time. If the mixture is heated to a high temperature (120–150 °C), the anhydride is reformed and reacts with the amine groups, leading to formation of a polyimide oligomer. Under this condition, the reaction between the half ester and amine does not take place. The initial resin was made using the molar ratio of the reactant 2:2.087:3.087 corresponding to a resin UPE of 1500 g/mole, and was termed PMR-15 [144–146]. Accordingly, the higher molecular weight resins PMR-30 and PMR-50 were developed. PMR resins made from BTDA were called 'first-generation PMR' (PMR-I). Methylene dianiline (MDA) used for the synthesis of PMR-1 is highly toxic and reported to be carcinogenic. Necessary precautions must be adopted with regard to handling of MDA. Hence efforts have been made to make PMR without using MDA. For instance, LARC RP46 resin was developed [147, 148] as an alternative to PMR-1 resin by replacing MDA with 3,4´-oxydianiline. Similarly, other aromatic amines such as 2,2-dimethyl benzidine and 2,2´,6,6´-tetramethyl benzidine were also tried as an replacement for MDA. However, such replacement often resulted in reduction of the thermo-oxidative stability of the polyimide product [149].

PMR-1 resins are widely used as commercial resins (marketed by SP Systems Imitec Inc., Hycomp. Inc., Eikos Inc.) for the fabrication of carbon fibre-reinforced composites with an upper use temperature of 316 °C [138]. However, for applications such as gas turbine engines, and missiles, the Polymer matrix must be able to resist thermal and thermooxidative degradation at higher temperatures (350–400 °C). Hence extensive research has been carried out in the last few decades to develop polymides with increasingly higher temperature service capability. This has led to the development of second-generation PMR resins (PMR-II). PMR-II resins are made in a similar a way as PMR-1 by replacing BTDA with fluorine-containing anhydrides such as 4,4´-(hexafluoroisopropylidene)-dipthalic acid (HFDE), 4,4´-(2,2,2-trifluoro-1-phenylethyle dine) dipthalic anhydride (3FDA) [150, 151]. The reaction scheme for the synthesis of 3F-PMR resin using 3FDA [151] is shown in **Figure 2.31**.

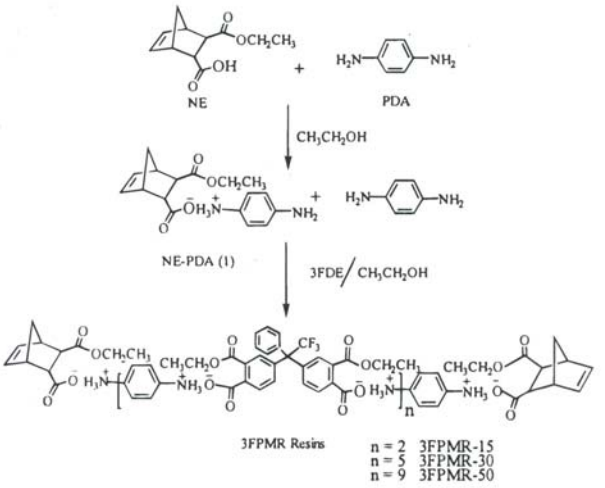

Figure 2.31 Chemistry of 3FPMR resin. Reproduced with permission from A.J. Hu, J.Y. Hao, T. He and S.Y. Yang, *Macromolecules*, 1999, **32**, 24, 8046 © 1999. ©1999, ACS

Due to a fluorine-containing monomer in the structure, PMR-11 resins exhibit better thermal and thermo-oxidative stability compared with PMR-1 resins of similar molecular weight and molecular-weight distribution. The UPE of the PMR prepolymer has an important role with respect to the processability and thermooxidative stability of the cured resin [152]. Higher molecular weight formulations offer the desired thermo-oxidative stability and toughness. **Figure 2.32** compares the thermooxidative stability of PMR and 3F-PMR resins of different molecular weights. The figure demonstrates the order of thermo-oxidative stability as 3F-PMR-50>3F-PMR-30>PMR-50>PMR-30. Thus 3F-PMR shows much better thermo-oxidative stability compared with PMR, and stability increases with increase in UPE of the oligomeric resins.

However, as the molecular weight of the prepolymer is increased, the melting temperature and melt viscosity also increase, so resin flow is severely restricted during processing [153]. Thus low molecular weight resins are preferable from a processing point of view. However, they often cannot match the therm-oxidative stability and toughness offered by high molecular weight resin formulations. Hence design of high molecular weight PMR prepolymer with better processabiliy is a great challenge. Chuang and co-workers [154] synthesised PMR-II (PMR-50) resin by replacing MDA with 2,2´-bis (trifluoromethyl)-4, 4´-diaminobiphenyl (BTDB). The substitution at the 2 and 2´ position of the biphenyl moiety forces the two phenyl rings into adopting a non-coplanar conformation, which reduces the melting point and T_g of the resin and imparts better flow characteristics [155].

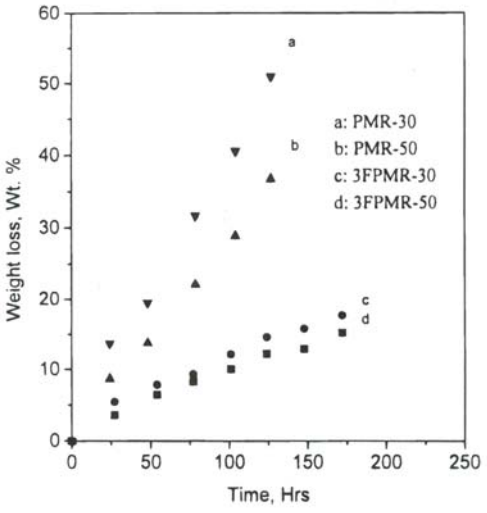

Figure 2.32 Thermo-oxidative stability of 3FPMR and PMR resin powder at 371 °C in air. Reproduced with permission from A.J. Hu, J.Y. Hao, T. He and S.Y. Yang, *Macromolecules*, 1999, **32**, 24, 8046 © 1999. ©1999, ACS

2.8.3 Crosslinking of polyimides

The crosslinking mechanism of PMR and other related addition polyimides is incompletely understood. Several mechanisms have been proposed [159–162]. A representative curing reaction of a fluorinated PMR polyimide (3FPMR) [151] resin is shown in **Figure 2.33**. The reaction involves imidisation, isomerisation and double Diels–Alder adduct formation. For nadic end-capped polyimides, retro Diels–Alder reactions of norborene end group take place, leading to the formation of maleimide groups and cyclopentadiene [163]. The formation of cyclopentadiene and occurance of retro Diels–Alder reaction were confirmed by a combined thermogravimetric analysis (TGA)–gas chromatography (GC)–mass spectroscopic analysis [164, 165]. The maleimide and cyclopentadiene undergo a thermally induced free-radical polymerisation reaction and produce cured 3D network structures. The crosslinking of ethynyl-terminated imide is free-radical propagation of the ethyne moiety to a linear conjugated polyene. The kinetic chain length of this reaction is unusually short and the termination first order. The reaction mechanism is not well understood. A major part of the ethyne groups dimerises to form an enyne structure.

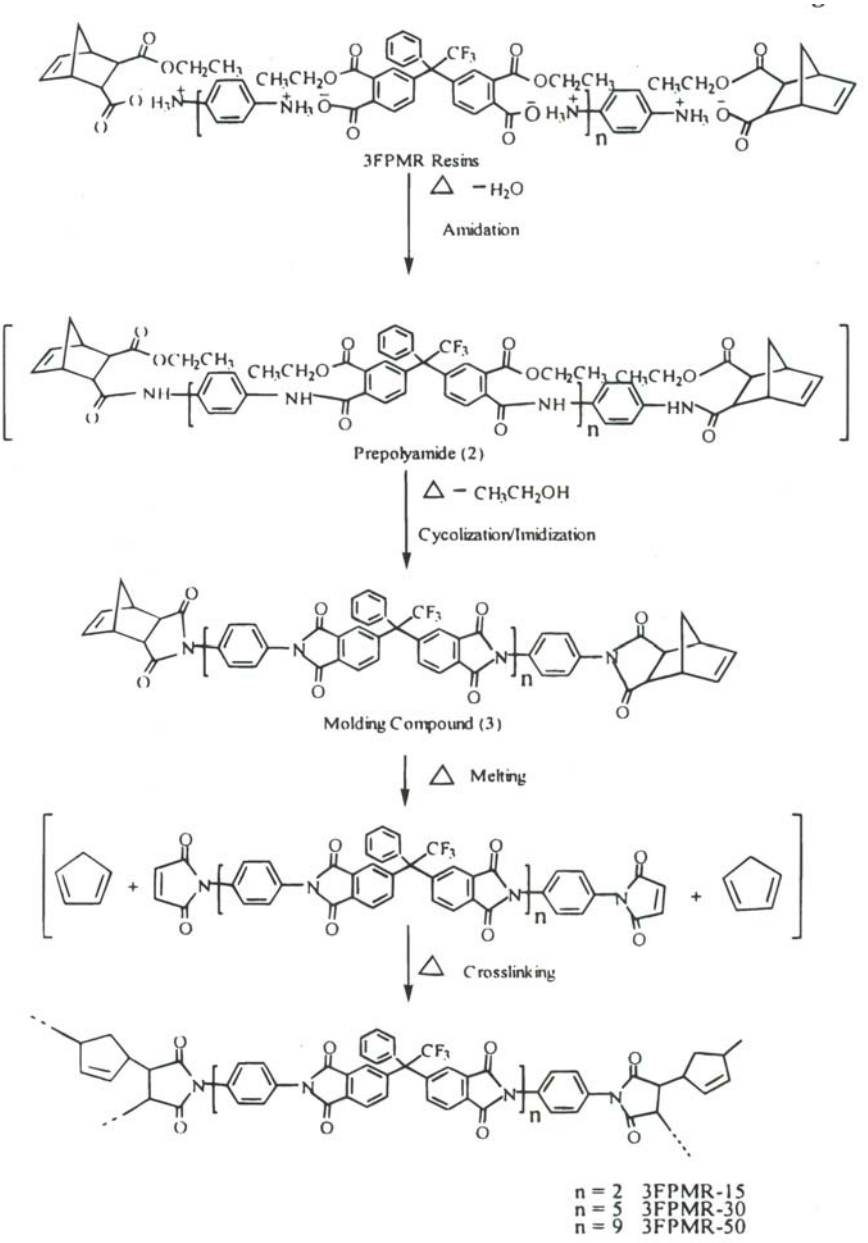

Figure 2.33 Chemical reactions of 3FPMR resins in thermal processing. Reproduced with permission from A.J. Hu, J.Y. Hao, T. He and S.Y.Yang, *Macromolecules*, 1999, **32**, 24, 8046 © 1999. ©1999, ACS

2.8.4 Curing of Polyimide Resins

Curing is an important process that differentiates between thermoplastic and thermosetting polyimides. As discussed in earlier sections, when the T_g of a thermoset resin reaches the curing temperature, vitrification takes place and the reaction becomes diffusion-controlled. Hence, one cannot expect a high T_g of a polyimide cured at a low temperature. To get a high T_g it is necessary to cure at a sufficiently high temperature for a longer time, which results in high crosslink density. For instance, a PMR-15 resin cured at 274 °C and 316 °C for few hours exhibits T_g values of 190 °C and 280 °C, respectively. A post-curing treatment in air at 316 °C for >16 hours is required to achieve the T_g close to 340 °C (**Table 2.15**). The different T_g values reported for cured and post-cured samples indicate that further heat treatment for a longer time also cause an increase in T_g to some extent. To avoid long thermal curing cycles, variable frequency microwave (VFM) processing can be used [166, 167]. VFM curing offers the polyimide network with nearly identical mechanical properties to thermally cured film. The most significant differences in properties between VFM and thermal cured polyimide involve a higher relative permittivity for the VFM film due to the slow evolution of volatile reaction byproducts.

2.8.5 Application of Polyimide Resins

The demand of polyimides originates from their outstanding thermal properties and thermo-oxidative resistance in combination with excellent mechanical properties. Polyimides burn but they have self-extinguishing properties. They have very low a dielectric constant and are resistant to ionising radiation. Among the low-cost thermoset resins, phenolic resin has a thermal stability comparable with polyimides. However, phenolic resin is extremely brittle and generally needs blending with other resins like epoxy/polyurethane or rubber for augmenting toughness. Such modifications significantly reduce their thermal stability and they cannot be used for high-temperature structural applications. Polyimides, due to their high strength and high heat resistance, often replace glass and metals (e.g., steel) in many demanding industrial applications. The thermosetting polyimides have aroused tremendous interest as advanced materials in civilian and defense applications. The various applications are summarised in **Table 2.16**.

The first application of polyimides was for wire enamel [168]. They are suitable for the parts where the materials are exposed to a harsh environment. The major use of PMR- based polyimides is in aircraft engines, missiles and reentry vehicles. Because of high temperature stability, polyimide composites find use as compressor seals in jet engines, automobile engines, exhaust system components, and self-lubricating bearings for high-temperature use. They are extensively used for bearings for appliances, seals

and gaskets for high temperature, pressure discs, sliding and guide rolls, and valve shafts in shutoff valves. They are also used for other high-temperature applications such as light ductwork for high temperatures, heat-resistant panels, and fire-resistant panels. Because of their self-extinguishing property, polyimides are used for the development of lightweight and flame-resistant composite structures.

Table 2.16 Major applications of polyimides

Sector	Field/industry	Application
Civil	Electronics, automobile, aircraft, mechanical engineering, aerospace, medical, fuel cell, environmental science	Wire insulation, tape, chip carrier, switches, liquid crystal display panels, foam insulation, baffles, bushings, seal rings, abrasive cutting wheels, composite structures, adhesives, gas separation membrane, high-temperature adhesive for semiconductor industries, pacemakers, eye lens implants, fuel cell membrane
Defence	Manufacturing, missile, rocket aircraft, spacecraft , mechanical engineering, energy devices	Bushings, bearing, nozzle flaps for aircraft engine, nose cone radomes, ablative coating for re-entry vehicles, disk in compressor valve systems, high- temperature adhesives, structural composites, structural adhesives

Due to a very high heat resistance and radiation resistance, polyimides are suitable for aerospace applications. The driving force to replace the metallic and ceramic materials by high-temperature polymers for aerospace applications is to reduce the weight of the spacecraft. A reduction in weight of a spacecraft significantly decreases the launching cost. It is estimated that a reduction of 0.5 kg from the launching payload saves an expenditure of $5000–30000, depending on the launch platform. Thus use of polyimides as a replacement for metallic and ceramic materials can reduce the launching cost to a great extent. Epoxy-based composites offer excellent mechanical properties and are widely used for structural applications, but they cannot offer heat resistance comparable with polyimides.

Polyimides have many applications in microelectronic industries. They are often used in the electronics industry for flexible cables, as friction elements in data processing equipment, and as insulating films on magnet wires. For example, in a laptop computer, the cable that connects the main logic board to the display (which must flex every time the laptop is opened or closed) is often a polyimide base with copper conductors. Polyimides are used as high-temperature adhesives in semiconductor industries and aerospace industries. They are used for the struts and chassis in cars as well as some

parts under-the-hood because they can withstand intense heat and corrosive lubricants, fuels, and coolants. They are also used in the construction of microwave cookware and other kitchen items and food packaging because of their thermal stability, resistance to oils, greases and their transparency to microwave radiation.

Recently, polyimides have drawn considerable attention for the development of membranes for fuel cells. In polymer membrane fuel cells, nafion is widely used as membrane. However, the nafion membrane cannot withstand high temperature (>80 °C), so research on the development of polyimide based fuel cell membranes has started [169–173]. Polyimides also find applications in the development of gas separation membranes because of their compact ring structure and less free volume, which restricts the passage of gases.

Another potential application is for the development of nonlinear optical (NLO) polymers. NLO Polymers posses dipoles which can be aligned by application of an electric field at a temperature higher than the T_g of the polymer. The dipole arrangement can be fixed by cooling the polymer to room temperature while maintaining the electric field. Such a system exhibits second harmonic generation. When radiation having frequency of w is passed through the material, the radiation is converted into one with frequency of 2 w. Thus such materials have potential use for frequency modulation. However, the diploes in a polymer with a moderate T_g relax very fast, leading to a loss in efficiency of second harmonic generation. Polyimides, because of their inherently high T_g and less free volume, are potential candidates for the development of NLO Polymer systems [174, 175].

2.9 Bismaleimide Resins

Bismaleimides are a relatively new class of polyimdes which have gained acceptance for wide industrial application. With respect to properties, bimaleimide resins are intermediate between PMR polyimides and epoxy resins. They offer thermal stability close to polyimides and epoxy-like autoclave processing. The unique features of bismaleimide resins include excellent physical property retention at elevated temperatures and in wet environments, non-flammabilty and processability [176]. Bismalemide resins are difunctional (or multifunctional) monomers or prepolymers with maleimide end groups. A general structure of bismaleimide and a synthetic route are presented in **Figure 2.34**. Bismaleimides are prepared by chemical dehydration of corresponding bismaleamic acid (intermediate product of an amine and excess maleic anhydride) [177]. The reaction involves several byproducts such as isoimide and acetanilides. Therefore, the yield of pure bismaleimide (obtained by recrystallisation) is generally low (<70%). By selecting an amine it is possible to design bismaleimide having a wide variety of chemical structures. Bismaleimides based on aromatic amines

are crystalline substances with high melting point. Because bismaleimides are processed in a melt state like thermoplastics, processability is directly related to the melting point of the resin. The melting point of a resin depends on the chemical structure and the desired processability can be achieved by judiciously selecting the precursor. The commercial bismaleimide resins are mostly made from MDA. .

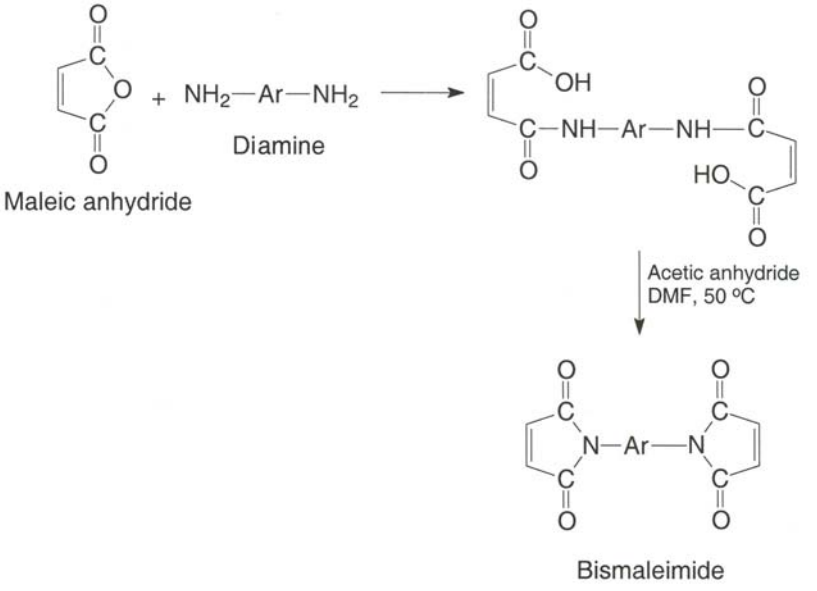

Figure 2.34 Reaction schemes for the synthesis of bismaleimide resin

MDA is highly toxic and reported to be carcinogenic. Necessary precautions must be adopted in regards handling of MDA. Hence bismaleimide-based on other aromatic diamines are of increasing interest [178, 179]. Bismaleimides can be used by itself, with another bismaleimide as a comonomer or as a chain-extended form using a suitable amine. When a bismaleimide is reacted with a stoichiometric amount of diamine, a linear polymer is formed which shows poor thermal stability [180]. The non-stoichiometric reaction of an aromatic diamine with a bismaleimide converts bismaleimide into a polyamino bismaleimide (**Figure 2.35**). The chain extension of bismaleimide using an amine allows further tailoring of crosslink density and properties of the resulting crosslinked network [181–185]. Sripadaraj and co-workers [186] reported *N*,*N*′-(4-aminophenyl)-p-quinone-based maleimide. They have also investigated chain extension of bismaleimides containing flexible ether linkages, i.e., 1,3-bis(4-maleimidophenoxy) benzene and 1,4- bus(4-maleimidophenoxy) benzene with *N*,*N*′-(4-aminophenyl)-*p*-quinone. The chain-extended product was characterised

by FT-IR analysis, which indicated the appearance of a weak-intensity band at 3470 cm^{-1} due to –NH stretching (see **Figure 2.35**) and at 2920 cm^{-1} and 2860 cm^{-1} due to aliphatic stretching. The imide linkage shows the two characteristic bands at 1790 cm^{-1} for symmetrical carbonyl stretching and at 1710–1730 cm^{-1} for asymmetrical carbonyl stretching. Chain-extended bismaleimide resins exhibit inferior thermal stability compared with neat bismaleimide.

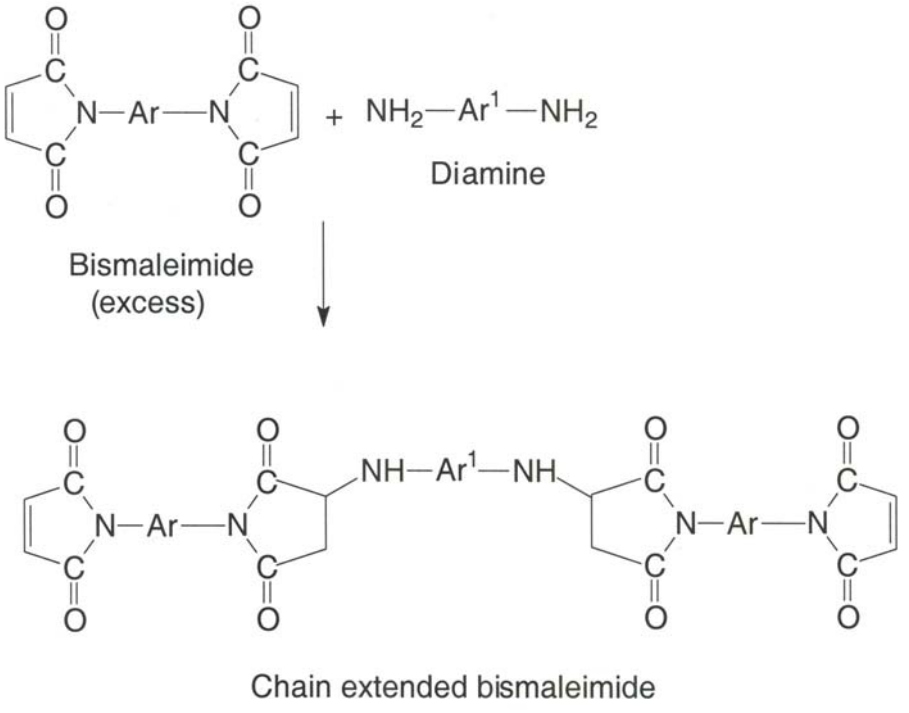

Figure 2.35 Chemistry of the chain extension of bismaleimide resin

2.9.1 Curing of Bismaleimides

The double bonds in bismalemide are highly electron-deficient due to two flanking carbonyl groups, and are reactive towards a bimolecular addition reaction. Hence the maleimide groups of a bismaleimide monomer or chain-extended prepolymer can undergo homopolymerisation to produce 3D network structures. To manipulate the structure and properties, different types of maleimide monomer or prepolymer can be used. The reactivity of such resins depends on their chemical structure and UPE.

In general, the presence of electron-withdrawing groups such as CO and SO_2 in the vicinity of maleimide groups increases the reactivity as the reaction proceeds through nuclephilic attack. The presence of electron-donating groups makes the corresponding maleimide group less nucleophillic and thereby reduces reactivity.

Bismaleimides can also be cured using a Diels–Alder comonomer [187]. When a bisdiene is reacted with excess bismaleimide, a prepolymer-carrying maleimide termination is formed as an intermediate, which can be further crosslinked to form a 3D cured network. Bis-(*o*-propenylphenoxy) benzophenone (Compimide TM123, Technochemie, Germany) is an example of a commercial Diels–Alder comonomer. CompimideTM123 is a low melting, low viscosity material and can be readily melt-blended with bismaleimide (BMI) and cured at high temperature to get a heat-resistant network.

2.9.2 Properties of Bismaleimide Resins

BMI can be cured by polyaddition reactions, which do not produce volatile side products. Cured bismeleimides can withstand service temperature up to 180 °C. By manipulating chemical structures, the thermal stability can be improved further and the service temperature extended up to 270 °C. Thus the thermal stability of bosmaleimides is higher than that of epoxy resin, but lower than that of PMR polyimides. However, bismaleimides offer better processability than PMR polyimide resins. Bismaleimide can be processed like epoxy resin by autoclave molding. At the same time, they exhibit mechanical properties and damage tolerance similar to epoxy resin. Another advantage of bismaleimides is that they are inherently fire-resistant. Because of excellent processability, good mechanical properties, very good thermal stability and adequate electrical properties, bismaleimides gained popularity for the development of high-performance composites and microelctronic components. Mechanical characterisation of bismaleimide resins are mostly studied in composite form, which will be discussed in subsequent chapters.

2.9.3 Applications of Bismaleimide Resins

Bimaleimides are often blended with other resins (e.g., epoxy) and unsaturated polyesters to improve their thermal stability. Aerospace composites are dominated by epoxy resins. Bismaleimides, due to their higher thermal stability and comparable mechanical properties, processability and cost with high-performance epoxies, are gaining acceptance in aerospace industries. They are used to design wings for extended supersonic aircraft [54]. They are also used as preferred matrices compared with epoxy for structural hinges (attached to the trailing edges of the wings) because such

structures experience engine exhaust in routine operation. Similarly, bismaleimides are used as replacements of metallic materials for helicopter tail booms, where the material is exposed to exhaust gases from the engine as well as experiencing a corrosive and fatigue-causing environment.

Bismaleimdes are often blended with other resins like epoxy resins and UPE resin for improvement of their thermal stability. Because of reactive maleimide groups which are Polymerisable by a free-radical mechanism, it is a potential blending component for free radically crosslinkable resins like UPE and VE. Recently, Li and co-workers [188] investigated the thermomechanical properties and morphology of copolymers of 4, 4′-bismaleimido-diphenyl methane and UPE resin. The bismaleimide was readily dissolved in UPE resin and underwent free-radical polymerisation with styrene (reactive diluent) to form alternating copolymers [189, 190]. Thus an intercrosslinking network of UPE and bismaleimide was formed. The effect of addition of bismaleimide on the thermal and mechanical properties of UPE resin is presented in **Table 2.17**. The results clearly indicate a significant increase in thermal stability as a result of incorporation of bismaleimide. However, the concentration of bismaleimide is kept to a minimum (5–10 wt %) to avoid drastic reduction in mechanical properties.

Table 2.17 Thermal and mechanical properties of bismaleimide-modified UPE resin network [188]

% of bismaleimide by weight	T_{md}/T_{50} (°C)	Heat distortion temperature (°C)	Tensile strength (MPa)	Impact strength (kJ/m^2)
0	412/402	54	68	6.3
5	420/409	69	63	5.8
8	424/413	80	53	4.3

T_{md} = temperature corresponding to maximum rate of weight loss
T_{50} = temperature corresponding to 50% weight loss

Because of high-temperature stability, bismaleimide composites find application in jet engines, automobile engines, exhaust system components and self-lubricating bearings for high-temperature use. They are extensively used for bearings for appliances, seals and gaskets for high-temperature use. They are also used for other high-temperature applications such as light ductwork for high temperatures, heat-resistant panels, and fire-resistant panels. Because of their self extinguishing property, bismaleimides are used for the development of lightweight and flame-resistant composite structures.

Bismaleimide resins are extensively used in multilayer printed circuit boards. They can also be used in insulation fibres for protective clothing. Due to their ability to adhere and retain adhesive strength at high temperature, bismaleimides are widely used as a base material for flexible printed circuit boards in the electrical and electronics industries. Bismaleimides are often linked with rubber chains for use as flexible linking molecules to reinforce the rubber compound for tyre applications. The double bond of bismaleimides readily reacts with all hydroxy or thiol groups found on the matrix to form a stable carbon–sulfur, carbon–nitrogen or carbon–carbon bond.

2.10 Cyanate Ester Resins

The third resin in the series of high-temperature thermosetting resins is cyanate ester resin or polycyanurates. The use of cyanate ester resin is limited to aerospace and defense application due to their high cost. Aryl cyanate monomer was first synthesised by Grigat and co-workers [191] and commercial production of cyanate ester (CE) resin started in the mid-1980s. CE resins are characterised by two or more cyanate functional groups (–O–C≡N–) with an aromatic or cycloaliphatic backbone.

In general, CE resins are prepared by reacting cyanogen chloride with an alcohol or phenol in the presence of a tertiary amine [192, 193]. Diethylcyanamide is formed as a gaseous by-product. More byproduct is formed if cynogen bromide is used instead of cyanogen chloride. Cyanogen bromide is preferable from a handling point of view because it is solid unlike cyanogen chloride (gas). To reduce the formation of undesirable byproducts, the reaction is carried out at low temperature for a longer time to reduce the formation of diethylcyanamide. The hydroxyl compounds used as precursors for the reaction can also act as catalysts for the trimerisation of CE resin product. This is why for preparation of CE resin with a long shelf-life it is necessary to ensure almost complete consumption of phenol or alcohol in the reaction [194, 195]. The unreacted phenol present in the resin catalyses the curing of CE resin and reduces the shelf-life.

Due to the high cost and health hazards associated with the handling of cyanogen halide, the source of cyanate ester resins are limited to only few companies (e.g., Lonza, Vantico, Mitsubisi Gas Chemicals). The commercial production of CE resin started in the mid-1980s. CE resin technology was licensed to Mitsubishi Gas Chemicals and Celanese. The range of CE resin products was expanded when CE resin activities were acquired by Vantico. Allied Signal commercialised a multifunctional CE resin in the trade name of Primaset (phenolic triazine) in 1991 [196]. In 1995, Lonza acquired the phenolic triazine family of resins from Allied Signal.

CE resins are available in liquid, semi-solid or low-melting solid form. CE resins contain cyanate monomers or a prepolymer, which is prepared by a controlled

cyclotrimerisation reaction of monomer in an inert atmosphere. CE resins are also commercially available in combination with a suitable impact modifier. For example, rubber-modified CE resin is supplied by Vantico under the trade name of XU-7178. Different types of resins are available with varying chemical structure of the backbone. The chemical structures of commercially available CE resins are presented in **Figure 2.36**.

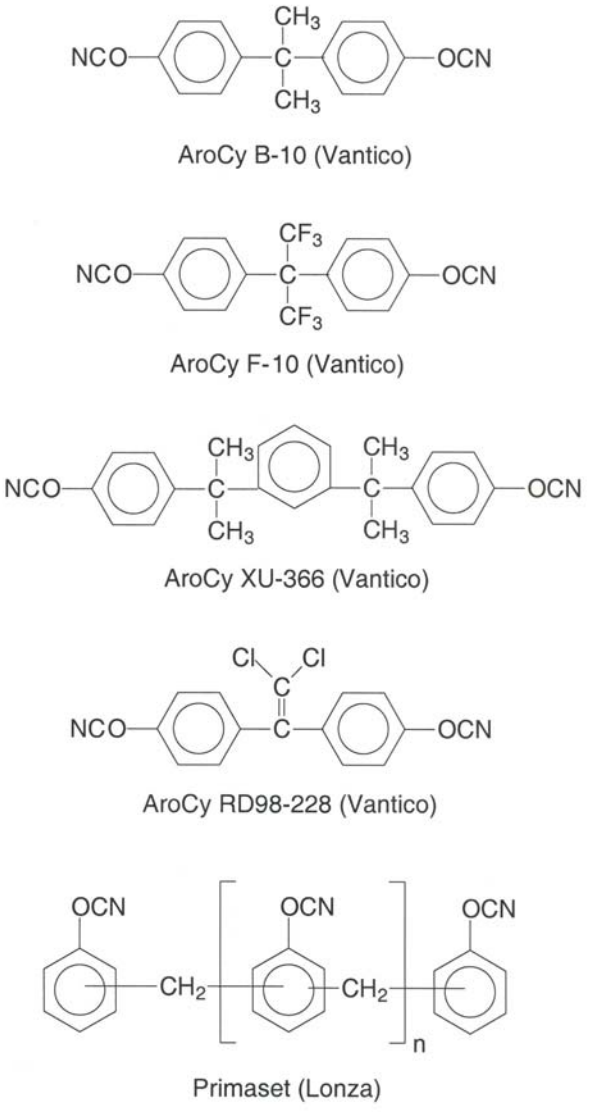

Figure 2.36 Chemical structures of commercially available cyanate ester resin

CE resins containing $–CF_3$ groups have been shown to exhibit low dielectric constant, water resistance, and higher thermal stability compared with their hydrocarbon counterpart [197, 198]. However, the fluorinated resins are high melting solids. For example, the melting point of 2,2-bis(4-cyanatophenyl)-1,1,1,3,3,3,3-hexafluoro propane (BAFCY) is 87 °C. Hence the resin can be melt-processed only at high temperature. Liquid resins can be impregnated with reinforcement and processed at a lower temperature. Ambient-temperature processing saves energy and is advantageous for application in intricate structures. The crystallinity of the CE resin can be reduced by introducing oligomeric spacer groups of random length between the terminal reactive cyanate groups. Such modification also reduces the crosslink density of the resulting network due to an increase in UPE between the crosslinks and is expected to improve the flexibility of the network [199–201].

Recently, Laskoski and co-workers [202] reported the synthesis of liquid fluorinated CE resin by incorporating aryl ether spacer groups between the reactive CE resins. A modified Ullmann reaction was utilised for the synthesis (**Figure 2.37**). First, a hydroxyl-terminated intermediate was prepared by reacting hexafluoro-bisphenol A with 1,3 tribromo benzene. The hydroxyl-terminated intermediate is then reacted with cyanogen bromide to get the cyanate ester prepolymer. The length of the spacer can be varied by changing the composition of the reactants. The prepolymer is a liquid and offers better processability. The cured resin has a T_g of 175 °C which is lower than the T_g of cured BAFCY (270 °C). The TGA results of cured resin (cured with chromium catalyst at a maximum temperature of 300 °C in an inert atmosphere) are presented in **Figure 2.38**. The sample showed weight retention of 95% at 430 °C and the onset of thermal decomposition takes place at about 425 °C. Thus the thermal stability is comparable with BAFCY.

Nair and co-workers [203] reported polycyanate esters of an imide-modified novolac of different maleimide content. The resins underwent a two-stage independent thermal curing through trimerisation of the cyanate groups, as well as addition polymerisation of maleimide moieties. On heating, cyanate esters were transformed into an imido-phenolic-triazine network polymer. The cured resins exhibited a higher initial decomposition temperature compared with the cured maleimide novolacs. However, the thermal stability was found to be inferior to the conventional phenolic-triazine resin.

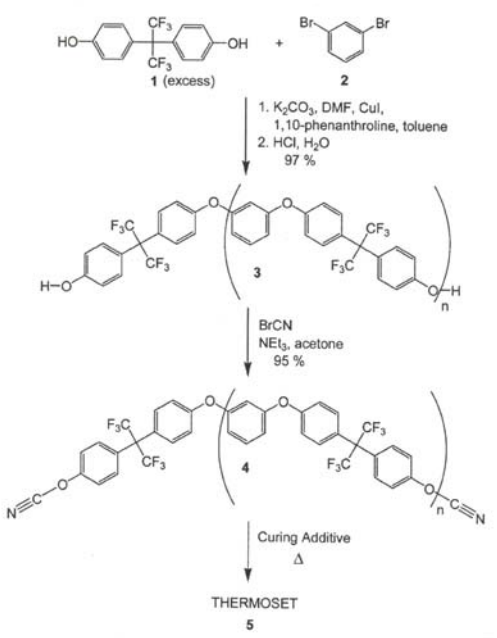

Figure 2.37 Reaction schemes for the synthesis and curing of liquid fluorinated cyanate ester resin. Reproduced with permission from M. Laskoski, D.D. Dominguez and T.M. Keller, *Journal of Materials Chemistry*, 2005, **15**, 161. ©2005, The Royal Society of Chemistry

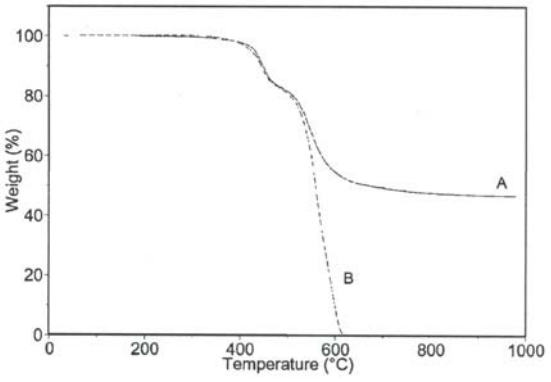

Figure 2.38 TGA thermograms of cured fluorinated cyanate ester resin under (A) nitrogen (B) air. Reproduced with permission from M. Laskoski, D.D. Dominguez and T.M. Keller, *Journal of Materials Chemistry*, 2005, **15**, 1611. ©2005, The Royal Society of Chemistry

2.10.1 Curing of CE resin

The curing of CE ester involves a simple cycotrimerisation reaction (**Figure 2.39**). The curing occurs via a thermally-activated addition reaction which produces no volatiles. The process allows the preparation of void-free castings and fibre-reinforced composites with a good surface finish [204]. The cyclotrimerisation addition reaction leads to the formation of a 3D crosslinked network consisting of triazine rings linked to the backbone structure through ether linkages. The autocatalytic reaction occurs without any catalyst at >200 °C. The use of catalyst offers the control of crosslinking reaction. The carboxylates and chelate salts of transition metals are the example of the commonest catalysts. The transition metals form a complex with the cyanate groups bridging three reactive groups together and encourage the trimerisation. By using catalysts, the curing temperature can be brought down to <100 °C. The curing reaction is highly exothermic. The heat evolved for curing of 1 mole of resin is about 105 kJ, which is about twice the value for epoxy (50–60 kJ/mole). Hence care must be taken to carry out the curing of CE resin. The high heat build up during curing may increase the temperature leading to the degradation of the resin. The CE resin degrades beyond 300 °C (**Figure 2.40**). The CE resins thermally decompose through a common mechanism which begins with thermolytic cleavage of the resin backbone and culminates with decyclisation of the cyanurate rings to produce a variety of volatile species [205] (**Figure 2.40**).

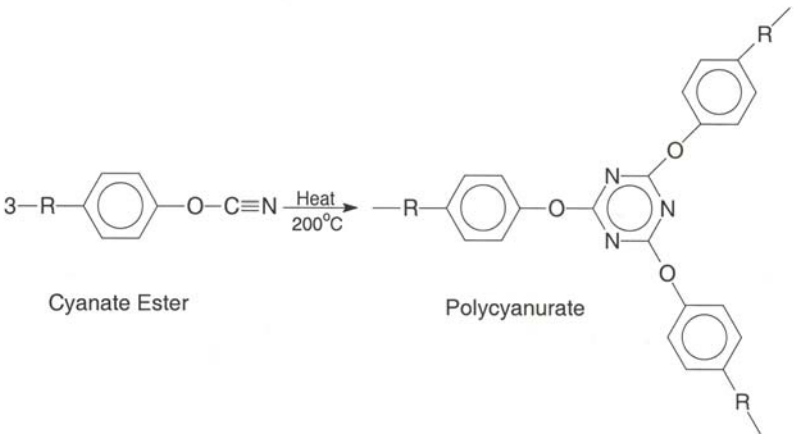

Figure 2.39 Mechanism of curing of cyanate ester resin

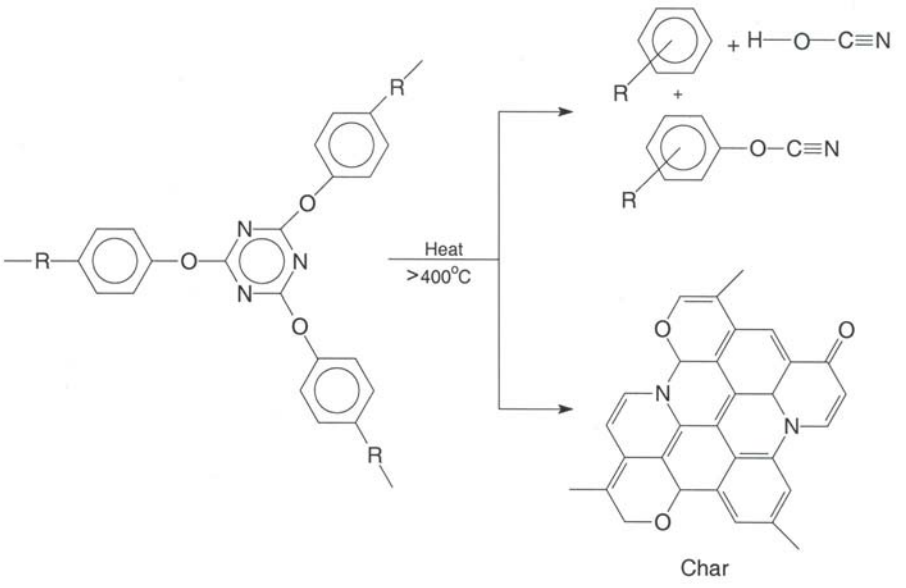

Figure 2.40 Chemistry of degradation of cured cyanate ester resin

This is why curing is carried out in different stages, including two or more initial curing stages followed by post-curing. The curing is generally carried out at 80–120 °C in the first stage, 120–180 °C in the second stage and post-curing at 250–300 °C. Curing of CE resin is sensitive to moisture and hence a dry atmosphere must be maintained for curing the resin. The cyanate group reacts with water to form a carbamate [206]. Carbamate is very unstable and decomposes into the amine and carbon dioxide. The amine further reacts with the cyanate group to form an isourea (**Figure 2.41**). The generated carbon dioxide produces blister in CE resin-based castings and composites.

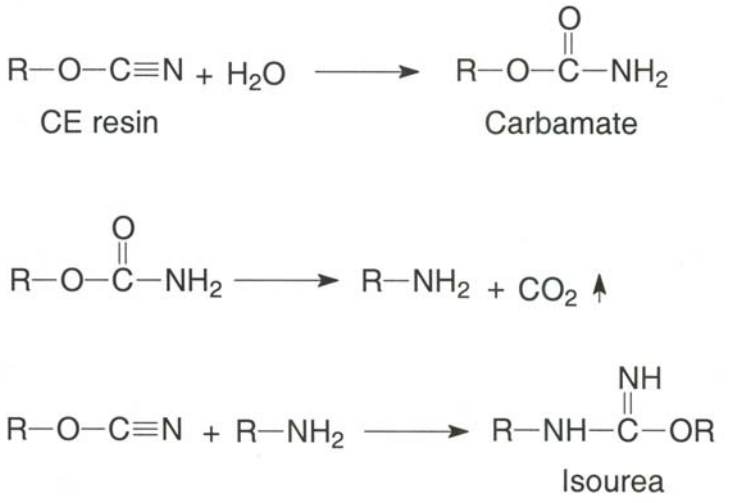

Figure 2.41 Reaction of cyanate ester resin with water to form carbamate and isourea

2.10.2 Properties of CE resins

A cured CE resin network consists of triazine rings linked to the backbone through ether linkages. Because of the presence of flexible ether linkages, cyanate esters exhibit higher flexibility compared with unmodified epoxy and bismaleimide resins. Because of the symmetric cyclic structure and very much fewer polar groups, it shows exceptionally low water absorption and dielectric loss. Moisture absorption for a high temperature-cured epoxy when kept in 100% humidity for 100 hours was >6%, whereas under a similar condition the CE resin showed water absorption of <2% [207]. The other interesting properties of CE resins include low cure shrinkage and low coefficient of thermal expansion. Typical thermomechanical properties of AroCy B-10 and Primaset PT-30 are presented in **Table 2.18**. PT resins are available as viscous liquids, semi-solids and a powdered material. The availability of resin in various consistencies (liquid and solid forms) provides the broad processing capabilities of PT resins by various techniques, i.e., hot melt (prepreg/adhesives), filament winding, resin transfer moulding and powder coating. The resins require initial cure and post-cure at elevated temperatures to achieve the maximum T_g of 350–400 °C. The resins offer outstanding thermal resistance. For instance, mechanical properties remain unaltered after ageing 200 h at 288 °C or 100 h at 315 °C.

Table 2.18 Thermomechanical properties of cyanate ester resin		
Properties	**AroCY B-10**	**Primaset PT-30**
Tensile strength (MPa)	73	48
Tensile strain (%)	3.8	1.9
Flexural strength (MPa)	162	79
Flexural modulus (GPa)	2.9	3.59
G_{1c} (J/m^2)	190	60
T_g (°C)	258	320
Dielectric constant at 1 GHz	2.58	2.97
Dissipation factor at 1 Hz	0.006	0.007

2.10.3 Applications of CE resins

CE resins failed to enter the aircraft and engineering composite industry due to their much higher cost compared with epoxy and bismaleimides, which predominate in these industries. The major use of CE resin is in aerospace applications. The driving force to replace metallic and ceramic materials by high-temperature polymers is to reduce weight, which significantly reduces the launching cost. CE resins find better acceptance for aerospace application compared with epoxy and bismaleimide due to their comparatively lower moisture absorption, increased flexibility and radiation resistance. CE resin-based composites can be processed in the same way as epoxy and bismaleimide, and are of special interest for space applications such as antennae, signal devices, and arrays.

The major use of CE resins is in the electronic industry, including printed wiring circuit boards, thin cards, multichip module laminates and ship encapsulants. CE resins have replaced epoxy and bismaleimide resins to a great extent for such microelectronic application due to their comparatively lower moisture absorption and dielectric dissipation factor.

Another important application for CE resin is for radomes. Effective exploitation of advance radar systems which involve communication of wide-band microwave (600 MHz to 100 GHz), targeting and tracking requires design of suitable window materials. The material should be transparent to the microwave but should simultaneously withstand the high temperature generated due to passage of such waves in the service condition and should also retain dimensional stability at high temperature. Because of the tendency of micro-cracking, epoxy and bismaleimides are not used for communication satellites. Radar transparency and micro-cracking

resistance make CE resins suitable for the conical radome nose-cone, which house the radar antennae of military and weather reconnaissance planes.

CE resins have the lowest dielectric constant and dissipation factor among the thermoset family. The only polymers that have lower dielectric constants and dissipation factors are Teflon and polyethylene, which are low-modulus materials. Low values of dielectric constant and dissipation factor are extremely desirable for aerospace applications because they allow an increase in signal speed and circuit density while simultaneously decreasing the power requirements and amount of heat generated relative to other materials. Thus use of CE resins resulted in increased transmission of microwaves through radome walls, antenna housings and stealth aircraft composites. Cyanate esters also find use as friction materials in brake linings, grinding wheels, and as high-performance adhesives and coatings [208].

PT resins are used in aircraft interior duct components, plastic ball grind arrays, and encapsulation of electronic components. Similar bismaleimide CE resins are often blended with other resins to improve thermal stability. The high water absorption and dielectric loss of epoxies limit their applications for printed circuit boards requiring high speed signal propagation and transport. Blending of CE resin can improve the properties mentioned previous in addition to improving thermal stability. Kim [209] studied the effect of blending of cyanate ester (AroCy L-10) on the cure behaviour and thermal stability of epoxy resin. Addition of 28.6% (40 parts per 100 parts of epoxy) of CE resin resulted in an increase in T_g by 40 °C and improvement of thermal stability (temperature corresponding to onset of weight loss). Similarly, addition of epoxy in CE resin improves the processability, tack/drape properties and reduces cost [210]. Development of such blend systems have significantly resolved the cost and processing issue of CE resins and broadened their applications.

References

1. J.P. Critchley, G.J. Knight and W.W. Wright, *Heat Resistant Polymers - Technologically Useful Materials*, Plenum Publishing Corporation, New York, NY, USA, 1983.

2. A. Knop, V. Bohmer and L.A. Pilato in *Comprehensive Polymer Science, Volume 5: Step Polymerisation – the Synthesis, Characterisation, Reactions and Applications of Polymers*, Eds., G.C. Eastmond, 1989, Chapter 35.

3. A. Knop and L.A. Pilato, *Phenolic Resins*, Springer, Berlin, Germany, Heidelberg, Germany and New York, NY, USA, 1979.

4. M. Komiyama, *Progress in Polymer Science*, 1993, **18**, 871.

5. Z. Lazlo-Hedvig, M. Szesztay and F. Tudos, *Angewandte Makromolekulare Chemie*, 1996, **241**, 57.

6. G. Casiraghi, G. Casnati, M. Cornia, G. Sartori and F. Bigi, *Makromolekulare Chemie,* 1981, **182**, 2973.

7. D. Ratna, A. K. Banthia and N.C. Maity, *Indian Journal of Chemical Technology*, 1995, **2**, 253.

8. J.A. Hiltz, S.G. Kuzak and P.A. Waitkus, *Journal of Applied Polymer Science*, 2001, **79**, 385.

9. T.R. Dargaville, F.N. Guerzoni, M.G. Looney, D.H. Solomon and X. Zhang, *Journal of Polymer Science: Part A: Polymer Chemistry*, 1997, **35**, 1399.

10. P.J. de Bruyn, L.M. Foo, A.S.C. Lim, M.G. Looney and D.H. Solomon, *Tetrahedron*, 1997, **53**, 13915.

11. X. Zhang, A.C. Potter and D.H. Solomon, *Polymer*, 1998, **39**, 1967.

12. X. Zhang, A.C. Potter and D.H. Solomon, *Polymer*, 1998, **39**, 399.

13. S. Markovic, B. Dunjic, A. Zlatanic and J. Djonlagic, *Journal of Applied Polymer Science*, 2001, **81**, 1902.

14. J. Arimond and B.B. Fitts, *Design Data for Phenolic Engine Components, Polymer Composites for Automotive Applications*, Society of Automotive Engineers Technical Papers Series, SAE, Washington, DC, USA, 1988, p.79.

15. D.V. Rosato and C.S. Grove, Jr., *Filament Winding*, Interscience, New York, NY, USA, 1964.

16. L. Pilato and M.J. Micano, *Advanced Composite Materials*, Springer-Verlag, Heidelburg, Germany, 1994.

17. G.M. Jenkins and K. Kawamura, *Polymeric Carbons*, Cambridge University Press, Cambridge, UK, 1976.

18. A.Knop and L.A. Pilato, *Phenolic Resins*, Springer, Berlin, Germany, 1985, p.156.

19. R.P. Lattimer, R.A. Kinsey, R.W. Layer and C.K. Rhee, *Rubber Chemistry and Technology*, 1989, **62**, 107.

20. *Applications of Electroactive Polymers*, Ed., B. Scrosati, Chapman & Hall, New York, NY, USA, 1993, p.251.

21. W. Wieczorek, D. Raduacha, A. Zalewska and J.K. Stevens, *Journal of Physical Chemistry*, 1998, **B102**, 8725.

22. K.M. Abraham, Z. Jiang and B. Carroll, *Chemistry of Materials*, 1997, **9**, 1978.

23. P.P. Chu, M.J. Reddy and J.Tsai, *Journal of Polymer Science: Polymer Physics Edition*, 2004, **42**, 3866.

24. D. Ratna, T. Abraham and J. Karger Kocsis, *Journal of Applied Polymer Science*, 2008, **108**, 2156.

25. D. Ratna, T. Abraham and J. Karger Kocsis, *Macromolecular Chemistry and Physics*, 2008, **209**, 723.

26. C. Liu, H. Qin and P.T Mather, *Journal of Materials Chemistry*, 2007, **17**, 1543.

27. H.D. Wu, P.P. Chu, C.M. Ma and F.C. Chang, *Macromolecules*, 1999, **32**, 3097.

28. H. Kosonen, J. Ruokolanien, M. Torkkeli, R. Serima, P. Nyholm and O. Ikkala, *Macromolecular Chemistry and Physics*, 2002, **203**, 388.

29. S.W. Kuo, C.L. Lin and F.C. Chang, *Macromolecules*, 2002, **35**, 278.

30. T.J. Fox, *Bulletin of the American Physical Society*, 1956, **1**, 123.

31. B. Meyer, *Urea-formaldehyde Resins*, Addison-Weslay Publishing Company, Inc. MA, USA, 1979.

32. F.J. Blais, *Amino Resins*, Reinhold Publishing Corporation, New York, NY, USA, 1959.

33. *Handbook of Thermoset Plastics*, 2nd Edition, Ed., S.H. Goodman, Noyes Publications, Park Ridge, New Jersey, USA, 1998.

34. T.L. Richardson, *Industrial Plastics: Theory and Application*, 2nd Edition, Delmar Publishers Inc., Albany, NY, USA, 1989, p.210.

35. K.A. Hodd, *Epoxy Resins*, Rapra Review Report No.38, Rapra Technology, Shrewsbury, UK, 1990.

36. Kirk-Othmer, *Encyclopedia of Chemical Technology*, *Volume 9*, 4th Edition, Eds., J.I. Kroscwitz and M. Howe Grant, Wiley, New York, NY, USA, 1994, p.730.

37. *Encyclopedia of Polymer Science and Engineering*, Volume 6, 2nd Edition, Eds., H.F. Mark and J.I. Kroscwitz, Wiley, New York, NY, USA, 1991, p.322.

38. *Epoxy Resin Chemistry,* Ed., R.S. Bauer, ACS Symposium Series No.114, American Chemical Society, Washington, DC, USA, 1979.

39. H. Lee and K. Neville, *Handbook of Epoxy Resins*, McGraw-Hill, New York, NY, USA, 1967.

40. D. Ratna, *Epoxy Composites: Impact Resistance and Flame Retardancy*, Rapra Review Report No.185, Smithers Rapra, Shrewsbury, UK, 2007.

41. C.J. Larez and G.A.P Mendoza, *Polymer Bulletin*, 1989, **22**, 513.

42. C.J. Larez and G.A.P Mendoza, *Polymer Bulletin*, 1990, **23**, 577.

43. V.I. Szmercsanyi, L.K. Maros and A.A. Zahran, *Journal of Applied Polymer Science*, 1966, **10**, 513.

44. L.G. Curtice, *Industrial and Engineering Chemistry Product Research and Development*, 1964, **3**, 218.

45. S. K. Gupta and R. T. Thampy, *Makromolekulare Chemie,* 1970, **139,** 103.

46. V. Zvonar and A. Sternscuss, *Plaste und Kautschuk*, 1960, **7**, 228.

47. Z. Ordelt and V. Soedin, *Macromolecular Chemistry*, 1962, **4, 1,** 110.

48. Z. Ordelt and V. Soedin, *Macromolecular Chemistry*, 1963, **63**, 153.

49. Z. Ordelt and F. Ciganek, *Chemicky Prumsyl*, 1964, **14,** 141.

50. W. Kemp, *Organic Spectroscopy*, 2nd Edition, Macmillan Education Ltd.,

Hong Kong, China, 1987.

51. Y.S. Yang and J.P. Pascault, *Journal of Applied Polymer Science*, 1997, **64**, 133.

52. Y.S. Yang and J.P. Pascault, *Journal of Applied Polymer Science*, 1997, **64**, 147.

53. P.J. Flory, *Journal of the American Chemical Society,* 1939, **61**, 3334.

54. C.C. Lin and K.H. Hsieh, *Journal of Applied Polymer Science*, 1997, **21**, 2711.

55. A.C. Tang and K.S. Yao, *Journal of Polymer Science:* 1959, **35**, 219.

56. Y.R. Fang, C.G. Lai, J.L. Lu and M.K. Chen, *Scientia Sinica,* 1975, **18**, 72.

57. S.A. Chen and K.C. Wu, *Journal of Polymer Science: Polymer Chemistry Edition*, 1982, **20**, 1819.

58. C.T. Kuo and S. Chen, *Journal of Polymer Science: Polymer Chemistry Edition*, 1989, **27**, 2793.

59. D. Beigzadeh, S. Sajjadi and F.A. Taromi, *Journal of Polymer Science: Polymer Chemistry Edition*, 1995, **33**, 1505.

60. *Reaction Polymers*, 2nd Edition, Eds., W.F. Gum, W. Riese and H. Ulrich, Hanser, Munich, Germany, 2000, p.153.

61. C.P. Hu and L. Lee, *Polymer*, 1993, **34**, 4516.

62. B. Mortaigne, B. Feltz and P. Laurens, *Journal of Applied Polymer Science*, 1997, **66**, 1703.

63. Y.J. Huang and C.C. Su, *Journal of Applied Polymer Science*, 1995, **55**, 323.

64. L. Suspene, D. Fourquier and Y.S. Yang, *Polymer*, 1993, **32**, 1593.

65. F. Baffa and J. Borrajo, *Journal of Applied Polymer Science*, 2006, **102**, 6064.

66. J.P. Lecointe, J.P. Pascault, L. Suspene and Y.S. Yang, *Polymer*, 1990, **33**, 3226.

67. P.J. Flory, *Principles of Polymer Chemistry*, Cornell University Press, Ithaca, NY, USA, 1975.

68. P. Eisenberg, J.C. Lucas and R.J.J. Williams, *Journal of Applied Polymer Science*, 1997, **65**, 755.

69. R. Bhatnagar and I.K.Verma, *Journal of Thermal Analytical Calorimetry,* 2005, **35**, 1241.

70. P. Siva, I.K.Verma, D.M. Patel and T.J.M. Sinha, *Bulletin of Materials Science*, 1994, **17**, 1095.

71. B.A. Zaitsev, inventor; no assignee, US 6143922, 2000. .

72. C.P. Hsu and L.J. Lee, *Polymer*, 1993, **34**, 4495.

73. K. Dusek in *Developments in Polymerisation – 3: Network Formation and Cyclisation in Polymer Reactions*, Ed., R.N. Haward, Applied Science Publishers, Barking, UK, 1982, Chapter 4.

74. S.V. Muzumdar and L.J. Lee, *Polymer Engineering and Science,* 1996, **36**, 943.

75. A. Zlatanic, B. Dunjic and J. Djonlagic, *Macromolecular Chemistry and Physics*, 1999, **200**, 2048.

76. A. Zlatanic, J. Djonlagic and B. Dunjic, *Macromolecular Chemistry and Physics*, 1998, **199**, 2029.

77. M.B. Launikitis, *Vinyl Ester Resins, Handbook of Composites*, Ed., G. Lubin, Van Nostrand Reinhold Co., New York, NY, USA, 1982, Section 3.

78. W.D. Cook, G. P. Simon, P.J. Burchill. M. Lau, T.J. Fitch, *Journal of Applied Polymer Science*, 1997, **64**, 769.

79. M. Skrifvars, P. Niemela, R. Koskinen and O. Hormi, *Journal of Applied Polymer Science*, 2004, **93**, 1285.

80. G.Y. Yang and C.P. Hu, *Journal of Applied Polymer Science*, 2002, **84**, 1629.

81. F.C. Schilling and A.E. Tonelli, *Macromolecules*, 1986, **19**, 1337.

82. A. LeBorgne, N. Spassky, C.L. Jun and A. Momtaz, *Macromolecular Chemistry*, 1988, **189**, 637.

83. S. Inoue and T. Aida, *Ring Opening Polymerisation*, Eds., K.J. Ivin and T. Saegusa, Elsevier Applied Science Publishers, London, UK, 1984, **1**, 185.

84. S.D. Gangnon, *Encyclopedia of Polymer Science and Engineering*, Wiley Interscience Publication, NY, USA, 1986, **6**, 273.

85. A.M. Eastman in *The Chemistry of Cationic Polymerisation*, Eds., P.H. Plesch, Pergamon Press, Elmford, NY, USA, 1963, Chapter 10.

86. P.Dreyfuss, M.P.Dreyfuss and Kirk-Othmer, *Encyclopedia of Chemical Technology*, 3rd Edition, Wiley and Sons Inc., NY, USA, 1982, **18**, 645.

87. T. Xavier, B. Didier and T. Lan, *European Polymer Journal,* 2000, **36**, 1745.

88. Z.W. Wicks, F. Jones and S. Pappas, *Organic Coating Science and Technology*, John Wiley and Sons, Hoboken, NJ, USA, 1992, **1**, p.188.

89. I. Ahmad, J.H. Zaidi, R. Hussain and A. Munir, *Polymer International,* 2007, **56**, 1521.

90. P.T. Gnanarajan, N. Padmanava, N.A. Sultan and G. Radhakrishnan, *Polymer International,* 2002, **51**, 195.

91. T. Mukaiyama and Y. Hoschino, *Journal of the American Chemical Society,* 1956, **78**, 1946.

92. Y. Zouohong, H. Jinlian, L. Yeqiu and Y. Lapyan, *Materials Chemistry and Physics*, 2006, **98**, 368.

93. J. Hu, Z. Yang, L. Yeung, F. Ji and Y. Liu, *Polymer International,* 2005, **54**, 584.

94. S.H. Lee, J.W. Kim and B.K. Kim, *Smart Materials Structure*, 2004, **13**, 1345.

95. T.L. Smith and Magnusson, *Journal of Polymer Science:* 1960, **13**, 391.

96. D. Ratna and K. Kocsis, *Journal of Materials Science*, 2007, **43**, 254.

97. A. Lendlein, S. Kelch and K. Kratz, *Kunstoffe*, 2006, **2**, 1, 54.

98. A. Lendlein and S. Kelch, *Angewandte Chemistry - International Edition*, 2002, **41**, 2034.

99. A. Metcalfe, A.C. Desfaits, I. Salazkin, L.H. Yahia, W.M. Sokolowski and J. Raymond, *Biomaterials*, 2003, **24**, 491.

100. M.F. Metzger, T.S Wilson, D. Schumann, D.L. Mathew and D.J. Maitland, *Biomedical Microdevices*, 2002, **4**, 1, 89.

101. H.M.Wache, D.J. Tartakowska, A. Hentrich and M.H. Wagner, *J. Mater. Sci. Mater. Med*, 2003, **14**, 109.

102. K. Gall, M. Mikulas, N. Munsi and M.Tupper, *Journal of Intelligent Material Systems and Structures*, 2000, **11**, 877.

103. M. Enomoto and K. Suehiro, *Textile Research Journal*, 1997, **67**, 601.

104. R. Langer and D.A. Tirrell, *Nature*, 2004, **428**, 487.

105. A. Lendlein and R. Langer, *Science*, 2002, **296**, 1673.

106. J.M. Hampikian, B.C. Heaton, F.C. Tong, Z. Zhang and C.P. Wang, *Materials Science and Engineering C*, 2006, **26**, 1373.

107. D.J. Maitland, M.F. Metzger, D. Schumann, A. Lee and T.S. Wilson, *Lasers in Surgery and Medicine*, 2002, **30**, 1, 1.

108. S.J. Tey, W.M. Huang and W.M. Sokolowski, *Smart Materials and Structures*, 2001, **10**, 321.

109. W.M. Huang, C.W. Lee and H.P. Teo, *Journal of Intellignt Material Systems and Structures*, 2006, **17**, 753.

110. J.W. Cho, J.W. Kim, Y.C. Jung and N.S. Goo, *Macromolecular Rapid Communications*, 2005, **26**, 5, 412.

111. G. Baer, T.S. Wilson, D.L. Mathews and D.J. Maitland, *Journal of Applied Polymer Science,* 2007, **103**, 3882.

112. S. Mondal and J.L. Hu, *Journal of Elastomers and Plastics*, 2007, **39**, 1, 81.

113. T. Takahashi, N. Hayashi and S. Hayashi, *Journal of Applied Polymer Science,* 1996, **60**, 1061.

114. H.S. Park, J.W. Kim, S.H. Lee and B.K. Kim, *Journal of Macromolecular Science B*, 2004, **43**, 447.

115. B.S. Lee, B.C. Chun, Y.C. Chung, K. Sul and J.W. Cho, *Macromolecules*, 2001, **34**, 6431.

116. J.R. Lin and L.W. Chen, *Journal of Applied Polymer Science,* 1998, **69**, 1563.

117. J.R. Lin and L.W. Chen, *Journal of Applied Polymer Science,* 1998, **69**, 1575.

118. H.M. Jeong, S.Y. Lee and B.K. Kim, *Journal of Materials Science*, 2000, **35**, 1579.

119. B.C. Chun, T.K. Cho and Y.C. Chung, *Journal of Applied Polymer Science,* 2007, **103**, 1435.

120. J.W. Cho, Y.C. Jung, B.C. Chun and Y.C. Chung, *Journal of Applied Polymer Science,* 2004, **92**, 2812.

121. H.H. Wang and U. Yuen, *Journal of Applied Polymer Science*, 2006, **102**, 607.

122. J.H.Yang, B.C. Chun, Y.C. Chung and J.H. Cho, *Polymer*, 2003, **44**, 3251.

123. M. Xu and F-K. Li, *Journal of Polymer Science,* 1999, **17**, 203.

124. F.K. Li, X.Y. Zhang, M.T. Wang, D.J. Ma, M. Xu, X.L. Luo, D.Z. Ma and B.K. Kim, *Journal of Applied Polymer Science*, 1997, **64**, 1511.

125. H.M. Jeong, B.K. Ahn, S.M. Cho and B.K. Kim, *Journal of Polymer Science: Polymer Physics Edition,* 2000, **38**, 3009.

126. H.M. Jeong, B.K. Ahn and B.K. Kim, *Polymer International,* 2000, **49**, 1714.

127. H.M. Jeong, B.K. Kim and Y.J. Choi, *Polymer*, 2000, **41**, 1849.

128. Y. Zhu, J.L. Hu, K.W. Yeung, Y.Q. Liu and H.M. Lien, *Journal of Applied Polymer Science,* 2006, **100**, 4603.

129. C.P. Buckley, C. Prisacariu and A. Caraculacu, *Polymer*, 2007, **48**, 1388.

130. J. Xu, W.Shi and W. Pang, *Polymer*, 2006, **47**, 457.

131. P. Ping, W. Wang, X. Chen and X. Jing, *Biomacromolecules*, 2005, **6**, 587.

132. W. Chen, C. Zhu and X. Gu, *Journal of Applied Polymer Science,* 2002, **84**, 1504.

133. B.K. Kim and S.H. Paik, *Journal of Polymer Science: Polymer Chemistry Edition*, 1999, **37**, 2703.

134. *Encyclopedia of Polymer Science and Engineering*, 2nd Edition, Volume 10, Eds., H.F. Mark, N.M. Biikles, C.G. Overberger and G. Menges, Wiley, New York, NY, USA, 1989.

135. *Polyimides: Synthesis, Characterisation and Applications*, Ed., K.L. Mittal, Plenum, New York, NY, USA, 1984.

136. S.Z.D. Cheng, S.K. Lee, J.S. Barley, S.L.C. Hsu and F.W. Harris, *Macromolecules*, 1991, **24**, 1883.

137. S.Z.D. Cheng, F.E. Arnold, A. Zhang, S.L.C. Hsu and F.W. Herris, *Macromolecules*, 1991, **24**, 5856.

138. J.A. Brydson, *Plastic Materials*, *4th Edition*, Butterworth-Scienftific, London, UK, 1982, p.499.

139. T.M. Bogert and R.R. Renshaw in *Resins for Aerospace*, Ed., C.A. May, ACS Symposium Series No.132, American Chemical Society, Washington, DC, USA, 1980, p.30.

140. I.K. Varma, *Advances in Composite Materials*, Ed., P. Ramakrishna, IBH, Oxford, UK, 1991, p.85.

141. P.M. Hergenrother, J.W. Connell and J.G. Smith, Jr., *Polymer*, 2000, **41**, 5073.

142. J.G. Smith, Jr., J.W. Connell and P.M. Hergenrother, *Journal of Composite Materials*, 2000, **34**, 614.

143. B.J. Jensen, R.G. Bryant, J.G. Smith, Jr. and P.M. Hergenrother, *Journal of Adhesion*, 1995, **54**, 57.

144. T.T. Serafini, P. Delvigs and G.R. Lightsey, *Journal of Applied Polymer Science,* 1972, **16**, 905.

145. P.M. Hergenrother, *ACS Polymer Preprints*, 1984, **25**, 97.

146. T.T. Serafini in *Resins for Aerospace*, Ed., C.A. May, ACS Symposium Series No.132, American Chemical Society, Washington, DC, USA, 1980, p.15.

147. R.D.Vannucci, *SAMPE Journal*, 1987, **19**, 1, 31.

148. W.X. Wang, Y. Takao and F.G. Yuan, *Journal of Composite Materials*, 1998, **32**, 16, 1508.

149. T.T. Serafini, R.D.Vannucci and W.B. Alston, *Second Generation PMR Polyimides*, NASA Technical Memorandum No.TMX-71894, NASA, WAShington, DC, USA, 1976.

150. *Comprehensive Polymer Science*, Volume 5, Eds., Sir G. Allen and J.C. Bevington, Pergamon Press, Oxford, UK, 1989, 423.

151. A.J. Hu, J.Y. Hao, T. He and S.Y. Yang, *Macromolecules*, 1999, **32**, 24, 8046.

152. D.L.Wilson, *British Polymer Journal*, 1988, **20**, 405.

153. P.L. Dynes, T.T. Liao, C.L. Hammermesh and E.E. Witucki in *Polyimides: Synthesis, Characterisation and Applications*, Ed., K.L. Mittal, Plenum, New York, NY, USA, 1984, 311-326.

154. K.C. Chuang, R.D. Vannucci, I. Ansari, L.L. Cerny and D.A. Scheiman, *Journal of Polymer Science: Polymer Chemistry Edition*, 1994, **32**, 1341.

155. H.G. Rogers, R.A. Gaudiana, W.C. Hollinsed, P.S. Kalyanaraman, J.S. Manello, C. Mcgrown, R.A. Minns and R. Sahatjian, *Macromolecules*, 1985, **18**, 1058.

156. W. Hatke, H.W. Schmidt and W. Heitz, *Journal of Polymer Science: Polymer Chemistry*, 1991, **29**, 1387.

157. C.A. Pryde, *Journal of Polymer Science: Polymer Chemistry Edition*, 1989, **27**, 711.

158. I.K. Varma, *Polymers and Composites - Recent Trends*, IBH, Oxford, UK, 1989.

159. M.A. Meador, J.C. Johnston and P.J. Cavano, *Macromolecules*, 1997, **30**, 515.

160. A.C. Wong and W.M. Ritchey, *Macromolecules*, 1981, **14**, 825.

161. Y. Liu, X.D. Sun, X.Q. Xie and D.A. Scola, *Journal of Polymer Science: Polymer Chemistry Edition*, 1998, **36**, 2653.

162. H.R. Lubowitz in *Proceedings of the 31st ACS Division of Organic Coatings and Plastics Chemisty Conference*, 1971, p.560.

163. R.W. Lauver, *Journal of Polymer Science*, 1979, **17**, 2529.

164. N. Odagiri, T.M. Yamashita and K. Toburko in *Proceedings of the 3rd Japan-US Conference on Composite Materials*, Tokyo, Japan, 1986, p.53.

165. D. Wilson, J.K. Wells, J.N. Hay, D. Lind, G.A. Owens and F. Johnson, *SAMPE Journal*, 1987, **18**, 242.

166. K.D. Farnsworth, R.N. Manepalli, S.B. Allen and P.A. Kohl, *International Journal of Microcircuits and Electronic Packaging*, 2000, **23**, 162.

167. K.D. Farnsworth, R.N. Manepalli, S.B. Allen and P.A. Kohl, *IEEE Transactions on Components and Packaging Technology*, 2001, **24**, 474.

168. M. Chanda and S.K. Roy, *Plastic Technology Handbook*, 3rd Edition, Marcel Dekker, New York, NY, USA, 1997, Chapter 4, p.638.

169. K. Okamoto, *Journal of Photopolymer Science and Technology*, 2003, **16**, 247.

170. N. Asano, M. Aoki, S. Suzuki, K. Miyatake, H. Uchida and M. Watanabe, *Journal of the American Chemical Society,* 2006, **128**, 1762.

171. G. Meyer, G. Gebel, L. Gonon, P. Capron, D. Marscaq, C. Marestin, and R. Marcier, *Journal of Power Sources*, 2006, **157**, 293.

172. M. Aoki, N. Asano, K. Miyatake and H. Uchida and M. Watanabe, *Journal of the Electrochemical Society*, 2006, **153**, A1154.

173. Y. Xu, C. Chen, P. Zhang, B. Sun and J. Li, *Journal of Chemical Engineering*, 2006, **51**, 1841.

174. J.Y. Do, S.K. Park, J.J. Ju, S. Park and M.H. Lee, *Optical Materials*, 2004, **26**, 223.

175. J.J. Ju, S.K. Park, S. Park, J. Kim, M.S. Kim and M.H. Lee, *Applied Physics Letters,* 2006, **88**, 241106.

176. *Advanced Thermoset Composites: Industrial and Commercial Applications*, Ed., J.M. Margolis, Van Nostrand Reinhold Co, New York, NY, USA, 1986.

177. H.N. Cole and W.F. Gruber, inventors; DuPont, assignee; US 3,127,414, 1964.

178. A. Nagai, A. Takahashi, M. Suzuki and A. Mukoh, *Journal of Applied Polymer Science*, 1992, **44**, 159.

179. H. Stenzenberger, *Journal of Applied Polymer Science*, 1973, **22**, 77.

180. J.V. Crivelo, *Journal of Polymer Science: Polymer Chemistry Edition*, 1973, **11**, 313.

181. I.K.Varma, Sangita and D. Ralli, *Polymer News*, 1987, **12**, 294.

182. I.K. Varma, A.K. Gupta and Sangita, *Journal of Polymer Science: Polymer Letters Edition*, 1982, **20**, 621.

183. I.K. Varma, A.K. Gupta, Sangita and D.S. Varma, *Journal of Applied Polymer Science*, 1983, **28**, 191.

184. I.K. Varma and S. Sharma, *European Polymer Journal*, 1984, **20**, 1101.

185. I.K. Varma and D.S. Varma, *Journal of Polymer Science: Polymer Chemistry Edition*, 1984, **22**, 1419.

186. K.Sripadaraj, N. Gupta and I.K. Varma, *Die Angewandte Makromolekulare Chemie*, 1998, **260**, 41.

187. H. D. Stenzenberger, *Advances in Polymer Science*, Springer Verlag, Berlin, Germany, 1994, **117**, 165.

188. Y. Li, L. Feng and L.C. Zhang, *Journal of Applied Polymer Science*, 2006, **100**, 593.

189. J.D. He, J. Wang and S.D. Li, *Acta Polymerica Sinica*, 2000, **5**, 559.

190. J.M.B. Rienda, *Journal of Macromolecular Science Chemistry*, 1977, **11**, 267.

191. E. Grigat and R. Putter, inventors; no assignee, DE 1,195,746, 1963.

192. *Chemistry and Technology of Cyanate Ester Resins*, Ed., I. Hamerton, Blackie Academic & Professional, Chapman & Hall, London, UK, 1994.

193. T. Fang and D. Shimp, *Progress in Polymer Science*, 1995, **20**, 61.

194. D. Shimp, *Polymeric Materials: Science and Enginmeering*, 1994, **70**, 561.

195. J.C. Abed, R. Mercier and J.E. McGrath, *Journal of Polymer Science: Part A Polymer Chemistry Edition*, 1997, **35**, 977.

196. S. Das and C.D. Prevorsek, inventors; Allied-Signal Inc., assignee; US 4,831,086, 1989.

197. A.W. Snow and L.J. Buckley, *Macromolecules*, 1997, **30**, 394.

198. M. Delucchi, S. Turri, A. Barbucci, M. Bassi, S. Novelli and G. Cerisola, *Journal of Polymer Science Part B: Polymer Physics Edition*, 2002, **40**, 1, 52.

199. G. Liang and M. Zhang, *Journal of Applied Polymer Science*, 2002, **85**, 2377.

200. T. Iijima, S. Katsurayana, W. Fukuda and M. Tomoi, *Journal of Applied Polymer Science*, 2000, **76**, 208.

201. J. Fan, X. Hu and C.Y. Yue, *Journal of Polymer Science Part B: Polymer Physics Edition*, 2003, **41**, 1123.

202. M. Laskoski, D.D. Dominguez and T.M. Keller, *Journal of Materials Chemistry*, 2005, **15**, 1611.

203. C.P.R. Nair, D. Mathew and K.N. Ninan, *European Polymer Journal*, 2001, **37**, 315.

204. H. Parvatareddy, P.H.T. Wilson and D.A. Dillard, *Composites Science and Technology*, 1996, **56**, 1129.

205. S.J. Ising and D.A. Shimp in *Proceedings of the SAMPE 34th International Symposium*, Reno, NV, USA, 1989, p.1326.

206. D.A. Shimp, J.R. Cristenson and S.J. Ising, *Cyanate Ester Resins - Chemistry, Properties and Applications*, Technical Bulletin, Ciba, Ardsley, NY, USA, 1991.

207. S. Robitaille in *MIL-17 - The Composite Materials Handbook*, Volume 2, ASTM International, West Conshohocken, PA, USA, 2002, p.126.

208. S.A. Srinivasan, J.C. Abed and J.E. McGrath, *Polymer Preprints*, 1994, **359**, 537.

209. B.S. Kim, *Journal of Applied Polymer Science*, 1997, **65**, 85.

210. G. Liang, M. Zhang, *Journal of Applied Polymer Science*, 2002, **85**, 2377.

3 Epoxy Resins

Epoxy resins are oxirane-containing oligomers, which cure through the reaction of epoxide groups with a suitable curing agent. The first production of epoxy resin occurred simultaneously in Europe and in the United States in the early 1940s. Today, a wide variety of epoxy resins of varying consistency are available.

Epoxy resins are unique among all the thermoset resins due to several factors [1–3]: minimum pressure is needed for fabrication of products normally used for thermosetting resins; cure shrinkage is much lower and hence lower residual stress in the cured product than that encountered in the vinyl polymerisation is used to cure unsaturated polyester resins; use of a wide range of temperatures by judicious selection of curing agents enables good control over the degree of crosslinking; and availability of the resin ranging from low viscous liquid to tack-free solids. Because of these unique characteristics and useful properties of the network polymers, epoxy resins are widely used [4, 5] in structural adhesives, surface coatings, engineering composites, and electrical laminates. Most of the composite applications utilise conventional difunctional epoxy as a matrix. However, many high-performance applications such as aerospace and critical defence applications require incorporation of epoxies of higher functionality, known as multifunctional epoxies. Tri- and tetrafunctional epoxy resins are available commercially. The chemical structures of difunctional and multifunctional epoxies are shown in **Figure 3.1** and the physicochemical properties of the resins are given in **Table 3.1**.

Table 3.1 Physicochemical properties of difunctional and multifunctional epoxy resins

Epoxy resin	Viscosity (Pa-s)	Epoxy equivalent (g/eq)	Functionality (eq/mol)
DGEBA	3.5	190	2
TGAP	0.6	95	3
TGDDM	94.5	100	4

DGEBA: Diglycidyl ether of bisphenol A
TGAP: Triglycidyl *p*-amino phenol
TGDDM: Tetraglycidylether of 4,4′ diaminodiphenyl methane

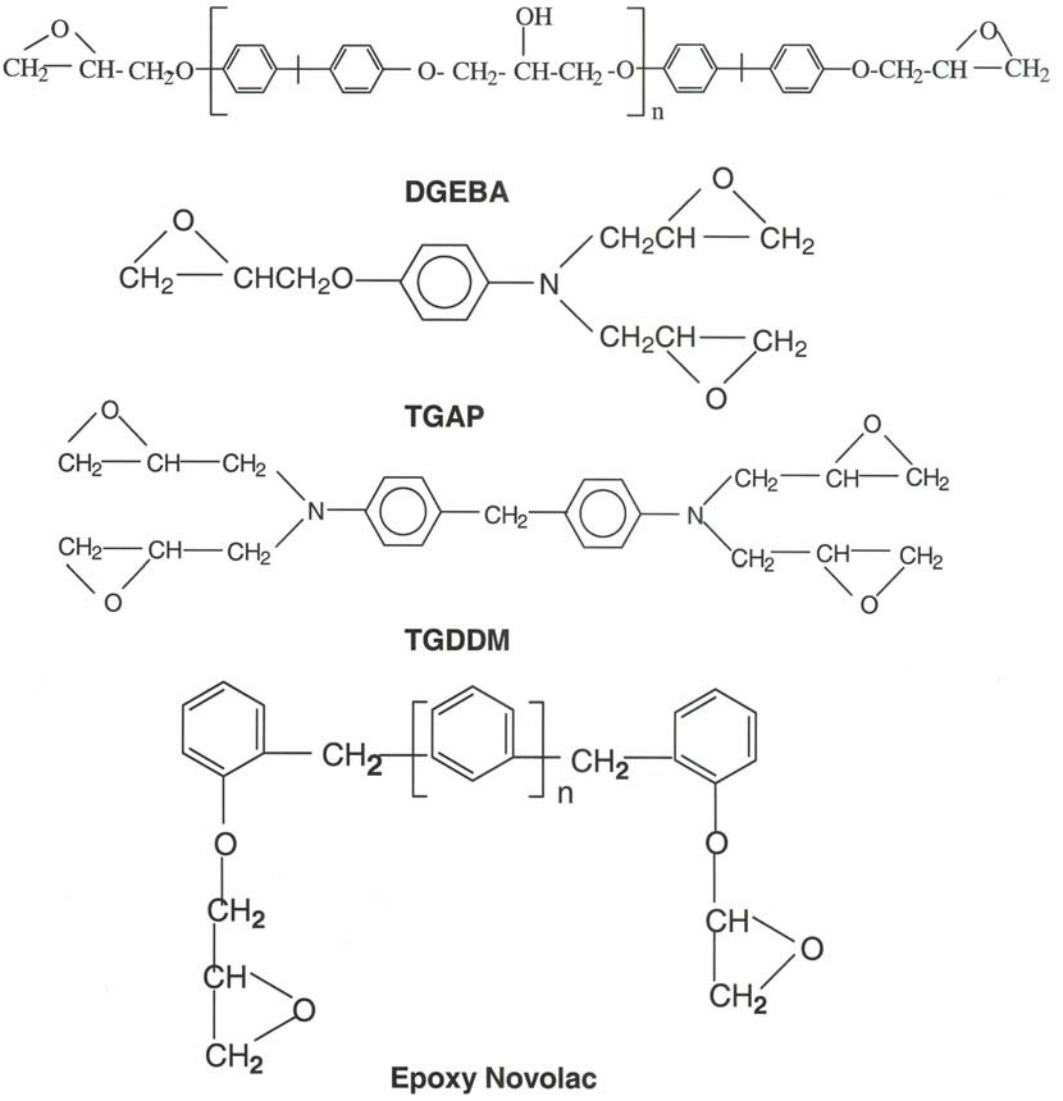

Figure 3.1 Chemical structures of difunctional and multifunctional epoxies.

3.1 Analysis and Characterisation of Epoxy Resins

3.1.1 Determination of Epoxy Equivalent

Epoxy resins are characterised by two or more epoxy groups in the structure. To cure an epoxy resin with a suitable hardener, accurate estimation of epoxy groups is crucial. 'Epoxy equivalent' is defined as the amount of resin that contains one mole of epoxy. Epoxy equivalent of an epoxy sample is determined by a standard titration method [6] using hydrogen bromide solution in acetic acid. The method is briefly described next.

About 100 mg of anhydrous sodium carbonate, 20 ml of chlorobenzene and 10 ml of glacial acetic acid are taken in an Erlenmeyer flask and magnetically stirred until all the carbonate dissolves. Four drops of 0.1% solution of crystal violet in acetic acid are added. The purple-coloured solution is titrated with hydrogen bromide solution (prepared by diluting about 6 ml of commercial reagent with 250 ml of acetic acid). The titre value is noted at the blue–green end point. About 300 mg of epoxy sample is titrated in a similar way. A blank titration is also carried out without any sample.

The epoxy equivalent (Z) is calculated from the following formula:

$$Z = W \times 53 \times V/(Vs - V0) \times Wp \tag{3.1}$$

where W, W_P are the weight (g) of sodium carbonate taken and the same for the sample, V and V_s are the volume of HBr/CH_3COOH solution required for titration of Na_2CO_3 and the same for the sample, in ml and V_0 is the blank titre value in ml.

3.1.2 Spectroscopic Characterisation

Epoxy resins are characterised by Fourier transform infrared (FT-IR) and nuclear magnetic resonance (NMR) spectroscopic analysis. Detailed description of various spectroscopic analyses has already been discussed in Chapter 1. In FT-IR spectra, peaks at 890 cm^{-1} to 910 cm^{-1} are attributed to an epoxy group. A hydroxyl group is indicated by a broad band at 4000 cm^{-1}. The characteristic proton NMR peaks for epoxy resin appear at 2.8–3.2 ppm.

3.1.3 Solubility Parameter

Solubility parameter is an important parameter to assess the compatibility of epoxy resin with an additive or modifier. Several modifiers and additives must be added with an epoxy resin to qualify the resin for diverse applications. Solubility parameter (δ) is defined as a square root of cohesive energy density [7]. Cohesive energy density is the amount of energy needed to completely remove unit volume of molecules from their neighbours to infinity, which is equal to the enthalpy of vapourisation divided by the molar volume. Thus the solubility parameter of small compounds or solvent can be determined easily from the corresponding heat of vapourisation data available in the literature. However, macromolecules mostly degrade before vapourisation, which is why the solubility parameter of a polymer is determined indirectly by examining its solubility or swelling efficiency in solvents using the 'like dissolves like' principle. Theoretically, the solubility parameters can be determined by van Kravelen's group contribution method [8]. Hansen [9] considered the contribution of three interaction forces (London dispersion force, polar force, H-bonding interaction) and introduced the concept of three-dimensional (3D) solubility parameters, δ_p, δ_p, and δ_h, corresponding to the three interactions. The overall solubility parameter can be expressed as follows:

$$\delta = \sqrt{\delta_d{}^2 + \delta_p{}^2 + \delta_h}^2 \tag{3.2}$$

Solubility parameters are determined by Hansen's iteration method from the 3D solubility parameters of the solvents in which the polymer is miscible [9, 10]. In this method, solubility of the polymer in various solvents is initially examined. The plots of the 3D solubility parameters of the solvents (available in the literature [8]) give a 3D spherical space, called 'Hansen's space'. If the distance between any two points is measured by a computation method, then the straight line connecting the two points situated at the longest distance will represent the diameter of the sphere, and the center of the sphere will represent the 3D solubility parameter of the polymer.

3.2 Epoxy Formulation

An epoxy formulation must contain a suitable curing agent and some optional ingredients, which are decided after considering the application in which the resin is going to be used. Examples of such ingredients are diluents, fillers or extenders. Diluents are used in an epoxy formulation to reduce the viscosity or to eliminate the need of solvents. Depending on the interaction of the diluents with the epoxy, diluents are grouped into two types: reactive diluents and non-reactive diluents. Reactive diluents are monoepoxide compounds, which participate in the curing reaction and

reduce the crosslink density. However, the addition of diluent is generally associated with a reduction in mechanical strength, modulus and glass transition temperature (T_g). Therefore, the amount of diluent must be optimised by critically analyzing the thermomechanical properties while keeping the technical specification for a particular application in mind. Common diluents and curing agents are presented in **Table 3.2**.

Table 3.2 Common curing agents and diluents for epoxy resins

Curing agent	Non-reactive diluent	Reactive diluent
Triethylene tetramine (TETA) 4,4´ Diaminodiphenyl methane (DDM) 4,4´ Diaminodiphenyl sulfone (DDS) Dicynamide (Dcy) Diethyl toluene diamine (DETDA) Pthalic anhydride Hexahydropthalic acid anhydride Dicyclopentadiene dianhydride Melltic anhydride	Dioctyl phthalate Nonyl phenol Dibutyl phthalate Furfuryl alcohol Pine oil Coal tar Castor oil	Diglycidylether of 1,4 butane diol Epoxidised soybean oil Epoxidised castor oil Diglycidyl ether of neopentyl glycol Butyl glycidyl ether 2-Ethylhexyl glycidyl ether Phenyl glycidyl ether *t*-Butyl glycidyl ether *o*-Cresyl glycidyl ether

3.2.1 Curing Agents

Due to the versatility of epoxy resins towards a wide variety of chemical reactions, epoxy resins can be cured using a range of materials with different types of curing conditions. The choice of curing agents (also called 'hardeners') depends on the curing conditions applicable and the final application of the resin. Epoxies can be cured with amines, thiols, and alcohols [2, 3]. The reaction proceeds through the cleavage of the oxirane ring through a nucleophillic addition reaction (**Figure 3.2**). Due to the involvement of an addition reaction, no volatile byproducts are formed during the curing of epoxy resins. Because the reactions of the epoxy monomers with the respective hardener are sometimes not fast enough for a specific application, accelerators are often added to the resin formulations. Lewis acids are used for

accelerating the reaction between an epoxy and an alcohol. The mechanism is shown in **Figure 3.3**. Similarly, alcohols, phenols or carboxylic acids are used as accelerators in amine-cured epoxies, and tertiary amines (e.g., benzyldimethylamine) are usually used in anhydride-cured epoxy systems.

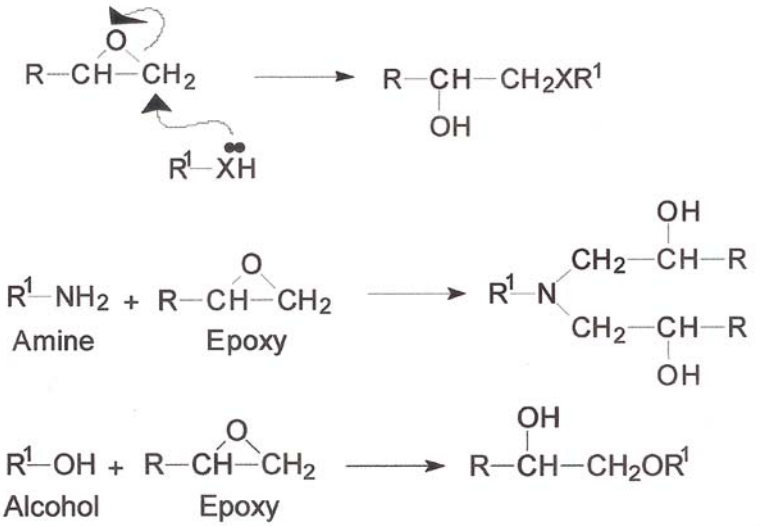

Figure 3.2 Mechanism of curing of epoxy resins.

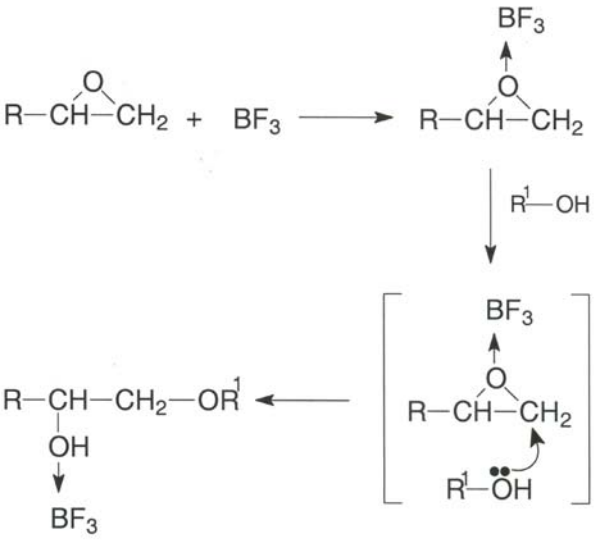

Figure 3.3 Mechanism of Lewis acid-catalysed curing of epoxy by alcohol.

Amines are widely used as hardeners for epoxy resins. The chemical structures of some commonly used amine curing agents are shown in **Figure 3.4**. During the curing reaction, two epoxy rings react with a primary amine (**Figure 3.2**). The first step is the reaction between the primary amine hydrogen with the epoxy group, followed by a reaction between the secondary amine hydrogen with another epoxy. Although a single activation energy and heat of reaction are experimentally obtained for both steps, the reactivities of primary and secondary amino groups may be different. The hydroxyl groups generated during the cure can also react with the epoxy ring, forming ether bonds (etherification). The etherification reaction competes with the amine–epoxy cure when the reactivity of the amine is low or when there is an excess of epoxy groups. The tendency of the etherification reaction to occur depends on the temperature and basicity of the diamines, and increases with the concentration of epoxy in the mixture. Secondary alcohols (continuously formed during cure) also catalyse the amine–epoxy reactions; this is called 'autocatalysis'. Thus the curing reaction occurs by two competitive mechanisms: an autocatalytic reaction (catalysed by the hydroxyl groups initially present in the epoxy prepolymer or those generated during the reaction) and a non-catalytic mechanism, which is second order in nature. The autocatalytic mechanism involves a ternary transition complex (**Figure 3.3**). At high temperature, the catalytic mechanism almost vanishes due to the difficulty of forming such a ternary complex. The second-order non-catalytic reaction takes place over the entire range of temperature. The kinetic equations are not discussed here because they have been stated in Chapter 1 for thermosets in general and are also applicable for epoxy resins.

Amines used for curing epoxy resins can be grouped into three categories: aliphatic, cycloaliphatic, and aromatic. The advantages and disadvantages of various amines are summarised in **Table 3.3**. The reactivity of the amine increases with its nucleophilic character: aliphatic > cycloaliphatic > aromatic. Thus, appropriate curing temperatures and catalysts (called 'accelerators') must be employed for curing. The network density of the cured resin can be adjusted by careful choice of chemistry and stoichiometry of the epoxy monomer and amine hardener. Increasing functionality combined with a low molecular mass of the components results in a highly crosslinked network.

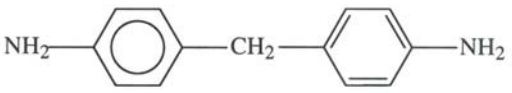

Diamino diphenyl methane (DDM)

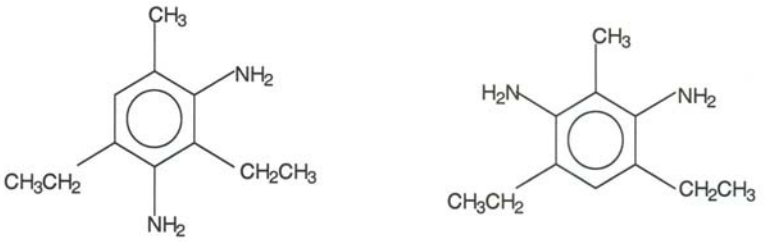

Diethyl toluene diamine (DETDA)

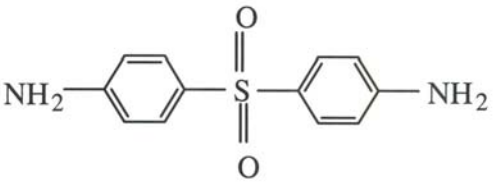

Diamino diphenyl sulfone (DDS)

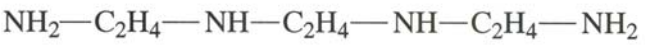

Triethylene tetramine (TETA)

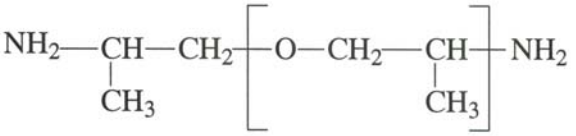

Jeffamine

Figure 3.4 Chemical structures of commonly used amine curing agents.

Table 3.3 Comparison of the properties of different types of curing agents for epoxy		
Type	**Advantage**	**Limitation**
Aliphatic amine	Low cost, low viscosity, easy to mix, room temperature-curing, fast reacting	High volatility, toxicity, short pot life, cured network can work up to 80 °C but not above
Cycloalipatic amine	Room temperature-curing, convenient handling, long pot life, better toughness and thermal properties of the resulting network compared with aliphatic amine-cured network	High cost, can work at a service temperature <100 °C poor chemical resistance poor solvent resistance
Aromatic amine	High T_g, better chemical resistance and thermal properties of the resulting network compared with aliphatic- and cycloaliphatic amine-cured network	Mostly solid, difficult to mix, Curing requires elevated temperature
Anhydride	High network T_g compared with amine curing agent, very good chemical and heat resistance of the resulting network	High temperature curing, long post-curing, necessity of accelerator, sensitive to moisture
Dcy	Low volatility, improved adhesion, good flexibility and toughness	Difficult to mix, high temperature curing and long post-curing
Polysulfide	Flexibility of the resulting network, fast curing	Poor ageing and thermal properties, odor
Polyamides	Low volatility, low toxicity, room temperature-curing, good adhesion, long pot life, better flexibility and toughness of the resulting network compared with aliphatic amine-cured networks	Low T_g of the resulting network, high cost and high viscosity

The advantage of aliphatic amines is that they can cure epoxy resins at ambient temperature. Other amines mostly require heat curing. Heat curing is difficult and impractical for fabrication of certain structures, and requires a significant amount of energy. Ambient curing saves energy and is advantageous for coating or adhesive

applications with intricate structures. Although the curing takes place at room temperature, for completion of the curing reaction it is necessary to post-cure at a high temperature. In this context, it is relevant to discuss the differential scanning calorimetry (DSC) analysis of a room temperature-curable epoxy/triethylene tetramine (TETA) system as reported by Ratna and co-workers [11]. The DSC thermogram of the epoxy/TETA system cured at room temperature for two days is shown in **Figure 3.5**. It shows a residual exotherm, indicating that the curing reaction is not complete. The same sample when post-cured at 100 °C for 2 hours showed no residual exotherm, indicating completion of the curing reaction.

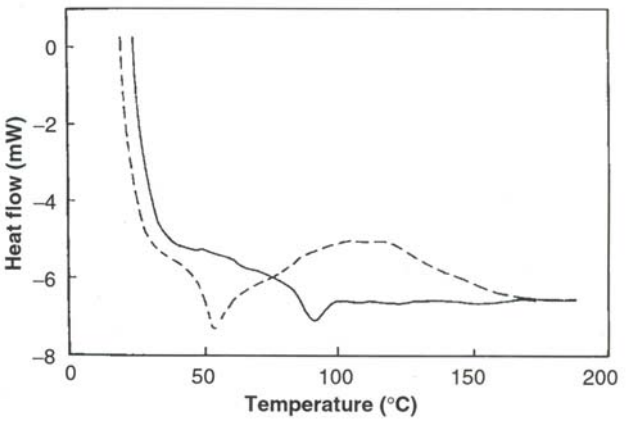

Figure 3.5 DSC thermogram of room temperature-curing epoxy (---) before and (-) after post-curing.

The major limitation of aliphatic amine-cured epoxy is that it cannot provide a network system with a T_g >120 °C [12]. To make an epoxy network with a high T_g, it is necessary to use aromatic amines, which require curing at high temperature [13, 14]. Epoxies cured with aromatic diamines can withstand high temperatures and are often used in structural composites. Reydet and co-workers [15] investigated the curing of epoxy using diaminodiphenyl methane (DDM), diaminodiphenylsulfone (DDS), 4,4´-methylenebis[2,6 diethyl aniline] (MDEA) and 4,4´-methylenebis [3-chloro 2,6-diethylaniline] (MCDEA). The evolution of epoxy conversion with time at 135 °C for epoxy/DDS, epoxy/MDEA and epoxy/MCDEA are shown in **Figure 3.6**. The conversion *versus* time plots for epoxy/DDS and epoxy/MCDEA at different temperatures are shown in **Figure 3.7**. The gelation (indicated by an arrow) time increases in the order MDEA>DDS>MCEDA. The reactivity of the amines can be explained in terms of basicity and steric hindrance. DDM is much more reactive

than the amine mentioned above. This is why kinetic characterisation of the epoxy/DDM system is very difficult. The reactivity decreases comparatively in MDEA due to steric hindrance. Due to the presence of an electron-withdrawing sulfone group, DDS is less reactive than MDEA. MCDEA is the least reactive due to the combined effects of steric hindrance as well as the electron-withdrawing effect of chlorine in the structure.

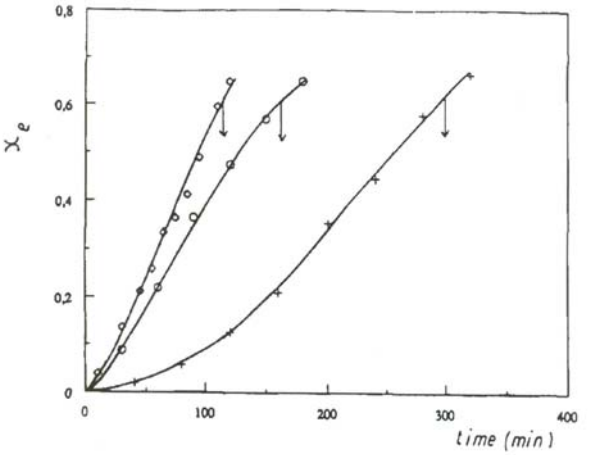

Figure 3.6 Epoxy conversion ***versus*** reaction time at 135 °C for different comonomers: (◊) DGEBA-MDEA; (0) DGEBA-DDS; (+) DGEBA-MCDEA. Arrows indicate gelation times. Reprinted with permission from E.G. Reydet, C.C. Riccardi, H. Sautereau and P.J. Pascault, *Macromolecules*, 1995, 28, 23, 7599 © 1995, American Chemical Society

After the amines, acid anhydrides are the next commonest hardeners for the curing of epoxy monomers. These epoxy systems are widely used for castings, especially in electronic applications. They find applications in circuit boards, as encapsulating material for integrated circuits, and as insulators in power current components. In contrast to the stepwise nature of the amine–epoxy cure, the acid anhydride–epoxy reaction proceeds via a chain-wise polymerization. This comprises an initiation by Lewis bases, propagation and termination or chain transfer steps. Some of the postulated reactions are shown in **Figure 3.8**. Initiation involves ring-opening of an epoxy monomer by a tertiary amine (the most widely used Lewis base), yielding zwitterions which contain a quaternary nitrogen cation and an active anion. The anion attacks an anhydride group at a very fast rate, leading to a species bearing a carboxylate anion as the active site. This ester is considered to be the initiator of the chain-wise polymerisation. The amount of Lewis base initiator determines the

number of active sites. The initiating species then reacts with an epoxy group, leading to an alkoxide species, which again attacks a cyclic anhydride. Propagation occurs through the alternating copolymerisation of epoxy and acid anhydride groups. The strictly alternating copolymerisation yielding polyesters has been confirmed by several studies [16]

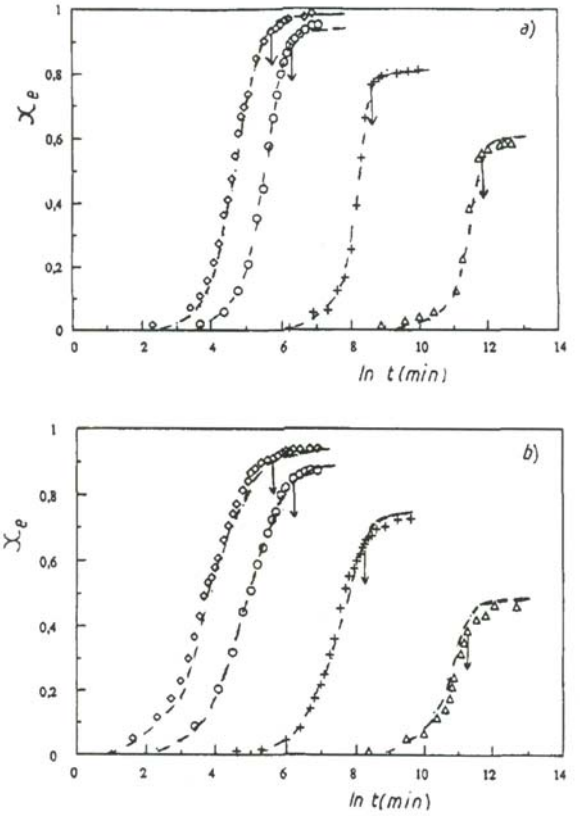

Figure 3.7 Epoxy conversion ***versus*** reaction time at different cure temperatures: (◊) 160 °C; (*0*) 135 °C; (+) 80 °C; (Δ) 30 °C; (- - -) diffusion model predictions. For (a) DGEBA-MCDEA; (b) DGEBA-DDS. Arrows (4) indicate vitrification times. Reprinted with permission from E.G. Reydet, C.C. Riccardi, H. Sautereau and P.J. Pascault, *Macromolecules*, 1995, 28, 23, 7599 © 1995, American Chemical Society

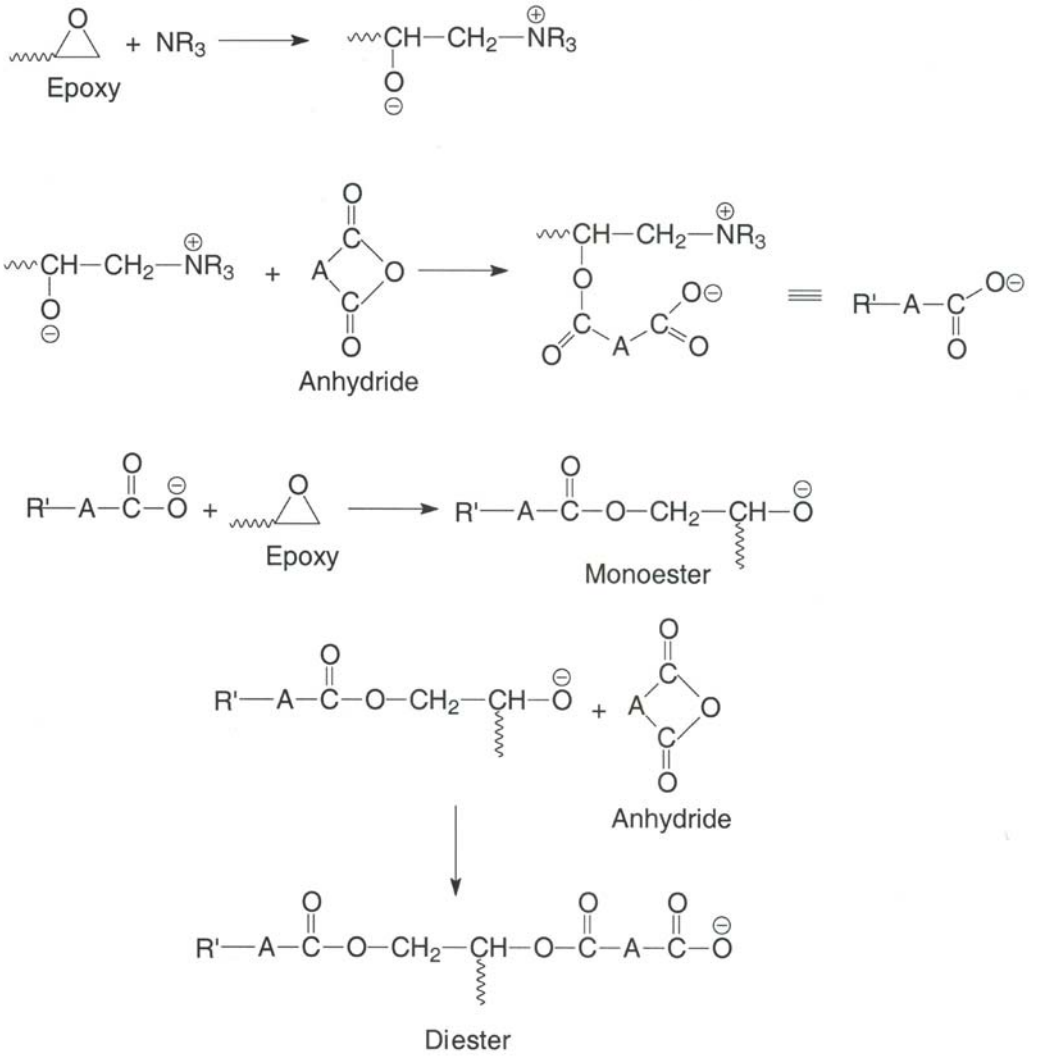

Figure 3.8 Mechanism of curing of epoxy using an anhydride.

3.3 Gelation and Vitrification

Effective use of a thermosetting system requires prediction of the cure kinetics of the system [17] to consistently obtain the maximum T_g and also to predict the flow behaviour of the curing resin, in particular to precisely locate when the sol–gel transition occurs. This is because the polymer can be easily shaped or processed only before the gel point, where it can still flow and can be easily formed with stresses applied relaxed to zero thereafter. Accurate knowledge of the gel point would therefore allow estimation of the optimum temperature and time for which the sample should be heated before being allowed to set the mould. The gel point can also be used to determine the activation energy for the cure reaction of the system [18].

The gel point of a crosslinking system is defined as the instant at which the weight-average molecular weight reaches infinity and as such is an irreversible reaction. A crosslinked polymer at its gel point is a transition state between a liquid and a solid. The polymer reaches its gel point at a critical extent of crosslinking (α_{gel}). Before the gel point, that is, $\alpha < \alpha_{gel,}$ the polymer is called a sol because it is typically soluble in appropriate solvent. Beyond gel point, that is, $\alpha > \alpha_{gel,}$ at least part of the polymer is typically not soluble in any solvent and is called a gel. Kinetically, gelation does not usually inhibit the curing process so the conversion rate remains unchanged. Hence it cannot be detected by a technique sensitive only to a chemical reaction (e.g., DSC, thermogravimetric analysis).

There are various methods to determine the gel point. Gel time for an epoxy resin is generally determined as per ASTM D3532-76. The time when the resin ceases to form strings by contact with a pick is taken as the gel point. The most sophisticated method for the determination of gel time of an epoxy system is by rheology. The basics of rheology were discussed in **Section 1.9.7**. Another process which a thermoset resin undergoes during cure is vitrification. It is defined as the point at which the T_g of the network has become identical to the cure temperature. At this point, material is transformed from a rubbery gel to a gelled glass.

Ratna and co-workers [19] compared the chemorheology of diglycidylether of bisphenol A (DGEBA), triglycidyl *p*-amino phenol (TGAP), and tetraglycidylether of 4,4 diaminodiphenyl methane (TGDDM) cured with diethyltoluene diamine (DETDA). Rheological measurements carried out with a controlled stress rheometer using a parallel plate assembly permitted the characterisation of the gelation and vitrification process during curing. The evolution of loss modulus (G˝) for DGEBA, TGAP and TGDDM against the curing time at 140 °C is shown in **Figure 3.9**. The point at which a clear increase in G˝ occurs is defined as a gel point, and G˝ maximum is defined as a vitrification point. It is evident from Figure 3.9 that TGAP and TGDDM show gelation and vitrification (loss modulus maximum), whereas for DGEBA the vitrification is not clear. This supports the work of Gilham [20] using

torsional brained analysis, which showed that vitrification is not necessarily observed because it can depend upon cure temperature and reaction kinetics. They found that at higher cure temperatures the time to vitrify increases relative to gelation, whereas the loss modulus peak becomes less intense until it reaches a point where it is so diffuse that it is not readily observed. Conversely, Varlay and co-workers [21] carried out flexural braid analysis of the highly crosslinked epoxy systems such as TGAP/DDS, and showed that vitrification always occurs soon after the gelation.

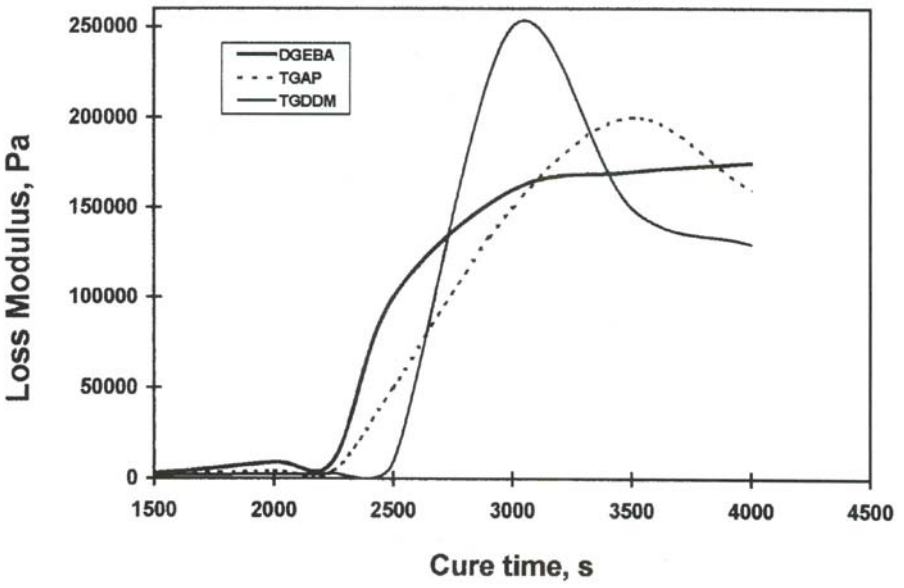

Figure 3.9 Evolution of loss modulus ***versus*** cure time at 140 °C (measured using a parallel plate rheometer). Reprinted with permission from D. Ratna, R. Varley and G.P. Simon, *Journal of Applied Polymer Science*, 2004, 92, 1604 © 2004,John Wiley and Sons Publishers

Gel point conversion is inversely proportional to the functionality of a monomer [22]. Hence the gel time is expected to decrease from DGEBA to TGDDM with increasing functionality of the resin. However, a reverse trend was reported by Ratna and co-workers [19] in their comparative study. The tetrafuntional resin (TGDDM) gels later compared with a difunctional resin (DGEBA). This is because epoxy resins are basically prepolymers, and their initial viscosity and increase in viscosity during curing have an important role in controlling the rate of the curing reaction. An increase in viscosity of the medium retards the chemical reaction attributed to the restricted molecular mobility. The increase in viscosity during cure is higher in the case of resins with a higher functionality. This explains why TGDDM gels later than TGAP and DGEBA.

Beyond gelation the system becomes highly viscous and then functionality rather than viscosity controls the curing, and thus TGDDM vitrifies sooner than TGAP (trifunctional epoxy). The maximum loss modulus value of TGDDM was found to be higher than that of TGAP. This can be explained in terms of the chemical structures of TGAP and TGDDM (**Figure 3.1**). The molecular weight between crosslinks (M_c) for the TGAP network is lower than that for the TGDDM network.

Gelation and vitrification are more clearly determined from a loss factor plot, as shown in **Figure 3.10** for a trifunctional epoxy (TGAP/DETDA) system [23]. This experiment clearly demonstrates the time required for curing an epoxy system at a particular temperature to get a required T_g can be quantitatively estimated. This is very important for the development of prepregs. When the T_g of the cured system reaches the cure temperature, the curing reaction becomes very slow. This is why when a multifunctional epoxy network without a post-curing treatment at a sufficiently high temperature is subjected to a dynamic mechanical analysis, it shows two loss peaks; one is for the partially cured network and other is for the fully cured network. Hence it is very important to give appropriate post-curing treatment to an epoxy system (especially multifunctional epoxy systems) to get a network with the desired T_g.

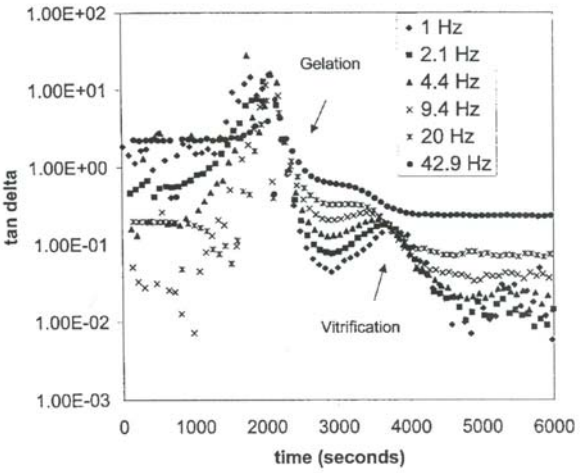

Figure 3.10 Loss factor *versus* temperature plot at various frequencies (measured using a parallel plate rheometer) showing gelation and vitrification. Reprinted with permission from D. Ratna, R. Varley and G.P. Simon, *Journal of Applied Polymer Science*, 2004, 92, 1604 © 2004, John Wiley and Sons Publishers

The different transformations observed during the cure of epoxy with a stoichimetric amount of curing agent are generally recorded in the form of a time–temperature–*trans*

formation (TTT) diagram [24, 25]. Such a diagram is built from the experimental determinations of the time to gel (t_{gel}) and the time to vitrify (t_{vit}) under isothermal conditions. Because the reaction rate varies exponentially with temperature, times are represented in a logarithmic scale. It also includes a char region which is reached after degradation at high temperatures. In a general curing procedure, the prepolymer system is employed in the liquid state. The curing temperature should range between the glass transition temperature of the gelled polymer ($T_{g,gel}$) and the glass transition temperature of the fully cured thermoset ($T_{g,\infty}$). In case of an isothermal cure, the ongoing reaction can be followed on a horizontal line in the TTT diagram. A TTT diagram for an epoxy novolac cured with a stoichiometric amount of DDS as reported by Oyanguren and Williams [26] is presented in **Figure 3.11**. The temperature at which the vitrification and gelation take place simultaneously is 65 °C. Because the reaction becomes diffusion-controlled at vitrification, the epoxy systems must be cured at a temperature >215 °C, which is the T_g of the fully cured epoxy network. Degradation may occur at high temperature, so the post-curing temperature must be set below the degradation temperature because degradation will cause a reduction in thermomechanical properties. The degradation temperature is chosen arbitrarily at 270 °C for the present system, but degradation depends on exposure time.

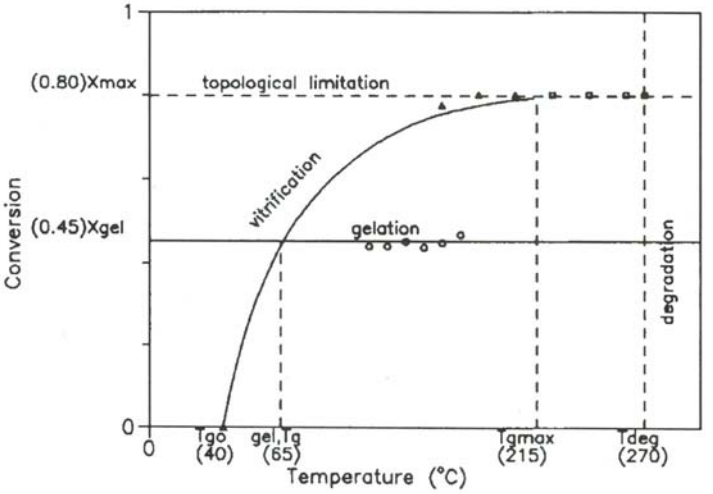

Figure 3.11 Conversion *versus* temperature transformation diagram showing conditions under which gelation, vitrification and chemical degradation take place, as well as restriction arising from topological limitations for novolac epoxy resin cured with DDS. Reprinted with permission from P.A. Oyanguren and R.J.J. Williams, *Journal of Applied Polymer Science*, 1993, 47, 1361 © 1993, John Wiley and Sons Publishers

3.4 Thermomechanical Properties

The properties of a cured epoxy network depend primarily on two factors: nature of the resin and nature of the curing agent. The functionality of an epoxy resin plays an important part in determining the thermomechanical properties. The properties of epoxy resins of various functionalities cured with DETDA are presented in **Table 3.4**. Multifunctional epoxies exhibit a higher T_g compared with the difunctional epoxy when cured with the same hardener. This is due to the increase in crosslink density as a result of an increase in epoxy functionality and the formation of a tighter network. This significantly reduces the free volume of the network, leading to an increase in the T_g.

Table 3.4 Viscoelastic properties of difunctional and multifunctional epoxies cured with DETDA [5]

Epoxy resin	E´ at RT (GPa)	T_g # (°C)	Tanδ peak temperature (°C)	Tan δ_{max}
DGEBA	1.2	195	217	0.6
TGAP	1.7	260	295	0.3
TGDDM	2.1	230	260	0.7

Temperature corresponds to the onset of modulus drop
RT: Room temperature

Positron annihilation lifetime spectroscopy (PALS) is normally applied to determine the free volume properties of a cured thermoset. The theory and methodology of PALS [27, 28] is briefly described next. The positron, an antiparticle of an electron, is used to investigate the free volume between polymer chains. The birth of the positron can be detected by the release of a gamma ray of characteristic energy. This occurs approximately 3 ps after positron emission when the ^{22}Na decays to ^{22}Ne. Once inside the polymer material, the positron forms one of the two possible types of positroniums, an *ortho*-positronium or a *para*-positronium, obtained by pairing with an electron abstracted from the polymer environment. The decay spectra are obtained by the 'death' event of the positron, *para*-positronium or *ortho*-positronium species. By appropriate curve fitting, the lifetimes of the various species and their intensity can be determined. The lifetime of an *ortho*-positronium (τ_3) and intensity (I_3) have been found to be indicative of the free volume in a polymer system because this is where the relevant species become localised. τ_3 is related to the size of the free volume sites and I_3 to their number concentration. The free volume properties of difunctional and multifunctional epoxies are shown in **Table 3.5**. The data clearly

showed a decrease in free volume as a result of increase in crosslink density due to the increase in functionality.

Table 3.5 Basic PALS data for difunctional and multifunctional epoxies cured with DETDA #		
Resin	**τ_3 (ns)**	**I_3 (%)**
DGEBA	1.76 ± 0.01	25.63 ± 0.23
TGDDM	1.69 ± 0.01	27.24 ± 0.22
TGAP	1.60 ± 0.02	26.84 ± 0.24
# taken from author's unpublished work		

The T_g of an epoxy network can be varied to a great extent by changing the hardener. The T_g values for DGEBA epoxy cured with different curing agents are shown in **Table 3.6,** which clearly demonstrates the tremendous effect of a hardener on the T_g. The adhesive property also depends on the chemistry of the hardener. The lap shear strength values of a few room temperature-curing adhesive formulations are given in **Table 3.7**. It is evident from the table that the adhesive strength of the same epoxy resin can be improved significantly by using polar curing agents [29]. The polyamide-based epoxy system offers better adhesive properties compared with amine-based hardeners. The adhesive strength can be further improved by various methods, which will be discussed in Chapter 4.

Table 3.6 Glass transition temperature (T_g) of DGEBA epoxy cured with various curing agents		
Curing agent	**T_g (°C)**	**Reference**
TETA	139	[10-12]
DDM	190	[4, 29]
DDS	189	[3, 4, 29]
DETDA	217	[13, 14]
Jeffamine-130	65	[53]
Jeffamine-800	0	[53]

Table 3.7 Bond strength data for epoxy resin and various hardener systems [29]	
Adhesive system	**Lap shear strength (MPa)**
DGEBA/TETA	3
DGEBA/Hexamethylene diamine	6
DGEBA/HY 848	7
DGEBA/HV 953u	9
HY 848 and HV 953u (Vantico) are polyamide-based hardeners	

3.5 Chiral epoxy resins

Optically active materials show a positive or negative value of specific rotation. Optical rotation is measured by using plane-polarised light with the help of a polarimeter. Epoxy resins are normally optically inactive. However, it has been demonstrated that by using a chiral monomer as starting material [30] or by introducing a chiral unit into a commercially available epoxy through chemical modification [31] an optically active resin can result. Ratna and co-workers [31] investigated the modification of epoxy with optically active L-leucine. L-leucine was modified by replacing the $-NH_2$ group with –Cl to get S-2-chloro, 4-methyl pentanoic acid (CMPA) using the dizonium salt route [32]. The reaction scheme for this modification is shown in **Figure 3.12**.

The specific rotation of CMPA is –27.32°. When CMPA is attached to an epoxy through the reaction between the –COOH group of CMPA and the epoxide group of the epoxy resin, the modified resin shows optical activity in the uncured and cured state (**Table 3.8**).

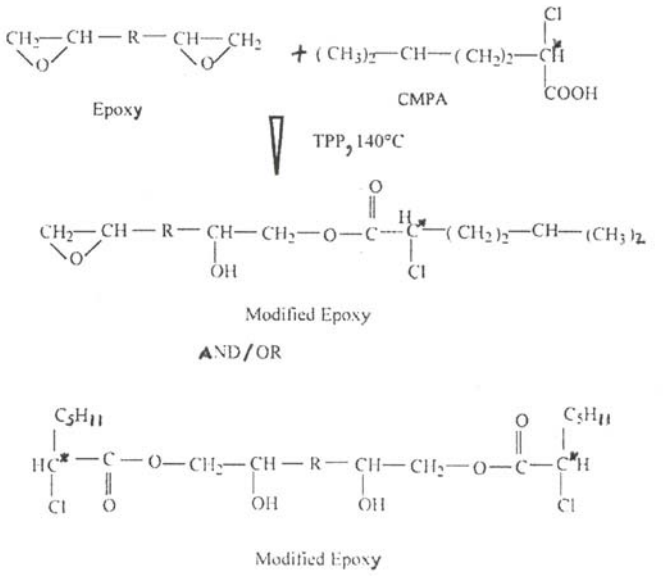

Figure 3.12 Reaction scheme for synthesis of chiral epoxy by chemical modification of DGEBA resin. Reprinted with permission from A.B. Samui, D. Ratna, J. Chavan and P.C. Deb, *Journal of Applied Polymer Science*, 2004, 92, 1604 © 2004, John Wiley and Sons Publishers

Table 3.8 Chiral properties of CMPA-modified epoxy [31]

No.	Ratio of epoxy and CMPA (mole/mole)	Specific rotation of solution $[\alpha]_D^a$ (°)	Optical rotation of film[a] α [b]
1	0.055/0	-0.004	-0.002
2	0.055/0.006	-1.52	-0.017
3	0.055/0.009	-1.61	-0.020
4	0.055/ 0.012	-1.70	-0.027
5	0.055/ 0.015	-2.23	-0.030
6	0.055/ 0.018	-4.34	--
7	0.055/ 0.026	-5.44	--
8	0.055/ 0.031	-7.61	--
9	0.055/ 0.037	-7.71	--
10	Pure CMPA	-27.32	-

[a] Film thickness was maintained at 0.7 mm
[b] Measured by polarimeter at 25 °C

3.6 Liquid crystalline epoxy

Liquid crystals exhibit a partially ordered state (anisotropic) which falls in-between the completely ordered solid state and completely disordered liquid state. It is sometimes referred to as the 'fourth state of matter'. In recent years, interest in liquid crystalline thermosets (especially liquid crystalline epoxy) has increased tremendously [33–44]. If the liquid crystal epoxy is cured in the mesophase, the liquid crystalline superstructure is fixed permanently in the polymer network, even at higher temperature. Liquid crystal epoxies are prepared using a liquid crystal monomer [33–38] or by chemical modification of epoxy resin [43] which incorporates liquid crystal unit in the epoxy structure. Liquid crystalline epoxy resins with different types of mesogen such as benzaldehyde azine [33], binaphthyl ether [34, 35], phenyl ester [36, 37] and azomethine ethers [38, 39] have been reported. Depending on the chemical nature of the mesogen, the related epoxies display a wide range of thermomechanical properties. The resins can be cured chemically with an acid or amine [40, 41] or by photochemical curing in the presence of a photo-initiator [3]. Broer and co-workers [42] demonstrated the fabrication of uniaxially oriented nematic networks from a diepoxy monomer in the presence of a photo-initiator.

Su [44] synthesised and studied main-chain thermotropic liquid crystalline thermosets based on biphenyl mesogen. They reported that the liquid crystal epoxy networks exhibited higher T_g and dielectric strength and lower thermal expansion compared with conventional epoxy networks. Recently, liquid crystal epoxy (monomers and polymers) containing photo-responsive moieties (e.g., azobenzene, stilbene, chalcone) were extensively investigated [45–47] due to their interesting photochemical and photophysical properties, which may lead to a wide range of applications. Chemically or photochemically cross-linkable epoxy groups and photo-labile –N=N– or =C units may be utilised for the fabrication of photo-aligned liquid crystalline recordable layers without the aid of an electric or magnetic field.

Liquid crystal epoxies bearing stilbine were first reported by Calundann and co-workers [45]. Ober and co-workers [46, 47] reported the synthesis and characterisation of liquid crystalline thermosets based on dihydroxy stilbene. Depending upon the molecular weight and polydispersity of the starting material, the polymers showed nematic or smectic mesophase. Carfagna and co-workers [33, 34, 48] reported the synthesis of epoxy-terminated stilbene monomer, which on curing with an amine curing agent generates smectic and nematic mesophases. They demonstrated the use of these materials in macroscopically oriented optical films [48]. When an electromagnetic field is applied to a liquid crystal epoxy sample in the uncured state, domains were oriented along a preferred direction. A subsequent crosslinking reaction 'locks' the molecules in the aligned conformation achieved

under the influence of an external field, and the structure is stabilised at the gel point. The alignment of the rigid molecular backbone remains stable over a wide range of temperature.

Choi and Cha [49] reported the synthesis of photo-crosslinkable liquid crystalline chalcone epoxy compounds for the fabrication of photo-aligned liquid crystalline layers. Photo-dimerisation and photo-polymerisation of compounds under linearly polarised ultraviolet (UV) light in the presence of a cationic photo-initiator were also reported. Koschienlny and co-workers [50] reported the synthesis of liquid crystalline azobenzene epoxy polymer, which has shown nematic mesophase having a narrow temperature range. Castell and co-workers [51] reported the synthesis of epoxy liquid crystalline monomers with azo groups in the central mesogenic core. They developed anisotropic networks of the resulting polymers by irradiation with linearly polarised light without magnetic or electric orientation by utilising photochemical cis–trans isomerisation of azobenzene moieties.

Ratna and coworker [43] synthesised liquid crystal epoxy by chemical modification of epoxy resins. Terephthaloyl chloride was reacted with 4-hydroxy benzoic acid to get terephthaloyl bis (4-oxybenzoic) acid which was characterised and further reacted with epoxy resin [diglycidyl ether of bisphenol A (DGEBA)] to get a liquid crystalline epoxy resin (LCEP). The reaction scheme is shown in **Figure 3.13**. Optical microcopy studies clearly show a smectic phase (**Figure 3.14**). The isotropisation takes place at 130 °C. LCEP can be cured in the similar way as commercially available DGEBA epoxy. The LCEP has been blended in various compositions with DGEBA and cured by using a room temperature curing hardener. The cured blends were found to show higher storage moduli and lowered glass transition temperatures (tan $\delta_{max,}$ from dynamic mechanical analysis) compared with that of the pure DGEBA network.

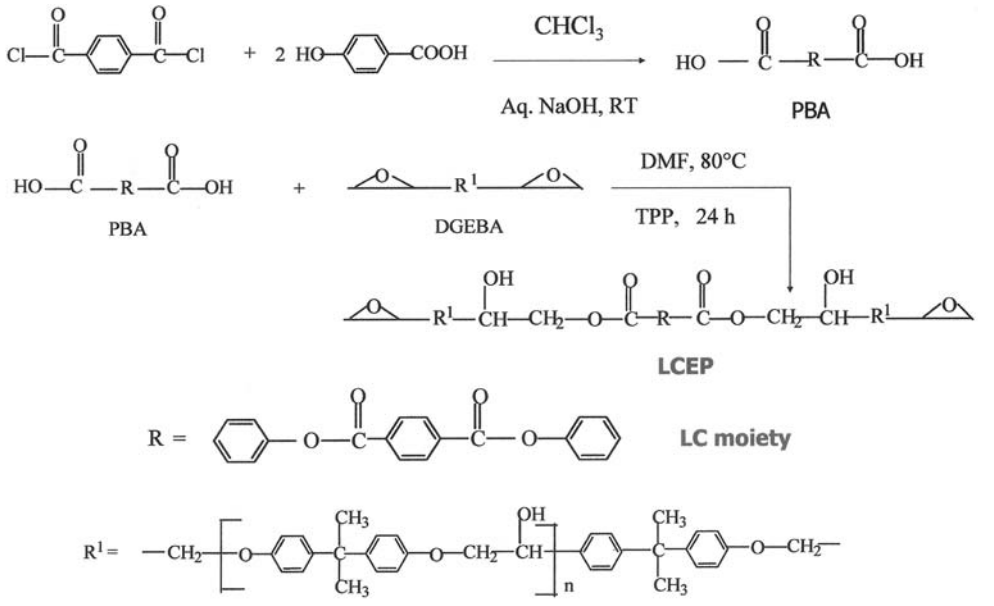

Figure 3.13 Reaction scheme for synthesis of liquid crystalline epoxy by chemical modification of DGEBA resin. Reprinted with permission from K. Sadagopan, D. Ratna and A.B. Samui, *Journal of Polymer Science Part A: Polymer Chemistry Edition*, 2003, 41, 3375 © 2003, John Wiley and Sons Publishers

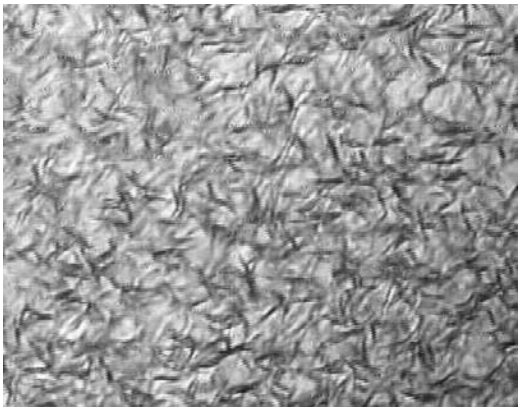

Figure 3.14 Optical microscopy photograph showing the smectic texture of liquid crystalline epoxy. Reprinted with permission from K. Sadagopan, D. Ratna and A.B. Samui, *Journal of Polymer Science Part A: Polymer Chemistry Edition*, 2003, 41, 3375 © 2003, John Wiley and Sons Publishers

3.7 Rubbery epoxy

Cured epoxy resins are usually glassy in nature because they exhibit a T_g well above room temperature [52]. However, the T_g can be reduced by using ether containing long-chain hardener, as demonstrated by Ratna and co-workers [53]. Loss factor *versus* temperature plots of epoxy networks generated by curing DGEBA epoxy with polyether amines having different chain lengths are presented in **Figure 3.15**. The corresponding thermomechanical properties are presented in **Table 3.9**. By varying the molecular weight of the polyether segment, a broad range of properties can be obtained. As expected, the T_g of the network decreases with increase in molecular weight of the polyether amine used. The decrease in the T_g is associated with a decrease in tensile strength and an increase in elongation at break. This behaviour is explained by the effect of two mechanisms: the reduction of crosslink density and the increase in the length of polyether segments. A rubbery epoxy network can therefore be made by using a polyether amine of suitable chain length.

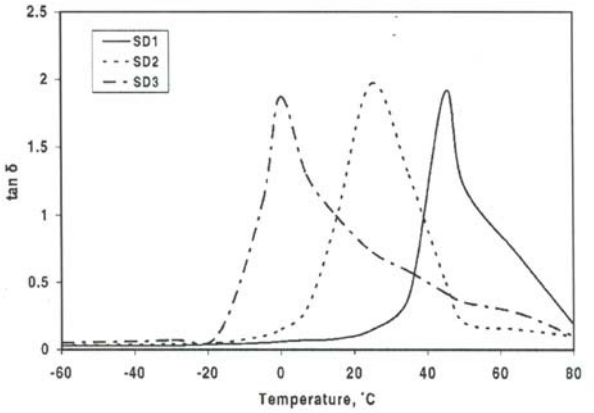

Figure 3.15 Plot of loss tangent *versus* temperature plots of epoxy networks cured with polyetheramine (Jeffemine) of various chain lengths: SD-1 (Jeff-300), SD-2 (Jeff-500) and SD-3 (Jeff-800). Reprinted with permission from D. Ratna, N.R. Manoj , L. Chandrasekhar and B.C. Chakraborty, *Polymers for Advanced Technologies*, 2004, 15, 10 , 583 © 2003, John Wiley and Sons Publishers

Table 3.9 Mechanical properties of epoxy networks cured with polyetheramine of various chain length [53]			
Epoxy network	**Molecular weight of polyether chain of Jeffamine (g/mol)**	**Tensile strength (MPa)**	**Elongation at break (%)**
SD 1	300	14.8	50
SD 2	500	2.4	75
SD 3	800	0.5	210

3.8 Applications of epoxy resin

Epoxy resins are widely used as adhesives, surface coatings, encapsulates and casting materials. They are used in industrial tooling applications to produce moulds, master models, laminates, castings, fixtures, and other industrial production aids. This 'plastic tooling' replaces metal, wood and other traditional materials, and generally improves the efficiency and lowers the overall cost or shortens the lead-time for many industrial processes. Epoxy resins are extensively used as a binder for marine paints, which is required to protect the naval structure from the corrosive marine environment.

Epoxy resins can be used as a matrix for making high-strength composites with glass, carbon and Kevlar fibers because they are chemically compatible with most substrates and tend to wet surfaces very easily. Such composites are exclusively used for aerospace applications. The aerospace industries are dominated by epoxy resins due to the excellent processability and useful properties of network polymers. This is because epoxy composites can satisfy the technical requirements of structural material for civil and military aerospace applications, namely flooring panels, ducts, wings and vertical and horizontal stabilisers. Such composites are also used to produce lightweight vehicle frames, racing cars, musical instruments, and industrial components with high strength to weight ratio.

The major use of epoxy resins is in the electronics industry. They are extensively used in motors, generators, transformers, switchgears, bushings, and insulators. Epoxy resins are excellent electrical insulators and protect electrical components from short circuiting, dust and moisture. In the electronics industry, epoxy resins are the primary resin used in moulding integrated circuits, transistors and hybrid circuits, and making printed circuit boards.

Liquid crystalline epoxies have potential applications for electro optics, acoustics, and in information technology. The rubbery epoxies exhibit very high damping factor (>1) and can be used for vibration damping applications, as discussed next.

3.8.1 Vibration damping applications

Vibration and its efficient control are a universal concern for product designers considering its occurrence in most machines, structures and dynamic systems. Vibration often leads to undesirable consequences such as unpleasant motions, noise and dynamic stresses that lead to fatigue and failure of structures, decreased reliability and degraded performance. The vibration produced in ships and submarines radiate as a noise in the sea which can be detected by the sound navigation system of enemy vessels. Hence, vibration damping application is relevant to civilian and defense sectors. Vibration damping is achieved by using a suitable viscoelastic material. Because a viscoelastic material shows maximum damping (**Section 1.9.6.2**) in the glass transition region, the damping material must be developed in such a way that the transition region covers the use temperature.

As discuused above, epoxy/polyetheramine offers the possibility to tailor mechanical and damping properties as a function of composition. Hence they can be effectively used as vibration damping materials. Epoxy-based vibration damping materials offer several technological advantages compared with rubber compound-based damping materials, such as high damping and easier application. They are naturally self-adhering and do not need extra adhesive for application.

The time–temperature superposition as discussed in **Section 1.9.6.3** is used to assess a vibration damping material because it assists in understanding the damping behaviour at very low and very high frequencies which are normally unavailable in machines. **Figure 3.16** shows the master curves of an epoxy-based damping material at three reference temperatures (0 °C, 25 °C, 50 °C). The peaks corresponding to the T_g shift gradually to the lower frequencies as the reference temperature decreases (from 100 Hz at a reference temperature of 50 °C to 10^{-7} Hz at 0 °C). Thus a material effective in damping at 50 °C may not work at ≤0 °C. For example, at 0 °C, the present damping material will have almost no damping at normal frequencies of interest (20–20,000 Hz). The frequency dependences of three damping materials with varying polyether chains (SD-1-Jeffemine-800, SD-2- Jeffemine 500, SD-3-Jeffemine 300) are presented in **Figure 3.17**. With increase in polyether chain length, the frequency corresponding to maximum damping increases. It is also necessary to consider the mode of application of the material, as discussed next.

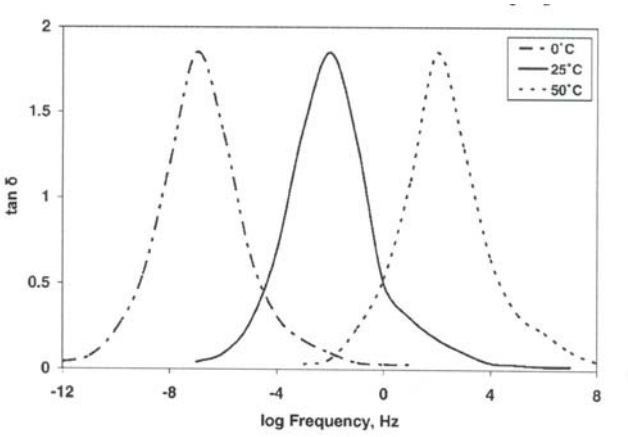

Figure 3.16 Master curves of loss tangent *versus* frequency for a rubbery epoxy at different reference temperatures. Reprinted with permission from D. Ratna, N.R. Manoj, L. Chandrasekhar and B.C. Chakraborty, *Polymers for Advanced Technologies*, 2004, 15, 10 , 583 © 2003, John Wiley and Sons Publishers

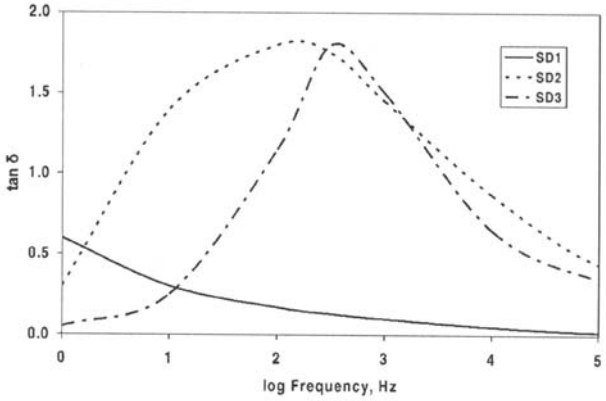

Figure 3.17 Master curve of loss tangent *versus* frequency plots of rubbery epoxy networks cured with polyetheramine (Jeffemine) of various chain lengths: SD-1 (Jeff-300), SD-2 (Jeff-500) and SD-3 (Jeff-800). Reprinted with permission from D. Ratna, N.R. Manoj, L. Chandrasekhar and B.C. Chakraborty, *Polymers for Advanced Technologies,* John Wiley and Sons Publishers, 2004, 15, 10 , 583 © 2003.

Polymers are commonly used in two different configurations to dissipate the mechanical energy of vibration as heat [54]: (i) free layer damping where energy is dissipated due to direct strains, i.e., alternate extension and compression of the viscoelastic layer; and (ii) constrained layer damping where shear strains in the viscoelastic layer cause damping of vibrations. In a constrained layer damping system, a thin layer of a viscoelastic material is applied over the vibrating substrate and covered with a stiff constraining layer such as metal or fibre reinforced plastic. Some of the applications of constrained layer damping are in aircraft and missile substructures, machinery supports, mounting platforms of electronic equipment, bridges and buildings. Though constrained layer damping treatment provides higher damping compared with free layer damping, the latter is more convenient to apply and retain damping over a wide frequency range [55]. Hence the mode of damping must be selected according to applications. For example, if the structure to be treated for vibration damping is intricate, then free layer damping is preferable compared with constrained layer damping.

In general, in constrained layer damping, polymeric sheets are used as viscoelastic materials, which are used to adhere to the substrate as well as the constraining layer. The advantages of the compositions studied are that they can be sprayed to the substrate, and secondary adhesives are not required. The strength of adhesion of epoxy materials to many substrates is essentially high. This is coupled with the high loss factor over a wide range of temperature and frequencies. Hence these materials offer less weight penalty, making it ideal for aircraft applications. More compositions can be tailor-made to suit mode and the range of application by simple blending of various epoxies and amines.

References

1. W.G. Potter, *Epoxide Resins*, Springer, New York, NY, USA, 1970.

2. C.A. May and G.Y. Tanka, *Epoxy Resin Chemistry and Technology*, Marcel Dekker, New York, NY, USA, 1973.

3. *Epoxy Resin Chemistry*, Ed., R.S. Bauer, ACS Symposium Series No.114, American Chemical Society, Washington, DC, USA, 1979.

4. H. Lee and K. Nevile, *Handbook of Epoxy Resins*, McGraw-Hill, New York, NY, USA, 1967.

5. A.B.Samui, B.C. Chakraborty and D. Ratna, *International Journal of Plastic Technology*, 2004, **8**, 279.

6. A.J. Durbetaki, *Analytical Chemistry*, 2000, **28**, 1956.

7. F.W. Billmeyer, *Textbook of Polymer Science*, 3rd Edition, Wiley, New York, NY, USA, 1984.

8. D.W. Van Krevelen, *Properties of Polymers*, Elsevier, Amsterdam, The Netherlands, 1976.

9. C. Hansen, *Hansen Solubility Parameters*, *A User's Handbook*, 2nd Edition, CRC Press, Boca Raton, FL, USA, 2007.

10. D. Ratna, M. Patri, B.C. Chakrabarty and P.C. Deb, *Journal of Applied Polymer Science*, 1997, **65**, 901.

11. D. Ratna, B.C. Chakraborty and P.C. Deb, *Journal of Polymer Materials*, 1997, **14,** 185.

12. D. Ratna and A.K. Banthia, *Polymer International*, 2000, **49**, 281.

13. D. Ratna and G.P. Simon, *Polymer Engineering and Science*, 2001, **41**, 1815.

14. D. Ratna, R. Varley and G.P. Simon, *Journal of Applied Polymer Science*, 2003, **89**, 9, 2339.

15. E.G., Reydet, C.C. Riccardi, H. Sautereau and P.J. Pascault, *Macromolecules*, 1995, **28**, 23, 7599.

16. L. Matejka, J. Lövy, S. Pokorny, K. Bouchal and K. Dušek, *Journal of Polymer Science Part A: Polymer Chemistry Edition*, **1983**, 21, 2873.

17. F. Boey and W. Qiang, *Polymer*, 2000, **41**, 2081.

18. F. Boey and W. Qiang, *Journal of Applied Polymer Science*, 2000, **76**, 1248.

19. D. Ratna, R. Varley and G.P. Simon, *Journal of Applied Polymer Science*, 2004, **92**, 1604.

20. X. Wang and J.K. Gillham, *Journal of Applied Polymer Science*, 1992, **45**, 2127.

21. R.J. Varley, D.G. Hawthorne, J. Hodgkin and G.P. Simon, *Journal of Polymer Science Part B: Polymer Physics Edition*, 1997, **35**, 1, 153.

22. P.J. Flory, *Principle of Polymer Chemistry*, Cornell University Press, Ithaca, New York, NY, USA, 1975.

23. D. Ratna, R. Varley and G.P. Simon, *Journal of Applied Polymer Science*, 2003, **89**, 2339.

24. H.E. Adabbo and R.J.J. Williams, *Journal of Applied Polymer Science*, 1982, **27**, 1327.

25. R.J.J. Williams in *Developments in Plastic Technology - 2*, Eds., A. Whelan and J. Craft, Elsevier, Barking, England, UK, 1985, 339.

26. P.A. Oyanguren and R.J.J. Williams, *Journal of Applied Polymer Science*, 1993, **47**, 1361.

27. D.M. Bigg, *Polymer Engineering and Science*, 1996, **36**, 737.

28. O. Becker, Y.B. Cheng, R.J. Varley and G.P. Simon, *Macromolecules*, 2003, **36**, 5, 1616.

29. D. Ratna, *Journal of Adhesion Science and Technology*, 2003, **17**, 12, 1655.

30. A. Hartwig, T.K. Mahato, T. Kaese and D. Wohrle, *Macromolecular Chemistry and Physics*, 2005, **206**, 1718.

31. A.B. Samui, D. Ratna, J. Chavan and P.C. Deb, *Journal of Applied Polymer Science*, 2004, **92**, 1604.

32. M. Nagata and M. Nakae, *Journal of Polymer Science Part A: Polymer Chemistry Edition*, 2001, **39**, 3043.

33. C. Carfagna, E. Amendola and M. Giamberini, *Macromolecular Chemistry and Physics*, 1994, **195**, 279.

34. C. Carfagna, E. Amendola and M. Giamberini, *Macromolecular Chemistry and Physics*, 1994, **195**, 2307.

35. C. Carfagna, E. Amendola and M. Giamberini, *Macromolecular Chemistry and Physics*, 1997, **198**, 3185.

36. D. Wohrle, A. Hartwig, G. Schnurpfeil, A. Harder and H. Schroder, *Polymers for Advanced Technologies*, 2000, **11**, 739.

37. W. Mormann and M. Brocher, *Macromolecular Chemistry and Physics*, 1994, **197**, 1841.

38. D. Ribera, A. Mantecon and A. Serra, *Macromolecular Chemistry and Physics*, 2001, **202**, 1658.

39. D. Ribera, A. Mantecon and A. Serra, *Journal of Polymer Science Part A: Polymer Chemistry Edition*, 2002, **40**, 4344.

40. S.M. Kelly, *Liquid Crystals*, 1998, **24**, 1, 71.

41. J.I. Mallon and P.A. Adams, *Journal of Polymer Science Part A: Polymer Chemistry Edition*, 1993, **31**, 2249.

42. D.J. Broer, J. Lub and G.N. Mol, *Macromolecules*, 1993, **26**, 1244.

43. K. Sadagopan, D. Ratna and A.B. Samui, *Journal of Polymer Science Part A: Polymer Chemistry Edition*, 2003, **41**, 3375.

44. W.F.A. Su, *Journal of Polymer Science Part A: Polymer Chemistry Edition*, 1993, **31**, 3251.

45. G.W. Calundann, H.A.A. Rasoul and H.K. Hall, Jr., inventors; Celanese Corporation, assignee; US 4,654,412, 1987.

46. A. Shiota and C.K. Ober, *Journal of Polymer Science Part A: Polymer Chemistry Edition*, 1996, **34**, 1291.

47. A. Shiota and C.K. Ober, *Polymer*, 1997, **38**, 5837.

48. C.Carfagna, E. Amendola and M. Giamberini, *Progress in Polymer Science*, 1997, **22**, 1607.

49. D.H. Choi and Y.K. Cha, *Bulletin of the Korean Chemical Society*, 2002, **23**, 587.

50. B. Koscienlny, A. Pfiatzmann and M. Fedtke, *Polymer Bulletin*, 1994, **32**, 529.

51. P. Castell, M. Galia and A. Serra, *Macromolecular Chemistry and Physics*, 2001, **202**, 1649.

52. D. Ratna, *Epoxy Composites: Impact Resistance and Flame Retardency*, Rapra Review Report No.185, Smithers Rapra, Shawbury, Shrewsbury, UK, 2007.

53. D. Ratna, N.R. Manoj , L. Chandrasekhar and B.C. Chakraborty, *Polymers for Advanced Technologies*, 2004, **15**, 10, 583.

54. J.D. Ferry, *Viscoelastic Properties of Polymers*, John Wiley, New York, NY, USA, 1980.

55. L.H. Sperling and J.J. Fay, *Polymers for Advanced Technologies*, 1991, **2**, 1, 49.

4 Toughened Thermoset Resins

Thermosets, because of their crosslinked structure, offer many useful properties such as high strength, good dimensional stability at elevated temperature, very low creep, solvent and water resistance. To get the desired thermomechanical properties, it is necessary to maintain a high crosslink density of the thermoset resin network. Unfortunately, these highly crosslinked glassy networks suffer from poor fracture resistance. Hence, since late 1960s, efforts have been made to toughen thermosets [1–10]. Although plasticisers are a very successful way of improving the ductility of a brittle thermoplastic, they do not work well for thermosets resins. This is because thermoset resins are characterised by a crosslinking reaction, as a result of which the modifier exudes out from the matrix or undergoes a macro-phase separation. Moreover, accumulation of free liquid plasticiser molecules at the fiber surface can act as a weak boundary layer and cause a substantial reduction in the mechanical performance of a composite. A similar problem arises for adhesive applications. The general strategies used to toughen thermoset resins are:

- introduction of flexible chain (e.g., ether linkages) into the network structure
- compatible blending with a flexible/ductile polymer
- reduction in crosslink density of the network
- introduction of a suitable filler (rubber, thermoplastic or rigid particles) as a second phase.

The first three approaches improve toughness by flexibilising the thermoset networks. Flexibilisation is achieved by various methods such as chemical modification of the resin, use of reactive diluents, long-chain curing agents and chain extension of the resin. However, the improvement in toughness due to flexibilisation using the first three strategies is associated with a significant sacrifice in the glass transition temperature (T_g) and mechanical properties. Mechanical properties of a thermoset resin can be adjusted by reinforcing it with high-strength inorganic fillers/fibres. However, a reduction in the T_g as a result of modification (flexibilisation) limits the applications of the cured resins at a high service temperature because at a temperature higher than the T_g the cured resin loses its dimensional stability and cannot hold the fibres as a

matrix. Similarly, a thermoset adhesive can offer good bond strength at a temperature higher than the T_g of the resin due to cohesive failure.

The fourth strategy provides a solution to this problem whereby the modifier is introduced as a separate phase so that it does not affect the bulk thermomechanical properties and simultaneously improves the fracture properties of the thermoset network. This approach is called 'second phase toughening', and offers a significant increase in toughness/impact strength without a significant sacrifice of thermomechanical properties (especially the T_g). This is particularly important if the material has to experience high temperature (e.g., aircraft applications). As will be discussed in subsequent sections, an epoxy network with desirable mechanical properties and a T_g of about 240–250 °C can be made by combining conventional difunctional and multifunctional epoxies. If the T_g is reduced further due to modification, then epoxy formulation cannot satisfy the requirement for aircraft application (T_g >200 °C). Hence, the technology of second phase toughening is extremely important for the development of advanced thermoset polymer materials. This can be achieved by using a rubber, thermoplastic or rigid fillers. However, the most effective toughening is achieved by using a suitable rubbery filler ('rubber toughening').

In this chapter, the general principles of rubber toughening and research on thermosetting resins will be reviewed. Rubber toughening has been most successfully exploited for epoxy resins, hence, studies on toughened epoxy will be discussed in Chapter 5. Though this book is dedicated to thermoset resins, toughening of thermoplastics [11–106] will also be briefly discussed for completeness and for better understanding of the subject.

4.1 Toughening of Thermoplastics

The earliest and most well known rubber-toughened thermoplastics are high-impact polystyrene (HIPS) [11, 12] and acrylonitrile–butadiene–styrene copolymer (ABS) [13, 14]. Both rubber-modified polymers possess greatly improved toughness as compared with unmodified polystyrene (PS) and styrene acrylonitrile copolymer. Styrene butadiene rubber (SBR) was previously used as a toughening agent. Initially, butadiene rubber (T_g of about –85 ° C) replaced SBR (T_g of about –50 °C) and increased its application over a wide range of temperature. Other thermoplastics which have been successfully toughened by introduction of a rubbery second phase include poly(vinyl chloride) (PVC) [15–17], poly(methyl methacrylate) (PMMA) [18–20], polypropylene (PP) [21–26], polycarbonate (PC) [27–30], poly (phenylene oxide) (PPO) [31-33] and Nylons [34–36].

HIPS materials were prepared by a melt or latex blending of rubber and PS during early attempts at making rubber-toughened plastics. However, in these multiphase polymers the rubber particles were only poorly bonded to the surrounding matrix. The interfacial adhesion problem was addressed by polymerising styrene in the presence of a rubber that gives well-bonded particles due to chemical grafting [37, 38]. The graft copolymer, formed during polymerisation, acts as a coupling agent and the ungrafted rubber acts as a toughening agent. The PS is produced due to homopolymerisation of styrene from the matrix. Graft copolymerisation via a bulk or bulk suspension process is currently the standard method for manufacture of HIPS [9]. HIPS materials prepared by the grafting route exhibit significantly higher toughness compared with those prepared by melt blending. Similarly, ABS and related polymers such as methacrylate–styrene–butadiene copolymers and toughened PMMA are prepared by techniques which lead to grafting reactions [9]. In these materials, such reactions are typically induced by first preparing rubber latex by emulsion polymerisation and then adding the monomer (e.g., styrene, acrylonitrile) to the reactor vessel and polymerising them in the presence of rubber latex [9]. Hardward and Mann [39] compared the properties of ABS polymers prepared by blending and grafting. They demonstrated that the direct blending route results in low particle/matrix adhesion and poor impact strength compared with grafted polymers.

The grafting strategy cannot be readily adopted in some materials such as rubber-toughened PVC and Nylon, so they are prepared by the conventional blending route. The criterion for a rubber to be an effective toughening agent is that the rubber should possess a solubility parameter sufficiently different from that of the matrix polymer to ensure a fine second phase dispersion, but close enough to promote adequate adhesion of the particles with the matrix [9, 40]. This requirement may limit the choice of rubber at the expense of mechanical properties. Block copolymers with hard and soft segments can overcome these limitations and broaden the scope of application of toughened plastics. As a result, block copolymers have been investigated extensively [41–49] to examine their suitability as toughening agents for several plastics, especially PS. Their soft segments provide the low modulus needed for dispersed particles to act as effective stress concentrators, while their hard segments can lead to the microdomains that act as physical crosslinks and can provide a mechanism of physical adhesion to the rigid matrix phase. It has been reported that a styrene-based block copolymer adheres well to PS and PPO, with which PS is miscible. The effectiveness of block copolymers as toughening agents heavily depends on their molecular architecture [33].

4.1.1 Mechanism of Toughening of Brittle Polymers

When a mechanical stress is applied to a brittle polymer, the polymer cannot dissipate the mechanical energy adequately. This inadequate energy dissipation causes

overstressing and results in the formation of cracks. These cracks propagate rapidly through the glassy material, leading to catastrophic failure of the material. To increase its fracture toughness, it is required to provide some mechanisms for the dissipation of mechanical energy while simultaneously limiting the growth and breakdown of voids and 'crazes' (see next for definition) to prevent premature crack initiation. Depending on the inherent nature of the matrix polymer, the major energy-dissipating mechanism may vary. Two important energy-dissipating mechanisms (shear yielding and crazing) are discussed next.

4.1.1.1 Shear Yielding

When a polymer starts to deform plastically under an applied stress, it is said to have 'yielded'. Shear yielding consists of a change of shape without a significant change in volume, and is the major energy-absorbing mechanism for toughened pseudo-ductile polymers [50–68] such as PC, PVC, and polyamides. Although shear yielding also operates in unmodified polymers, it does so only in highly localised regions around the crack tip. In rubber-toughened thermoplastics, each rubber particle initiates shear yielding. Shear yielding is therefore propagated throughout the matrix and enhanced to a great extent. When a multiphase material is subjected to a uniaxial stress, the necking, drawing and orientation hardening occurred indicating shear deformation. The toughened matrix undergoes localised plastic deformation around virtually every rubber particle when the particles are uniformly dispersed in the matrix [50].

To understand the role of rubber particles in enhancing the shear yielding mechanism, various micromechanisms have been proposed. Most convincing among these is rubber cavitations, first identified by Haff and co-workers [51] and Donald and Kramer [52]. This micromechanism not only explains the enhanced shear yielding in rubber-toughened polymers but also accounts for the stress whitening observed during the fracture of rubber-toughened polymers. Stress whitening is observed during the mechanical stretching of a polymer, which cannot be explained by the shear yielding mechanism without considering rubber cavitations.

4.1.1.2 Rubber Cavitation

In rubber-modified plastics, under triaxial tensile stresses, voiding can be initiated inside the rubber particles. Once the rubber particles are cavitated, the hydrostatic tension in the material is relieved, with the stress state in the thin ligaments of the matrix between the voids being converted from a triaxial to a more uniaxial tensile stress state. This new stress state is favourable for the initiation of shear bands. In other words, the role of rubber particles is to cavitate internally, thereby relieving

the hydrostatic tension and initiating the ductile shear yielding mechanism [53–58]. The process of rubber cavitation and the associated matrix shear yielding are found in rubber-modified PC [59–62], PVC [63–65], poly(butylene terephthalate) (PBT) [66] and Nylon [67–69]. Depending on the nature of the matrix, rubber cavitation may initiate shear yielding or crazing. For plastics having a high entangle density or a thermoset with very high crosslink density, crazing is suppressed [70] and shear yielding is initiated to a great extent. For a very brittle polymer, even though rubber cavitation can occur to a very large extent, but this does not lead to matrix shear yielding [62]. This is why in very brittle polymers the major energy-dissipating mechanism is crazing initiated by rubber cavitation.

Dompus and Groeninckx [71, 72] recently developed a criterion for internal cavitation which has been treated as an energy balance between strain energy relieved by cavitation and surface energy required to create a new surface. It is given by the following equation:

$$U_{total} = U_{strain} + U_{surface}$$

$$= -\pi/12\, K_r\, \Delta^2\, d_o^{\,3} + \gamma\, \pi\, \Delta^{2/3}\, d_o^{\,2} < 0 \qquad (4.1)$$

Where K_r, Δ, d_o, and γ are the rubber bulk modulus, relative volume strain, rubber particle diameter and surface energy per unit area, respectively.

Accordingly, the cavitation of rubber is dependent on the elastic and molecular properties of rubber, rubber particle size and on applied volume strain, which again depends on the difference in the Poisson ratio between the matrix and the rubber. Cavitation resistance increases with the decrease in particle size and difference in the Poisson ratio [73]. From **Equation 4.1** it is clear that the bigger rubber particles cavitate more easily that the smaller rubber particles. A critical particle size for cavitation in the range 100–200 nm has been estimated [71, 72]. The same critical particle size is found for effective toughening in rubber-toughened PVC [74, 75], Nylon [76, 77], PMMA [78–80] and PC [53]. This explains the experimental observation of the little toughening effect when the particle size is reduced to <0.1 μm. If rubber cavitation is favoured for bigger particles, then why should we use sufficiently smaller rubber particles (<5 μm) for effective toughening? This will be addressed shortly.

4.1.1.3 Crazing

When a triaxial stress is applied to a brittle polymer, microvoiding is initiated in the matrix because it cannot easily deform. The localised yielded region therefore consists of an interpenetrating system of voids and polymer fibrils (1-μm diameter) called a

craze. A craze can grow indefinitely in length following minor principal trajectories. The craze also grows in width, although craze opening is limited to 0.5–1.0 μm [81]. Unlike a crack, a craze can transmit loads across faces, and this energy dissipation is called 'crazing'. In rubber-toughened brittle plastics, crazing is the major energy-dissipating mechanism [88–94] because shear yielding cannot be initiated. From optical microscopy studies on HIPS, Bucknall and Smith [82] concluded that the function of rubber particles is to initiate multiple crazes in the PS matrix. Subsequent studies [82–87] have reported the results of transmission electron microscopy (TEM) analysis of thin sections of various rubber-modified polymers by first staining the unsaturated rubber phase with osmium tetraoxide. These results confirmed that crazes frequently initiate from rubber particles.

The role of rubber cavitation on the initiation of shear yielding has been discussed in **Section 4.1.1.2**. In brittle polymers, cavitated rubber particles on relieving the stress cannot initiate shear deformation. How rubber cavitation favours the crazing mechanism is important. Bucknall and coworkers [87] proposed that rubber particles have two separate (but equally important) functions. First, under an applied tensile stress, crazes are initiated at the points of maximum stress concentrations and grow approximately normal to the applied stress. Second, the rubber particles are 'craze terminators', preventing the growth of very large crazes. Many small crazes are therefore generated, in contrast to the few large crazes formed in the same polymer in the absence of rubber particles. The multiple crazing that occurs throughout a comparatively large volume of rubber-modified materials explains the high energy absorption in fracture tests and exclusive stress whitening which accompanies deformation and failure.

4.1.2 Morphological Aspects

Phase morphology is a key issue for effective rubber toughening. It is generally believed that there is an optimal rubber particle size which is closely related to the nature of the post-yield deformation mechanism of matrix materials that can be triggered by rubber particles. Very brittle polymers such as PS require relatively large particles of the order of several microns [95–98]. This is because large particles are more effective in crazing, which is the major energy-dissipating mechanism for brittle polymers [81–94]. If the rubber particle size is less than craze thickness, then a growing craze may engulf the rubber particles smaller than the craze thickness rather than having its growth arrested. If the growth of crazes is not arrested then the crazes may combine and form a bigger craze, which may act as a defect and lead to catastrophic failure of the material. Note that the rubber cavitation micromechanism is also more effective for bigger particles.

More ductile polymers such as PPO, polyamides and PC deform by shear yielding and require relatively smaller particles for toughening than the materials that craze [99–101]. When toughness value is plotted against particles size at a constant amount of rubber and interphase adhesion, a sharp brittle tough transition occurs at a critical rubber particle diameter, d_c [102, 103]. When the average particles size (d) is smaller than d_c, a blend is tough; when d is larger than d_c, the blend is brittle [35, 103]. For example, Nylon 6 and Nylon 6,6 are not effectively toughened unless the rubber particles are considerably smaller than 1 μm [104]. The optimal particle size for toughening PPO is well below than that for PS [105] but probably larger than the optimal range for certain polyamides [104] or for styrene acrylonitrile copolymers [106, 107]. The critical particle size depends on the amount of rubber, i.e., decreasing with decreasing amount of rubber. The lower limit of the optimal particle size range effective for rubber toughening can be explained in terms of reduction in effectiveness of rubber cavitation with decreasing size and engulfment of smaller rubber particles by the growing crazes. The higher limit of particle size can be explained by considering the fact that the particles, bigger than the optimum size, cannot serve as effective stress concentrators. Instead, these bigger rubber particles act as defects and lead to catastrophic failure of the material. The existence of a higher limit of the optimal particle size range can also be very precisely explained using the concept of matrix ligament thickness (MLT) (see **Section 4.3.3.3**).

4.2 Toughening of Thermosets

Unlike the modification of thermoplastics, which often requires only simple physical blending of a particular elastomeric modifier, the toughening of thermosets by rubbery second phase is achieved almost exclusively through chemistry, and is a challenge to the expertise of polymer chemists. A useful final product with improved durability and applicability is a major concern of materials scientists and engineers who are responsible for answering this challenge. There are two approaches for incorporating rubber into a thermoset network: (i) direct dispersion of preformed core-shell particles; and (ii) blending with a liquid rubber ('liquid rubber toughening'). Liquid rubber toughening has been more extensively investigated and exploited.

4.3 Liquid Rubber Toughening

In this method, a liquid rubber is blended with a thermoset resin before curing [108–200]. Various liquid rubbers used for toughening thermoset resins are presented **Table 4.1**. The toughening effect of a particular modifier is largely dependent on the molecular weight (M_W) and functionality of a particular liquid rubber. When selecting the rubber, it must:

- be a low molecular weight liquid to ensure easy miscibility with a thermoset resin
- have functional groups capable of reacting with the base thermoset resin
- have borderline miscibility with the thermoset resin.

Table 4.1 Liquid rubbers used for toughening of a thermoset	
Name of liquid rubber	**Abbreviation/source/reference**
Carboxyl-terminated copolymer of butadiene and acrylonitrile	CTBN, Goodrich company
Amine-terminated copolymer of butadiene and acrylonitrile	ATBN, Goodrich company
Vinyl-terminated copolymer of butadiene and acrylonitrile	VTBN, [195]
Hydroxyl-terminated polybutadiene	HTBN, [195]
Hydroxyl-terminated polyether	HTE, [195]
Carboxyl-terminated poly (butyl acrylate)	[2, 110]
Vernoria oil	[2, 10, 111]
Epoxidised soyabean oil	ESO [2, 10, 11]
Epoxy-terminated siloxane oligomer	[2, 10]
Poly (ethylene phthalate)	PEP [253]
Carboxyl-terminated poly (ethylene glycol) adipate	CTPEGA [2, 10]
Carboxyl-terminated poly (propylene glycol) adipate	CTPPGA [2, 10]
Epoxy-functionalised hyperbranched polymer	Perstrop, HBP (epoxy), [108]
Hydroxy-functionalised hyperbranched polymer	Perstrop, HBP (OH), [10, 108, 203, 204]
Carboxyl-terminated poly (2-ethyl hexyl acrylate)	CTPEHA [109, 110]
Carboxyl-randomised poly (2-ethyl hexyl acrylate)	CRPEHA, [2, 10]
Hydroxyl-terminated poly (propylene oxide-block-ethylene oxide)	[10, 110]
N-phenylmaleimide styrene copolymer	PMS, [254]
Isocyanate end-capped poly butadiene	[227]

'Borderline miscibility' means that the rubber is initially miscible with the resin, making a homogeneous solution, and undergoes reaction-induced phase separation leading to the formation of a two-phase microstructure. Scanning electron microscopy (SEM) photographs of a carboxyl-terminated butadiene-acrylonitrile liquid rubber (CTBN)-toughened epoxy network is shown in **Figure 4.1**. It clearly shows a uniform dispersion of spherical rubber particles in the epoxy matrix. Such rubber-modified resin networks with a two-phase microstructure show improved fracture toughness as the rubber particles dispersed and bonded to the matrix act as the centres for dissipation of mechanical energy. The detailed mechanisms of toughening and roles of rubber particles will be discussed shortly. The principle of reaction-induced phase separation is discussed next considering the thermodynamics of mixing.

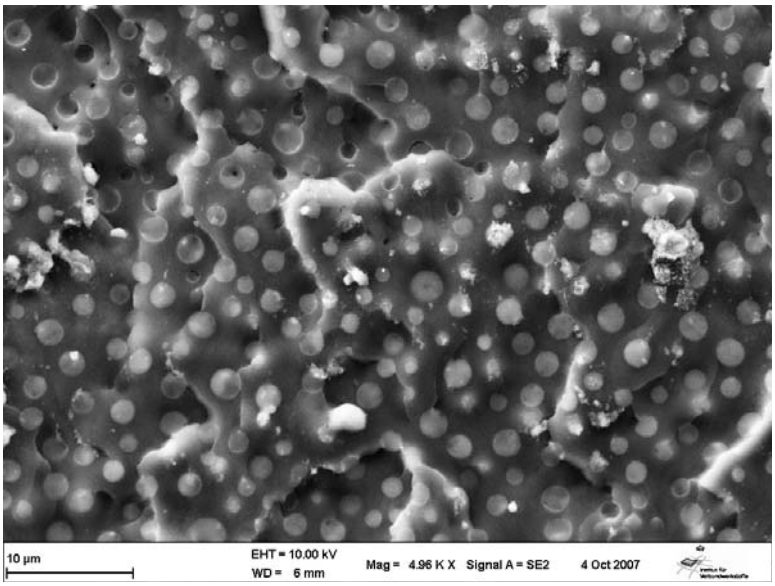

Figure 4.1 SEM photographs of a CTBN-toughened epoxy network showing two-phase morphology

4.3.1 Reaction-Induced Phase Separation

The thermodynamic condition for compatibility of a resin and a rubber is that the free energy change of mixing (ΔG_m) at constant pressure (P) and temperature (T), should be negative [108]:

$$(\Delta_{G_m})_{P,T} < 0 \tag{4.2}$$

Combining the Flory–Huggins equation and the Hildebrand equation, the free energy of mixing can be expressed as:

$$\Delta G_m/V = \varphi_R \varphi_r (\delta_R - \delta_r)^2 + RT(\varphi_R/V_R \,.\, \ln \varphi_R + \varphi_r / V_r \,.\, \ln \varphi_r) \quad (4.3)$$

where ϕ_R and ϕ_r are the volume fractions, δ_R and δ_r are the solubility parameters, V_e and V_r are the molar volume of the resin and rubber, respectively, V is total volume, R is the universal gas constant, and T is the temperature.

Because ϕ_R and ϕ_r are fractions, the second term is always negative. The equation clearly explains why high temperature and low molar volume (molecular weight) favour miscibility because both factors decrease the free energy of mixing (thermodynamic spontaneity). For a fixed resin/rubber composition, ΔG_m at constant temperature depends on δ_r, i.e., the chemical nature of rubber and V_r, which is dependent on the molecular weight of the rubber. A toughening agent must be designed (in terms of chemistry and molecular weight) so that the free energy of mixing is marginally negative at the curing temperature. The rubber will then be compatible with the resin before the curing but with the advancement of curing reaction, V_R and V_r, will increase due to the increase in molecular weight of the rubber and the resin and, at a certain stage, ΔG_m will become positive. At that point rubber starts to undergo phase separation and it is called the 'cloud point'. The process continues until the gelation point, where the phase separation is arrested due to the tremendous increase in viscosity. The final network is obtained after a heat treatment called 'post –curing'. The process is schematically described in **Figure 4.2**.

If $(\delta_R - \delta_r)$ is very low, then ΔG_m will be highly negative and entropy change (during curing) can not make ΔG_m negative before gelation, leading to the formation of a single-phase morphology. If $(\delta_R - \delta_r)$ is very high, then ΔG_m will be positive at curing temperature and rubber will be immiscible at the initial stage itself, leading to a macro-level phase separation. If the phase separation starts at a very early stage of curing then rubber particles will coalesce, leading to the formation of bigger particles. If phase separation starts at a latter stage of curing, the rubber may not get the chance to phase separate completely. Hence, it is necessary to design the toughening agent for a particular thermoset considering miscibility criteria. For example, carboxyl-terminated polybutadiene undergoes macro-phase separation when blended with an epoxy, and is not a suitable toughening agent for epoxy. This is because the solubility parameter of butadiene is much lower than that of epoxy and it is immiscible with epoxy. However, a carboxyl-terminated copolymer of butadiene and acrylonitrile with 20–30 wt% of acrylonitrile (polar acrylonitrle increases the solubility parameter) has a close proximity of solubility parameter with an epoxy resin, and is an effective toughening agent for epoxy. The copolymers are commercially produced by Goodrich Company, and are known in the trade as Hycar CTBN. CTBN with higher acrylonitrile content

has better miscibility with the epoxy resin in terms of the solubility parameter, and undergoes phase separation at a later stage of curing, resulting in a lower amount of phase separated rubber. CTBN with an acrylonitrile content >30 wt%, results in a single-phase morphology and the modifier acts as a flexibiliser rather than a toughening agent.

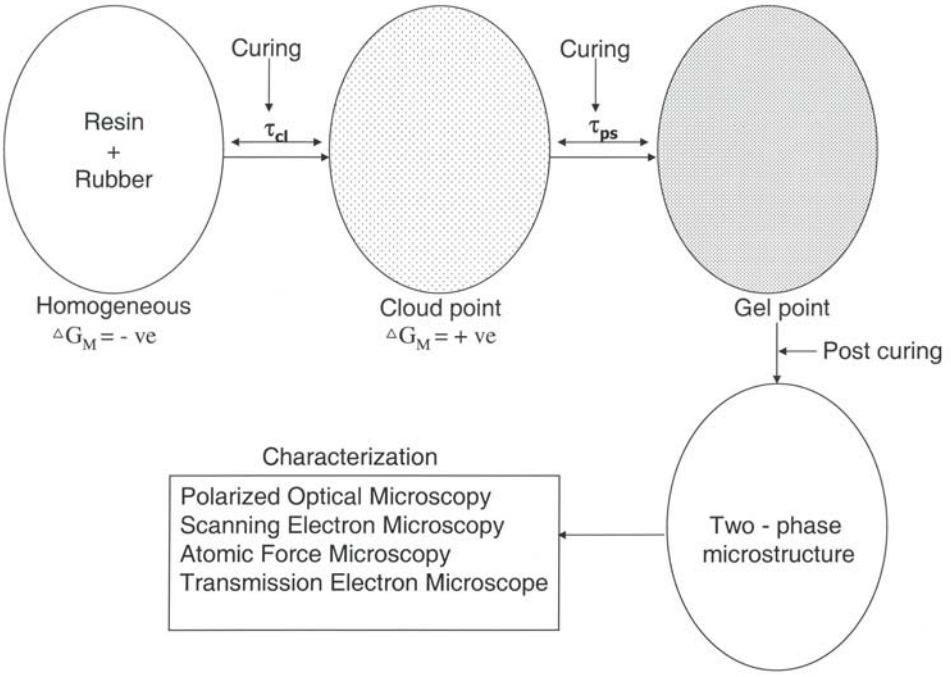

Figure 4.2 Description of reaction-induced phase separation in rubber-modified thermoset resin

Complete phase separation is always desirable because residual rubber remains miscible with the resin and reduces the T_g of the resin network. The other factor (apart from the nature of rubber), which plays an important part in the development of morphology is the cure condition. The morphology is controlled by the initial cure temperature. The post curing has no role in the development of morphology [109-111], although it affects the final properties of the cured network. The time from cloud point to gelation is the effective phase separation time (t_{ps}). For complete phase separation, the t_{ps} must be higher than the time required for diffusion of rubber from the resin medium (t_{diff}). The diffusivity is the controlling factor of phase separation if $t_{diff} > t_{ps}$.

The diffusivity of rubber in the resin medium (D_r) is considered to be proportional to the temperature and viscosity ratio through the Stokes–Einstein equation [112]:

$$D_r = kT/6\pi Rr\,\eta R \tag{4.4}$$

where k is the Boltzman constant, R_r is the radius of rubber adducts, η_R is the viscosity of the resin, and T is absolute temperature.

The characteristic time scale for diffusion in two dimensions is:

$$t_{diff} = L^2 / 2\,D\gamma \tag{4.5}$$

A length scale (L) can be assigned from the average two-dimensional distance between domain centres obtained from micrographs of the cured specimen. Monternal and co-workers [110] reported that the system viscosity at cloud point (η_{cp}) is the most fundamental parameter rather than the t_{ps} and t_{diff} for morphology development in rubber-toughened thermosets. They correlated the system viscosity with the particle size ($\bar{D}$) of the dispersed phase. A straight line with negative slope was obtained when ln η_{cp} was plotted against $\bar{D}$. The same validity was verified by Verchere and co-workers [111] for epoxy/CTBN systems using two types of CTBN. They reported that correlation was found for both systems independently of the cure temperature and initial rubber concentration. Different systems show different fittings, indicating that other factors such as thermodynamic miscibility have an important role.

4.3.2 Mechanism of Toughening of Thermosets

Several theories have been proposed to explain the toughening effect of rubber particles on the brittle thermoset matrix. These are based on the fractographic features and fracture properties of rubber-toughened thermoset networks. Garg and Mai [113] proposed 13 mechanisms to explain the impact behaviour of rubber-toughened epoxy systems:

- Shear band formation near rubber particles
- Fracture of rubber particles after cavitation
- Stretching of rubber particles
- Debonding of rubber particles
- Tearing of rubber particles
- Trans-particle fracture

- Debonding of hard particles
- Crack deflection by hard particles
- Voiding and cavitation of rubber particles
- Crazing
- Plastic zone at craze tip
- Diffuse shear yielding
- Shear band/craze interaction.

Among these mechanisms, a few important mechanisms are discussed next [114–195].

4.3.2.1 Rubber Bridging and Tearing

According to bridging and tearing mechanism [114, 115] when a crack opens up during its advancement, the rubber particles are stretched between the crack surfaces, behind the crack tip and bridge the crack surfaces. Yee and Pearson [118] studied a highly crosslinked rubber-modified epoxy system, and attributed the enhancement in toughness to the rubber bridging mechanism. Similar evidence was reported by others [114–117]. The model is based on the assumption that crosslinked thermoset resins are truly brittle materials and incapable of localised plastic deformation. Thus the mechanical energy is absorbed exclusively by the rubber particles, not the matrix. However, even in a highly crosslinked thermosets some plastic deformation occurs. Because the absorbed energy is utilised to stretch and tear rubber particles, the fracture energy can be estimated quantitatively:

$$G_{1c} = G_{1ce} (1–V_p) + 4 \Gamma V_p (1– 6/ \lambda 2 + \lambda + 4) \quad (4.6)$$

where V_p ,Γ are the volume fraction and tear energy of the rubbery particles; G_{1ce} and G_{1c} are the fracture energy of the unmodified and rubber-modified thermoset matrix, respectively.

However, this theory has several drawbacks. It can only explain the modest increase in toughness and cannot explain the dramatic increase in fracture energy reported in many rubber-toughened epoxy systems. There are many discrepancies between reported data for improvement in toughness for thermoset resins due to the sensitivity of the toughening effect to the curing condition and inherent matrix ductility [119, 120]. The effect of G_{ic} on test temperature and strain rate cannot be explained using

the previous equation because the dependence of Γ is exactly the reverse that of G_{ic}. Moreover, the theory cannot explain the stress whitening observed in fracture surface analysis. Hence, this mechanism cannot be considered to be a major energy-dissipating mechanism for highly crosslinked thermoset resins.

4.3.2.2 Crazing

A second hypothesis to explain the toughening of a thermoset network involves conventional crazes being initiated and growing in the thermoset matrix. In some rubber-toughened thermoplastics such as HIPS, multiple crazing as stress concentrators around rubber particles has been established as the major toughening mechanism [88–94]. Donald and Kramer [121, 122] showed that in thermoplastic resins there is a transition from crazing and shear yielding as the length of the polymer chain between physical entanglements decrease below ~20 nm. Thus crazing is less probable in highly crosslinked thermoset resins. Van den Boogaat [123] observed crazes at the tips of moving cracks in partially cured epoxy. In fully cured resins, crazes were not found [121].

Sultan and McGarry [124, 125] identified the microcavitation at the crack tip as crazing, and the proposed mechanism has been used to explain the toughening behaviour of CTBN-modified epoxy networks. Lilley and Holloway [126] reported seeing crazes in the vicinity of the crack tips in some epoxy resins, although the features they showed could have been micro-cracks. Morgan and co-workers [127–129] showed craze-like entities in TEM images obtained from strained films of epoxy resins. They claimed that crazes resulted from local regions of low crosslink density, but the crazes were relatively short (~1 μm) and appeared to be bridged by drawn polymer. Hence, no firm evidence has been found for crazing for toughened thermoset resins [130, 131].

4.3.2.3 Shear Yielding and Crazing

As discussed earlier, shear yielding is the most probable and effective mechanism for toughening a crosslinked thermoset system. However, two or more mechanisms may act simultaneously in a complex multiphase system. Bucknall and co-workers proposed [9] that massive crazing and shear flow are the two energy-absorbing mechanisms in rubber-modified epoxies. They used tensile creep dilatometry and determined the volume strain ($\Delta V/V_0$) to study the contribution of shear yielding and crazing on toughening of a thermoset resin [132, 133]. This study was based on the assumption that shear yielding creates no change in volume, whereas crazing is associated with volume change. Therefore the slope of the volume strain $\Delta V/V_0$

against longitudinal strain curve should be zero for a pure shear yielding process, and equal to unity for a pure crazing process. Intermediate slopes would be produced by proportionate mixing of the two processes. Hence, by assuming the rule-of-mixture, it is possible to determine the contributions of the two mechanisms. Bucknall and co-workers investigated rubber-modified epoxies using this method and found that volume strain and toughness increased with rubber content. They concluded that a combination of shear yielding and massive crazing were the toughening mechanisms for thermoset resins.

However, volume dilation cannot be unambiguously and exclusively attributed to crazing; voiding can cause volume dilation [134–136]. No other supporting evidence to corroborate volumetric data has been reported. Several authors have cast doubt on the existence of crazes in a tightly crosslinked glassy polymer [114, 115, 137, 138] despite reports of their presence [126, 130, 131]. Hence, even if crazes are present in rubber-modified thermoset networks, their contribution in improving the toughness of highly crosslinked thermoset networks is not convincing.

4.3.2.4 Cavitation and Shear Yielding

A direct relationship between toughness and plastic zone size was reported by Bascom and coworkers [139, 140] in rubber-toughened epoxy adhesives. They proposed that cavitation caused by triaxial tension above the crack tip increases the size of the plastic zone, and that plastic flow of the epoxy matrix and elongation of the particles also contribute to toughness. The spectroscopic evidence for cavitation of rubber particles have been reported for various rubber-modified thermoset systems [141–143]. SEM photographs of the fracture surface of an epoxy-terminated vinyl-terminated poly (butadiene–acrylonitrile) (ETBN)-modified vinyl ester (VE) resin is shown in **Figure 4.3**, and clearly shows cavitation of rubber particles [195]. Cavitations in the particle or in the matrix/particle interface and plastic shear yielding of the thermoset matrix are the micro-deformation mechanisms occurring at the crack tip that dissipate energy and produce the toughening effect. This was further supported by the fact that modified a VE matrix that shows cavitation results in higher toughness [195] compared with a matrix in which cavitation was not observed (see **Section 4.4**).

The fractographic features of stress-whitened regions indicate several deformation processes. Hole formation suggests that there has been a dilational deformation because holes are larger in diameter than the non-deformed particles seen in the rapid crack growth region [134–136]. This dilational deformation is consistent with the triaxial stress field known to be present at the crack tip [143]. These stresses lead to the rapture of the rubber particles, which then relax back into the enlarged cavity and give the appearance of holes. Results from several studies support this idea, but the

most convincing is that of Kinloch and co-workers [144]. They exposed the whitened region of the fracture surface to an organic fluid to swell the rubber. SEM images revealed that the hole had become hillocks. Several workers [145–147] attempted to capture any rubber particle that may have been ejected from the holes during crack growth, but none of the efforts have produced evidence that particles are ejected. Thus this result suggests that microvoids are produced during crack growth by cavitation of rubber particles.

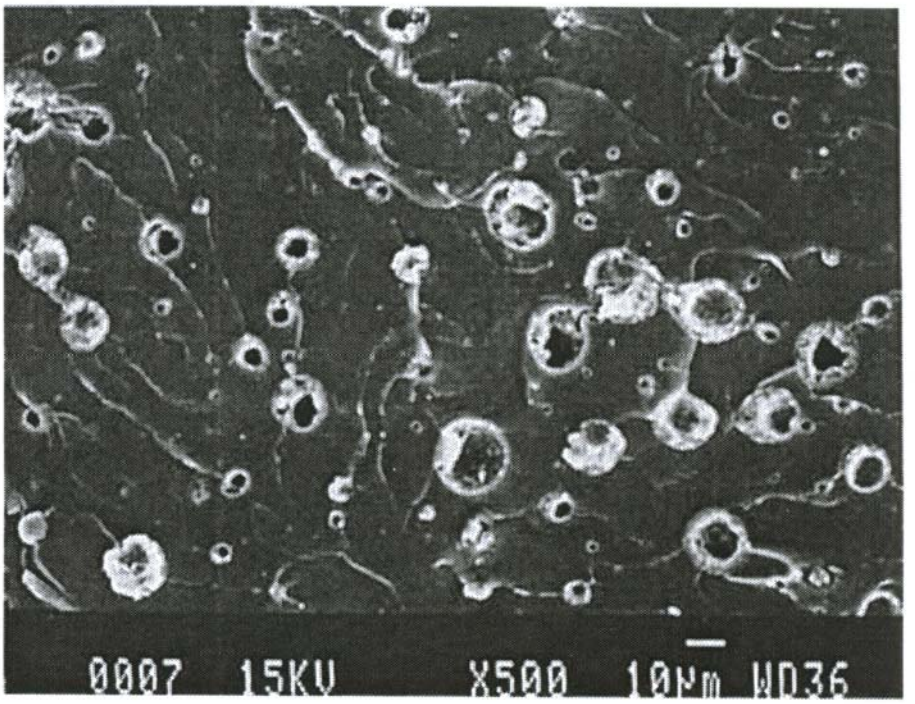

Figure 4.3 SEM photograph of the compact tension fracture surface of 4 phr (parts per hundred grams of resin) ETBN-modified VE resin showing cavitated particles. Propagation was from left to right. The specimen was stained with osmic acid. Reprinted with permission from J.S. Ullett and R.P. Chartoff, *Polymer Engineering and Science*, 1995, 35, 13, 1086 © 1995, John Wiley and Sons Publishers

Cavitation is followed by the onset of a shear localisation process, which would not have taken place in the net resin under the same conditions. Rubber cavitation and

associated shear yielding have been discussed in **Section 4.2.1.2** for rubber-toughened thermoplastics. The difference in elastic modulus of a glassy thermoset and rubber is much higher than the corresponding difference in their bulk modulus. Hence, at the crack tip, where the hydrostatic tensile component is large, the magnitude of the concentrated devioteric stress in the vicinity of rubber particles is insufficient to promote shear yielding. The internal cavitation of the rubber particles relieves the plain strain constrain by effectively reducing the bulk modulus. After an effective reduction, the magnitude of the concentrated deviatoric stresses become sufficient for shear yielding. The voids left behind by the cavitated rubber particles act further as stress concentrators. Theoretical model calculations show that they reduce the octahedral shear stress to yield [148] and they grow and promote the formation of plastic zone between voids [149]. Shear band formation is enhanced in such a void-like solid [150–151].

All these theoretical predictions are consistent with the results observed by Yee and Person [120, 131], which clearly show shear bands between cavitated particles in rubber-toughened epoxy materials. They also found that the ability of CTBN rubber to toughen epoxy is closely related to CTBN rubber cavitation, which is seen as thick dark circle within the rubber particles under optical microscopy. The need of internal cavitation of rubber particles has been questioned by others [152, 153], but these researchers have considered only the case of uniaxial tension, which have been shown to be quite different than the triaxial stress seen at the crack tip.

Li and co-workers [154] studied the fracture behaviour of unmodified and CTBN-modified epoxies under hydrostatic pressure. They found that when rubber cavitation is suppressed by superimposed hydrostatic pressure, the fracture toughness of CTBN modified epoxy is no higher than that of the unmodified thermoset resin network. This implies that stress concentration by rubber particles alone will not necessarily induce massive shear yielding and increase fracture toughness. Hence, rubber cavitation is very important to the toughening of rubber-modified epoxies; without cavitation these rubber particles can cause stress concentration, but they are not effective in toughening. From the previous discussion it is clear that, although all four mechanisms have some support from experimental observations, the most accepted mechanism is rubber cavitation and associated shear yielding.

According to Evans and co-workers [155, 156], no single mechanism can explain the toughening effect of a thermoset network by rubber particles. They proposed a synergistic model which takes all the possible mechanisms (including rubber bridging, void growth, shear banding) into consideration. The synergistic relationship between the rubber bridging mechanism and the other two mechanisms was based on the assumption that the fracture energies increase proportionately with the size of the process zone. The validity of this relationship has not been accurately validated.

Yee [157] cast doubt on the synergism in the toughening mechanism observed in rubber-modified plastics. Huang [158, 159] calculated the contribution of different mechanisms, and concluded that the localised shear yielding initiated by rubbery particles is a major toughening mechanism. Plastic void growth is another important toughening mechanism at higher test temperatures, and the contribution increases sharply with rising temperature. The rubber bridging mechanism can also play a part if the ability of the matrix to undergo plastic deformation is suppressed.

4.3.3 Microstructural Features

Microstructural features of the dispersed rubbery phase have a major effect on the toughness of multiphase thermoset networks. The morphogical parameters are dependant on the nature of the resin, toughening agent and the cure condition. Various morphological parameters and the molecular parameters which control the morphology are listed in **Table 4.2**. It is very difficult to study the effect of individual parameters on the toughening effect because the parameters are interrelated. In many studies, several crucial features have been changed simultaneously. Moreover, the parameters are interrelated and it is difficult to change one parameter without affecting others. For example, if we want to study the effect of the functionality of rubber by changing functionality, this changes the solubility parameter and affects the other morphological parameters. However, attempts have been made here to correlate fracture behaviour and microstructural features of toughened networks based on the literature.

Table 4.2 Parameters Influencing rubber toughening [2]

Molecular parameters		Morphological parameters	Processing parameters
Epoxy	Rubber		
Matrix ductility	Polarity	Rubber volume fraction	Initial cure temperature
Functionality	Molecular weight	Particle size	Post cure temperature and time
Molecular weight	Functionality	Particle size distribution	-
Curing agent (type and concentration)	Concentration	Matrix ligament thickness	-
Viscosity	Viscosity	Particle to matrix adhesion	-

4.3.3.1 Volume Fraction

The fracture energy of toughened thermoset resins increases with increase in concentration of elastomer until it becomes difficult to obtain the desired particle–matrix morphology. Bucknall and Yoshii [160] determined the fracture energy of rubber-modified epoxy resins, all containing 8.7% *w/w* of CTBN rubber but with various rubbery phase volume fractions, by varying the curing condition. They varied the rubber volume fraction from 0 to 0.2, and reported a linear relationship between fracture energy and volume fraction of rubber for different epoxy resin hardener systems using a CTBN rubber. Different rubber volume fractions for a modified epoxy system with same concentration of rubber were achieved by changing cure conditions. As noted earlier, the morphology of a rubber-toughened thermoset system is tremendously influenced by curing conditions.

Kunz and coworkers [161, 162] found for CTBN- and amine-terminated copolymer of butadiene and acrylonitrile (ATBN)-modified epoxies that, once a volume fraction of about 0.1 had been achieved in the polymer, further increase in volume fraction resulted in only minor increase in the value of fracture energy. The apparent discrepancy can be attributed to the use of matrices with different inherent ductility, curing conditions and test conditions employed [163, 164]. Fracture energy in rubber-toughened epoxy is dependent on the test temperature and test rate [164–166]. The fracture energy increases with increase in the test temperature and decreases in test rate below the T_g.

Kinloch and Hunston [163, 167] and others used the concept of time–temperature superpositioning, and separated the effect of changing the volume fraction and the properties of the matrix phase. No definite relationship between fracture energy and volume fraction of rubber was observed. The maximal value of volume fraction that can be achieved is about 0.2–0.3. Attempts to produce higher volume fraction result in phase inversion and loss of mechanical fracture properties. Though in most of the studies [168, 169], phase inversion was reported at a volume fraction >20%, in some recent studies inversion has been reported [170, 171] at a very low volume fraction (~2%) of rubber.

4.3.3.2 Particle Size

Several studies have suggested that particle size may influence the extent and type of micro-mechanism and so affect measured toughness. Sultan and McGarry [125, 126] proposed that large particles (0.1–1 μm in diameter) cause crazing, and are five-times more effective in toughening the thermoset than small particles (about 0.01 μm in diameter), which initiates shear yielding. However, evidence for crazing is not

convincing (see **Section 1.3.1.3.2**). Furthermore, volume fraction was not determined in these studies.

Kunz and co-workers [114, 115] reported that large (40 μm diameter) particles are not as efficient in providing an increase in fracture energy as smaller (1 μm diameter) particles. Many authors [131, 132, 172, 173] reported that the fracture energy of rubber-toughened thermosets is independent on particle size, but mean particle size was varied only between 0.5 μm and 5 μm. Pearson and Yee [174] studied the effect of particle size on the fracture properties of rubber-toughened epoxy networks having a particle size 0.2–200 μm. They found that large particles (100 μm diameter) are not as effective in providing a toughening effect whereas small particles (0.1 μm diameter) appear to be the most efficient, and provides a more than tenfold increase in fracture energy. Hence, rubber particle size should be in the range 0.1 μm to 10 μm for effective toughening of a thermoset network.

The origin of this size dependence arises from the part played by the particles, which is governed by the size of the process zone. Large rubber particles lying outside the process zone can act only as bridging particles, and provide only a modest increase in fracture energy. Small rubber particles which lie in the process zone are forced to cavitate by the large hydrostatic stress component present in the process zone and contribute to the increase in fracture energy.

4.3.3.3 Matrix Ligament Thickness (MLT)

Wu [175–177] proposed that the MLT, i.e., surface-to-surface inter-particle distance is a fundamental parameter. For effective toughening, mean matrix ligament thickness (τ) should be less than that of the critical value (τ_c) where brittle–tough transition occurs. The τ_c is independent of rubber volume fraction, particle size and characteristics of the matrix alone at a given test temperature and rate of deformation. For blends with dispersed spherical particles, the τ_c can be related to the rubber particle size and rubber volume fraction (ϕ_r) by the following equation [177]:

$$\tau_c = d_o [k (\pi/6\varphi_r)1/3 - 1] \quad (4.7)$$

where k is a geometric constant and d_o is particle diameter. τ_C is reported to be 0.30 μm for a Nylon/rubber blend.

The existence of critical MLT for effective rubber toughening can be explained [72, 177, 178] in the light of two basic mechanisms: rubber cavitation followed by the formation of shear bands, and crazing. A low MLT maintains the connectivity of the yielding process, which then propagates over the entire deformation zone and makes

the blend tough. This happens if $\tau < \tau_c$. If crazing is the major energy-dissipating mechanism, high MLT causes the formation of secondary crazes at the highly stressed region of the ligament. These then propagate rapidly, leading to the catastrophic failure of the materials.

Using the critical MLT concept, the effect of particle size on the toughness of modified thermoset resin can be explained. If we consider the rubber cavitaion mechanism (which is accepted as a major energy-dissipating mechanism in toughened thermosets), then bigger particles should perform better because cavitation resistance decreases with increase in particle size. Recall equation 4.1, where the power of particle size (d0) is more for the negative term. However, particle should be sufficiently small to satisfy the critical MLT condition. For a given volume fraction, the critical MLT is achieved by decreasing the particle size and improving the dispersion. This concept works very well for most systems, a decrease in particle size corresponding to a lower brittle–tough transition temperature. However, very small particles (<0.1 μm) cannot cavitate and therefore do not release the hydrostatic tension in the material to promote ductile shear yielding [179]. A minimum particle size below which the brittle–tough transition no longer shifts to lower temperatures has been found in several systems.

Other researchers [161, 180] have claimed that optimal particle size involves a bimodal distribution of small and large particles. They reported that rubber-modified networks having a bimodal distribution of particles exhibit higher fracture toughness than that of the matrix having a unimodal distribution of particles. Bimodal distributions were achieved using bis phenol A (BPA), BPA acts as a chain extender and significantly reduces crosslink density. It is well known that the toughness of a matrix increases with decrease in crosslink density. Hence, these claims have neglected the effect of crosslink density, which has been shown to be quite substantial [181–192]. Yee and Pearson [174] disproved the effect of bimodal particle distribution on several morphological scales. They did not find a synergistic effect combining 0.2 μm particles with 2 μm particles, and 2 μm particles with 100 μm particles.

4.3.3.3 Interfacial Adhesion

Matrix–rubber particle adhesion is an important parameter for rubber toughening. For effective rubber toughening, rubber particles must be well bonded to the thermoset matrix. The poor intrinsic adhesion across the particle–matrix interface causes premature debonding of particles, leading to catastrophic failure of the materials. Nearly all the studies [9, 193, 2–10] have been concerned with reactive rubbers as toughening agents, and showed that dispersed particles have interfacial chemical bonds as a consequence of chemical reactivity.

Some authors have refused to accept the role of interfacial adhesion on the toughening of thermoset resins. Lavita and co-workers [190] reported that non-reactive rubber can toughen BPA-modified epoxy, but the mechanism was not fully discussed. Huang and co-workers [194] showed that when the second phase consists of micron-size rubber particles, the interfacial bonding has only a modest effect on the fracture properties of blends.

4.4 Toughening of Vinyl Ester (VE) Resins

The various general strategies for toughening thermoset resins discussed in earlier sections have been utilised to toughen VE resins. Incorporation of flexible units into the dimethacrylate backbone by reacting a CTBN with the VE resin system has been reported [195–197]. The CTBN is chemically bonded through terminal ester groups with 2,2–bis (4-hydroxyphenyl) propane units during manufacture [198]. Incorporation of such flexible units into the crosslinked structure improves the fracture toughness at the cost of thermomechanical properties. To achieve improved fracture toughness without a significant sacrifice of themomechanical properties, blends or interpenetrating networks with two-phase morphology have been investigated. Rubber toughening of VE resins can be achieved by two different methods. The first method is to blend with preformed core-shell particles. Additions of core-shell rubber particles have been found to increase the toughness of VE resin-based fibre-reinforced composite systems [199]. The second method is a liquid rubber toughening (see next).

4.4.1 Liquid Rubber Toughening

As discussed in earlier sections, a thermoset toughener must be soluble with the resin at the beginning and undergo phase separation during the curing reaction. This leads to the formation of a two-phase microstructure. However, most of the commercially available or developed modifiers (for epoxy resin) suffer from poor miscibility with VE resins. The poor compatibility between the liquid rubber and the resin tends to result in large particles with poor interfacial adhesion [200, 201]. Pham and Barchill [198] reported a particle size of 40 μm using an hydroxyl-terminated polybutadiene (HTPB) rubber. Suitable modification of the toughеners [50] or VE resin [51] and the use of a compatibiliser [52] have been reported for successful toughening of VE resins.

Initial compatibility can be improved by the use of rubber with the reactive functional groups to enable rubber molecules to react with the resin to produce an adduct. This strategy can significantly promote the compatibility of the rubber, leading to a blend with smaller particle size. Rubber particles with size up to 0.1 μm have been reported

using a vinyl-terminated poly (butadiene–acrylonitrile) rubber (VTBN) [202]. Pham and Burchill [198] modified HTBN by reaction with a diisocyanate and various alcohols to increase the compatibility between the rubbery phase and the VE resin.

Ullett and Chartoff [195] investigated fracture behaviour of VE resins toughened with various rubbers such as CTBN, VTBN, ETBN, and hydroxyl-terminated polyether (HTE). They analyzed the morphology and reported single-phase particles using VTBN and two-phase particles using ETBN and CTBN. Two-phase particles-containing systems led to a greater increase in toughness than those containing single-phase particles. Examination of the fracture surfaces of these systems revealed that the toughening mechanisms for the systems with the two-phase particles were cavitation and shear yielding as evident from SEM photographs for the compact tension fracture surface of 4 parts per hundred grams of resin (phr) ETBN-modified VE resin (**Figure 4.3**). Only crack bridging and particle deformation were observed for systems with single-phase particles [195]. For example, SEM photographs for compact tension fracture surface of 4phr VTBN-modified VE resin is presented in **Figure 4.4**: particles appear to have been stretched. Dreerman and co-workers [201] investigated the effect of modification with VTBN and ETBN on the fracture properties of VE resin. For VTBN and ETBN, the latter was the most effective in increasing toughness. They also observed the internal structure in ETBN particles, and suggested that it implied a dual-phase structure in the rubber particles. The toughening effect depends on several factors such as type of rubber [195], rubber volume fraction [196, 201], morphology of rubber particles [195], cure regimen [195], testing rate [198, 201] and the compatibility or chemistry of the rubber/matrix system [198].

Results on fracture properties of rubber-toughened VE resin have been contradictory. For example, Liao and co-workers [202] observed impact toughness to increase with addition of VTBN, whereas Dreerman and co-workers [201] observed no improvement in toughness using VTBN. This can be explained in terms of difference in size of rubber particles generated during reaction-induced phase separation in the two systems investigated by the two research groups. Liao and co-workers [202] found very small particle sizes (up to 10 nm) and Dreerman and co-workers [201] observed particle sizes >1 μm. They suggested that the very small particle size obtained was due to the gelation of VE resins at an early stage in the reaction, which prevented aggregation of the rubber molecules. The origin of discrepancies in toughness results can also be explained by noting that fracture behaviour is sensitive to test conditions and inherent matrix properties (especially ductility). The pure resin material was found [198, 202] to fail catastrophically using the three-point bend with single notch but, when tested using compact tension sample geometry [195] or the much slower double–torsion method [198], stick/slip or stable crack propagation was observed. Dreerman and co-workers [201] and Ullett and Chartoff [195] found that additions of rubber changed the fracture mode from catastrophic failure to stick/slip. Pham and Burchill [198] observed

no change in the failure mode with the addition of rubber using the three-point bend with single notch, but all samples failed catastrophically. Toughness values determined in the study of Pham and Burchill by the single-edge-notch three-point bend technique were lower than those determined by a double-torsion technique. This observation highlights the influence of test conditions on measurements of fracture toughness. Karger-Kocsis and coworkers [203, 204] investigated the reactive hyperbranched polymers (HBP) for toughening a vinyl ester–urethane hybrid (VEUH) resin [203, 204]. The toughening effect was influenced by the ratio of architecture and terminal groups (vinyl/hydroxyl ratio). Less compact star-like polymers with long, flexible arms with high vinyl functionality resulted in the highest improvement in toughness. Such HBP copolymerise with VE resin and styrene and allow polyaddition reactions (with polyisocyanate), leading to the formation of a regular crosslinked network structure. An approximate fourfold increase in fracture toughness was reported by adding 20 wt% of HBP with long, flexible arms with high vinyl functionality, and they also investigated the interpenetrating structure of VE resin and epoxy [205]. They studied various combinations of the interpenetrating polymer network (IPN) system using different types of epoxies, and reported significant improvement in toughness using an aliphatic epoxy system.

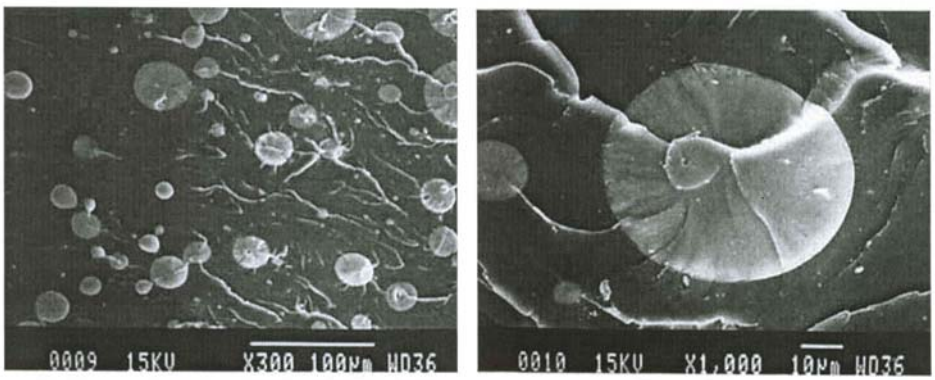

Figure 4.4 SEM photographs of the compact tension fracture surface of 4 phr VTBN-modified VE resin showing a) transition from fast fracture to crack-initiation region and b) close-up of one particle. Propagation was from left to right. The specimen was stained with osmic acid. Reprinted with permission from J.S. Ullett, and R.P.Chartoff, *Polymer Engineering and Science*, 1995, 35, 13, 1086 © 1995, John Wiley and Sons Publishers

4.5 Modification of unsaturated polyester (UPE) resins

Curing of UPE resin is associated with large volume shrinkage (7–10%) [206]. This is attributed to the extensive intramolecular or cyclisation reactions of UPE molecules and the formation of a compact microgel structure during cure [207]. Cure shrinkage induces a series of defects in the final product such as sink mark, surface waviness, and cracks. This complicates the fabrication of a high-quality surface and maintaining dimensional stability of a part made of UPE resin. Addition of non-reactive additives such as thermoplastic polyurethane, PMMA, and poly(vinyl acetate; PVAc) offers a unique solution to this problem. These additives are called 'low profile additives' (LPA) [208–213].

Depending on the chemical structure and molecular weight, LPA can be compatible or incompatible with the uncured UPE resin. However, after curing, both compatible and incompatible LPA lead to the formation of a two-phase microstructure. This reaction-induced phase separation is favoured by the reduction in combinatorial entropy due to curing. Detailed thermodynamic analysis of such reaction-induced phase separation in thermosets has been discussed in **Section 4.3.1**. The phase separation is mostly described through a nucleation and growth process [214]. Li and Lee [215] proposed a phase separation mechanism through spinodal decomposition for the low-temperature cure of UPE–PVAc systems. It was pointed out that the time between the onset of phase separation and gelation is the phase separation time, which determines the final morphology of modified UPE resin network. Boyard and co-workers [216] confirmed the spinodal decomposition mechanism in a similar system by using small-angle laser light scattering.

At the early stages of curing, microgels of polyesters are formed because of the strong tendency towards intramolecular cyclisation (a characteristic of chain growth polymerisation). With further progress in curing, LPA and the unreacted styrene separate from these microgels in a matrix, which surrounds and isolates the microgels. Subsequently, the microgels contact each other leading to the formation of a co-continuous morphology. Bulliard and co-workers [217] carried out a detailed SEM analysis to study the characteristic morphologies of an UPE/PVAc (LPA) system. SEM photographs for the modifier UPE system (cured for 90 minutes) with different concentrations of PVAc are presented in **Figure 4.5**. The polished cured UPE resin exhibits single-phase morphology. It is referred to as 'flake-like' if the surface is a fracture surface because cracks then appear, as in glassy materials. The addition of PVAc induces a two-phase structure. At a low concentration in PVAc (**Figure 4.5b**), the PVAc-enriched phase forms domains of about 20 μm in diameter dispersed in the continuous polyester phase. The PVAc-enriched phase is composed of a globular structure. Small inclusions of PVAc are visible in the continuous polyester phase. Increasing the concentration over 5 wt% led to a transition in morphology, which

was composed of fine polyester globules a few microns in size that seemed to be connected to each other: they were the polyester microgels. This connected globule structure implies a two-phase morphology of interconnected domains of a polyester-rich phase regularly dispersed in a matrix enriched in PVAc. This morphology is referred to as a 'co-continuous' morphology. For a concentration of 14 wt% of PVAc, this interconnected globule morphology implies a step of coarsening and growth of the structure between phase separation and gelation. The structure that was shown to be co-continuous after phase separation would tend to form spherical domains of polyester because of the differences in the interfacial tension between the phases (as reported in epoxy-based systems) and because of intramolecular cyclisation of polyester molecules. The morphology comprises three elements: i) microgel particles; ii) LPA layer; and iii) lightly styrene crosslinked polyester chain and polystyrene chain between the LPA covered microgel particles between the LPA-covered microgel. The overall morphology is represented by a model which is a combination of the three elements mentioned previously. The mechanical behaviour can be approximately represented by the Takayanagi models [218, 219].

Several studies have elaborated the origin of function of LPA. The formation of micro-cracks/micro-voids has been assigned as the origin of volume shrinkage control of UPE resins by non-reactive LPA [220–223]. Pattison and co-workers [206, 220] proposed that as crosslinking of LPA-containing UPE resins proceeds, strain due to polymerisation develops in the system, particularly at the interface of LPA phase and crosslinked UPE phase. This strain can increase to a point where stress cracking propagates through the week LPA phase. In this process, the strain is relieved, leading to the generation of micro-cracks and micro-voids or both. The decrease in volume due to cure shrinkage is compensated by the space generated by micro-cracks or micro-voids.

Reactive LPA such as PVAc-*b*-PMMA, PVAc-*b*-PS with many peroxide linkages along the skeleton of LPA have also been developed. Reactive LPA, in addition to micro-cracking, reduce the inherent cure shrinkage of the resin and thereby decrease overall volume shrinkages. Dong and co-workers [223] investigated a series of reactive LPA and found that volume shrinkage control can not be explained in terms of the formation of micro-cracks or micro-voids. If micro-voiding and micro-cracking is the sole mechanism of volume shrinkage control, then a system with a smaller volume fraction of micro-voids would lead to a higher volume shrinkage, which was not found to be the case. Besides micro-void formation, the intrinsic polymerisation shrinkage is also an important factor in determining volume shrinkage control during cure of UPE/LPA systems.

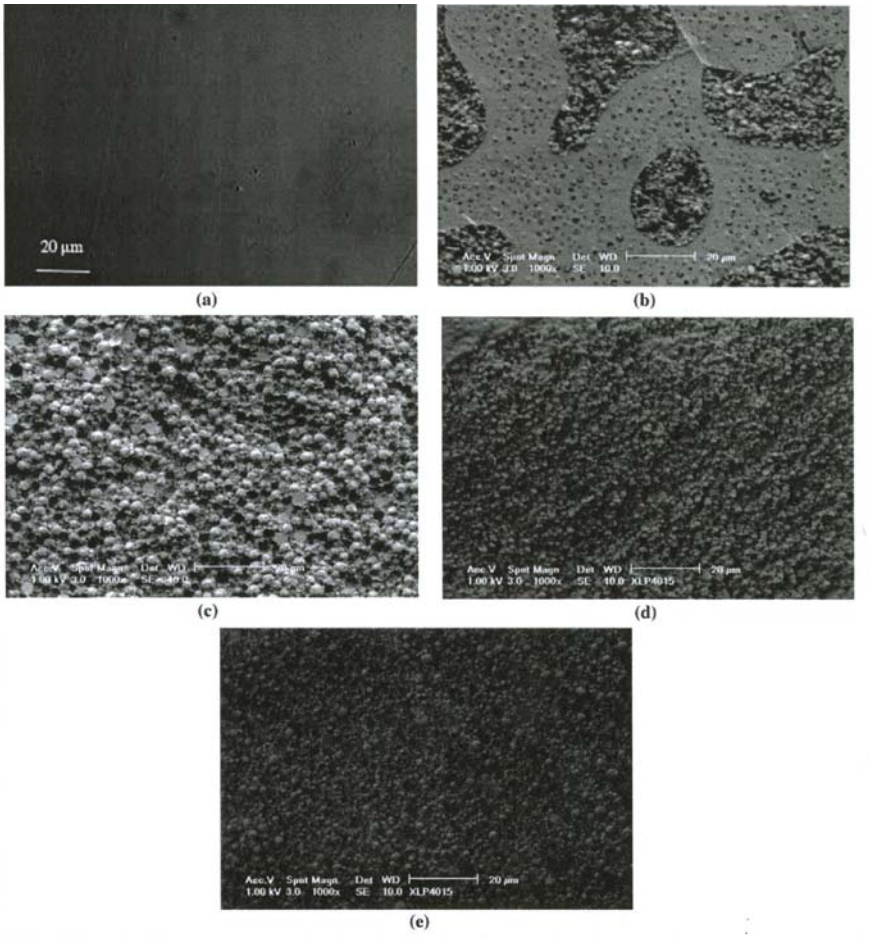

Figure 4.5 SEM photographs for the modifier UPE system (cured for 90 minutes) with different concentrations of PVAc: a) 0, b) 5, c) 6, d) 11, and d) 14 wt%. All samples were etched in 2-butanone, except (a). Reprinted with permission from X. Bulliard, V. Michaud and J-A.E. Manson, *Journal of Applied Polymer Science*, 2006, 102, 3877 © 2006, John Wiley and Sons Publishers

UPE resins are blended with several materials such as rubber or thermoplastics to improve their impact strength and fracture properties. Solid and liquid rubbers are dispersed in the resin for enhancement of toughness. The commercial toughening agents are CTBN and ATBN. Various grades of CTBN and ATBN are available with

different molecular weight and acrylonitrile content. The toughening effect of an elastomer additive depends on phase separation to provide the final morphology and to control the rubber particle size and volume fraction [224]. The toughening effect is often modest due to the low chemical reactivity of the rubber towards polyester end groups. To initiate chemical bonding, condensation of hydroxyl or carboxyl -terminated liquid rubbers and the polyester reactants has been tried, resulting in polyesters containing rubber segments in the main chain [225]. Other examples of chemically reactive rubbers are methacrylate end-capped carboxyl-terminated nitrile rubber [226] or isocyanate end-capped poly butadiene [227] or epoxy-terminated nitrile rubber [228]. Block copolymers of UPE with polyurethanes (PU), polyureas, polysiloxanes, polyimides, polyoxazolines, or polyglycols have also been reported [229]. Attempts have been made to modify UPE resins with dicyclopentadiene [230], bismaleimide [231] and poly(-caprolactone)-perfluro polyethers [232] and epoxy [233].

IPN strategy has also been used for such modifications. Alcoholic and carboxyl end groups of the resin can be blocked by isocyanates that form covalent urethane bonds [234, 235]. Chou and Lee [234] studied the morphology–kinetics–rheology relationship of polyurethane-unsaturated polyester IPN. They found that the polyurethane-rich phase formed the dispersed domains in the continuous UPE rich phase. The interaction between the two reactive systems may give rise to a synergistic effect on the properties of IPN. The interactions have been attributed to an increase in crosslink density because of mutual interpenetration of network chains [236]. Other specific interactions such as grafting [237] and opposite charged group interactions [238] between the two networks are possible reasons for property enhancement.

Cherian and co-workers [239] recently investigated IPN of polyester and polyurethane prepolymers based on various polyols such as hydroxyl-terminated natural rubber, HTPB, polyethylene glycol, and castor oil (containing the glyceride ester of ricinoleic acid). Urethane linkages are formed by the reaction between terminal hydroxyl and carboxyl groups of UPE and isocyanate groups of a polyurethane prepolymer. The schematic representation of polyurethane-UPE IPN is shown in **Figure 4.6**. The effect of incorporation of polyurethane on the strength and toughness properties of IPN is shown in **Figure 4.7** and **Figure 4.8**, respectively. It is evident that the tensile strength and toughness increase as result of incorporation of polyurethane in the IPN form, and maximum property enhancement was achieved in case of HTBP-based polyurethane.

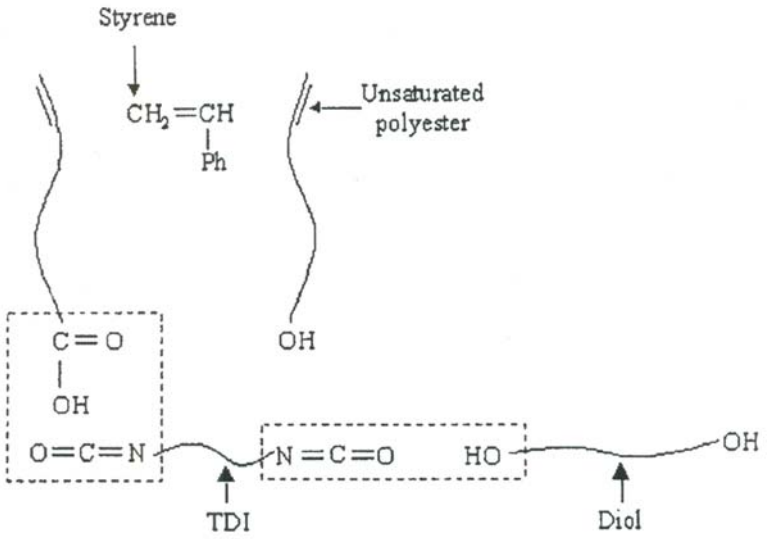

Figure 4.6 Schematic representation for the formation of PU-UPE IPN. Reprinted with permission from A.B. Cherian, B.T. Abraham, E.T. Thachil, *Journal of Applied Polymer Science*, 2006, 100, 449 © 2006, John Wiley and Sons Publishers

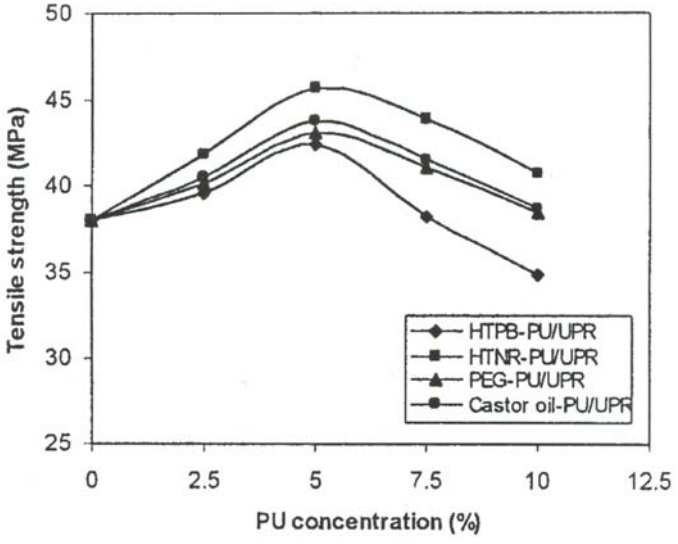

Figure 4.7 Tensile strength of PU-UPE IPN *versus* PU concentration. Reprinted with permission from A.B. Cherian, B.T. Abraham and E.T. Thachil, *Journal of Applied Polymer Science*, John Wiley and Sons Publishers, 2006, 100, 449 © 2006, John Wiley and Sons Publishers

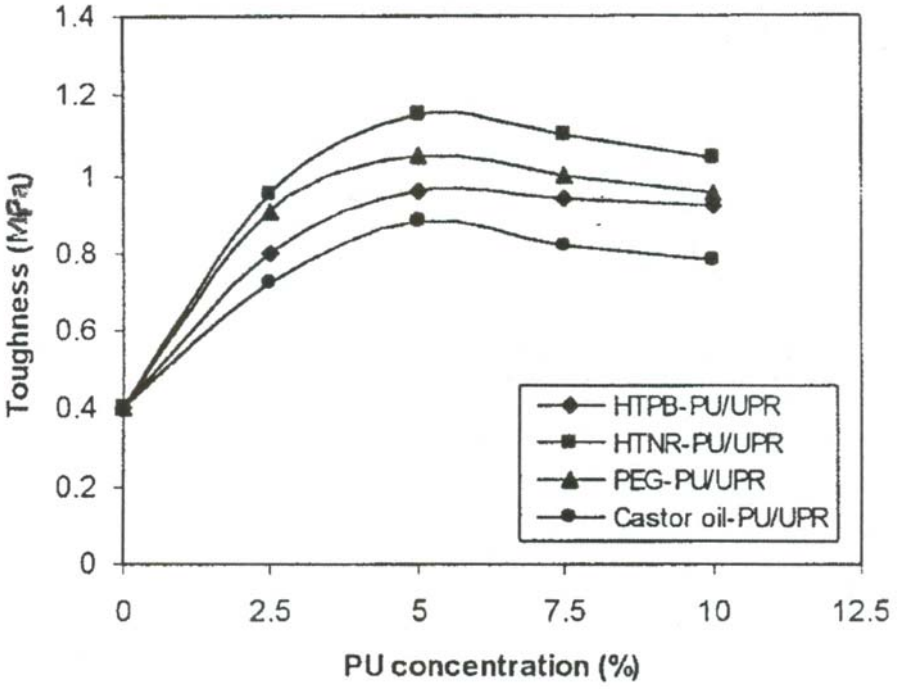

Figure 4.8 Toughness of PU-UPE IPN *versus* PU concentration. The effect of incorporation of PU on toughness properties of PU-UPE IPN. Reprinted with permission from A.B. Cherian, B.T. Abraham, E.T. Thachil, *Journal of Applied Polymer Science*, 2006, 100, 449 © 2006, John Wiley and Sons Publishers

4.6 Toughening of phenolic resins

The brittleness of phenolic resin can be reduced using derivatives of phenol (such as dihydroxydiphenyl ether) in the main reaction with formaldehyde [240]. The toughness increases due to the incorporation of ether linkages in the network. Novolac resin has been modified with flexible carboxylic acid like adipic acid [241] (**Figure 4.9**). Such modified novolac resins on curing with hexamethylene tetramine produce tougher networks due to the introduction of flexible aliphatic chains and reduction in crosslink density of the networks. Investigation of various dicarboxylic acids and various concentrations revealed that 0.0007 mole adipic acid was the optimal level of modification. An increase in strain from 3% to 7% and an increase in compression strength from 99 MPa to 142 MPa were achieved as a result of the modification.

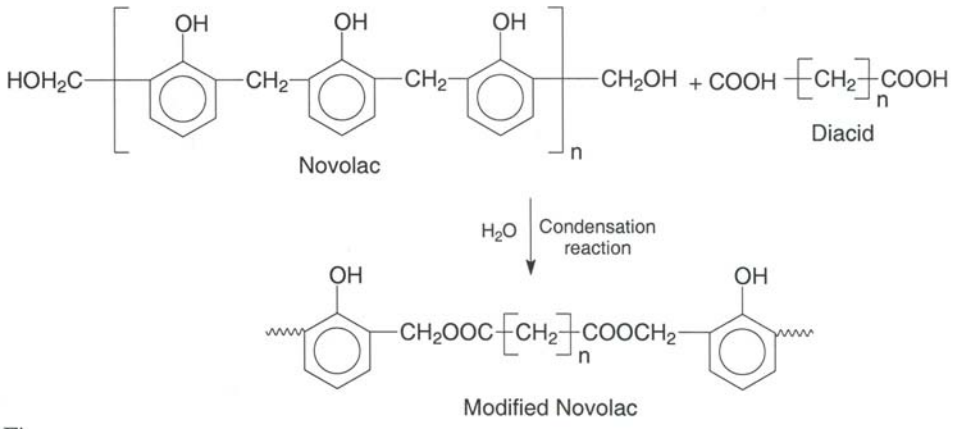

Figure 4.9 Chemical modification of novolac-type phenolic resin by a diacid

Blending of rubber has been tried out for toughening phenolic resin. Phenolic-nitrile rubber (NBR) was developed in the early 1950s, which has found wide applications [242] such as structural adhesives, O-rings, and gaskets. However, it was reported that when NBR is mixed with resole and cured, they phase separate into undesirably large domains with low adhesion between the phases [243]. A discussed earlier, for an effective toughening effect the domain size and interfacial adhesion are important.

Addition of *p*-cresol formaldehyde (PCF) into phenolic/NBR blends resulted in reduction in the domain size of the dispersed phase and improvement in mechanical properties [244]. PCF resin has an intermediate polarity compared with NBR and resole and can react faster with NBR. Therefore, PCF molecules are likely to be concentrated at the phenolic/NBR interface and act as an external compatibilising agents [245]. Thus compatibility and chemical bonding between NBR and phenolic resin is improved, leading to the enhancement in properties. The other materials used as toughening agents of phenolic resin include elastomers such as natural rubber and nitrile rubber [246, 247], reactive liquid polymers [248] and thermoplastics such as polysulfone, polyamide, polyethylene oxide [249, 250].

Gietl and co-workers [251] recently investigated the efficiency of various types of toughening agents such as CTBN, ATBN and core-shell rubber particles. They found the best performance using ATBN rubber.

4.7 Toughening of polyimide, bismaleimide and cyanate ester resins

Rubber toughening of high-temperature resins such as polyimide (PI), bismaleimide (BMI) and cyanate ester resins (CE) resins is not very successful because addition of rubber reduces the thermal stability of the resin drastically. The toughness of such resins is improved by changing the chemical structure or by blending with engineering thermoplastics or other thermoset resins. Toughness of PI and BMI resins are mostly improved by using the amines containing ether linkages and chain extension strategy as discussed in a previous chapter. BMI and CE resins can be blended with epoxy to improve processability and toughness. However, such modifications are associated with a reduction in water absorption owing to the strong polarity of epoxy groups [252]. Cyanate esters have been successfully modified by bismaleimides. However, the modified resins are extremely sensitive to curing conditions and it is very difficult to guarantee the good quality of the cured product.

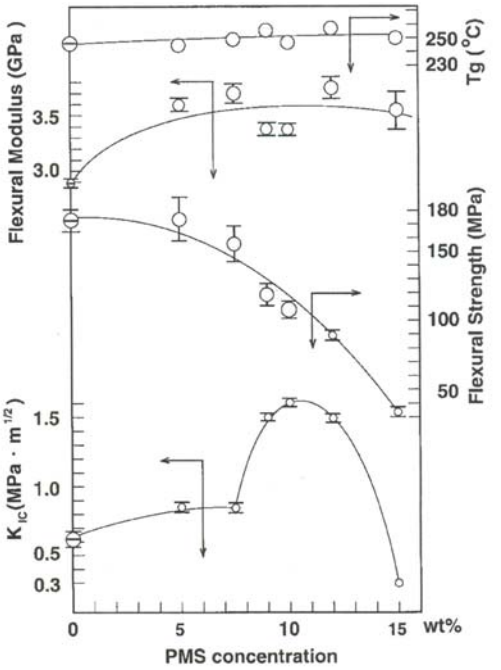

Figure 4.10 Physical properties of the modified cyanate ester resins as a function of PMS (***N***-phenylmaleimide styrene copolymer) concentration Θ, control and O, PMS (M_w 129,000 or 133,000). Reprinted with permission from T. Iijima, T. Maeda and M. Tomoi, *Journal of Applied Polymer Science*, 1999, 74, 2931 © 1999, John Wiley and Sons Publishers

Poly (ethylene phthalate) (PEP) has been successfully utilised to toughen BMI and CE resins [253]. However, the low water absorptivity of the parent resin was significantly deteriorated. Iijima and co-workers [254] used *N*-phenylmaleimide styrene copolymer (PMS) for toughening BMI and CE resins. The effect of modification of CE resin with PMS (molecular weight = 129000 g/mol) on thermomechanical properties and fracture toughness of the modified network is presented in **Figure 4.10**. The fracture toughness increases remarkably at 9–12 wt% PMS loading and decreases thereafter. The increase in toughness is associated with a modest reduction in flexural strength and slight increase in moduli. The thermal properties of the modified resins are comparable with those of unmodified resins.

Recently, Yang and co-workers [255] modified CE resins using an epoxidised polysiloxane, produced by the reaction between an epoxy resin and amido siloxane. Epoxidation of the siloxane with epoxy improves the miscibility with CE resin, and thus macro phase separation can be avoided. The modified resin offers better processability compared with the unmodified resin. A significant improvement in impact strength was achieved while maintaining the desirable flexural strength. For example, the unmodified CE resin (cured) exhibits an Izod impact strength of 5.4 kJ/m^2, whereas the modified resin with 18 wt% polysiloxane exhibits an impact strength of 9.7 kJ/m^2.

References

1. A.J. Kinloch and R.J. Young, *Fracture Behaviour of Polymers*, Applied Science Publishers, London, UK, 1983.

2. D. Ratna, *Epoxy Composites: Impact Resistance and Flame Retardency*, Rapra Review Report No.185, Smithers Rapra, Shawbury, Shrewsbury, UK, 2005.

3. S.N. Tong, D.S. Chen and T.K. Kwei, *Polymer Engineering and Science*, 1985, **25**, 54.

4. P.J. Madec and E. Marecha, *Journal of Polymer Science Part A: Polymer Chemistry Edition*, 1978, **16**, 3165.

5. S.N. Tong, C. Chen and P.T.K. Wu in *Rubber Toughened Plastics*, Ed., C.K. Riew, Advances in Chemistry Series No.222, American Chemical Society, Washington, DC, USA, 1989, p.375 .

6. J.M. Brown, S. Srinivasan, A. Rau, T.C. Word, J.E. MaGrath, A.C. Loos, D. Hood and D.E. Kranbeuhl, *Polymer*, 1996, **37**, 1691.

7. J. Borrajo, C.C. Riccardi, R.J.J. Williams, Z.Q. Cao and J.P. Pascault, *Polymer*, 1995, **36**, 3541.

8. A.J. Kinloch, S.J. Shaw and D.A. Tod in *Rubber Modified Thermoset Resins*, Eds., C.K. Riew and J.K. Gillham, Advances in Chemistry Series No.208, American Chemical Society, Washington, DC, USA, 1984, p.101.

9. C.B. Bucknall, *Toughened Plastics*, Applied Science Publishers Ltd, London, UK, 1977.

10. D. Ratna, *Jouirnal of Adhesion Science and Technology*, 2003, **17**, 1655.

11. H. Keskkula, A.E. Platt and R.F. Boyer in *Encyclopedia of Chemical Technology*, 2nd Edition, Wiley Interscience, New York, NY, USA, 1969, **19**, p.85.

12. J.L. Amos, *Polymer Engineering and Science*, 1974, **14**, 1.

13. L.E. Daly, inventor; US Rubber Company, assignee; US 2439, 202, 1948.

14. C.W. Childers and C.F. Fisk, inventors; US Rubber Company, assignee; US 2820773, 1958.

15. *History of Polymer Science and Technology*, Ed., R.B. Semour, Marcel Dekker, New York, NY, USA, 1982.

16. *Encyclopedia of Polymer Science and Technology*, Volume 1, Eds., D.M. Kulich, P.D. Kelley and J.E. Pace, John Wiley and Sons, New York, NY, USA, 1985, p.338.

17. A.W. Carlson, T.A. Zones and J.L. Martin, *Modified Plastics*, 1957, **44**, 155.

18. R.G. Bauer, R.M. Pierson, W.C. Mast, N.C. Blatso and L. Shepherd in *Multicomponent Polymer Systems*, Advances in Chemistry Series No.99, American Chemical Society, Washington, DC, USA, 1971, p.251.

19. B.D. Gesner, *Journal of Applied Polymer Science*, 1967, **11**, 2499.

20. C.J.G. Plumer, P. Bengnelin and H.H. Kausch, *Polymer*, 1996, **37**, 7.

21. B.Z. Jang, D.R. Ulhmann and J.B. Vandersande, *Journal of Applied Polymer Science*, 1985, **30**, 2485.

22. A.K. Gupta and S.N. Purwar, *Journal of Applied Polymer Science*, 1984, **30**, 1799.

23. A.K. Gupta and S.N. Purwar, *Journal of Applied Polymer Science*, 1984, **31**, 535.

24. A.K. Gupta, K.R. Srinivasan and P. Krishnakumar, *Journal of Applied Polymer Science*, 1991, **42**, 2595.

25. C.B. Bucknall and C.J. Page, *Journal of Materials Science*, 1982, **17**, 808.

26. F.C. Stehling, T. Huff, C.S. Speed and G. Wissler, *Journal of Applied Polymer Science*, 1981, **26**, 2693.

27. A.F. Yee, *Journal of Materials Science*, 1977, **12**, 757.

28. A.F. Yee, W.V. Olszewski and S. Miller in *Toughness and Brittleness of Plastics*, Eds., R.D. Deanin and A.M. Crugnala, Academic Press, New York, NY, USA, 1976, p.97.

29. J. Karger-Kocsis and I. Csikai, *Polymer Engineering and Science*, 1987, **27**, 241.

30. C.K. Riew and R.W. Smith in *Rubber Toughened Plastics*, Ed., C.K. Riew, Advances in Chemistry Series No.222, American Chemical Society, Washington, DC, USA, 1989, p.225.

31. H.E. Bair, *Polymer Engineering and Science*, 1970, **10**, 247.

32. M. Kramer, *Applied Polymer Symposia*, 1971, **15**, 227.

33. I. Park, H. Keskula and D.R. Paul, *Journal of Applied Polymer Science*, 1992, **45**, 1313.

34. S. Wu, *Journal of Applied Polymer Science*, 1988, **35**, 549.

35. S.Wu, *Polymer*, 1955, **26**, 1855.

36. R.J.M. Borggreve, R.J. Gaymans, J. Schuijer and J.F. Ingen Housz, *Polymer*, 1987, **28**, 1489.

37. A. Echte in *Rubber Toughened Plastics*, Ed., C.K. Riew, Advances in Chemistry Series No.222, American Chemical Society, Washington, DC, USA, 1989, p.15.

38. G.E. Molau and H. Keskkula, *Journal of Polymer Science, Part A: Polymer Chemistry Edition*, 1966, **4**, 1595.

39. R.N. Haward and J. Mann, *Proceedings of the Royal Society*, 1964, **A282**, 120.

40. A.J. Kinloch, *Journal of Materials Science*, 1980, **15**, 2141.

41. H. Keskkula in *Polymer Compatibility and Incompatibility*, Ed., K. Sol, Harwood Academic Publishers, London, UK, 1982, p.323.

42. N.R. Legge, S. Devison, H.E.De La Mare, G. Halden and M.K. Martin in *Applied Polymer Science*, Eds., R.W. Tess and G.W. Poehlein, American Chemical Society Symposia Series No.285, American Chemical Society, Washington, DC, USA, 1985, p.175.

43. J.R. Campbell, S.Y. Hobbs, T.J. Shea and D.J. Smith in *Multiphase Macromolecular Systems*, Ed., B.M. Culbertson, Contemporary Topics in Polymer Science No.6, Plenum Press, New York, NY, USA, 1990, p.439.

44. S.L. Aggarwall, *Polymer*, 1976, **17**, 938.

45. A.L. Bull and G. Molden, *Journal of Elastomers and Plastics*, 1977, **9**, 281.

46. A.F. Yee and J. Diamant, *Polymer Preprints*, 1978, **9**, 1, 92.

47. W.J. Coumans, D. Heikens and S.D. Sjoerdsma, *Polymer*, 1980, **21**, 103.

48. S.L. Aggarwall, R.A. Livigni, *Polymer Engineering and Science*, 1992, **45**, 1313.

49. D. Trifonova and S. Vasileva, *Journal of Materials Science*, 1992, **27**, 3657.

50. S. Newman and S. Strella, *Journal of Applied Polymer Science*, 1965, **9**, 2297.

51. F. Haff, H. Breuer and J. Stabenow, *Journal of Macromolecular Science and Physics*, 1977, **B-14**, 387.

52. A.M. Donald and E.J. Kramer, *Journal of Materials Science*, 1982, **17**, 1765.

53. G. Signa, P. Lomellini and M. Merlotti, *Journal of Applied Polymer Science*, 1989, **37**, 1527.

54. F.A. Flexman, *Polymer Engineering and Science*, 1979, **19**, 564.

55. S.Y. Hobbs, R.C. Bopp and V.H. Watkins, *Polymer Engineering and Science*, 1983, **23**, 380.

56. G. Weber and J. Schoeps, *Angewandte Makromolekulare Chemie*, 1985, **136**, 45.

57. F. Speroni, E. Castoldi, P. Fabri and T. Casirangi, *Journal of Materials Science*, 1989, **24**, 2165.

58. T. Kunori and P.H. Geil, *Journal of Macromolecular Science and Physics*, 1980, **B 18**, 135.

59. D.S. Parker, H.J. Sue, J. Huang and A.F. Yee, *Polymer*, 1985, **31**, 2267.

60. A.F. Yee, *Journal of Materials Science*, 1977, **12**, 757.

61. F.C. Chang, J.S. Wu and L.H. Chu, *Journal of Applied Polymer Science*, 1992, **44**, 491.

62. R.A. Bubech, D.J. Buckley, E.J. Kramer and H.R. Brown, *Journal of Materials Science*, 1991, **26**, 49.

63. H. Breuer, F. Haff and J. Stabenow, *Journal of Macromolecular Science and Physics*, 1977, **14**, 387.

64. F. Haff, H. Breuer, A. Echte, B.J. Schmitt and J. Stabenow, *Journal of Scientific and Industrial Research*, 1981, **40**, 659.

65. A. Tse, E. Shin, A. Hittner, E. Baer and R. Laakso, *Journal of Materials Science*, 1991, **26**, 2823.

66. D.J. Hourston, S. Lane and H.X. Zhang, *Polymer*, 1991, **32**, 2215.

67. F.W. Billmeyer, *Textbook of Polymer Science*, 3rd Edition, Wiley, New York, NY, USA, 1984.

68. R.J.M. Borggreve, R.J. Gaymans and J. Schuijer, *Polymer*, 1989, **30**, 71.

69. R.J.M. Borggreve, R.J. Gaymans and H.M. Eichenwald, *Polymer*, 1989 **30**, 78.

70. E.J. Kramer and L.L. Berger in *Crazing in Polymers, Volume 2*, Ed., H-H. Kausch, Advances in Polymer Science Series No. 91, Springer-Verlag, Berlin, Germany, 1990, p.1.

71. D. Tompas and G. Groeninckx, *Polymer*, 1994, **35**, 22, 4743.

72. D. Tompas and G. Groeninckx, *Polymer*, 1994, **35**, 22, 4751.

73. Y. Huang and A.J. Kinloch, *Polymer*, 1992, **33**, 5338.

74. M. Morton, M. Cizmecioglu and R. Lhila in *Polymer Blends and Composites in Multiphase Systems*, Ed., C. D. Han, Advances in Chemistry Series No.206, American Chemical Society, Washington, DC, USA, 1984, p.221.

75. D.L. Dunkelberger and E.P. Doughterty, *Journal of Vinyl Technology*, 1990, **12**, 212.

76. K. Dijkstra and G.H.T. Bolscher, *Journal of Materials Science*, 1994, **29,** 16, 4286.

77. A.J. Oshinski, H. Keskula and D.R. Paul, *Polymer*, 1992, **33**, 268.

78. S. Wu, *Polymer International*, 1992, **29**, 229.

79. C. Wrotecki, P. Heim and P. Gaillard, *Polymer Engineering and Science*, 1991, **31**, 213.

80. H. Liang, W. Jiang, J. Zhang and J. Bingzheng, *Journal of Applied Polymer Science*, 1996, **59**, 505.

81. E.J. Kramer and L.L. Berger in *Advances in Polymer Science*, 1990, **2**, 91/92, 1.

82. C.B. Bucknall and R.R. Smith, *Polymer*, 1965, **6**, 437.

83. M. Matuo, *Polymer*, 1966, **7**, 421.

84. R.P. Kambour and D.R. Russel, *Polymer*, 1971, **12**, 237.

85. M. Matuo, A. Ueda and Y. Kondon, *Polymer Engineering and Science*, 1970, **10**, 253.

86. J.D. Moore, *Polymer*, 1971, **12**, 478.

87. C.B. Bucknall, D. Clayton and W.E. Keast, *Journal of Materials Science*, 1972, **7**, 1443.

88. M. Matsuo, C. Nozaki and Y. Jyo, *Polymer Engineering and Science*, 1969, **9**, 197.

89. P. Beahan, A. Thomas and M. Bevis, *Journal of Materials Science*, 1976, **11**, 1207.

90. K. Kato, *Journal of Electron Microscopy*, 1968, **14**, 220.

91. K. Kato, *Polymer Engineering and Science*, 1967, **7**, 1, 38.

92. H.H. Kausch, *Polymer Fracture*, 2nd Edition, Springer Verlag, Berlin, Germany, 1987.

93. I. Narisawa, M. Ishikawa and H. Ogata, *Journal of Materials Science*, 1980, **15**, 2059.

94. G.H. Michler, *Colloid and Polymer Science*, 1989, **267**, 377.

95. R.N. Haward and C.B. Bucknall, *Pure and Applied Chemistry*, 1976, **46**, 227.

96. I.V. Yannas and R.R. Luise, *Journal of Macromolecular Science and Physics*, 1982, **B-21**, 443.

97. A.M. Donald and E.J. Kramer, *Journal of Materials Science*, 1982, **17**, 1765.

98. H. Keskkula, M. Schwarz and D.R. Paul, *Polymer*, 1986, **27**, 211.

99. M.A. Maxwell and A.F. Yee, *Polymer Engineering and Science*, 1981, **21**, 205.

100. S.T. Wellinghoff and E. Baer, *Journal of Applied Polymer Science*, 1978, **22**, 2025.

101. R.J.M. Borggreve, R.J. Gaymans, J. Schuijer and J.F. Ingen Housz, *Polymer*, 1987, **28**, 1489.

102. S. Wu, *Journal of Polymer Science, Part B: Polymer Physics Edition*, 1983, **21**, 699.

103. S. Wu and A. Mongalina, *Polymer*, 1990, **31**, 5, 972.

104. R.J.M. Borggreve, R.J. Gaymans and A.R. Luttmer, *Die Makromolekulare Chemie - Macromolecular Symposia*, 1988, **16**, 195.

105. G.D. Cooper, G.F. Lee, A.K. Katchman and C.P. Sannk, *Materials Technology*, 1981, Spring, 12.

106. C.B. Bucknall and I.C. Drinkwater, *Journal of Materials Science*, 1973, **8**, 1800.

107. R.R. Durst, R.M. Griffith, A.J. Arbenic and W.J. Van Essen in *Toughness and Brittleness of Plastics*, Ed., R.D. Deanin, Advances in Chemistry Series No.154, American Chemical Society, Washington, DC, USA, 1976, p.239.

108. D. Ratna, R. Varley and G.P. Simon, *Journal of Applied Polymer Science*, 2003, **89**, 9, 2339.

109. D. Ratna and A.K. Banthia, *Macromolecular Research*, 2004, **12**, 1, 11.

110. S. Manternal, J.P. Pascault and H. Sautereau in *Rubber Toughened Plastics*, Ed., C.K. Riew, Advances in Chemistry Series No.222, American Chemical Society, Washington, DC, USA, 1989, p.193.

111. D. Verchere, J.P. Pascault, H. Sautereau, S.M. Moschair, C.C. Riccardi and R.J.J. Williams, *Journal of Applied Polymer Science*, 1991, **42**, 701.

112. P.J. Flory, *Principles of Polymer Chemistry*, Cornell University Press, Ithaca, NY, USA, 1975.

113. A.C. Garg and Y-W. Mai, *Composites Science and Technology*, 1988, **31**, 179.

114. S. Kunz-Douglass, P.W.R. Beamont and M.F. Ashby, *Journal of Materials Science*, 1980, **15**, 1109.

115. S. Kunz-Douglass and P.W.R. Beamont, *Journal of Materials Science*, 1981, **16**, 3141.

116. J.A. Sayre, S.C. Kunz and R.A. Assink in *Rubber Modified Thermoset Resins*, Eds., C. K. Riew and J.K. Gillham, Advances in Chemistry Series No. 208, American Chemical Society, Washington, DC, USA, 1984, p.215.

117. A.N. Gent, *Science and Technology of Rubber*, Academic Press, New York, NY, USA, 1978, p.419.

118. R.A. Pearson and A.F. Yee, *Journal of Materials Science*, 1989, **24**, 2571.

119. A.C. Meeks, *Polymer*, 1974, **15**, 675.

120. A.C. Soldatos and A.S. Burhans in *Multicomponent Polymer Systems*, Advances in Chemistry Series No.99, American Chemical Society, Washington, DC, USA, 1971, p.531.

121. A.M. Donald and E.J. Kramer, *Journal of Materials Science*, 1982, **17**, 1871.

122. E.J. Kramer in *Crazing in Polymers*, Ed., H.H. Kausch, Advances in Polymer Science Series No. 52/53, Springer-Verlag, Berlin, Germany, 1983, Chapter 1.

123. A.Van den Boogaart in *Physical Basis of Yield in Glassy Polymers*, Ed., Z.R.N. Haward, Institute of Physics, London, UK, 1979.

124. J.N. Sultan, R.C. Liable and F.J. McGarry, *Journal of Applied Polymer Symposia*, 1971, **16**, 127.

125. J.N. Sultan and F.J. McGarry, *Polymer Engineering and Science*, 1973, **13**, 29.

126. J. Lilley and D.G. Halloway, *Philosophical Magazine*, 1973, **28**, 215.

127. R.J. Morgan and J.E. O'Neel, *Journal of Materials Science*, 1982, **12**, 295.

128. R.J. Morgan, E.T. Mones and W. J. Steele, *Polymer*, 1982, **23**, 295.

129. R.J. Morgan, J.E. O' Neel and D.B. Miller, *Journal of Materials Science*, 1979, **14**, 109.

130. A.F. Yee and R.A. Pearson, *Journal of Materials Science*, 1986, **21**, 2462.

131. R.A. Pearson and A.F. Yee, *Journal of Materials Science*, 1986, **21**, 2475.

132. C.B. Bucknall, F.F.P. Cote and I.K. Partdridge, *Journal of Materials Science*, 1986, **21**, 301.

133. C.B. Bucknall and T. Yoshii in *Proceedings of the Plastic and Rubber Institute International Conference on Deformation, Yield and Fracture of Polymers*, Cambridge, UK, 1976, p.131.

134. H. Breuer, F. Haff and J. Stabenow, *Journal of Macromolecular Science and Physics*, 1977, **14**, 3, 387.

135. M.A. Maxwell and A.F. Yee, *Polymer Engineering and Science*, 1981, **21**, 205.

136. R. Ramsteiner, *Polymer*, 1979, **20**, 839.

137. J. Mijovik and J.A. Koutsky, *Polymer*, 1979, **20**, 1095.

138. R.J. Young in *Development of Polymer Fracture 1*, Ed., E.H. Andrews, Applied Science Publishers, London, UK, 1979, p.183.

139. W.D. Bascom and D.L. Hunston in *Proceedings of the Plastic and Rubber Institute International Conference on Toughening of Plastics*, London, UK, 1978, p.221.

140. W.D. Bascom and D.L. Hunston in *Rubber Toughened Plastics*, Ed., C.K. Riew, Advances in Chemistry Series No.222, American Chemical Society, Washington, DC, USA, 1989, p.135.

141. A.J. Kinloch, S.J. Shaw, D.A. Tod and D.L. Hunston, *Polymer*, 1983, **24**, 1355.

142. A.J. Kinloch and D.L. Hunston, *Journal of Materials Science, Letters*, 1986, **5**, 909.

143. A.J. Kinloch in *Rubber Toughened Plastics*, Ed., C.K. Riew, Advances in Chemistry Series No.222, American Chemical Society, Washington, DC, USA, 1989, p.67.

144. A.J. Kinloch, S.J. Shaw, D.A. Tod and D.L. Hunston, *Polymer*, 1983, **24**, 1341.

145. D.L. Hunston, J.L. Bitner, J.L. Rushford, J. Oroshnik and W.S. Rose, *Journal of Elastomers and Plastics*, 1980, **12**, 133.

146. C.C. Chau and J.C.M. Li, *Journal of Materials Science*, 1981, **16**, 1858.

147. D.R. Uhlmann, *Faraday Discussions*, 1979, **68**, 87.

148. A.L. Gurson, *Journal of Engineering Materials*, 1977, **99**, 2.

149. A. Needleman, *Journal of Applied Mechanics,* 1972, **39**, 964.

150. H. Yamamoto, *International Journal of Fracture*, 1978, **14**, 347.

151. V. Tvergaard, *International Journal of Fracture*, 1981, **17**, 389.

152. M.E.J. Dekkers, S.Y. Hobbs and V.H. Watkins, *Journal of Materials Science*, 1988, **23**, 1225.

153. F.J. Guild and R.J. Young, *Journal of Materials Science*, 1989, **24**, 2454.

154. D. Li, A.F. Yee, I.W. Chen, S.C. Chang and K. Takahashi, *Journal of Materials Science*, 1994, **29**, 8, 2205.

155. A.G. Evans, Z.B. Ahmad, D.G. Gilbert and P.W.R. Beaumont, *Acta Metallurgica*, 1986, **34**, 79.

156. K.T. Faber and A.G. Evans, *Acta Metallurgica*, 1983, **31**, 565.

157. A.F. Yee and R.A. Pearson, *Journal of Materials Science*, 1991, **26**, 2273.

158. Y. Huang and A.J. Kinloch, *Journal of Materials Science*, 1992, **27**, 2763.

159. Y. Huang and A.J. Kinloch, *Journal of Materials Science Letters*, 1992, **11**, 484.

160. C.B. Bucknall and T. Yoshii, *British Polymer Journal*, 1978, **10**, 53.

161. S.C. Kunz, J.A. Sayre and R.A. Assink, *Polymer*, 1982, **23**, 1897.

162. J.A. Sayre, S.C. Kunz and R.A. Assink in *Rubber Modified Thermoset Resins*, Eds., C.K. Riew and J.K. Gillham, Advances in Chemistry Series No.208, American Chemical Society, Washington, DC, USA, 1984, p.215.

163. A. J. Kinloch and D.L. Huntston, *Journal of Materials Science Letters*, 1987, **6**, 137.

164. A.J. Kinloch, G.A. Kodokian and M.B. Jamarani, *Journal of Materials Science*, 1987, **22**, 4111.

165. B.J. Cardwell and A.F. Yee, *Polymer*, 1993, **34**, 8, 1695.

166. H. Huange and A.J. Kinloch, *Journal of Adhesion*, 1993, **41**, 5.

167. D.L. Hunston, A.J. Kinloch, S.J. Shaw and S.S. Wang, *Adhesive Joints*, Ed., K.L. Mittal, Plenum Press, NY, USA, 1984, p.789.

168. K. Fulin and U.L. Chung, *Journal of Materials Science*, 1994, **29**, 1198.

169. A.R. Siebert in *Rubber Modified Thermoset Resins*, Eds., C.K. Riew and J.K. Gillham, Advances in Chemistry Series No.208, American Chemical Society, Washington, DC, USA, 1984, p.179.

170. A. Lowe, O.H. Kwon and Y.H. Mai, *Polymer*, 1996, **37**, 4, 565.

171. H.R. Daghyani, L. Ye, Y.W. Mai and J.S. Wu, *Journal of Materials Science Letters*, 1994, **13**, 18, 1330.

172. L.C. Chen, J.K. Gillham, S.J. Kinloch and S.J. Shaw in *Rubber Modified Thermoset Resins*, Eds., C.K. Riew and J.K. Gillham, Advances in Chemistry Series No.208, American Chemical Society, Washington, DC, USA, 1984, p.261.

173. Y.B. Zeng, L.Z. Zang, W.Z. Peng and Q. Yu, *Journal of Applied Polymer Science*, 1991, **42**, 1905.

174. R.A. Pearson and A.F. Yee, *Journal of Materials Science*, 1991, **26**, 3828.

175. A. Mongolina and S. Wu, *Polymer*, 1988, **29**, 2170.

176. S. Wu and A. Mongolina, *Polymer*, 1990, **31**, 972.

177. S. Wu, *Journal of Applied Polymer Science*, 1988, **35**, 549.

178. S.D. Sjoerdsma, *Polymer Communications*, 1989, **30**, 106.

179. D. Tompas and G. Groeninckx, *Polymer*, 1994, **35**, 4760.

180. A.J. Kinloch and D.L. Hunston, *Journal of Materials Science Letters*, 1987, **6**, 137.

181. J.P. Bell, *Journal of Applied Polymer Science*, 1970, **14**, 1901.

182. J.P. Bell, *Journal of Polymer Science*, 1987, **A-2**, 6, 13.

183. J.D. Lemay, B.J. Swetlin and F.N. Kelley in *Characterization of Highly Crosslinked Polymers*, Eds., S.S. Labana and R.A. Dickie, ACS Symposium Series No.243, American Chemical Society, Washington, DC, USA, 1984, p.165.

184. S.L. Kim, M.D. Skibo, J.A. Manson, R.W. Hertzberg and J. Janisjewski, *Polymer Engineering and Science*, 1978, **18**, 1093.

185. B.W. Cherry and K.W. Thomson, *Journal of Materials Science*, 1981, **16**, 1913.

186. R.A. Pearson and A.F. Yee, *ACS Polymeric Materials Science and Engineering Preprints*, 1983, **186**, 316.

187. G. Levita, A. Marchetti and E. Butta, *Polymer*, 1985, **26**, 1110.

188. G. Levita, A. Marchetti, A. Lazzeri and V. Frosini, *Polymer Composites*, 1987, **8**, 141.

189. G. Lavita, S. Depetris, A. Marchetti and A. Lazzeri, *Journal of Materials Science*, 1991, **26**, 2348.

190. G. Levita in *Rubber Toughened Plastics*, Ed., C.K. Riew, Advances in Chemistry Series No.222, American Chemical Society, Washington, DC, USA, 1989, p.93.

191. G.A. Crosbie and M.G. Philips, *Journal of Materials Science*, 1985, **20**, 182.

192. A.J. Kinloch, S.J. Shaw and D.A. Tod in *Rubber Modified Thermoset Resins*, Eds., C.K. Riew and J.K. Gillham, Advances in Chemistry Series No.208, American Chemical Society, Washington, DC, USA, 1984, p.101.

193. K.A. Hodd, *Epoxy Resins*, Rapra Review Report No.38, Rapra Technology, Shawbury, Shrewsbury, UK, 1990.

194. Y. Huang, A.J. Kinloch, R. Bertsch and A.R. Siebert in *Toughened Plastics I – Science and Engineering*, Eds., C.K. Riew and A.J. Kinloch, Advances in Chemistry Series No.233, American Chemical Society, Washington, DC, USA, 1993, p.189.

195. J.S. Ullett and R.P. Chartoff, *Polymer Engineering and Science*, 1995, **35**, 1086.

196. J.S. Ullett and R.P.Chartoff, *ACS Polymeric Materials Science and Engineering Preprints*, 1993, **70**, 100.

197. A.R. Siebert, C.D. Guiley, A.J. Kinloch, M. Fernando and E.P.L. Heijnsbrock in *Toughened Plastics II: Novel Approaches in Science and Engineering*, Eds., C.K. Riew and A.J. Kinloch, Advances in Chemistry Series No.252, American Chemical Society, Washington, DC, USA, 1996, p.151.

198. S. Phas and P.J. Burhcill, *Polymer*, 1995, **36**, 3279.

199. P.J. Burchill, A. Kootsooks and M. Lau, *Journal of Materials Science*, 2001, **36**, 4239.

200. P.J. Pearce, A.R. Siebert, D.R. Egan, C.D. Guiley and R.S. Drake, *Journal of Adhesion*, 1995, **49**, 245.

201. E. Dreerman, M. Narkis, A. Siegmann R. Joseph, H. Dodiuk and A.T. Dibenedetto, *Journal of Applied Polymer Science*, 1999, **72**, 647.

202. F.H. Liao, N.J. Chu, and S.N. Tong, *Journal of Applied Polymer Science*, 1988, **35**, 797.

203. J. Karger-Kocsis, J. Frohlich, O. Gryshchuk, H. Kautz, H. Frey and R. Mulhaupt, *Polymer*, 2004, **45**, 4, 1185.

204. O.Gryshchuk, N. Jost and J. Karger-Kocsis, *Polymer*, 2002, **43**, 17, 4763.

205. J. Karger-Kocsis, O.Gryshchuk and N. Jost, *Journal of Applied Polymer Science*, 2003, **88**, 8, 2124.

206. V.A. Pattison, R.R. Hindersinn and W.T. Schwartz, *Journal of Applied Polymer Science*, 1974, **18**, 2763.

207. Y.S. Yang and L.J. Lee, *Polymer*, 1988, **29**, 1793.

208. K.E. Atkins in *Sheet Molding Compounds: Science and Technology*, Ed., H.G. Kia, Hanser Publishers, New York, NY, USA, 1993, Chapter 4.

209. L. Suspene, D. Fourquier and Y.S.Yang, *Polymer*, 1991, **32**, 1593.

210. C.B. Bucknall, I.K. Partridge and M.J. Phillips, *Polymer*, 1991, **32**, 638.

211. Y.J. Huang and C.M. Liang, *Polymer*, 1996, **37**, 401.

212. Y.J. Huang, C.J. Chu and J.P. Dong, *Journal of Applied Polymer Science*, 2000, **78**, 543.

213. Y.J. Huang, T.S. Chen, J.G. Huang and F.H. Li, *Journal of Applied Polymer Science*, 2003, **89**, 3336.

214. M. Kinkelaar, B. Wang and L. Lee, *J. Polymer*, 1994, **35**, 3011.

215. W. Li and J. Lee, *Polymer*, 2000, **41**, 697.

216. N. Boyard, M. Vayer, C. Sinturel and R. Erre, *Journal of Applied Polymer Science*, 2005, **95**, 1459.

217. X. Bulliard, V. Michaud and J.-A.E. Manson, *Journal of Applied Polymer Science*, 2006, **102**, 3877.

218. M. Takayanagi, K. Imada and T. Kojiyama, *Journal of Polymer Science Part C,* 1966, **15**, 263.

219. Y.J. Huang and J.C. Horing, *Polymer*, 1998, **39**, 3683.

220. V.A. Pattison, R.R. Hindersinn and W.T. Schwartz, *Journal of Applied Polymer Science*, 1975, **19**, 3045.

221. Z. Zhang and S. Zhu, *Polymer*, 2000, **41**, 3861.

222. J.P. Dong, J.G. Huang, F.H. Lee, J.W. Roan and Y.J. Huang, *Journal of Applied Polymer Science*, 2004, **91**, 3388.

223. J.P. Dong, S.G. Chiu, M.W. Hsu and Y.J. Huang, *Journal of Applied Polymer Science*, 2006, **100**, 967.

224. L. Suspene, Y.Y.Show and P.J. Pierre in *Rubber Toughened Plastics*, Eds., C.K. Riew and A.J. Kinloch, Advances in Chemistry Series No.233, American Chemical Society, Washington, DC, USA, 1993.

225. V.M. Rosa, J.Karger-Kocsis and M.I. Felisberti, *Journal of Applied Polymer Science*, 2001, **81**, 3280.

226. F.J. McGarry, E.H. Rowe and C.K. Riew, *Polymer Engineering and Science*, 1978, **18**, 2.

227. M. Malinconico, E.Martuscelli, G. Ragosta and M.G. Volpi, *International Journal of Polymer Materials*, 1987, **11**, 317.

228. G.A. Crosbie and M.G. Phillips, *Journal of Materials Science*, 1985, **20**, 182.

229. C.K. Riew in *Rubber Toughened Plastics*, Ed., C.K. Riew, Advances in Chemistry Series No.222, American Chemical Society, Washington, DC, USA, 1989, p.230.

230. H.T. Chiu and S.C. Chen, *Journal of Polymer Research*, 2001, **8**, 183.

231. B. Gawdzik, T. Matynia and E. Chmielewska, *Journal of Applied Polymer Science*, 2001, **82**, 2003.

232. M. Messori, M. Toselli, F. Pilati and C. Tonelli, *Polymer*, 2001, **42**, 9877.

233. Z.G. Shaker, R.M. Browne, H.A. Stretz, P.E. Cassidy and M.T. Blanda, *Journal of Applied Polymer Science*, 2002, **84**, 2283.

234. Y.C. Chou and L. Lee, *Polymer Engineering and Science*, 1995, **35**, 976.

235. L. Valette and C-P. Hsu, *Polymer*, 1999, **40**, 2059.

236. K.C. Frisch, D. Klempner and H.L. Frisch, *Polymer Engineering and Science*, 1982, **22**, 1143.

237. P.R. Scarito and L.H. Sperling, *Polymer Engineering and Science*, 1979, **19**, 297.

238. J.K. Yeo, L.H. Sperling and D.A. Thomas, *Journal of Applied Polymer Science*, 1983, **26**, 3283.

239. A.B. Cherian, B.T. Abraham and E.T. Thachil, *Journal of Applied Polymer Science*, 2006, **100**, 449.

240. Y. Takase, M. Nishi, T. Yamagishi and Y. Nakamoto, *Polymer Preprints*, 2005, **54**, 397.

241. T.B. Iyim, *Journal of Applied Polymer Science*, 2007, **106**, 46.

242. N.J. DeLollis, *Adhesives, Adherends, Adhesion*, Krieger Publishing, Huntington, NY, USA, 1980, p.105.

243. P.S. Achary, G. Chockalingam and R. Ramaswamy, *Journal of Adhesion Science and Technology*, 1988, **6**, 415.

244. P.S. Achary and R. Ramaswamy, *Journal of Applied Polymer Science*, 1998, **69**, 1187.

245. *Polymer Blends, Volume 2,* Eds., D.R. Paul and S. Newman, Academic Press, New York, NY, USA, 1978, p.9.

246. P.S. Achary, G. Chockalingam and R. Ramaswamy, *Journal of Applied Polymer Science*, 1998, **69**, 1187.

247. C.C. Kaynak and O. Agatay, *Polymer Testing*, 2006, **25**, 296.

248. G. Camino, E. Alba and P. Buonfico, *Journal of Applied Polymer Science*, 2001, **82**, 1346.

249. J.T. Carter, *Plastics, Rubber and Composites Processing and Applications*, 1991, **16**, 157.

250. H. Wu, C.C. Ma and J. Lin, *Journal of Applied Polymer Science*, 1997, **63**, 911.

251. T. Gietl, H. Lengsfeld and V. Altstadt, *Journal of Materials Science*, 2006, **41**, 8226.

252. G.Z. Liang and M.X. Zhang, *Journal of Applied Polymer Science*, 2002, **85**, 2377.

253. T. Iijima, H. Shiono, W. Fukuda and M. Tomoi, *Journal of Applied Polymer Science*, 1997, **65**, 1349.

254. T. Iijima, T. Maeda and M. Tomoi, *Journal of Applied Polymer Science*, 1999, **74**, 2931.

255. C. Yang, A. Gu, H. Song, Z. Fang and L. Tong, *Journal of Applied Polymer Science*, 2007, **105**, 2020.

5 Toughened Epoxy Resins

In Chapter 4, toughening of thermoset resins was discussed in a general way. Among the commercially available thermosetting resins, epoxy resins have been the most extensively studied, and toughening technology has been exploited in the field of adhesive and fibre-reinforced composites. This is due to the inherent ductility of the cured epoxy resins and versatile epoxy resin chemistry. In this chapter, the toughening of epoxy resin will be discussed specifically.

5.1 Chemical Modification

Unlike thermoplastics, non-reactive liquid plasticisers are not successful in improving the toughness and bond strength of epoxy resins. This is because after the formation of a network, as a result of curing, the modifier exudes out from the matrix or undergoes macro-phase separation. Moreover, the accumulation of free liquid plasticiser molecules at the substrate surface can act as a weak boundary layer in the adhesive joints, leading to a substantial decrease in adhesive joint strength [1, 2]. Reactive diluents, which are basically monoepoxide compounds, are used as plasticisers for epoxy. The use of a long-chain hardener is reported in the literature as a solution to this problem of low bond strength [3, 4], as discussed in Chapter 3.

Ratna and colleagues [5–8] reported the chemical modification of diglycidyl ether of bis-phenol A (DGEBA) with carboxyl-terminated poly(ethylene glycol) adipate (CTPEGA). CTPEGA was prepared by the condensation polymerisation of polyethylene glycol (PEG) with an excess amount of adipic acid using *p*-toluene sulfonic acid as a catalyst. The epoxy resin was prereacted with CTPEGA in presence of triphenyl phosphine (TPP) as a catalyst till no carboxyl group was found by titration. The reaction is basically a carboxyl-epoxy esterification reaction, as proposed by Romanchick and co-workers [9]. The product was epoxy end-capped PEG adipate which can be cured in the same way as epoxy. A large excess of epoxy resin was used for end capping the CTPEGA to prevent further polymerisation. The reaction is illustrated in **Figure 5.1**. The modified epoxy can be cured in the same way as epoxy, leading to the formation of a crosslinked network. The stress–strain diagram for the modified networks containing varying concentrations of CTPEGA [6] is shown in

Figure 5.2. As the concentration of CTPEGA increases, the tensile strength decreases and percentage elongation at break increases slowly. This can be attributed to the increase in flexibility of the matrix as a result of the incorporation of flexible ether linkage (–O–) into the matrix. Moreover, due to the pre-reaction of epoxy with CTPEGA, the molecular weight (Mw) between crosslinks increases, which enhances the flexibility of the matrix. CTPEGA can be further reacted with diaminodiphenyl sulfone (DDS) to make an amine-terminated polysulfone (ATPS) [7] (**Figure 5.3**). ATPS can be used as hardener-cum-flexibiliser for epoxy resins [8].

Though chemical modification as discussed previously resulted in a significant improvement in flexibility, the major downside of this approach is that it is associated with a significant decrease in modulus and the glass transition temperature (T_g) (**Table 5.1**). This problem can be overcome by using second phase toughening strategy as discussed in Chapter 4. The various toughening agents reported will be discussed under four subsections: liquid rubber toughening, core-shell particle toughening, thermoplastic toughening, and rigid particle toughening.

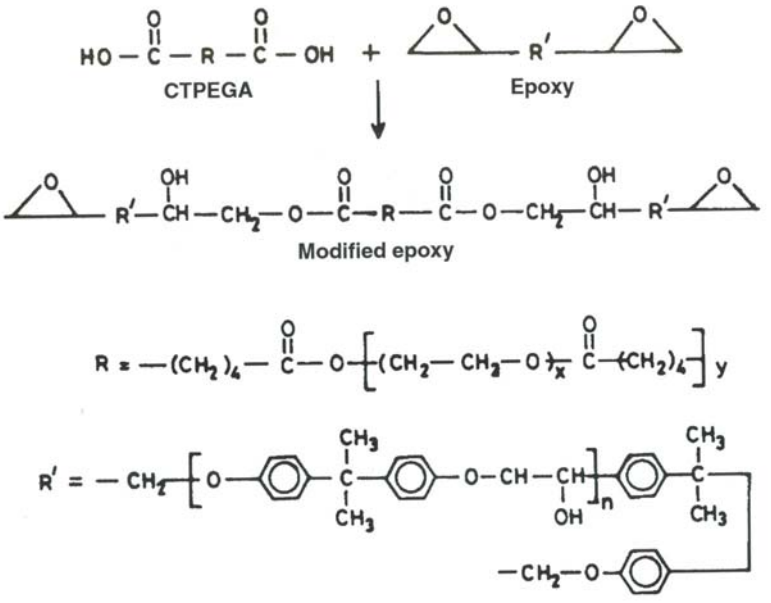

Figure 5.1 Chemical modification of epoxy resin with carboxyl-terminated poly (ethylene glycol) adipate (CTPEGA). Reprinted with permission from D. Ratna, A.B. Samui and B.C. Chakraborty, *Polymer International*, 2004, **53**, 1882. ©2004, John Wiley and Sons Publishers,

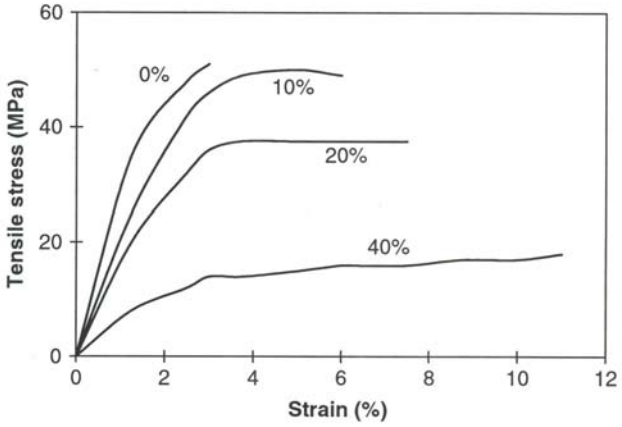

Figure 5.2 Stress–strain diagrams for modified epoxy networks containing varying concentrations of CTPEGA. Reprinted with permission from D. Ratna, A.B. Samui and B.C. Chakraborty, *Polymer International*, 2004, **3**, 1882. ©2004, John Wiley and Sons Publishers

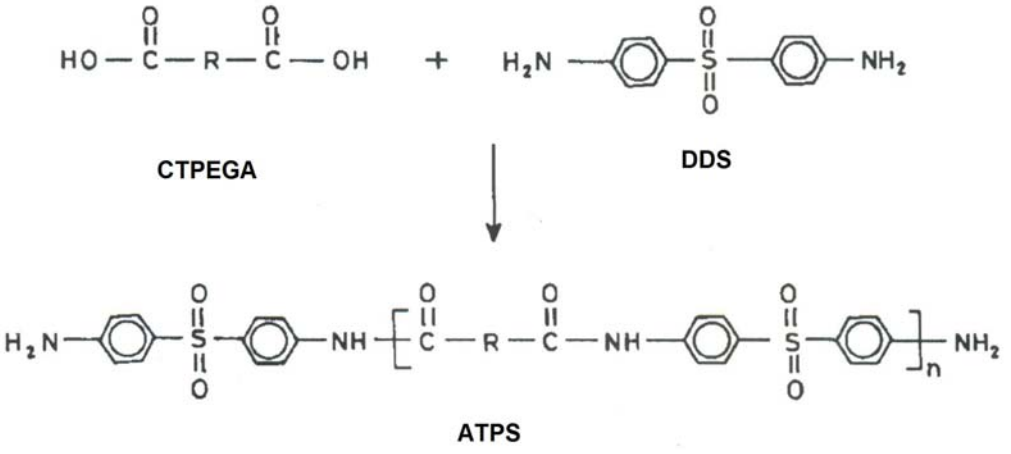

Figure 5.3 Synthesis of amine-terminated polysulfone (ATPS). Reprinted with permission from D. Ratna, M.Patri, B.C. Chakraborty and P.C. Deb, *Journal of Applied Polymer Science*, 1997, **65**, 901. ©1997, John Wiley and Sons Publishers

Table 5.1 Effect of chemical modification on the thermomechanical properties of epoxy [6]				
Concentration of CTPEGA (phr)	**Tensile strength (MPa)**	**Flexural strength (MPa)**	**Impact strength (J/m)**	**T_g (°C)**
0	54	135	19	115
10	48	120	26	90
20	39	98	32	75
30	28	50	27	65
40	18	20	24	50

5.2 Rubber Toughening

In rubber toughening, an elastomeric modifier is incorporated into the epoxy matrix as a second phase (as discussed in **Chapter 4**), which is why improvement in toughness is achieved without a significant sacrifice of the T_g and mechanical properties. The toughening agents reported so far can be classified as commercial, other rubber-based, acrylate-based and hyperbranched polymer-based modifiers.

5.2.1 Commercial Toughening Agents

The commercial toughening agents used widely are carboxyl-terminated copolymer of butadiene and acrylonitrile (CTBN) and amine-terminated copolymer of butadiene and acrylonitrile (ATBN) from Goodrich Company. A multifunctional liquid rubber (nitrile-diene-acrylamide terpolymer) for toughening epoxy composites and coatings was developed by the Wolverine Gasket division of Eagle-Picher Industries (Inkster, MI, USA) [10]. A new additive that increases the strength and toughness of amine-cured epoxy resins has been commercialised by Uniroyal Limited (Elmira, Canada). NASA has discovered [11] that fibre-reinforced epoxy composites can be made tougher by incorporating a bromine-containing additive, which resulted in a substantial increase in flexural and impact strength. Addition of a small amount of CTBN or ATBN further improved these properties.

5.2.2 Rubber-based Toughening Agents

Apart from carboxyl and amine-terminated nitrile rubbers, the rubbers having other end groups like amine [12-14], mercaptan [15, 16] hydroxyl [17] and epoxy [18,

19] have also been examined. Riew and co-workers [20] showed that ATBN could be added to the amine curatives which could then be mixed with the epoxy resin. Unfortunately, ATBNs are not universally soluble in amine curatives. Among the reactive ended nitrile rubbers, CTBN gives the best performance. The better adhesive strength of the CTBN-modified epoxy in comparison with epoxy system modified with NBR with other reactive groups can be attributed to the better adhesion of CTBN-modified epoxy with the substrate due to the presence of carboxyl groups.

Cunliff and co-workers [21, 22] in a series of articles described the generation of rubber-modified epoxy prepared by anionic polymerisation of monomers such as isoprene, butadiene and acrylonitrile. Their method ensures the reaction of anionic functional rubber with epoxy, which then guarantees the reaction of epoxy end-capped rubber to the matrix. They found all the rubbers increased the shear strength of the epoxy-based adhesive system. However, they did not carry out detailed fracture analysis. The main problem with their techniques was the instability of the rubber particles, which tended to coalesce upon standing. Meek [23] investigated the use of preformed acrylonitrile-butadiene-styrene powder as a toughening agent. He found that the fracture energy value surpassed the same for CTBN-modified system.

Rezaiford and co-workers [24] reported that significant toughness enhancement could be achieved by using poly(methyl methacrylate) (PMMA)-grafted natural rubber instead of CTBN. Carboxyl-terminated polyisobutylene [25] and polysulfide [26, 27] rubbers are also reported as effective modifier for DGEBA resin using different types of amine hardeners. Mizutani [28] reported an anhydride-cured transparent toughened epoxy network using hydroxyl-terminated liquid polycloroprene rubber as a toughening agent. Modified networks containing 0–10 vol% of liquid rubber lead to a completely phase separated microstructure. However, the modified networks are transparent because the refractive index of rubber is comparable with that of the epoxy.

Siloxane rubbers, because of attractive properties such as high chain flexibility, extremely low T_g (about –100 °C), low surface tension and surface energy and hydrophobic behaviour, have been used for toughening epoxy resins. Poly (dimethyl siloxane) oligomer (PDMS) is not compatible with epoxy resin because pure PDMS has a calculated solubility parameter of about 7.6 (cal/mole).s, which is much lower than that of epoxy resin (δs = 7.4-7.8) [29]. Due to its extreme incompatibility with epoxy resin, it is macroscopically immiscible or exudes out from the crosslinked matrix during the curing process. Pure PDMS therefore has little use as a toughening agent for epoxy. 2-Aminopropyl siloxane is better as a modifier for epoxy [30], but is not highly miscible either. The mechanical properties of siloxane-modified epoxy networks depend on the method of modification. For example, the modulus of silicone-modified epoxy is lower when modification is carried out in toluene solution compared with modified networks made in melt [30, 31].

The compatibility is increased by copolymerising dimethyl siloxane with diphenyl siloxane or dimethyl fluoropropylsiloxane [30]. Such copolymers having a controlled structure and can be successfully used as toughening agents [32, 33]. Konzol and co-workers [34] reported that the miscibility of PDMS can be increased by introducing polycaprolactam (PCL) block into PDMS. Hydroxyl-terminated block copolymers having a basic structure (PCL)2-*b*-PDMS-*b*-(PCL)2 with a controlled composition leads to a phase separated system with uniformly dispersed elastomeric particles with size in the order of 20 nm. Incorporation of about 5 wt% of such modifier resulted in twofold increase in toughness. Tong and co-workers [35–37] showed that the miscibility of PDMS with epoxy can be improved by grafting the PDMS with glycidyl methacrylate (GMA). The graft segments of PMMA and PGMA on the siloxane particles surface enhance their compatibility with the epoxy and ensure homogeneous distribution of particles, leading to an effective toughening effect.

Riffle and co-workers [38, 39] developed an epoxy-terminated siloxane oligomer and used it successfully for the toughening of epoxy resin. The epoxy-terminated oligomer was further reacted with piperzine to get a secondary amine group end-capped oligomer which can be used to cure and modify epoxy resins. Silicone-epoxy block copolymers have also been investigated [40] as toughening agents for epoxy. Lanzetta and co-workers [41] modified epoxy resin by hydroxyl-terminated block copolymer of PDMS and polyoxyethylene (PDMS-*co*-PEO) elastomer and functionalised saturated polybutene. These modified networks exhibit a better oxidative stability but do not produce similar effects reported in the literature for CTBN and ATBN on the mechanical properties of epoxy.

Polyepichlorohydrin (PECH) is reported to be a toughening agent for epoxy in patents [42, 43] and published literature [44]. The structure of PECH, with its pendent chloromethyl groups and terminal-hydroxyl groups, gives great flexibility in the variation of interactions that could be introduced by pre-reaction or curing reaction. The degree of toughening depends on the $\bar{M}_w$ (weight average molecular weight) of the PECH and on the curing temperature. Optimal properties were achieved with PECH of highest $\bar{M}_w$ of 3400 g/mole. The PECH-modified epoxy exhibits similar thermomechanical and hot-wet properties as CTBN-modified epoxy.

Epoxy groups containing triglyceride oils viz. Vernoria oil [45, 46], epoxidised soybean oil (ESO) [47, 48] and castor oil [49, 50] have been utilised to toughen epoxy resins. Direct mixing of epoxidised oil and epoxy resin followed by curing of the mixture does not lead to a two-phase microstructure and offers only a plasticising effect. The two-phase microstructure was obtained by using prepolymer of ESO and amine hardener instead of pure ESO. The high molecular weight of the prepolymer compared with pure ESO reduces its compatibility with the epoxy and favours phase separation [47, 48]. The optimal modifier concentration was found to be 10–20 phr. At >30 phr of rubber concentration, phase inversion takes place.

Samajima and co-workers [51] described a poly(ether ester)-based modifier made from dimethyl terepthalate, butanediol and poly (tetramethylene ether) glycol. They have demonstrated that the elastomer also phase separates and increases flexural strength of epoxy over that of unmodified epoxy. Carboxyl terminated poly (propylene glycol) adipate (CTPPGA) has been used as liquid rubber for the development of ambient temperature-curing epoxy adhesive [52]. The effects of concentration and molecular weight of the liquid rubber, on the impact and adhesive properties of the modified epoxy resin have been studied. It was reported that for effective toughening, the Mw must be >5000 g/mole and the addition of 15 wt% of such CTPPGA resulted in a threefold increase in lap shear strength and a fivefold increase in T-peel strength.

Polyurethane (PU) oligomer has been investigated as a modifier for epoxy resins by Wang and Chen [53, 54]. They developed hydroxyl-, amine- and anhydride-terminated PU prepolymer by reacting the isocyanate-ended PU oligomers with bisphenol-A, DDS, and benzophenone tetracarboxylic anhydride, respectively. Evaluating the oligomers having different reactive groups, they found that hydroxyl-terminated oligomers offer the best toughening effect. Incorporation of about 20 wt% of this oligomer into epoxy matrix resulted in a fivefold increase in fracture energy compared with the unmodified epoxy.

Laeuger and co-workers [55, 56] reported the toughening of anhydride-cured DGEBA resin by using diol and bis (4-hydroxy benzoate)-terminated poly (tetrahydrofuran) liquid rubber. The morphology development occurs via spinodal decomposition and is monitored by transmission electron microscopy (TEM) and small angle light scattering. The liquid rubbers react with DGEBA to form segmented liquid rubbers with poly (tetrahydrofuran) and poly (hydroxy ether) segments. The bis (4-hydroxy benzoate) terminated poly (tetrahydrofuran) gives better performance compared with the diol-terminated one as far as mechanical and fracture properties are concerned. Modification with 20–30 phr of poly (propylene carbonate) resulted [57] in 30% improvement of lap shear strength and 75% increase in impact strength.

5.2.2 Acrylate-Based Toughening Agents

Commercially available liquid rubber (CTBN, ATBN)-toughened epoxy often shows outstanding fracture properties, and the technology is exploited in engineering adhesives [58]. However, because the butadiene component of the elastomer contains unsaturation, it would appear to be a site for premature thermal and/or oxidative instability, and such modified resins are not suitable for application at high temperature. One would imagine that excessive crosslinking could take place with time which would detract from otherwise desirable improvements accomplished with these structures. Second, there is some limitation in its use due to a possibility of the

presence of traces of free acrylonitrile, which is carcinogenic. Hence, considerable efforts have been made to develop saturated liquid rubbers alternative to CTBN [59, 60].

Functionalised acrylic oligomers can be shown to exhibit considerable utility as toughening agents for epoxy due to the following reasons.

(i) The T_g of various acrylates are well below room temperature (~30 °C). Moreover, some of these acrylates are known for their high damping peak which in turn may be helpful for toughening of epoxy resin from a mechanistic point of view.

(ii) Even at room temperature low molecular weight acrylate oligomers which are elastomeric in nature are viscous liquids.

(iii) Low molecular weight acrylates are compatible with DGEBA resin because the difference in solubility parameter of certain acrylates is relatively small.

(iv) Due to lack of unsaturation, the oxidative stability and aging resistance of acrylates are much superior compared with unsaturated rubbers such as CTBN.

(v) Acrylate monomer can be conveniently polymerised or copolymerised by conventional technology.

5.2.2.1 Synthesis of Functionalised Acrylate Rubbers

Ratna and co-workers [61–68] extensively reported on acrylate-based liquid rubbers for toughening epoxy resins. Various acrylate-based modifiers have been synthesised, namely carboxyl-terminated poly(2-ethyl hexyl acrylate) (CTPEHA), carboxyl-randomised poly(2-ethyl hexyl acrylate) (CRPEHA), amine-terminated poly(2-ethyl hexyl acrylate) (ATPEHA) and poly(2-ethyl hexyl acrylate) oligomer with terminal and pendent reactive groups (carboxyl or amine). CTPEHA or ATPEHA can be prepared by bulk polymerisation of EHA using a carboxyl- or amine-ended initiator and chain-transfer agent. A typical synthetic process for CTPEHA is briefly described next.

CTPEHA of various molecular weights was synthesised [60, 63] by bulk polymerisation, using 4,4´-Azobis (4-cyanovaleric acid) (ABCVA) (Aldrich) as a free radical initiator and dithiodiglycolic acid (DTDGA) as a chain transfer agent. The reaction was carried out in a three-necked reaction flask (500 ml) fitted with a stirrer, a thermometer pocket, and a gas inlet. Approximately, 100 g (0.54 mole) of EHA monomer was put into the reaction flask and rapidly brought to the desired temperature. After the system was well purged with nitrogen gas, 3.0 g of ABCVA

(2 mol%) and the required amount of DTDGA (2.3–11.3 g, 2–10 mol%) were added. The reaction was allowed to occur for 1 h with stirring. The mixture was then diluted with toluene (200 ml), cooled to room temperature and left overnight. The unreacted ABCVA and DTDGA precipitated out and were removed by filtration. Unreacted monomer and solvent were removed under vacuum on a rotary evaporator until a constant weight was obtained.

The initiator ABCVA on dissociation generates carboxyl-ended free radicals which initiate monomer molecules to produce the growing macro radicals. These growing macro radicals evidently react with DTDGA through cleavage of the sulphur–sulphur bond to form carboxyl end-capped oligomers. This reaction reduces the probability of chain termination of growing acrylate radicals by combination and disproportionation. A tentative reaction mechanism is shown in **Figure 5.4**. Because acrylates are known to terminate through combination of free radicals rather than disproportioation, the functionality of the liquid rubber should theoretically be 2. However, the process mentioned previously generates liquid rubber with functionality in the range of 1.6–1.9 eq/mole (**Table 5.2**). The deviation of the value of functionality from the theoretical value of 2 can be attributed to the chain transfer to monomer. In order to keep the functionality close to 2, it is necessary to synthesise the liquid rubbers by bulk polymerisation. In case of solution polymerisation, the solvent competes with the functionalised chain transfer agent in the chain transfer process and significantly reduces the functionality. Solution polymerisation produces almost monofunctional resin (**Table 5.2**).

Table 5.2 Physicochemical properties of acrylate rubbers [61, 63]

Solvent	DTDGA Concentration (mole %)	$\bar{M}_n$ [a]	$\bar{M}_n$ [b]	$\bar{M}_w$ [b]/ $\bar{M}_n$ [b]	Functionality (f) (eq/mole)
Nil	2	9500	8000	7.8	1.8
Nil	5	7000	4700	8.2	1.7
Nil	10	3600	2400	7.3	1.9
Dioxan	2	2360	1900	2.3	1.2
THF	2	2700	2200	2.7	1.3

[a] The number average molecular weight ($\bar{M}_n$) was measured by vapour pressure osmometer

[b] weight average molecular weight ($\bar{M}_w$) was measured by gel permeation chromatography

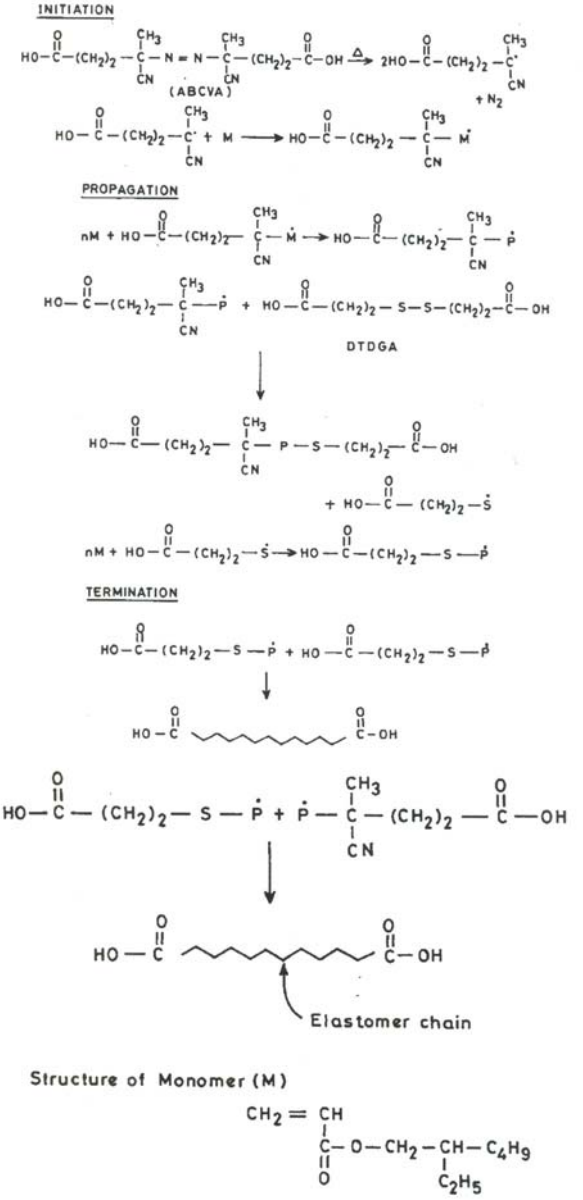

Figure 5.4 A tentative reaction mechanism for formation of carboxyl-terminated poly(2-ethyl hexyl acrylate) (CTPEHA) from free radical polymerisation of EHA in the presence of 4, 4′-azobis (4-cyanovaleric acid) (ABCVA) as a free radical initiator and dithiodiglycolic acid (DTDGA) as a chain transfer agent. (P• = nM•) Reprinted with permission from D. Ratna, A.K. Banthia and P.C. Deb, *Journal of Applied Polymer Science*, 2000, **78**, 716. ©2000, John Wiley and Sons Publishers

5.2.2.2 Acrylate-Modified Epoxy

The acrylate modification of epoxy resins is carried out in two ways: a one-stage method and two-stage method. In the former, the modifier is directly blended with the resin/hardener mixture. In a two-stage process the modifier is pre-reacted with the epoxy resin and the pre-reacted resin further cured with a suitable hardener. For the modification of high temperature-curing epoxy systems, any of the previously mentioned processes can be adopted. For room temperature-curing epoxy systems, a two-stage modification method is recommended because generally the modifiers react with the epoxy at a much slower rate compared with a curing agent. For example, when a carboxyl-functionalised modifier is directly blended with a room temperature-curing epoxy system (resin + hardener) the modifier cannot form chemical bonds with the epoxy because a epoxy-carboxyl reaction does not take place at room temperature. Hence, in order to initiate chemical bonding of the modifier with the epoxy, it is necessary to adopt the pre-reaction method for modification of a room temperature-curing epoxy system.

In general, the modified resin shows a higher gel point compared with the unmodified resin due to the lower reactivity of the unmodified resin as a result of chain extension and dilution effect. The effects of CTPEHA modification (using a two-stage method) on gel time and T_{peak} (temperature corresponding to the exothermic peak obtained in differential scanning calorimetry (DSC)) are shown in **Table 5.3**. As expected, both the gel time and Tpeak increase with increasing concentration of CTPEHA. However, when CTPEHA modification is carried out by the one-stage method (i.e., by direct blending of CTPEHA with epoxy without pre-reaction), the T_{peak} was found to decrease. This can be explained by considering the accelerating effect of carboxyl groups of CTPEHA on the epoxy–amine reaction. The behaviour can be interpreted in terms of intermolecular transition state of the epoxy–amine reaction. According to this mechanism, strong hydrogen bonding species such as acids and alcohols stabilise the transition state and strongly accelerate the reaction (as discussed in Chapter 3).

Acrylate rubbers are initially miscible with the epoxy resin and undergo phase separation during curing, leading to the formation of a two-phase microstructure. Such a two-phase microstructure with uniformly dispersed rubber particles often offers outstanding fracture properties as the rubber particles dissipate the mechanical energy by various mechanisms (as discussed in **Chapter 4**). The effect of addition CTPEHA on the impact strength of the modified epoxy is shown in **Figure 5.5**. The impact strength of modified epoxy increases with increasing CTPEHA concentration, attains a maximum at 10–15 phr and decreases thereafter. The decrease in impact strength beyond an optimal concentration is attributed to the deviation from uniformly dispersed morphology as a result of agglomeration.

Table 5.3 Effect of CTPEHA modification on gel time, T_{peak} and T_g of modified epoxy cured with DETDA [64]				
Concentration of CTPEHA (phr)	**Gel time (min)**	**T_{peak} (°C)**	**Viscosity (Pa-s)**	**T_g # (°C)**
0	43	195	2.8	203
5	48	205	9.1	198, –60
10	51	210	14.8	196, –60
15	53	215	18.1	185, –55
20	61	217	23.2	174, –58
# Values determined from DSC analysis of cured network using the same cure schedule; the two T_g values refer to the epoxy-rich phase (high value) and CTPEHA-rich phase (low value)				

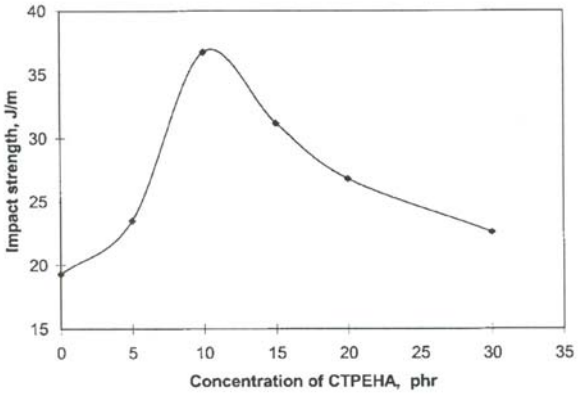

Figure 5.5 Effect of CTPEHA content on impact strength of a modified epoxy network. Reprinted with permission from D. Ratna, A.K. Banthia and P.C. Deb, *Journal of Applied Polymer Science*, 2001, **80**, 1792. ©2001, John Wiley and Sons Publishers

Morphology depends on the functionality and Mw of the rubber. Intial cure temperature also has an important role in deciding morphological development for a particular rubber-modified system. The post-curing temperature has no role in morphological development because the phase separation is arrested at gelation due to a tremendous increase in viscosity. The theoretical reasons for the effect of these parameters have already been discussed in section 4.3.1. Because the impact property of the modified network depends on the resulting morphology, adjustment of initial

cure temperature is equally important as the selection of correct liquid rubber. For example, CTPEHA-modifed epoxy contaning 10 phr CTPEHA and cured with diethyl toluene diamine (DETDA) shows a significant enhancement in impact properties when the resin is cured at 140 °C compared with the unmodified epoxy. When the same system is cured at 180 °C, the cured resin displays a much lower impact strength. The results can be explained by considering the fact that at a higher temperature the curing reaction is so fast that the geletion is reached immediately and the dissolved rubber does not get sufficient time to undergo phase separation. Scanning electron microscopy (SEM) photographs of fracture surfaces of the modified epoxy/DETDA systems cured at 160 °C and 180 °C are shown in **Figure 5.6**. The modified system cured at 180 °C shows almost single-phase morphology with very little phase-separated rubber. This explains the poor impact performance of the epoxy system cured at 180 °C as it has already been explained in section 4.3.2 that phase-separated rubber particles initiate the shear yielding by various mechanisms and effectively enhance the toughness of the matrix, whereas the dissolved rubber plasticises the matrix and causes a nominal increase in toughness.

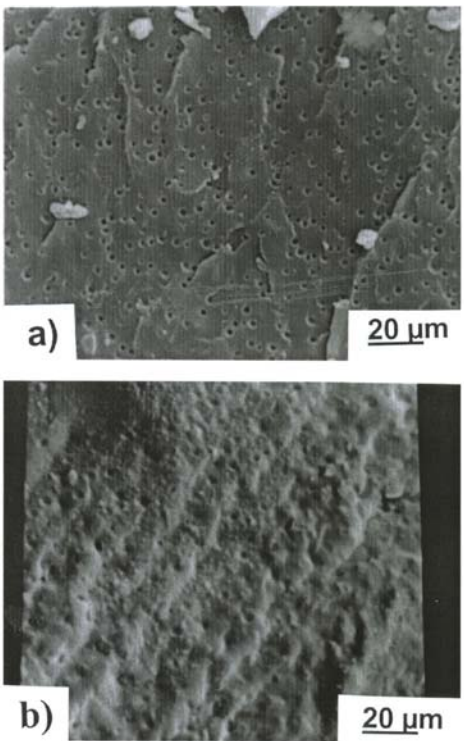

Figure 5.6 SEM photographs of fracture surfaces of CTPEHA-modified epoxy/DETDA systems cured at (a) 140 °C and (b) 180 °C. Reprinted with permission from D. Ratna, *Polymer*, 2001, **42**, 4209. ©2001, Elsevier Publishing Company

Thus a complete phase separation can be achieved for such acrylate liquid rubbers by increasing the $\bar{M}_w$ of the liquid rubber and decreasing the cure temperature within the processing window. The T_g values for CTPEHA (number average moleculer weight, $\bar{M}_n$ = 3600 g/mole) modified epoxy (cured with DETDA) are presented [64] in **Table 5.3**. The modified DSC analysis shows two T_g, one for epoxy network and other is due to phase-separated CTPEHA. Since CTPEHA forms chemical bonds with the epoxy, it is expected that the T_g of phase-separated CTPEHA will be higher than the T_g of pure CTPEHA. However, it was observed [64, 48] that the T_g of phase-separated CTPEHA (–45 °C) is lower than pure CTPEHA (– 60 °C). This can be explained by considering thermal shrinkage stress [48]. Triaxial thermal shrinkage stress develops in the dispersed domain phase on cooling through epoxy T_g because the coefficient of thermal expansion of rubbery state is larger than that of the glassy state. The triaxial stress increases the free volume of the rubbery CTPEHA particles and depresses the T_g of the precipitated CTPEHA. It is also evident from **Table 5.4** that up to 10 phr CTPEHA concentration there is no significant change in epoxy, which suggests almost a complete phase separation.

Table 5.4 A comparison of toughening effects of various modifiers for epoxy matrix

Liquid rubber	Optimum concentration	Curing agent	Improvement in property	Reference
CTBN	15 phr	HY 960[a]	400% T-peel strength	[4]
CTBN	15 phr	Piperidine	100% T-peel strength	[2, 3]
CTPPGA	15 phr	HY 960[a]	400% T-peel strength	[52]
CTPEHA	10 phr	HY 951[b]	100% impact strength	[63]
ESR	20 wt%	HY 960[a]	100% lap shear strength	[47]
PECH	10 phr	Pipyridine	66% fracture toughness K_{IC}	[44]
PU prepolymer	Not established	DDS	400% fracture energy G_{IC}	[53, 54]
BA, VBGE, St terpolymer	20 wt%	DDS	80% fracture energy G_{IC}	[73, 74]
HBP	5 wt%	Isophorone-diamine	600% G_{IC}	[75, 78]
HBP	15 wt%	DETDA	300% impact strength	[76]

[a] Tris-2,4,6-(*N*,*N*-dimethyl amino methyl) phenol

[b] Trimethylene tetramine

Increase in the molecular weight of liquid rubber favours phase separation. Hence to ensure complete phase separation, it is necessary to use liquid rubber with sufficiently high weight-average molecular weight ($\bar{M}w$). However, beyond a certain $\bar{M}w$, the liquid rubber undergoes phase separation at a very early stage, leading to the agglomeration and macrophase separation (**Figure 5.7**). The fracture surface of an epoxy network modified with CTPEHA (having a number-average molecular weight of 10,000 g/mole) shows agglomerated particles having a size >10 micron. The optimal molecular weight is reported to be about 7000 g/mole for CTPEHA [61, 62] and 3000 g/mole for CRPEHA [65].

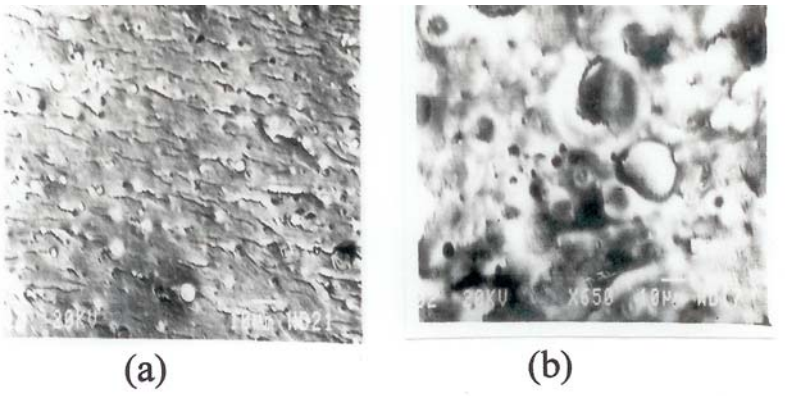

Figure 5.7 SEM microphotographs of the fracture surfaces of a TETA-cured epoxy network modified with CTPEHA of different molecular weight a) $\bar{M}_n$= 3600 g/mole b) $\bar{M}_n$ = 9500 g/mole. Reprinted with permission from D. Ratna, A.K. Banthia and P.C. Deb, *Journal of Applied Polymer Science*, 2000, **78**, 716. ©2000, John Wiley and Sons Publishers

In order to study the effect of functionality on toughening effect, various acrylate rubbers having only a pendent carboxyl group and both the terminal and pendent groups have been investigated. The acrylate rubber with pendant carboxyl groups (i.e., CRPEHA) can be prepared by copolymerising EHA and acrylic acid. The advantage of CRPEHA over CTPEHA is that CRPEHA can be made by solution polymerisation, which offers better control over polymerisation reaction compared with bulk polymerisation (method of preparation for CTPEHA). The synthesis of CTPEHA using solution polymerisation produces almost monofunctional resins (**Table 5.2**). The impact strength of the liquid acrylate rubber-modified epoxy networks as a function of carboxyl functionality of the liquid rubber is shown in **Figure 5.8**. Impact strength increases with an increase in carboxyl functionality, attains a maximum,

and then decreases [66]. It appears that an increase in chemical interaction of the liquid rubber and the epoxy matrix leads to the initial increase in impact strength of the matrix.

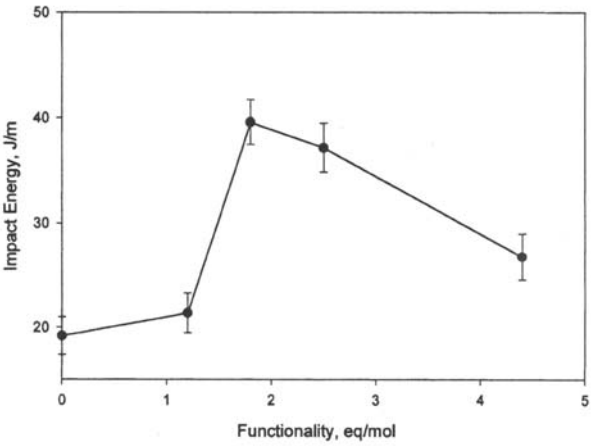

Figure 5.8 Effect of carboxyl functionality of carboxyl-randomised poly (2-ethyl hexyl acrylate) (CRPEHA) on impact strength of a modified epoxy network. Reprinted with permission from D. Ratna and G. P. Simon, *Polymer*, 2001, **42**, 7739. ©2001, Elsevier Publishing Company

However, the increase in toughness cannot be attributed to only the increase in rubber particle to matrix adhesion as the thermal analysis results indicate that the Tg value of the modified networks (all containing same amount of rubber) decreases with an increase in functionality of the resin. The depression of epoxy T_g in a rubber-modified system arises due to residual rubber, which remains dissolved in the epoxy matrix. Hence for a particular composition, the amount of dissolved rubber increases with an increase in functionality of the rubber. The dissolved rubber increases the ductility of the epoxy matrix. This has a twofold effect on toughness: (i) improvement of toughness due to a plasticising effect and (ii) increase in effectiveness of the toughening process imparted by the rubber particles. The toughening mechanism highlights the role of inherent ductility of the matrix in influencing the toughness of multiphase network. For example, a decrease in the stress needed for localised shear yielding should obviously assist in increasing the toughness if all other microstructural features are unchanged [68]. Rubber toughening of brittle tetraglycidyl methylene dianiline (TGMDA)-based networks has resulted in minimum improvement of fracture energy in contrast with the comparatively ductile DGEBA-based networks [69, 70]. Lavita and co-workers [70] plotted the fracture energy of toughened thermoset *versus* the fracture energy

of the unmodified epoxy which represents an amplification factor of 10. TGMDA-based resin formulation cured with pipyridine (PIP) is more amenable to toughening by addition of CTBN than the DDS-hardened system because of the lower ductility of the latter [70]. The fracture energy of TGMDA-PIP is four-times greater than that of the TGMDA-DDS system but fracture energy of the CTBN-modified (20 phr) TGMDA-PIP system is 24-times greater than that of the toughened TGMDA-DDS system [71, 72]. This is because the rubber-rich particles, as stress concentrators, induce plastic deformation of highly brittle matrix to a far lesser extent. Hence, the increase in rubber particle to matrix adhesion and the flexibilising effect of dissolved rubber contribute to the improvement in toughness.

A decrease in toughness above an optimum value of the functionality of the liquid rubber can be explained in terms of solubility parameter and chemical interactions. The solubility parameter of epoxy is higher than acrylate rubber (PEHA). With the introduction of carboxyl functionality the solubility parameter of the acrylate oligomer increases. When the functionality reaches an optimum value, the solubility parameter difference between the epoxy and acrylate rubber ($\delta_e \sim \delta_r$) becomes less than 0.1. As a result the decrease in combinatorial entropy cannot compensate for the enthalpy term (recall **Equation 4.3, Chapter 4**) and the free energy change of mixing does not become positive before gelation. Hence the rubber with higher functionality cannot phase separate and leads to a single-phase morphology. This explains the decrease in impact strength of acrylate modified epoxy when the functionality goes beyond an optimum value. The nominal enhancement in impact strength results due to plasticising effect of the dissolved rubber. In addition, the liquid rubber having higher functionality undergoes extensive chemical reaction with the epoxy, which further makes the phase separation more difficult.

Iijima and co-workers [73, 74] used an acrylic elastomer containing pendent epoxy groups to reduce the brittleness of DGEBA resin cured with diamino diphenyl sulfone (DDS). The elastomers were prepared by copolymerisation of butyl acrylate (BA), vinyl benzyl glycidyl ether (VBGE) and styrene (St) or acrylonitrile. The addition of 20% of the terpolymer (74 mole% BA, 18 mole% VBGE and 8 mole% St) resulted in an 80% increase in fracture energy of the cured resin at the slight expense of its mechanical properties.

5.2.3 Hyperbranched polymer (HBP) - based toughening agents

The modification of epoxy with linear elastomers, as discussed in previous sections, is associated with a considerable increase in viscosity, which is disadvantageous from a processing point of view. The problem can be overcome by using dendritic HBP toughening agents [75, 76]. Due to the compact, three-dimensional (3D)

structure of dendritic polymers, these molecules mimic the hydrodynamic volume of spheres in solution or melts, and flow easily past each other under applied stress. This results in a low melt viscosity, even at high molecular weights, due to a lack of restrictive interchain entanglements [77]. Dendritic polymers have been shown to exhibit melt and solution viscosities that are an order of magnitude lower than their linear analogues of similar M_w. The high density of functional terminal groups on dendritic polymers also offer the potential for tailoring their compatibility with epoxy through conversion of dendritic polymer end groups to chemically suitable moieties or through in-situ reaction to form covalently bound networks. These two properties (low viscosity and tailorable compatibility) make HBP excellent candidates as flow additives that could act simultaneously as toughening agents. These polymers are commercially available e.g., Bolton. A schematic representation of hydroxyl and epoxy-functionalised HBP are shown in **Figure 5.9**.

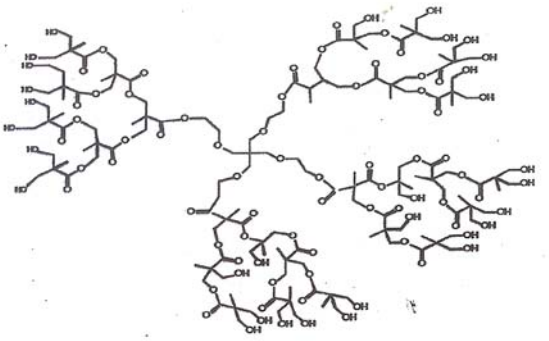

Hydroxy-functionalized HBP

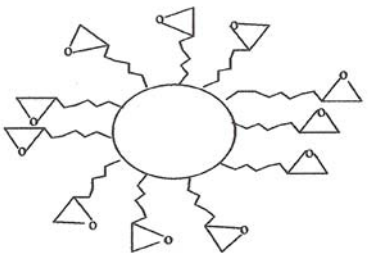

Epoxy-functionalized HBP

Figure 5.9 Chemical structures of hydroxyl and epoxy-functionalised hyperbranched polymers (HBP)

Boogh and co-workers [78, 79] first investigated the effect of incorporation of HBP on the fracture properties of epoxy resins. They reported an increase in critical strain energy release rate (G_{1c}) by a factor of 6 as a result of addition of 5 wt% of epoxy functionalised HBP in the epoxy matrix. Ratna and co-workers [80–86] studied extensively the blends of epoxies (difunctional and multifunctional) and HBP with various functionalities such as epoxy and hydroxyl. A significant toughening effect was demonstrated. A comparison of the toughening effect of various toughening agents is presented in **Table 5.4**.

Epoxy-functionalised HBP is not miscible with epoxy at room temperature but becomes miscible at higher temperature (100 °C). With the advancement of curing reaction, the HBP undergoes phase separation, leading to the formation of a two-phase microstructure as shown by optical microscopic analysis (**Figure 5.10**). It was confirmed from dynamic mechanical analysis and microscopic studies that the HBP phase separates completely up to 15 wt% of HBP concentration. The loss factor *versus* temperature plots for epoxy/HBP (epoxy-functionalised) is shown in **Figure 5.11**. The plot clearly shows two relaxation peaks; one is at high temperature for epoxy and other is at low temperature for the HBP. There is no change in epoxy T_g up to 15 wt% of HBP, suggesting complete phase separation.

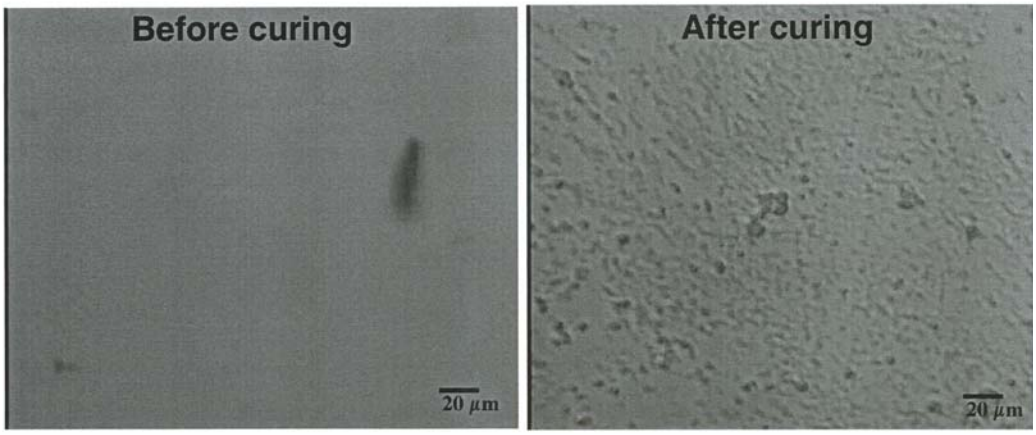

Figure 5.10 Optical microscopy photographs of epoxy/HBP/DETDA mixture (a) before curing (b) after curing. Reprinted with permission from D. Ratna, *Composites A*, 2008, **39**, 462. ©2008, Elsevier Publishing Company

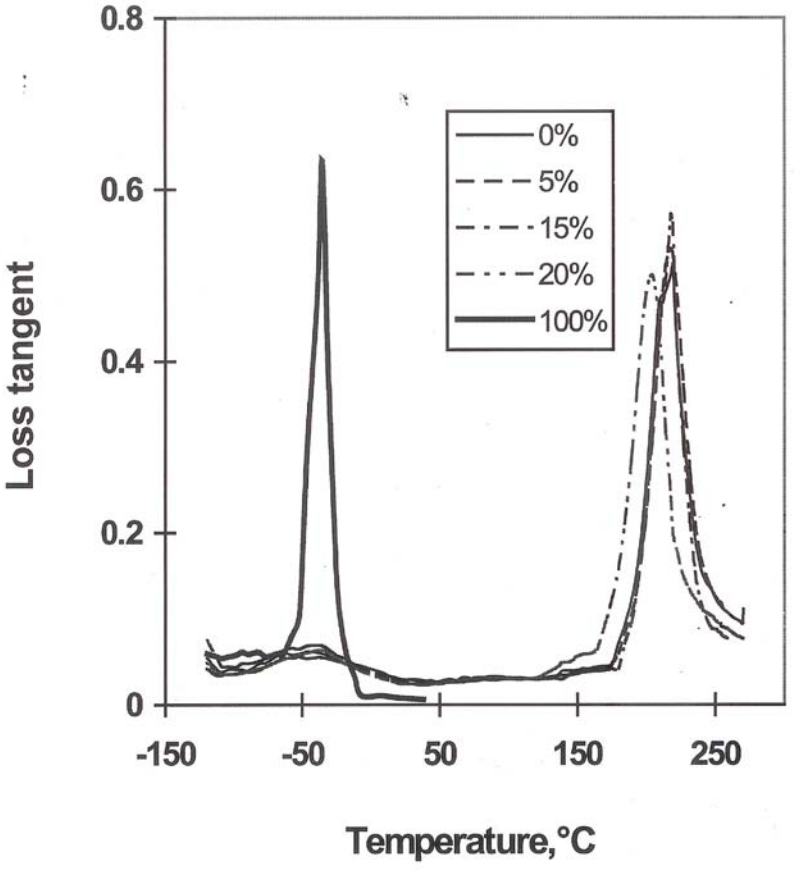

Figure 5.11 Loss tangent versus temperature plots of epoxy, epoxy-functionalised HBP and epoxy/HBP blends cured with DETDA

The effect of addition of epoxy-functionalised and hydroxyl-functionalised HBP on gelation at 160 °C for epoxy/HBP blends is shown in **Figure 5.12**. The figure indicates that addition of epoxy-functionalised HBP has hardly any effect on gelation and vitrification, although HBP is known to cure at a slower rate compared with that of epoxy resin. This behaviour is different from that observed in the case of other liquid rubbers such as CTPEHA (discussed earlier), where a significant increase in gel time was observed. In those cases, the delay was attributed to the viscosity effect, which retards the movement of reactive molecules. Blending of HBP with epoxy, however, does not lead to a significant change in viscosity and hence the reaction rate remains unaffected. The viscosity of HBP at 25 °C (15 Pa-s) is about three-times lower than that of the acrylate-based liquid rubber CTPEHA (42 Pa-s). Addition of hydroxyl-

functionalised HBP was found to decrease the gel time of epoxy/HBP blends [81–83] (**Figure 5.12**). This indicates that hydroxyl-functionalised HBP blends undergo curing faster than epoxy alone. This can be explained by considering the accelerating effect of HBP on the epoxy–amine reaction as discussed in Chapter 3.

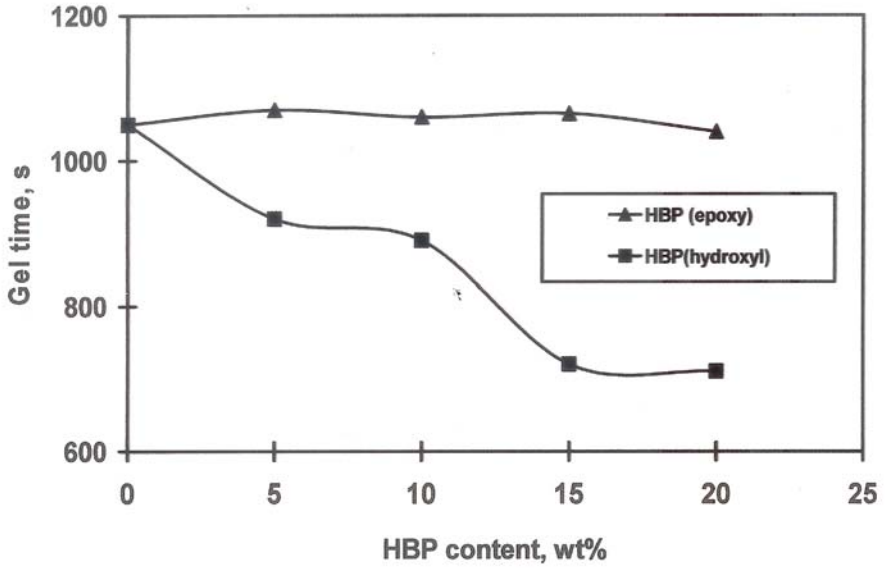

Figure 5.12 Effect of addition of hydroxyl and epoxy-functionalised hyperbranched polymers (HBP) on the gel time of modified epoxy

5.3 Core-Shell Particle Toughening

Liquid rubber toughening is associated with a reaction-induced phase separation process during which the rubber (initially miscible with epoxy) undergoes phase separation and generates morphology with a two-phase microstructure. The phase separation process depends upon the formulation, processing and curing conditions. Incomplete phase separation can result in a significant lowering of T_g. Moreover, the rubber phase that separates during the cure is difficult to control and may result in an uneven particle size. The differences in morphology and volume of the separated phase affect the mechanical performance of the product. The factors that affect the fracture toughness of the modified epoxy such as morphology, particle

size and composition are interdependent, hence it is very difficult to study the effect of an individual parameter. These problems can be minimised by using insoluble preformed particles directly [87–89]. Since the size, morphology and composition, shell thickness and crosslink density of the rubbery cores can be controlled separately by employing emulsion polymerisation techniques, the effects of various parameters on the toughening of epoxies can be investigated individually. The control of the particle parameters by emulsion polymerisation has been extensively studied, and various efficient technologies developed [90–93]. Monodisperse latex particles with a diameter from submicron to micron range can be prepared by sequential seeded emulsion polymerisation [87], sequential swelling process [89] and dispersion polymerisation [90, 91]. Cohesive strength, which is influenced by crosslink density of the rubber phase, can be controlled by the conversion of polymerisation and the amount of crosslinking agent [93]. Interfacial architecture can be controlled by changing the following parameters: (1) thickness of the shell (which depends on the ratio of the shell-core materials and polymerisation mechanism); (2) chemical bonding and physical interaction between particles and matrix (which can be enhanced by introducing functional groups onto the surface of the shell); (3) grafting between the shell and core and (4) weight-average molecular weight ($\overline{M}w$) of shell materials. Various morphologies of the composite such as core shell, occluded or multilayer, can be achieved through two- or multiple-stage emulsion polymerisation [94]. Typically, core shell morphology latex particles can be made by semicontinuous process under a monomer 'starved' condition [95].

Preformed particles are incorporated into the epoxy matrix by simple mechanical mixing. The dispersibility of the particles can be improved by: 1) introducing crosslinking into the shell or 2) using comonomer-like acrylonitrile or GMA, which increases the interfacial adhesion by polar or chemical interaction [96, 97]. Quan and co-workers [98] reported that for poly (butadiene-co-styrene) core poly (methyl methacrylate) (PMMA) shell particles, the cluster size reduces from 3–5 μm to 1–3 μm as a result of using 5 wt% crosslinker (divinyl benzene). They also found that the cluster size could be further reduced to 1–2 μm by using a methyl methacrylate-acrylonitrile (MMA-AN) or methyl methacrylate-glycidyl methacrylate (MMA-GMA) copolymer shell composition.

Lin and co-workers [99, 100] prepared reactive core shell particles (CSP) with butyl acrylate as a core and MMA-GMA copolymer as a shell, and used them as toughening agents for DGEBA epoxy. They found that shell-crosslinked CSP had a higher toughening effect than core-crosslinked CSP. They also reported the tremendous effect of comonomer-like GMA on the toughening effect. This seemed to contradict Sue's [97] observation that chemical bonding of CSP to the epoxy matrix did not significantly contribute to the toughening performance.

5.4 Thermoplastic Toughening

As discussed in earlier sections, rubber toughening resulted in a dramatic improvement in the impact properties of cured epoxy. However, the presence of rubber phase decreases the modulus and thermal stability of the materials and increases the tendency of water absorption with an accompanying loss of properties at elevated temperatures. Moreover, reactive rubbers such as CTBN have been reported to be ineffective modifiers for a highly crosslinked system based on epoxy having a functionality >2 (i.e., 3 or 4). This is because the rubber-rich particles, as stress concentrators, induce the plastic deformation of a highly crosslinked matrix to a far less extent, and dissipation of fracture energy by enlargement of the deformation zone can barely be attained [71, 72]. The search for an alternative method to rubber toughening led to the development of thermoplastic-toughened epoxy.

The thermoplastics which have been reported as efficient modifiers for epoxy resin can be classified as: a) engineering thermoplastics b) amorphous thermoplastics and c) crystalline thermoplastics.

5.4.1 Engineering Thermoplastics

Tough and ductile engineering thermoplastics have been experimented for modifying epoxy resin [101–104]. The chemical structures of a few commonly used thermoplastic modifiers are given in **Figure 5.13**. Because of the high modulus and high T_g of engineering thermoplastics, the modified epoxy resin will reach (or even exceed) the corresponding values for the unmodified resin. Unlike rubber toughening where significant reduction in stiffness and modulus was observed at ambient temperature, thermoplastic-toughened epoxy reduction in stiffness becomes significant only at temperature near to the T_g of the thermoplastic moiety [105].

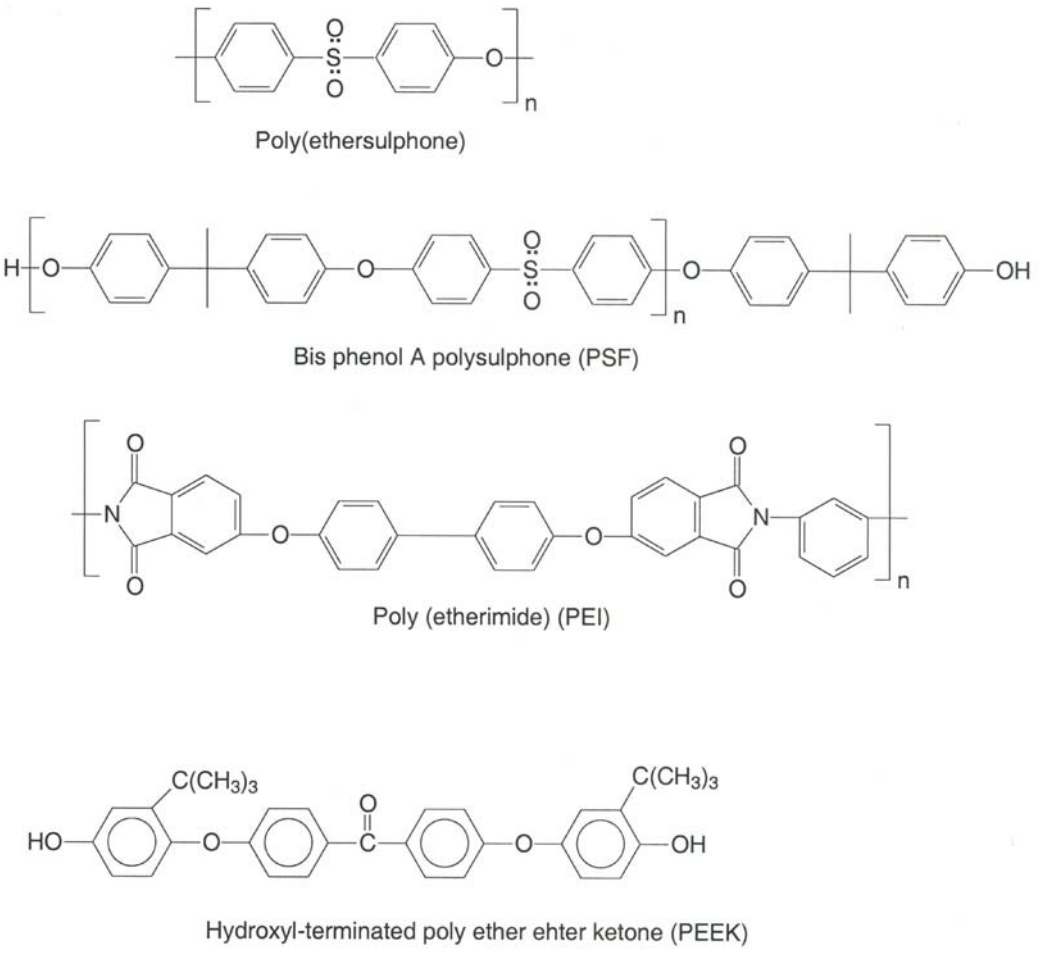

Figure 5.13 Chemical structures of some thermoplastic modifiers used to toughen epoxy resins

The earliest studies on the addition of thermoplastics into epoxy resins were by Bucknall and Partridge [106] using poly(ether sulfone) (PES) and by Diamant and Moulton [107] using poly(ether imide) (PEI), by physical blending of epoxy and respective thermoplastics using methylene dichloride as a solvent. Using trifunctional (Ciba Giegy, MY 051) and tetrafunctional (Ciba Giegy, MY 720) epoxy, they reported little improvement in fracture energy of the modified epoxy networks cured by dicyanamide (Dicy) and DDS. Additionally, Bucknall and Partridge [108] found that the fracture energies and fatigue properties of fibre-reinforced composites were relatively insensitive to the thermoplastic. Part of the explanation for the ineffectiveness of PES as a toughening agent in this study may derive from the morphology of the

systems under observation the Bucknall and Partridge reported that they did not find any phase separation in three of the systems studied (PES/MY720/Dicy, PES/MY720/DDS, PES/MY720/ERL 0570/DDS). However, phase separation was observed in the PES/ERL 0510/Dicy and PES/MY 720/ERL 0510/Dicy systems. They concluded that the type and concentration of resin and hardener influenced the morphology of the PES-rich phase, and that the addition of PES has no significant effect upon the creep and fracture toughness of epoxy resin, irrespective of phase separation and morphology.

Raghva [109, 110] studied the influence of microstructure on the mechanical properties of a modified epoxy system derived from a tetrafunctional epoxy and an aromatic anhydride. Characterising the resulting morphology, he found that Victex 100 P (PES with M_w 145,000) gave a higher percentage of large round particles (1–5 μm) as compared with the agglomerated particles by Victex 100 P (PES with M_w = 85,000). He reported that there was only a marginal improvement in the fracture toughness for both blend systems over the unmodified epoxy network at and below room temperature, but a significant improvement in fracture toughness was observed at higher test temperature. He concluded that the lack of improvement of fracture toughness observed in these systems may be the cured epoxy resin's high crosslink density inhibited the primary toughening mechanism, i.e., formation of shear bands.

Hedrick and co-workers [111, 112] considered poor interfacial adhesion to be the main reason for the inability of commercial thermoplastics (non-reactive) in improving the toughness of epoxy resin. They used phenolic –OH-ended bisphenol-A-based PES and amine-terminated PES oligomers as toughening agents, and claimed that this approach resulted in a remarkable increase in fracture energy. The theory is similar to liquid rubber toughening. The thermoplastic modifier having reactive ends reacts with the epoxy resin. Excess epoxy resin essentially produces an epoxy end-capped thermoplastic, with the modifier preventing further polymerisation. Initially, the thermoplastic is compatible with the epoxy resin but, as M_w increases due to the curing reaction, the homogeneous mixture starts phase separating by spinodal decomposition, resulting in the development of a two-phase microstructure.

The thermodynamic feasibility of phase separation (positive ΔGm) at a certain stage of the curing reaction can be attributed to the substantial decrease in combinatorial entropy of mixing (ΔSm) due to the increase in M_w. The extent of phase separation (and hence the resulting morphology) largely depend on system viscosity and gel period. When the phase separation proceeds, the periodic distance increases simultaneously. Simultaneously, phase connectivity will be interrupted by the increase in interfacial tension, resulting in dispersed droplets. Once the interruption has taken place, the dispersed droplets grow in size without changing their loci because they are dispersed

in a matrix of high T_g. The droplets make contact with one another to yield a globular structure [113, 114]. A nucleation and growth mechanism has been used to describe the morphology of epoxy/thermoplastic blends. Using a suitable model, it possible to predict the fraction, composition and average radius of the dispersed phase segregated during the thermoset polymerisation, based on the thermodynamic consideration as discussed in Chapter 4 for rubber-modified epoxy systems, and the constitutive equations of the rate of nucleation, coalescence and growth. Another origin of phase separation is spinodal decomposition, which is usually assigned to the textures displaying some degree of connectivity ('co-continuous' structure). Unlike rubber-modified epoxy, thermoplastic modified-epoxy systems mostly display co-continuous morphology.

The popularity of PES as a toughening agent of epoxy is due to its good oxidative, thermal and hydrolytic stability as well as good mechanical properties [115, 116]. Once the -OH-terminated bis-phenol-A-based PES was found to be successful for toughening the epoxy matrix, efforts have been concentrated on amine-terminated oligomers of PES, which can be synthesised by adding stoichiometric amounts of amino phenol as the end capping agent [117, 118]. Pac and co-workers [119] used PES with pendent amino groups as the modifier for epoxy resin. Like amine-terminated PES, they can be used as such or after modification with maleic anhydride. It has been found that with increase in $-NH_2$ content, the toughness increases initially, passes through a maximum, and then decreases. Similar observations were reported by Lin and co-workers [120] while investigating PEI as a modifier. The initial increase in fracture toughness with increase in $-NH_2$ content is due to the increase in interfacial adhesion between the epoxy matrix and the dispersed PES particles, which prevents the debonding of particles. The decrease in fracture energy after an optimum $-NH_2$ concentration can be attributed the higher miscibility of PES containing higher $-NH_2$ content with epoxy resin, leading to a single-phase morphology of the modified network, which is undesirable for toughening.

Other engineering thermoplastics have also been examined and found to be effective e.g., polyetherimide [121-124], poly(ether ketones) (PEK) [125, 126], poly(phenylene oxide) [127-129], and liquid crystalline polymers [130, 131].

5.4.2 Amorphous Thermoplastics

Aromatic polyesters were investigated to examine their suitability as a toughening agent for epoxy, and found to be effective for a highly crosslinked system. Liquid rubber is less efficient in toughening a highly crosslinked system. Iijima and co-workers [132, 133] synthesised a series of polyesters by the reaction of 1,2 ethane diol and aromatic dicarboxylic acid. The latter and the derivatives contained pthalic anhydride,

isopthalic acid, dimethyl terepthalate and dimethyl 2,6-naphthalene dicarboxylate. These polyesters were reported to be soluble with epoxy without using any solvent at the initial stage but during the curing reaction undergo phase separation, leading to the formation of a two-phase microstructure.

The glass transition temperatures of polyesters are higher than room temperature (intermediate between reactive liquid rubber and engineering thermoplastics). Their effectiveness was barely influenced by polyester structure and depended on Mw and content of the polyester. Maximum fracture toughness was obtained by 20 wt% addition of polyester. Fracture resistance gradually increases with increasing M_w of the polyester, passes through a maximum, and then starts decreasing. The optimum M_w is dependent on the nature of the polyester.

N-phenyl-maleimide-styrene copolymer (PMS) and *N*-phenylmaleimide-*N*-cyclo hexylmaleimide styrene terpolymer (PHMS) were also reported [134, 135] to be effective modifiers for DGEBA resin. PMS was also an effective modifier for liquid amino cresol-type trifunctional epoxy resin [136]. These copolymers can be prepared by radical polymerisation, and hence the high M_w could be easily achieved. It is rather difficult to get engineering thermoplastics with high M_w because they are generally prepared by polycondensation. In polycondensation, the M_w of the product is sensitive to stoichiometry and hence synthesis of high molecular weight polymer requires maintenance of purity level, which requires stringent purification.

Studies show that the most suitable composition for modification of epoxy resin is the inclusion of 10 wt% of PMS with weight average molecular weight ($\bar{M}_w$) of 344,000 g/mole. The copolymers of still higher M_w are difficult to handle because of an increase in viscosity of the uncured epoxy mixture. The disadvantage of this particular system is that the fracture resistance is achieved at the cost of medium deterioration of flexural strength. This can be attributed to the poor interfacial adhesion between epoxy and PMS due to the absence of reactive groups in PMS and PHMS. The decrease in flexural strength was suppressed to some extent by introducing pendent hydroxyl phenyl groups using the hydroxyl-containing monomer-like hydroxyl styrene *N*-(*p*-hydroxyl) phenyl maleimide [137].

5.4.3 Crystalline Thermoplastics

Crystalline thermoplastics have also been utilised in modifying resin. Among the crystalline thermoplastics, PEO is most extensively investigated [138–141]. The presence of a polyether chain helps to impart flexibility. The -OH groups of PEO react with epoxy at elevated temperature and form a compatible blend with single-phase morphology or two-phase microstructure depending on the M_w of PEO and curing conditions.

Kim and Robertson [142] reported the toughening by particulate inclusions of three crystalline polymers such as poly(butylene terepthalate) (PBT), Nylon 6, and poly(vinylidene fluoride) (PVDF) of a crosslinked epoxy that cannot be toughened significantly by liquid rubber. This improvement in toughness was achieved without a loss of long Young's modulus or yield strength. Nicholson and Robertson [143] reported a systematic exploration of the relationship between thermal history, morphology and mechanical properties of PBT-epoxy blend. They found that 5 wt% of a thermoplastic PBT could increase the fracture energy (G1c) of a brittle anhydridecured epoxy from 180 to 2000 J/m2 with appropriate control over the resulting morphology. An exceptionally higher toughening ability of PBT in comparison with Nylon 6 and PVDF can be attributed to phase transformation of PBT at the crack tip [142, 143].

5.4.4 Morphology and Microstructural Aspects

Unlike rubber-toughened epoxy polymers, the relationship between the microstructure and toughness of thermoplastic-toughened epoxy polymers is not fully understood. Several studies have been initiated the focusing on fracture properties and fractrography of thermoplastic-toughened epoxy systems to establish the definitive relationships between microstructure and fracture properties. However, as discussed in detail next, the complex nature of materials precludes straightforward interpretations.

In contrast with liquid rubber-modified epoxy systems, which tend to form a simple particulate structure, the microstructure of thermoplastic-toughened epoxy networks change from one form to the other with an increase in thermoplastic concentration [144, 145]. Initially, at a low concentration of thermoplastic in the epoxy/thermoplastic blend, the thermoplastic beomes miscible in the epoxy matrix and generates single-phase morphology. On subsequent increase in thermoplastic concentration, phase separation occurs, leading to the development of a two-phase microstructure. The microstructure changes to particulate, co-continuous and finally to phase inverted [146, 147]. In the sample containing the particulate structure, the particle size increases with increase in modifier concentration. Min and co-workers [146, 147] identified a partial phase-inverted structure (intermediate between co-continuous and phase-inverted structure) in their phenolic hydroxyl-ended polysulfone (M_n = 10,000 g/mole) and in a modified epoxy system at 15 wt% modifier concentration.

The microstructure of the modified epoxy networks largely depends on the cure condition. For a multistep cured system, the final microstructure depends on initial cure temperature, and post-curing condition has no role in microstructure development because phase separation gets arrested at gelation. An increase in initial cure temperature causes increase in particle size due to a decrease in system viscosity.

These observations are similar to those observed in a rubber-toughened epoxy system. Yamanka and co-workers [114] observed a phase-inverted co-continuous structure by decreasing the cure temperature in their PES-modified epoxy system. They reported that a decrease in the cure temperature slowed down the rate of phase separation (based on spinodal decomposition process) without significantly reducing the rate of the chemical reaction. This arrested the phase separation at an early stage of phase separation and finally resulted in an interconnected globular epoxy particle in a co-continuous modifier-rich matrix.

Using a PES with a reactive functional group, Mackinnon and co-workers [148] reported that phase separation was needed to record a significant increase in toughness, but discontinuities in the plot of toughness (G_{1c} or K_{1c}) *versus* the concentration of added thermoplastic were not observed as microstructure changed from one form to another. Wilkinson and co-workers [149] used a reactively terminated polysulfone to modify thermo setting bis-maleimide resins and reported no correlation between toughness and various microstructures.

Considering other engineering thermoplastics, Bucknall and Gilbert [124] found that phase separation was needed to record a significant increase in toughness of epoxy polymers modified with PEI, but did not observe discontinuities in the toughness *versus* the concentration of added thermoplastic as the microstructure changed from one form to another. Hourtson and Lane [150] investigated the toughening of a trifunctional epoxy cured with DDS using PEI (Ultem-1000) as a modifier and reported that fracture toughness increases significantly at 15 wt% of modifier concentration when phase inversion starts. Murakami and co-workers [151] concluded that a morphology possessing particle of PEI rich phase is sufficient for toughening. Kinloch and co-workers [152] studied the relationship between microstructure and fracture properties of high-temperature curing epoxy systems using PES modifier having reactive end groups and varying the concentration from 0 phr to 140 phr. Toughness of the system does not begin to increase until phase separation of the thermoplastic copolymer occurs (at about 8 phr). Up to this point, no significant increase in fracture toughness was observed. As the concentration of PES is further increased, the toughness value increases steadily. They reported greater increase in toughness when the level of added thermoplastic exceeds about 55 phr and this is approximately the concentration at which co-continuous thermoplastic phase is first observed. However, they did not get discontinuities as microstructure changed from particulate to co-continuous to phase-inverted. Therefore it appears that phase separation is required to achieve a significant increase in the toughness of thermoplastic-modified epoxy polymers, which is in broad agreement with the observation reached by other authors [125, 151].

5.4.5 Mechanism of Toughening

For rubber-toughened epoxy, it is well established that shear yielding by rubber cavitations and voiding is the main mechanism of toughening. For thermoplastic toughened-epoxy, it is contradictory. Kim and Brown [153] investigated the fracture properties of a glassy oligomer (undisclosed composition)-modified epoxy system and suggested that plastic yielding of epoxy-rich and thermoplastic-rich phases were the active toughening mechanisms. Bucknall and Gilbert [124] and Hedrick and co-workers [119] concluded that ductile tearing in the thermoplastic-rich phase is the major toughening mechanism, but they did not observe plastic yielding of the thermoplastic-rich phase. According to these views, the first stage of fracture is the brittle fracture of the epoxy-rich phase, leaving the more ductile thermoplastic-rich phase bridging behind the advancing crack front. Both groups of workers supported their suggestion by observing the plastic drawing and ductile failure of the thermoplastic-rich phase on the fracture surfaces of the materials. Iijima and co-workers [127] also supported the ductile drawing and tearing mechanism studying the *N*-phenyl malemide-styrene copolymer-toughened epoxy system. However, other authors have not observed The significant ductile tearing of the thermoplastic-rich phase. Diliello and co-workers [154] claimed that for a tetraglycidyl ether of 4,4´-diaminodiphenyl methane (TGDDM)/diamino di phenyl sulfone (DDS) system toughened with PEI, the toughening mechanism was due to the plastic deformation of PEI phase while it was part of the dispersed phase.

5.4.6 Effect of Matrix Crosslink Density

In previous sections, it has been discussed that rubber toughening is extremely successful in the modification of difunctional epoxy for toughness improvement. However, though rubber modifiers can dramatically increase the fracture toughness of difunctional epoxy, they cannot toughen the multifunctional epoxy significantly. Hence it is interesting to know the performance of thermoplastic modifier in this respect. To establish this comparative performance, various types of thermoplastics have been investigated using the difunctional epoxy (DGEBA) as well as highly crosslinked epoxies such as triglycidyl amino phenol (TGAP) and tetraglycidyl diaminodiphenyl methane (TGDDM) [149, 155]. Fracture energy (K_{1c}) *versus* PEI content plots for various epoxy systems [156] are shown in **Figure 5.14**. The toughenability using a thermoplastic modifier is better for highly crosslinked epoxies compared with the conventional difunctional epoxy. This is the advantage of thermoplastic toughening compared with rubber toughening, where toughenability decreases with increasing crosslink density, and rubber modification is virtually ineffective for highly crosslinked epoxy systems. Thus thermoplastic modifiers can toughen difunctional epoxies moderately (to a lesser extent compared with rubbery modifiers) as well as

multifunctional functional epoxy systems to a significant extent (better than rubbery modifiers).

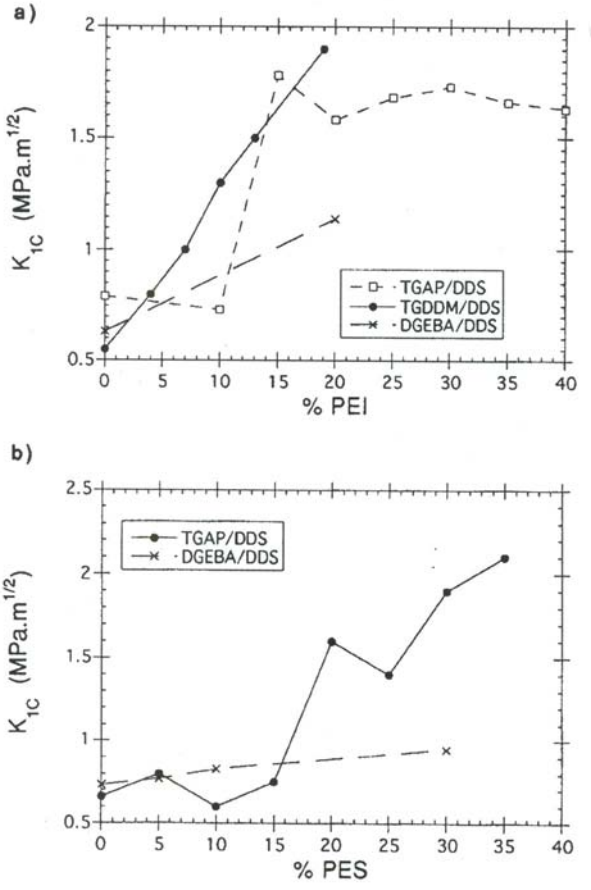

Figure 5.14 Fracture energy (K_{1c}) *versus* weight percent of thermoplastic modfier plots for difunctional and multifunctional epoxy systems (a) PEI (b) PES. Reprinted with permission from J.H. Hodgkin, G.P. Simon and R. Varley, *Polymers for Advanced Technologies*, 1998, **9**, 1, 3. ©1998, John Wiley and Sons Publishers,

5.6 Rigid Particle Toughening of Epoxy

The third approach taken to improve the crack resistance of epoxy resin is the incorporation of rigid an inorganic filler into the glassy epoxy matrix. The energy-

dissipating mechanism for rigid filler-toughened epoxy is believed be 'crack pinning'. According to this mechanism, when a sharp crack crack approaches a layer of rigid particles, the crack front is pinned, perhaps due to the development of sufficient adhesion between the particles and the matrix. The crack is then bowed, creating a new surface area before fracture. However, unlike rubbery fillers which can cavitate, get stretched and remain well bonded due to the chemical interaction to sustain the imposed load, the rigid filler cannot deform, cavitate and or easily get debonded from the matrix, leading to catastrophic failure of the material. It is difficult also to achieve a good dispersion of such materials in the epoxy matrices. This is why the rigid particles cannot enhance the toughness of the matrix to a great extent like rubbery fillers and, in most of cases, achieving and reproducing the dispersion of such fillers remains a problem. Some of the works utilising this approach of toughening are briefly reviewed next.

Among the various rigid fillers, glass beads and alumina [157–159] have been investigated most extensively. Kinloch [160] examined epoxy resin toughened with CTBN and glass beads. This hybrid particle composite showed greater tougheness than the composition containing CTBN alone. A similar observation was reported by Geisler and Kelly [161] using alumina particles. Lange and Redford [162] used aluminium trihydrade to modify epoxy networks and found an enhancement in toughness which depended on volume fraction and particle size of the rigid filler. Molony and co-workers [163, 164] reported a considerable improvement in fracture toughness using angular-shaped silica particles ranging 60–300 μm in diameter. Cured epoxy resin filled with such silica particles in size from <1 μm to about 100 μm were used as packaging materials for integrated circuits [164]. Nakumura and co-workers [165] used angular-shaped silica prepared by crushing fused natural raw silica. Studying the particles of six sizes of range 2–47 μm, they found that fracture toughness increases with increase in particle size.

5.7 Summary and Conclusion

Epoxy resins are a class of versatile thermosetting resins which finds a wide scope of applications (as discussed in Chapter 3). However, the poor fracture toughness of epoxy limits their application, especially in structural applications. Toughness can be improved by chemically modifying the resin with a flexible modifier or by reducing the crosslink density (long-chain hardener and epoxy with high epoxy equivalent). However, this approach is associated with a significant deterioration in thermomechanical properties. The improvement in toughness without significant deterioration in thermomechanical properties can be achieved by incorporating a suitable filler (rubber, thermoplastic or rigid fillers) as a second phase. Addition of rubbery filler often results in a dramatic increase in fracture toughness of difunctional

epoxy, which can be attributed to the energy dissipating mechanism, namely rubber cavitation followed by shear yielding. Rubber toughening is generally achieved by blending liquid rubber which is initially miscible with the epoxy and undergoes phase separation with advancement of the curing reaction, leading to the formation of a two-phase microstructure. The toughening effect depends on the morphological parameters, i.e., particle size, particle size distribution, matrix ligament thickness, and particle to matrix adhesion, which are controlled by molecular parameters such as Mw and functionality of the rubber and epoxy equivalent of the resin. Initial cure temperature also plays an important part in deciding the morphology. However, rubbery fillers are not effective in toughening multifunctional epoxy with higher crosslink density. Multifunctional epoxy resins are successfully toughened by using thermoplastic-based toughening agents. Rigid fillers like alumina and glass beads are also reported to enhance the epoxy network by a crack pinning mechanism, but are not as effective as rubbery fillers.

References

1. C.A. May and G.Y. Tanka, *Epoxy Resin Chemistry and Technology*, Marcel Dekker, New York, NY, USA, 1973.

2. D. Ratna and A.K. Banthia, *Polymer International*, 2000, **49**, 281.

3. *Epoxy Resin Chemistry*, Ed., R.S. Bauer, ACS Symposium Series No.114, American Chemical Society, Washington, DC, USA, 1979.

4. P.S. Achary, P.B. Latha and R. Ramaswamy, *Journal of Applied Polymer Science*, 1990, **41,** 151.

5. D. Ratna, M. Patri, B.C. Chakraborty, C. Madhavan and P.C. Deb, *Bulletin of Materials Science*, 1995, **18**, 1013.

6. D. Ratna, A.B. Samui and B.C. Chakraborty, *Polymer International*, 2004, **53**, 1882.

7. D. Ratna, B.C. Chakraborty and P.C. Deb, *Journal of Polymer Materials*, 1997, **14**, 185.

8. D. Ratna, M. Patri, B.C. Chakraborty and P.C. Deb, *Journal of Applied Polymer Science*, 1997, **65**, 901.

9. W.A. Romanchick, J.E. Sohn and J.F. Gaibel in *Epoxy Resins Chemistry II*, Ed., R.S. Bauer, ACS Symposium Series No. 221, American Chemical Society, Washington, DC, USA, 1983, p.93.

10. *Plastics Technology*, 1988, **34**, 13.

11. *Composites and Adhesives Newsletter*, 1990, **7**, 1, 4.

12. S. Kaushal and Kishore, *Journal of Materials Science Letters*, 1992, **11,** 2, 86.

13. S. Kaushal, K. Tankala, R.M.V.G.K. Rao and P. Kishore, *Journal of Materials Science*, 1991, **26**, 6293.

14. G. Levita, A. Marchetti and E. Butta, *Polymer*, 1985, **26**, 1110.

15. T.T. Wang and H.M. Zupko, *Journal of Applied Polymer Science*, 1981, **15**, 1211.

16. K. Nakao and K. Yamanka, *Journal of Adhesion*, 1992, **37**, 15.

17. C.K. Riew, *Rubber, Chemistry and Technology*, 1985, **58**, 622.

18. E.H. Rowe, A.R. Siebert and R.S. Darke, *Modern Plastics*, 1970, **47**, 110.

19. C.K. Riew, E.H. Rowe and A.R. Siebert in *Toughness and Brittleness of Plastics*, Eds., R.D. Deanin and A.M. Crugnala, Advances in Chemistry Series No. 154, American Chemical Society, Washington, DC, USA, 1976, p.326.

20. C.K. Riew, *Rubber, Chemistry and Technology*, 1981, **54,** 2, 374.

21. A.V. Cunliffe, M.B. Huglin, P.J. Pearce and D.H. Rechards, *Polymer*, 1975, **16**, 622.

22. A.V. Cunliffe, M.B. Huglin, P.J. Pearce and D.H. Rechards, *Polymer*, 1975, **16**, 514.

23. A.C. Meeks, *Polymer*, 1974, **15**, 675.

24. A.H. Rezaiford, K.A. Hodd, D.A. Tod and J.M Barton, *International Journal of Adhesion & Adhesives*, 1994, **14**, 153.

25. R. Slysh in *Epoxy Resins*, Advances in Chemistry Series No.92, American Chemical Society, Washington, DC, USA, 1970, p.108.

26. T.J. Kemp, A. Wilford, O.W. Howarth and T.C.P. Lee, *Polymer*, 1992, **33**, 1860.

27. R.A. Peter and T.J. Logan, *Adhesive Age*, 1975, **17**.

28. K. Mizutani, *Journal of Materials Science*, 1993, **28**, 2178.

29. E.M. Yorkgitis, C. Tran, N.S. Eiss, Jr., T.Y. Hu, I. Yilgor, G.L. Wilkes and J.E. McGrath in *Rubber Modified Thermoset Resins*, Eds., C.K. Riew and J.K. Gillham, Advances in Chemistry Series No.208, American Chemical Society, Washington, DC, USA, 1984, p.137.

30. E.M. Yorkgitis, N.S. Eiss, C. Tran, G.L. Wilkes and J.E. McGrath, *Advances in Polymer Science*, 1985, **72**, 79.

31. J.L. Hedrick, B. Haider, T. Russel and D.C. Hofer, *Macromolecules*, 1988, **21**, 1967.

32. P. Liu, L. He, J. Song, X. Liang and H. Ding, *Journal of Applied Polymer Science*, 2008, **109**, 1105.

33. Y. Zheng, K. Chonung, X. Jin, P. Wei and P. Jiang, *Journal of Applied Polymer Science*, 2008, **107**, 3127.

34. L. Konczol, W. Doll, V. Buchholz and R. Mulhaupt, *Journal of Applied Polymer Science*, 1994, **54**, 815.

35. J.D. Tong, R.K. Bai, Y.F. Zou, C.Y. Pan and S. Ichimura, *Journal of Applied Polymer Science*, 1994, **52**, 1373.

36. J.D. Tong, R.K. Bai, C.Y. Pan and E.J. Goethals, *Journal of Applied Polymer Science*, 1995, **57**, 895.

37. J.D. Tong, R.K. Bai, Y.F. Zou, C.Y. Pan and S. Ichimura, *Macromolecular Reports*, 1993, **A30**, 5, 407.

38. J. Riffle, A.K. Banthia, D.C. Webster and J.E. McGrath, *Organic Coatings and Plastics Chemistry Preprints*, 1980, **42**, 122.

39. J. Riffle, R.G. Freelin, A.K. Banthia and J.E. McGrath, *Journal of Macromolecular Science Chemistry*, 1981, **15**, 5, 967.

40. M. Ochi and H. Yamana, *Kobunsi Ronbunshi*, 1992, **49**, 499.

41. N. Lanzetta, P. Laurienzo, M. Malinconico, E. Martuscelli, G. Rongosta and M.G. Valpe, *Journal of Materials Science*, 1992, **27**, 786.

42. C.K. Riew, A.R. Siebert and E.H. Rowe, inventors;The BF Goodrich Company, assignee; US 4107116, 1978.

43. K. Sakamoto, inventor; Nitto Kasei Co. Ltd. and Osaka Soda Co. Ltd., assignees; US 3945972, 1976.

44. M.B. Jackson, L.N. Edmond, R.J. Varley and P.G. Warden, *Journal of Applied Polymer Science*, 1993, **48**, 1259.

45. I. Frischinger and S.K. Dirlikov, *ACS Polymeric Materials Science and Engineering*, 1991, **65**, 178.

46. I. Frischinger and S.K. Dirlikov, *ACS Polymeric Materials Science and Engineering*, 1993, **70**, 1.

47. D. Ratna and A. K. Banthia, *Journal of Adhesion Science and Technology*, 2000, **14**, 15.

48. D. Ratna, *Polymer International*, 2001, **50**, 179.

49. S.K. Dirlikov, I. Frischinger, M.S. Islam and T.J. Lepkowski in *Biotechnology and Polymers*, Ed., C.G. Gebelain, Plenum Press, New York, NY, USA, 1991.

50. R.A. Ruseckaite, D.P. Fasce and R.J.J. Williams, *Polymer International*, 1993, **30**, 3, 297.

51. H. Samejima, T. Fukuzawa, H. Toda and M. Saga, *Industrial and Engineering Chemistry Products Research and Development,* 1983, **22**, 10.

52. P.S. Achary, C. Gouri and R. Ramamurty, *Journal of Applied Polymer Science*, 1991, **42**, 743.

53. H.H. Wang and J.C. Chen, *Journal of Applied Polymer Science*, 1995, **57**, 671.

54. J.M. Zeilingki, M.S. Vratsanos, J.H. Laurer and R.J. Spoutek, *Polymer*, 1996, **37**, 75.

55. P. Albert, J. Läuger, J. Kressler and R. Mülhaupt, *Acta Polymerica*, 1995, **46**, 1, 68.

56. J. Läuger, P. Albert, J. Kressler, W. Gronski and R. Mülhaupt, *Acta Polymerica*, 1995, **46**, 1, 74.

57. J. Wang, Y. Huang and G. Cong, *Gaofenzi Xuebao*, 1994, **7**, 2, 181.

58. D. Ratna, *Journal of Adhesion Science and Technology*, 2003, **17**, 12, 1655.

59. D. Ratna, *International Journal of Plastics Technology*, 2004, **8**, 2, 279.

60. D. Ratna, *Epoxy Composites: Impact Resistance and Flame Retardency*, Rapra Review Report No.185, Smithers Rapra, Shawbury, Shrewsbury, UK, 2005.

61. D. Ratna, A.K. Banthia and P.C. Deb, *Journal of Applied Polymer Science*, 2001, **80**, 1792.

62. D. Ratna, *Polymer International*, 2001, **50**, 179.

63. D. Ratna, A.K. Banthia and P.C. Deb, *Journal of Applied Polymer Science*, 2000, **78**, 4, 716.

64. D. Ratna, *Polymer*, 2001, **42**, 4209.

65. D. Ratna and A.K. Banthia, *Polymer International*, 2000, **49**, 309.

66. D. Ratna and G. P. Simon, *Polymer*, 2001, **42**, 7739.

67. S. Kar, D. Gupta, A.K. Banthia and D. Ratna, *Polymer International*, 2003, **52**, 1332.

68. J. Diamant and R.J. Moulton, *SAMPE Quarterly*, 1984, **16**, 1, 13.

69. T. Iijima, N. Yoshioka and M. Tomoi, *European Polymer Journal*, 1992, **28**, 573.

70. G. Levita in *Rubber Toughened Plastics,* Ed., C.K. Riew, Advances in Chemistry Series No.222, American Chemical Society, Washington, DC, USA, 1989, p.93.

71. P.J. Pearce, B.C. Ennis and C.E.M. Morris, *Polymer Commications*, 1988, **29**, 93.

72. P.J. Pearce, C.E.M. Morris and B.C. Ennis, *Polymer*, 1996, **37**, 1137.

73. T. Iijima, M. Tomoi, J. Yamasaki and H. Kakiuchi, *European Polymer Journal*, 1990, **26**, 145.

74. M. Tomoi, H. Yamazaki, H. Akada and H. Kakiuchi, *Angewandte Makromolekulare Chemie*, 1988, **163**, 63.

75. R. Mezzenga, L. Boogh and J.A.E. Manson, *Composites Science and Technology*, 2001, **61**, 5, 787.

76. D. Ratna, R. Varley, R.K. Singh and G. P. Simon, *Journal of Materials Science*, 2003, **38**, 1, 147.

77. P.J. Flory, *Principles of Polymer Chemistry*, Cornell University Press, Ithaca, NY, USA, 1975.

78. L. Boogh, B. Pettersson and E.J. Manson, *Polymer*, 1999, **40,** 2249.

79. R. Mezzenga, L. Boogh and E.J. Manson, *Journal of Polymer Science: Polymer Physics Edition,* 2000, **38,** 1883.

80. D. Ratna and G. P. Simon, *Journal of Polymer Materials*, 2002, **19**, 349.

81. D. Ratna and G. P. Simon, *Polymer Engineering and Science*, 2001, **41**, 1815.

82. D. Ratna and G. P. Simon, *Polymer*, 2001, **42**, 8833.

83. D. Ratna, R. Varley, R.K. Singh and G. P. Simon, *Journal of Materials Science*, 2003, **38**, 147.

84. D. Ratna, O. Becker, R. Krishnamurthy, G.P. Simon and R. Varley, *Polymer*, 2003, **44**, 24, 7449.

85. D. Ratna, R. Varley and G.P. Simon, *Journal of Applied Polymer Science*, 2004, **92**, 1604.

86. D. Ratna, *Composites*, 2008, **A39**, 462.

87. H.J. Sue, *Polymer Engineering and Science*, 1991, **31**, 270.

88. A. Maazouz, H. Santerean and J.F. Genard, *Polymer Bulletin*, 1994, **33**, 67.

89. A. Maazouz, H. Sautareau and J.F. Gerard, *Polymer Bulletin*, 1994, **33**, 67.

90. J. Ugelstad, P.C. Mork, K.H. Kaggurud, T. Ellingsen and A. Berge, *Advances in Colloid and Interface Science*, 1980, **13**, 101.

91. K.E.J. Barret, *Disperson Polymerisation in Organic Media*, Wiley, New York, NY, USA, 1975.

92. S. Shen, E.D. Sudol and M.S. El-Aasser, *Journal of Polymer Science Part A: Polymer Chemistry Edition*, 1993, **32**, 1393.

93. M.P. Markel, V.L. Dimonie, M.S. El-Aasser and J.W. Vanderhoff, *Journal of Polymer Science Part A: Polymer Chemistry Edition*, 1987, **25**, 1219.

94. J.E.L. Joensson, H. Hassander, L.H. Jansson and B. Toernell, *Macromolecules,* 1991, **24**, 126.

95. S. Lee and A. Rudin in *Polymer Latexes: Preparation, Characterisation and Applications*, Eds., E.S. Daniels, E.D. Sudol and M.S. El-Aasser, ACS Symposium Series No. 492, 1992, p.234.

96. K-F. Lin and Y-D. Shieh, *Polymer Materials Sci. Eng*, 1997, **76**, 358.

97. H.J. Sue, E.L. Garcia-Maitin and N.A. Orchard, *Journal of Polymer Science, Polymer Physics Edition*, 1993, **31**, 595.

98. J.Y. Qian, R.A. Pearson, V.L. Dimonie and M.S. El-Aasser, *Journal of Applied Polymer Science*, 1995, **58**, 139.

99. K-F. Lin and Y-D. Shieh, *Journal of Applied Polymer Science*, 1998, **70**, 2313.

100. K-F. Lin and Y-D. Shieh, *Journal of Applied Polymer Science*, 1998, **69**, 2069.

101. K. Mimura. H. Ito and H. Fujuka, *Polymer*, 2000, **41**, 4451.

102. I. Martinez, M.D. Martin, A. Eceiza, P. Oyanguren and I. Mondragon, *Polymer*, 2000, **41**, 1027.

103. I. Mondragon, M.A. Corcuera, M.D. Martin, A. Valea, M. Franco and V. Bellenguer, *Polymer International*, 1998, **47**, 152.

104. R.J. Varley, D.G. Hawthorne, J. Hodgkin and G.P. Simon, *Journal of Polymer Science Part B: Polymer Physics Edition*, 1997, **35**, 153.

105. B.S. Kim, T. Ciba and T. Inoue, *Polymer*, 1993, **34**, 2809.

106. C.B. Bucknall and I.K. Partridge, *Polymer*, 1983, **24**, 639.

107. J. Diamant and R.J. Moulson in *Proceedings of the 29th National SAMPE Symposium*, Covina, CA, USA, 1994, p.422.

108. C.B. Bucknall and I.K. Partridge, *Polymer Engineering and Sci*ence, 1986, **26**, 54.

109. R.S. Raghava in Proceedings of the *29th National SAMPE Symposium*, Covina, CA, USA, 1984, p.1384.

110. R.S. Raghava, *Journal of Polymer Science, Part B: Polymer Physics*, 1988, **26**, 65.

111. J.L. Hedrick, I. Yilgor, G.L. Wilkes and J.E. McGrath, *Polymer Bulletin*, 1985, **13**, 201.

112. J.L. Hedrick, M.J. Jureck, I. Yilgor and J.E. McGrath, *Polymer Preprints*, 1985, **26**, 293.

113. K. Yamanka and T. Inoue, *Polymer*, 1989, **30**, 662.

114. C. Girodet, E. Espuche, H. Sautereau, B. Chabert, R. Ganga and E. Valot, *Journal of Materials Science*, 1996, **31**, 2997.

115. T.E. Attwood, P.C. Dawson, J.L. Freeman, J.B. Rose and P.A. Staniland, *Polymer*, 1981, **22**, 1096.

116. P.M. Hergenother, B.J. Jensen and S.J. Havens, *Polymer*, 1988, **25**, 357.

117. J.L. Hedrick, D.K. Mahanty, B.C. Johnson, R. Biswanathon, J.A. Hinkley and J.E. McGrath, *Journal of Polymer Science Part A: Polymer Checmistry Edition*, 1986, **23**, 287.

118. J.L. Hedrick, I. Yilgor, M. Jureck, J.C. Hedrick, G.L. Wilkes and J.E. McGrath, *Polymer*, 1991, **32**, 2020.

119. S.J. Pac, G.D. Lyle, R. Mercier and J.E. Mcgrath, *Polymer*, 1993, **34**, 885.

120. S.J. Li, B.L. Hsu and S.Z.D. Cheng, *ACS Polymeric Materials Science and Engineering*, 1994, **70**, 51.

121. S.C. Kim, H.R. Brown, *Journal of Materials Science*, 1987, **22**, 2509.

122. A. Murakami, D. Saunders, K. Osihi, T. Yoshiki, M. Saitoo, O. Watanabe and M. Takezawa, *Journal of Adhesion*, 1992, **39**, 227.

123. W.G. Liu, T.L. Yu, W.Y. Chen and J.C. Chen, *Journal of Applied Polymer Science*, 1996, **61**, 2423.

124. C.B. Bucknall and A.H. Gilbert, *Polymer*, 1989, **30**, 213.

125. B.Z. Zang, J.Y. Lian, L.R. Hwang and W.K. Shih, *Journal of Reinforced Plastics*, 1989, **8**, 312.

126. T. Iijima, T. Tochimoto and M. Tomoi, *Journal of Applied Polymer Science*, 1991, **43**, 1685.

127. R.A. Pearson and A.F. Yee, *Polymer*, 1993, **34**, 3568.

128. R.W. Venderbosch, J.G.L. Nelissen, H.G.H. Meijer and P.J. Lemstra, *Die Makromolekulare Chemie - Macromolecular Symposia*, 1993, **75**, 73.

129. A.F. Yee and R.A. Pearson, *ACS Polymeric Materials Science and Engineering*, 1990, **63**, 311.

130. L.N. Carfangna, E. Amendola, C. Carfagna, Jr., and A.G. Filippov, *Journal of Applied Polymer Science*, 1992, **44**, 1465.

131. K. Sodagapan, D. Ratna and A.B. Samui, *Journal of Polymer Science Part A: Polymer Chemistry Edition*, 2003, **41**, 3375.

132. T. Iijima, N. Arai, W. Fukuda and M. Tomoi, *European Polymer Journal*, 1995, **31**, 3, 275.

133. T. Iijima, T. Tochimoto, M.Tomoi and H. Kakiuchi, *Journal of Applied Polymer Science*, 1991, **43**, 463.

134. T. Iijima, N. Arai, K. Kakematsu, W. Fukuda and M. Tomoi, *European Polymer Journal*, 1992, **28**, 1539.

135. T. Iijima, K. Sato, W. Fukuda and M.Tomoi, *Journal of Applied Polymer Science*, 1993, **48**, 1859.

136. T. Iijima, S. Miura, W. Fukuda and M. Tomoi, *European Polymer Journal*, 1993, **29**, 1103.

137. T. Iijima, S. Mirua, W. Fukuda and M. Tomoi, *Journal of Applied Polymer Science*, 1995, **57**, 819.

138. X. Luo, S. Zeng, Z. Naibin and Ma Dezhu, *Polymer*, 1994, **35**, 2619.

139. Q. Guo, X. Peng and Z. Wang, *Polymer*, 1991, **32**, 53.

140. Q. Guo, X. Peng and Z. Wang, *Polymer Bulletin*, 1989, **21**, 593.

141. Q. Guo, *Polymer*, 1993, **34**, 70.

142. J. Kim, and R.A. Robertson, *Journal of Materials Science*, 1992, **27**, 3000.

143. M.E. Nichols and R.E. Robertson, *Journal of Materials Science*, 1994, **29**, 5916.

144. A.M. Romano, F. Garbassi and R. Bragila, *Journal of Applied Polymer Science*, 1994, **52**, 1775.

145. C.D. Wingerd and C.L. Beatty, *Journal of Applied Polymer Science*, 1990, **41**, 2539.

146. B.G. Min, Z.H. Stachurski and J.H. Hodgkin, *Journal of Applied Polymer Science*, 1993, **50**, 1511.

147. B.G. Min, J.H. Hodgkin and Z.H. Stachurski, *Journal of Applied Polymer Science*, 1993, **50**, 1065.

148. A.J. Mackinnon, S.D. Jenkins, P.T. McGrail and R.A. Patrick, *Macromolecules*, 1992, **25**, 3492.

149. S.P. Wilkinson, S.C. Liptac, P.A. Wood, J.E. McGrath and T.C. Ward in the *Proceedings the 23rd International SAMPE Conference*, Kiamesha, NY, USA, 1991, p.201.

150. D.J. Hourston and S. Lane, *Polymer*, 1992, **33**, 1379.

151. A. Murakami, D. Saunders, K. Osihi, T. Yoshiki, M. Saitoo, O. Watanabe and M. Takezawa, *Journal of Adhesion*, 1992, **39**, 227.

152. A.J. Kinloch, M.L. Yuen and S.D. Jenkins, *Journal of Materials Science*, 1994, **29**, 3781.

153. C. Kim and H.R. Brown, *Journal of Materials Science*, 1987, **22**, 2589.

154. V. Diliellow, E. Martuscelli, P. Musto, G. Ragosta and G. Scarinzi, *Angewandte Makromolekulare Chemie*, 1993, **213**, 93.

155. S. Horiuchi, A.C. Street, T. Ougizawa and T. Kitano, *Polymer*, 1994, **35**, 5283.

156. J.H. Hodgkin, G.P. Simon and R.J. Varley, *Polymers for Advanced Technologies*, 1998, **9**, 3.

157. J. Spanoudakis and R.J. Young, *Journal of Materials Science*, 1984, **19**, 473.

158. J. Spanoudakis and R.J. Young, *Journal of Materials Science*, 1984, **19**, 487.

159. R.J. Young, D.L.Maxwell and A.J. Kinloch, *Journal of Materials Science*, 1986, **21**, 380.

160. A.J. Kinloch, D.L. Maxwell and R.J. Young, *Journal of Materials Science*, 1985, **20**, 3797.

161. B. Geisler and F.N. Kelley, *Journal of Applied Polymer Science*, 1994, **54**, 177.

162. F.F. Lange and K.C. Reinford, *Journal of Materials Science*, 1971, **6**, 1197.

163. A.C. Moloney, H.H. Kausch, T. Kaiser and H.R. Beer, *Journal of Materials Science*, 1983, **18**, 208.

164. A.C. Moloney, H.H. Kausch, T. Kaiser and H.R. Beer, *Journal of Materials Science*, 1984, **19**, 1125.

165. Y.Nakamura, M.Yamaguchi, A.Kitayma, M. Ocubo and T. Matsumoto, *Polymer*, 1991, **32**, 3221.

6 Thermoset Composites

Introduction

A composite is defined as a combination of two or more materials with a distinguishable interface. On the basis of the nature of matrices, composites can be classified into four major categories: polymer matrix composite (PMC), metal matrix composite (MMC), ceramic matrix composite (CMC) and carbon matrix composite or carbon carbon composites. PMC can be processed at a much lower temperature compared with MMC and CMC. Over the last three decades, the use of PMC, especially fibre-reinforced plastic (FRP) composites, has increased tremendously, and this dramatic growth is expected to continue. The composites possess many useful properties such as high specific stiffness and strength, dimensional stability, adequate electrical properties and excellent corrosion resistance. The implications are easy transportability, high payload for vehicle, low stress for rotating parts, and high ranges for rockets and missiles, which make them attractive for the civilian and defense applications. For a given design load, the weight component is much lower if manufactured with a composite than with a metal. The high specific stiffness and strength of PMC offers the potential for reduced fuel consumption and increased range with passenger aircraft, and enhances the stealth performance for military aircrafts [1, 2].

Depending on the types of polymer matrices, PMC are classified as thermoset resin composites or thermoplastic resin composites. The composite industries are dominated by thermoset resins. This is because of their availability, relative ease of processing, lower cost of capital equipment for processing and low material cost. Because thermosetting resins are available in oligomeric or monomeric low-viscosity liquid forms, they have excellent flow properties to facilitate resin impregnation of fibre bundles and appropriate wetting of the fibre surface by the resin. They are characterised by a crosslinking reaction or curing, which converts them into a three-dimensional (3D) network form (insoluble, infusible). Due to the crosslinked structure, thermoset composites offer better creep properties and environmental stress cracking resistance compared with many thermoplastics (e.g., polycarbonates) [3, 4].

Thermoset composites can be broadly grouped into FRP composites, particulate composites and nanocomposites [5, 6] depending on the reinforcement used (**Table 6.1**). Different forms of reinforcements used for making thermoset composites are given in **Figure 6.1**. Thermoset-based FRP offer very high strength and the opportunity to tailor the material properties through the control of fibre and matrix combinations and processing conditions. The FRP composite and particulate composites are microcomposites because reinforcement sizes are at the micro level. In recent years, considerable attention has been focused on the development of nanocomposites where the enforcement size reduces to the nano level. Nanocomposites will be discussed in Chapter 7.

Table 6.1 Types of thermoset composites and manufacturing processes

Composites	Reinforcement	Process
Fibre-reinforced plastic composite	Glass fibre, carbon fibre, Kevlar fibre, basalt fibre	Wet lay-up and compression moulding, prepreg lay-up with vacuum bagging and autoclave curing, filament winding with oven curing, pultrusion, resin transfer moulding (RTM), vacuum bag moulding, liquid composite moulding (LCM), structural reaction engineering moulding
Particulate microcomposite	Silica, carbon black, calcium carbonate, glass bead, glass balloons, silicon carbide	Mechanical mixing and casting, compression moulding, matched-die moulding
Nanocomposite	Nano silica, nano calcium carbonate, nano titania, nanoclay, carbon nanofibres , carbon nanotubes	Mechanical mixing and sonication followed by casting or compression moulding

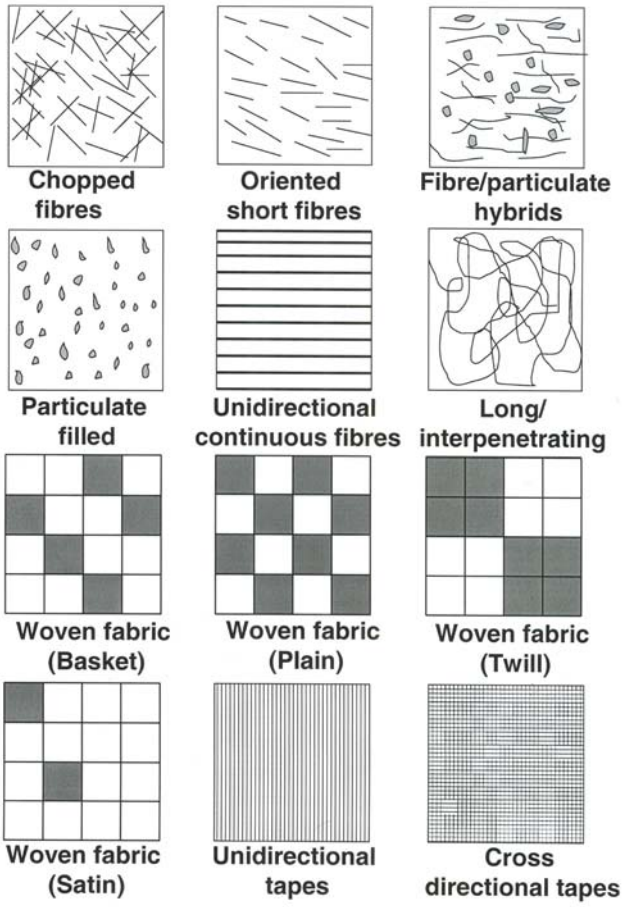

Figure 6.1 Schematic representations of various types of reinforcements used to make thermoset-based composites

6.1 Constituents of FRP Composites

FRP composites comprise two major constituents: the thermosetting resin matrix and the fibre reinforcement. Unlike blends, in composites the constituents (fibres and matrix) grossly retain their identities and simultaneously produce properties that can never be achieved with either of the constituents acting alone. The fibres are usually of high strength and rigidity and predominantly responsible for the load-bearing capacity of composites. The role of matrix resin is to keep the fibres in a desired location and orientation. The fibres must be separated from each other to avoid mutual

abrasion during deformation of the composites. The load applied into the composite is distributed into the fibres through the matrix. Because fibres are mostly brittle, the resin is the source of toughness for a composite. However, as will be discussed in subsequent sections, impact property (toughness) cannot be simply predicted from the constituents because the toughness originates from various complex mechanisms.

Table 6.2 Physical properties of commercially available fibres used for making thermoset composites

Material fibres	Tensile modulus (GPa)	Tensile strength (GPa)	Density (g/cm^3)	% Strain at break	Specific strength
E-glass	72.4	3.5	2.54	2.30	1.38
S-glass	85.5	4.6	2.48		1.85
Carbon (high modulus)	390	2.1	1.90	0.6	1.1
Carbon (high strength)	240	2.9	1.77	1.1	1.64
Boron	385	2.8	2.63	-----	1.1
Silicon carbide	400	3.5	3.5	-----	1.0
Silica	72.4	5.8	2.19	-----	2.65
PBT (heat treated)	331	4.2	1.58	-----	2.65
Kevlar-49	130	2.8	1.45	2.25	1.87
Kevlar-29	6	2.8	1.44		1.8
Spectra-900	117	2.6	0.97		2.8
Spectra-1000	172	3	0.97	2.33	3.2
Polyester	<18	0.8	1.38	15	0.6
Silicon nitride	380	11	3.2	-	3.44
Sisal	7-13	0.5	1.41	4.5	-
PBT: Polybutylene terephthalate					

The thermosetting resins used as matrices in FRP composites have been discussed in Chapter 2. The other constituent (fibre) and the interface between the matrix and the fibre merit attention. A wide variety of fibres are available for use in composites. The physical properties of the available fibres are presented in **Table 6.2**. The most commonly used fibres are glass, carbon and Kevlar fibres. Each

type of fibre can have a different shape, size and orientation (**Figure 6.1**). A wide variety of composites can be made using the same matrix, which may differ with respect to the type, amount, length, and orientation of fibres. Fibre hybridisation can be further exploited to tailor the properties of a composite. On the basis of length, fibres are designated in two ways: short fibres and long continuous fibres. Continuous fibre-reinforced composites contain reinforcements having lengths much greater than their cross-sectional dimensions. A composite is considered to be discontinuous or a short fibre composite if its properties vary with fibre length. If the length of the fibre is such that a further increase in length does not result in further increase in elastic modulus or strength of the composite, the composite is considered to be continuous fibre-reinforced. Most continuous fibre-reinforced composites contain fibres which are comparable in length to the overall dimension of the composite part. Thus, continuous fibre-reinforced composites offer higher strength compared with short fibre-based composites. Hence short fibre composites are used for secondary structural applications, whereas continuous fibre composites are utilised in primary structural applications and considered to be high-performance engineering materials. The mechanical properties of a composite also depend on fibre orientation. The maximum mechanical performance is achieved when all the fibres are oriented in the fibre axis direction.

6.2 Composite Interface

The properties of a composite not only depend on the nature of constituents i.e., matrix and fibre, but also largely depend on the interface. The high strength of fibres can be realised in composites only by designing the interface judiciously. Otherwise, failure may take place at a weak interface. An interface is a boundary demarcating the distinct phases between the matrix and fibre. At the interface, there can be chemical and physical interactions between the fibre and matrix, and also there can be voids, adsorbed gases and surface chemical groups. Bascom and Drzal [7] cited several possible polymer fibre interactions: selective adsorption of matrix components, conformational effects, penetration of polymer molecules into the fibre surface, diffusion of low molecular weight components from the fibre, and catalytic effects of the fibre surface on resin curing [8]. An interface is represented in **Figure 6.2**. Another term often used to indicate the region where the fibre and resin are chemically and or mechanically combined is the ‘interphase’. Depending on the processing condition, chemical reactions, generated volumetric changes, and stresses will be different at the interface. Thus the resultant interface will be very complex.

For good interfacial strength there should be a good wetting of the fibre surface by the resin. In this regard it is necessary to discuss surface tension and contact angle

and their relationship with wetting of the fibre by the resin. Better wetting results in better interfacial bonding between the fibres and the resin matrix, leading to better performance of the composites.

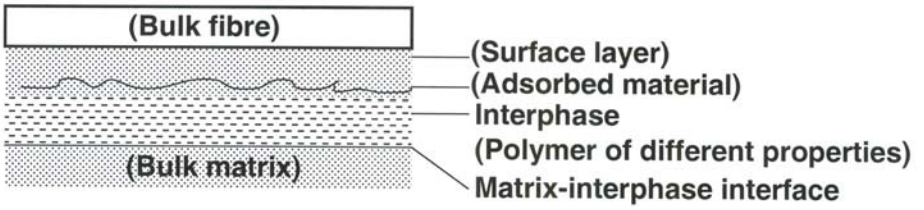

Figure 6.2 Possible representation of interface in fibre-reinforced thermoset composites

6.2.1 Surface Tension and Contact Angle

The molecules on the surface of a liquid are always in a state of unsaturation of molecular forces. Unlike a molecule in the bulk which is attracted by other molecules from all directions, the molecules on the surface are pulled inwards by other molecules deeper inside the liquid and are not attracted as intensely by the molecules in the neighbouring medium (be it vacuum, vapour or air). This is why a net force acts on them, pulling them towards the interior. The force is manifested as the formation of 'convex meniscus' on a liquid because the relaxation time of the liquid is in the order of microseconds. This is known as surface tension. It is defined as the force along a line of unit length, where the force is parallel to the surface but perpendicular to the line. The value of surface tension increases with increasing polarity of the liquid. Various methods for the determination of surface tension can be found in the literature [9]. The surface molecules in a solid also face a similar situation, but the atoms or molecules in a solid cannot rearrange themselves spontaneously like in a liquid (higher relaxation time), which is why the surface appears to be unaffected by disturbances.

If a liquid is placed on a solid surface then, depending on the nature of surface, the liquid will spontaneously form a droplet or spread out into a film. If a droplet is formed then there will be a value of contact angle, which is the angle which the tangent to the surface makes with the solid surface. The contact angle can be correlated with the surface tension values of the corresponding solid and liquid in the equilibrium condition:

$$\gamma_S = \gamma_{\text{ß}} + \gamma_L \cos\theta \tag{6.1}$$

where γ_S, $\gamma_{L,}$ and γ_s are the surface tensions of solid and liquid and interfacial surface tension, repsectively. Adhesion between the solid fibre and liquid resin can be thermodynamically defined as the `work of adhesion`(W_A), which is the energy required for generation of two new surfaces and elimination of an interface:

$$W_A = \gamma_L + \gamma_S - \gamma_{\text{ß}} \tag{6.2}$$

Combining **Equations 6.1** and **6.2** we get:

$$W_A = \gamma_L (1 + \cos\theta) \tag{6.3}$$

When Θ = 0, W_A = two times the surface tension of the liquid.

As Bascom and Drzal [9] pointed out, this force should not be confused with the work of disrupting an adhesively bonded interface between the reinforcing fibre and the matrix resin, which includes many substantial energy-absorbing and energy-dissipating mechanisms. Although these expressions apply to the equilibrium condition, they can be utilised to understand the wetting process in resin-reinforcement systems of composites. If Θ >90°, then the liquid is a non-wetting one for that particular solid. If Θ >90°, then the process is called 'wetting'. The lower the value of Θ, the higher is the extent of wetting. When Θ = zero, a droplet does not form and the liquid is said to be 'spreading'.

6.2.2 Fibre Surface Treatment

The design strategy of the interface will change depending on the nature of the matrix as well as the nature of the fibre. Reinforcing fibres are never used in the state they are manufactured. They are used after subjecting them to suitable physical or chemical treatments.

6.2.2.1 Glass Fibre

The surfaces of freshly prepared glass fibres absorb water very quickly. This results in the formation of a hydroxilated surface. If exposure to moisture is continued, critical size flaws are generated due water absorption. This process considerably reduces the strength of the glass fibres [10, 11]. The intensity of water absorption and surface oxidation can vary depending on the composition of the glass fibre. Thus the glass

surface must be protected from the chemical attack of water. Organo-functional silanes are widely used for surface protection. Silane molecules, having three hydrolysable groups and one functional group capable of reacting with the matrix, are usually applied to the glass surface. The silanol groups react with surface hydroxyl groups and form stable siloxane bonds, which are not attacked by water. In commercial glass fibres, the formulation applied for surface protection is called 'sizes', which is a mixture of a suitable silane coupling agent, binder, antistatic agent, lubricants and other ingredients. An approximately 0.1 μm thick coating is applied. Thus the `sizing` surface treatment not only provides the corrosion protection to the fibre, but also provides protection for the fibre surface from surface damage during handling, and aids in the infiltration of the matrix into the fibre during processing of composites.

6.2.2.2 Carbon Fibre

Unlike glass fibre surfaces, carbon fibre surfaces are not so reactive. Most carbon fibre surfaces consist of graphite planes which are very stable. However, the surface generated during carbonisation or graphitisation is not suitable to withstand the high shear required for composite applications. During chemical treatment, the native fibre surface is etched away and reactive functional groups are produced on the surface. Thus a fresh surface capable of withstanding much higher shear loading, coupled with the formation of reactive groups, leads to much improved compatibility and bonding of carbon fibres with the matrix. The edges and corner of the planes and the resulting crystallites are susceptible only to chemical reaction and utilised for surface modification.

Various surface modification techniques that can effectively promote interfacial bonding have been reported [12–16] (**Figure 6.3**). The modification techniques can be broadly classified into two categories: oxidative methods and non-oxidative methods. In oxidative methods, the fibres are oxidised with liquid oxidising agents (e.g., concentrated nitric acid) or by gases (e.g., air, oxygen, carbon dioxide, ozone). Oxidation can also be carried out using an electrochemical technique using electrolytes such as caustic soda, phosphoric acid, potassium dichromate, and potassium permanganate. In this process, fibres are moved continuously through an electrolytic bath. The fibres act as the anode. The electrochemical techniques offer fast and uniform surface modification. Oxidation of the fibre surface is associated with the generation of functional groups (e.g., carbonyl, carboxyl, hydroxyl) on the fibre surface. The implantation of polar organic groups significantly enhances the compatibility and interfacial bonding between the reinforcing fibre and the matrix resin.

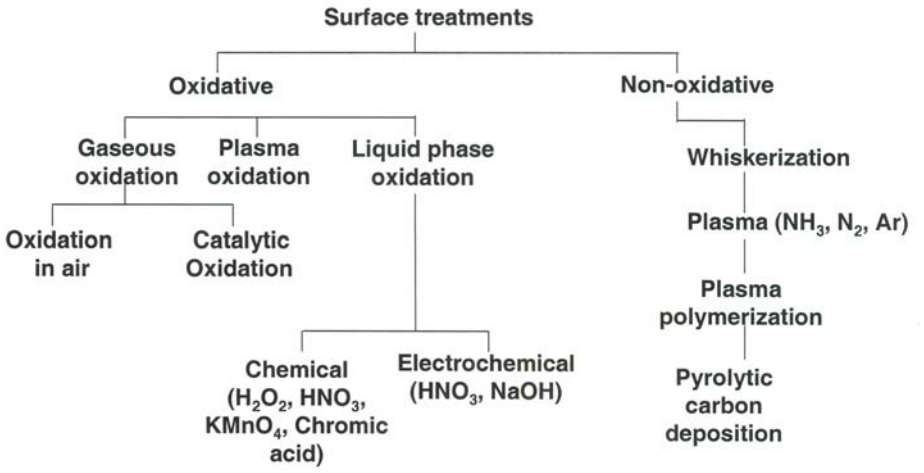

Figure 6.3 Various surface treatment techniques for modification of fibres to improve interfacial adhesion in fibre-reinforced thermoset composites

In a non-oxidative process, the fibre surface is roughened by the deposition of whiskers, which provides the sites for mechanical anchorage and significantly increases interfacial adhesion. Plasma treatment with ammonia produces amine groups on the surface and effectively increases the interfacial bonding for epoxy-based composites due to the possibility of chemical reaction between the epoxy groups of the matrix resin with the amine groups of the fibres. The plasma polymerisation process provides a polymeric layer on the fibre surface, and promoting compatibility. It was observed that fibres after being subjected to plasma coating treatment exhibited higher tensile strength compared with untreated carbon fibres. This indicates that the plasma coating probably healed some of the surface flaws of the fibre. Thus, depending on the nature of the matrices, plasma treatment promotes interfacial bonding by various mechanisms such as removal of native weak surfaces and contaminants, which increases the surface roughness of the fibres. This enhances mechanical locking and implantation of specific functional groups, which can react with the polymer matrix.

Various other methods of modification (mentioned in **Figure 6.3**) can also be utilised. For intermediate modulus fibres, only 20% of the fibre surface contains reactive functional groups. Further increase in surface reactivity usually results in a loss of strength due to the generation of flaws in the fibre. To protect the treated surface from damage during handling, a thin layer of polymer coating (which is essentially identical to the matrix to be used for the fabrication of composite) of thickness ~0.1 μm is given.

6.2.2.3 Polymeric Fibre

Polymer-based reinforcing fibres are not sensitive to oxidation or mechanical damage due to handling. They do not require sizing (necessary for glass fibres) or 'finishing' (necessary for carbon fibres). However, the surfaces of polymeric fibres are low-energy surfaces that require some surface treatment to improve wettability. The various surface preparation techniques shown in **Figure 6.3** are also partially applicable for the modification of polymeric fibres. Surface treatment improves interfacial adhesion between the matrix and fibres. This can be attributed to the removal of low-energy contaminants from the fibre surface, increase in surface roughness, and implantation of reactive groups capable of reacting with the matrix [17, 18].

6.3 Processing of Composites

The final properties of a composite material depend not only on the nature of the matrix and fibre, but also to a great extent on processing of such materials. The properties of composites made from the same resin and reinforcements may vary widely depending on the processing technique and processing parameters used for their fabrication. Composite materials have found application in low-tech application (e.g., toys, household appliances) as well as high-tech applications (e.g., aerospace and biomedical applications). The growing awareness and increasing confidence in composite materials prompted concerned scientists to develop/perfect the existing processing techniques and to introduce newer techniques. With the growth of industries and requirements, the mass production of composites has increased. Mass production demands shortened production time, quality control and greater repeatability. While selecting a particular processing technique, apart from the final properties of composites, the cost and volume production have to be considered. In this section, various processing techniques used for the fabrication of thermoset fibre-reinforced composites are discussed. A comparison of advantages and limitations of various processes are presented in **Table 6.3**.

6.3.1 Contact Moulding

Contact moulding is a simple and well known method for fabrication of fibre-reinforced thermoset composites. Thermoset resins which cure at room temperature such as unsaturated polyester, vinyl ester, and epoxy are used to make glass, jute or carbon fibre-reinforced composites using contact moulding. A wide variety of structures can be fabricated using this technique without limitation with respect to the size and complexity of the shape of the structure. However, the process is very labour-intensive and time-consuming, so is used only for a short run or one-off production.

Table 6.3 Comparison of various processing techniques			
Process	**Advantage**	**Limitation**	**Preferred matrix**
Contact moulding	Low tooling cost, simple process, no shape restriction	Labor-intensive, high volatile emission, slow production rate	Epoxy, polyester, vinyl ester
Compression moulding	Low cycle time, low volatile emission, structural integrity	High tooling cost, average finish	Epoxy, polyester, vinyl ester, polyimide, cyanate ester
RTM	Variety of reinforcement, closed mould, good tolerance	Medium production time	Epoxy
RIM	Fast cycle automation	Resin selectivity	Polyurethanes
Pultrusion	continuous process, low tooling cost, easy to handle	Joining difficulty, shape restriction	Polyester
Filament winding	continuous process, control of fibre orientation, automation	Expensive tooling, slow production rate, shape restriction	Epoxy, polyester
Prepreg moulding	High-quality product, reproducibility, no need of impregnation, minimum material wastage	High cost	Epoxy, bismaleimides, polyimide

The process requires only one mould or moulding tool. The mould can be made from wood, plaster of Paris or metal. Wood and plaster of Paris moulds are used for one-time moulding whereas a metal mould is ideal for longer runs. A release agent (e.g., waxes, polyvinyl alcohol) is applied onto the surface of the mould. The release agent prevents the final fabricated product from sticking to the mould. This is followed by application of a gel-coat by using a spray gun or a painting brush. A gel-coat is generally a resin-rich layer of thickness about 0.5-mm which provides a smooth, hard surface and prevents fibre reinforcements appearing on the surface. The gel-coat can be provided with a particular colour using a suitable colourant on request depending on the application. The mould is then coated with a resin layer and pre-sized reinforcement is laid over the resin layer. Alternate layers of resin and fibre reinforcements are applied until the required thickness is built up. The fibres

are continually rolled to ensure appropriate wetting of the fibres, expulsion of air and consolidation of materials. Glass content of 25–30 wt% can be achieved for random glass mat-based composites whereas up to 50 wt% can be achieved using fine glass fabric.

To increase the production rate, spray-up technique is used instead of a hand lay-up technique. This technique employs a multiple-headed spray gun. The resin mixture and chopped fibres are discharged simultaneously by using the spay gun on the surface of the mould where they are deposited to a uniform thickness. Sheets, storage vessels, auto body parts, boat hulls, truck bodies and building components are made using this process.

6.3.2 Compression Moulding

This process has been described in a previous chapter as a means to process unreinforced resins. Fibre-reinforced composites can be fabricated in a similar way. The resin and fibre can be combined by usual hand lay-up or spray-up techniques. Glass fibre content up to 70 wt% or 50 vol% can be achieved for fibre composites processed by this technique. Press moulding offers obvious advantages like fast cycle time, good finish, structural integrity and high reinforcement content.

6.3.3 Resin Transfer Moulding

Resin transfer moulding (RTM) offers fabrication of a composite structure with dimensional tolerances and good surface finish. Simultaneously, the process is less costly compared with autoclave moulding. The popularity of this process has increased in recent years due to the increased use of resin-transfer moulded composites in automotive and aerospace industries. A schematic diagram of the RTM process is shown in **Figure 6.4**. This process consists of filling a mould cavity by injecting a resin through one, or several, points depending on the size of the component. The reinforcements are placed in the interior of the mould before closing and locking it firmly. The closed-mould pressure injection system allows faster gelling as compared with contact moulded parts. Use of closed moulds produces good tolerances and control of emission of volatiles. The basic difference between RTM and compression moulding is that in RTM the resin is inserted into the mould which contains the reinforcement whereas, in compression moulding, reinforcement and resin remain in the mould, where heat and pressure are applied.

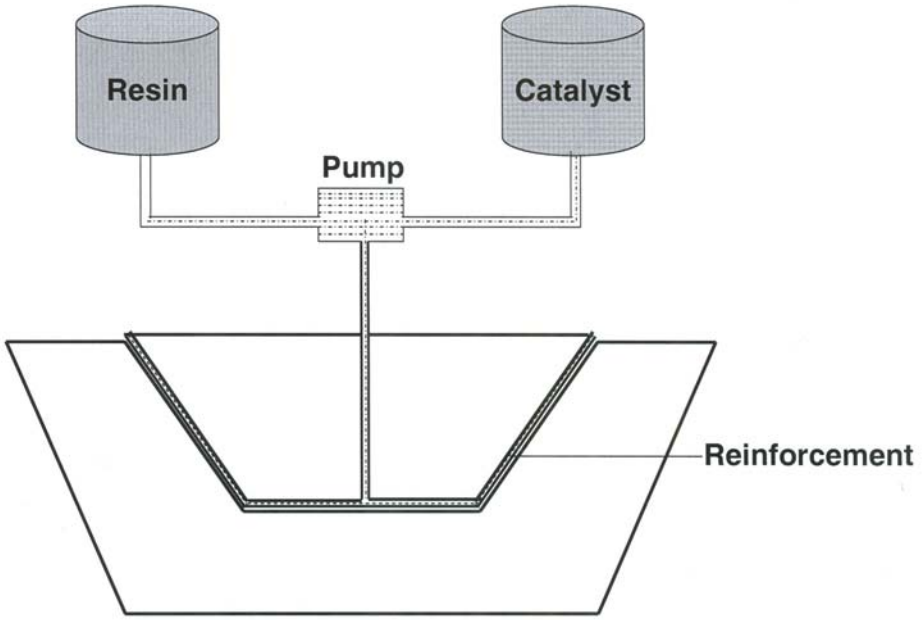

Figure 6.4 Resin transfer moulding (RTM) (schematic)

In this process, the reinforcement (rovings, mat, and fabric) is cut into the desired shape using a knife/scissor or pattern cutter, and shaped into a preform by laying up individual layers of fabrics with the correct orientation. The preform is normally pre-rigidised by using a fast curing resin, or a small amount of thermoplastic binder is added on the surface of the reinforcement which softens on heating and helps to set the reinforcement in shape. For high-performance applications, the preform is compressed under pressure using matched lightweight tooling. Once the preform is ready, it is inserted into the mould and the mould is closed. Resin is injected into the mould cavity. The resin flows under pressure through the reinforcement preform and impregnates the fibres by expelling air in the cavity. The injection of resin is continued until the resin starts flowing from the vent areas of the mould. The preform must not extend beyond the pinch-off area in the mould to keep the mould safely closed. The mould is kept at the curing temperature for several minutes or hours depending on the resin system. When the curing process ends, the item is removed from the mould and subjected to a post-curing treatment to complete the residual curing reaction of the resin. RTM offers rapid production, ease to vary the reinforcement and use of inclusion if required, a quality product and low volatile emission. Propeller blades, panels, compressor casings, bumper beams, missiles, helicopter components, and satellite discs can be made this way. RTM:

- offers good surface finish on both sides of mouldings

- allows items with close dimensional tolerances to be made
- offers fabrication of composites with high fibre volume fraction up to 65%
- involves low pressure injection
- involves low tooling cost compared with other sophisticated moulding process
- offers fabrication of the high- and low-thickness laminates
- involves low material wastage
- offers processing with low volatile emission
- can be used to mould complex structural and hollow shapes

6.3.4 Reaction Injection Moulding (RIM)

RIM is a relatively new process. It can be used for processing of unfilled resin as well as fibre-reinforced composites. The process was discussed in **Chapter 1**. The process is similar to RTM (discussed previously) with some variation in mould release and reinforcement sizing to optimise resin chemistry with the process. The low viscosity reactant systems facilitate composite materials production, so-called structural RIM composites [19, 20] in which continuous fibre reinforcement mats are placed in mould cavities before injection. Capital investment and operational cost in RIM are therefore much less than those for conventional injection moulding. Polymerisation of a monomer is usually initiated by heat. However, in RIM, the polymerisation is initiated by impingement mixing (not by heat). Hence it is possible to activate polymerisation at relatively low temperature. Unlike RTM, in RIM the mould-fill times are very low (~1 s) and a cycle time of <60 s is typical. The process is used for the rapid and automated production of large, thin and complex-shaped parts.

6.3.5 Pultrusion

Pultrusion is a simple technique which is employed mostly for fabrication of products based on unsaturated polyester resins (or other resins like epoxy, vinyl ester) and continuous strand mats (fibre or fabric). A pultrusion machine consists of creel for supplying fibre, a resin tank, forming dies, machined dies with a temperature control facility, a puller and a saw for cutting the product from a continuous composite product. The continuous strand mats are passed through a bath containing a mixture of resin and curatives. In the resin bath, the fibre is passed through a series of rods to remove entrapped air and excess resin to ensure complete wetting of the fibre.

The resin-impregnated fibres or fabrics are then pulled through a series of forming dies. The final die is heated to cure the resin system to produce a rigid composite structure. Depending on the tool cross-section, products of different profiles can be made. The cured profile is continuously pulled out of the die, which provides the driving force for impregnation of fibres to be forced through the die. The process is called pultrusion because the raw materials are pulled through the combining, shaping and curing operations. The process has a similarity with extrusion which is generally used for processing of thermoplastics. The difference is that in extrusion the thermoplastic is forced through the die from inside by a rotating screw; in pultrusion the thermoset material is pulled through the die orifice from the outer side. Solid and hollow products with high stiffness and strength can be made using this technique. A fibre volume fraction of >50 vol% fibre can be made using this process. Typical products made by pultrusion are ladders, stanchions, pipes, aerial booms, and building parts. Putrusion offers advantages such as high specific strength of the product, easy handling and various product profiles. The disadvantages are expensive tooling, and difficulty in joining the products.

6.3.6 Filament Winding

Filament winding is an important continuous processing technique widely used in defence sectors for fabrication of structures like pressure vessels, drive shafts and radomes. The basic difference between filament winding and pultrusion is that the latter involves placement of fibre in the longitudinal direction whereas filament winding has reinforcement in the hoop direction. This involves laying down of resin-impregnated reinforcement in the form of rovings or tapes onto a mandrel. A continuous length of roving or tape of fibres is passed through a bath containing resin and curatives. Before winding over a mandrel the excess resin is squeezed out. The winding process is continued till the desired thickness is achieved. The mandrel is then subjected to initial cure according to the recommended cure schedule of the matrix resin. The component is then pulled off the mandrel for post-curing. Depending on the shape of the mandrel, components of different sizes and shapes can be produced. By adjusting the manner and direction of fibre lay down, various patterns (e.g., helical, hoop, polar) can be achieved. Generally, the mandrel is rotated continuously in one direction and the fibre source parallel to it. Synchronisation of rotation and reciprocation is necessary to provide total cover of the mandrel surface. The process offers the possibility to tailor the orientation of reinforcement to match the direction and magnitude of applied loads. A successful development of product using a filament winding process requires judicious selection of winding type, mandrel design and winding equipment. Components with complex shapes can be made by using a multi-axis winding spindle. The process produces high-quality components, and can be automated to produce high-volume products.

6.3.7 Prepreg Moulding

6.3.7.1 Prepreg

Fibres pre-pregnated with matrix resin cured to B-stage (tacky semi-solid form) are called prepreg. Depending on the nature of fibres, prepregs can be of various types: unidirectional prepreg, woven fabric prepreg, multidirectional tape-prepreg and tow prepregs. Prepregs are grouped into two categories on the basis of applications: general-purpose prepregs and high-performance prepregs. The latter are used for aerospace applications. Solvent impregnation is the common process for manufacturing prepreg tapes. The fabric or a ribbon is passed through a bath containing resin solution. The fabric absorbs the resin solution, after which the fabric is passed through a series nip-roller. During this process the excess resin is squeezed off and wetting of the fibre is ensured. The rollers are designed in consideration of the fibre-to-resin ratio. The solvent is used to reduce the viscosity of the resin mixture. Lower viscosity promotes better impregnation. The impregnated ribbons or fabrics are then passed through a heated drying chamber for solvent removal. Dried fabrics are then partially cured to attain a state of restricted flow but adequate tack. Such prepregs are then covered with plastic film from both sides, wound on a drum and stored in a refrigerator (preferably at less than –15 °C).

6.3.7.2 Moulding of Prepregs

Prepregs are ready-made materials for moulding with optimised composition for specific purposes. Hence by using prepregs, manufacturers can avoid the cumbersome process of stocking of resins, hardeners and reinforcements [21]. The process is simple because resin impregnation is excluded as a variable in contrast with other process like contact or compression moulding in which resin impregnation is an important parameter. The process offers good alignment of reinforcements, minimum material wastage and high-quality products.

The prepreg sheets are cut to a specific shape with a template as per requirement. A gel coat is applied on the mould surface. As soon as the gel coat is partially cured, the prepreg layers are laid on top of one another in appropriate orientation. Prepreg-based composites can be made by vacuum bag moulding (**Figure 6.5**) or by application of pressure in an autoclave (autoclave moulding). The vacuum bag configuration shown in **Figure 6.5** consists of various release layers and air bleed layers to make the surface non-sticky and to absorb the excess resin coming out from the prepregs, respectively. The set-up can be used for application of vacuum, or the entire set-up can be put in an autoclave to cure the composite under heat and pressure.

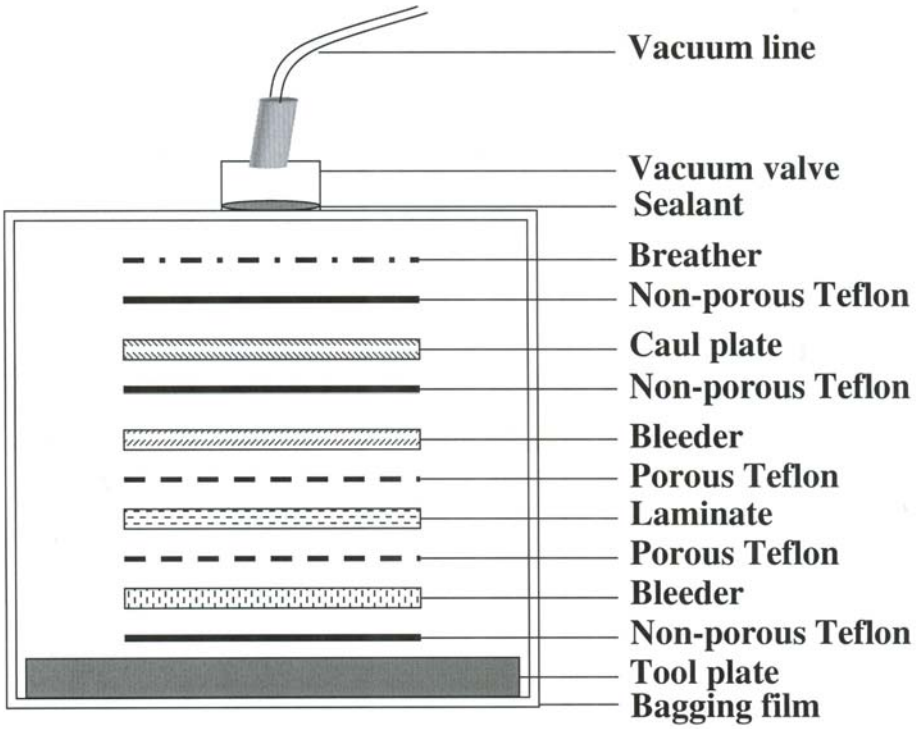

Figure 6.5 Typical vacuum bag configuration used for processing of prepregs

Prepreg moulding offers the highest level of uniformity and excellent properties of the composites. Prepreg-moulded composites are extensively used in aerospace industries, where the ultimate mechanical properties and lightness are the major consideration rather than production rate and cost. The composites made by autoclave moulding exhibit better properties compared with those prepared by vacuum bag moulding. This is because autoclave can exert more pressure than that is generally achieved in vacuum bag moulding and thus results in greater packing-up and void elimination.

6.4 Analysis and Testing of Composites

Analysis and testing of composites includes the quality control of matrix resins and reinforcements, which have been discussed in earlier sections. The composition of a composite i.e., resin content and fibre contents, should be accurately determined for quality control.

6.4.1 Determination of Glass Content

The glass content for composite samples are determined by a resin burn-off test according to ASTM D3171-99. The wt% glass (x) is determined from the following formula:

$$x = \frac{w}{w_o} \times 100 \tag{6.4}$$

wo and w are the initial weight and weight after the matrix burn-off, respectively.

The vol% glass (y) is determined from the formula given next:

$$y = \frac{x}{x + (100 - x)\dfrac{d_g}{d_e}} \tag{6.5}$$

d_g and d_e are the densities of glass and epoxy, respectively.

6.4.2 Mechanical Testing of Composites

Composites are tested in similar ways as unreinforced resins, as discussed in Chapter 1. In some cases, different ASTM standards are used. The ASTM standards used for testing of composites are presented in **Table 6.4**. For example, tensile testing of a composite is carried out using ASTM D3039. Uncured resins are mostly tested with dumbbell-shaped specimens, whereas composites are mostly tested with rectangular specimens. Because composites require much a higher load to break compared with the corresponding casting, tabbed specimens are used (**Figure 6.6**).

6.4.3 Interlaminar Shear Stress (ILSS)

The ILSS of a thermoset composite is generally determined using a short beam shear (SBS) test (ASTM D2344) and a double-notched shear test (ASTM D3846-99). In addition, a four-point bending test (ASTM D790) is also used for the measuring the ILSS of laminates. A review of analytical and experimental data reveals that the three-point or four-point SBS test at best represents a quality control test and cannot correctly provide the actual ILSS. This is because in many instances failure does not occur through an interlaminar shear, but instead by indentation and/or flexure. For compressive testing, the loading heads cause indentation deformation and

concentration of compressive and transverse shear stresses. These stresses individually or in combination exceed the material strength before interlaminar failure occurs. Thus it is extremely difficult to pinpoint the failure load that is used in calculation of the ILSS [22]. Defects or waviness of textile fabric composites further deteriorates the compression strength [23] and causes compression failure on the loading side. Short [24] also developed a method with sandwiched specimen to measure the ILSS of graphite-epoxy composites.

Figure 6.6 A representation of tabbed specimens used for tensile testing of fibre-reinforced composites

Table 6.4 ASTM standards for various tests of thermoset composites	
Test methods	**ASTM standard**
Three-point and four-point flexural test	D790M
Short-beam test	D2344
Impact test	D3029
Tensile test	D3039
Constituent content test	D3171
Compressive test	D3410
In-plane shear test	D3518
Density measurement test	D3800
Interlaminar shear test	D3846
In-plane shear test	D4255
Shear test	D5379
Interlaminar fracture toughness test	D5528
Bearing response test	D5961
Damage resistance test	D6264

6.5 Prediction of Composite Strength and Rigidity

A theoretical analysis for predicting the functional properties of a material is very important to materials scientists to design materials for a particular application. This is more important in multiphase and multi-component systems like a composite. Such theoretical analysis can be utilised to save lot of time for experiments which are otherwise necessary for designing a material for a particular application. Extensive works have been carried out to predict the rigidity and strength of a polymer composite material from the corresponding constituent properties and their proportions [25–28]. Such predictions are valid for only a composite with a fairly good interface. This means processing parameters are to be taken care of to validate the prediction.

In multicomponent systems, a statistical approach is used for the prediction of a particular property. A statistical approach requires the knowledge of the distribution of the individual phases. In a composite it is very difficult to ascertain the distribution of individual phases. Hence a statistical approach cannot be used to predict the mechanical properties of a composite. This is why a two-phase model in which average stresses and strains are considered to exist in each of the phases is used. If we assume that fibre and matrix experience equal strain, then a parallel model can be used to

predict the elastic modulus under longitudinal loading and the composite modulus can be correlated with modulus of the constituents by the following equation:

$$Y_c = Y_f V_f + Y_m V_m \tag{6.6}$$

$$V_f + V_m = 1 \tag{6.7}$$

where Y_c is the composite modulus, Y_f is the fibre modulus, Y_m is the matrix modulus, V_f is the fibre volume fraction and V_m is the matrix volume fraction. Typically, Y_f is much higher than Y_m and V_f is equal or greater than $V_{m,}$ hence the previous equation can be approximated to:

$$Y_c = Y_f V_f \tag{6.8}$$

This suggests that the longitudinal modulus of a unidirectional composite is practically dictated by the axial modulus of the fibres. If the load is applied in a transverse direction or in the case of shear loading, the parallel model mentioned previously cannot be applied. Rather the matrix and fibre can be considered to act in series. Assuming an iso-stress condition where the matrix and fibre carry the same load, the transverse modulus of the composite can be expressed by the following equations:

$$Y_c = \frac{Y_m Y_f}{Y_m V_f + Y_f V_m} \tag{6.9}$$

$$\frac{1}{Y_c} = \frac{V_f}{Y_f} + \frac{V_m}{Y_f} \tag{6.10}$$

Similarly, under shear loading, the shear modulus (G_c) of a composite can be expressed as:

$$\frac{1}{G_c} = \frac{V_f}{G_f} + \frac{V_m}{G_m} \tag{6.11}$$

where G_c, G_f and G_m are the shear modulus of the composite, fibre and matrix, respectively.

Hirsch [29] proposed a model considering the stress transfer between fibre and matrix. The model is a combination of parallel and series model and can be expressed as:

$$Y_c = x(Y_f V_f + Y_m V_m) + (1-x)\frac{Y_m Y_f}{Y_m V_f + Y_f V_m} \tag{6.12}$$

where x is a parameter which determines the stress transfer between the fibre and the matrix. It is always assumed that x is determined mainly by fibre orientation, fibre length and the stress amplification effect at the fibre ends.

Combining **Equations 6.6** and **6.7** we get:

$$Y_c = (Y_f - Y_m)V_f + Y_m \tag{6.13}$$

This is the well-known rule-of-mixture which describes a rather idealised situation and can predict the modulus only for continuous fibre-reinforced composites where there is sufficient stress transfer from the matrix to the fibre. However, short fibres are usually much shorter than the specimen length. For short fibres we must consider the matrix–fibre stress transfer. When the matrix is under stress, the maximum stress transferred to the fibre is described by the interfacial stress transfer (τ). The stress transfer depends on the fibre length (l), so that at some critical length, l_c, the stress transferred is large enough to break the fibre. The stress transferred to the fibre builds up to its maximum value (σ_f that which causes breakage) over a distance l_c from the end of the fibre. This means that the long fibres carry load more efficiently than short fibres.

In other words, the short fibres offer lower effective modulus for reinforcement purposes compared with continuous fibres. This was first considered by Cox [30], who showed that for aligned fibres the composite modulus is given by the following equation:

$$Y_c = (\eta_l Y_f - Y_m)V_f + Y_m \tag{6.14}$$

where η_l is the length efficiency factor, which is described by the following equations:

$$\eta_l = 1 - \frac{Tanh(a.l/D)}{a.l/D} \tag{6.15}$$

$$a = \sqrt{\frac{-3Y_m}{2Y_f \text{ h } V_f}} \tag{6.16}$$

From **Equation 6.15** it is clear that as the value of aspect ratio (*l/D*) increases, the value of η_l (<1) increases and approaches to unity for a high value of aspect ratio (*l/D* >50). This indicates that that fillers with higher aspect ratio offer better reinforcing effect compared with the one with lower aspect ratio.

Another assumption for the equation based on rule-of-mixture is that all the fibres are aligned. In case of short fibres, this assumption does not hold. Hence it is necessary to consider the orientation effect. Thus for non-aligned, short fibres, the composite modulus is given by the following equation:

$$Y_c = (\eta_0 \eta_1 Y_f - Y_m)V_f + Y_m \tag{6.17}$$

where η_0 is the orientation efficiency factor. This has values of $\eta_0 = 1$ for aligned fibres, $\eta_0 = 3/8$ for fibres aligned in plane and $\eta_0 = 1/5$ for randomly oriented fibres. At a low V_f, the measure of reinforcement, which takes into account of the magnitude of the stiffness increase and the amount of fibre, is represented by the following equation:

$$\frac{dY_C}{dV_f} \approx \eta_0 \eta_1 Y_f - Y_m \tag{6.18}$$

A similar calculation can be used to derive an equation for composite strength. For very long aligned fibres the composite strength is:

$$\sigma_C = (\sigma_f - \sigma_m)V_f + \sigma_m \tag{6.19}$$

where σ_C, σ_f and σ_m are the tensile strength of composite, fibre and matrix, respectively. The equation shows a similar trend as was found for the modulus. That is, the reinforcement is reduced as the fibre length is decreased. For medium length fibres ($l > l_c$) the composite strength can be expressed by the following equation:

$$\sigma_C = (\eta_s \sigma_f - \sigma_m)V_f + \sigma_m \tag{6.20}$$

where η_s is the strength efficiency factor and given by $\eta_s = (1 - l_c/2l)$. When l is greater than the critical fibre length (l_c), there is good load transfer between the fibre and the matrix and the fibre breaking takes place at a higher applied stress. However, if l is lower than the critical fibre length (l_c), matrix cannot effectively transfer the load to the fibres and hence fibres do not experience enough load for breaking. As a result, failure takes place through fibre pull-out from the matrix. Under this situation, the strength can be expressed as follows:

$$\sigma_C = (\tau\, l/D - \sigma_m)V_f + \sigma_m \tag{6.21}$$

Another common model is that developed by Halpin and Tsai [31, 32], which may be used for calculating the in-plane stiffness of a single, transversely isotropic sheet having all the fibres unidirectionally aligned in plane of the sheet. The values of moduli calculated from the equations agree reasonably well with the experimental values for a variety of reinforcement geometries including fibres, flakes and ribbons. One of the advantages of the Halpin and Tsai equations that they cover the particulate-reinforced case (which can be considered as fibre with aspect ratio 1) as well as the continuous fibre-reinforced case, where the aspect ratio of the fibre tends to infinity. For aligned fibre composites, the Halpin–Tsai model gives the composite modulus to be:

$$Y_C = Y_m \frac{(1-\xi\eta V_f)}{(1-\eta V_f)} \tag{6.22}$$

where $\xi = 2l/D$ and $\eta = \dfrac{Y_f/Y_m - 1}{Y_f/Y_m + 1}$

For randomly oriented composites, the expression becomes slightly more complicated, as presented next:

$$\frac{Y_C}{Y_m} = \frac{3}{8}\left[\frac{1+\xi\eta_L V_f}{1-\eta_L V_f}\right] + \frac{5}{8}\left[\frac{1+2\eta_T V_f}{1-\eta_T V_f}\right] \tag{6.23}$$

where $\eta_L = \dfrac{Y_f/Y_m - 1}{Y_f/Y_m + \xi}$ and $\eta_T = \dfrac{Y_f/Y_m - 1}{Y_f/Y_m + 2}$

The Halpin–Tsai equation can explain the experimental results fairly well at low volume fraction of fibre. However, the modulus of a composite, calculated using the Halpin–Tsai equation often shows lower value in comparison with experimental data. At a low fibre volume fraction, the change in modulus as a function of fibre concentration can be expressed by the following equation:

$$\frac{dY_C}{dV_f} \approx \frac{3}{8} Y_m \eta_L (\xi + 1) + \frac{15}{8} Y_m \tag{6.24}$$

The equation can be successfully used to predict the mechanical properties (strength and modulus) of a composite up to a certain volume fraction of fibres. At higher fibre volume fractions, the results shows a negative deviation.

6.6 Thermomechanical Properties of Thermoset Composites

6.6.1 Thermal Properties

The thermal properties of a composite are mainly governed by the resin because the inorganic fibres are highly heat resistant. The glass transition temperature (T_g) of the matrix is very important for the performance of a composite. At a temperature higher than the T_g of the matrix, the composite loses its dimensional stability and cannot be used for load-bearing applications. Hence knowledge of the T_g of the matrix in the composite is essential from the application point of view. The T_g of a matrix in the form of a composite is generally measured my dynamic mechanical analysis (DMA), though differential scanning calorimetry (DSC) and DMA are normally used to determine the T_g of a pure matrix resin [33]. The loss factor *versus* temperature plots of glass fibre-reinforced composites using epoxies of different functionalities as matrices are shown in **Figure 6.7**.

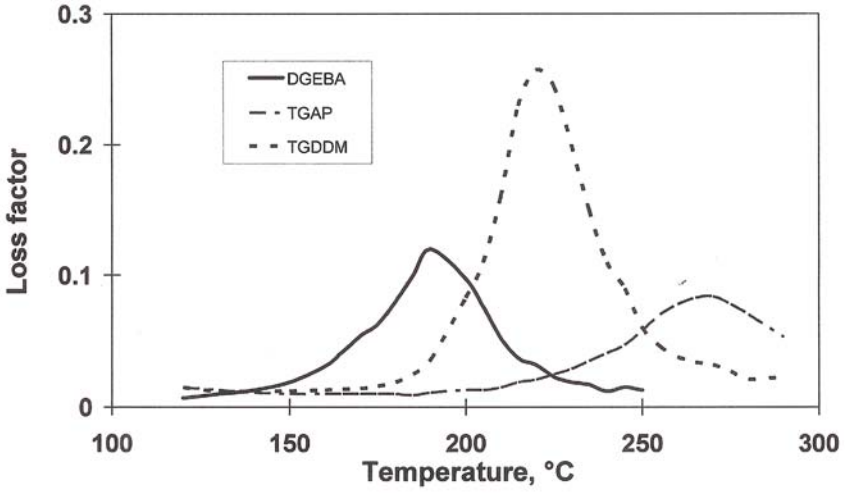

Figure 6.7 Loss factor *versus* temperature plots of glass fibre-reinforced composites based on epoxies of different functionalities as matrices

Comparing these data with those for unreinforced resin (presented in **Table 3.4, Chapter 3**), it can be observed that a composite sample shows a relaxation peak at a temperature lower than that obtained in the case of the corresponding bulk cured resin. For example, the tanδ peak temperature (T_g) for a trifunctional epoxy resin (TGAP)-based glass fibre-reinforced plastic (GFRP) composite was 268 °C, whereas the value for the unreinforced cured epoxy was 284 °C [34]. Theocaris and Papanicolaou [35] reported that the temperature of tanδ peak of an epoxy resin was significantly higher (25 °C) in the bulk resin than that in a GFRP composite containing the same resin. Ghosh and co-workers [36, 37] reported similar effects in the case of jute fibre-reinforced composites. This can be explained by considering the effect of organosilane coating, which is used for commercial fibres to increase their adhesion with the matrix. The organosilane coating with unreactive organic groups leads to an interface with many unrestrained or free end groups, which result in a reduction in the crosslink density of the polymer network in the interface region [38]. The plasticised region then yields decreased internal friction and thereby causes a reduction in relaxation temperature.

6.6.2 Mechanical Properties

In contrast to thermal properties, the mechanical properties of a composite depend mostly on the type, content and orientation of the fibre used as the reinforcement. The mechanical properties of glass fibre-reinforced unsaturated polyester (UPE) resin composites [39] are shown in **Table 6.5**. The mechanical strength of a composite is mostly dictated by the fibres due to much higher strength of inorganic fibres compared with any thermoset resin. Thus the mechanical strength of a composite increases with increase in fibre content up to an optimal concentration. Increasing fibre concentration beyond the optimum concentration results in the formation of flaws inside the composite. This leads to a drastic reduction in mechanical properties. Processing of flawless composites using a minimum amount of resin is a real challenge. As evident from **Table 6.5**, the fibre glass orientation has a great influence on mechanical properties of glass-reinforced composites. For constant fibre content, the unidirectional composites showed much higher tensile properties and flexural modulus when tested in the fibre direction. Unidirectional composites are highly anisotropic. In the fibre direction they show the maximum tensile strength, whereas if the measurement is carried out in a direction transverse to the fibre direction, the tensile strength of the composite tends to be almost identical as the strength of the unreinforced matrix resin.

Table 6.5 Properties of glass fibre-reinforced UPE resin [39]					
Fibre type	**Glass content (%)**	**Tensile strength (MPa)**	**Tensile modulus (GPa)**	**Flexural strength (MPa)**	**Flexural modulus (GPa)**
Nil	0	59	5.4	88	3.9
Chopped – stretched mat	50	288	16.7	197	14.5
Roving fabric	60	314	19.5	317	15.0
Woven glass fabric	70	331	25.8	403	17.4
Unidirectional roving fabric	70	611	32.5	403	29.4

Ratna and co-worker [40] evaluated the GFRP and carbon fibre-reinforced plastic (CFRP) composites based on difunctional and multifunctional epoxies for their mechanical properties (**Table 6.6**). Details of the chemistry and properties of various epoxy resins are shown in Chapter 3. It is expected that tetrafunctional epoxy resin (TGDDM)-based composites would exhibit superior properties compared with difunctional epoxy (DGEBA)-based composites made using a similar method. However, the mechanical properties of TGDDM-based composites were inferior compared to those based on difunctional epoxy. The anomalous behaviour of composites may be due to the very high viscosity of tetrafunctional epoxy (**Table 3.1, Chapter 3**) which hinders impregnation with the fibres [41]. This can be explained in terms of ILSS, which is considered to be the bonding strength between the fibre and the resin. The ILSS of a TGDDM-based composite was 20 MPa, compared with 32 MPa for a DGEBA-based composite. The lower ILSS value for a TGDDM-based composite clearly supports the phenomenon of poor resin impregnation due to the higher viscosity of TGDDM.

Trifunctional epoxy (TGAP)-based composites also do not show good mechanical properties because of their highly brittle nature. This can be attributed to the inherent brittleness of the resin due to very low molecular weight between crosslinks. However, when TGDDM is blended with TGAP, the viscosity decreases and the mechanical properties of the composites improve due the improvement of impregnation of resin mixture into the fibre. The mechanical properties of FRP composites based on the multifunctional epoxy blend (TGDDM/TGAP = 50/50 *w/w*) are superior to the same based on difunctional epoxy resin (**Table 6.6**). The improvement in impregnation as a result of blending is reflected from the increase in ILSS from 20 MPa to 35 MPa. The results mentioned previously have been reported for composites made by hand lay-up

followed by compression moulding. This discrepancy may not arise if a sophisticated processing like autoclave moulding is used.

Table 6.6 Mechanical properties of FRP composites based on difunctional and multifunctional epoxies [40, 65, 71]

Composition of composites	Flexural strength (MPa)	Flexural modulus (GPa)	Impact strength (J/m)
TGDDM/GF	350	20	700
TGAP/GF	330	19	700
TGDDM+TGAP/GF (50:50)	440	21	900
DGEBA/GF	400	19	950
DGEBA/CF	730	53	600
TGDDM+TGAP/CF (50:50)	780	55	600

GF = glass fibre
CF = carbon fibre

6.7 Toughened Composites

As discussed earlier, thermoset composites offer many interesting properties and have wide applications in various fields. However, thermoset-based FRP composites are known to be highly susceptible to internal damage caused by a low velocity impact, which may lead to severe safety and reliability problems. Hence, improvement of damage tolerance of FRP composites by enhancing their impact strength has been the subject of considerable research interest [42–50].

The impact response of a composite is a complex phenomenon unlike the mechanical strength measured at a small strain rate. As discussed in earlier sections, the modulus of a composite material can be predicted from the same values for the constituents i.e., matrix and fibre. In many cases, even simple rule-mixture can explain experimental results. However, no such theoretical analysis can be successfully utilised for the assessment of impact properties of a composite. When an impact load is subjected to a composite structure it absorbs the impact energy by energy-absorbing or energy-dissipating mechanisms. The first is an elastic non-failure response due to the rearrangement of the reinforcement and the other is energy absorption through

creation of damaged areas. Matrix fibre delamination is one of the important energy absorption mechanisms and the increase in absorbed energy is linearly related to an increase in delaminated area [42–44]. Fibre breakage, fibre pull-out and fibre debonding are other important energy-dissipating mechanisms. Because of involvement of these energy-dissipating mechanisms, a composite exhibits much higher toughness than that expected from the toughness of individual components. For example, the impact strength of cured epoxy is about 20 J/m, the impact strength of glass is lower than that of the cured epoxy. However, the impact strength of an epoxy-glass fibre composite is about 900 J/m, which is about an order of magnitude higher than the value for epoxy or glass.

There are several methods to enhance the toughness of FRP composites: matrix toughening, interleaving (insertion of interlaminer 'interleaf' layers), short fibre reinforcement and stitching [45–48]. The impact strength of a thermoset composite can be improved by using high strain fibre or fibre hybridisation [49, 50]. However, high strain fibres often show lower modulus and hence cannot satisfy the requirement for dimensional stability in high-performance engineering applications [51]. This approach is particularly exploited for the application of composites under high-incident-energy condition (e.g., ballistic applications) [52].

Interleaving involves incorporation of a tough resin layer in the interface which enhances the plastic deformation at the interface which is otherwise highly elastic. Wimolkiatisak and Bell [53] electropolymerised a high-temperature thermoplastic (3-carboxy phenyl maleimide-styrene copolymer) interphase onto graphite fibre and evaluated the fibre-reinforced epoxy composites. The improvement in critical strain energy factor of about 100% and notched impact strength of about 60% were achieved while maintaining the interlaminar shear strength at around the same value as for controlled composites. The disadvantage of interleaving is that the improvement in toughness is associated with a reduction in stiffness, heat deflection temperature and poor tolerance to adverse environment [54]. In addition, interleaving reduces the ability of a composite to elastically store energy due to interlaminar hysteretic losses.

Short fibre reinforcement is another effective technique for making toughened composites. Unlike interleaving, it does not rely on the generation of plastic deformation for consumption of mechanical energy. Short fibre reinforcement enhances the toughness of a composite by increasing the energy consumption for a given damage area using semi-elastic failure mechanism of fibre pull-out or fibre breakage. Generally, short fibre loading ranges from 1 wt% to 4 wt%. It can be deposited parallel to the ply surface or oriented translaminarly through the thickness of the ply. The short fibre reinforcement resulted in an increase in toughness of 100–300% [55]. Scanning electron microscopy (SEM) analysis indicated the generation of increased levels of

fibre bridging, crack deviation and crack bifurcation due to the addition of short fibres [56].

The impact strength and damage tolerance of a composite can also be significantly enhanced by the introduction of z-direction fibres (3D fibres) or stitching. Cox and co-workers [57] investigated tensile behaviour of graphite/epoxy composites with 3D woven interlock reinforcements and reported the contributions of various mechanisms of fracture. Through-thickness reinforcement can maintain transverse damage almost constant over the depth of the composite. It also helps in crack bridging [58–61]. As far as the mode I failure is concerned, the stitching yarns carry most of the load at the crack tip, reducing the stress intensity in the surrounding matrix. The stitching provides a crack closure force and thus increases the load required to propagate the crack through the matrix. It was reported that the bridging effect was most prominent in the 90°/90° interface and negligible for the 0°/0° interface. Hence stitched composites display higher interlamimar fracture toughness and offer better damage resistance. The damage area was found to be significantly reduced due to the incorporation of stitching for a constant impact loading. In contrast to the composites made from two-dimensional fabrics, which fail catastrophically, in stitched composites, the failure process usually proceeds gradually through a combination of various mechanisms such as matrix micro-cracking, fibre-matrix debonding, fibre breakage, stress distribution and delamination.

At the same time, unlike interleaving where energy absorption is reduced, the stitching has been shown to improve energy absorption [62–64]. The nature of stitch and yarn has an important role in determining the behaviour of composite materials under impact condition. The knot strength controls the fibre´s ability to crimp without breaking, while the denier indicates the volume percent of stitching fibre and also degree of in plane fibre disruption. There also exists an optimum value for stitch pitch (number of stitches per unit length), such as weaving of fibre in another direction. The number of stitches per unit length should be sufficient to be effective in suppressing the extent of damage induced by the impact. However, resin impregnation becomes more and more difficult with increasing value of stitch pitch. For achieving good mechanical properties of a composite, resin impregnation is very much an essential. Hence the 3D fibres have to be designed accordingly. It is sometimes necessary to modify a thermoset resin formulation by introducing diluents to make it less viscous to ensure sufficient resin impregnation. Use of too much diluent may affect properties of the composites, so it is necessary to optimise the amount of diluent to be added.

6.7.1 Resin Toughening

Using a particular reinforcement, low-velocity-impact resistance (desirable for structural applications) of a particulate or FRP composite can be greatly improved

by increasing the toughness of the matrix. The various methods for toughening of thermoset resins were discussed in **Chapters 4** and **5**. Few examples will be discussed here to highlight their potential for composite applications.

Ratna and co-workers [65] evaluated GFRP composites (glass content almost 45 vol%) based on carboxyl-terminated poly (ethylene glycol) [CTPEGA]-modified epoxy cured with an ambient temperature-curing amine hardener (see **Chapter 5**). Flexural stress *versus* strain curves for the GRFP composites (containing 0-40 phr of CTPEGA) are shown in **Figure 6.8.** The knee on the stress–strain curves and the stiffness represented by the lower portion of the curve are identical for all FRP samples. This indicates that the flexural modulus of a composite is mostly dominated by the fibre. As expected, a significant increase in flexural strain and toughness was observed without abruptly changing the strength and modulus up to 20 phr of CTPEGA concentration. Beyond a concentration of 20 phr, an abrupt decrease in strength and modulus takes place. The area under the curve gives an indication of the toughness of the material. The increase in toughness (as a result of modification) of the composites is much lower compared with that observed in the unreinforced matrix (reported in **Figure 5.2, Chapter 5**). The poor translation of resin toughness into GFRP composites can be attributed to fibre constraints, suppressing the inelastic resin deformation at the crack tips [66, 67].

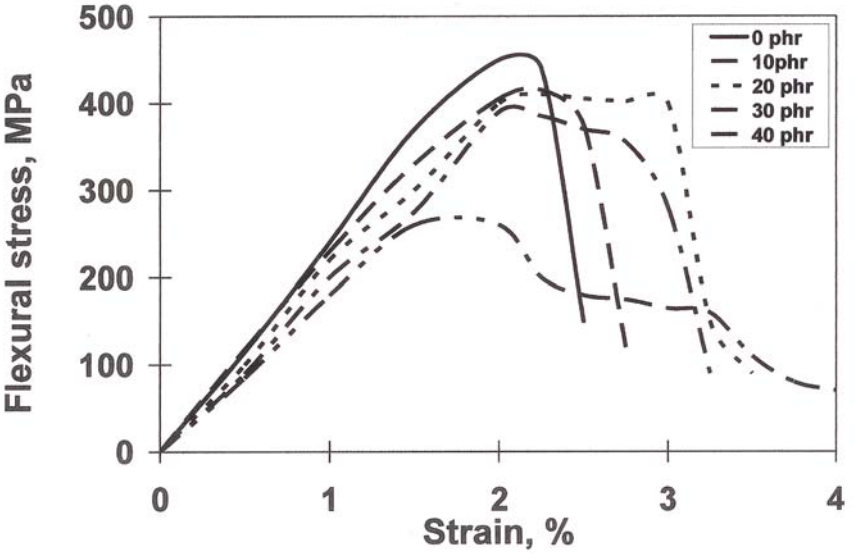

Figure 6.8 The flexural stress *versus* strain curves for glass fibre-reinforced CTPEGA-modified epoxy-based composites (containing 0-40 phr of CTPEGA) Reprinted with permission from D. Ratna, T.K. Chongdar and B.C. Chakraborty, *Polymer Composites*, 2004, **25**, 165. © 2004, John Wiley and Sons Publishers

Impact strength and ILSS data of various composites based on epoxy (DGEBA)- and CTPEGA-modified epoxy are presented in **Table 6.7**. The composites based on CTPEGA-modified epoxy show higher impact strength compared with that based on unmodified epoxy, and its value passes through a maximum (20 phr CTPEGA concentration) with increasing CTPEGA concentration. The ILSS of the unmodified epoxy-based composite is higher than that of a composite made using 20% CTPEGA-modified epoxy, although the impact strength of the modified epoxy-based was much higher compared with the unmodified epoxy-based composite. This indicated that the reduction in ILSS is associated with an increase in impact strength up to a certain value of ILSS. This is attributed to the fact the strong adhesion can limit the energy absorption mechanisms like fibre debonding, pull-out and post-debonding friction during the fracture process, leading to brittle failure of the composites [68, 69]. However, a satisfactory adhesion is required to avoid debonding before the failure [69, 70]. Hence it is not necessary for a composite to have very high ILSS to exhibit very good overall mechanical properties. A moderate ILSS value (needs to be optimised) results in balanced strength and toughness properties.

Table 6.7 Impact and ILSS data for various toughened DGEBA epoxy composites [40]

Modifier	Concentration of modifier (wt%)	Impact strength J/m^{-1} GFRP	Impact strength J/m^{-1} CFRP	ILSS of GFRP (MPa)
CTPEGA	0	950±50	500±25	32.5
CTPEGA	10	1120±40	-	29.2
CTPEGA	20	1350±45	-	26.4
HBP	0	900±40	540±30	-
HBP	10	1150±45	510±25	-
HBP	15	1325±35	500±20	-

As discussed in **Chapter 5**, CTPEGA forms a compatible blend with the epoxy (DGEBA) and improves the impact strength by enhancing the plastic deformation. Such modification always reduces the T_g and restricts the use of the related composites for high-temperature applications. To solve this problem, a second-phase toughening strategy is used. The modifier is selected in such a way that it is miscible with the thermoset resin, initially and, while processing of the composite, it undergoes a reaction-induced phase separation, leading to the formation of a two-phase microstructure. Because the modifier is introduced in a separate phase,

it affects the T_g of the composites significantly. Hence such composites can be used for high-temperature applications. If a composite is used at a temperature higher than the T_g of the matrix, its dimensional stability is lost and it becomes unsuitable for structural applications. The composites made with such modified resin systems exhibit considerably higher impact strength and damage tolerance due to increase in the toughness of the matrix resin. The toughening of resins has been thoroughly discussed in **Chapter 5**. In this section, the properties of the composites based on the modified two-phase resin systems will be discussed taking an epoxy/hyperbranched polymer (HBP) blend system as a reference.

Ratna [71] studied epoxy/HBP-based GFRP and CFRP composites. **Figure 6.9** compares the effects of incorporation of HBP on the T_g for castings and composites. The T_g of an epoxy/blend in the composite form is lower than the same epoxy/blend in the casting form. The difference originates from the interaction of epoxy with the organosilane coating of glass fibres (as discussed in **Section 6.6.1**). Apart from the difference in the T_g of epoxy or blend in different forms (reinforced or unreinforced), the effects of incorporation of HBP on the T_g are different in castings and in composites. For castings, there is no change in the T_g of epoxy/HBP blends up to 15 wt% of HBP whereas, for composites, the reduction in epoxy T_g was observed as a result of incorporation of HBP for all the compositions. The decrease in the T_g for cured rubber modified-epoxy systems arises from the incomplete phase separation and plasticisation phenomenon caused by the dissolved rubber that has been noted in various rubber-modified epoxy formulations [72, 73]. Hence the quantity of dissolved HBP for a particular blend is more in the composite form than in the casting form. This indicates that the presence of fibres initiates partial miscibility of the HBP with the epoxy matrix due to the chemical interaction of the epoxy/HBP blend with the fibre at the interface. The thermodynamic consideration explaining the previous observation is given next.

For composites, the free energy change of the system of three components, epoxy, HBP and fibre, can be described as:

$$\Delta G_m = \Delta G_{EF} + \Delta G_{HF} - \Delta G_{EH} \tag{6.25}$$

where ΔG_{EH} is the free energy of mixing between epoxy and HBP, ΔG_{EF} and ΔG_{HF} are the free energy of interaction of the two components with the fibre surface. Because both components are strongly adsorbed to the fibre surface, ΔG_m will always be negative and hence the equilibrium phase diagram is shifted to a higher compatibility. This explains why epoxy/HBP blend shows more compatibility in composites compared with that in casting.

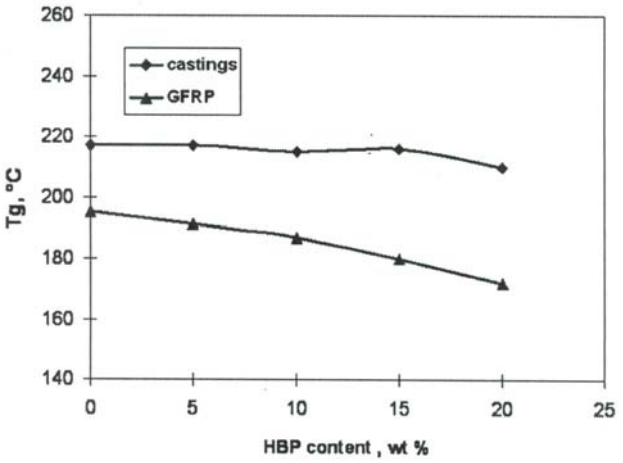

Figure 6.9 Effects of incorporation of HBP on the T_g of modified epoxy in castings and glass fibre-reinforced composites. Reprinted with permission from D. Ratna, *Composites A*, 2008, **39**, 462. © 2008, Elsevier Publishing Company

SEM photographs of the fracture surfaces of epoxy/HBP blend (15 wt% HBP) in various forms such as castings, GFRP and CFRP composites are shown in **Figure 6.10**. In the case of castings, HBP particles are uniformly distributed throughout the matrix as already discussed in Chapter 5. In composites, the particles are comparatively bigger and the uniformity in particle size distribution is lost to a certain extent. GFRP and CFRP composites exhibit similar morphologies. This indicates that the fibres simply act as nucleating agents and there is not much effect of the nature of the fibre on the resulting morphology. However, the two types of composites discussed previously differ drastically in their impact behaviour. Because epoxy/HBP blends are tougher than the unmodified epoxy alone, it is expected that the composites based on epoxy/HBP blend would be tougher than the unmodified epoxy-based composites. As expected, the GFRP composites offer a significant improvement in impact strength (**Table 6.7**). Such a toughening effect is not observed for CFRP composites (**Table 6.7**). The fracture property of CFRP composites is reported [74, 75] to be governed by the interfacial adhesion and internal stress development during cure, which can be manipulated by material and process tailoring. Thus these aspects need to be analyzed critically. However, the apparent difference in behaviour of HBP-modified epoxy-based GFRP and CFRP composites prepared under the same conditions can be explained in the light of the inherent properties of the fibres (**Table 6.2**). Carbon fibres are much more brittle (tensile strain = 1%) compared with glass fibres (tensile elongation = 2.5%) [76]. This is also reflected in the impact behaviour of GFRP and CFRP composites. The impact strength of unmodified epoxy-based CFRP composite

is 500 J/m compared with 950 J/m for the corresponding GFRP composite. It is well established that dispersed rubber particles enhance the toughness of the epoxy system by cavitations of rubber particles followed by shear yielding, and that their effectiveness decreases with increase in the rigidity of the system [77, 78]. Highly brittle carbon fibre imposes restriction on the induction of plastic deformation by rubber particles. Failure of CFRP composites is due to fibre breaking.

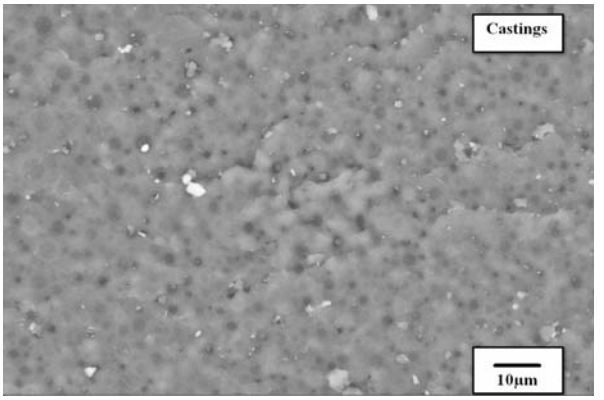

Figure 6.10a SEM photographs of the fracture surfaces of epoxy/HBP blend (15 wt% HBP) in castings form. Reprinted with permission from D. Ratna, *Composites A*, 2008, **39**, 462. © 2008, Elsevier Publishing Company

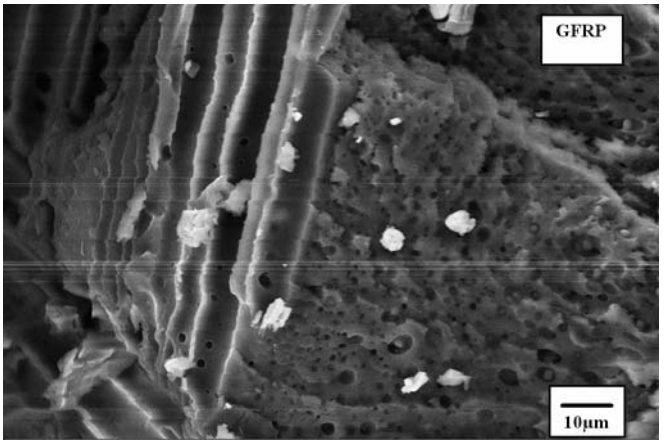

Figure 6.10b SEM photographs of the fracture surfaces of epoxy/HBP blend (15 wt% HBP) in glass fibre reinforced plastic (GFRP) form. Reprinted with permission from D. Ratna, *Composites A*, 2008, **39**, 462. © 2008, Elsevier Publishing Company

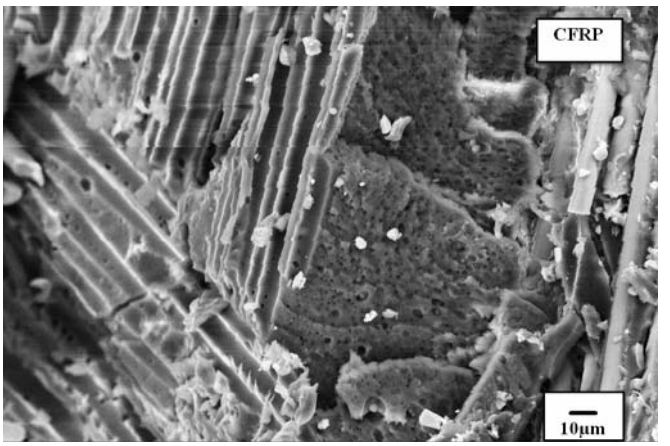

Figure 6.10c SEM photographs of the fracture surfaces of epoxy/HBP blend (15 wt% HBP) in carbon fibre-reinforced plastic (CFRP) form. Reprinted with permission from D. Ratna, *Composites A*, 2008, **39**, 462. © 2008, Elsevier Publishing Company

References

1. L.T. Drzal in *Epoxy Resin and Composites II*, Ed., K. Dusek, Advanced Polymer Science Series, Springer-Verlag, Berlin, Germany, 1986, p.75.

2. *Composite Materials in Aircraft Structures*, Ed., D.H. Middleton, Longman, New York, NY, USA, 1990.

3. A.A. Bakker, R. Jones and R. Callinan, *Journal of Composite Materials*, 1985, **15**, 154.

4. B.Z. Jang, *Science and Engineering of Composite Materials*, 1991, **2,** 1, 29.

5. D. Ratna, *Epoxy Composites: Impact Resistance and Flame Retardency*, Rapra Review Report No.185, Smithers Rapra, Shawbury, Shrewsbury, UK, 2005.

6. M. Okamoto, *Polymer/Layered Silicate Nanaocomposites,* Rapra Review Report No.163, Smithers Rapra, Shawbury, Shrewsbury, UK, 2003.

7. W.D. Bascom and L.T. Drzal, *The Surface Properties of Carbon Fibre and their Adhesion to Organic Polymers,* NASA Contract Report No. 4084, NAS 1-17918, NASA, Washington, DC, USA, 1987.

8. P.S. Chua, *Polymer Composites*, 1987, **8,** 308.

9. A.J. Walter, *Physics Education*, 1972, **7**, 8, 491.

10. E.A. Plueddmann, *Silicate Coupling Agents*, Plenum Press, New York, NY, USA, 1982.

11. C. Shen, L.S. Liu and J.T. Yeh, *Polymers and Polymer Composites*, 1999, **7**, 1, 21.

12. L.T. Drzal, M. Rich and P. Lloyd, *Journal of Adhesion*, 1983, **16**, 1, 1.

13. K.J. Hook, R.K. Agrawal and L.T. Drzal, *Journal of Adhesion*, 1990, **32**, 157.

14. T. Takahagi and A. Ishitani in *Molecular Characterization of Composite Interfaces*, Eds., H. Ishida and G. Kumar, Plenum Press, New York, NY, USA, 1985.

15. H. Zhang, Z. Zhang and B. Claudia, *Composite Science Technology*, 2004, **64**, 2021.

16. Y. Yang, F. He, M. Wang and B. Zhang, *Journal of Materials Science*, 1998, **33**, 3651.

17. D. Ratna, R. Kushwaha, V. Dalvi, N.R. Manoj, A.B. Samui and B.C. Chakraborty, *Journal of Adhesion Science and Technology*, 2008, **22**, 1, 93.

18. D.S. Bag, V.A. Kumar and S. Maiti, *Journal of Applied Polymer Science*, 1999, **71**, 1041.

19. C.W. Macosko, *RIM - Fundamentals of Reaction Injection Moulding*, Hanser Publishers, New York, NY, USA, 1989.

20. E. Haberstroh and I. Kleha, *Macromolecular Materials and Engineering*, 2000, **289**, 108.

21. *Advanced Materials Newsletter*, 1991, **13**, 1.

22. J.M. Whitney, *Interlaminar Response of Composite Materials*, Ed., N.J. Pagano, Composite Materials Series No.5, Elsevier, Amsterdam, The Netherlands, 1989, **p.**161.

23. C. Emehel and K.N. Shivakumar, *Journal of Reinforced Plastics and Composites*, 1997, **16**, 1, 86.

24. S.R. Short, *Composites*, 1995, **26**, 431.

25. C.L. Tucker and E. Liang, *Composites Science and Technology*, 1999, **59**, 655.

26. W.D. Callister, Jr., *Materials Science and Engineering: An Introduction*, 6th Edition, John Wiley and Sons, New York, NY, USA, 2003.

27. A. Kelly and W.R. Tyson, *Journal of the Mechanics and Physics of Solids*, 1965, **13**, 329.

28. G.P. Carman and K.L. Reifsnider, *Composites Science and Technology*, 1992, **43**, 137.

29. T.J. Hirsch in *Proceedings of the American Concrete Institute International Conference on Advances in Concrete and Structure*, 1962, **59**, 427.

30. H.L. Cox, *Journal of Applied Physics*, 1952, **3**, 1, 72.

31. B.W. Rosen, *Fibre Composite Materials*, American Society for Metals, Metals Park, OH, USA, 1965, p.58.

32. L.E. Nielson, *Mechanical Properties of Polymers and Composites*, Marcel Dekker, New York, NY, USA, 1974. [2 volumes]

33. T. Murayama, *Dynamic Mechanical Analysis of Polymeric Materials*, Elsevier Science Publishing Co., Amsterdam, The Netherlands, 1978.

34. D. Ratna, T.K. Chongder and B.C. Chakraborty, *Polymer International*, 2000, **49**, 815.

35. P.S. Theocaris and G.C. Papanicolaou, *Colloid and Polymer Science*, 1980, **258**, 1044.

36. P. Ghosh and N.R. Bose, *Journal of Applied Polymer Science*, 1995, **58**, 2177.

37. P. Ghosh, N.R. Bose, B.C. Mitra and S. Das, *Journal of Applied Polymer Science*, 1997, **65**, 2467.

38. V.B. Gupta, L.T. Drzal, C.Y.C. Lee and M.J. Rich, *Journal of Macromolecular Science B*, 1985, **23**, 435.

39. M. Grayson and D. Eckroth in *Encyclopedia of Chemical Technology*, 3rd Edition, John Wiley and Sons, 1982, Volume 18, p.575.

40. A.B. Samui, B.C. Chakraborty and D. Ratna, *International Journal of Plastics Technology*, 2004, **8**, 279.

41. I.M. Low, P. Schmidt, J. Lane and M. McGrath, *Journal of Applied Polymer Science*, 1994, **54**, 2191.

42. J.P. Slow and V.P.W. Shim, *Journal of Composite Materials*, 1998, **32**, 1178.

43. A. Kessler and A.K. Bledzki, *Polymer Composites*, 1999, **20**, 269.

44. A.A.J.M. Peijs, S.W. Venderbosch and P.J. Lemstra, *Composites*, 1990, **25**, 522.

45. W.J. Cantwell and J. Morton, *Composites*, 1991, **22**, 347.

46. I.K. Patridge and D.D.R. Cartie, *Composites*, 2005, **A 36**, 55.

47. M.V. Hosur, U.K. Vaidya, C. Ulven and J.S. Tuskegee, *Composite Structures*, 2004, **64**, 455.

48. J.C. Chen, C.K. Lu, C.H. Chiu and H. Chin, *Composites*, 1994, **25**, 251.

49. R.C.L. Dutra, B.G. Soares, E.A. Campose and J.L.G. Silva, *Polymer*, 2000, **41**, 3841.

50. M-S. Sohn and X-Z. Hu, *Composites Science and Technology*, 1998, **58**, 211.

51. D.F. Adams and R.S. Zimmerman, *SAMPE Journal*, 1986, **22**, 10.

52. R.L. Ellis, F. Lalande, H. Jia and C.A. Rogers, *Journal of Reinforced Plastics and Composites*, 1998, **17**, 147.

53. A.S. Wimolkiatisak and J.P. Bell, *Journal of Applied Polymer Science*, 1992, **46**, 1899.

54. S. Abrate, *Applied Mechanics. Review*, 1991, **44**, 155.

55. L. Walker and X. Hu, *Scripta Materialia*, 1999, **41**, 575.

56. L. Walker, M.S. Sohn and X. Hu, *Composites Part A*, 2002, **33**, 893.

57. B.N. Cox, M.S. Dadkhan and W.L. Morris, *Composites Part A*, 1996, **27**, 447.

58. D. Shu and Y. Mai, *Composites Science and Technology*, 1993, **47**, 1, 25.

59. D. Shu and Y. Mai, *Composites Science and Technology*, 1993, **49**, 165.

60. L.K. Jain and Y.W. Mai, *Composites Science and Technology*, 1994, **51**, 331.

61. W.C. Chung, B.Z. Zang, T.C. Chang, L.R. Hwang and R.C. Wilcox, *Materials Science and Engineering*, 1989, **A112**, 157.

62. S.T. Jenq and S.L. Sheu, *Composite Structures*, 1993, **25**, 427.

63. P.J. Hogg, *Materials Technology*, 1993, **8**, 1, 51.

64. K. Dransfield, D.C. Baillie and Y.W. Mai, *Composites Science and Technology*, 1994, **50**, 305.

65. D. Ratna, T.K. Chongdar and B.C. Chakraborty, *Polymer Composites*, 2004, **25**, 165.

66. J.M. Scott and D.C. Phillips, *Journal of Materials Science*, 1995, **10**, 551.

67. W.D. Bascom, J.L. Bitner, R.J. Moulton and A.R. Siebert, *Composites*, 1980, **11**, 9.

68. P. Marshall and J. Price, *Composites*, 1991, **22**, 53.

69. B. Zinger, S. Shkolnik and H. Hoecker, *Polymer*, 1989, **30**, 628.

70. A.S. Crasto, S.H. Own and R.V. Subramaniam, *Polymer Composites*, 1988, **9**, 1, 78.

71. D. Ratna, *Composites A*, 2008, **39**, 462.

72. M. Murli, D. Ratna, A.B. Samui and B.C. Chakraborty, *Journal of Applied Polymer Science*, 2007, **103**, 1723.

73. S. Kar, D. Gupta, A.K. Banthia and D. Ratna, *Polymer International*, 2003, **52**, 1332.

74. Y. Eom, L. Boogh, V. Michaud and J-A.E. Månson, *Polymer Composites*, 2002, **23**, 1044.

75. J. Verry, Y. Winkler, V. Michaud and J-A.E. Månson, *Composites Science and Technology*, 2005, **65**, 1527.

76. W.D. Bascom, J.L. Bitner, R.J. Moulton and A.R. Siebert, *Composites*, 1980, **11**, 1, 9.

77. G. Levita, S. Petris, A. Marchetti and A. Lazzer, *Journal of Materials Science*, 1991, **26**, 2348.

78. D. Ratna and A.K. Banthia, *Macromolecular Research*, 2004, **12**, 1, 11.

7 Thermoset Nanocomposites

Introduction

In the previous chapter, particulate and fibre-reinforced thermoset composites have been discussed in detail. Those are the examples of microcomposites because the reinforcement sizes are in the micro scale. Wood is a classic example of natural composite where cellulose fibers act as a reinforcement in a lignin matrix. The oldest example of man-made composite material is concrete where macro size (diameter > 1 mm) steel rods are used for reinforcement. In the course of time, materials scientists have reduced the sizes of reinforcements from the macro to the micro scale. This is because a reinforcement with smaller size offers a better opportunity to control their orientations and interactions with the matrix. Since such interactions play an important role in determining the overall mechanical properties of a composite, the composite property can be manipulated to a great extent [1] by reducing the size of the reinforcement. That is why today microcomposites have formed the basis of multicrore industries. The recent trend in composite research is to further reduce the reinforcement size up to the nanoscale. The composites made with nanometer-sized reinforcements are called nanocomposites. In a nanocomposite, it is not necessary for the reinforcement to be nano-sized in all dimensions but at least in one dimension, it should be in nanoscale (1-100 nm). For example carbon nanotube has a diameter in nanoscale but length in microscale. Though the materials with size ranging from 1 to 100 nm are defined as nanomaterials, to realise the actual nano-effect the size should be less than 20 nm. The unique properties of nanomaterials arise due to a tremendous increase in surface area when a conventional material is converted to a nanomaterial. For example, the surface area of nanotubes of a diameter of 1 nm is 1000 times higher than the same volume of short fibres of a diameter of 1 μm.

Though nanocomposites or nanostructured inorganic organic hybrid materials are considered as a novel class of materials, they are available naturally. Nature has long demonstrated the propensity to synthesise organic-inorganic hybrids as exemplified by several ubiquitous materials such as bones, abalone, shell of molluscs and marine sponges. For example, nacre (available in abalone shell) is composed of 99 vol% aragonite ($CaCO_3$) and 1 vol% biopolymer. Nacre is 2 times harder and 1000 times

tougher than its main component aragonite [2]. Such a remarkable enhancement in properties due to the presence of only 1 vol% of biopolymer is the result of a highly controlled structure, which nature produces by a process called biomineralisation. It is very difficult for mankind to match such a controlled structure. So similar to many other technologies, nanocomposite technology is also an outcome of man's attempt to mimic nature.

In this context, it is relevant to mention an example of old man-made hybrid material which was produced without a proper understanding of nanoscience [3]. This is a painting called 'Maya blue' available in Bunampark, Maxico. The painting is a wonderful discovery which retains its intense blue colour even after experiencing the harsh jungle atmosphere for the several centuries. A careful analysis of the painting indicates that the colouring pigment is indigo (not so stable) and it is encapsulated within the channels of clay minerals playgorskite. Hence the material is nanostructured in nature which is responsible for the remarkable stability offered by the painting despite constituting a colouring pigment (indigo), which itself is not so stable.

7 Themoset Nanocomposites

In the last two decades, extensive works have been done to develop various types of organic-inorganic hybrid materials. Various routes [3] for synthesis of such hybrid nanocomposites are presented in **Figure 7.1**. One successful approach to achieve such nanocomposites is the in situ polymerisation of metal alkoxides in organic matrices [4-6]. Inorganic components, especially silica have been formed by the hydrolysis and condensation of a mononuclear precursor such as tetraethoxysilane (TEOS) in many polymer systems. Due to the loss of volatile by products formed in the hydrolysis/condensation reaction, it is difficult to control sample shrinkage after molding. Self-assembly is another important method for the synthesis of nanocomposites. This is mostly carried out through block copolymerisation which may lead to a hierarchical structure [7, 8]. The third approach is to intercalate the polymer materials in a layered silicate, which leads to the formation of a polymer/clay nanocomposites (PCN). Nanocmposites can also be made by directly dispersing nanomaterials like carbon nanotube (CNT), nanoscale mesoporus silica (NMS) and polyhedral oligomeric silsesquioxane (POSS) in a thermoset matrix.

The main advantage of a nanocomposite is the property tradeoffs associated with the conventional composites. For example, nanomodification can improve the stiffness without sacrificing toughness, can enhance barrier properties without sacrificing transparency and offer flame retardancy without deteriorating mechanical property

and colour. The advantages of nanocomposites over conventional composites are given below:

- Efficient reinforcement with minimal loss of ductility and impact strength.
- Much lower weight penalty compared to filled polymers and conventional polymer composite systems, as nanocomposites contain a very little amount of inorganic fillers.
- Outstanding barrier properties without requiring a multilayered design.
- Improved heat stability and flame resistance characteristics.
- Improved chemical and weather resistance properties.
- Improved biodegradability for a pristine biodegradable polymer.
- Retained transparency for a pristine transparent polymer.

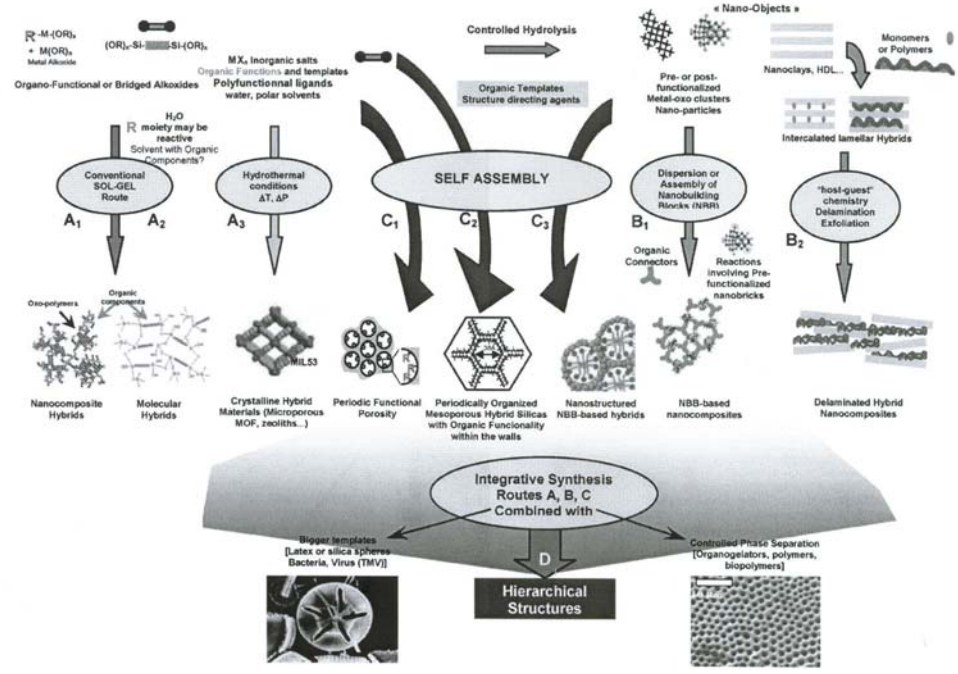

Figure 7.1 Scheme of main chemical routes for the synthesis of organic-inorganic hybrids. Reprinted by permission of The Royal Society of Chemistry, C. Sanchez, P. Julian, P. Pellerille and M. Popall, *Journal of Materials Chemistry*, 2005, **15**, 3559. ©2005, Royal Society of Chemistry

In nanocomposites, a significant mechanical reinforcement is achieve by the incorporation of only a low level of clay (< 5%) in contrast to microcomposites where a high level of filler incorporation is required for even a modest improvement in properties. Rubbery modifiers and rigid fillers are very often used to adjust the mechanical properties of a polymer for various applications [9]. The superiority of a nanofiller over conventional modifiers lies in the fact that nanomodification offers an improvement in mechanical properties in all aspects. The addition of a conventional filler in a polymer matrix often leads moderate increase in modulus at the cost of strength and elongation at break. However, nanofiller, if dispersed properly can lead to increase in all the three properties modulus, strength, % elongation (impact strength). The impermeable inorganic nano layers like nanoclay, CNT etc. mandate a tortuous pathway for a permeant to transverse the nanocomposite. The enhanced barrier characteristics, chemical resistance and reduced solvent uptake of the polymer nanocomposites make them suitable for various applications. The nanomposites especially polymer/clay nanocomposites shows flame retardant properties which will be discussed in detailed shortly. Key evidence for the resilience of nanocomposites to combustion includes:

- An increase in heat distortion temperature
- An increase in peak heat release temperature
- A change in char structure
- A decrease in char permeability
- A decrease in rate of mass loss
- A tendency to self extinguish

7.1 Thermoset/clay nanocomposites

Polymer/clay nanocomposites (PCN)are a new class of nanocomposite that makes use of clay materials, which are cheap and well known fillers for polymer materials. The research on polymer-clay intercalation has been reported before 1980s [10]. However, these works were not taken in the history of polymer/clay nanocomposites as these did not result in a dramatic improvement in the physical and engineering properties of the polymers. The researchers at Toyota, Japan demonstrated for the first time that clay (so called filler) can do miracles in 1993 [11, 12]. While searching for a lightweight material for automotive applications they successfully developed a nylon-6/clay nanocomposite, which results in a dramatic improvement in properties compared to the pristine polymer. Subsequently, the technique was extended to thermoset resins leading to the formation of thermoset nanocomposites.

7.1.1 Principle of polymer/clay nanocomposite formation

The model structure of layered silicates such as montmorillonite [13] is shown in **Figure 7.2**. The crystal lattice of the single 0.95 nm thick layer consists of two tetrahedral sheets fused to one octahedral sheet of either aluminum or magnesium hydroxide (2:1 layer). These 2:1 layers are not electrostatically neutral. The excess layer charge, caused by isomorphous substitutions of Si^{4+} for Al^{3+} in the tetrahedral lattice and Al^{3+} for Mg^{2+} in the octahedral sheet, is balanced by interlayer cations, which are commonly Na^{+}, Ca^{2+} or Mg^{2+} ions. The number of sites of the isomorphous substitution determines the surface charge density and hence significantly influence the surface and colloidal properties of the layered silicate [14]. The charge per unit cell is thus a significant parameter necessary to describe the layered silicates. The intermediate value for the charge per unit cell of smectites ($x \approx 0.25–0.6$) compared to talc ($x \approx 0$) or mica ($x \approx 1–2$) enables cation exchange and gallery swelling for this group of layered silicate, making them suitable for the formation of thermoset nanocomposites [15, 16]. The negative surface charge determines the cation exchange capacity (CEC) [meq/100 g], which is the key factor to the organic surface modification. The crystallites are composed of as many as 100 individual layers stacking together, known as tactoids. The primary particles consist of compact face to face stacking or low angle intergrowth of individual tactoids. Finally, weak agglomerations of these primary particles form the powders, which are agglomerates. Conventionally, theses are called as 'particles'. It is necessary to break such agglomerates in order to make a nanocomposite. The strong hydrophilic nature of the clay surface results in a high interfacial tension with organic materials, making the layered silicate difficult to intercalate and disperse homogeneously in a polymer matrix. That is why *in situ* polymerisation or blending of a polymer with clay leads to a conventional microcomposite with a particle size of about 5 to 15 μm [17] as shown in **Figure 7.3**.

The fundamental principle behind the formation of a PCN is that the monomer is able to move in and react within the interlayer galleries. In order to facilitate the organic material to penetrate into the gallery space, alkyl ammonium cations are introduced into the clay by a simple ion exchange method as the alkali cations residing in the clay gallery are exchangeable [18]. A typical laboratory method for modification of clay is described below. At first Na^{+} and or NH_4^{+} exchanged clays are obtained by the reaction of aqueous NaCl and or NH_4Cl solution (~1.0 M) with the pristine clay at elevated temperature (70-80 °C) for a specific period of time (~24 h). The resulting products are washed with distilled water until no chloride ion is detected while adding a dilute $AgNO_3$ (~0.1 N) solution. Then it is air-dried. This hydrophilic exchanged clay is then used to get organophilic alkyl ammonium exchanged clays by the following procedure. At first the neutral alkyl amine [$CH_3(CH_2)_{n-1}NH_2$, n = 4-8] is dissolved in ethyl alcohol and added to 1.0 N aqueous HX solution (X = Cl or Br) with constant stirring at about 60 °C to get alkylammonium halide salts. Sometimes alkyl diamines

or amino acids are also used. The Na^+ /NH_4^+ exchanged clay is dispersed thoroughly into the alkyl ammonium halide salt solution under vigorous stirring condition at 60-70 °C for 3-6 h. The precipitate formed is isolated by filtration and washed several times with warm deionised water and water-alcohol mixture until no trace of chloride is detected while treating with dilute $AgNO_3$ solution. The treated clay is dried at 80 °C in a vacuum oven, until it was dried properly. The drying can also be done by freeze drying process after dispersion of the modified clays in deionised water.

This simple method offers a wide scope of modification of clay with different types of onium ion as presented in **Figure 7.4**. Such modification serves two purposes; it introduces a hydrophobic character into the clay gallery and it also increases the d-spacing. The modified clay is termed as organo-clay or nanoclay. The hydrophobicity of the clay gallery increases with increase in the number of carbon atoms present in the alkyl ammonium cation. However, it is difficult to introduce an alkyl ammonium cation with a large number of carbon atoms. Generally, the number of carbon atom should be eight or above to generate the required hydrophobicity. Blending of a polymer or *in situ* polymerisation with a suitably designed organo-clay, leads to the formation of a nanocomposite.

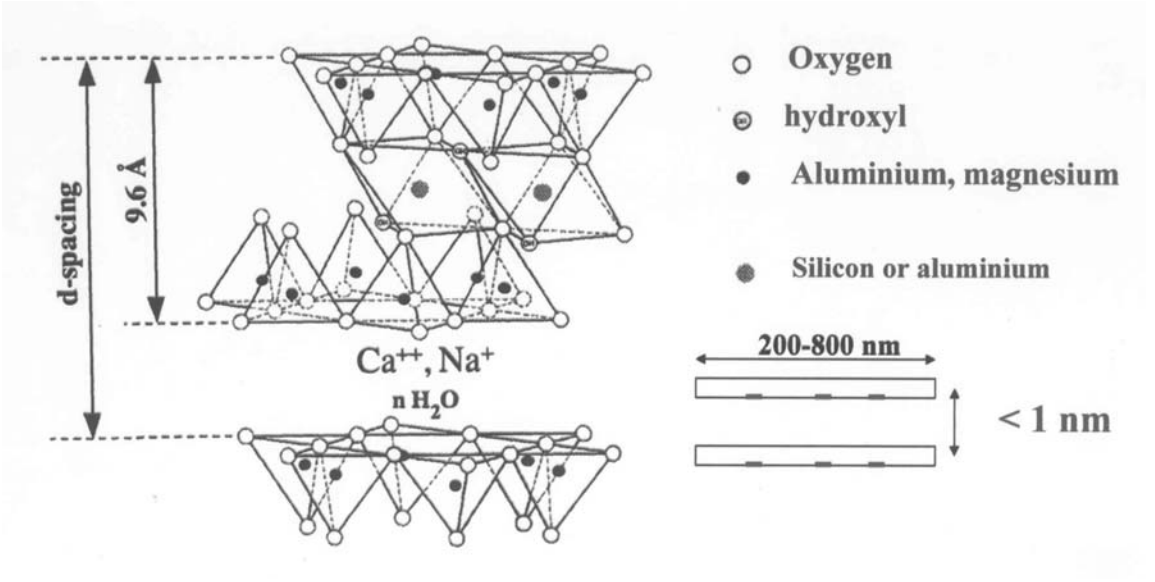

Figure 7.2 Model structure for montmorilonite clay

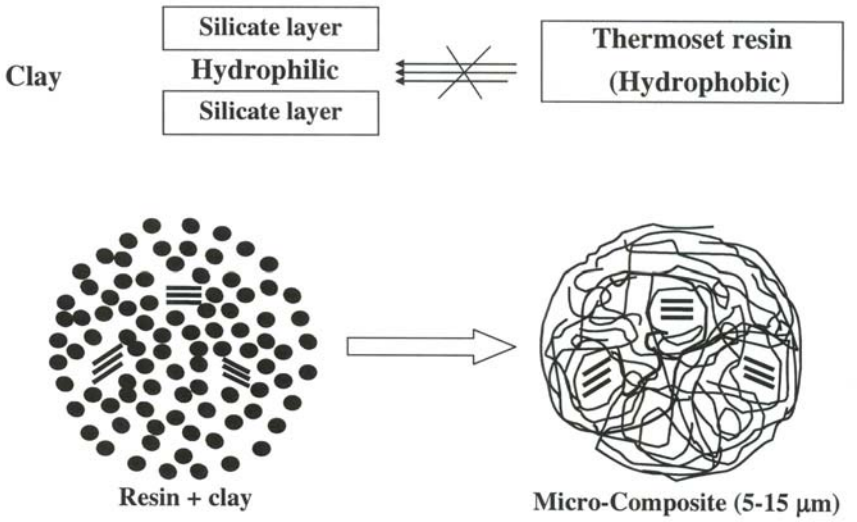

Figure 7.3 Blending of a thermoset resin with pristine clay

In general two idealised polymer layered silicate structures are possible: intercalated and exfoliated. Schematic representations of conventional, intercalated and exfoliated or delaminated nanocomposites are shown in **Figure 7.5**. In an intercalated nanocomposite the insersion of polymer into the clay structure occurs in a crystallographically regular fashion and a few molecular layers of polymer typically occupy the gallery region. Consequently, the properties of an intercalated composite usually resemble those of the ceramic host. In contrast, in an exfoliated nanocomposite, the individual 1 nm thick clay layers are dispersed in a continuous polymer matrix and segregated from one another by average distances that depend on the clay loading. Hence, an exfoliated nanocomposite has a monolithic structure with properties related to those of the starting polymer.

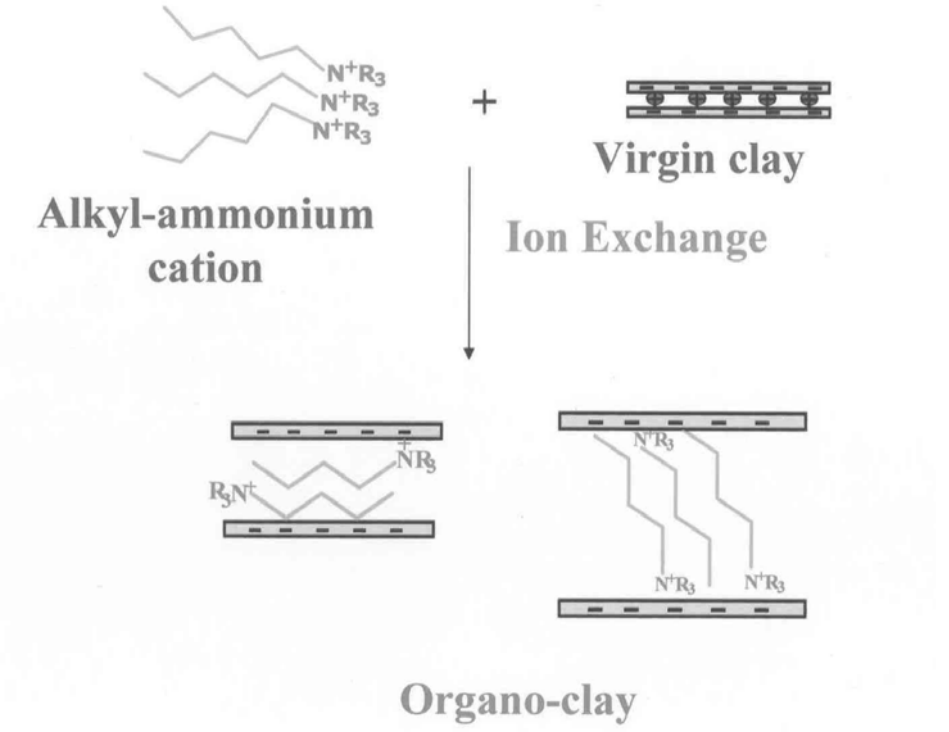

Figure 7.4 Modification of clay with alkyl ammonium cation by ion-exchange method

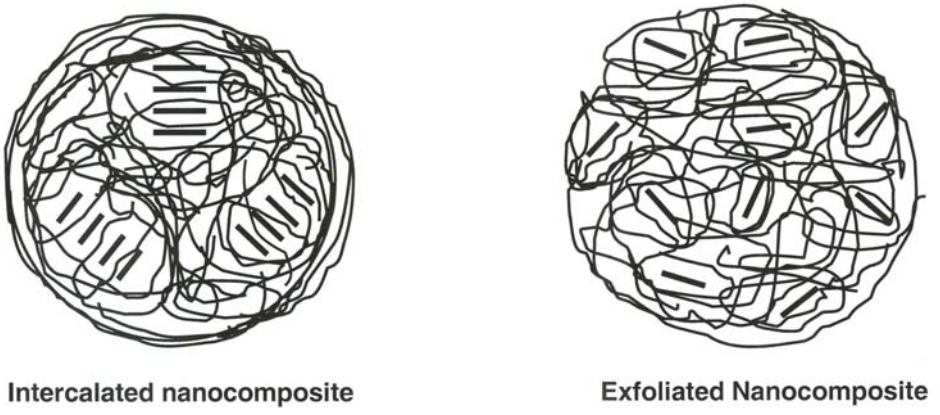

Figure 7.5 Schematic representations of intercalated and exfoliated nanocomposites

7.1.2 Methods of nanocomposite synthesis

The process for synthesising a polymer nanocomposite by various researchers can be classified into four categories namely monomer intercalation (*in situ* polymerisation), covulcanisation, common solvent and polymer melt blending. Rubber-based nano composites are made by covulcanisation method where the nanoclay is dispersed in the rubber directly or using some liquid rubber and vulcanised [19]. In a melt mixing technique, the intercalation or exfoliation of clay particles occurs during melting of polymer either statically or under shear. The efficiency of intercalation using this method may not be as good as that of *in situ* polymerisation technique. However, the approach can be applied by the polymer processing industry to produce nanocomposites based on traditional polymer processing techniques, such as extrusion and injection molding [20, 21]. This process also eliminates the use of hazardous solvents used in solution technique. Therefore, this technology has played an important role in proliferating the application of PCN.

Common solvent technique is based on a solvent system in which the polymer or pre-polymer is soluble and the silicate layers are swellable. The layered silicate is first swollen in a solvent, such as water, chloroform, or toluene. When the polymer and layered silicate solutions are mixed, the polymer chains intercalate and displace the solvent within the interlayer of the silicate. Upon solvent removal, the intercalated structure remains, resulting in the formation of PCN. Polyimide based nanocomposites are made by using a common solvent like dimethyl acetamide (DMAc) [22].

Nanocomposites based on the other thermosetting resins like epoxy, polyurethane, unsaturated polyester resins etc. are made by *in situ* polymerisation method and the resulting morphology of the nancomposite depends on various factors e.g., layered silicate charge density, the nature of interlayer exchanged ion, cure condition, nature of resin, curing agent and their composition [23-25]. *In situ* polymerisation of layered silicate nanocomposite was first reported for the synthesis of Nylon 6 polymer nanocomposites [11, 12]. In this method, the organoclay is initially swollen by the liquid monomer (ε-caprolactam) enabling polymer formation outside and inside the interlayer galleries. The layered silicate gallery surface was pre-treated with 12-aminolauric acid which takes part with the ε- caprolactam in the reaction. In some of the early studies the layered silicate was added directly to the resin/hardener mixture [26, 27]. However, the more established methods of thermoset nanocomposite formation [28] include the pre-intercalation of the layered silicate by swelling in the resin for a period of time prior to the curing followed by the addition of a suitable curing agent and crosslinking. A flowchart describing the synthesis of a thermoset/clay nanocomposite is shown in **Figure 7.6**. Sonication is used in many cases to break the tactoids. Another processing techniques that have been examined include the use of a three-roll mill to impart high shear forces into the system [29]. For such

processing, the clay is added to the epoxy which initially becomes more viscous and opaque, attaining clarity after shearing,

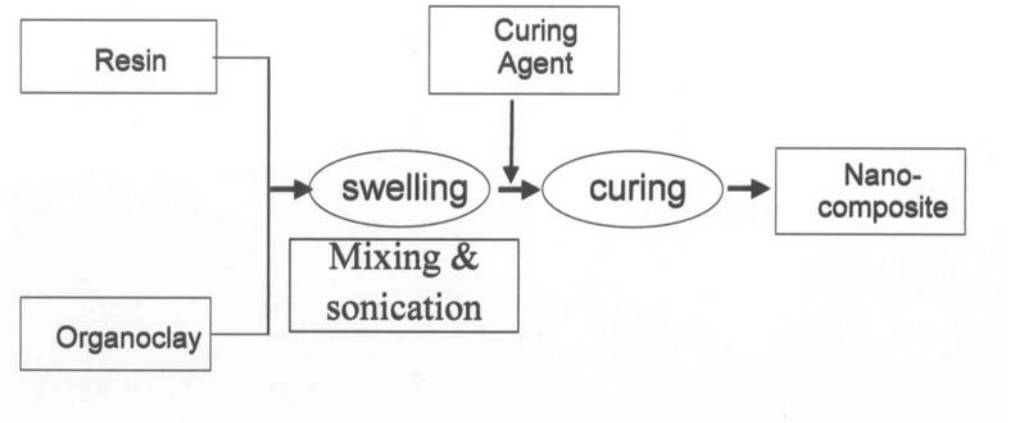

Figure 7.6 A flowchart describing the synthesis of a thermoset/clay nanocomposite

7.1.3 Characterisation of PCN

The key question regarding the structure of a thermoset/clay nanocomposite system is whether a true nanocomposite has formed or not. If not, the material is comparable to a conventional filled microcomposite. Generally, wide angle X-ray diffraction (WAXD) analysis and transmission electron microscopy (TEM) are used to elucidate the structure of a nanocomposite. Due to its easiness and availability, WAXD is most commonly used to establish the nanocomposite structure [30, 31]. By monitoring the position, shape, and intensity of the basal reflections from the distributed silicate layers, the nanocomposite structure (intercalated or exfoliated) may be identified. The X-ray technique is often applied to identify nanocomposite structures through Bragg's relation, which is given below:

$$\lambda = 2d \sin\theta \qquad \text{(Equation 7.1)}$$

where λ is the wavelength of the X-ray used (λ =1.5405 Å), d is the spacing between specific diffraction lattice planes and θ is the measured diffraction angle. The increase in d as a result of intercalation will be reflected through a decrease in θ as λ is constant. Thus any shift of peak in X-ray spectrum of the composite is an indication of the formation of an intercalated nanocomposite. If a crystalline order is manifested as a peak corresponding to the same basal spacing as in the pristine silicate, we

have a conventional composite material. Increase in the basal spacing indicates the formation an intercalated composite. An extensive layer separation associated with the delamination of the original silicate layers in the polymer matrix results in the eventual disappearance of any coherent X-ray diffraction from the distributed silicate layers. Hence the absence of any corresponding peak is an indication of delamination of the clay platelets leading to the formation of an exfoliated nanocomposite. The typical XRD plots of clay and epoxy based intercalated and exfoliated nanocomposites [32] are shown in **Figure 7.7**. The clay shows d100 peak at $2\theta = 3.9$, which corresponds to a d-spacing of 2.26 nm. This indicates that modification of clay with organic ions, not only makes the clay surface hydrophobic but also results in a tremendous increase in d-space (d-space for untreated clay < 1 nm), which facilitates the penetration of liquid resin into the interlayer galleries. In the intercalated nanocomposite, the peak shifted to a position at $2\theta = 3.9$, corresponding to the d-spacing of 4.42 nm. The absence of d100 peak in the other nano composite, indicates an extensive delamination leading to the formation of an exfoliated nanocomposite. The origin of results of different morphology for the epoxy systems will be discussed later.

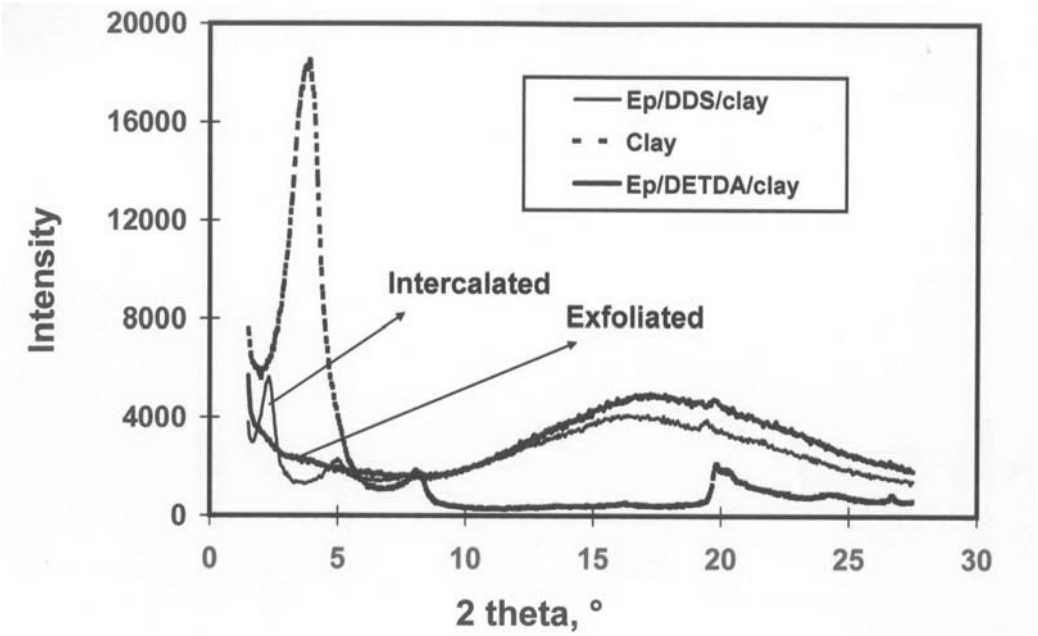

Figure 7.7 XRD plots of organoclay (modified with octadecyl ammonium cation), epoxy/DDS/clay (intercalated) and epoxy/DETDA/clay (exfoliated) nanocomposites. Reprinted from D.Ratna, N.R. Manoj, R.K. Singh Raman, R. Varley and G.P. Simon, *Polymer International*, 2003, **52**, 9, 1403 © 2003 John Wiley and Sons Publishers

Although WAXD offers a convenient method to determine the interlayer spacing of the silicate layers in the original layered silicates and in the intercalated nanocomposites (< 8 nm), it can not provide sufficient information about the spatial distribution of the silicate layers or any structural inhomogeneities in nanocomposites. Further complicacy arises due to the fact that some layered silicates initially do not exhibit well-defined basal reflections. This makes it difficult to investigate the peak broadening and change in intensity systematically. The elucidation of exact structure of nanocomposite can be done by TEM, which allows a qualitative understanding of the internal structure, spatial distribution of the various phases, and views of the defect structure through direct visualisation. It may be noted that very thin (<70 nm) and uniform samples are necessary for getting informative TEM pictures. A TEM picture of epoxy/DETDA based nanocomposite [30] made using an octadecyl ammonium cation modified montmorilonite clay is shown in **Figure 7.8**. XRD analysis of the same nanocomposite system (**Figure 7.7**) indicates exfoliation. However, as is evident from the TEM image that the tactoids are still present. This indicates the morphology falls in between the intercalated and exfoliated nanostructure, though XRD shows exfoliation. The advantage of XRD is that it provides the changes in layer spacing quantitatively unlike TEM, which gives only qualitative information. However, when the layer spacing exceeds 8-9 nm, the XRD feature weakens and remains no longer useful. Hence it is recommended that both WAXD and TEM should be applied as complementary tools to characterise and describe the morphology of a nanocomposite. Small angle X-ray scattering (SAXS) is used to measure crystallite sizes [33]. The XRD analysis can also be extended to determine three-dimensional orientation as demonstrated by Bafna and co-workers [34] and Sinha Ray [31]. Nowadays, small angle neutron scattering and dynamic light scattering are being used [35] to understand the underlying structural aspects of the silicates layers as well as the conformations of polymers in layered silicate based nanocomposites.

High resolution SEM and AFM are increasingly becoming tools for characterising nanocomposites. However, for a clearer picture TEM is necessary. The interlayer distance determined from AFM is generally higher than that obtained from WAXD [36]. This can be explained by considering the fact that AFM tip may deplete or distort the flexible silicate layers dispersed in a rigid thermoset matrix. Since all these measurements involve only a very small area, care must be taken to not to neglect the characterisation in larger-scale inhomogenities. Such inhomogenities could not be detected at a very high magnification. Hence it is recommended to analyse a specimen microscopically in both the higher and lower magnifications.

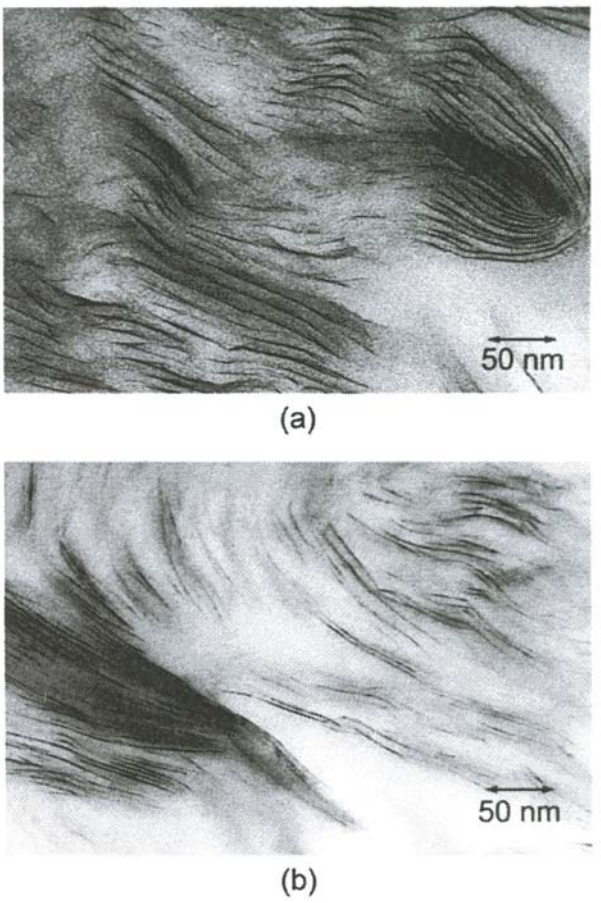

Figure 7.8 TEM micrographs of epoxy/DETDA/clay (modified with octadecyl ammonium cation) nanocomposite cured at a) 100 °C and b) 160 °C. Reprinted with permission from O. Becker, Y.B. Cheng, R.J. Varley and G.P. Simon, *Macromolecules*, 2003, **36**, 5, 1616 © 2003, American Chemical Society

VanderHart and co-workers [37] used solid-state NMR (^{1}H & ^{13}C) spectroscopy for the first time as a tool to study the morphology, surface chemistry and to a very limited extent the dynamics of exfoliated PCN. This method uses the reduction in the spin-spin relaxation time, T_{H_1}, of a nanocomposite when compared with the neat system, as an indicator for the organoclay layer separation. It was shown that the paramagnetic Fe^{3+} ions in the crystal lattice of the montmorillonite provide an additional relaxation mechanism of the protons. The additional relaxation depends on average Fe^{3+}–^{1}H distance, which is determined by clay concentration and dispersion of clay in the matrix.

7.1.4 Controlling Factors for nanocomposite formation

The thermodynamic spontaneity of the interacalation process is determined by an interplay of entropic and enthalpic factors [38, 39]. The confinement of the polymer inside the interlayer results a decrease in the overall entropy of the polymer chains. However, the entropic penalty may be compensated by the increased conformational freedom of the tethered surfactant chains in a less confined environment, as the layers separate out. Even then, there is an overall decrease in entropic factor as the increase in gallery height is very small. Thus the degree of layer separation depends on the establishment of very favorable polymer surface interaction to over come the penalty of polymer confinement. There are two different types of interactions, unfavorable apolar interaction and the favorable polar interaction, which originates from the Lewis acid/Lewis base character of the layered silicates. Thus depending on the interactions and entropic factors three possible equilibrium states are generated namely immiscible (conventional), intercalated and exfoliated.

The first condition of penetration of polymer/monomer into the clay galleries is the polarity matching between the clay gallery and the polymer or monomer. The modification of clay with alkylammonium cations increases the hydrophobicity of the galleies to match the polarity with the polymer/monomer to be intercalated. The hydrophobicity increases with an increase in the number of carbon atoms in the alkyl ammonium cation. It may be noted that incorporation of alkyl ammonium cation becomes more difficult with increase in the number of carbon atoms in the cation. Lan and co-workers [40] used a series of alkylammonium ions, $CH_3(CH_2)_{n-1}NH^{3+}$, exchanged montmorillonite with n = 4, 8, 10, 12, 16 and 18, to study the intercalation of epoxy and observed that the number of carbon atoms in the alkylammonium ion greatly affects clay expansion before cure [40]. It was concluded that an alkylamine cation with number of carbon atoms more than 8, was necessary for the successful formation of a nanocomposite. Zilg and co-workers [41] carried out a similar study using a fluorhectorite clay and reported that the number of carbon atom in the alkyl ammonium cation had to exceed six to promote intercalation or exfoliation. A chain length of higher than eight units did not further improve the exfoliation process. Wang and Pinnavaia [42] studied a series of primary to quaternary onium (octadecylammonium) ions modified clays and observed that primary and secondary onium ion-modified clays produces exfoliated nanocomposites in an aromatic amine cured epoxy system, whilst the tertiary and quaternary ion-modified clays generates only intercalated one. This effect has been attributed to the higher acidity and stronger Brönsted-acid catalytic effect of the primary and secondary onium ions on the intergallery epoxy-amine curing reaction.

For a highly hydrophobic polymers like polypropylene (PP), the modification of clay gallery with an onium ion having the highest possible number of carbon atoms

can not introduce sufficient hydrophobicity to match the polarity of the clay gallery with PP. Modification of polypropylene is necessary to match the polarity of the clay gallery with PP. PP nanocomposites have been successfully made by modifying PP with maleic anhydride [43]. Ratna and co-workers [32] investigated intercalation of epoxy/DDS and epoxy /DETDA systems using an octadecyl ammonium ion modified clay. Under the same processing conditions, epoxy/DDS system produces an intercalated nanocomposite and epoxy/DETDA system produces an exfoliated nanocomposite as evident from XRD analysis shown in **Figure 7.7**. The difference in results due to the change in curing agent may be attributed to a higher polarity of DDS compared to DETDA. Moreover, DETDA is liquid and offers lower viscosity of the epoxy/hardener mixture compared to DDS which is a solid. The lower prepolymer viscosity favors penetration of polymer molecules into the clay gallery which leads to the exfoliation. This indicated that exfoliation depended on the nature of thermoset system used especially on the viscosity of the resin/hardener system.

High processing temperature have been used to improve intercalation. It was found that higher cure temperatures offered better exfoliation of the organosilicate in the epoxy matrix [44, 45]. This improved exfoliation was mainly ascribed to the higher molecular mobility and diffusion rate of the resin and hardener into the clay galleries, leading to an improved balance between inter and extragallery reaction rate. Simon and coworkers [30] investigated the effect of curing temperature on intercalation of epoxy by preparing composites at different temperatures and characterising them by XRD analysis. **Figure 7.9** shows the XRD plots of nanocomposites prepared using different curing temperatures. It is evident that d001 peak shifted toward lower value (indicative of increase in d-spacing) with increasing curing temperature. This clearly indicated that an increase in cure temperature favours the intercalation. However, since the window of processing temperatures is limited by the side reactions, thermal degradation, the variation of cure temperature alone may not be sufficient to form a fully dispersed true nanocomposite.

When an organoclay is dispersed in a thermoset resin mixture, the resin mixture penetrates into the gallery and the curing reaction occurs both inside the gallery and outside the gallery which are called intragallery and extragallery reactions, respectively. For expansion of the clay gallery and delamination, the intragallery reaction should be slightly higher than extragallery reaction so that clay platelets are pushed apart. In case of epoxy resin, the alkyl ammonium cations (present in the galleries) catalyse the epoxy/amine reaction. Hence the intragallery reaction is faster than the extragallery reaction. For other thermosets, this can be achieved by attaching a reactive moiety with the alkyl ammonium cation. For example a schematic drawing of synthesis of polyimide/clay nanocomposite using nonreactive and reactive modifier [46] are shown in **Figure 7.10**. In the first case (a) the modifier contains NH3+ and –COOH group. NH^{3+} replaces Na^{+} and form ionic bond with the silicate layers and the –COOH

group does not react with amic acid (precursor of PI). In second case (b) the modifer contains two $–NH_2$ groups; the protonated one forms ionic bond with the silicate layers and the other $–NH_2$ group can react with the dianhydride end group of polyamic acid as shown in **Figure 7.10**. The incorporation of a reactive moiety helps the clay platelets to push apart leading to a higher extent of intercalation or exfoliation. Lan and co-workers [40] emphasised the importance of the balance between intergallery and extragallery reaction rates, as well as the accessibility of the resin and hardener mixture to the clay galleries for the exfoliation process. It is reported that the monomers penetrate and swell the silicate layers until a thermodynamic equilibrium is reached between the polar resin molecules or resin/hardener blend, and the high surface energy of the silicate layers. Actually further increases in the distance between organoclay platelets require the driving force in terms of elastic forces generated due to curing reaction or homopolymerisation to overcome the attractive electric forces between the negative charge of the silicate layers and the counterbalancing cations in the galleries. Decreasing polarity during reaction of the resin in the galleries displaces the equilibrium and encourages further monomer to diffuse into, and react within, the silicate galleries. Yebassa and co-workers [47] investigated the effect of processing parameters on the morphology of vinyl ester resin based nanocomposites and observed that shearing and sonication during the cure improve the exfoliation process. They also reported that treatment of clay with a reactive amine and addition of comonomer like styrene favour exfoliation.

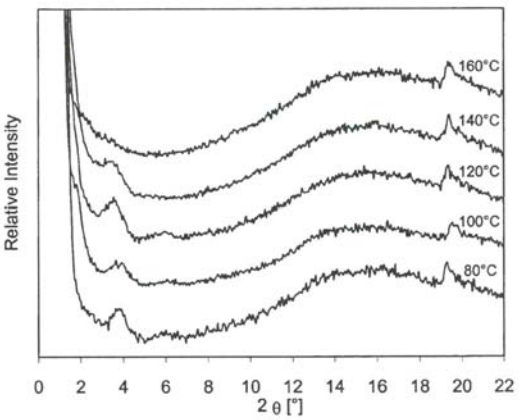

Figure 7.9 XRD plots of an epoxy/DETDA/clay (modified with octadecyl ammonium cation) nanocomposite cured at different temperature profile. Reprinted with permission from O. Becker, Y.B. Cheng, R.J. Varley and G.P. Simon, *Macromolecules*, 2003, **36**, 5, 1616 © 2003, American Chemical Society

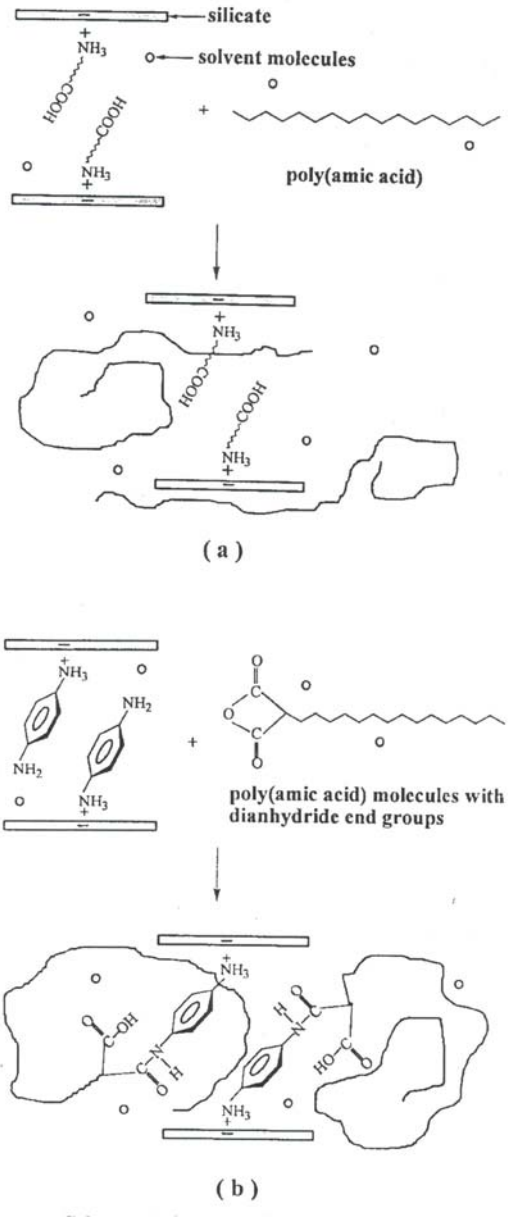

Figure 7.10 Schematic drawing of montmorilonite intercalated by poly (amic acid) and (a) nonoreactive swelling agent containing one functional group NH^{3+} (reversible) and (b) reactive swelling agent having double functional groups NH^{3+} and NH^{2} (irreversible). Reprinted with permission from H.L. Tyan, Y. Liu and K. Wei, *Chemistry of Materials*, 1999, **11**, 7, 1942 © 1999, American Chemical Society

It has been demonstrated by *in situ* SAXS studies of an epoxy nanocomposite that the d-spacing increases with the advancement of curing reaction [48]. Only mixing of resin with the clay did not result in a significant increase in d-spacing. Chen and co-workers [49] divided the interlayer expansion mechanism into three stages. Stage one is the initial interlayer expansion due to resin and hardener intercalation into the silicate galleries. The second stage is the interlayer expansion state where the interlayer spacing steadily increases due to intergallery polymerisation. The third stage of interlayer expansion is characterised by a decreased interlayer expansion rate. In some cases, a slight decrease in interlayer spacing could be observed before cessation of gallery change, due to restrictions on further extragallery change because of gelation.

Park and Jana suggested [50] the possible mechanism of nanoclay exfoliation in epoxy clay nanocomposites. They considered various opposing forces, which simultaneously act when a thermoset resin cures in presence of clay as shown in **Figure 7.11**. They theorised that the primary force behind clay layer exfoliation in this nanocomposite system is elastic force. The elastic force exerted by the crosslinked epoxy molecules inside the clay galleries pushed out the outer most clay layers from the tactoids against the opposing forces arising from electrostatic and van der Waals attractions. The study suggested further that a complete exfoliation of clay structure can be produced if the ratio of shear modulus to complex viscosity is maintained in such a way so that the elastic forces inside the galleries outweigh the viscous forces offered by the extra gallery resin. The authors also studied the effects of quaternary ammonium ions in epoxy clay nanocomposite system on the curing rate, catalytic and plasticisation actions. The study indicated that the degree of exfoliation strongly depends on the ratio of storage modulus of intragallery crosslinking epoxy molecules. The plasticisation effect, which lowers the storage modulus was found to be present in both aliphatic and aromatic epoxy and also a strong function of the nature of curing agent. However, in aromatic system plasticisation effect is less compared to the corresponding aliphatic one and thus there is a difference in exfoliation behaviour of the nanocomposite. The aliphatic epoxy shows better exfoliation.

The use of a low reactive aromatic diamine as a curing agent, favors exfoliation by retarding the crosslinking reaction in the extragallery region as reported by Kong and Park [51]. By analyzing the real time small angle XRD patterns they suggested that the exfoliation occurred in a stepwise manner. The first step is the intercalation of epoxy into the intergallery region of alkyl chain of clay. The second increase is by the clay layer folding, translating and expanding from the self polymerisation of epoxy with the catalytic effect of protonated alkyl amine and the third increase originates from the cross-linking of epoxy resin with the alkyl amine and the hardener in the intergallery region.

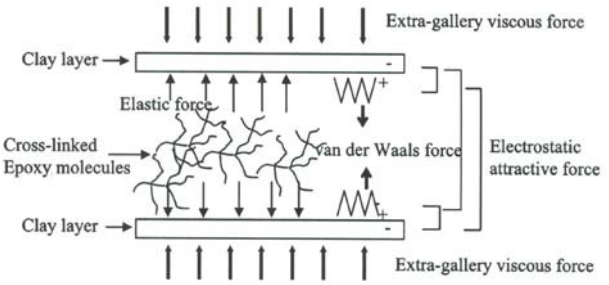

Figure 7.11 Schematic illustration of forces acting on a pair of clay layers during intercalation and exfoliation. Reprinted with permission from J. Park and S.C. Jana, *Macromolecules*, 2003, **36**, 22, 8391 © 2003, American Chemical Society

7.1.6 Properties of PCN

Messersmith and Giannelis [52] carried out the dynamic mechanical characterisation of an anhydride-cured epoxy-based nanocomposites and reported 58% increase in glassy storage modulus due to the incorporation of 4 vol% of layered silicate. Ratna and co-workers [32] reported similar observation using an aromatic amine cured epoxy. The dynamic modulus *versus* temperature plots for DETDA-cured epoxy system and the corresponding nano composites [32] are shown in **Figure 7.12**. The storage modulus of the nanocomposite is significantly higher compared to the neat epoxy. About 50% increase in storage modulus was achieved as a result of incorporation of 5 wt% of clay into the glassy epoxy matrix. Although neither crosslinking density nor the modulus of such exfoliated silicate layers are known, this behaviour can be attributed to the extraordinarily large aspect ratio of exfoliated silicate layers which is frequently assumed to exceed 1000. The increase in modulus is more prominent in rubbery state, which shows about 300% improvement. The nanocomposites show higher T_g compared to the neat epoxy network. This can be explained by considering the confinement of polymer chain as a result of intercalation into the interlayer gallery of the clay. However, in case of highly crosslinked thermoset systems, a decrease in Tg was reported as a result of incorporation of organoclay [30]. The probable reasons are the reduction in crosslink density due to addition of nanoclay as happened in glass fibre reinforced composites or the plasticisation of the crosslinked matrix by the unreacted resins/hardener present in the network. Note that it is difficult to pin point the exact reason due to complexity of the cure reaction and possible side reaction involved especially when the resin is cured at more than 150 °C.

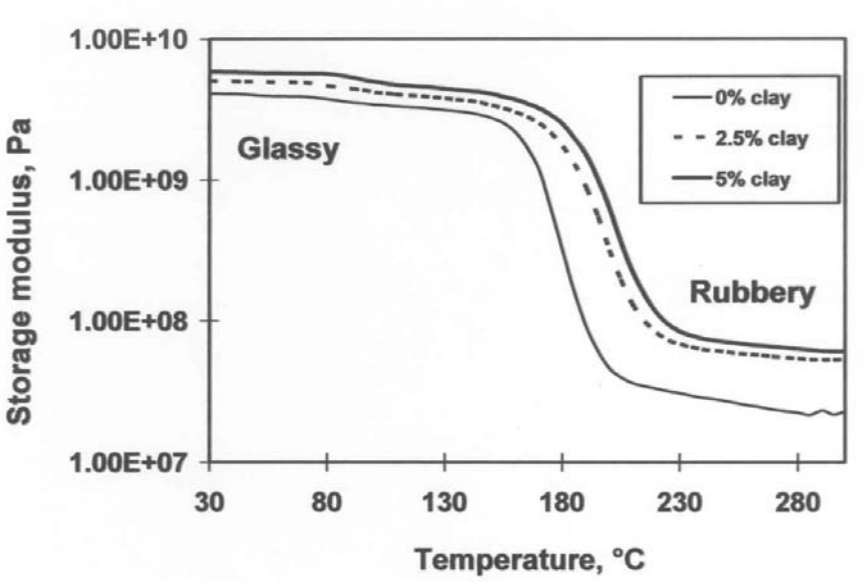

Figure 7.12 The dynamic modulus *versus* temperature plots for DETDA-cured epoxy system and the corresponding nanocomposites containing 2.5 wt% and 5 wt% clay (modified with octadecyl ammonium cation). Reprinted from D. Ratna, N.R. Manoj, R.K. Singh Raman, R. Varley and G.P. Simon, *Polymer International*, 2003, **52**, 9, 1403 © 2003, John Wiley and Sons Publishers

Zilg and co-workers [53] characterised the tensile properties of anhydride cured epoxies using various organoclays (modification with different alkyl ammonium cations). All systems investigated exhibited an increase in Young's modulus, although in several cases, decreases in tensile strength and failure strain were observed. It is thought that the loss in tensile strength might be related to an inhomogeneous network density due to the different cure rates of the intergallery and extragallery reactions or due to the internal stresses developed in the material. Pinnavaia and coworkers [54] found that *m*-phenyl diamine-cured epoxy (high T_g) based PCN showed only a marginal improvement of tensile strength and modulus compared to the pristine epoxy network. On the other hand a significant reinforcement was observed for polyether amine cured epoxies (low T_g) [55]. Ratna and co-workers [56] studied the reinforcing effect of a octadecyl ammonium cation modified clay on polyetheramine cured (low T_g) epoxy systems. The reinforcing effect as evident from the plots of tensile strength and % elongation at break as a function clay concentration for a polyether amine cured rubbery epoxy is shown in **Figure 7.13**. The incorporation of 15 wt% clay into a rubbery epoxy resulted in about 800% increase in tensile strength. It was also noted that the value of % improvement in tensile strength increases with increasing

% elongation of the matrix. This can be explained by considering the phenomenon that under tensile loading the clay platelets undergo orientation towards the applied load. Higher flexibility of the matrix facilitates the orientation of clay platelets resulting in better strengthening effect. As in this case the room temperature is above T_g, the elasticity of the matrix increased thus some amount of applied stress will be transferred to the clay platelets.

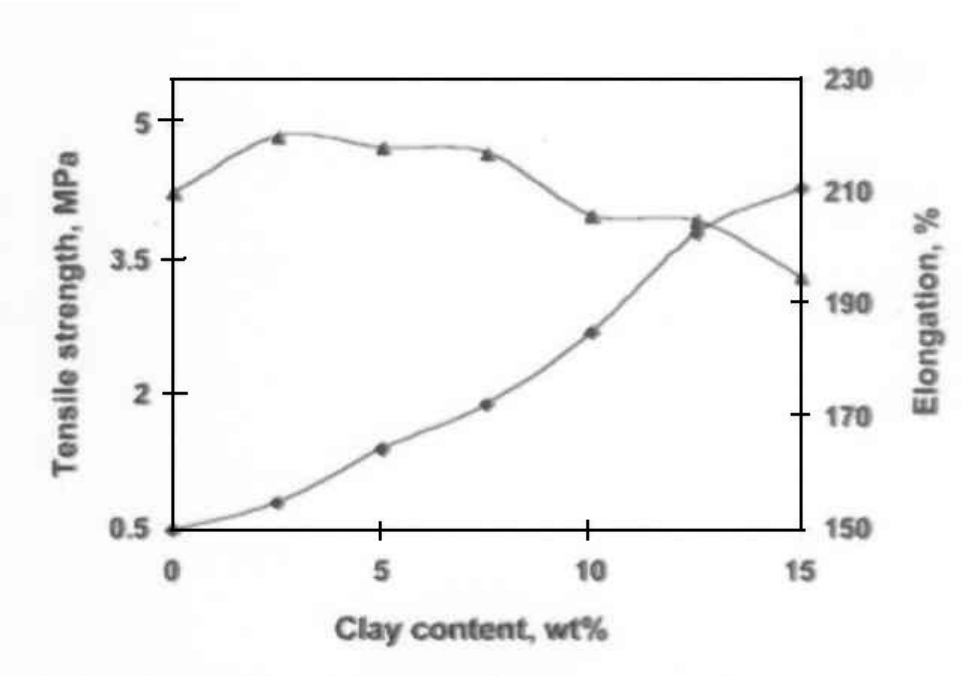

Figure 7.13 Effect of clay loading on tensile properties of rubbery epoxy network: tensile strength (-■-■) and % elongation at break (-■-■-). Reprinted from D. Ratna, B.C. Chakraborty, H. Dutta and A.K. Banthia, *Polymer Engineering and Science*, 2006, **46**, 1667 © 2006, John Wiley and Sons Publishers

The PCN also characterised by a reduced permeability [57, 58] with respect to moisture, solvents etc. The permeability of a nanocomposite can be expressed in terms of clay concentration and aspect ratio as given below:

$$P_{nanocomposite} = \frac{(1-\phi)P_{matrix}}{1+\phi\alpha/2} \tag{7.2}$$

Where P is the permeability, ϕ is the volume fraction and α is the aspect ratio of the layered silicate used. The permeability of a nanocomposite can be enhanced by using higher concentration of layered silicate with higher aspect ratio. Note that the clay concentration should not exceed the optimum concentration beyond which layered silicates are agglomerated. That means the layered silicate should be well dispersed. The reduced permeability in case of nanocomposite can be explained by considering a "tortuous path" concept. Because of the presence of impervious silicate layers, a permeant has to follow a tortuous path compared to a smooth one in pure polymer as shown in **Figure 7.14**.

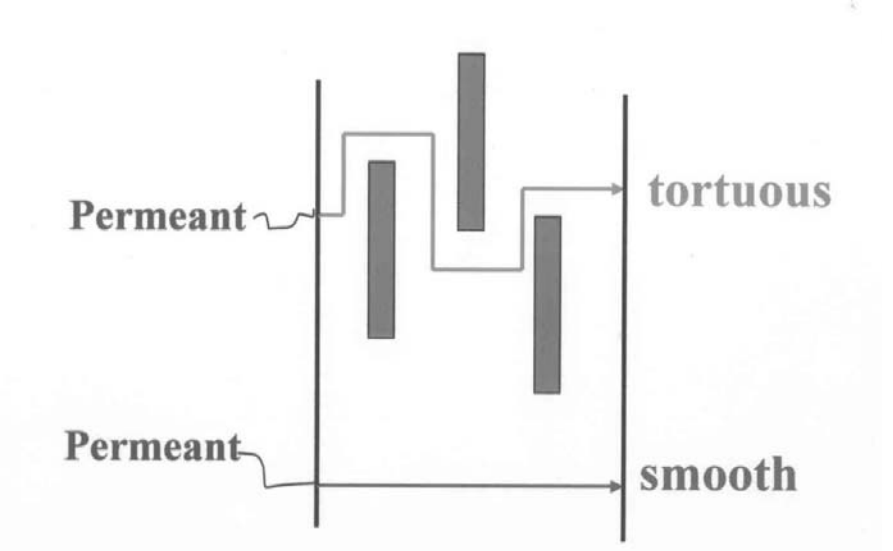

Figure 7.14 A tortuous model for permeability of thermoset/clay nanocomposites

Shah and Gupta [59] investigated moisture diffusion through vinyl ester-based nanocomposites using two different organoclays and showed that the clays were effective in reducing the diffusion coefficient and permeability. However, they did not get any correlation between the morphlogy and water diffusion properties. Ratna and co-workers [56] carried out the swelling study of rubbery epoxy-based nanocomposites in chloroform to asses the solvent resistance. The solvent uptake in terms of weight gain as a function of time is shown in **Figure 7.15**. It was observed that the rubbery epoxy disintegrates into pieces after exposure of about 2 h, whereas the nanocomposites survives the exposure up to 6 h without any damage. This clearly indicates that the solvent and water resistance of thermoset systems can be reduced significantly and application of themoset can be broadened.

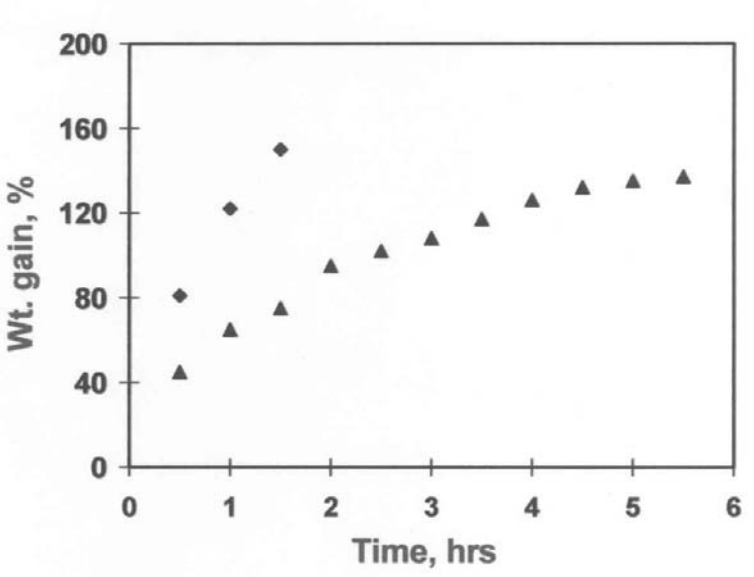

Figure 7.15 Swelling study (in chloroform) of a rubbery epoxy (-■-■) and 15 wt% clay containing nanocomposite (-■-■-) Reprinted with permission from D. Ratna, B.C. Chakraborty, H. Dutta and A.K. Banthia, *Polymer Engineering and Science*, 2006, **46**, 1667 © 2006, John Wiley and Sons Publishers

7.2 POSS and silica-based nanocomposites

Polyhedral oligomeric silsesquioxanes (POSS) are a class of cage-like molecules which have been investigated recently as effective nanofillers for thermoset resins [60-64]. A typical POSS monomer possesses the structure of a cube (octameric framework) with eight organic corner groups. Depending on the nature of R group POSS monomer can be nonfunctional (no reactive group), monofunctional (one reactive group) and polyfunctional (more than one reactive group). Polymerisation of a multifunctional POSS monomer produces cage like molecule with a general formula $[RSiO_{3/2}]n$ where n is an even number in the range of 6-12 and R can be various types of organic groups, one or more of which is/are reactive or polymerisable. POSS materials are derived from the hydrolysis and condensation of trifunctional organosilanes [60]. POSS can be dispersed in a thermoset matrix to make POSS-based nanocomposites and the morphology depends on the degree of reaction between the POSS and the thermoset resin. Williams and coworkers [61] investigated the effect of incorporation of POSS on the dynamic mechanical properties and static compression properties of epoxy/POSS nanocomposites and reported an increase in dynamic glassy modulus from

2.8 GPa to 3.43 GPa and uniaxial compression strength (at 25 °C) from 80 MPa to 100 MPa due to the incorporation of 50 wt % POSS. The studies on modification of epoxy resins by a series of octasilsesquioxanes (with a variety R groups such as aminophenyl and dimethyl siloxylpropylgylcidyl ether groups) indicated [62, 63] that the dynamical mechanical properties, fracture toughness, and the thermal stability of the epoxy hybrids were closely dependent on the types of R group, tether structure between epoxy matrices and the defects in silsesquioxanes cages.

Ni and Zheng [63] designed a novel amphiphilic macromolecule i.e., POSS-capped poly(ε-caprolactone) (PCL), which has both the organic (PCL) and inorganic (silsesquioxane cage structure) portions. POSS-capped PCL was synthesised via a ring-opening polymerisation of ε-caprolactone using 3-hydroxypropylheptaphenyl POSS as the initiator. The PCL sub-chain is miscible with the epoxy whereas octaphenyl-POSS is immiscible with the epoxy resin before and after the curing reaction. POSS-PCL forms a homogeneous solution with epoxy/4,4′-bis methylenebis (2-chloroaniline) (MOCA) system suggesting that no phase separation takes place before the curing. During the curing reaction-induced phase separation takes place via self-assembly leading to the formation of a nanostructured epoxy as shown in **Figure 7.16**. The hydrophobic character of the surface increases with an increase in the concentration of POSS as evident from the static contact angle measurements because the inorganic portion gets enriched on the surface. The contact angle of the cured epoxy/MOCA system with respect to water was 85.2° whereas the same for a nanocomposite containing 40 wt% POSS-capped PCL was 96.2°.

A reactive filler or modifier can be incorporated into a thermoset resin in two different ways; it can be directly blended and cured (chemical bonding occurs during curing) or the modifier/filler is first prereacted with the thermoset resin followed by curing which is known as pre-react method. The effects of the direct blending and prereact methods on the morphology of the modified networks have been elaborately discussed for liquid rubber modified epoxy system in **Chapters 4** and **5**. However, for thermoset/POSS composites, most of the studies have used direct blending method. Recently Zucchi and co-workers [64] analysed the effect of a prereaction for an aromatic amine-cured epoxy system using two types of monofunctional POSS namely glycidyloxypropyl-heptaisobutyl POSS (iBu-GlyPOSS) and glycidyloxypropyl-heptaphenyl POSS (iPh-GlyPOSS). The difference between the two POSS is the nature of inert group; iBu-GlyPOSS contains seven isobutyl groups whereas iPh-GlyPOSS contains seven phenyl groups. The presence phenyl groups causes stronger POSS-POSS interactions and that is why iPh-GlyPOSS is not compatible with the epoxy/amine mixture on direct blending. However, when iPh-GlyPOSS is prereacted with the epoxy it makes a homogeneous solution which on curing produces a two phase nanostructure. Thus epoxy/iPh-GlyPOSS composites can only be made by a prereact method. On the other hand, the presence of iBu groups weakens the POSS-POSS interactions, which makes

it possible to process epoxy/iBu-GlyPOSS composites by both a direct blending and a prereaction method. Note that isobutyl group is less compatible with the epoxy and the hardener which are aromatic in nature. This factor favors the phase separation of POSS from the epoxy matrix. The SEM photographs for the fracture surfaces of epoxy/iBu-GlyPOSS composites made without prereaction and with prereaction are shown [64] in **Figure 7.17**. The composites made with a prereaction show a globular morphology with micron size POSS-rich phase. On the other hand when the same composite is made after prereacting iBu-GlyPOSS with the epoxy followed by curing, irregular clusters (composed by a set of small individual domains) are formed. Thus prereaction produced a significant change in morphology of the nanocomposites. This is because in case of nonreacted POSS the reaction-induced phase separation takes place rapidly in the early stage of pregel region which produces a globular morphology. The prereaction enhances the compatibility of POSS with the epoxy as a result the phase separation takes place slowly at the later stage of pregel region leading to the formation of clusters. Due to its better compatibility with the epoxy/MOCA system, iPh-GlyPOSS does not undergo any reaction–induced phase separation and mostly remains dissolved in the matrix resulting in a reduction in T_g of the nanocomposites.

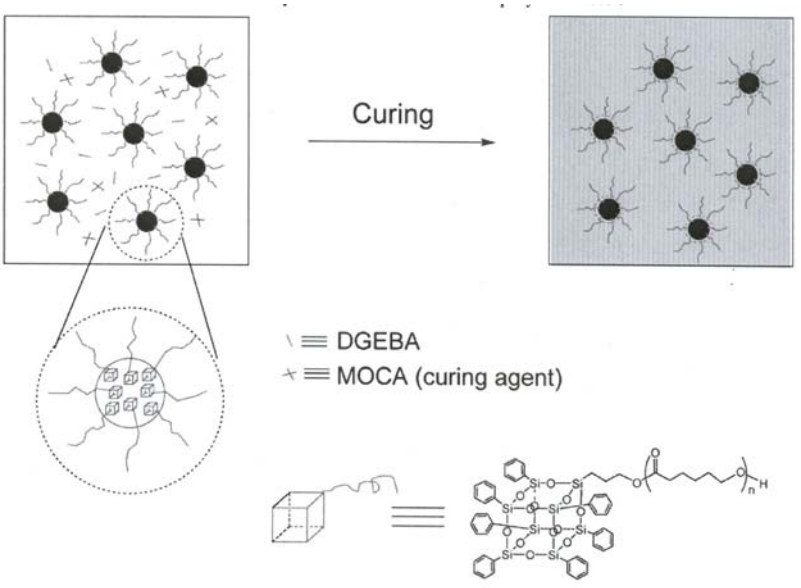

Figure 7.16 Preparation of POSS-based nanostructured epoxy thermoset. Reprinted with permission from Y. Ni and S. Zheng, *Macromolecules*, 2007, **40**, 19, 7009 © 2007, American Chemical Society

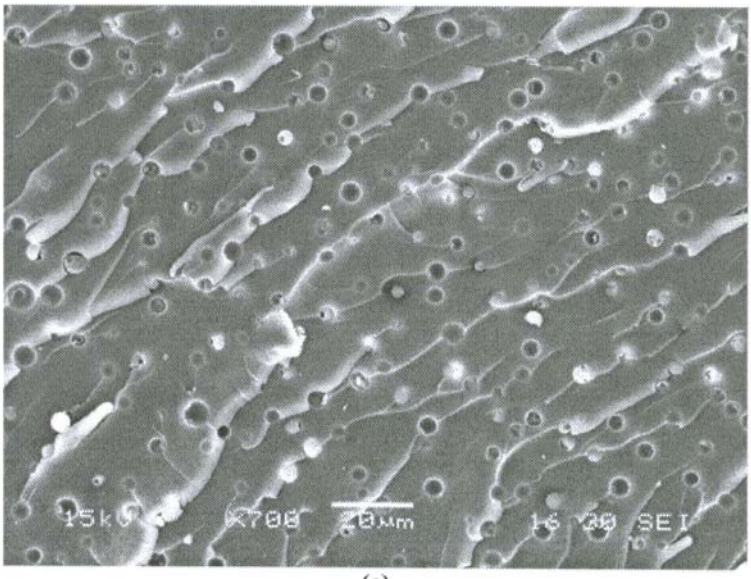

(a)

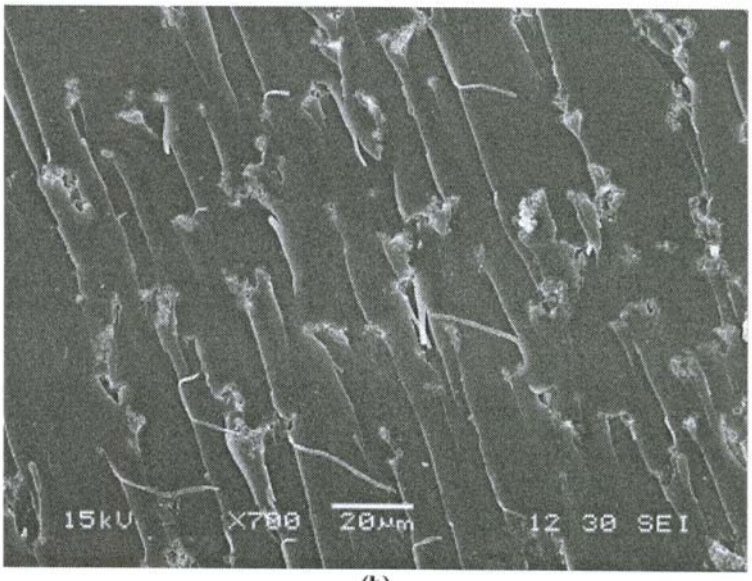

(b)

Figure 7.17 SEM micrographs of final morphologies generated in an epoxy network modified with iBu-GlyPOSS: a) nonreacted iBu-GlyPOSS b) prereacted iBu-GlyPOSS. Reprinted with permission from I.A. Zucchi, M.J. Galante, R.J.J. Williams, E. Franchini, J. Galy and J-F. Gerard, *Macromolecules*, 2007, **40**, 4, 1274 © 2007, American Chemical Society

As evident from the above discussion POSS can effectively enhance the properties of a thermoset. However, the high cost of POSS limits its application for various applications. Recently, nanoscale mesoporus silica (NMS) has been viewed as a suitable candidate for reinforcement of thermoset resin because of its excellent thermal and mechanical stability and inherent air void inside the nanochannels. The major advantage of NMS over POSS is that NMS is much cheaper compared to POSS. NMS can be easily dispersed in a polar resin through polar interactions and covalent bonding. Recently, Cheng and co-workers [65] have successfully dispersed NMS in polyimide (PI) through chemical bonding approach. The outline of synthesis of PI/NMS nanocomposite is shown in **Figure 7.18**. NMS containing large number of silanol groups inside the mesopore channels and on the surface was reacted with 3-aminopropyltrimethoxysilane (APTMS) to prepare an amino-functionalised NMS (**Figure 7.18**). The modification involves reaction between the hydrolysable $Si(OMe)_3$ moiety of APTMS and silanol groups of NMS. The amine-functionalised NMS is then converted to anhydride-functionalised one by reacting the same with ODPA(4,4′-oxydipthalic anhydride). Further reaction with 2-bis-[4-(4-aminophenoxy) phenyl] propane (BAPP) followed by imidisation produces the PI/NMS nanocomposite. NMS-based nanocomposites offer better compatibility compared to other nanocomposites and show lower dielectric constant than the corresponding pure poly imide. The covalent functionalisation route discussed above resulted in a good dispersion of NMS in PI matrix. The TEM images of a PI/NMS nanocomposites containing different concentrations of NMS are shown in **Figure 7.19**. It can be observed that the nanocomposite displays an effective dispersion even at higher concentration of NMS (10 wt%). Note that it is very difficult to maintain a uniform dispersion of nanomaterials beyond 5 wt% of filler loading. The chemical interaction of PI chains NMS through amino group is the driving force to attain such good dispersion.

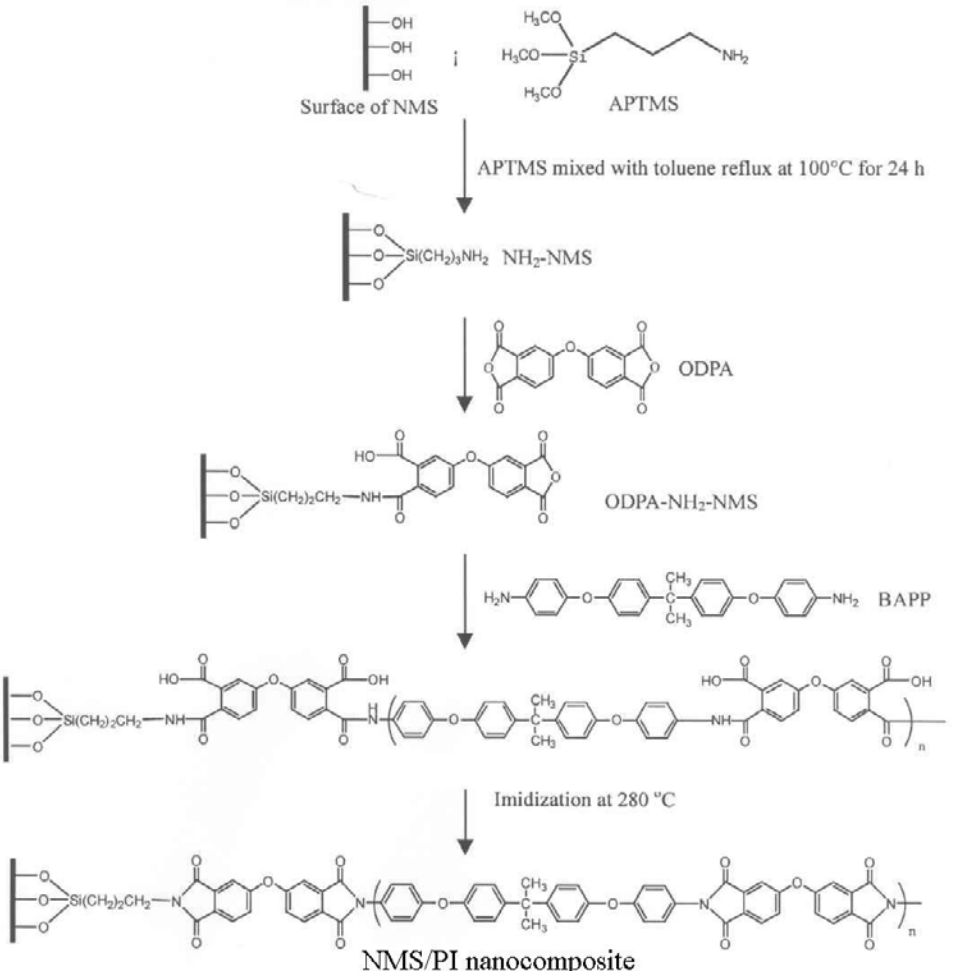

Figure 7.18 Synthesis of NMS/polyimide nanocomposite. Reprinted with permission from C. Cheng, H. Cheng, P. Cheng and Y. Lee, *Macromolecules*, 2006, **39**, 7583 © 2006, American Chemical Society

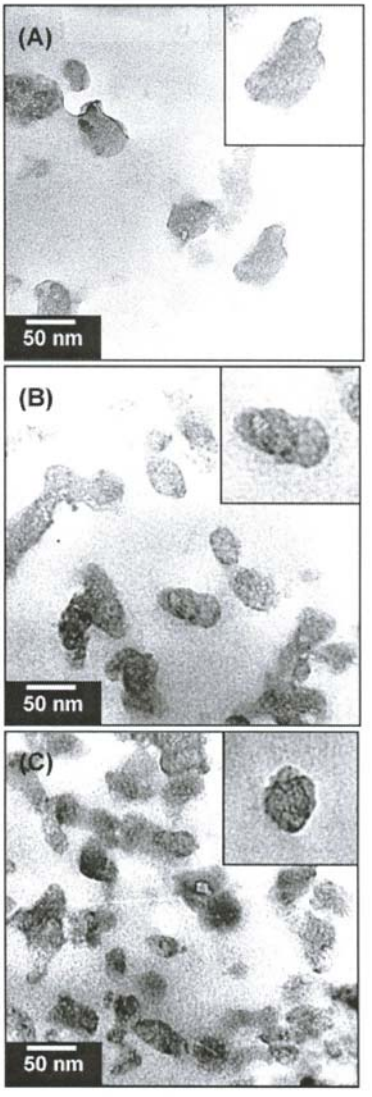

Figure 7.19 The TEM images of a PI/NMS nanocomposite containing (A) 1 wt% (B) 3 wt% and (C) 10 wt% of amino-functionalised NMS. Reprinted with permission from C. Cheng, H. Cheng, P. Cheng and Y. Lee, *Macromolecules*, 2006, **39**, 7583 © 2006, American Chemical Society

7.3 Block copolymer-based nanocomposite

Block compolymers show an interesting property of selfassembling on polymeric length scale (nanostructure) into well defined ordered nanostructure when blended with a suitable polymer [66, 67]. The resulting morphology depends on various factors like molecular weight, block symmetry and interblock repulsive strength developed as a result of contact of dissimilar copolymer blocks. Amphiphilic block copolymers of poly(ethylene-*alt*-propylene) (PEP) and poly(ethylene oxide) (PEO) have been successfully used to generate self assembled nanostructures with epoxy. Grubbs and co-workers [68] investigated both unreactive and reactive amphiphilic block copolymers to prepare epoxy-based nanocomposites. They have used a block copolymer, which consists of two blocks; one block is a random copolymer of methyl acrylate (MA) and glycidyl methacrylate (GMA) and other one is polyisoprene. The epoxy groups of GMA can react with the amine group of the curing agent and participate in the curing reaction. Initially, MA/GMA copolymer block is solvated in epoxy and phase separation occurs due the desolvation as a result of curing. The principle of such reaction-induced phase separation has already been discussed in chapter 4 and 5. A comparison of phase separation processes of unreactive and reactive block copolymers is shown in **Figure 7.20**.

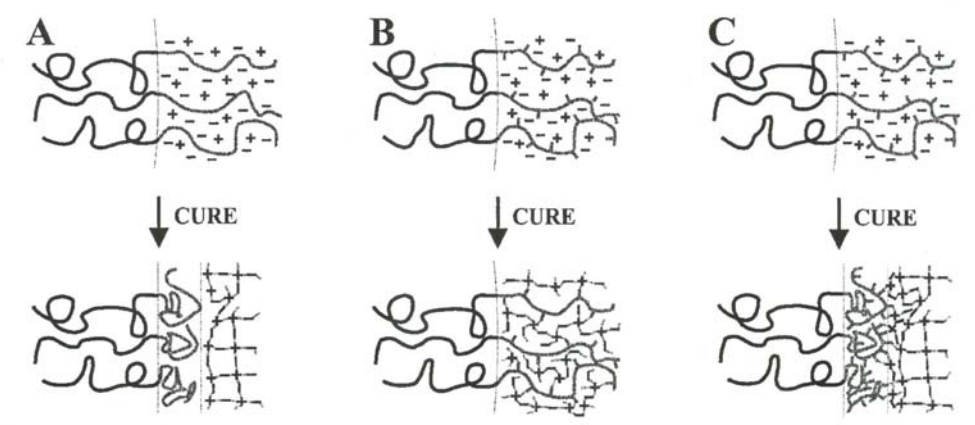

Figure 7.20 A comparison of phase separation processes of unreactive and reactive block copolymers from epoxy matrix. Reprinted with permission from R.B. Grubbs, J.M. Dean, M.E. Broz and F.S. Bates, *Macromolecules*, 2000, **33**, 9522 © 2000, American Chemical Society

7.4 CNT-based nanocomposites

Since the discovery of carbon nanotubes (CNT) by Ijima in 1991 [69] and investigation of its properties by others subsequently, considerable attention has been made on carbon nanotube based nanocomposite in recent years [70]. Carbon nanotubes are seamlessly rolled sheets of hexagonal array of carbon atoms with a diameter ranging from few Angstroms to several tens of nanometer across. These nanometer-sized tubes exist in two forms, single wall carbon nanotubes (SWCNT) in which the tube is formed from only a single layer of carbon atoms and multi wall carbon nanotubes (MWCNT), in which the tube consists of several layers of coaxial carbon tubes. A graphite sheet can be rolled up in many ways to form an SWCNT. The rolling action disturbs the symmetry of the planar system and an axial direction is imposed. Thus various types of tubes are formed namely metallic, semi-metalic or semiconducting. The exceptionally high strength (10-50 GPa) and elastic modulus (~1 TPa) of these tubes render them ideal candidate as ultra-strong reinforcement for composites. In addition CNT exhibit extremely high electrical and thermal conductivity. Due to their one-dimensional nature, charge carriers can travel through nanotubes without scattering. As a result nanotubes can carry very large current densities (up to 100 MA/cm2). Hence unlike layered silicate they can be used to make conducting composites. The related composites offer many interesting application like sensor, actuators, electrolytes and conductive composites.

The technology of polymer/CNT nanocomposites, is less matured compared to the contemporary technology of PCN. The probable reasons are difficulty in synthesis of CNT in large scale and their dispersion in a thermoset matrix unlike layered silicates which are easily available and the related intercalation chemistry is well understood. Typically, CNT tend to agglomerate as bundles in solvents or in the host resin and if dispersed, reagglomerate soon thereafter due to electrostatic attraction. Uniform dispersion within the polymer matrix and improved nanotube/matrix wetting and adhesion are critical issues in the processing of these nanocomposites. Slipping of nanotubes when they are assembled in ropes significantly affects the elastic properties of the composite. In addition to slipping of tubes that are not bonded to the matrix in a composite, the aggregates of nanotube ropes effectively reduce the aspect ratio of the reinforcement [69].

As established for microfibre reinforced composite, matrix-CNT interfacial bonding is a critical parameter, which controls the efficiency of stress transfer from CNT to matrix and the efficiency of stress transfer in turn dictates the mechanical properties of the composites. Since the magnitude of CNT strength is very high (almost 10 times higher than typical carbon fibre) a very high interfacial shear strength may be required for more efficient strengthening of polymers with CNT. Thus the current interest in using CNT and anticipated potential applications for CNT-reinforced

polymer composites demands a better understanding of CNT-matrix interfacial characteristics.

Initial academic research on polymer/CNT nanocomposites has been focused on single wall carbon nanotubes (SWCNT) because of their simpler structure. However, the extremely high cost of SWCNT considerably restricts the commercialisation of CNT based composites. However, the production of multiwall carbon nanotube (MWCNT) has already been scaled up by industry and MWCNT are available in sufficient quantities and at reasonable cost. Therefore, nowadays, research interest has been diverted towards the technological proliferation of MWCNT-based systems. Research efforts have been made to improve the dispersion using various strategies like ultrasonication, high shear mixing, aid of surfactants, chemical modification etc. Surface oxidation by acid treatments, which generates polar groups, has been proven as an effective way to improve the dispersion [71] of CNT. Once such polar groups (-OH, -COOH) are introduced into CNT, the surface can be tailored to make them suitable for dispersion in various polymer matrices by covalent grafting methods using both "graft to" [72, 73] and "graft from" [74, 75] approaches. The "graft to" approach is to graft polymer chains onto the nanotube surface by direct esterification or amidation reactions and the "graft from" approach involves growth of polymer chains from an initiator covalently immobilised on the nanotube surface (surface–initiated polymerisation). Recently, Coleman and co-workers [76] published an exhaustive review on covalent functionalisation of CNT and various aspects of polymer/CNT composites. The disadvantage of chemical functionalisation is that it destroys the Π-electron clouds of CNT to a certain extent and reduces the inherent conductivity of CNT. Another strategy to achieve good dispersion of CNT (without affecting the Π-electron clouds) is to use surfactants (ionic or non-ionic type) which trigger the debundling of CNT by physical interactions and promote dispersion [77, 78]. Ratna and co-workers [79] modified MWCNT with a half-neutralised salt of sebasic acid where the Na+ interact with the Π-electron clouds of MWCNT (cation-Π interaction) and the other –COOH groups of the modifier form H-bonding with the polymers like PEO. They have demonstrated a clear improvement in dispersion and the mechanical properties of the resulting composites.

Thermoset/CNT nanocomposites are processed [80, 81] in a similar way as PCN are prepared. Generally sonication is used to disperse CNT in the resin. Zhou and co-workers [82] incorporated 0-0.4 wt% of MWCNT in epoxy matrix by sonication technique and evaluated their mechanical properties. Improvement in property in all respects was observed up to 0.3 wt% of nanotube. Beyond this concentration the strength and elongation decrease though the modulus keeps increasing. As a result of addition of 0.3 wt% nanotube the tensile strength increases from 93.5 MPa to 121 MPa and % elongation increases from 4.0 wt% to 7.5 wt%. Schadler and co-workers [83] evaluated mechanical properties a MWCNT-epoxy nanocomposites

in both tension and compression. They reported better reinforcement in terms of improvement in modulus (3.63 GPa to 4.5 GPa) in compression than that in tension (3.1 GPa to 3.71 GPa). This indicates a better load transfer in compression than in tension as confirmed by Raman spectroscopy. This can be explained by considering the fact that the load transfer in compression can be thought of as a hydrostatic pressure effect while the stress transfer in tension depends on matrix to nanotube bonding. Recently, Miyagawa and co-workers [84] have used fluorinated single-wall CNT for making anhydride cured epoxy nanocomposite by sonication method as the fluorine atoms present in the nanotubes helps to disrupt the Van der Waals forces between the nanotubes leading to homogeneous dispersion. However, during sonication the fluorine atoms form free radical and resulted in partial breakage of the epoxy rings.

Gong and co-workers [85] used surfactants as a wetting agent to improve dispersion and showed about 30 % increase in dynamic storage modulus and increase in T_g from 63 °C to 88 °C, due to the addition of 1 wt% of nanotubes. However, effective load transfer from the matrix to nanotube is only possible when there is chemical interaction between the nanotube and matrix so that the nanotube forms as integral part of the matrix. Yaping and co-workers [86] functionalised MWCNT with amino groups by treating with an ethanol solution of triethylene tetramine and used the amino-functionalised CNT for reinforcing epoxy resin. The reported an optimum MWCNT concentration of 0.6 % where about 100% increase in flexural strength was achieved.

Zhu and co-workers [87] treated SWCNT with dicarboxylic acid peroxide to generate alkyl carboxyl groups attached to SWCNT. The treated SWCNT are further reacted with diamine to make amine-functionalised SWCNT. These amino groups (covalently attached to SWCNT) can readily react with epoxy resin along with the added curing agent. Thus a crosslinked structure with covalent bonds between nanotubes and epoxy matrix. Addition of 1 wt% of such modified nanotube resulted in about 25% increase in tensile strength and 30% increase in both modulus and % elongation. This behaviour is quite different from the one observed when conventional microfiller are incorporated into polymer matrix i.e., elongation at failure froms drastically when particulate or short fibres are incorporated into a polymer matrix. It may be noted that addition of 1 wt% of pristine SWNT in epoxy under similar condition resulted in little enhancement in mechanical properties. This clearly demonstrates that through suitable modification it is possible to realise the real nano effect in CNT-reinforced composites.

7.5 Nanoreinforcement and toughening

Thermoset nanocomposites with well dispersed layered silicate or CNT, offer improved thermal stability and elastic modulus as discussed in the earlier sections. However,

the results on the effect of nanomodification on fracture toughness are contradictory. Some studies reported reduction in toughness due to addition of nanofiller [88] and other studies indicated reduction in toughened as a result of nanomodification [89]. Thermoset resins are as such brittle and often required to be toughened using a suitable modifier. Thermoset resins can effectively toughened by the modification with rubbers as discussed in **Chapter 4** and **5**. However, rubber modification is accompanied with a substantial decrease in modulus. Hence the conventional toughening strategy can be coupled with the nanoreinforcement strategy to make a really strong and tough material. The ternary blending strategy (simultaneous nanoreinforcement and toughening) is schematically represented in **Figure 7.21**. This requires the control of both the nanostructure (dispersion of nanofiller) and micro structure (dispersion of rubber). Few studies have been carried out to examine the outcome of the above mentioned strategy. However, further further research activities are required to be carried out to come to a meaningful conclusion. The works done so far are reviewed next.

The chemorheology and morphology of a ternary system consisting of an epoxy resin, CTBN liquid rubber and an organoclay modified with octadecyl ammonium cation have been investigated [90]. Analysis of both the nanostructure and microstructure indicate that although the intercalate the layered silicate alone, it does not do so to the same extent as the epoxy resin. Indeed, in the ternary blend, the clay remained in the epoxy-rich phase and the rubber phase separated into fine particles. Flexural testing indicated that the clay was able to compensate some of the modulus sacrificed as a result of rubber addition. The toughness was found to increase with the addition of clay alone and, of course, rubber alone. However, no synergistic toughening effect was observed. Frölich and co-workers [91] investigated a system in which epoxy was mixed with hydroxyl-terminated poly (propylene oxide-block-ethylene oxide) as the rubber, with a synthetic fluorohectorite clay treated with bis (2-hydroxyethyl) methyl tallow alkyl ammonium ions. The clay was first blended with the rubber, before being dispersed into the reactive epoxy mixture. Modification of the rubber allowed variation in miscibility and differing morphologies and properties. When the rubber was miscible, it imparts only plasticising effect and the intercalated clay led to the improved toughness. If the rubber is sufficiently modified, such as with methyl stearate, then both the nanostructure and microstructure coexist. The TEM pictures of various samples are shown in **Figure 7.22**. The phase-separated morphology leads to a significant increase in toughness, with only a modest decrease in modulus.

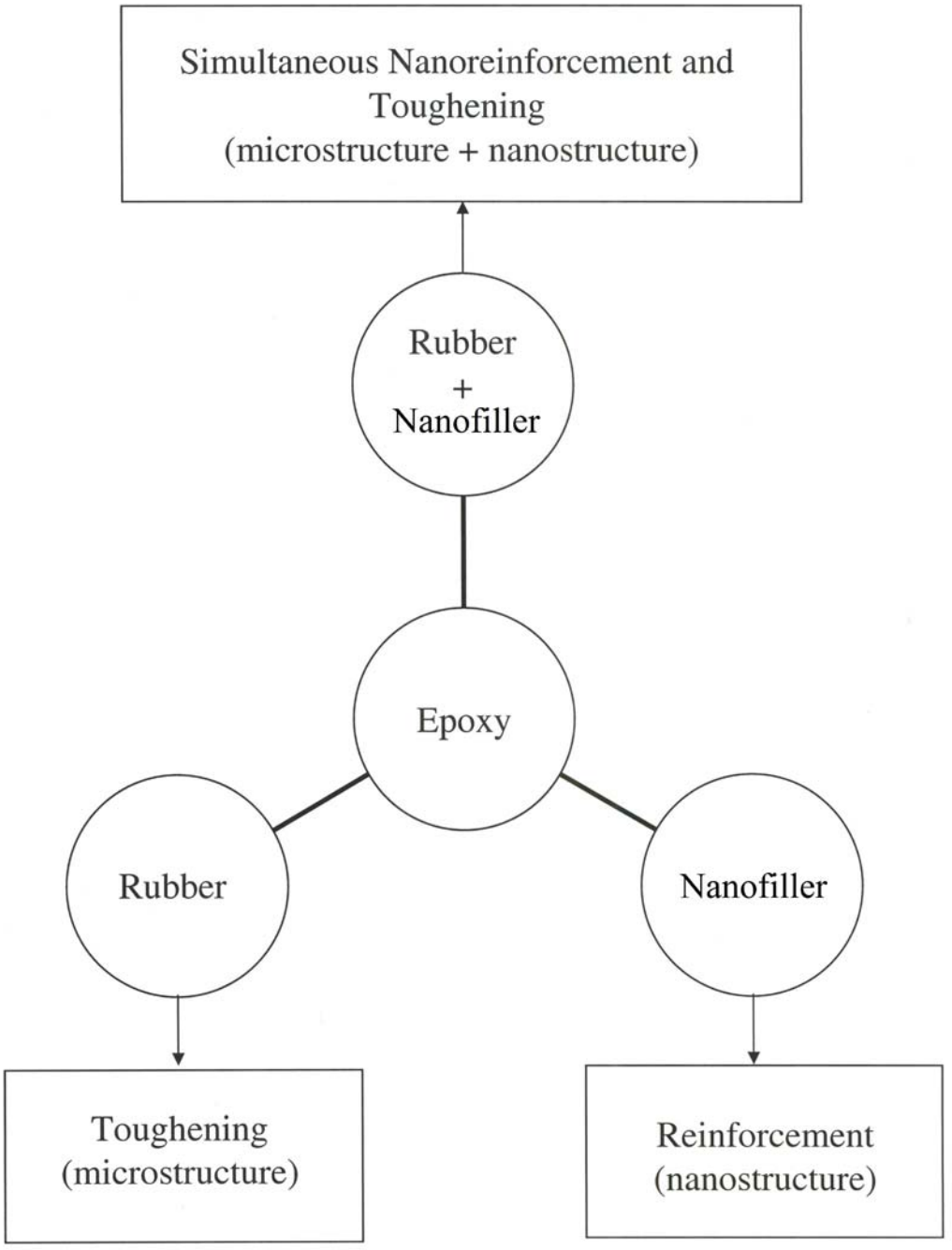

Figure 7.21 Schematic representations of simultaneous nanoreinforcement and toughening of thermoset resins

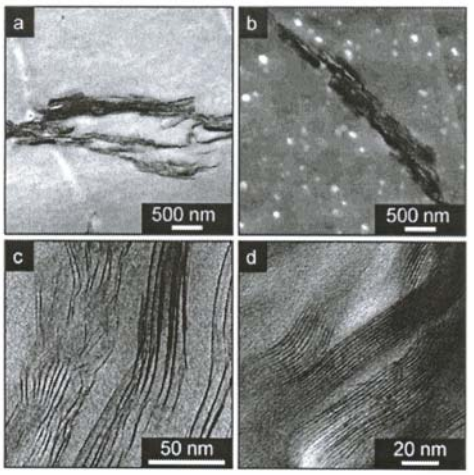

Figure 7.22 Transmission electron micrographs of epoxy hybrid nanocomposites. Images shown are examples for composites with (a) dissolved PPO in epoxy matrix (b) phase separated PPO-stearate spheres in epoxy matrix (c) PPO-modified epoxy/clay nanocomposite (d) PPO-stearate-modified epoxy/clay nanocomposite. Reprinted with permission from J. Frohlich, R. Thomann and R. Mulhaupt, *Macromolecules*, 2003, **36**, 7205 © 2003, American Chemical Society

Ratna and co-workers [92] investigated a ternary system containing epoxy, epoxy-functionalised hyperbranched polymer (HBP) and an octadecyl ammonium ion modified nanoclay. Investigation of the morphologies of these materials showed that the epoxy nanocomposite had a well-dispersed structure an average d-spacing of 8-9 nm. However, analysis and low magnification indicates the presence of tactoids. The thermomechanical properties of ternary systems with varying compositions are given in **Table 7.1**. It is clear that the incorporation of clay is able to compensate for the reduction in modulus as a result of rubber modification. However, the impact strength of the ternary system was found to be lower than epoxy/HBP blend alone. This can be explained by considering the fact the reaction-induced phase separation of HBP is disturbed to some extent due to the presence of clay as evident from SEM photographs shown in **Figure 7.23**. The toughening effect in liquid rubber modified system largely depends on the microstructure, which is likely to be affected by the presence of a third component. Hence this issue has to be addressed properly for the development of a strong and tough three component materials consisting of a thermoset resin, a liquid rubber and a nanofiller. Choi and co-workers [93]

investigated a similar epoxy-based ternary system where they used a core-shell rubber (CSR) modifier, in which no reaction-induced phase separation is involved. They used cubic silsesquioxane (cubes typically 1.2-1.5 nm diameter) as a nanofiller. The stress-strain plots of the ternary systems containing different concentration of CSR are shown in **Figure 7.24**. It is clear from the figure that the toughness (area under the stress-strain plot) increases gradually with increase in CSR concentration while the modulus remained constant. Similar observation was reported for vinyl ester resin based ternary system [92]. Apart from the blending of thermoplastic and rubber with as a thermoset to improve the toughness property, various toughened interpenetrating network (IPN) systems have also been reported. IPN are made by designing a system where at least one monomer can be simultaneously or sequentially polymerised with the immediate presence of others. Karger-Kocsis and co-workers [93] reported vinyl ester (VE)/epoxy interpenetrating networks (VE/EP IPN), which shows a considerable higher toughness compared to the pristine VE resin [55]. However, IPN materials exhibit low modulus and glass transition temperature [94]. With the motivation to improve the modulus and Tg, the same group has investigated VE/EP/clay nanocomposites using closite 30B and another synthetic flurohectorite clay. The nanocomposites were made by adding the treated-clays to the pre-mixed equally-proportioned VE/EP resin mixture. The addition of the clay was found to further decrease the thermal and fracture properties. The epoxy resin appeared to encapsulate the clays, which showed some level of intercalation. The fracture energy of the nanocomposite system containing 5 wt% clay was found to be two times higher compared to the same for the unreinforced resin. The fracture energy decreased drastically with further increase in clay concentration, which was attributed to a fundamental change in the failure mode. The increase in toughness at lower concentration of clay was not a nano-phenomenon, rather due to the toughening effects of the softer interphase between encapsulated clay and the matrix. The course non-intercalated silicate particles (adhered to the bulk by a soft interface) act as stress concentrator and initiate extensive shear deformation.

Table 7.1 Properties of ternary blends of epoxy, epoxy-functionalised HBP and nanoclay [92]

Blend composition Epoxy/HBP/clay	Flexural strength (MPa)	Flexural Modulus (MPa)	Impact strength (J/m)	T_g (°C)
100/0/0	112	2920	740	192
100/15/0	109	2510	2250	182
100/0/5	146	4090	1060	206
100/15/5	135	3630	1540	192

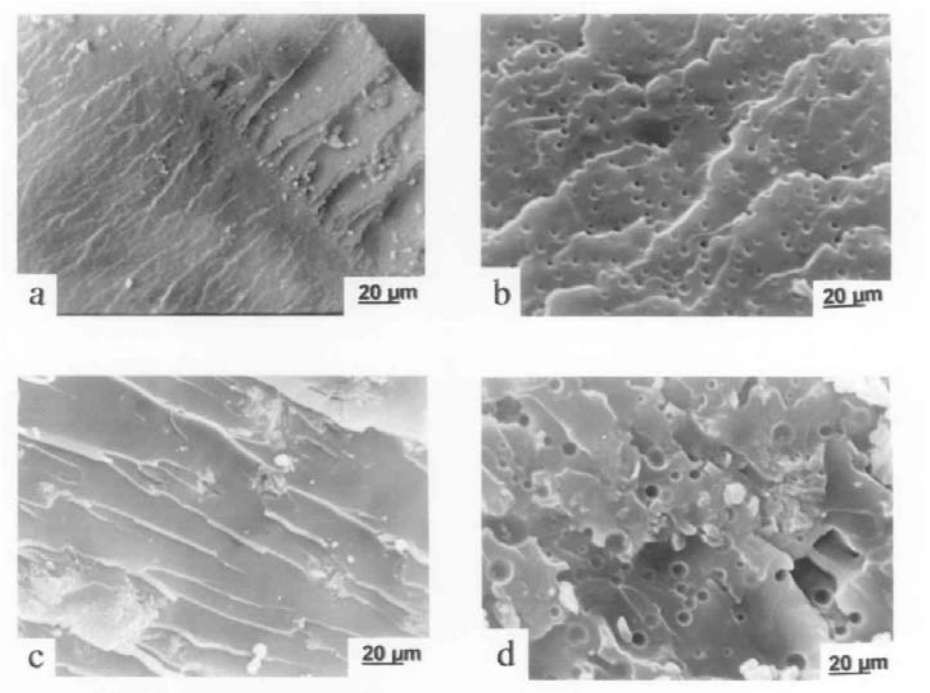

Figure 7.23 SEM micrographs for fracture surfaces of a) neat epoxy b) epoxy/HBP c) epoxy/clay d) epoxy/HBP/clay. Reprinted with permission from D. Ratna, O. Becker, R. Krishnamurty, G.P. Simon and R. Varley, *Polymer*, Elsevier Publishers, 2003, **44**, 24, 7449 © 2003

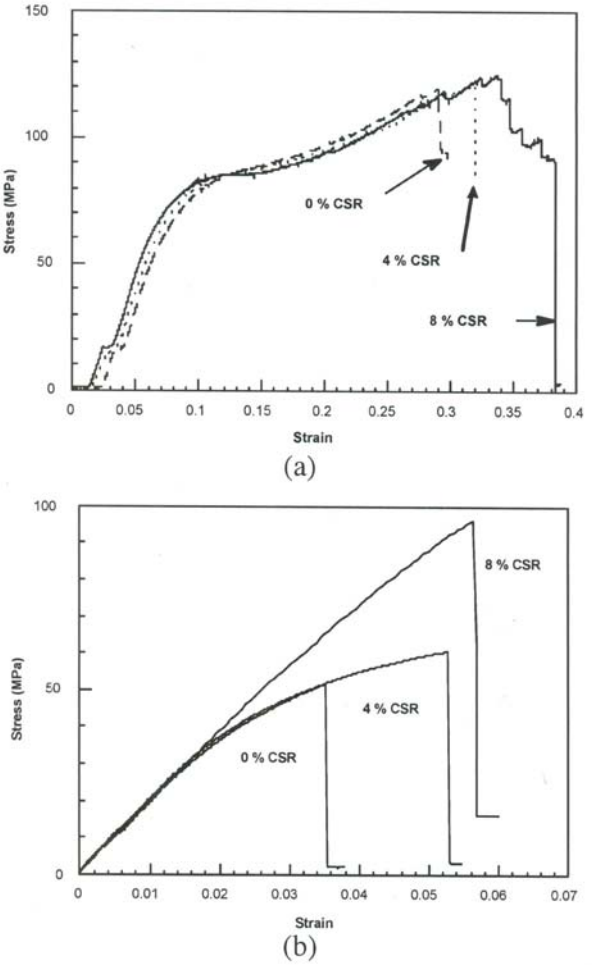

Figure 7.24 Room temperature mechanical tests of the ternary systems (epoxy + cubic silsesquioxane + CSR) containing different concentration of CSR (a) compression (b) tension. Note that the strain scales for (a) and (b) are different. Reprinted with permission from J. Choi, A.F. Yee and R.M. Laine, *Macromolecules*, 2004, **37**, 3267. © 2004, American Chemical Society

7.6 Nanotechnology and flammability

A thermosetting resin composition is required to be fire retardant to ensure reliability and human safety. The flame retardancy is a major concern in the applications where fire can occur namely, aircraft cabin, ships, submarines, offshore drilling platforms and rail carriages. A number of studies have been carried out to examine the effect of high temperature or fire on the load bearing properties of polymer laminates and sandwich structures [97, 98]. It was concluded that thermal softening of the polymer matrix and reinforcement, creep and decomposition of polymer matrix, deteriorate the tension properties, whereas matrix softening and delamination cracking are responsible for the reduction of compression properties. Among the thermoset resin discussed in previous sections phenolic, polyimides, amino resins are inherently flame retardant. Epoxies, PU, UPE are flammable and are to be modified in order to reduce their flammability for fire sensitive applications. Such modification can be done by either chemically modifying the resin or by incorporating additives called flame retardants. Before discussing the role of nanotechnology on the fire retardancy of thermoset resin it is necessary to discuss about the basics of flame retardancy and conventional flame retardants. The relevant testing for assessment of flammability and smoke behaviour of the thermoset resins have already been discussed in **Chapter 1**.

7.6.1 Mechanism of flame retardancy

Like the mechanical and thermal properties, flame retardancy of a thermoset resin polymer is in some way connected to both the number of cross-links and to the strength of the bonds that make up their cross-linked structure. A highly crosslinked thermoset system containing N-C bonds are more fire resistant compared to a less crosslinked network [99]. Flammability of a thermoset can be further reduced by blending them with an additive called flame retardant. A material which inhibits or even suppress the combustion process is called flame retardant. The functions of a flame retardant in the solid, liquid or gas phase can be broadly divided into two categories namely physical action and chemical action. However, it should be kept in mind that combustion is a complex process where all the mechanisms operate simultaneously. The most common physical action is the formation of a protective layer. Under an external heat flux, the flame retardant produces a shield with a low thermal conductivity that can reduce the heat transfer from the heat source to the material. This restricts the passage of volatile degradation products from the matrix which supports the continuous fueling of the fire [100]. As a result the degradation rate is reduced. Other physical actions are cooling and dilution effect caused by the modifier. Some flame retardants evolve inert gases on decomposition and dilute the fuel in the solid and gaseous phases so that the lower ignition limit of the gas mixture is not exceeded.

The interfering effect on combustion due to chemical action mostly takes place in condensed or gas phase. Combustion is believed to proceed through a free radical mechanism. The flame retardant can interfere the process by scavenging the free radicals. The example of such chemical reaction will be discussed in subsequent sections. The material may form a carbonaceous char as a result of chemical reaction which protects the polymer from fire by physical action discussed above. The carbonaceous material formed from the additives plays two different chemical roles in the flame retardancy process. It contains free radical species, which react with the gaseous free radical products formed during the degradation of the polymer. These species may also play a part in termination steps in the free radical reaction. An intumescent flame retardants (IFR) consists of three main components: an acid source, a carbon source and a gas source. Polyphosphates-pentaerytritol-melamine system has been successfully used to develop intumescent coating and additive for thermosets [101]. The solid first begins to melt and dissipates thermal energy in the process. A state of viscoelastic material is achieved which can trap the evolving gases. This material starts to expand and grow, i.e., to intumesce. The intumescent coating so formed no longer traps the evolving gases when the internal pressure increases and it degrades under the heat flux and thus protects the structure. The final state consists of a carbonaceous residue constituted of polyaromatic and phopshorus oxides.

7.6.2 Conventional flame retardants

7.6.2.1 Inorganic flame retardants

Inorganic fillers are well known flame retardants and smoke suppressants for polymers in general and thermosetting resins in particular. The main advantage of inorganic fillers is that they are nontoxic. However, the flame retardant efficiency of inorganic fillers is so low that that a very high loading of filler is required to be incorporated in order to achieve an adequate flame retardancy. For example aluminium trihydrate is most commonly used inorganic flame retardant which is incorporated in amounts up to 300% of the resin level. These extremely high loadings pose processing problem and deteriorate the mechanical properties of a composite substantially. The use of a combinations of aluminum trihydrate with ammonium polyphosphate or red phosphorus significantly reduces the loading (~50%) to achieve an optimum flame retardancy. Red phopshorus, an allotropic form of phopshorus, is not spontaneously flammable and is thermally stable up to 450 °C. A silane treated grade of aluminum trihydrate (more expensive) is also available which is easier to incorporate the thermoset resin system.

7.6.2.2 Halogen containing flame retardants

Thermoset resins are made fire resistant either by modifying the resin (or any component) with halogen or by using a halogen containing flame retardants. Halogenated polyols (brominated polyol, dibromo neopentyl glycol) are advantageously used for making flame retardant PU. The polyols with aliphatically bound bromine like dibromo neopentyl glycol, tribromo neopentyl glycol are more effective than the polyols with aromatically bound bromine, which do not decompose at the lower temperature range of the burning of polymer. The polyester polyol containing hexachloroendomethylene tetrahydro phthalic acid structures are frequently used for the synthesis of flame retardant PU. Chlorinated paraffins (CP) and decabromobiphenyl oxide (DB) [102] are generally blended with epoxy and polyester resins to improve flammability. However, low molecular weight of CP or DB has a problem of migration. The migration problem can be solved by using brominated epoxy resins, which are mostly derived from diglycidyl ether of bisphenol-A (DGEBA) and tetrabromo bisphenol-A (TBBA) with a suitable catalyst [103]. Brominated epoxies of different grades are commercially available by Atul and Vantico. Halogen-containing compounds release of hydrogen halide during decomposition, which interrupts the chain reaction. Due to participation of halogen containing compound in combustion [104] the highly reactive ·OH and ·H radicals are replaced by the less reactive halogen X as shown below:

$$R\text{-}X + P\text{-}H \longrightarrow H\text{-}X + R\text{-}P$$

$$H\text{-}X + H\cdot \longrightarrow H_2 + X\cdot$$

$$H\text{-}X + OH\cdot \longrightarrow H_2O + X\cdot$$

where RX and PH represent the flame retardant and the polymer, respectively. This strongly reduces the combustion rate. The effectiveness of halogens deceases in the order: HI > HBr > HCl > HF. Brominated and chlorinated organic compounds are generally used because iodides are thermally unstable at processing temperatures and the effectiveness of fluorides is too low. The choice depends on the type of polymer, for example, in relation to the behaviour of the halogenated flame retardant under processing conditions (stability, melting, distribution) and/or the effect on properties and long-term stability of the resulting material.

Generally halogen containing flame retardants are used in combination with a metal oxide like antimony trioxide to achieve synergistic effect. During fire the antimony trioxide reacts with the chlorine of the flame retardant or polymer and forms antimony halides which create a blanket of gaseous layer. This acts as a gas barrier between the fuel gas and condensed phase. The reaction scheme is shown in **Figure 7.25**. The problem in general with halogenated flame retardants is that during

combustion the burning is associated with release of toxic and corrosive gases, like hydrogen halides, which is a potential health hazard. Also they can cause the severe degradation of polymer chain to combustible monomer or similar species [104]. In recent years the research on the development of environment friendly, so called "green flame retardants" has received considerable attention. The need has not only been expressed by acute government regulations but equally and persuasively by various social concerns for the environment.

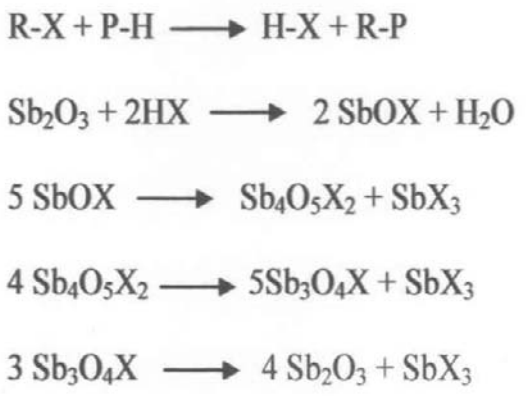

Figure 7.25 Reaction scheme for combustion of halogen containing compound in presence of Sb_2O_3

7.6.2.3 Phopshorus Containing Flame Retardant

Organophopshorus compounds have high flame retardant efficiency in thermoset resins and also been found to generate less toxic gases and smoke compared to halogen containing compounds [105]. Hence, the replacement of halogen-containing fire retardant by a phopshorus-containing one has a noteworthy benefit in terms of environmental protection. The mechanisms of flame retardancy have already been discussed in earlier sections. The presence of phopshorus helps to form a carbonaceous char or a barrier layer of polyphosphoric acid on burning of the polymer in condensed phase [104, 106]. A chemical vapour-phase mechanism is found to be effective in those cases where the phopshorus-containing degradation products are capable of being vapourised at the temperature of the pyrolysing surface. Triphenyl phosphine oxide and triphenyl phosphate have been shown to break down in the flame to small molecular species such as PO, HPO_2, PO_2, P_2. The rate controlling hydrogen atom

concentration in the flame has been shown to reduce in presence of these species. Studies on the systems with phopshorus atom in the chain as well as with the volatile phase species indicate that condensed phase mechanism is more effective than vapour phase mechanism [107].

Phophorous-based flame retardant system can be made modifying the resin or curing agent to incorporate phopshorus into their chemical structure or by using reactive or nonreactive phopshorus containing flame retardants. The reactive types flame retardant exhibit much better flame retardancy and overcome several drawbacks associated with physical blends of the epoxy and the flame retardants [108]. For phopshorus-containing epoxy resin and phopshorus containing curing agents (amine, acid or anhydride) can be used to make flame retardant epoxy resin. A conventional epoxy can be modified with phenyl phosphate or a phopshorus-containing diol bis (3-hydroxyphenyl) phenyl phosphonate to prepare phopshorus containing epoxies [109] as shown in **Figure 7.26**. By the judicious selection of curing agent of the epoxy, the fire-retardant property can be manipulated taking advantage of phopshorus-nitrogen synergism. Note that the synergistic property occurs probably due to the formation of P-N bonded intermediates, which are better phosphorylating agents than those of the related phopshorus compounds without nitrogen [107]. However, introduction of phopshorus in the resin backbone or in the curing agents may affect the curing behaviour and thermomechanical properties of the cured resin. It is necessary to detailed kinetics and mechanical properties before selecting for a particular application.

Hergenenrother and co-workers [110] synthesised the epoxy and the diamine curing agents containing phopshorus and evaluated the resins for composite applications. The optimised formulations showed excellent flame retardation with phopshorus content as low as 1.5 wt%. The flame retardancy is achieved without any sacrifice in the properties due to the incorporation of phopshorus. Braun and co-workers [111] investigated the influence of the oxidation state of phopshorus on the decomposition and fire behaviour of epoxy-based composites highlighting the potential for optimising flame retardancy while maintaining the mechanical properties of epoxy/CF composites. They used phosphene oxide, phosphinate, phosphonate, and phosphates (phopshorus content about 2.6 wt%) and found that with increasing the oxidation state of the phopshorus, additional charring was observed. So, the thermally stable residue increases whereas the flame inhibition, which plays an important role for the fire performance of the composites, decreases. The study of the decomposition behaviour indicates that phopshorus-containing groups influence the decomposition of the epoxy, resulting in a clear multi-step decomposition with mass losses between approximately 15 to 20 wt% in subsequent processes after the main decomposition step. The mass loss of the main decomposition process is reduced as a result of incorporation of phopshorus.

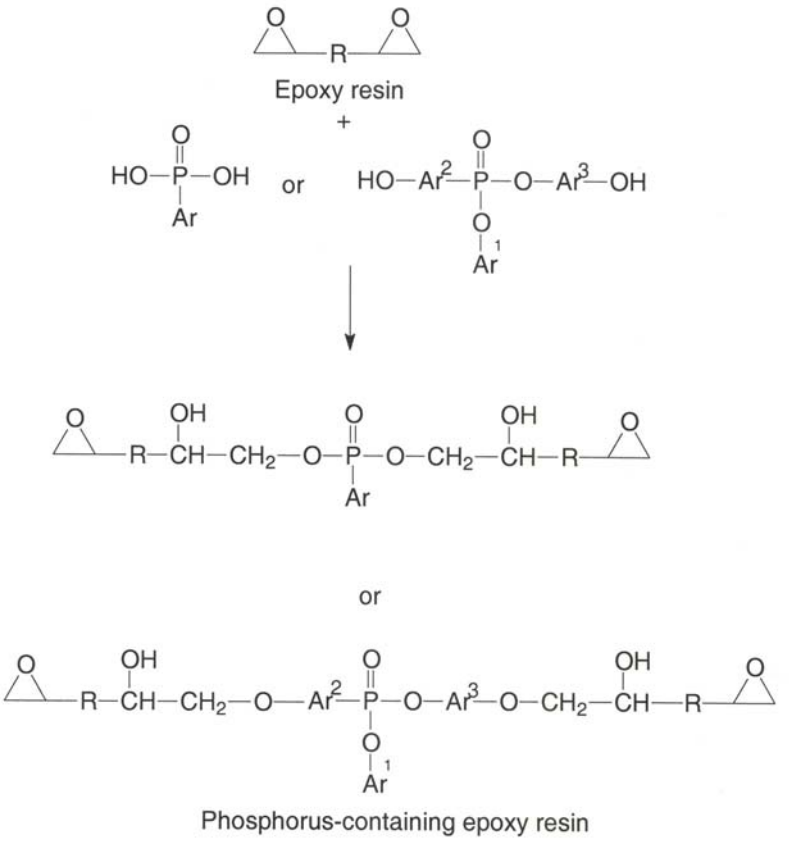

Figure 7.26 Synthesis of phopshorus-containing epoxy from conventional epoxy

DOPO (9,10 dihydro-9-oxa-10-phosphaphenanthrene-10-oxide) has been widely used to make flame retardant thermoset system. DOPO-based compounds have been shown [112, 113] to induce a significant improvement in the flame retardancy of epoxies, while at the same time avoiding many disadvantages such as poor compatibity, migration of compound and release of toxic gases upon burning as compared to conventional flame retardants. DOPO can be used as such or it can be reacted with the resin or DOPO-based resin can be synthesised. For example DOPO-based epoxy resin is synthesised by first reacting DOPO with *p*-benzoquinone to get hydroxyl derivative of DOPO. The DOPO derivative is further reacted with epiclorohydrin in presence of a base catalyst to prepare DOPO-bases epoxy resins. The reaction scheme is shown in **Figure 7.27**. The beauty of this system is that the flame retardancy can be improved at a phopshorus content as low as 3 wt%, thereby limiting the processing difficulties and the often severe degradation of the thermomechanical

properties of the base resin. Recently, a novel phopshorus-modified polysulfone was developed [114], which can act as a flame retardant-cum-impact modifier for an epoxy thermoset. Incorporating the modifier in an amine-cured difunctional epoxy they could enhance both the toughness and the flame retardancy without a significant sacrifice in thermomechanical properties. Also it was possible to generate a network of higher T_g under certain curing condition due to the formation of an interlocked epoxy-thermoplastic network. In order to explain the fire property, the decomposition behaviour has been investigated. The possible decomposition pathway for DGEBA/DDS network is shown [114] in **Figure 7.28**. The analysis of decomposed product indicates formation of gases like SO_2, CO, CH_4 etc.

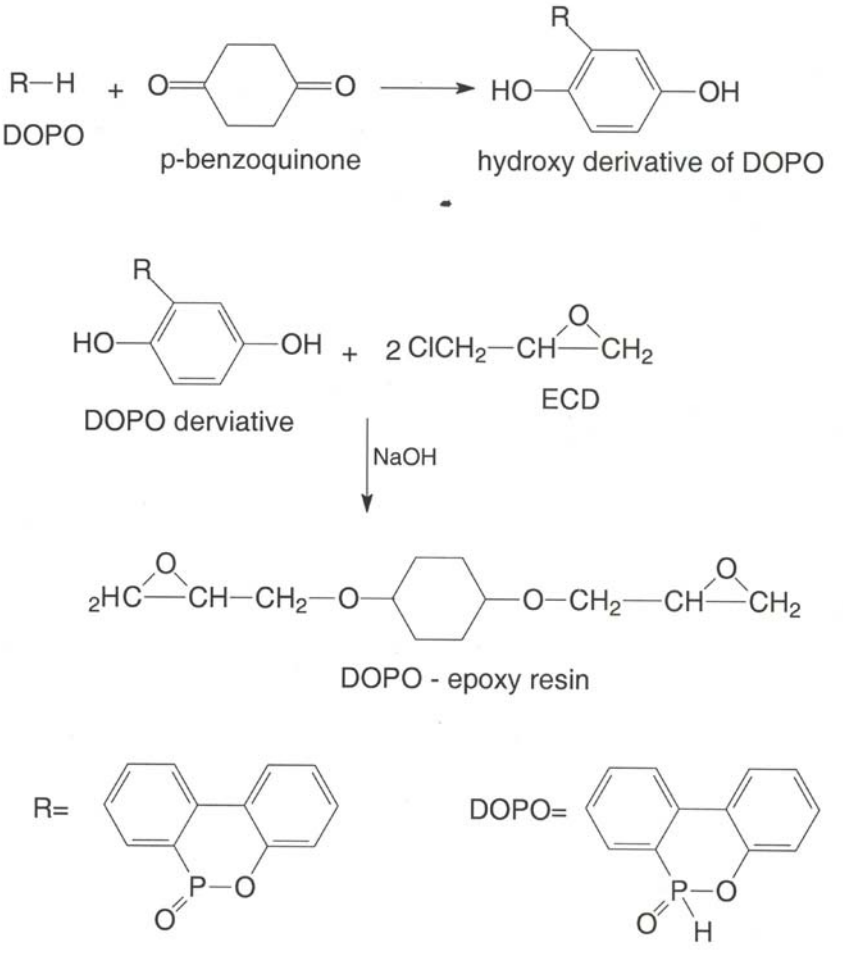

Figure 7.27 Synthesis of DOPO-based epoxy

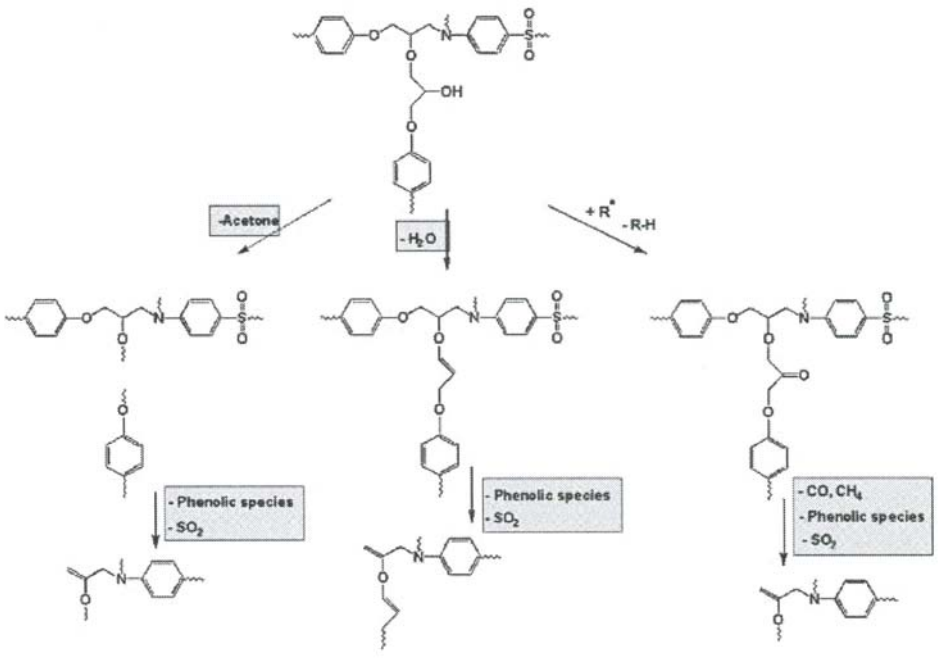

Figure 7.28 Part of Possible Decomposition Pathway for DGEBA-DDS Epoxy Material. Verified Decomposition Products are shown in Grey and Charring/Cross-linking is indicated by Zigzag Line. Reprinted with permission from U. Braun, U. Knoll, B. Schartel, T. Hoffman, D. Pospiech, J. Artner, M. Ciesielski, M. Doring, R.P. Graterol, J.K.W. Sandler and V. Altstadt, *Macromolecular Chemistry and Physics*, 2006, **207**, 16, 1501. © 2006, Wiley-VCH Verlag GmbH & Co KgaA

7.6.2.4 Nanoclay Based Flame Retardant

Polymer/clay nanocomposites have been examined extensively for their flammability characteristics [115, 116]. It was reported that if the samples were examined using a cone calorimeter, the peak heat release rate and mass loss rate. For example the cone calorimeter profile of a PU system and its nanocomposite as investigated by Berta and co-workers [117] are shown in **Figure 7.29**. The figure compares the weight loss, mass loss rate and heat release rate (HRR) of the nanocomposite and the corresponding PU matrix. It is evident that an incorporation of 2.5 wt% of organoclay resulted in a significant decrease in weight loss, mass loss rate and heat release profile. The nanocomposite gives a reduction in HRR of 43% and the total heat released is reduced to more than 80% in compared to the PU matrix. It is not clear which type of

nanocomposite (intercalated or exfoliated) improves the combustion behaviour more. This is because it is difficult to prepare exfoliated nanocomposites without changing other parameters which affect flammability of a polymer. Moreover, in most cases the morphology of a polymer/clay nanocomposite system falls in between the intercalated and exfoliated nanostructure. It may be noted that the time of ignition values of the nanocomposites were similar or slightly lower compared to the corresponding matrix. This is probably due to the early decomposition of the organic modifier on the clay surface, which catalyses the polymer degradation.

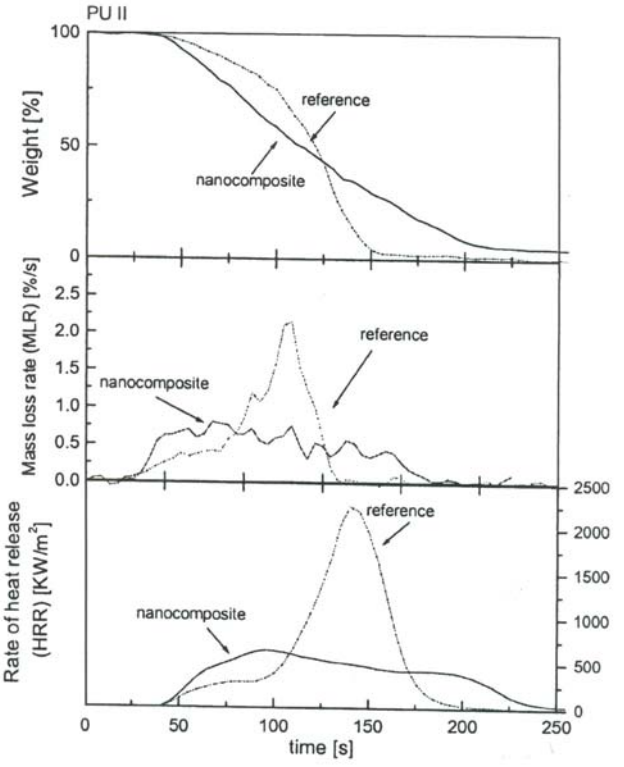

Figure 7.29 Cone calorimeter profiles of PU and PU/clay nanocomposite. Reprinted with permission from M. Berta, C. Lindsay, G. Pans and G. Camino, *Polymer Degradation and Stability*, 2006, **91**, 1179. © 2006 Elsevier Publishers

The investigation on the mechanisms of thermal stabilisation and flammability reduction in nanocomposites reveals that an addition of organoclays into a thermoset resin can substantially aid flame retardancy by encouraging the formation of a carbonaceous char in the condensed phase [118, 119]. The nanoscale dispersed lamellae of clay, either intercalated or exfoliated in polymer matrix, all enhance the

formation of charring upon burning [120]. After pyrolysis, the nanocomposite forms a char with a multilayered carbonaceous silicate structure. The exfoliated clay layers firstly collapse into an intercalated structure, which is transformed into a multilayered carbonaceous-silicate structure later [120, 121]. The carbonaceous char builds up on the surface during burning and insulates the underlying materials. This limits the passage of degradation products from the matrix which supports the continuous fueling of the fire [104]. In case of the presence of char forming additives the nanoclay reinforce the char and makes it more impervious. It was reported that the formation of a hard crust on burning of the nanocomposite, which can be observed on the surface of the residue. A TEM picture of the crust at the boarder between polymer and the residue as reportrd by Hartwig and co-workers [122] is presented in **Figure 7.30**. It can be seen that the silicate is concentrated close to the interface of the residue and that particles are the main component of the residue. The particles contain silicon and aluminum which shows that they are originated from the clay. However, the layered structure of the clay is destroyed in the residue.

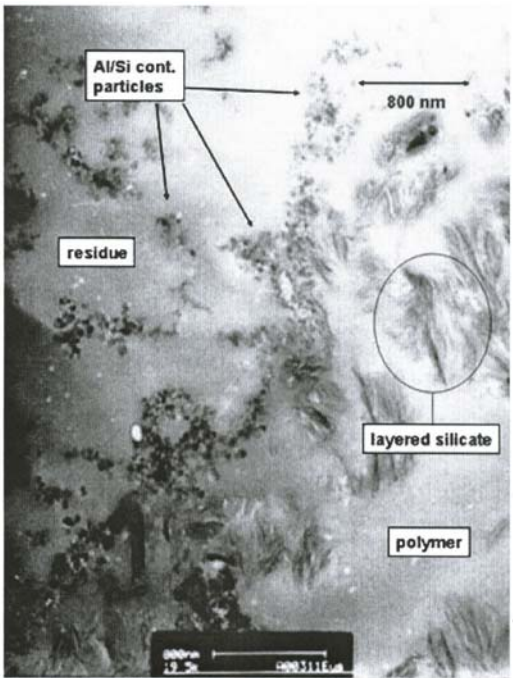

Figure 7.30 TEM image of the ignited polymer sample containing the sodium bentonite in the region between the decomposed and the intact polymer. Reprinted with permission from A. Hartwig, D. Putz, B. Schartel, M. Bartholmai and M.Wendschuh-Josties, *Macromolecular Chemistry and Physics,* 2003, **204**, 2247 © 2003, Wiley-VCH Verlag GmbH & Co KgaA

Hartwig and co-workers [122] examined the cone calorimetric analysis of three different epoxy samples: unmodified epoxy resin (E+T), layered silicate epoxy resin nanocomposite with 4.7 wt% ammonium bentonite (E+T+trimethylamine (TMA)) and layered silicate epoxy resin nanocomposite with 4.7 wt% phosphonium bentonite (E+T+TPP). The comparison of heat release rates and total heat release for the three epoxy samples are presented in **Figure 7.31**. The external heat flux of 70 kW/m2 was maintained for all the samples. The unmodified resin shows sharp peak whereas the nanocomposites show platue-like behaviour. The drastic reduction in peak heat release rate shows a typical improvement in fire resistance. The phosphonium bentonite-based nanocomposite shows superior flame resistance behaviour compared to the ammonium bentonite-based nanocomposite. The advantages of organoclay over conventional flame retardants are manifolds: no generation of toxic gases (truly green flame retardant) and no discolouration. Use of organoclay improves the mechanical properties unlike conventional flame retardants which usually cause a deterioration in the thermo mechanical properties [22-26]. However, it is usually found that such clay additions are not themselves sufficiently effective to be classified as a flame retardant. The clay modified polymer compositions perform poorly when tested by the industrially significant UL-94 standard with respect to extinction time [123]. The failure is attributed to the adsorbed onium salt present in the clay (making it organophilic) which increases the early ignition. Also at high temperature the onium ions present in the galleries of the clay undergo decomposition destroying the nanocomposite structure.

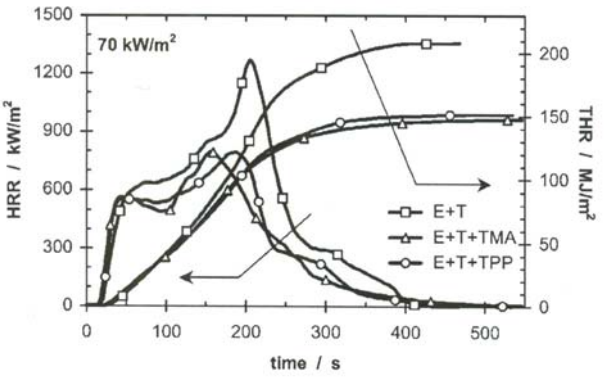

Figure 7.31 Cone calorimetric analysis of three different epoxy samples: unmodified epoxy resin (E+T), layered silicate epoxy resin nanocomposite with 4.7 wt% ammonium bentonite (E+T+TMA) and layered silicate epoxy resin nanocomposite with 4.7 wt% phosphonium bentonite (E+T+TPP). Reprinted with permission from A. Hartwig, D. Putz, B. Schartel, M. Bartholmai and M.Wendschuh-Josties, *Macromolecular Chemistry and Physics*, 2003, **204**, 2247 © 2003, Wiley-VCH Verlag GmbH & Co KgaA

7.6.2.5 Combination Organoclay and Other Flame-Retardants

It has been established by recent studies that the presence of a nanofiller (organoclay) enhances the compatibility of an incompatible blend. For example scanning transmission X-ray microscopy images [124] of PS/PMMA (30/70) and PS/PMMA/Closite 30B (27/63/10) taken after annealing at 190 °C are presented in **Figure 7.32**. It was observed that the size of the dispersed particles decreases due to the addition of clay into PS/PMMA blend indicating the improvement in compatibility. The results have been attributed to the barrier effect or specific interaction of both the polymers with the clay, which resulted in a change in free energy of mixing. The modern flame retardants are basically organic molecules with halogen or phopshorus groups, and are not well dispersed in polymer system. Hence it can be postulated that the presence of clay might enhance the compatibility between the polymer and the fire retardant resulting in an improvement in fire properties. Thus by using a small amount of clay, it is possible to significantly reduce the amount of conventional fire retardant additives, required for an optimum flame retardancy. The conventional flame retardants have always some detrimental effects on the mechanical properties of the polymer system, hence by using nanoclay, such detrimental effects can be minimised and compensated. Synergistic effects of inorganic flame retardants (aluminum trihydrate) and phopshorus based flame retardants with nanoclay, were reported for thermoset resins like epoxy [125] and vinyl ester [126]. TEM and pyrolysis gas chromatography-mass spectrometry measurements of serially burned samples indicate that the clays play various roles on quenching the flame, such as promoting the char formation, improving the dispersion of fire-retardants and catalysing the chain reaction for dissociation of halogenated compounds. However, Simon and co-workers [127] observed no synergistic effect while studying a tetrafunctional epoxy/clay nanocomposite and a phopshorus containing flame retardant. The synergistic effect of nanoclay and conventional fire retardant (decabromodiphenyl oxide plus antimony trioxide) was also investigated for thermoplastic-based nanocomposite systems e.g., polypropylene-*g*-maleic anhydride system [120]. The synergy between the brominated fire retardant and antimony trioxide was found in nanocomposite system whereas no synergy was observed in the virgin polymer matrix.

7.7 Application of nanocomposites

Nanocomposites have potential applications in various industries namely automotive, packaging, aerospace, electronics, biomedical and defense. Various applications are briefly presented in **Table 7.2**. The first successful use of polymer/clay nanocomposites was in automotive industries. Reseacher at Toyata could reduce the weight of the automobile parts about 40% by using nanomaterials compared to the conventional

materials. Subsequently, the technology was adopted by other automotive companies. Thus the use of nanocomposites in automotive industries is likely to reduce the fuel consumption and the related carbon dioxide emissions to a great extent.

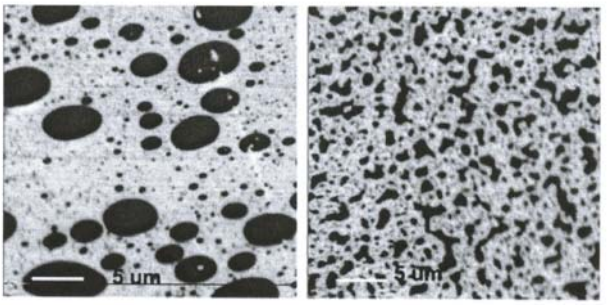

Figure 7.32 Scanning transmission X-ray microscopy images of PS/PMMA (30/70) and PS/PMMA/Closite 30B (27/63/10) taken after annealing at 190 °C. Reprinted with permission from M. Si, T. Araki, H. Ade, A.L.D. Kilcoyne, R. Fisher, J.C. Sokolov, M.H. Rafailovich, *Macromolecules*, 2006, **39**, 4793 © 2006, American Chemical Society

The unique mechanical and barrier properties of nanocomposites justify their potential applications in structural and packaging applications. Very thin nanocomposite films can be used as wrapping materials for vegetables and fruits for long storage due to their inherent very low permeability to oxygen and moisture. Specific examples include packaging of processed meats, cheese, confectionary and boil-in-the-bag foods. Since the nanocomposite film with much lower thickness compared to pristine polymer film can serve the packaging purpose, the solid waste and burden of the soldier can be reduced significantly. Thus nanocomposite has potential applications in defence technology.

Table 7.2 Application of polymer nanocomposites	
Field of application	**Area/advantages**
Automotive	Timing belt cover, engine cover, door handles, bumper etc.
Food packaging	a. Enhancement of shelf life of food b. Reduction of solid waste c. Reduction in overall logistic burden of war fighter
Fuel Tanks	a. Low fuel transmission b. Material for fuel tank and fuel line component of vehicles
Aerospace	a. Low level of incorporation b. Less weight penalty
Plastic film industries	Enhancement of transparency and haze reduction
Naval	Reduced water diffusion coupled with flame retardancy
Barrier coating	Reduced permeability
Medical	Dental filling material, artificial intestine
Electrical and electronic industries	Electrodes, sensors, gas separation membrane, fuel cell membrane, solid polymer electrolytes for batteries and supercapacitors
Smart devices	Remote sensing actuators
General	Impellers, blades for vacuum cleaner, power hoods and covers for electronic equipment

The low gas permeability of nanocomposites can be exploited for the development of gas separation membranes, where restricted and preferential permeability of gases are the prime requirement. Nanotechnology can be used for the development of high performance proton-exchange membrane fuel cell (PEMFC). Fuel cells are an unconventional energy source and provide energy without environmental pollution and are going to be the future energy sources. The role of the membrane is to allow proton transport from the anode to the cathode and to act as a separating barrier between hydrogen and oxygen. Presently, Nafion® (DuPont) is widelly used as a membrane in PEMFC. However, it is permeable to methanol, very expensive and limited to only low temperature applications. The use of PEMFC membrane at higher temperature (80 °C) is required in order to increase the yield of the cell. By using nanomaterials like layered silicate or CNT it is possible to control the properties like moisture retention, chemical stability and proton conductivity of a conventional thermoset based membrane so that they can compete with Nafion in terms of exchange property and at the same time offer better thermal stability.

Since thermoset nancomposites show much lower water permeability compared to the corresponding matrix polymer, they have potential applications in the Navy. The electronic instruments (e.g., transducer) have to work under water for navigation and ranging purposes. It is necessary to encapsulate such instruments with a suitable polymeric material. The nanocomposite based encapsualting materials can offer longer life because of their lower water permeability. The thermoset resin and nanoclay combination can be integrated into glass or carbon fibre reinforced composites for the development of FRP structures for underwater applications. Thus by utilising nanotechnology the life of materials can be significantly extended for underwater applications.

Polymer nanocomposites have potential applications in the field of vibration damping. Vibration damping is necessary to avoid undesirable consequences such as unpleasant motions, noise and dynamic stresses. Polymers (viscoelastic materials) are generally used to damp the vibration. For an effective vibration damping, a material should have both high modulus and loss factor. When a polymer is blended with conventional fillers the modulus increases moderately along with a drastic reduction in loss factor. By using nanomaterials the modulus can be improved considerably without a significant sacrifice or even increase in loss factor. Hence such nanocomposite materials are going to find wide applications in the field of vibration damping.

Thermoset/CNT composites can be used as conducting composites for various applications. One such example is antistatic coating. Polymers because of insulating nature often find problem arising due to the storage of static electricity. This problem can be solved by incorporating small amount of CNT. Thermoset/CNT composites are the future materials for aerospace application because of their antistatc property and radiation resistance. Shape memory polymers (SMP)/CNT composites have potential applications in remote sensing actuators. PU-based SMP have already been discussed in **Chapter 2**. Most of the SMPs reported so far exhibit thermally induced shape memory effect. Heat is a very good stimulus but it is very difficult to control remotely. The SMP/CNT nanocomposite system is expected to offer electrically induced actuation, which can be controlled remotely, via Joule heating (current is passed through the conductive percolative network of the nanotubes within the SMP system).

Recent works on conducting polymer based nanocomposite and liquid crystalline polymer-based nanocomposites show promise for electronic applications [15, 16]. Conductive polymer based nanocomposites present remarkable electrochemical behaviour, attracting interest in applications that include modified electrodes, biosensors, solid state batteries, smart windows and other electrochemical devices. Poly pyrole (Ppy)-clay nanocomposite exhibit a redox chemistry approximately 1 V more negative than the chemically synthesised Ppy. Although the capacitances of the materials are similar, the charge discharge plateau is also shifted approximately 1

V [15]. These observations could be related to the close interaction of the polymer with anionic clay layers, stabilising the Ppy cationic form. The conductivity of polyethylene oxide-based electrolyte (containing Li ions) can be significantly enhanced by incorporating a small amount of clay. The PEO based electrolyte shows lower ionic conductivity due to high crystallinity of PEO and formation ion pairs (ion pair effect). The small anions get attached with cation strongly and move as ion pair under electrical field which significantly reduces the effective cation conductivity. Modification of PEO-based electrolyte with 7.5% organoclay resulted in an increase in conductivity by several times [129]. Such a dramatic change in conductivity due to the incorporation of clay can be explained by two reasons; firstly the clay increases the amorphous content of PEO which participate in conduction of ions. Secondly when Li ion enter into the galleries of clay the silicate layers act as anion and under the electric field only the Li ion moves causing an increase in effective cation conductivity.

Thermoset based liquid crystalline materials have been discussed in chapter 3. When an electric field is applied the LC orient themselves in the direction of the field and once the electric field is turned off the reformation takes place immediately. When clay is dispersed in LC matrix, the clay platelets anchor the LC and prevent to reform into the original random distribution. Such systems can find applications like adjustable light-controlling glass, erasable optical storage battery, thermo-optical sensor, optical shutter etc. The same strategy can be used in non linear optical material to increase the relaxation time of the aligned dipoles. NLO polymers posses the dipoles, which can be aligned by the application of electric field at a temperature higher than Tg of the polymer. The dipole arrangement can be fixed by cooling the polymer to room temperature, keeping the electric field on. Such poled system exhibits an interesting property of second harmonic generation. When a radiation having a frequency of w is passed through the material, the radiation is converted into one with frequency of 2 w. Thus such materials have potential use for frequency modulation and many other interesting applications. However, the dipoles in a polymer with moderate T_g relax very fast leading to a loss in efficiency of the second harmonic generation. Incorporation of clay is expected to reduce the relaxations of the dipoles in the same way as in the LC systems discussed above.

7.8 Summary and Outlook

The two decades have witnessed an extensive research and development in the field of thermoset nanocomposites. The physics and chemistry of intercalation of clay (layered silicate) in thermoset resin have been understood to a great extent though synthesis of fully exfoliated thermoset-based nanocomposites still remains as a challenge. More research is necessary to study the feasibility of integrating the nanoreinforced thermoset resins into the fibre-reinforced plastics to develop composite structure not

only with an improved strength but with improved water and solvent resistance. Such composites will have tremendous potential for use in civil and defence sectors. It has been demonstrated that reinforcing effect is much more effective in a rubbery matrix rather than in a highly brittle glassy matrix. Research will continue in this field focusing more on using low T_g thermoset matrices, and the thermosets with liquid crystalline and nonlinear optical properties.

Organoclays offer fire retardancy without any environmental hazard ("green" flame-retardants). Note that the use of conventional flame retardants (FR) is associated with environmental hazards, deterioration in mechanical properties and discolouration. However, nanoclays are not sufficiently effective when used alone. They can be used in combination with other FR to achieve the required fire properties with a minimum amount of FR and to compensate the degradation in thermomechanical properties of the composites occurring due to the addition of FR. Chemically reactive phopshorus-containing flame retardants, in addition with organoclays, are going to be the future materials for the development of high performance flame retardant thermoset composites. Note that phopshorus-containing FR are reported to be better in terms of environmental protection compared to the halogen-based ones. In addition phopshorus-containing modifiers, can simultaneously act as a flame retardant and as an impact modifier for thermoset (as has been recently demonstrated for epoxy resins, [114]).

Though both the technologies, namely thermoset/clay and thermoset/CNT are contemporary, the former is more matured compared to the later. Hence, future works on thermoset nanocomposites is going to consider carbon nanotube (CNT) in a bigger way. Since the magnitude of CNT strength is very high (almost 10 times higher than that of a typical carbon fiber), very high interfacial shear strength may be required for a more efficient strengthening of polymers with CNT. Recent strategies of using functionalised CNT, and cation-Π interactions show a considerable promise and are likely to be the subjects of major focus in the near future.

The toughening strategy can be coupled with a suitable nanoreinforcement by using a nanofiller like nanoclay and CNT, to produce strong and tough composites. The control of both microstructures and nanostructures is required for achieving the optimum properties. In a liquid rubber-toughened system, the presence of clay disturbs the reaction-induced phase separation resulting in a change in microstructure. Thus extensive studies are needed to look into the various aspects for optimisation of both the microstructures and nanostructures.

References

1. B.M. Novak, *Advanced Materials,* 1993, **5**, 422.

2. P. Westbrock and F. Marin, *Nature*, 1998, **394**, 256.

3. C. Sanchez, P. Julian, P. Pellerille and M. Popall, *Journal of Materials Chemistry,* 2005, **15**, 3559.

4. G. Philipp and H. Schimdt, *Journal of Non-Crystalline Solids,* 1984, **80**, 283.

5. G. Philipp and H. Schimdt, *Journal of Non-Crystalline Solids,* 1986, **82**, 31.

6. M. Kakimoto, Y.Iyoku, A.Morikawa, H. Yamaguchi and Y. Imai, *Polymer Preprints*, 1994, **35**, 393.

7. S. Mann, S.L. Burkett, S.A. Davis, C.E. Fowler, N.H. Mendelson, S.D. Sims, D. Walsh and N.T. Whilton, *Chemistry of Materials,* 1997, **9**, 2300.

8. T.P. Lodge, *Macromolecular Chemistry and Physics*, 2004, **204**, 265.

9. D. Ratna and A.K. Banthia, *Macromolecular Research*, 2004, **12**, 11.

10. D.J. Greenland, *Journal of Colloid Science,* 1963, **18**, 647.

11. A. Usuki, Y. Kojima, M. Kawasumi, A.Okoda, Y. Fukushima, T. Kurauchi and O. Kamigaito, *Journal of Materials Research,* 1993, **8**, 1179.

12. Y. Kojima, A. Usuki, M. Kawasumi, A. Okada, T. Kurauchi and O. Kamigaito, *Journal of Polymer Science Part A: Polymer Chemistry Edition*, 1993, **31**, 983.

13. M. Zanetti, S. Lomakin and G. Camino, *Macromolecular Materials and Engineering*, 2000, **279**, 1, 1.

14. B.K.G. Theng, *The Chemistry of Clay-Organic Reactions*, Wiley, New York, NY, USA, 1974.

15. E.P. Giannelis, *Advanced Materials,* 1996, **8**, 1, 29.

16. M. Kawasumi, *Journal of Polymer Science Part A: Polymer Chemistry Edition*, 2004, **42**, 3, 819.

17. D. Ratna, *Journal of Polymer Materials*, 2002, **19**, 2, 143.

18. N. Karak, *Journal of Polymer Materials*, 2006, **23**, 1, 1.

19. S. Verghese, K.G. Gatos, A.A. Apostolov and J. Karger-Kocsis, *Journal of Applied Polymer Science*, 2004, **92**, 543.

20. A. Usuki, H. Hasegawa and M. Kato, *Advances in Polymer Science,* 2005, **179**, 135.

21. Y. Tang, Y. Hu, S. Wang, J. Gui, Z. Chen and W. Fan, *Polymers for Advanced Technology,* 2003, **14**, 733.

22. P.C. LeBaron, Z. Wang and T.J. Pinnavaia, *Applied Clay Science,* 1999, **15**, 1, 11.

23. D. Ratna, *Epoxy Composites: Impact Resistance and Flame Retardancy,* Rapra Review Report No.185, Rapra Technology, Shawbury, Shrewsbury, UK, 2005.

24. N.A. Salahuddin, *Polymers for Advanced Technology*, 2004, **5**, 5, 251.

25. T. Lan, P.D. Kaviratna and T.J.Pinnavia, *Chemistry of Materials,* 1994, **6**, 573.

26. Z. Wang, T. Lan and T.J. Pinnavaia, *Chemistry of Materials,* 1996, **8**, 2200.

27. T. Lan and T.J. Pinnavia, *Chemistry of Materials,* 1994, **6**, 2216.

28. J.M. Brown, D. Curliss and R.A. Vaia, *Chemistry of Materials,* 2000, **12**, 3376.

29. A.Yasmin, J.L. Abot and I.M. Daniel, *Scripta Materiala*, 2003, **49**, 1, 81.

30. O. Becker, Y.B. Cheng, R.J. Varley and G.P. Simon, *Macromolecules*, 2003, **36**, 1616.

31. S. Sinha Ray and M. Okamoto, *Progress in Polymer Science*, 2003, **28**, 1539.

32. D. Ratna, N.R. Manoj, R.K. Singh Raman, R. Varley and G.P. Simon, *Polymer International*, 2003, **52**, 9, 1403.

33. I.J. Mathias, R.D. Davis and W.L. Jarrett, *Macromolecules*, 1999, **32**, 7958.

34. A. Bafna, G. Beaucage, F. Mirrabella and S. Mehta, *Polymer*, 2003, **44**, 1103.

35. T. McNally, W.R. Murphy, Y.L. Chun, R.J. Turner and G.P. Brennan, *Polymer*, 2003, **44**, 2761.

36. C. Chen and D. Curliss, *Nanotechnology*, 2003, **14**, 643.

37. D.L. VanderHart, A. Asano and J.W. Gilman, *Macromolecules*, 2001, **34**, 3819.

38. R.A. Vaia, K.D. Jandt, E.J. Kramer and E.P. Giannelis, *Macromolecules*, 1995, **28**, 8080.

39. Y. Ke, J. Lü, X. Yi, J. Zhao and Z. Qi, *Journal of Applied Polymer Science*, 2000, **78**, 808.

40. T. Lan, P.D. Kaviratna and T.J. Pinnavaia, *Chemistry of Materials,* 1995, **7**, 2144.

41. C . Zilg, R. Thomann, J. Finter and R. Mülhaupt, *Macromolecular Materials and Engineering*, 2000, **280/281**, 1, 41.

42. Z. Wang and T.J. Pinnavaia, *Chemistry of Materials,* 1998, **10**, 1820.

43. M. Okamoto, P.H. Nam, P. Maiti, T. Kotaka, N. Hasegawa and A. Usuki, *Nano Letters*, 2001, **1**, 6, 295.

44. T.B. Tole and D.P. Anderson, *Composites Science and Technology*, 2002, **62**, 1033.

45. X. Kornmann, R. Thomann, R. Mulhaupt, J. Finter and L.A. Berglund, *Polymer Engineering and Science,* 2002, **42**,1815.

46. H.L. Tyan, Y. Liu and K. Wei, *Chemistry of Materials,* 1999, **11**, 7, 1942.

47. D. Yebassa, S. Balakrishnan, E. Feresenbet, D. Raghavan, P.R. Start and S.D. Hudson, *Journal of Polymer Science Part A: Polymer Chemistry Edition*, 2004, **42**, 1310.

48. C. Chen and D. Curliss, *Journal of Applied Polymer Science*, 2003, **90**, 2276.

49. J.S. Chen, M.D. Poliks, C.K. Ober, Y. Zhang, U. Wiesner and E.P. Giannelis, *Polymer*, 2002, **43**, 4895.

50. J. Park and S.C. Jana, *Macromolecules*, 2003, **36**, 22, 8391.

51. D. Kong and C.E. Park, *Chemistry of Materials,* 2003, **15**, 419.

52. P.D. Messersmith and E.P. Giannelis, *Chemistry of Materials,* 1994, **6**, 1719.

53. C. Zilg and R. Mulhaupt and J. Finter, *Macromolecular Chemistry and Physics*, 1999, **200**, 661.

54. T. Lan, P.D. Kaviratna and T.J. Pinnavia, *Journal of Physics and Chemistry of Solids*, 1996, **57**, 1005.

55. T. Lan and T.J. Pinnavia, *Chemistry of Materials,* 1994, **6**, 2216.

56. D. Ratna, B.C. Chakraborty, H. Dutta and A.K. Banthia, *Polymer Engineering and Science,* 2006, **46**, 12, 1667.

57. O. Becker, R.J. Varley and G.P. Simon, *European Polymer Journal*, 2004, **40**, 1, 187.

58. K. Yano, Y. Kojima, A. Usuki, A. Okada, T. Kurachi and O. Kamigaito, *Journal of Polymer Science Part A: Polymer Chemistry Edition*, 1993, **31**, 2493.

59. A.P. Shah, R.K. Gupta, H.V.S. Gangarao and C.E. Powell, *Polymer Engineering and Science*, 2002, **42**, 1852.

60. D.P. Fasce, R.J.J. Williams, F. Mechin, J.P. Pascault, M.F. Llauro and R. Petiaud, *Macromolecules*, 1999, **32**, 15, 4757.

61. D.P. Fasce, R.J.J. Williams, R. Balsells, Y. Ishikawa and H. Nanami, *Macromolecules*, 2001, **34**, 11, 3534.

62. S.A. Pellice, D.P. Fasce and R.J.J. Williams, *Journal of Polymer Science Part B: Polymer Physics Edition*, 2003, **41**, 13, 1451.

63. Y. Ni and S. Zheng, *Macromolecules*, 2007, **40**, 19, 7009.

64. I.A. Zucchi, M.J. Galante, R.J.J. Williams, E. Franchini, J. Gally and J.F. Gerard, *Macromolecules*, 2007, **40**, 4, 1274.

65. C. Cheng, H. Cheng, P. Cheng and Y. Lee, *Macromolecules*, 2006, **39**, 7583.

66. M.W. Matsen and F.S. Bates, *Macromolecules*, 1996, **29**, 1092.

67. P.M. Lipic, F.S. Bates and M.A. Hillmyer, *Journal of the American Chemical Society*, 1998, **120**, 8963.

68. R.B. Grubbs, J.M. Dean, M.E. Broz and F.S. Bates, *Macromolecules*, 2000, **33**, 9522.

69. S. Ijima, *Nature*, 1991, **354**, 1, 56.

70. E.T. Thostenson, Z. Ren and T. Chou, *Composites Science and Technology*, 2001, **61**, 13, 1899.

71. Y. Lin, M.J. Meziani and Y-P.J. Sun, *Materials Chemistry,* 2007, **17**, 1143.

72. D. Bhaskaran, J.R. Dunlap, J.W. Mays and M.S. Bratcher, *Macromolecular Rapid Communications*, 2005, **26**, 481.

73. B. Zhao, H. Hu, A. Yu, D. Perea and R.C. Haddon, *Journal of the American Chemistry Society*, 2005, **127**, 8197.

74. C.Y. Hong, Y.Z. You and C.Y. Pan, *Chemistry of Materials*, 2005, **17**, 2247.

75. A.M. Shanmugharaj, J.H. Bae, R.R. Nayak and S.H. Ryu, *Journal of Polymer Science Part A: Polymer Chemistry*, 2007, **45**, 460.

76. J.N. Coleman, U. Khan, W.J. Blau and Y.K. Gun'ko, *Carbon*, 2006, **44**, 1624.

77. B. Vigolo, A. Penicaud, C. Coulon, C. Sauder, R. Pailler, C. Journet, P. Bernier and P. Poulin, *Science*, 2000, **290**, 1331.

78. P.M. Ajayan, L.S. Schadler, C. Giannaris and A. Rubio, *Advanced Materials*, 2000, **12**, 750.

79. D. Ratna, T. Abraham, S. Siengchin and J. Karger-Kocsis, *Journal of Polymer Science Part B: Polymer Physics Edition*, 2009, **47**, 12, 1156.

80. R. Andrews and M.C. Weisenberger, *Current Opinion in Solid State and Materials Science*, 2004, **8**, 1, 31.

81. P. Puglia, L. Valentini and J.M. Kenny, *Journal of Applied Polymer Science*, 2003, **88**, 452.

82. Y.X. Zhou, P.X. Wu, Z.Y. Cheng, J. Ingram and S. Jeelani, *Express Polymer Letters,* 2008, **2**, 1, 40.

83. L.S. Schadler, S.C. Giannaris and P.M. Ajayan, *Applied Physics Letters*, 1998, **73**, 3842.

84. H. Miyagawa and L.T. Drzal, *Polymer*, 2004, **45**, 15, 5163.

85. X. Gong, J. Liu, S. Baskaren, R.D. Voise and J.S. Young, *Chemistry of Materials*, 2000, **12**, 1049.

86. Z. Yaping, Z. Aibo, C. Qinghua, Z. Jiaoxia and N. Rongchang, *Materials Science and Engineering*, 2006, **A435**, 1, 145.

87. J. Zhu, H. Peng, F.R. Macious, J.L. Margrave, V.N. Khabashesku, A.M. Imam, K. Lozano and E.V. Barrera, *Advanced Functional Materials*, 2004, **14**, 643.

88. F.H. Gojny, M.H.G. Wichmann, U. Kopke, B. Fiedler and K. Schulte, *Composites Science and Technology*, 2004, **64**, 2363.

89. Y.T. Vu, G.S. Rajan, J.E. Mark and C.L. Myers, *Polymer International*, 2004, **53**, 1071.

90. O. Becker and G.P. Simon, *Advances in Polymer Science,* 2005, **179**, 1, 29.

91. J. Frohlich, R. Thomann and R. Mulhaupt, *Macromolecules*, 2003, **36**, 7205.

92. D. Ratna, O. Becker, R. Krishnamurty, G.P. Simon and R. Varley, *Polymer*, 2003, **44**, 24, 7449.

93. J. Choi, A.F. Yee and R.M. Laine, *Macromolecules*, 2004, **37**, 3267.

94. A.K. Subramaniyan and C.T. Sun, *Composites*, 2007, **A 38**, 1, 34.

95. J. Karger-Kocsis, O. Gryshchuk and N. Jost, *Journal of Applied Polymer Science*, 2003, **88**, 8, 2124.

96. J. Karger-Kocsis, O. Gryshchuk, J. Frohlich and R. Mullhaupt, *Composites Science and Technology*, 2003, **63**, 2045.

97. T. Keller C. Tracy and A. Zhou, *Composites Part A*, 2006, **37**, 7, 1286.

98. J.V. Bausano, J.J. Lesko and S.W. Case, *Composite Part A*, 2006, **37**, 7, 1092.

99. S.V. Levchik and E.D. Weil, *Polymer International*, 2004, **53**, 1901.

100. G.H. Chen, B.Yang and Y.Z. Wang, *Journal of Applied Polymer Science*, 2006, **102**, 4978.

101. V.I. Kodolov, S.G. Shuklin, A.P. Kuznetsov, L.G. Makarova, S.G. Bystrov, O.V. Demicheva and T.A. Rudakova, *Journal of Applied Polymer Science*, 2002, **85**, 1477.

102. C.P. Yang and T.M. Lee, *Journal of Applied Polymer Science*, 1987, **34**, 2733.

103. S.W. Shalaby and E.M. Pearce, *Internation Polymer Materials*, 1974, **3**, 1, 81.

104. A.E. Grand and C.A. Wilkie, *Fire Retardency in Polymeric Materials*, Marcel Dekker Inc., new York, NY, USA, 2000.

105. C.S. Wang and J.Y. Shieh, *European Polymer Journal*, 2000, **36**, 433.

106. C.S. Wang and C.H. Lin, *Journal of Applied Polymer Science*, 2000, **75**, 429.

107. U. Braun and B. Schartel, *Journal of Fire Science*, 2005, **23**, 5.

108. C.H. Lin and C.S. Wang, *Polymer*, 2001, **42**, 1869.

109. P. Jain, V. Choudhury and I.K. Verma, *Journal of Macromolecular Science C: Polyer Reviews*, 2002, **42**, 2, 139.

110. P.M. Hergenrother, C.M. Thompson, J.G. Smith, J.W. Connell, J.A. Hinkley, R.E. Lyon and R. Moulton, *Polymer*, 2005, **46**, 14, 5012.

111. U. Braun, A.I. Balabanovich, B. Schartel, U. Knoll, J. Artner, M. Ciesielski, M. Doring, R. Perez, J.K.W. Sandler, V. Altstadt, T. Hoffman and D. Pospiech, *Polymer*, 2006, **47**, 26, 8495.

112. X. Wang and Q. Zhang, *European Polymer Journal*, 2004, **40**, 385.

113. T. Hoffmann, D. Pospiech, L. Hausler, H. Komber, D. Voigt, C. Harnisch, C. Kollmann, J. Sandler and V. Altstadt, *Macromolecular Chemistry and Physics*, 2005, **206**, 423.

114. U. Braun, U. Knoll, B. Schartel, T. Hoffman, D. Pospiech, J. Artner, M. Ciesielski, M. Doring, R.P. Graterol, J.K.W. Sandler and V. Altstadt, *Macromolecular Chemistry and Physics*, 2006, **207**, 16, 1501.

115. Y. Hu, S. Wang, Z. Ling, Y. Zhuang, Z. Chen and W. Fan, *Macromolecular Materials and Engineering*, 2003, **288**, 272.

116. J.W. Gilman, *Applied Clay Science,* 1999, **15**, 1, 31.

117. M. Berta, C. Lindsay, G. Pans and G. Camino, *Polymer Degradation and Stability*, 2006, **91**, 1179.

118. J.W. Gilman, C.L. Jackson, A.B. Morgan, R. Harris, E. Manias, E.P. Giannelis, M. Wuthenow, D. Hilton and S.H. Philips, *Chemistry of Materials,* 2000, **12**, 1866.

119. S. Bourbigot, E. Devaux and X. Flambard, *Polymer Degradation and Stability*, 2002, **75**, 397.

120. M. Zanetti, G. Camino, D. Canavese, A.B. Morgan and C.A. Wilkie, *Chemistry of Materials,* 2002, **14**, 1, 189.

121. J. Innes and A. Innes, *Plastic Flame Retardants: Technology and Current Development*, Rapra Review Report No.168, Rapra Technology, Shawbury, Shrewsbury, UK, 2003.

122. A. Hartwig, D. Putz, B. Schartel, M. Bartholmai and M. Wendschuh-Josties, *Macromolecular Chemistry and Physics*, 2003, **204**, 2247.

123. A.B. Morgan, *Polymers for Advanced Technology,* 2006, **17**, 4, 206.

124. M. Si, T. Araki, H. Ade, A.L.D. Kilcoyne, R. Fisher, J.C. Sokolov and M.H. Rafailovich, *Macromolecules*, 2006, **39**, 4793.

125. Y. Wang, Q. Zhang and Q. Fu, *Macomolecular Rapid Communications*, 2003, **24**, 231.

126. B. Schartel, U. Knoll, A. Hartwig and D. Puetz, *Polymers for Advanced Technology,* 2006, **17**, 218.

127. G. Chigwada, D.D. Jiang and C.A. Wilkie, *Proceedings of the Fall Meeting 2004, ACS Polymeric materials: Science and Engineering*, Philadelphia, PA, USA, 2004, p.156.

128. M. Hussain and G.P. Simon, *Journal of Materials Science Letters*, 2003, **22**, 1471.

129. D. Ratna, S. Divekar, P. Sivaraman, A.B. Samui and B.C. Chakraborty, *Polymer International*, 2007, **56**, 900.

Abbreviations and Acronyms

τ	Matrix ligament thickness
Δ	Relative volume strain
δ	Solubility parameter
γ	Surface energy per unit area
Γ	Tear energy
η	Viscosity
ΔG_m	Free energy of mixing
^{13}C-NMR	Carbon 13 nuclear magnetic resonance
^{1}H-NMR	Proton nuclear magnetic resonance
3D	Three-dimensional
3FDA	4,4′-(2,2,2-Trifluoro-1-phenylethyledine) diphthalic anhydride
3FPMR	Fluorinated PMR polyimide
ABS	Acrylonitrile–butadiene–styrene copolymer
AFM	Atomic force microscope
APTMS	3-Aminopropyltrimethoxysilane
ASTM	American Society for Testing and Materials
ATBN	Amine-terminated copolymer of butadiene and acrylonitrile
BAFCY	2,2-Bis(4-cyanatophenyl)-1,1,1,3,3,3,3-hexafluoro propane

BAPP	2-Bis-[4-(4-aminophenoxy)phenyl] propane
BD	Butanediol
BEBP	4,4′-Bis-(2-hydroxyethoxy)biphenyl
BFPA	Poly[(tetra methylene fumerate)-*co*-(tetramethylene phthalate)]
BMI	Bismaleimide
BMPA	Poly[(tetramethylene maleate)-*co*-(tetramethylene phthalate)]
BPA	Bisphenol-A
BPO	Benzoyl peroxide
BPSA	Poly[(tetramethylene phthalate)-*co*-(tetramethylene succinate)]
BTDA	3,3′,4,4′-Benzophenone tetracarboxylic acid anhydride
BTDB	2,2′-Bis (trifluoromethyl)-4, 4′-diaminobiphenyl
CE	Cyanate ester
CEC	Cation exchange capacity
CF	Carbon fibre
CFRP	Carbon fibre-reinforced plastic
CMC	Ceramic matrix composite
CMPA	4-Methyl pentanoic acid
CNT	Carbon nanotube(s)
CP	Chlorinated paraffin
CPOM	Cross-polarised optical microscopy
CRPEHA	Carboxyl-randomised poly(2-ethyl hexyl acrylate)
CSR	Core-shell rubber
CTBN	Carboxyl-terminated copolymer of butadiene and acrylonitrile

CTPEGA	Carboxyl-terminated poly(ethylene glycol) adipate
CTPEHA	Carboxyl-terminated poly(2-ethyl hexyl acrylate)
CTPPGA	Carboxyl-terminated poly(propylene glycol) adipate
DB	Decabromobiphenyl oxide
Dcy	Dicynamide
DDM	4,4´ Diaminodiphenyl methane
DDS	4,4´-Diaminodiphenyl sulfone
DETDA	Diethyl toluene diamine
DGEBA	Diglycidyl ether of bisphenol A
DMA	Dynamic mechanical analysis
DMAc	Dimethyl acetamide
DMPA	Dimethylol propionic acid
d_o	Rubber particle diameter
DOPO	9,10 Dihydro-9-oxa-10-phosphaphenanthrene-10-oxide
DP_n	Degree of polymerisation, number average
DSC	Differential scanning calorimeter/ry
E´	Dynamic storage modulus
ECD	Epichlorohydrin
E_g	Glassy dynamic modulus
EP	Epoxy
EPDM	Ethylene propylene diene rubber
ESO	Epoxidised soyabean oil
ETBN	Epoxy-terminated vinyl-terminated poly(butadiene–acrylonitrile)

f	Functionality
FFA	Furfuryl alcohol
FRP	Fibre reinforced plastic(s)
FT-IR	Fourier transform infrared
G	Fracture energy
GC	Gas chromatography
G_C	Shear modulus
GF	Glass fibre
GFRP	Glass fibre-reinforced plastic
G_{1c} mode	Fracture energy
GMA	Glycidyl methacrylate
GPC	Gel permeation chromatography
HBP	Hyperbranched polymer(s)
HDI	1,6-Hexamethylene diisocyanate
HDT	Heat distortion temperature
HFDE	4,4´-(Hexafluoroisopropylidene)-diphthalic acid
HIPS	High-impact polystyrene
HMTA	Hexamethylene tetramine
HRR	Heat release rate
HTE	Hydroxyl-terminated polyether
HTPB	Hydroxyl-terminated polybutadiene
iBu-GlyPOSS	Glycidyloxypropyl-heptaisobutyl POSS
IFR	Intumescent fire retardant

ILSS	Inter laminar shear strength
iPh-GlyPOSS	Glycidyloxypropyl-heptaphenyl POSS
IPN	Interpenetrating polymer network(s)
IR	Infrared
IVW	Institute of Composite Materials, Kaiserlauten, Germany
Jeffamine	Polypropyletheramine
k	Boltzman constant
K_r	Rubber bulk modulus
LCEP	Liquid crystalline epoxy resin
LCM	Liquid composite moulding
LOI	Limiting oxygen index
LPA	Low profile additives
MA	Methyl acrylate
M_c	Molecular weight between crosslinks
MCDEA	4,4´-Methylenebis[3-chloro 2,6-diethylaniline]
MDA	Methylene dianiline
MDEA	4,4´-Methylenebis[2,6 diethyl aniline]
MDI	4,4´-Diphenylmethane diisocyanate
MEKP	Methyl ethyl ketone peroxide
MF	Melamine–formaldehyde
MLT	Matrix ligament thickness
MMC	Metal matrix composite
M_n	Number average molecular weight

MOCA	4,4´-Bis methylenebis (2-chloroaniline)
M_w	Molecular weight
M_w/M_n	Polydispersity index
MWCNT	Multiwall carbon nanotube
NASA	National Aeronautics and Space Administration
NBR	Phenolic-nitrile rubber
NLO	Nonlinear optical
NMP	*N*-Methyl pyrrolidone
NMR	Nuclear magnetic resonance
NMRL	Naval materials research laboratory
NMS	Nanoscale mesoporus silica
PALS	Positron annihilation lifetime spectroscopy
PBT	Poly(butylene terephthalate)
PC	Polycarbonate
PCF	*P*-Cresol formaldehyde
PCL	Polycaprolactone
PCLU	PCL-based polyurethane
PCN	Polymer-clay nanocomposite(s)
PDI	1,6-Diphenyl diisocyanate
PDMS	Poly(dimethyl siloxane) oligomer
PECH	Polyepichlorohydrin
PEG	Polyethylene glycol
PEI	Poly(ether imide)

PEMFC	Proton-exchange membrane fuel cell
PEO	Poly(ethylene oxide)
PEP	Poly(ethylene phthalate)
PEP	Poly(ethylene-alt-propylene)
PES	Poly(ether sulfone)
PET	Poly(ethylene terepthalate)
PF	Phenol formaldehyde
PGA	Polyglycolide
PGC	Poly(glycolide-*co*-caprolactone)
PGE	Phenyl glycidyl ether
PGly	Hyperbranched polyglycerol
phr	Parts per hundred of resin
PI	Polyimide
PLLA	Poly(L-lactide)
PMC	Polymer matrix composite(s)
PMMA	Poly(methyl methacrylate)
PMR	Polymerisation of monomer reactants
PMS	*N*-Phenylmaleimide styrene copolymer
POSS	Polyhedral oligomeric silsesquioxane
PP	Polypropylene
ppm	Parts per million
PPO	Poly(phenylene oxide)
Ppy	Polypyrole

PS	Polystyrene
PU	Polyurethane(s)
PVAc	Poly(vinyl acetate)
PVC	Poly(vinyl chloride)
R	Universal gas constant
RIM	Reaction injection moulding
RT	Room temperature
RTM	Resin transfer moulding
SAXS	Small angle X-ray scattering
SBR	Styrene butadiene rubber
SBS	Short beam shear test
SEM	Scanning electron microscope
SMA	Shape memory alloys
SMP	Shape memory polymer(s)
St	Styrene
SWCNT	Single wall carbon nanotube
TBBA	Tetrabromobisphenol-A
TBO	*t*-Butyl peroxide
T_c	Crystallisation temperature
TDI	2,4-, or 2,6-Toluene diisocyanate
t_{diff}	Time required for diffusion
TEM	Transmission electron microscope
TEOS	Tetraethoxysilane

TETA	Triethylene tetramine
T_g	Glass transition temperature(s)
TGA	Thermogravimetric analysis
TGAP	Triglycidyl *p*-amino phenol
TGDDM	Tetraglycidylether of 4,4′ diaminodiphenyl methane
t_{gel}	Time to gel
TGMDA	Tetraglycidyl methylene dianiline
THF	Tetrahydrofuran
TMA	Trimethylamine
TPP	Triphenyl phosphine
t_{ps}	Phase separation time
TTT	Time–temperature–*trans* formation
t_{vit}	Time to vitrify
UF	Urea–formaldehyde resins
UL-94	Underwriters Laboratory test
UPE	Unsaturated polyester
UV	Ultraviolet
V	Molar volume
VBGE	Vinyl benzyl glycidyl ether
VE	Vinyl ester
VEUH	Vinyl ester–urethane hybrid
VFM	Variable frequency microwave
VOC	Volatile organic compound(s)

VPO	Vapour pressure osmometer
VTBN	Vinyl-terminated poly(butadiene–acrylonitrile) rubber
WAXD	Wide-angle X-ray diffraction
WAXS	Wide-angle X-ray sattering
X_c	Crosslink density
XRD	X-ray diffraction
ΔS_m	Combinatorial entropy of mixing
υ_p	Volume fraction
Φ	Volume fraction

Index

D

F

G

H

I

J

L

M

R

S

T

U

V

W

X

Y

Published by Smithers Rapra, 2009

Handbook of Thermoset Resins is designed as a stand-alone guide to Thermoset Resins, an important class of polymer materials. The book begins with a general introduction to thermoset resins – including network concept, curing, processing, and testing – and ends with thermoset nanocomposites, a subject of much current interest. The objective of *Handbook of Thermoset Resins* is to provide focused and detailed information on synthesis, characterizations, applications, and toughening of thermoset resins. In contrast to thermoplastics, where the toughening is achieved by simple physical blending, the same is achieved in thermoset resins exclusively through chemistry and presents a greater challenge to polymer scientists, as highlighted in this book.

This book also presents a detailed review of the recent advances on thermoset-based composites and nanocomposites. Finally, *Handbook of Thermoset Resins* highlights the future directions of research in various areas of thermoset resins.

With such broad technical content, covering the basic concepts and recent advances, the book serves as both a useful textbook and as a handbook for students, researchers, engineers, R&D scientists from academia, research laboratories and industries (related to resins, fibre composites, adhesive, paints, rubbers, printing inks, and more).

Scientists and researchers in the field of polymer science in general and thermoset resins in particular will find *Handbook of Thermoset Resins* very useful in developing a knowledge-base in the subject as well as planning their future research works.

SMITHERS
iSmithers

Shawbury, Shrewsbury, Shropshire, SY4 4NR, UK
Telephone: +44 (0)1939 250383
Fax: +44 (0)1939 251118
Web: www.rapra.net